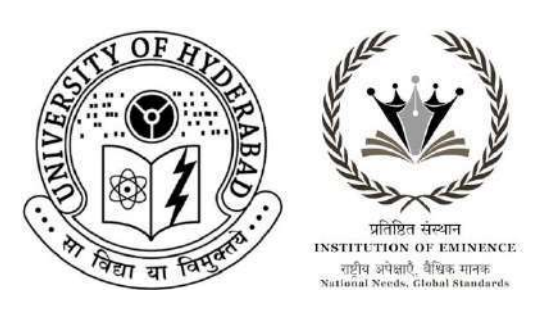
Protein engineering of Arabidopsis thaliana hydroxynitrile lyase (AtHNL) improves promiscuous nitroaldolase and retro-nitroaldolase activity

A thesis Submitted to University of Hyderabad for the award Doctor of Philosophy in Biochemistry

By Badipatla Vishnu Priya 17LBPH06



Department of Biochemistry
School of Life Sciences
University of Hyderabad
Hyderabad-500046
Telangana, India

November 2022



University of Hyderabad

Hyderabad -500046, India

Certificate

This is to certify that this thesis entitled "Protein engineering of Arabidopsis thaliana hydroxynitrile lyase (AtHNL) improves promiscuous nitroaldolase and retro-nitroaldolase activity" submitted by Badipatla Vishnu Priya bearing registration number 17LBPH06 in partial fulfilment of the requirement for the award of Doctor of Philosophy in the Department of Biochemistry, School of Life Sciences, is a bonafide work carried out by her under my supervision and guidance.

This thesis is free from plagiarism and has not been submitted previously in part or in full to this University or any other University or Institution for the award of any degree or diploma.

Part of this thesis has been presented in the following conferences:

Badipatla Vishnu Priya*, D.H. Sreenivasa Rao, Rubina Gilani, Surabhi Lata, Nivedita Rai, Mohd. Akif, Santosh Kumar Padhi "Improvement of catalytic efficiency and enantioselectivity of an engineered Hydroxynitrile lyase towards promiscuous retro nitroaldolase activity"- poster presented at International Symposium "Chemical Wisdom by Her" organized by Department of Chemistry, Deshbandhu College (DU) held on 31st January, 2022.

Badipatla Vishnu Priya*, Rubina Gilani, Nivedita Rai, Santosh Kumar Padhi "The promiscuous nitroaldolase activity of a plant hydroxynitrile lyase vs. its natural activity of cyanogenesis"- poster presented at National Seminar on "Biomolecular interactions in development and diseases" organized by Department of

Biochemistry, UoH held on 26-28th September, 2019.

Badipatla Vishnu Priya*, Rubina Gilani, Nivedita Rai, Santosh Kumar Padhi "Understanding the promiscuous nitroaldolase activity of a hydroxynitrile lyase vs. its natural cyanohydrin cleavage activity" - poster presented at BioQuest-2019 organized by School of Life Sciences, UoH held on 11th March 2019.

Published in the following journal:

Badipatla Vishnu Priya a, D.H. Sreenivasa Rao a.1, Rubina Gilani a.1, Surabhi Lata b.1, Nivedita Rai a, Mohd. Akif b, Santosh Kumar Padhi a*. Enzyme engineering improves catalytic efficiency and enantioselectivity of hydroxynitrile lyase for promiscuous retro-nitroaldolase activity. Bioorganic Chemistry, 120 (2022) 105594. (Chapter 2)

Further the student has passed the following courses towards fulfilment of coursework requirement for Ph.D.

Course code	Name	Credits	Pass/Fail
BC 801	Analytical Techniques	4	Passed
BC 802	Research ethics, Data analysis and Biostatistics	3	Passed
BC 803	Lab seminar and Records	5	Passed

Supervisor

Dr. Santosh Kumar Padhi Assistant Professor Department of Biochemistry School of Life Sciences University of Hyderabad Hyderabad-500 046. India Head, Dept. of Biochemistry

Dept. of Biochemistry
SCHOOL OF LIFE SCIENCES
UNIVERSITY OF HYDERABAD
HYDERABAD-500 046.

Dean, School of Life Sciences 23/11/22



University of Hyderabad Hyderabad -500046, India

Declaration

I, Badipatla Vishnu Priya, hereby declare that this thesis entitled "Protein engineering of Arabidopsis thaliana hydroxynitrile lyase (AtHNL) improves promiscuous nitroaldolase and retro-nitroaldolase activity" submitted by me under the guidance and supervision of Dr. Santosh Kumar Padhi, is an original and independent research work. I also declare that it has not been submitted previously in part or in full to this University or any other University or Institution for the award of any degree or diploma.

Date: 23 11 2022

Signature of the Student

Signature of the Supervisor

(Dr. Santosh Kumar Padhi) Dr. Santosh Kumar Padhi Assistant Professor Department of Biochemistry School of Life Sciences University of Hyderabad Hyderabad-500 046. India

Dedicated to my amma and nanna...

Acknowledgements

Undertaking this Ph.D. has been a truly life-changing experience and a roller coaster ride for me and it would not have been possible to complete it without the support and guidance that I received from many people. At this juncture, I would like to express my deepest gratitude to all those people for their help and probably words will fall short to convey my endless emotions.

Firstly, I would like to express my sincere and profound sense of gratitude to my supervisor **Dr.**Santosh Kumar Padhi for his continuous support, endless encouragement, and constant guidance throughout my Ph.D. study with his patience and knowledge. I am deeply indebted to him for training me in the interdisciplinary field of biology and chemistry. He has been a great mentor in mapping my PhD. journey and has been the backbone in molding me as a researcher capable of handling multi-functional activities with proper planning and execution. He is a gem of a person who is always ready to provide whatever support a student needs, always motivates in accomplishing our targets and encourages us whenever we are low. I shall be forever obliged for his timely guidance, boundless motivation and never-ending support.

I'm extremely grateful to my doctoral committee members: **Prof. N. Siva Kumar** and **Prof. Sharmishta Banerjee** for their critical comments and invaluable suggestions throughout my Ph.D. programme.

I would like to express my deepest thanks to **Prof. Krishnaveni Mishra**, Head, Department of Biochemistry and **Prof. Mrinal Kanti Bhattacharyya**, former Head, Department of Biochemistry for providing encouragement and necessary facilities for carrying out the research work.

I would like to extend my sincere thanks to **Prof. S. Dayananda**, **Prof. K.V.A. Ramaiah**, **Prof. MNV Prasad**, and **Prof. P. Reddanna** Deans of the School of Life Sciences for allowing me to use all the central facilities of school.

My sincere thanks to all the **faculty members** of the department of biochemistry and school of life sciences for their timely help.

I'm extremely grateful to **Dr. T. Saravanan** from the School of Chemistry, University of Hyderabad for his kind help to record NMR spectra used in my Ph.D. thesis work.

Major thanks to UOH-Infrastructure and School of Life Sciences facilities provided by **DST-COE**, **DBT-CREB**, **UGC-SAP UPE**, **CSIR** & **ICMR**.

I'm also very thankful to the funding bodies **UGC-SAP**, **DST-SERB**, **CSIR** & **IOE-UOH** for providing funding to our lab.

I also would like to thank **University of Hyderabad** (UoH) for providing me with the fellowship.

Many thanks to Chary sir, Prabhu sir and all other non-teaching staff of Department of Biochemistry and School of Life Sciences for their help.

I would like to thank all my previous and present lab-mates **Dr. Nisha Jangid, Dr. D.H.** Sreenivasa Rao, Ghufrana Abdus Sami, Ayon Chatterjee, Mohit Rajoria, Sukadev Rana, **Totha Vinay Kumar, A.P. Uha, Praneeta, and Nivedita Rai** for their help and co-operation during my research work.

I would also like to thank all the Bachelor's and Master's project students **Rubina Gilani, Lucas, Shalini Mishra and Monalisa** who worked with me during my Ph.D.

A big thanks to **S.Dheeraj**, **Karishma**, **Jeevani**, and **Prashanth** for helping me with the NMR facility.

I would like to thank to my Seniors & Friends – **Pankaj Kumar**, **Nachiketh**, **Shiraz** & **Surabhi** for their help and support. I also thank all my SLS and hostel friends.

My heartfelt thanks to all my beloved friends: Malathi Akka, C. Nitya, K. Praneeth Kumar, A. Priyanka, Y. Sri Ram, V. Govinda Raju and my Karra samu friends: G. Vasantha Lakshmi, M. Sudarshan Reddy, and V. Neeraja.

My special thanks to **Jyothi ma'am** with whom I spend good time with fun and have discussion over research work as well as personal issues. I am extremely grateful for her constant support, encouragement, and guidance.

Finally, I would like to thank my family members **Amma**, **Nanna**, **Annayya & Monu** for their unconditional love, affection, care, and support. This endeavor would not have been possible without their patience, encouragement, and motivation. They stood by me against all odds and gave me all the persistence, courage, and willpower to deal with all the uncertainties of life. To have them with me is my biggest blessing and fortune in life.

Lastly, I thank God, the Almighty, for the boundless blessings he has bestowed on my life. I am truly grateful for his unconditional and endless love, mercy, grace, and timely guidance. I offer my humble pranams at thy feet.

ABSTRACT

Application of enzymes as catalyst is emerging in academics and industries due to their high selectivity, environment friendly nature, and sustainable reaction conditions. Being not evolved to catalyze non-natural reactions, they often require modifications for industrial and research applications. Altering wild type enzymes usually produces potential biocatalysts with a wide range of desirable properties, suitable for industrial application. Hydroxynitrile lyases (HNLs) are a class of enzymes emerged as potent biocatalysts in the global market for the synthesis of various valuable optically pure compounds, i.e., α -cyanohydrins, and β -nitroalcohols. Based on the protein structure, enantioselectivity and presence of cofactor, HNLs are diverse in nature; yet their application in biotechnology industry is restricted with several limitations such as poor enantioselectivity, limited yield and not being evolved to accept unnatural substrates. In the current study, a plant HNL was engineered to achieve desired biocatalytic properties, such as increased enantioselectivity, conversions, stability, selectivity and broad substrate selectivity, while catalyzing a promiscuous reaction.

Here, we engineered a HNL and employed the variants to synthesize/prepare enantiopure β -nitroalcohols using the promiscuous Henry (nitroaldol) and retro-Henry (retro-nitroaldol) reactions. Enantiopure β -nitroalcohols are chiral drug intermediates that have diverse applications in pharmaceutical, agrochemical, and cosmetic industries. HNL catalyzed stereoselective synthesis of chiral β -nitroalcohols is considered to be one of the most predominant methods among other biocatalytic approaches as it involves an atom economy approach, and does not require additional steps of substrate synthesis. So far, *Arabidopsis thaliana* hydroxynitrile lyase (*At*HNL) is the only HNL reported for both stereoselective cleavage (retro-nitroaldolase activity) and synthesis (nitroaldolase activity) of chiral β -nitro alcohols. Unlike (*R*)-selective *Gt*HNL and *Ac*HNL which requires cofactor, *At*HNL doesn't require any cofactor for catalysis. The synthetic scope of the HNL catalyzed promiscuous nitroaldol reaction is high compared to the chiral cyanohydrin synthesis because the later reaction involves the use of hydrogen cyanide and hence is not preferred by the industries.

AtHNL catalyzing this promiscuous nitroaldol reaction is however limited by low enantioselectivity, poor yield, and narrow substrate scope. In addition to these limitations, no AtHNL engineering has been done to investigate its binding pocket towards this promiscuous

reaction. The mutational and modeling studies done so far are confined to understand the natural cyanogenesis reaction only. To address the above limitations, we envisioned to engineer AtHNL and explore the variants towards promiscuous retro-nitroaldol and nitroaldol reaction to obtain enantiocomplementary β -nitroalcohols.

We engineered AtHNL by altering residues in its binding site at Phe179, Phe82, and Tyr14. Protein engineering has enhanced the promiscuous retro-nitroaldolase activity, i.e., stereoselective cleavage of racemic 2-nitro-1-phenyl ethanol (NPE) of AtHNL. Screening of the variants library towards the retro-Henry reaction has identified F179N with ~2.4 fold greater catalytic efficiency (k_{cat}/K_M) than the WT. Further it showed enantioslectivity (E) of 137.6, which is ~1.7 fold more than the WT. Computational studies have supported the strong substrate binding by the F179N and a better orientation of the substrate in the active site of F179N, which is similar with the data observed from kinetics. Based on the interactions between (R)-NPE and AtHNL wild type at different time intervals from the molecular dynamic simulations study, a plausible retro-nitroaldol mechanism was proposed. Finally, a preparative scale synthesis of (S)-NPE using crude cell lysates of F179N under optimized conditions was performed. This resulted in 48.6% isolated yield of (S)-NPE with 93% ee, including ~20% ethyl acetate impurity.

The AtHNL variants were studied in the synthesis of (R)- β -nitroalcohols to address the limitations such as low enantioselectivity, poor yield, and narrow substrate scope. The F179, F82 and Y14 library were screened towards the synthesis of (R)-NPE from benzaldehyde by asymmetric Henry reaction. Selected variants were further studied towards the enantioselective nitroaldol reaction with a wide range of substrates (aldehydes) along with nitromethane as a nucleophile. The AtHNL engineering was proven productive with several aromatic aldehydes containing single, double and triple substitutions in the aromatic ring, substituents at different positions of aromatic ring having both electron-donating and withdrawing groups, as substrates in the chiral β -nitroalcohol synthesis. Our study of the substrate scope of dozen of selected AtHNL variants in the synthesis of diverse (R)- β -nitroalcohols revealed that the variants F179N, F179W, Y14M, Y14F and Y14M-F179W have improved the enzyme's activity significantly. This study uncovered several AtHNL variants which have successfully improved the promiscuous Henry reaction activity, broad substrate selectivity, and enantioselectivity.

In final objective of the thesis, the selected AtHNL variants of the previous study were tested to synthesize (R)-1-(4-methoxyphenyl)-2-nitroethanol, an industrially useful chiral intermediate.

Combining this enzymatic synthesis, a chemo-enzymatic method was developed to synthesize a chiral intermediate of (R)-Tembamide, i.e., (R)-2-amino-1-(4-methoxyphenyl)-2-ethanol, an industrially significant active pharmaceutical ingredient. This involves a two-step process, (a) enzymatic synthesis of (R)-1-(4-methoxyphenyl)-2-nitroethanol, followed by, (b) a chemical reduction of the enzymatic product. The double variant Y14M-F179W showed the highest % conversion (70%) than other variants with > 99% ee in the synthesis of (R)-1-(4-methoxyphenyl)-2-nitroethanol. Further, this product was reduced to (R)-2-amino-1-(4-methoxyphenyl)-2-ethanol using a simple HCOOH/Zn in methanol at room temperature. We successfully made a clean and green combination of an engineered AtHNL along with a chemical catalyst to efficiently synthesize the (R)-Tembamide drug intermediate, i.e., (R)-2-amino-1-(4-methoxyphenyl)-2-ethanol in a preparative scale.

Keywords: β -nitroalcohols, *Arabidopsis thaliana* hydroxynitrile lyase, biocatalysis, promiscuity, protein engineering.

LIST OF CONTENTS

ACKNOWLEGEMENTS	i
ABSTRACT	iv
LIST OF TABLES.	xiii
LIST OF SCHEMES	xv
LIST OF FIGURES	
Chapter 1: Introduction	1
1.1. Protein engineering and its importance	2
1.2. Hydroxynitrile lyase	3
1.2.1. Classification of HNLs	4
1.2.2. Arabidopsis thaliana HNL (AtHNL)	7
1.3. Importance of HNL engineering.	8
1.4. Catalytic promiscuity	9
1.4.1. Nitroaldolase activity	10
1.4.2. Retro-nitroaldolase activity	11
1.5. Enantiopure β- nitroalcohols	11
1.5.1. Importance of enantiopure β- nitroalcohols	11
1.5.2. Various synthetic chemical transformations of β-nitro alcohols	11
1.5.3. Asymmetric synthesis of β -nitroalcohols.	15
1.5.3.1. Asymmetric synthesis of β -nitroalcohols by chemical catalysts	16
1.5.3.2. Importance of biocatalysis.	16
1.5.3.3. Asymmetric synthesis of chiral β -nitroalcohols by biocatalytic approaches	17
1.6. Promiscuous catalytic activity by HNL in synthesis of enantiopure β -nitroalcohols.	18
1.6.1. HNLs (non-engineered) catalyzed synthesis of enantiopure β -nitroalcohols	18
1.6.2. Engineered HNL catalyzed synthesis of enantiopure β-nitroalcohols	20
1.6.3. Engineered HNL catalyzed synthesis of enantiocomplementary β -nitroalcohols u	sing retro-
nitroaldol reaction	22
1.7. Engineered HNL catalyzed other promiscuous reactions	23

1.8. Requirement of HNL engineering for promiscuous synthesis of enantiopure β -nitroalcoh	nols.25
1.9. Objectives.	26
1.10. References	27
Chapter 2: AtHNL engineering to increase catalytic efficiency and enantiosele towards the promiscuous retro-nitroaldol reaction	_
2.1. Introduction	45
2.2. Objectives.	47
2.3. Materials and methods	47
2.3.1. Chemicals and materials	47
2.3.2. Primers employed in this work	48
2.3.3. Mutagenesis	48
2.3.3.1. Creation of <i>At</i> HNL variants (F82A, F179A)	48
2.3.3.2. Creation of SSM library at F82, F179, and Y14	49
2.3.3.3. Creation of <i>At</i> HNL double variants	49
2.3.4. Enzyme purification	50
2.3.5. CD spectroscopy measurements	50
2.3.6. Cyanogenesis and retro-nitroaldolase activity of <i>At</i> HNL and its variants	51
2.3.7. Determination of kinetic parameters of AtHNL variants for cyanogenesis and	retro
nitroaldol reaction	51
2.3.8. Synthesis of racemic NPE	52
2.3.9. At HNL variant catalyzed preparation of (S) - β -nitroalcohol using retro-nitroaldol reactions.	tion.52
2.3.10. Computational details.	53
2.3.10.1. Molecular docking studies	53
2.3.10.2. Molecular dynamic simulations	53
2.3.10.3. Binding free energy calculations	54
2.3.11. Preparative scale synthesis of (<i>S</i>)-NPE	55
2.3.11.1. Optimization of biocatalytic parameters for preparative scale synthesis of (S)-NPI	
2.3.11.2. Preparative scale synthesis.	56
2.4. Results.	56
2.4.1 SDS-PAGE of purified AtHNL and its variants	56

2.4.2. Steady state kinetics of <i>At</i> HNL toward cyanogenesis and retro-nitroaldol reaction59
2.4.3. CD spectroscopy measurements of AtHNL and its variants (F82A, F179A and F179A -
F17A)61
2.4.4. Steady state kinetics of AtHNL-F82A and AtHNL-F179A variants towards cyanogenesis
and retro-nitroaldol reaction
2.4.5. Cyanogenesis and retro-nitroaldolase activity of <i>At</i> HNL library of variants65
2.4.6. Kinetics analysis of <i>At</i> HNL variants for retro-nitroaldolase activity
2.4.7. <i>At</i> HNL variants catalyzed preparation of (<i>S</i>)-β-nitroalcohol
2.4.8. Study of <i>At</i> HNL double variants towards the retro-nitroaldol reaction80
2.4.9. Computational studies
2.4.9.1. Docking studies to identify hot spots in <i>At</i> HNL binding site84
2.4.9.2. Study of the binding pocket of <i>At</i> HNL87
2.4.9.3. Molecular docking and interaction studies to understand the substrate binding and
enantioselectivity of the variants
2.4.9.4. RMSD and RMSF analysis
2.4.9.5. Evaluation of binding free energy of substrate complex with WT and mutant proteins91
2.4.9.6. Plausible retro-nitroaldol mechanism based on MDS study of substrate interaction91
2.4.10. Preparative scale synthesis of (S)-NPE using AtHNL-F179N94
2.5. Discussion
2.5.1. Kinetic studies of AtHNL toward cyanogenesis and retro-nitroaldol reaction99
2.5.2. Docking studies to identify hot spots in <i>At</i> HNL binding site
2.5.3. Alanine mutants (Phe82 and Phe179) of AtHNL show higher selectivity for retro-
nitroaldolase activity over cyanogenesis
2.5.4. Study of the binding pocket of <i>At</i> HNL
2.5.5. Semi-rational engineering: creating saturation libraries at positions Y14, F82 and F179103
2.5.6. Cyanogenesis and retro-nitroaldolase activity of <i>At</i> HNL library of variants
2.5.7. Kinetics analysis of AtHNL variants for retro-nitroaldolase activity
2.5.8. <i>At</i> HNL variants catalyzed preparation of (S)-β-nitroalcohol
2.5.9. Study of <i>At</i> HNL double variants towards the retro-nitroaldol reaction
2.5.10. Molecular docking and interaction studies to understand the substrate binding and
enantioselectivity of the variants

2.5.11. RMSD and RMSF analysis	108
2.5.12. Evaluation of binding free energy of substrate complex with WT and mutant	proteins109
2.5.13. Plausible retro-nitroaldol mechanism based on MDS study of substrate inter-	raction109
2.5.14. Preparative scale synthesis of (S)-NPE using AtHNL-F179N	110
2.6. Conclusions.	111
2.7. References	112
Chapter 3: Enantioselective synthesis of diverse (R) - β -nitroalcohols by engin	
using promiscuous nitroaldol reaction	117
3.1. Introduction	118
3.2. Objectives	120
3.3. Materials and methods	121
3.3.1. Chemicals and materials	121
3.3.2. Mutagenesis	121
3.3.2.1. Creation of SSM library at F82, F179, and Y14	121
3.3.2.2. Creation of <i>At</i> HNL double variants	121
3.3.3. Enzyme expression and purification	122
3.3.4. HNL assay	122
3.3.5. Synthesis of racemic β-nitroalcohols	123
3.3.6. Screening of <i>At</i> HNL and its variants for (<i>R</i>)-NPE synthesis	123
3.3.7. At HNL variant catalyzed preparation of various (R)- β -nitroalcohols us	sing nitroaldol
reaction	123
3.4. Results.	124
3.4.1. SDS-PAGE of purified <i>At</i> HNL and its variants	124
3.4.2. Screening of <i>At</i> HNL and its variants for (<i>R</i>)-NPE synthesis	124
3.4.3 NMR characterization of the racemic β-nitroalcohols	143
3.4.4. Chiral resolution of racemic β-nitroalcohols by HPLC	143
3.4.5. AtHNL variant (62.5 U) catalyzed synthesis of various (R)-β-nitroalcohols u	sing nitroaldol
reaction	148
3.4.6. Enantioselective synthesis of various (R)- β -nitroalcohols by nitroaldol reaction	on using higher
amount of AtHNL variants (125 U)	175

3.4.7. At HNL double variants catalyzed synthesis of various (R) - β -nitroalcoho	ls using nitroaldol
reaction	181
3.5. Discussion.	189
3.5.1. Screening of <i>At</i> HNL and its variants for (<i>R</i>)-NPE synthesis	189
3.5.2. Chiral resolution of racemic β -nitroalcohols by HPLC	190
3.5.3. At HNL variants catalyzed synthesis of various (R) - β -nitroalcohols	using nitroaldol
reaction	191
3.6. Conclusions	198
3.7. References	199
Chapter 4: Development of a chemo-enzymatic method for synthe intermediate of (R) -Tembamide, using engineered At HNL	
4.1. Introduction	209
4.2. Objectives.	211
4.3. Materials and methods	211
4.3.1. Chemicals and materials	211
4.3.2. Mutagenesis	212
4.3.2.1. Creation of SSM library at F179, and Y14	212
4.3.2.2. Creation of <i>At</i> HNL double variants	212
4.3.3. Enzyme expression and purification	212
4.3.4. HNL assay	212
4.3.5. Synthesis of racemic 1-(4-methoxyphenyl)-2-nitroethanol	212
4.3.6. AtHNL variant catalyzed synthesis of various (R)-1-(4-methoxyphen	ıyl)-2-nitroethanol
using nitroaldol reaction	213
4.3.7. Preparative scale synthesis of (R) -1- $(4$ -methoxyphenyl)-2-nitroethanol	213
4.3.8. Preparative scale synthesis of (R) -Tembamide drug intermediate, i.e.,	(R)-2-amino-1-(4-
methoxyphenyl)-2-ethanol	213
4.4. Results	214
4.4.1. NMR characterization of racemic 1-(4-methoxyphenyl)-2-nitroethanol a	and 2-amino-1-(4-
methoxyphenyl) ethanol	214
4.4.2. Chiral resolution of racemic 1-(4-methoxyphenyl)-2-nitroethanol by HPL	.C215

4.4.3. At HNL variant (125 U) catalyzed synthesis of (R) -1- $(4$ -methoxy	phenyl)-2-nitroethano
using nitroaldol reaction	216
4.4.4. Preparative scale synthesis of (R) -1- $(4$ -methoxyphenyl)-2-nitroethan	ol using Y14M-F179W
crude cell lysate	220
4.4.5. Preparative scale synthesis of (R) -Tembamide drug intermediate,	i.e., (R)-2-amino-1-(4-
methoxyphenyl)-2-ethanol	222
4.5. Discussion	224
4.5.1. AtHNL variants (125 U) catalyzed synthesis of (R)-1-(4-methox)	yphenyl)-2-nitroethano
using nitroaldol reaction	224
4.5.2. Preparative scale synthesis of (R) -1- $(4$ -methoxyphenyl)-2-nitroethan	ol using Y14M-F179W
crude cell lysate followed by synthesis of (R)- Tembamide drug intermedia	ate, i.e., (R)-2-amino-1-
(4-methoxyphenyl)-2-ethanol	225
4.6. Conclusions	226
4.7. References	226
Chapter 5: Conclusions and future prospects	230
Future prospects	236
List of publications	238

LIST OF TABLES

Table	Title	Page
2.1	List of Primers used in this study. Italicized nucleotides are the site of mutation	48
2.2	The percentage of α-helix of WT, F82A, F179A and, F82A-F179A	61
2.3	Kinetic parameters of wild type AtHNL and variants using MN and NPE in	62
	cyanogenesis and retro-nitroaldol reaction, respectively	
2.4	Production of AtHNL mutant proteins in U per liter from purification	65
2.5	Steady-state kinetic parameters of purified AtHNL WT and variant libraries	73
	for the retro-nitroaldol reaction	
2.6	Steady-state kinetic parameters of purified AtHNL double variants for the	81
	retro-nitroaldol reaction.	
2.7	Docking results of MN and NPE with AtHNL	86
2.8	Binding energy and active site distance to substrate calculation results for (R)-	89
	NPE and (S)-NPE in WT and modelled mutant proteins docking.	
2.9	Catalytic triad distance in nm between Ca atoms of proteins in WT and its	90
	mutant.	
2.10	Average MMPBSA free energy of substrate complex with WT and its mutant.	91
2.11	Active site distance to substrate at different time points from MDS study.	92
2.12	Optimization of retro-nitroaldolase activity of cell lysates of F179N at	95
	different enzyme units and time points.	
2.13	Optimization of retro-nitroaldolase activity of cell lysates of F179N (200 U)	95
	using different % v/v of toluene.	
2.14	Optimization of retro-nitroaldolase activity of cell lysates of F179N (200 U)	95
	using higher contents of toluene	
3.1	Primers used to prepare Y14M-F179W double variant in this study. Italicized	122
	nucleotides are the site of mutation.	

3.2a	Enantioselective synthesis of (R)-NPE catalysed by F82 saturation library	125
	variants.	
3.2b	Enantioselective synthesis of (R)-2-nitrophenyl ethanol catalysed by F179	126
	saturation library variants.	
3.2c	Enantioselective synthesis of (R)-2-nitrophenyl ethanol catalysed by Y14	127
	saturation library variants	
3.3	HPLC conditions and retention times of aldehydes and racemic β-	144
	nitroalcohols.	
3.4	AtHNL variants (62.5 U) catalysed enantioselective synthesis of (R) - β -	150
	nitroalcohols.	
3.5	AtHNL variants (125 U) catalysed enantioselective synthesis of (R)-β-	176
	nitroalcohols.	
3.6	AtHNL double variants catalyzed enantioselective synthesis of (R) - β -	182
	nitroalcohols.	
4.1	HPLC conditions and retention time of 4-methoxybenzaldehyde and racemic	216
	1-(4-methoxyphenyl)-2-nitroethanol.	_

LIST OF SCHEMES

Scheme	Title	Page
1.1	HNL catalyzed (a) natural cyanogenesis reaction, (b) synthesis of chiral	4
	cyanohydrins.	
1.2	HNL catalyzed synthesis of chiral β-nitroalcohols.	10
1.3	Retro-Henry reaction catalyzed by <i>Hb</i> HNL and <i>At</i> HNL.	11
1.4	Various synthetic chemical transformations of a β-nitro alcohol adduct.	15
1.5	Asymmetric Henry reaction using a chemical catalyst.	16
1.6	HbHNL catalyzed stereoselective addition of (a) nitromethane to	19
	aldehydes, (b) nitroethane to benzaldehyde.	
1.7	AtHNL catalyzed asymmetric synthesis of (R) - β -nitro alcohols.	20
1.8	GtHNL and AcHNL catalyzed synthesis of A) enantioselective Henry	21
	products, and B) diastereoselective Henry products.	
1.9	AtHNL catalyzed synthesis of (S)- $β$ -nitroalcohols by retro-Henry reaction.	22
1.10	AtHNL-F179N catalyzed synthesis of (S)-2-nitro-1-phenylethanol by retro-	23
	Henry reaction.	
2.1	Retro-nitroaldol reaction (top), and conventional cyanogenesis (bottom) by	46
	AtHNL.	
2.2	Proposed mechanism of retro-nitroaldolase activity by AtHNL based on	94
	MDS study of (R)-NPE interaction (not based on X-ray structure).	
3.1	Biocatalytic asymmetric Henry reaction in synthesis of (<i>R</i>)-β-nitroalcohols	120
	using engineered AtHNLs.	
3.2	Screening of AtHNL variants towards enantioselective synthesis of (R)-	125
	NPE.	
3.3	AtHNL variants in the enantioselective synthesis of diverse (R) - β -	149
	nitroalcohols.	
4.1	Chemo-enzymatic synthesis of (R) -Tembamide drug intermediate i.e., (R) -	210
	2-amino-1-(4-methoxyphenyl)-2-ethanol using engineered <i>At</i> HNL.	

LIST OF FIGURES

Figure	Title	Page
1.1	Overview of protein engineering.	3
1.2	Overview of classification of HNLs based on the enantioselectivity, presence	7
	of cofactor and protein structure.	
1.3	Examples of pharmaceuticals, biologically active molecules, and natural	14
	products derived from enantiopure a) (S)- β -nitroalcohol adducts, b) (R)- β -	
	nitroalcohol adducts and c) chiral β-nitroalcohol diastereomers.	
1.4	Major biocatalytic approaches for the synthesis of chiral β-nitroalcohols.	18
2.1	SDS-PAGE analysis of Ni-NTA purified <i>At</i> HNL and its variants. Lane M:	59
	standard protein marker.	
2.2	Michaelis-Menten curve for wild type <i>At</i> HNL with rac-MN as substrate.	60
2.3	Michaelis-Menten curve for wild type <i>At</i> HNL with rac- NPE as substrate.	61
2.4	Comparison of CD spectra of wild type <i>At</i> HNL with variants F82A, F179A and F82A-F179A.	62
2.5	Michaelis-Menten curve for F82A variant with rac-MN as substrate.	63
2.6	Michaelis-Menten curve for F179A variant with rac-MN as substrate.	63
2.7	Michaelis-Menten curve for F82A variant with rac-NPE as substrate.	64
2.8	Michaelis-Menten curve for F179A variant with rac-NPE as substrate.	64
2.9	Cyanogenesis and retro-nitroaldolase activity of AtHNL variants modified at	66
	position F82 (left), F179 (middle), and Y14 (right).	
2.10	Michaelis-Menten curve for F179C variant with rac-NPE as substrate.	67
2.11	Michaelis-Menten curve for F179H variant with rac-NPE as substrate.	67
2.12	Michaelis-Menten curve for F179I variant with rac-NPE as substrate.	68
2.13	Michaelis-Menten curve for F179L variant with rac-NPE as substrate.	68
2.14	Michaelis-Menten curve for F179M variant with rac-NPE as substrate.	69
2.15	Michaelis-Menten curve for F179N variant with rac-NPE as substrate.	69
2.16	Michaelis-Menten curve for F179P variant with rac-NPE as substrate.	70
2.17	Michaelis-Menten curve for F179T variant with rac-NPE as substrate.	70
2.18	Michaelis-Menten curve for F179V variant with rac-NPE as substrate.	71
2.19	Michaelis-Menten curve for F179W variant with rac-NPE as substrate.	71
2.20	Michaelis-Menten curve for Y14L variant with rac-NPE as substrate.	72
2.21	Michaelis-Menten curve for Y14M variant with rac-NPE as substrate.	72

2.22	Retro- nitroaldol reaction of <i>At</i> HNL variants in the preparation of (<i>S</i>)-NPE.	74
2.23	HPLC spectrum of the standards: benzaldehyde, (<i>R</i>)- and (<i>S</i>)-NPE.	75
2.24	HPLC spectrum of the control reaction where enzyme was replaced by 20 mM KPB buffer shows no enantioselective cleavage of rac-NPE.	75
2.25	HPLC spectrum of wild type <i>At</i> HNL showing enantioselective cleavage of rac-NPE.	75
2.26	HPLC spectrum of the variant F179N showing enantioselective cleavage of rac-NPE.	76
2.27	HPLC spectrum of the variant F82A showing enantioselective cleavage of rac-NPE.	76
2.28	HPLC spectrum of the variant F179A showing enantioselective cleavage of rac-NPE.	76
2.29	HPLC spectrum of the variant F179L showing enantioselective cleavage of rac-NPE.	77
2.30	HPLC spectrum of the variant F179T showing enantioselective cleavage of rac-NPE.	77
2.31	HPLC spectrum of the variant F179W showing enantioselective cleavage of rac-NPE.	77
2.32	HPLC spectrum of the variant F179I showing enantioselective cleavage of rac-NPE.	78
2.33	HPLC spectrum of the variant F179M showing enantioselective cleavage of rac-NPE.	78
2.34	HPLC spectrum of the variant F179V showing enantioselective cleavage of rac-NPE.	78
2.35	HPLC spectrum of the variant F179H showing enantioselective cleavage of rac-NPE.	79
2.36	HPLC spectrum of the variant F179C showing enantioselective cleavage of rac-NPE.	79
2.37	HPLC spectrum of the variant F179P showing enantioselective cleavage of rac-NPE.	79
2.38	HPLC spectrum of the variant Y14L showing enantioselective cleavage of rac-NPE.	80

2.39	HPLC spectrum of the variant Y14M showing enantioselective cleavage of rac-NPE.	80
2.40	Michaelis-Menten curve for F82A-F179W variant with rac-NPE as substrate.	81
2.41	Michaelis-Menten curve for F82A-F179N variant with rac-NPE as substrate.	82
2.42	Michaelis-Menten curve for F82A-F179V variant with rac-NPE as substrate.	82
2.43	Retro-nitroaldol reaction of <i>At</i> HNL variants in the preparation of (<i>S</i>)-NPE.	83
2.44	HPLC spectrum of the double variant F82A-F179W in the enantioselective cleavage of rac-NPE.	83
2.45	HPLC spectrum of the double variant F82A-F179V in the enantioselective cleavage of rac-NPE.	84
2.46	HPLC spectrum of the double variant F82A-F179N in the enantioselective cleavage of rac-NPE.	84
2.47	Modelled At HNL complex shows interaction of the enzyme with substrate as seen in Table 2.7, A. with (R) -MN, B. with (R) -NPE, C. superimposed model complexes of At HNL- (R) -MN and At HNL- (R) -NPE (The amino acids 5Å around the active site interacting with the substrates are shown.	86
2.48	Superimposed model complexes of $AtHNL-(R)-MN$ and $AtHNL-(R)-NPE$ (The amino acids 5Å around the active site interacting with the substrates are shown comprising of the $AtHNL$ binding pocket.	87
2.49	Important interactions between the enzyme and (<i>R</i>)-NPE in A) WT+(<i>R</i>)-NPE (enlarged active site shows H-bonds), B) F179N+(<i>R</i>)-NPE.	88
2.50	A) Backbone RMSD vs. Time B) RMSF vs. Residue Number for WT+ NPE (red), F179N +NPE (blue).	90
2.51	Active site interacting residues for WT complex with (<i>R</i>)-NPE at interval of 10-50 ns MDS.	92
2.52	HPLC spectrum of F179N cell lysate catalyzed (200 U) enantioselective cleavage of rac-NPE at 6 h.	96
2.53	HPLC spectrum of F179N cell lysate catalyzed (200 U) enantioselective cleavage of rac-NPE in 65% v/v of toluene at 4 h.	96
2.54	HPLC spectrum of F179N cell lysate catalyzed (200 U) enantioselective cleavage of rac-NPE in 65% v/v of toluene at 3 h.	97
2.55	¹ H NMR of NPE obtained by of F179N cell lysate catalyzed enantioselective cleavage followed by column purification.	97
2.56	¹³ C NMR of NPE obtained by of F179N cell lysate catalyzed enantioselective cleavage followed by column purification.	98

2.57	HPLC spectrum of preparative scale synthesis of F179N cell lysate catalyzed enantioselective cleavage of rac-NPE at 3 h after column purification, 92.88% <i>ee</i> .	98
3.1	SDS-PAGE analysis of Ni-NTA purified <i>At</i> HNL double variants. Lane M:	124
	standard protein marker.	
3.2	Primary screening of <i>At</i> HNL variants altered at positions F82, F179 and Y14	125
	in the synthesis of (R)-NPE. The 2 h analysis data is considered and used	
	here to draw the heat map.	
3.3	HPLC spectrum of wild type <i>At</i> HNL showing enantioselective synthesis of	128
	(R)-NPE at 2 h.	
3.4	HPLC spectrum of F82A showing enantioselective synthesis of (R)-NPE at	128
	2 h.	
2.5	LIDLO Consideration of EQUIVAL and the state of the Alexander of the Alexa	120
3.5	HPLC spectrum of F82K showing enantioselective synthesis of (<i>R</i>)-NPE at	129
2.6	2 h.	129
3.6	HPLC spectrum of F82T showing enantioselective synthesis of (<i>R</i>)-NPE at 2 h.	129
3.7	HPLC spectrum of F82R showing enantioselective synthesis of (<i>R</i>)-NPE at	129
3.7	2 h.	129
3.8	HPLC spectrum of F82S showing enantioselective synthesis of (<i>R</i>)-NPE at	130
3.0	2 h.	130
3.9	HPLC spectrum of F82P showing enantioselective synthesis of (<i>R</i>)-NPE at	130
3.5	2 h.	150
3.10	HPLC spectrum of F82Q showing enantioselective synthesis of (<i>R</i>)-NPE at	130
	2 h.	
3.11	HPLC spectrum of F179A showing enantioselective synthesis of (<i>R</i>)-NPE at	131
	2 h.	
3.12	HPLC spectrum of F179H showing enantioselective synthesis of (<i>R</i>)-NPE at	131
	2 h.	
3.13	HPLC spectrum of F179S showing enantioselective synthesis of (<i>R</i>)-NPE at	131
	2 h.	
3.14	HPLC spectrum of F179C showing enantioselective synthesis of (<i>R</i>)-NPE at	132
	2 h.	
3.15	HPLC spectrum of F179P showing enantioselective synthesis of (<i>R</i>)-NPE at	132
	2 h.	
3.16	HPLC spectrum of F179R showing enantioselective synthesis of (<i>R</i>)-NPE at	132
	2 h.	

3.17	HPLC spectrum of F179N showing enantioselective synthesis of (<i>R</i>)-NPE at 2 h.	133
3.18	HPLC spectrum of F179Q showing enantioselective synthesis of (<i>R</i>)-NPE at 2 h.	133
3.19	HPLC spectrum of F179G showing enantioselective synthesis of (<i>R</i>)-NPE at	133
3.13	2 h.	100
3.20	HPLC spectrum of F179I showing enantioselective synthesis of (<i>R</i>)-NPE at	134
3.21	2 h. HPLC spectrum of F179E showing enantioselective synthesis of (<i>R</i>)-NPE at	134
3.21	2 h.	134
3.22	HPLC spectrum of F179L showing enantioselective synthesis of (<i>R</i>)-NPE at 2 h.	134
3.23	HPLC spectrum of F179M showing enantioselective synthesis of (<i>R</i>)-NPE at 2 h.	135
3.24	HPLC spectrum of F179T showing enantioselective synthesis of (<i>R</i>)-NPE at	135
	2 h.	
3.25	HPLC spectrum of F179V showing enantioselective synthesis of (<i>R</i>)-NPE at 2 h.	135
3.26	HPLC spectrum of F179K showing enantioselective synthesis of (<i>R</i>)-NPE at	136
	2 h.	
3.27	HPLC spectrum of F179Y showing enantioselective synthesis of (<i>R</i>)-NPE at 2 h.	136
3.28	HPLC spectrum of F179W showing enantioselective synthesis of (<i>R</i>)-NPE	136
	at 2 h.	
3.29	HPLC spectrum of F179D showing enantioselective synthesis of (<i>R</i>)-NPE at	137
	2 h.	
3.30	HPLC spectrum of Y14A showing enantioselective synthesis of (<i>R</i>)-NPE at	137
	2 h.	
3.31	HPLC spectrum of Y14C showing enantioselective synthesis of (<i>R</i>)-NPE at	137
	2 h.	
3.32	HPLC spectrum of Y14Q showing enantioselective synthesis of (R)-NPE at	138
	2 h.	
3.33	HPLC spectrum of Y14H showing enantioselective synthesis of (<i>R</i>)-NPE at	138
	2 h.	
3.34	HPLC spectrum of Y14N showing enantioselective synthesis of (R)-NPE at	138
	2 h.	
·		·

3.35	HPLC spectrum of Y14P showing enantioselective synthesis of (R)-NPE at	139
	2 h.	
3.36	HPLC spectrum of Y14S showing enantioselective synthesis of (R)-NPE at	139
	2 h.	
3.37	HPLC spectrum of Y14D showing enantioselective synthesis of (<i>R</i>)-NPE at	139
	2 h.	
3.38	HPLC spectrum of Y14F showing enantioselective synthesis of (R)-NPE at	140
	2 h.	
3.39	HPLC spectrum of Y14M showing enantioselective synthesis of (<i>R</i>)-NPE at	140
	2 h.	
3.40	HPLC spectrum of Y14V showing enantioselective synthesis of (<i>R</i>)-NPE at	140
5.10	2 h.	1.0
3.41	HPLC spectrum of Y14W showing enantioselective synthesis of (<i>R</i>)-NPE at	141
3.11	2 h.	111
3.42	HPLC spectrum of Y14L showing enantioselective synthesis of (<i>R</i>)-NPE at	141
3.12	2 h.	111
3.43	HPLC spectrum of Y14E showing enantioselective synthesis of (<i>R</i>)-NPE at	141
3.13	2 h.	111
	211.	
3.44	HPLC spectrum of Y14T showing enantioselective synthesis of (R)-NPE at	142
	2 h.	
3.45	HPLC spectrum of Y14K showing enantioselective synthesis of (R)-NPE at	142
	2 h.	
3.46	HPLC spectrum of Y14G showing enantioselective synthesis of (<i>R</i>)-NPE at	142
	2 h.	
3.47	HPLC spectrum of Y14I showing enantioselective synthesis of (<i>R</i>)-NPE at 2	143
	h.	
3.48	HPLC spectrum of Y14R showing enantioselective synthesis of (<i>R</i>)-NPE at	143
	2 h	
3.49	HPLC spectrum of the standards: benzaldehyde, (<i>R</i>)- and (<i>S</i>)-NPE.	144
3.50	HPLC spectrum of the standards: <i>trans</i> cinnamaldehyde, and corresponding	145
	(S)- and (R)- β -nitroalcohols.	
3.51	HPLC spectrum of the standards: 3-chlorobenzaldehdye, and corresponding	145
	(R)- and (S) -β-nitroalcohols.	
3.52	HPLC spectrum of the standards: 4-chlorobenzaldehdye, and corresponding	145
	(R)- and (S) -β-nitroalcohols.	
3.53	HPLC spectrum of the standards: 4-fluorobenzaldehdye, and corresponding	146
	(R)- and (S) -β-nitroalcohols.	

3.54	HPLC spectrum of the standards: 3-methylbenzaldehdye, and corresponding	146
	(R)- and (S) -β-nitroalcohols.	
3.55	HPLC spectrum of the standards: 4-methylbenzaldehdye, corresponding (<i>R</i>)-	146
	and (S)- β -nitroalcohols.	
3.56	HPLC spectrum of the standards: 4-nitrobenzaldehdye, and corresponding	147
	(R)- and (S) -β-nitroalcohols.	
3.57	HPLC spectrum of the standards: 3-methoxybenzaldehdye, and	147
	corresponding (R)- and (S)- β -nitroalcohols.	
3.58	HPLC spectrum of the standards: 2,4-dimethoxybenzaldehdye, and	147
	corresponding (R)- and (S)- β -nitroalcohols.	
3.59	HPLC spectrum of the standards: 3,4,5-trimethoxybenzaldehdye,	148
	corresponding (R)- and (S)- β -nitroalcohols.	
3.60	HPLC spectrum of the standards: 4-benzyloxybenzaldehdye, corresponding	148
	(R)- and (S) -β-nitroalcohols.	
3.61	HPLC spectrum of control reaction at 3 h where enzyme is replaced by 20	151
	mM KPB and benzaldehyde used as the substrate.	
3.62	HPLC spectrum of wild type AtHNL showing enantioselective synthesis of	151
	(<i>R</i>)-2-nitro-1-phenylethanol at 3 h using benzaldehyde as the substrate.	
3.63	HPLC spectrum of the F179W variant showing enantioselective synthesis of	151
	(<i>R</i>)- 2-nitro-1-phenylethanol at 3 h using benzaldehyde as the substrate.	
3.64	HPLC spectrum of the F179N variant showing enantioselective synthesis of	152
	(R)- 2-nitro-1-phenylethanol at 3 h using benzaldehyde as the substrate.	
3.65	HPLC spectrum of the Y14F variant showing enantioselective synthesis of	152
	(R)- 2-nitro-1-phenylethanol at 3 h using benzaldehyde as the substrate.	
3.66	HPLC spectrum of the Y14M variant showing enantioselective synthesis of	152
	(R)- 2-nitro-1-phenylethanol at 3 h using benzaldehyde as the substrate.	
3.67	HPLC spectrum of control reaction at 3 h where enzyme is replaced by 20	153
	mM KPB and <i>trans</i> cinnamaldehyde used as the substrate.	
3.68	HPLC spectrum of wild type AtHNL showing enantioselective synthesis of	153
	(R)- (E)-1-nitro-4-phenylbut-3-en-2-ol at 3 h using <i>trans</i> cinnamaldehyde as	
	the substrate.	
3.69	HPLC spectrum of the F179W variant showing enantioselective synthesis of	153
	(R)- (E)-1-nitro-4-phenylbut-3-en-2-ol at 3 h using <i>trans</i> cinnamaldehyde as	
	the substrate.	
3.70	HPLC spectrum of the F179N variant showing enantioselective synthesis	154
	of (R)- (E)-1-nitro-4-phenylbut-3-en-2-ol at 3 h using trans	
	cinnamaldehyde as the substrate.	

	1	
3.71	HPLC spectrum of the Y14F variant showing enantioselective synthesis of (<i>R</i>)- (<i>E</i>)-1-nitro-4-phenylbut-3-en-2-ol at 3 h using <i>trans</i> cinnamaldehyde	154
	as the substrate.	
3.72	HPLC spectrum of the Y14M variant showing enantioselective synthesis of	154
	(R)- (E)-1-nitro-4-phenylbut-3-en-2-ol at 3 h using <i>trans</i> cinnamaldehyde as	
	the substrate.	
3.73	HPLC spectrum of control reaction at 3 h where enzyme is replaced by 20	155
	mM KPB and 3-chlorobenzaldehyde used as the substrate.	
3.74	HPLC spectrum of wild type <i>At</i> HNL showing enantioselective synthesis of	155
	(R)-1-(3-chlorophenyl)-2-nitroethanol at 3 h using 3-chlorobenzaldehyde as	
	the substrate.	
3.75	HPLC spectrum of the F179W variant showing enantioselective synthesis of	155
	(R)-1-(3-chlorophenyl)-2-nitroethanol at 3 h using 3-chlorobenzaldehyde as	
	the substrate.	
3.76	HPLC spectrum of the F179N variant showing enantioselective synthesis of	156
	(R)-1-(3-chlorophenyl)-2-nitroethanol at 3 h using 3-chlorobenzaldehyde as	
	the substrate.	
3.77	HPLC spectrum of the Y14F variant showing enantioselective synthesis of	156
	(R)-1-(3-chlorophenyl)-2-nitroethanol at 3 h using 3-chlorobenzaldehyde as	
	the substrate.	
3.78	HPLC spectrum of the Y14M variant showing enantioselective synthesis of	156
	(R)-1-(3-chlorophenyl)-2-nitroethanol at 3 h using 3-chlorobenzaldehyde as	
	the substrate.	
2.70		1.57
3.79	HPLC spectrum of control reaction at 3 h where enzyme is replaced by 20	157
2.00	mM KPB and 4-chlorobenzaldehyde used as the substrate.	1.57
3.80	HPLC spectrum of wild type <i>At</i> HNL showing enantioselective synthesis of	157
	(<i>R</i>)-1-(4-chlorophenyl)-2-nitroethanol at 3 h using 4-chlorobenzaldehyde as	
2 01	the substrate. HDLC encetrum of the F170W varient showing apartic selective synthesis of	157
3.81	HPLC spectrum of the F179W variant showing enantioselective synthesis of	157
	(<i>R</i>)-1-(4-chlorophenyl)-2-nitroethanol at 3 h using 4-chlorobenzaldehyde as the substrate.	
3.82		158
3.82	HPLC spectrum of the F179N variant showing enantioselective synthesis of (<i>R</i>)-1-(4-chlorophenyl)-2-nitroethanol at 3 h using 4-chlorobenzaldehyde	138
2 02	as the substrate. HDLC encetrum of the V14E varient showing anontic selective synthesis of	150
3.83	HPLC spectrum of the Y14F variant showing enantioselective synthesis of	158
	(<i>R</i>)-1-(4-chlorophenyl)-2-nitroethanol at 3 h using 4-chlorobenzaldehyde as the substrate.	
	the substrate.	

3.84	HPLC spectrum of the Y14M variant showing enantioselective synthesis of (<i>R</i>)-1-(4-chlorophenyl)-2-nitroethanol at 3 h using 4-chlorobenzaldehyde as the substrate.	158
3.85	HPLC spectrum of control reaction at 3 h where enzyme is replaced by 20 mM KPB and 4-fluorobenzaldehyde used as the substrate.	159
3.86	HPLC spectrum of wild type <i>At</i> HNL showing enantioselective synthesis of (<i>R</i>)-1-(4-fluorophenyl)-2-nitroethanol at 3 h using 4-fluorobenzaldehyde as the substrate.	159
3.87	HPLC spectrum of the F179W variant showing enantioselective synthesis of (<i>R</i>)- 1-(4-fluorophenyl)-2-nitroethanol at 3 h using 4-fluorobenzaldehyde as the substrate.	159
3.88	HPLC spectrum of the F179N variant showing enantioselective synthesis of (R) -1- $(4$ -fluorophenyl)-2-nitroethanol at 3 h using 4-fluorobenzaldehyde as the substrate.	160
3.89	HPLC spectrum of the Y14F variant showing enantioselective synthesis of (<i>R</i>)-1-(4-fluorophenyl)-2-nitroethanol at 3 h using 4-fluorobenzaldehyde as the substrate.	160
3.90	HPLC spectrum of the Y14M variant showing enantioselective synthesis of (<i>R</i>)-1-(4-fluorophenyl)-2-nitroethanol at 3 h using 4-fluorobenzaldehyde as the substrate.	160
3.91	HPLC spectrum of control reaction at 3 h where enzyme is replaced by 20 mM KPB and 3-methylbenzaldehyde used as the substrate.	161
3.92	HPLC spectrum of wild type <i>At</i> HNL showing enantioselective synthesis of (<i>R</i>)-1-(3-methylphenyl)-2-nitroethanol at 3 h using 3-methylbenzaldehyde as the substrate.	161
3.93	HPLC spectrum of the F179W variant showing enantioselective synthesis of (R) -1-(3-methylphenyl)-2-nitroethanol at 3 h using 3-methylbenzaldehyde as the substrate.	161
3.94	HPLC spectrum of the F179N variant showing enantioselective synthesis of (R) -1-(3-methylphenyl)-2-nitroethanol at 3 h using 3-methylbenzaldehyde as the substrate.	162
3.95	HPLC spectrum of the Y14F variant showing enantioselective synthesis of (<i>R</i>)-1-(3-methylphenyl)-2-nitroethanol at 3 h using 3-methylbenzaldehyde as the substrate.	162
3.96	HPLC spectrum of the Y14M variant showing enantioselective synthesis of (<i>R</i>)-1-(3-methylphenyl)-2-nitroethanol at 3 h using 3-methylbenzaldehyde as the substrate.	162
3.97	HPLC spectrum of control reaction at 3 h where enzyme is replaced by 20 mM KPB and 4-methylbenzaldehyde used as the substrate.	163
		

3.98	HPLC spectrum of wild type AtHNL showing enantioselective synthesis of	163
	(<i>R</i>)-1-(4-methylphenyl)-2-nitroethanol at 3 h using 4-methylbenzaldehyde as	
	the substrate.	
3.99	HPLC spectrum of the F179W variant showing enantioselective synthesis of	163
	(<i>R</i>)-1-(4-methylphenyl)-2-nitroethanol at 3 h using 4-methylbenzaldehyde as	
	the substrate.	
3.100	HPLC spectrum of the F179N variant showing enantioselective synthesis of	164
	(<i>R</i>)-1-(4-methylphenyl)-2-nitroethanol at 3 h using 4-methylbenzaldehyde as	
	the substrate.	
3.101	HPLC spectrum of the Y14F variant showing enantioselective synthesis of	164
	(R)- 1-(4-methylphenyl)-2-nitroethanol at 3 h using 4-methylbenzaldehyde	
	as the substrate.	
3.102	HPLC spectrum of the Y14M variant showing enantioselective synthesis of	164
	(R)- 1-(4-methylphenyl)-2-nitroethanol at 3 h using 4-methylbenzaldehyde	
	as the substrate.	
3.103	HPLC spectrum of control reaction at 3 h where enzyme is replaced by 20	165
	mM KPB and 4-nitrobenzaldehyde used as the substrate.	
3.104	HPLC spectrum of wild type AtHNL showing enantioselective synthesis of	165
	(<i>R</i>)- 1-(4-nitrophenyl)-2-nitroethanol at 3 h using 4-nitrobenzaldehyde as the	
2.105	substrate.	1.67
3.105	HPLC spectrum of the F179W variant showing enantioselective synthesis of	165
	(<i>R</i>)- 1-(4-nitrophenyl)-2-nitroethanol at 3 h using 4-nitrobenzaldehyde as the	
2.106	substrate.	1.00
3.106	HPLC spectrum of the F179N variant showing enantioselective synthesis of	166
	(<i>R</i>)- 1-(4-nitrophenyl)-2-nitroethanol at 3 h using 4-nitrobenzaldehyde as the substrate.	
3.107	HPLC spectrum of the Y14F variant showing enantioselective synthesis of	166
3.107	(R)-1-(4-nitrophenyl)-2-nitroethanol at 3 h using 4-nitrobenzaldehyde as the	100
	substrate.	
3.108	HPLC spectrum of the Y14M variant showing enantioselective synthesis of	166
3.100	(<i>R</i>)-1-(4-nitrophenyl)-2-nitroethanol at 3 h using 4-nitrobenzaldehyde as the	100
	substrate.	
3.109	HPLC spectrum of control reaction at 3 h where enzyme is replaced by 20	167
	mM KPB and 3-methoxybenzaldehyde used as the substrate.	· ·
3.110	HPLC spectrum of wild type At HNL showing enantioselective synthesis of (R)-	167
	1-(3-methoxyphenyl)-2-nitroethanol at 3 h using 3-methoxybenzaldehyde as the	
	substrate.	
	·	

3.111	HPLC spectrum of the F179W variant showing enantioselective synthesis of (R)- 1-(3-methoxyphenyl)-2-nitroethanol at 3 h using 3-methoxybenzaldehyde	167
	as the substrate.	
3.112	HPLC spectrum of the F179N variant showing enantioselective synthesis of (<i>R</i>)-1-(3-methoxyphenyl)-2-nitroethanol at 3 h using 3- methoxybenzaldehyde as the substrate.	168
2 112		1.00
3.113	HPLC spectrum of the Y14F variant showing enantioselective synthesis of (<i>R</i>)-	168
	1-(3-methoxyphenyl)-2-nitroethanol at 3 h using 3-methoxybenzaldehyde as the substrate.	
3.114	HPLC spectrum of the Y14M variant showing enantioselective synthesis of (<i>R</i>)-1-(3-methoxyphenyl)-2-nitroethanol at 3 h using 3-methoxybenzaldehyde as the substrate.	168
3.115	HPLC spectrum of control reaction at 3 h where enzyme is replaced by 20 mM KPB and 2,4-dimethoxybenzaldehyde used as the substrate.	169
3.116	HPLC spectrum of wild type At HNL showing enantioselective synthesis of (R) -1-	169
3.110	(2, 4-dimethoxyphenyl)-2-nitroethanol at 3 h using 2,4-dimethoxybenzaldehyde as the substrate.	10)
3.117	HPLC spectrum of the F179W variant showing enantioselective synthesis of (R)-	169
	1-(2, 4-dimethoxyphenyl)-2-nitroethanol at 3 h using 2,4-dimethoxybenzaldehyde as the substrate.	
3.118	HPLC spectrum of the F179N variant showing enantioselective synthesis of (<i>R</i>)- 1- (2, 4-dimethoxyphenyl)-2-nitroethanol at 3 h using 2,4-dimethoxybenzaldehyde as the substrate.	170
3.119	HPLC spectrum of the Y14F variant showing enantioselective synthesis of (<i>R</i>)- 1- (2, 4-dimethoxyphenyl)-2-nitroethanol at 3 h using 2,4-dimethoxybenzaldehyde as the substrate.	170
3.120	HPLC spectrum of the Y14M variant showing enantioselective synthesis of (<i>R</i>)- 1-	170
3.120	(2, 4-dimethoxyphenyl)-2-nitroethanol at 3 h using 2,4-dimethoxybenzaldehyde as the substrate.	1,0
3.121	HPLC spectrum of control reaction at 3 h where enzyme is replaced by 20	171
	mM KPB and 3,4,5-trimethoxybenzaldehyde used as the substrate.	
3.122	HPLC spectrum of wild type <i>At</i> HNL showing enantioselective synthesis of	171
3.122	(R)-1-(3,4,5-trimethoxyphenyl)-2-nitroethanol at 3 h using 3,4,5-	1/1
	trimethoxybenzaldehyde as the substrate.	
3.123	HPLC spectrum of the F179W variant showing enantioselective synthesis of (<i>R</i>)-1-(3,4,5-trimethoxyphenyl)-2-nitroethanol at 3 h using 3,4,5-trimethoxybenzaldehyde as the substrate.	171
3.124	HPLC spectrum of the F179N variant showing enantioselective synthesis of (<i>R</i>)-1-(3,4,5-trimethoxyphenyl)-2-nitroethanol at 3 h using 3,4,5-trimethoxybenzaldehyde as the substrate.	172

3.125	HPLC spectrum of the Y14F variant showing enantioselective synthesis of (R) -1- $(3,4,5$ -trimethoxyphenyl)-2-nitroethanol at 3 h using 3,4,5-trimethoxybenzaldehyde as the substrate.	172
3.126	HPLC spectrum of the Y14M variant showing enantioselective synthesis of (<i>R</i>)-1-(3,4,5-trimethoxyphenyl)-2-nitroethanol at 3 h using 3,4,5-trimethoxybenzaldehyde as the substrate.	172
3.127	HPLC spectrum of control reaction at 3 h where enzyme is replaced by 20 mM KPB and 4-bezyloxybenzaldehyde used as the substrate.	173
3.128	HPLC spectrum of wild type <i>At</i> HNL showing enantioselective synthesis of (<i>R</i>)-1-(4-benzyloxyphenyl)-2-nitroethanol at 3 h using 4-benzyloxybenzaldehyde as the substrate.	173
3.129	HPLC spectrum of the F179W variant showing enantioselective synthesis of (<i>R</i>)-1-(4-benzyloxyphenyl)-2-nitroethanol at 3 h using 4-benzyloxybenzaldehyde as the substrate.	173
3.130	HPLC spectrum of the F179N variant showing enantioselective synthesis of (<i>R</i>)- 1- (4-benzyloxyphenyl)-2-nitroethanol at 3 h using 4-benzyloxybenzaldehyde as the substrate.	174
3.131	HPLC spectrum of the Y14F variant showing enantioselective synthesis of (<i>R</i>)- 1- (4-benzyloxyphenyl)-2-nitroethanol at 3 h using 4-benzyloxybenzaldehyde as the substrate.	174
3.132	HPLC spectrum of the Y14M variant showing enantioselective synthesis of (<i>R</i>)- 1- (4-benzyloxyphenyl)-2-nitroethanol at 3 h using 4-benzyloxybenzaldehyde as the substrate.	174
3.133	HPLC spectrum of <i>At</i> HNL WT (125 U) catalyzed synthesis of (<i>R</i>)-β-nitroalcohol of 4-benzyloxybenzaldehyde at 3 h.	176
3.134	HPLC spectrum of <i>At</i> HNL WT (125 U) catalyzed synthesis of (<i>R</i>)-β-nitroalcohol of 4-fluorobenzaldehyde at 3 h.	177
3.135	HPLC spectrum of the F179N variant (125 U) catalyzed synthesis of (<i>R</i>)-β-nitroalcohol of benzaldehyde at 3 h.	177
3.136	HPLC spectrum of the F179N variant (125 U) catalyzed synthesis of (<i>R</i>)-β-nitroalcohol of 4-fluorobenzaldehyde at 3 h.	177
3.137	HPLC spectrum of the F179N variant (125 U) catalyzed synthesis of (<i>R</i>)-β-nitroalcohol of 3-chlororobenzaldehyde at 3 h.	178
3.138	HPLC spectrum of the F179N variant (125 U) catalyzed synthesis of (<i>R</i>)-β-nitroalcohol of 3-methylbenzaldehyde at 3 h.	178
3.139	HPLC spectrum of the F179N variant (125 U) catalyzed synthesis of (<i>R</i>)-β-nitroalcohol of 4-benzyloxybenzaldehyde at 3 h.	178
3.140	HPLC spectrum of the Y14M variant (125 U) catalyzed synthesis of (<i>R</i>)-β-nitroalcohol of benzaldehyde at 3 h	179
3.141	HPLC spectrum of the Y14M variant (125 U) catalyzed synthesis of (<i>R</i>)-β-nitroalcohol of 4-fluorobenzaldehyde at 3 h.	179

3.142	HPLC spectrum of the Y14M variant (125 U) catalyzed synthesis of (<i>R</i>)-β-nitroalcohol of 4-benzyloxybenzaldehyde at 3 h.	179
3.143	HPLC spectrum of the Y14F variant (125 U) catalyzed synthesis of (<i>R</i>)-β-nitroalcohol of 4-chlorobenzaldehyde at 3 h.	180
3.144	HPLC spectrum of the Y14F variant (125 U) catalyzed synthesis of (<i>R</i>)-β-nitroalcohol of 4-fluorobenzaldehyde at 3 h.	180
3.145	HPLC spectrum of the Y14F variant (125 U) catalyzed synthesis of (<i>R</i>)-β-nitroalcohol of 4-nitrobenzaldehyde at 3 h.	180
3.146	HPLC spectrum of the Y14F variant (125 U) catalyzed synthesis of (<i>R</i>)-β-nitroalcohol of 4-benzyloxybenzaldehyde at 3 h.	181
3.147	HPLC spectrum of the Y14M-F179W catalyzed enantioselective synthesis of (<i>R</i>)-β-nitroalcohol of benzaldehyde at 3 h.	183
3.148	HPLC spectrum of the Y14M-F179W catalyzed enantioselective synthesis of (<i>R</i>)-β-nitroalcohol of <i>trans</i> cinnamaldehyde at 3 h.	183
3.149	HPLC spectrum of the Y14M-F179W catalyzed enantioselective synthesis of (<i>R</i>)-β-nitroalcohol of 4-fluorobenzaldehyde at 3 h.	183
3.150	HPLC spectrum of the Y14M-F179W catalyzed enantioselective synthesis of (<i>R</i>)-β-nitroalcohol of 4-chlorobenzaldehyde at 3 h.	184
3.151	HPLC spectrum of the Y14M-F179W catalyzed enantioselective synthesis of (<i>R</i>)-β-nitroalcohol of 4-nitrobenzaldehyde at 3 h.	184
3.152	HPLC spectrum of the Y14M-F179W catalyzed enantioselective synthesis of (<i>R</i>)-β-nitroalcohol of 2,4-dimethoxybenzaldehyde at 3 h.	184
3.153	HPLC spectrum of the Y14M-F179W catalyzed enantioselective synthesis of (<i>R</i>)-β-nitroalcohol of 3-chlorobenzaldehyde at 3 h.	185
3.154	HPLC spectrum of the Y14M-F179W catalyzed enantioselective synthesis of (<i>R</i>)-β-nitroalcohol of 3-methylbenzaldehyde at 3 h.	185
3.155	HPLC spectrum of the Y14M-F179W catalyzed enantioselective synthesis of (<i>R</i>)-β-nitroalcohol of 4-methylbenzaldehyde at 3 h.	185
3.156	HPLC spectrum of the Y14M-F179W catalyzed enantioselective synthesis of (<i>R</i>)-β-nitroalcohol of 3-methoxybenzaldehyde at 3 h.	186
3.157	HPLC spectrum of the Y14M-F179W catalyzed enantioselective synthesis of (<i>R</i>)-β-nitroalcohol of 3,4,5-trimethoxybenzaldehyde at 3 h.	186
3.158	HPLC spectrum of the Y14M-F179W catalyzed enantioselective synthesis of (<i>R</i>)-β-nitroalcohol of 4-benzyloxybenzaldehyde at 3 h.	186
3.159	HPLC spectrum of the Y14M-F179W (125 U) catalyzed enantioselective synthesis of (<i>R</i>)-β-nitroalcohol of benzaldehyde at 3 h.	187
3.160	HPLC spectrum of the Y14M-F179W (125 U) catalyzed enantioselective synthesis of (<i>R</i>)-β-nitroalcohol of <i>trans</i> cinnamaldehyde at 3 h.	187
3.161	HPLC spectrum of the Y14M-F179W (125 U) catalyzed enantioselective synthesis of (<i>R</i>)-β-nitroalcohol of 4-fluorobenzaldehyde at 3 h.	187

3.162	HPLC spectrum of the Y14M-F179W (125 U) catalyzed enantioselective	188
	synthesis of (R) - β -nitroalcohol of 4-chlorobenzaldehyde at 3 h.	
3.163	HPLC spectrum of the Y14M-F179W (125 U) catalyzed enantioselective	188
	synthesis of (R) - β -nitroalcohol of 4-nitrobenzaldehyde at 3 h.	
3.164	HPLC spectrum of the Y14M-F179W (125 U) catalyzed enantioselective	188
	synthesis of (R) - β -nitroalcohol of 4-benzyloxybenzaldehyde at 3 h.	
4.1	¹ H NMR spectrum of 1-(4-methoxyphenyl)-2-nitroethanol.	214
4.2	¹³ C NMR spectrum of 1-(4-methoxyphenyl)-2-nitroethanol.	215
4.3	HPLC spectrum of the standards: 4-methoxybenzaldehdye, (R)- and (S)-	216
4.4	enantiomers of 1-(4-methoxyphenyl)-2-nitroethanol. AtHNL variants catalysed enantioselective synthesis of (R)-1-(4-	217
4.4	methoxyphenyl)-2-nitroethanol.	217
4.5	HPLC spectrum of control reaction at 3 h where enzyme is replaced by 20	217
	mM KPB and 4-methoxybenzaldehyde was used as the substrate.	
4.6	HPLC spectrum of wild type AtHNL (125 U) catalyzed nitroaldol reaction	218
	showing enantioselective synthesis of (R)-1-(4-methoxyphenyl)-2-	
	nitroethanol at 3 h.	
4.7	HPLC spectrum of F179N (125 U) catalyzed nitroaldol reaction showing	218
	enantioselective synthesis of (<i>R</i>)-1-(4-methoxyphenyl)-2-nitroethanol at 3 h.	
4.8	HPLC spectrum of F179W (125 U) catalyzed nitroaldol reaction showing	218
	enantioselective synthesis of (<i>R</i>)-1-(4-methoxyphenyl)-2-nitroethanol at 3 h.	
4.9	HPLC spectrum of Y14M (125 U) catalyzed nitroaldol reaction showing	219
	enantioselective synthesis of (R) -1-(4-methoxyphenyl)-2-nitroethanol at 3 h.	
4.10	HPLC spectrum of Y14F (125 U) catalyzed nitroaldol reaction showing	219
	enantioselective synthesis of (R) -1-(4-methoxyphenyl)-2-nitroethanol at 3 h.	
4.11	HPLC spectrum of Y14M-F179W (125 U) catalyzed nitroaldol reaction	219
	showing enantioselective synthesis of (R)-1-(4-methoxyphenyl)-2-	
	nitroethanol at 3 h	
4.12	HPLC spectrum of Y14M-F179W cell lysate (200 U) catalyzed nitroaldol	220
	reaction showing enantioselective synthesis of (R)-1-(4-methoxyphenyl)-2-	
	nitroethanol at 2 h.	
4.13	HPLC spectrum of Y14M-F179W cell lysate (1000 U) catalyzed nitroaldol	220
	reaction showing enantioselective synthesis of (R)-1-(4-methoxyphenyl)-2-	
	nitroethanol at 2 h.	
4.14	HPLC spectrum of Y14M-F179W cell lysate catalyzed preparative scale	221
	enantioselective synthesis of (R)-1-(4-methoxy nitro phenyl) ethanol at 2 h	
	after column purification, >99 % ee.	
_		_

4.15	¹ H NMR spectrum of (<i>R</i>)-1-(4-methoxyphenyl)-2-nitroethanol.	221
4.16	¹³ C NMR spectrum of (<i>R</i>)-1-(4-methoxyphenyl)-2-nitroethanol.	222
4.17	Crude ¹ H NMR spectrum of (<i>R</i>)-2-amino-1-(4-methoxyphenyl) ethanol.	223
4.18	Crude ¹³ C NMR spectrum of (<i>R</i>)-2-amino-1-(4-methoxyphenyl) ethanol.	223

Chapter I: Introduction

1.1. Protein engineering and its importance

In the recent times protein engineering has gained substantial importance in the field of biocatalysis^{1,2}. Enzymes in nature are potent to accelerate different reactions which are used in the production of pharmaceuticals, fuels, agro and fine chemicals in bioprocess technologies. However, enzymes in-vitro require modifications for industrial and research applications as they evolved under various physiological conditions benefitting the organisms in which they live in, not for the non-natural reactions and reaction conditions. Driven by the importance, the number of examples of engineered enzymes in industries is continuously increasing. Enzyme engineering involves modification of protein sequence by various techniques, e.g., site directed mutagenesis (SDM), site saturation mutagenesis (SSM), and directed evolution (DM), which often generates library of variants. Screening of these variants are usually carried out aiming to improve desired biocatalytic properties, e.g., increased activity, affinity, selectivity (chemo, regio, and stereo), stability and tolerance of broad substrate, pH and temperature (Figure 1.1). The growing applications of protein engineering has made a revolutionary change in the traditional biocatalysis. Apparently tailoring natural enzyme in the laboratory has become almost inevitable especially for the industrial application of enzymes as a biocatalyst.

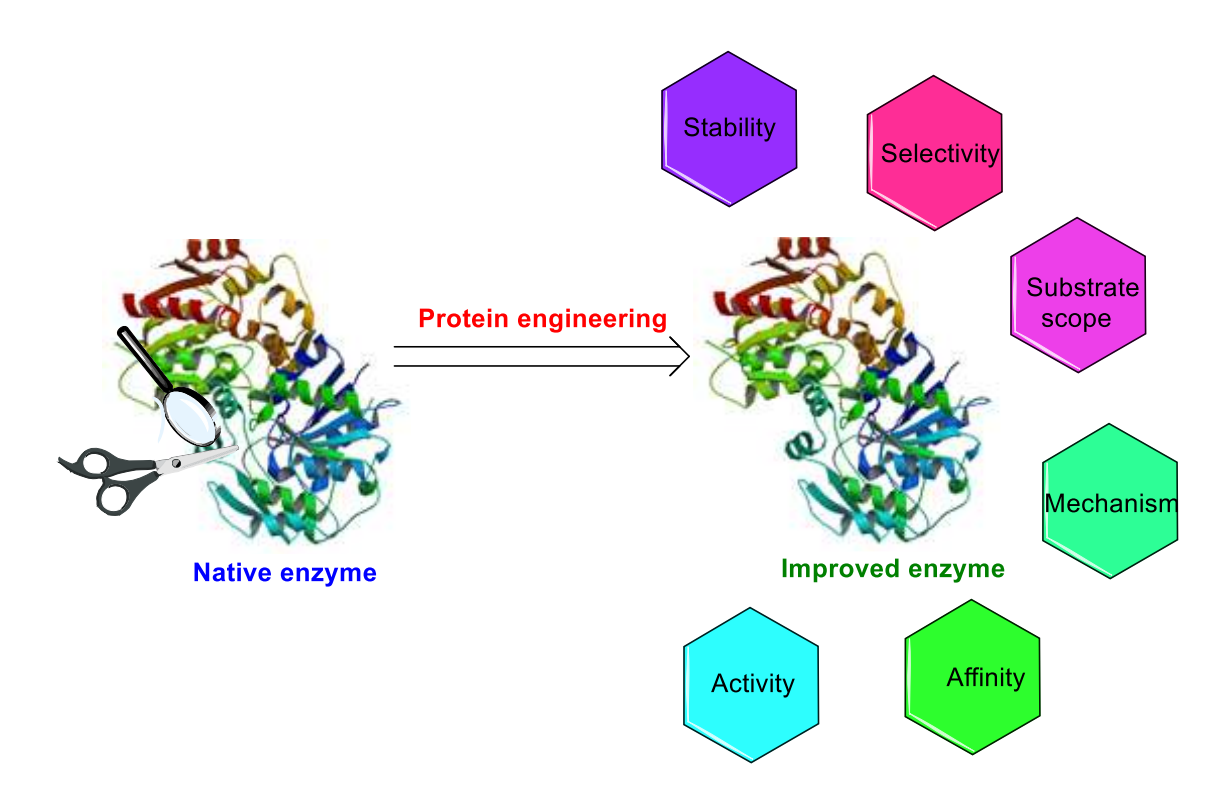


Figure 1.1: Overview of protein engineering.

1.2. Hydroxynitrile lyase

Hydroxynitrile lyases (HNLs) also called oxynitrilases (E.C. 4.1.2.x) are the enzymes mostly found in higher plants. They are also reported in some bacteria, fungi, ferns, lichens and arthropods. In nature, they catalyze the cyanogenesis, i.e., breakdown of a cyanohydrin molecule into corresponding carbonyl compound and hydrogen cyanide, a C-C bond cleavage reaction^{3,4}. The cyanide released serves as both a defense against predators and a nitrogen source for metabolic purposes such as biosynthesis of asparagine, etc. (**Scheme 1.1.a**). *In vitro* HNLs also catalyze stereoselective synthesis of α -cyanohydrins by nucleophilic addition of a cyanide into an electrophilic carbonyl center. This is a stereoselective C-C bond forming reaction, an important transformation in organic syntheses (**Scheme 1.1.b**)^{5–8}. This reaction plays an important role due to its synthetic utility and importance of the chiral cyanohydrins as building blocks of many drugs,

fine chemicals and agro chemicals. The ability of HNLs to synthesize diverse enantiopure compounds made way to emerge themselves as very important biocatalysts over time. HNLs have gained importance in organic synthesis towards the production of a wide range of enantiopure chiral products which are highly valuable in the global market.

a) Sugar
$$O \stackrel{R}{\longleftarrow} CN$$
 $\stackrel{\beta\text{-glycosidase}}{\searrow}$ $O \stackrel{R}{\longleftarrow} CN$ $O \stackrel{\beta\text{-glycosidase}}{\searrow}$ $O \stackrel{R}{\longleftarrow} CN$ $O \stackrel$

Scheme 1.1: HNL catalyzed (a) natural cyanogenesis reaction, (b) synthesis of chiral cyanohydrins.

1.2.1. Classification of HNLs

HNLs are derived from a convergent evolution. They are classified into several groups based on their (i) enantioselectivity, (ii) presence of co-factor and (iii) protein structure (**Figure 1.2**).

- (i) Based on the enantioselectivity or absolute configuration of the product formed, HNLs are classified into two classes:
- (a) (R)-selective HNLs: They produce (R)-products, e.g., Arabidopsis thaliana HNL (AtHNL)⁹, Prunus amygdalus HNL (PaHNL)¹⁰, Linum usitatissimum HNL (LuHNL)¹¹, Chamberlinius hualienensis HNL (ChuaHNL)¹², Parafontaria tonominea (PtonHNL)¹³, Prunus serotine (PsHNL)¹⁴, Prunus amygdalus turcomanica (PatHNL)¹⁵, Prunus mume (PmHNL)^{16,17},

Amygdalus pedunculata Pall (ApHNL)¹⁸, Passiflora edulis (PeHNL)^{19,20}, Prunus communis (PcHNL)²¹, Prunus armeniaca L. (ParsHNL)^{22–24}, Acidobacterium capsulatum ATCC 51196 (AcHNL)²⁵ and Granulicella tundricula (GtHNL)²⁶, etc.

- (b) (S)-selective HNLs: They produce (S)-products, e.g., Baliospermum montanum HNL (BmHNL)²⁷, Hevea brasiliensis HNL (HbHNL)²⁸, Manihot esculenta HNL (MeHNL)²⁹ and Sorghum bicolor HNL (SbHNL)³⁰, etc.
- (ii) Based on the cofactor presence they can be categorized into the following two types:
- (a) FAD-containing HNLs: These HNLs contain FAD cofactor in their structure, e.g., *Pa*HNL and other Prunus sp. HNLs.
- (b) Non-FAD based HNLs: These HNLs do not have any FAD with them, e.g., (*R*)-selective HNLs: *At*HNL, *Phlebodium aureum* HNL (*Pha*HNL)³¹, *Lu*HNL, *Passiflora edulis* HNL (*Pe*HNL) and *Xylella fastidiosa* HNL (*Xf*HNL)^{32,33}, and (*S*)-selective HNLs: *Sorghum bicolor* HNL (*Sb*HNL), *Ximenia americana* HNL (*Xa*HNL)³⁴, *Hb*HNL, *Me*HNL and *Bm*HNL.
- (iii) Based on the protein structure, HNLs can be categorized into nine superfamilies. They are
- (a) α/β hydrolase fold: Enzymes belonging to this superfamily have a core of an α/β sheet rather than a barrel. Thus, these enzymes contain 8 β -strands connected by 6 α -helices and a conserved catalytic triad (nucleophile-histidine-aspartate). HNLs from α/β hydrolase fold superfamily include HbHNL, MeHNL, AtHNL and BmHNL.
- (b) Serine carboxypeptidases: Enzymes in this superfamily exists in heterodimeric form, which is made-up by two pairs of chain A and B. Both chains are linked with glycosylated cysteine. *Sb*HNL is the single example of this family. *Sb*HNL contains catalytic triad Asp, His, and Ser similar to other HNLs.

- (c) FAD containing oxidoreductases: HNLs from this superfamily show maximum similarity (30% sequence similarity) with glucose-methanol-choline (GMC)-oxidoreductase but they do not show any oxidase activity. HNLs from *Prunus* sp. are main examples in this category.
- (d) Zn^{2+} dependent alcohol dehydrogenase: LuHNL is only the example of this family. It displays structure similarity to alcohol dehydrogenases (ADHs) which catalyzes both the oxidation and reduction of a wide range of alcohols and aldehydes. LuHNL and ADHs also have a conserved Zn^{2+} binding domain but LuHNL doesn't exhibit any ADH activity.
- (e) Cupin superfamily: Cupin fold HNLs are majorly bacterial HNLs. Ex: *Burkholderia phytofirmans* HNL (*Bp*HNL)³⁵, *Pseudomonas mephitica* HNL (*Psm*HNL)³⁵, *Granulicella tundricola* HNL (*Gt*HNL), and *Acidobacterium capsulatum* HNL (*Ac*HNL). HNLs from this superfamily exhibit a maximum identity with cupin fold superfamily proteins as they contain conserved barrel domain.
- (f) bet v1 fold: Davallia tyermannii HNL $(DtHNL)^{36}$ is the only the example of this family. DtHNL is the first protein with a bet v1fold exhibiting HNL activity with a new catalytic center.
- (g) $\alpha+\beta$ barrel fold: *Passiflora edulis* (*PeHNL*) is the only the example of this family. It contains a central β -barrel in the middle of a dimer.
- (h) Lipocalin superfamily: *Chamberlinius hualienensis* HNL (*Chua*HNL) and *Parafontaria laminate* (*Plam*HNL)³⁷ are the examples of this family. These HNLs have high similarity to the folding pattern of the other lipocalin proteins. The structural features of the lipocalin fold HNLs comprises of a large cup shaped cavity, which is composed of structurally conserved regions (SCRs). Their tertiary structure consists of 6 or 8 stranded β-barrels stabilized by one, two, or three sulfide bridges.

(i) A dimeric protein with a unique amino acid sequence not homologous to any other HNLs. Nandina domestica Thunb HNL (NdHNL-L)³⁸ belongs to this category.

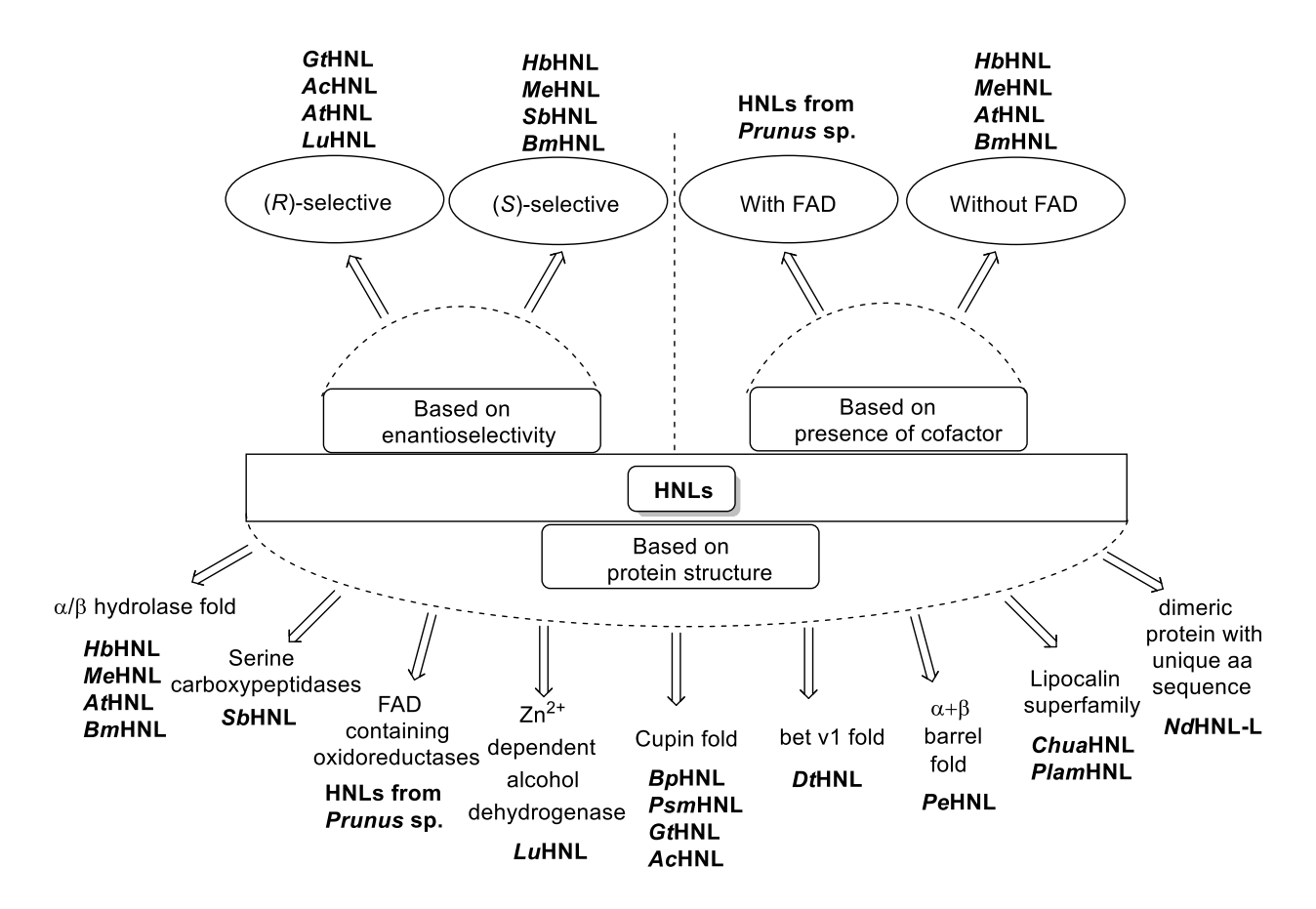


Figure 1.2: Overview of classification of HNLs based on the enantioselectivity, presence of cofactor and protein structure.

1.2.2. Arabidopsis thaliana HNL (AtHNL)

AtHNL is the first (R)-selective HNL (EC:4.1.2.10) that belongs to α/β-hydrolase superfamily from a non-cyanogenic plant⁹. It is structurally related to the (S)-selective HbHNL, MeHNL and BmHNL of α/β-hydrolase superfamily³⁹. Predominantly, AtHNL shows 45% identity and 67% similarity in sequence with the (S)-selective HbHNL. Despite of such high sequence similarity AtHNL shows opposite stereoselectivity in cyanohydrin synthesis. The opposite stereopreferences of AtHNL and HbHNL is due to the opposite routes of proton abstraction during cyanogenesis.

Based on the analysis of the complexes of the enzyme with (R)- and (S)-mandelonitrile (MN), it was predicted that in AtHNL, the proton is abstracted from the OH-group of (R)-MN by the histidine and moves back via the serine residue to the cyanide (clockwise), whereas in HbHNL the proton is abstracted from the (S)-MN via serine and moves back to cyanide by histidine (counterclockwise). In 2012, it was crystallized (PDB ID: 3DQZ), which confirmed its dimeric form and revealed that AtHNL's active site consists of a catalytic triad i.e., Ser^{81} -His²³⁶-Asp²⁰⁸, the three residues that are conserved in other α/β -hydrolase fold HNLs³⁹. The insights of binding of the cyanohydrins to the active site of AtHNL using modelling was also studied in comparison with HbHNL. Modelling and mutational studies revealed that Asn¹² side chain, main chain NH of Phe⁸², and Ala¹³ play a crucial catalytic role in cyanogenesis, while Thr¹¹ and Lys²³⁶ are vital in case of HbHNL. In 2015, Rui et al investigated the catalytic mechanism of AtHNL catalyzed cyanogenesis using QM/MM approach⁴⁰. AtHNL is known to have a broad substrate selectivity and high enantioselectivity towards a wide range of substrates, aliphatic and aromatic aldehydes in the enantioselective synthesis of diverse (R)-cyanohydrins^{9,41–43}. Its promiscuous catalytic activity in the stereoselective synthesis of β -nitroalcohols is discussed later.

1.3. Importance of HNL engineering

HNLs are diverse enzymes with respect to their source, sequence, structural fold and catalytic site, which might be the probable reason for them to show a varied degree of selectivity, i.e., chemo, regio, and stereo and substrate acceptance in their catalysis. Despite of such natural diversity many HNLs fail to fulfill the criteria of an industrial biocatalyst probably because they are not being evolved to accept unnatural substrates, catalyze in unnatural conditions. Hence, their use is far away from biotechnology industry. The industrial application of the non-engineered HNLs is thus restricted to the catalytic potential of the nature evolved catalytic site. However, there are examples

where different HNLs have been engineered for improved biocatalytic properties. Some of them are applied in various industrial applications, yet most of them lacks efficiency to synthesize chiral unnatural cyanohydrins and β-nitroalcohols that find industrial application. Engineering HNLs is an efficient approach to decrease such limitations. HNL engineering not only improves catalytic properties such as catalytic efficiency, enantioselectivity, acceptance of various substrates but also provides information about reaction mechanism of the enzyme. In 2011, Dadashipour and Asano have reviewed elaborately about HNLs³. Wiedner et al in 2016 have discussed in a book chapter about HNLs in biocatalytic synthesis of chiral cyanohydrins⁴⁴ and in the same year Bracco et al, have reviewed about the HNL catalyzed synthesis of enantiopure chiral cyanohydrins⁶. Several new HNLs were discovered in the past one-decade, new approaches developed in discovering diverse HNLs⁴ and many HNLs were engineered for biocatalysis.

1.4. Catalytic promiscuity

A few enzymes have the ability to catalyze reactions other than their natural ones. Such property is called catalytic promiscuity, and the enzymes are called promiscuous enzymes. Catalytic promiscuity in enzymes enables them to use the same active site to catalyze distinctly different chemical transformations that may differ in the functional group involved or the catalytic mechanism^{45–48}. This ability of the enzyme to catalyse multiple and mechanistically distinct reactions play a crucial role in developing new, novel and significant synthetic routes from the traditional biotransformations. Increasing demands for enantiopure compounds using efficient and versatile synthetic methods has certainly prompted to change from traditional biocatalysis to develop new enzymes with catalytic promiscuity. Although finding this kind of catalytically promiscuous enzymes is difficult in nature as they are accidental, using protein engineering one

can gain or improve enzyme promiscuity towards many biotransformations using different reaction conditions and many unnatural substrates^{49,50}.

Apart from the stereoselective cleavage and synthesis of chiral cyanohydrins few HNLs also catalyze stereoselective cleavage and synthesis of chiral β -nitro alcohols which are their promiscuous reactions. While stereoselective synthesis of β -nitro alcohols is also known as Henry reaction (nitroaldolase activity), the cleavage is called retro-Henry reaction, which is due to retro nitroaldolase activity.

1.4.1. Nitroaldolase activity

The most important biocatalytic method to synthesize chiral β -nitroalcohols involves enantioselective C-C bond formation between nucleophilic nitro alkane with an aldehyde or ketone (electrophilic in nature). This is a nitroaldol reaction or Henry reaction catalyzed by only a few HNLs (**Scheme 1.2**). The first and foremost asymmetric Henry reaction was done by Sasai and his co-workers in 1992⁵¹. As per literature many metal and nonmetal-based catalysts are used in this reaction^{52–70} only a few enzyme-catalyzed Henry reactions are reported. Among them, $HbHNL^{28}$ catalyzed reaction showed a better enantioselectivity. The other HNLs which are reported for nitroaldolase activity are bacterial HNLs, eg: $GtHNL^{71}$, $AcHNL^{71}$ and plant HNLs, eg: $AtHNL^{72}$ and $BmHNL^{73}$. GtHNL and AcHNL have also shown diastereoselective nitro-aldolase activity⁷¹.

Scheme 1.2: HNL catalyzed synthesis of chiral β -nitroalcohols.

1.4.2. Retro-nitroaldolase activity

This involves the stereoselective cleavage of one enantiomer of a racemic β -nitroalcohol based on the stereopreference of the HNL resulting in the production of an aldehyde as the cleavage product, and the complementary enantiomer that remains unreacted (**Scheme 1.3**). This approach is also known as the asymmetric retro-Henry reaction. *Hb*HNL and *At*HNL are reported to show retro-nitroaldolase activity^{74–77}. The substrate scope of the *At*HNL is extended to synthesize a broad range of (*S*)- β -nitroalcohols.

OH NO₂ (S)- selective OH NO₂ (R)- selective
$$AtHNL$$
 $CH_3NO_2 + PhCHO + CH_3NO_2 + P$

Scheme 1.3: Retro-Henry reaction catalyzed by *Hb*HNL and *At*HNL.

1.5. Enantiopure β- nitroalcohols

1.5.1. Importance of enantiopure β - nitroalcohols

Enantiopure β -nitro alcohols are versatile chiral intermediates in the synthesis of a wide range of chiral molecules with functional diversity. They are the vital chiral molecules and precursors of several pharmaceuticals, fine and agro chemicals which makes them industrially significant. **Figure 1.3** represents some key molecules that could be synthesized using chiral β -nitro alcohols as precursors.

1.5.2. Various synthetic chemical transformations of β -nitro alcohols

An optically pure β -nitro alcohol consists of a nitro and a hydroxyl group, attached to the vicinal carbon centers of which either one or both are asymmetric. The potential transformations of these two functional groups produces a wide variety of synthetic products with one or more different

functionalities (**Scheme 1.4**)^{53,78}. The β -nitro alcohols upon dehydration gives rise to conjugated nitro alkenes⁵². They undergo reduction to form β -amino alcohols and they can also undergo denitration process. They also oxidise to form nitro carbonyl compounds and α -hydroxy carbonyl compounds via the Nef reaction^{79,80}. These nitroalkenes, β -amino alcohols and nitro carbonyl compounds are valuable synthetic intermediates and can undergo a variety of nucleophilic and cycloaddition reactions to form various bioactive drugs and natural products.

Nitroalkenes obtained from dehydration methods are employed in the synthesis of (a) various nitrogen- containing natural products known for their biological activities such as indoles, primary amines, various pyrrole derivatives, isoindoles via retro Diels-Alder reaction, (b) antibiotics like lycoricidine and multiple coupling reagents like 2-nitro-2-propenyl-2,2-dimethylpropanoate (NPP) which helps in convergent syntheses, and (c) 2-nitro-1,3-dienes which are potential reagents for cycloaddition. Reduction of nitroalkenes is commonly used in the synthesis of a wide range of nitroalkanes^{78,81}. This approach is used in the synthesis of phenylethylamines which are of biochemical and pharmacological significance. Nitroalkanes are also building blocks of several heterocyclic derivatives such as γ -lactones and spiroketals lactams via Nef reaction. The reduction of nitro group followed by cyclization gives rise to a wide range of pyrrolidines and piperidines derivatives. Several polyheterocyclic derivatives are obtained by the nitronate anion-cyclization of nitroalkanes. The reduction of nitro group from α -nitroketone by denitration is an efficient method for the preparation of various natural products such as (Z)- jasmone, dihydrojasmone and various pheromones^{81,82}.

The β -amino alcohol moiety is a very important structural motif extensively seen in several natural and synthetic biologically active molecules such as antibiotics, alkaloids, enzyme inhibitors, and β -blockers^{83,84}. A few examples of different drug molecules and natural products having β -

nitroalcohol backbone with (S)- stereoselectivity are, (S)-chelonin A (antimicrobial)⁸⁵, (S)tembamide (anti-HIV)⁸⁶, (S)-toliprolol, (S)-moprolol⁸⁷, (S)-propranolol⁸⁸, (S)-norphenylephrine⁸⁹, (β-adrenergic receptor blocking agents), (S)-sotalol (antiarrhythmic agents)⁹⁰, and (S)-miconazole (antifungal)⁹⁰ (**Figure 1.3a**). Similarly, examples of various significant drugs and natural products having β -nitroalcohol backbone with (R)- stereoselectivity are (R)-tembamide⁹¹ (shows hypoglycemic activity), (R)-isoproterenol⁹² (β_1 -adrenergic receptor agonist), (R)-salmeterol⁹³ (β_2 adrenoreceptor agonist), (R)-clorprenaline (β_2 -adrenoreceptor agonist), (R)-salbutammol (β_2 adrenoreceptor agonist), (R)-arbutamine (a mixed β_1 - β_2 adrenoreceptor agonist), (R)phenylephrine (α_1 -adrenoreceptor agonist), (R)-adrenaline (neurotransmitter)⁹⁴ and (R)denopamine⁹⁵ (β_1 -adrenoreceptor agonist) (**Figure 1.3b**). Some of the natural products, biologically active molecules, and drug molecules are having β-nitroalcohol diastereomers in their structural backbone. Lipids and lipid-like molecules such as (R,S)-sphingosine⁹⁵ and (R,S)spisulosine 96 also fall under this category. Some of the drugs such as (R,S)-ephedrine 97 , (R,S)metaraminol⁹⁸, (R,S)-methoxamine⁹⁹, (R,R)-chloramphenicol¹⁰⁰, and AZD-5423¹⁰¹ also come under this group (**Figure 1.3c**).

c)
$$\bigcap_{14}^{OH} \bigcap_{NH_2}^{OH} \bigcap_{NH_2}^{OH}$$

Figure 1.3: Examples of pharmaceuticals, biologically active molecules, and natural products derived from enantiopure a) (S)-β-nitroalcohol adducts, b) (R)-β-nitroalcohol adducts and c) chiral β-nitroalcohol diastereomers.

Scheme 1.4: Various synthetic chemical transformations of a β-nitro alcohol adduct.

1.5.3. Asymmetric synthesis of β -nitroalcohols

The various synthetic transformations that have been used so far for the synthesis of enantiopure β -nitroalcohols can be broadly classified into the following two types.

- a) Chemical method
- b) Biocatalytic method

1.5.3.1. Asymmetric synthesis of β-nitroalcohols by chemical catalysts

Several established methods have been reported for the synthesis of chiral β -nitroalcohols that used chemical catalysts and majorly by Henry reaction (**Scheme 1.5**). As per literature many metals and non-metal-based catalysts are used in the asymmetric synthesis of β -nitroalcohols. Different catalysts such as the rare earth metal alkoxides, rare earth hexamethyldisilazides and binaphthol (BINOL) – rare earth metal complexes have been reported in the asymmetric synthesis of β -nitroalcohols⁵²⁻⁷⁰.

Scheme 1.5: Asymmetric Henry reaction using a chemical catalyst.

1.5.3.2. Importance of biocatalysis

Currently, a tremendous revolution towards a green and ecofriendly catalysis for the synthesis of chiral molecules is emerging in the global market. A lot of complications arise in the reactions catalyzed by chemical catalysts such as formation of various undesired side products due to the ability of strong bases to catalyse unwanted side reactions that include Aldol, Cannizzaro and water elimination reactions. Apart from being hazadarous and non-eco-friendly the chemical catalysts used in the reactions are too costly. These glitches in the chemical catalysis have led to an increase in the demand for an alternative way, i.e., enzyme based catalysis or biocatalysis. Over the years enzymes have been exploited in laboratories to carry out diverse chemical reactions. Enzyme based catalysis have created a different field of organic synthesis, biocatalysis, and have been used in the synthesis of a wide range of valuable enantiopure chiral products. Enzymes catalyze a broad range

of industrially significant biochemical transformations with high efficacy and selectivity. Unlike the chemical catalysts, they are chemo-, regio- and stereoselective in nature. Most of the enzymes possess a high catalytic turnover that implies the amount of substrate converted to product in a unit time is very high for them. Such high selectivity, turnover and efficacy is almost impossible to achieve using a chemical catalyst. The advantages of biocatalysis are given below.

- ➤ They provide a simple, sustainable, clean and cost-effective green catalysis.
- > They are nonhazardous and ecofriendly and avoid the usage of toxic/metal/hazardous catalysts.
- > They are biodegradable.
- ➤ They work under mild reaction conditions such as pH and temperature, which reduces the side reactions of the process and makes fewer byproducts.
- ➤ Biocatalysts are highly selective in nature.
- ➤ They do not require protection of functional groups in the substrate.
- ➤ They are reusable by immobilization.

1.5.3.3. Asymmetric synthesis of chiral β -nitroalcohols by biocatalytic approaches

Miner et al. in 2012 described two main biocatalytic approaches towards the synthesis of β -nitroalcohols⁷⁹. In 2021, Padhi et al. reviewed six major biocatalytic approaches to synthesize chiral β -nitroalcohols¹⁰². They are (a) kinetic resolution of racemic β -nitroalcohols, mostly catalyzed by lipases, (b) dynamic kinetic resolution that uses multienzymes or a chemoenzymatic system, (c) asymmetric reduction of α -nitroketones catalyzed by alcohol dehydrogenase (ADH) or corresponding whole cells, and (d) halohydrin dehalogenase (HheC) catalyzed enantioselective epoxide ring-opening (e) Henry reaction by direct C-C bond formation between a carbonyl and

nitroalkane substrate, mostly catalyzed by a HNL, (f) stereoselective cleavage of racemic β -nitroalcohols (retro-Henry reaction), (**Figure 1.4**). Among all the above biocatalytic routes the most important one is to synthesize chiral β -nitroalcohols using Henry reaction catalyzed by HNLs.

Figure 1.4: Major biocatalytic approaches for the synthesis of chiral β -nitroalcohols.

1.6. Promiscuous catalytic activity by HNL in synthesis of enantiopure β-nitroalcohols

Few HNLs which are known for their stereoselective synthesis of enantiopure β -nitroalcohols are summarized below.

1.6.1. HNLs (non-engineered) catalyzed synthesis of enantiopure β-nitroalcohols

In 2006, Purkarthofer et al. reported the first biocatalytic enantioselective nitroaldol synthesis using *Hevea brasiliensis* HNL (*Hb*HNL), an (*S*)-selective HNL²⁸. Using *Hb*HNL, they have examined the addition of nitromethane to benzaldehyde which gave (*S*)-2-nitro-1-phenylethanol in 63% yield with 92% *ee* (**Scheme 1.6.a**). The reaction was carried out in phosphate buffer pH

7.0, in presence of the organic solvent *tert*-butyl methyl ether (TBME) at room temperature for 48 h. They have also done the *Hb*HNL catalyzed reaction of nitroethane and benzaldehyde which gave a diastereomeric mixture of 2-nitro-1-phenylpropanol in 67% yield (**Scheme 1.6.b**). They obtained 90% (1*S*, 2*R*)-2-nitro-1-phenylpropanol as the main product.

a) R-CHO +
$$CH_3NO_2$$
 phosphate buffer/TBME 1:1 OH PH 7, rt, 48 h

b) Ph-CHO +
$$CH_3CH_2NO_2$$
 \xrightarrow{HbHNL} Ph $\stackrel{QH}{R}$ $\stackrel{NO_2}{R}$ + $\stackrel{Ph}{R}$ $\stackrel{NO_2}{R}$ 1R,2S $\stackrel{QH}{R}$ $\stackrel{NO_2}{R}$ + $\stackrel{QH}{R}$ $\stackrel{NO_2}{R}$ $\stackrel{Ph}{R}$ $\stackrel{NO_2}{R}$ $\stackrel{Ph}{R}$ $\stackrel{NO_2}{R}$ $\stackrel{Ph}{R}$ $\stackrel{NO_2}{R}$ $\stackrel{Ph}{R}$ $\stackrel{NO_2}{R}$ $\stackrel{Ph}{R}$ $\stackrel{NO_2}{R}$ $\stackrel{Ph}{R}$ $\stackrel{NO_2}{R}$ $\stackrel{R}{R}$ $\stackrel{R$

Scheme 1.6: *Hb*HNL catalyzed stereoselective addition of (a) nitromethane to aldehydes, (b) nitroethane to benzaldehyde.

In 2007, Griengl *et al* studied the *Hb*HNL catalyzed nitroaldol reaction with various aromatic, hetero-aromatic and aliphatic aldehydes and nitromethane¹⁰³. The reaction was carried out at room temperature in a biphasic aqueous-organic system with TBME as organic solvent. Initially, they performed experiments with 50 mM phosphate buffer at pH 7.0. Later, they switched on to citrate phosphate buffer) pH 5.5 to decrease the non-enzymatic deprotonation of nitromethane that takes place at pH 7.0. The corresponding addition of nitroethane to benzaldehyde produced two stereocenters simultaneously and a diastereomeric mixture of 2-nitro-1-phenylpropanols was

obtained. The *anti/syn* ratio was 9:1 and the enantiomeric excess of the *anti-*isomer was 95%. Thus, the product mixture contains about 90% of the main product (1*S*,2*R*). But no engineering of *Hb*HNL was done in any of these works. Apart from *Hb*HNL, *At*HNL is also reported to perform nitroaldol reaction. In 2011, Asano et al. used *At*HNL in an aqueous–organic biphasic system to synthesize (*R*)- β -nitro alcohols⁷² (**Scheme 1.7**).

$$\begin{array}{c} At \text{HNL} \\ \text{O} \\ \text{R} \\ \text{H} \end{array} + \begin{array}{c} \text{CH}_3 \text{NO}_2 \\ \hline \\ \text{rt, 2 h} \end{array} \xrightarrow{\text{rt, 2 h}} \begin{array}{c} \text{OH} \\ \text{R} \\ \end{array}$$

R=Ph, and other aromatic aldehydes, i.e., 2-Me,3-Me,4-Me, 2-OMe,3-OMe,4-OMe, 2-Cl,3-Cl,4-Cl,4-F,4-Br

Scheme 1.7: At HNL catalyzed asymmetric synthesis of (R)- β -nitro alcohols.

1.6.2. Engineered HNL catalyzed synthesis of enantiopure β-nitroalcohols

Bekerle-Bogner et al. tested both GtHNL and AcHNL for stereoselective synthesis of β -nitro alcohols¹⁰⁴. GtHNL engineering has resulted in mutants with higher enantioselectivity, and improved activity. SDM on AcHNL and GtHNL has produced several mutants that enhanced the substrate selectivity and stereoselectivity of the enzymes especially towards the enantioselective and diastereoselective synthesis of Henry products (**Scheme 1.8**). While GtHNL was almost inactive, wt AcHNL showed only 37.5% conversion and 79% ee of (R)-product in 24 h in the synthesis of (R)-2-nitro-1-phenylethanol. A study of the various mutants of GtHNL and AcHNL prepared earlier, e.g., A40H, A40R, and A40H-V42T-Q110H toward the synthesis of Henry products revealed that all of them show higher % conversion and ee than their wt. For example, AcHNL-A40H resulted in 73% conversion and 99.3% ee of (R)-2-nitro-1-phenylethanol in 4 h, while AcHNL-A40R showed 73% conversion and 96% ee after 24 h. Similarly, in case of GtHNL,

the mutants A40H, A40R and A40H-V42T-Q110H have shown 74 and 95.5, 75 and 94, and 73 and 94.5% of conversion and % *ee* respectively in the synthesis of (*R*)-2-nitro-1-phenylethanol¹⁰⁴.

Five mutants of *Gt*HNL (A40R and A40H-V42T-Q110H) and *Ac*HNL (A40H, A40R and A40H-V42T-Q110H) have shown broad substrate selectivity¹⁰⁴. They catalyzed the synthesis of (*R*)-nitroaldol products of aromatic, i.e., 2-chlorobenzaldehyde, as well as aliphatic aldehydes, i.e., cyclohexanecarboxaldehyde and hexanal in 31- 97% conversion and 23-99% *ee*. These five mutants were also tested for diastereoselective synthesis of Henry products by coupling benzaldehyde and nitroethane. The wild type as well as all the five mutants produced up to 88% *ee* of the (*R*)-*anti* product, i.e., (1*R*,2*S*)-2-nitro-1-phenylpropanol. They studied the effect of various metal ions, i.e., Mn²⁺, Ni²⁺, Co²⁺, Fe²⁺, and Zn²⁺ on the *Gt*HNL-A40H-V42T-Q110H catalysis toward stereoselective synthesis of Henry products. They observed a slower reaction with the Zn²⁺ bound enzyme, in contrary the Co²⁺, Fe²⁺ bound enzymes showed faster rate than the normal Mn²⁺ containing triple mutant. This result shows that, *Gt*HNL catalyzed Henry reaction is not specific to Mn²⁺ rather other metal ions, e.g., Co²⁺, Fe²⁺ can also be used.

a)
$$R + CH_3NO_2 = \frac{GtHNL / AcHNL mutein}{KPB pH 6 / TBME (1:1)} + \frac{OH}{R(R)} NO_2$$
 $R = 2 - CIC_6H_4$, cyclohexyl, $R = 2$

Scheme 1.8: *Gt*HNL and *Ac*HNL catalyzed synthesis of A) enantioselective Henry products, and B) diastereoselective Henry products.

1.6.3. Engineered HNL catalyzed synthesis of enantiocomplementary β -nitroalcohols using retro- nitroaldol reaction

In 2010, Yurvev et al. worked on biocatalytic retro-Henry reaction where the enantioslective cleavage of racemic 2-nitro-1-phenylethanol using HbHNL was carried out to produce (R)- β -nitroalcohols in 95% ee, 49% conversion⁷⁴. In 2014, Kazlauskas et al. engineered HbHNL and tested the mutants for the retro-Henry reaction¹⁰⁵. They found a variant HbHNL-L121Y, which catalyzed the cleavage of 2-nitro-1-phenylethanol 4.8 times more efficiently (specific activity 0.62 Umg¹) than the wild type (0.13 Umg⁻¹). A triple variant HbHNL-L121Y-F125TL146M showed better specific activity (0.71 Umg¹) and 3.3 times higher k_{cat} than the wild type. In 2019, our group has synthesized ten aromatic (S)- β -nitroalcohols using AtHNL catalyzed retro-Henry reaction with optimized biocatalytic reaction conditions⁷⁶ (**Scheme 1.9**). At least half a dozen aromatic (S)- β -nitroalcohols were synthesized showing 99% ee and 47% conversion and enantioselectivity up to 84. Subsequently a celite immobilized AtHNL was explored to catalyze retro-Henry reaction to produce a series of (S)- β -nitroalcohols under optimized conditions⁷⁷.

Scheme 1.9: *At*HNL catalyzed synthesis of (*S*)-β-nitroalcohols by retro-Henry reaction.

Recently, we have engineered AtHNL and the variants were used to synthesize (S)- β -nitroalcohol via retro-Henry reaction (Scheme 1.10). The AtHNL-F179N variant showed ~ 2.4 -fold k_{cat}/K_m

than the native enzyme towards retro-nitroaldolase activity. The same variant has also shown increased enantioselectivity (*E* value) of 138 vs. 81 by the wild type for the same reaction.

Scheme 1.10: *At*HNL-F179N catalyzed synthesis of (*S*)-2-nitro-1-phenylethanol by retro-Henry reaction.

1.7. Engineered HNL catalyzed other promiscuous reactions

Apart from stereoselective and synthesis of chiral cyanohydrins and β -nitroalcohols, few HNLs are reported to exhibit activity for other biotransformations. In 2010, Kazlauskas et al. used two amino acid substitution in a plant esterase salicylic acid binding protein 2 (SABP2) to shift it to a HNL¹⁰⁶. Thus, they produced a variant SABP2-G12T-M239K, which showed its activity towards release of cyanide form mandelonitrile and lost its activity for ester hydrolysis. In 2014, substitution was done in *Hb*HNL to convert its HNL activity to esterase activity¹⁰⁷. The substitutions at Thr11 and Lys236 to Gly in *Hb*HNL decreased 100-fold HNL activity towards the cleavage of mandelonitrile, at the same time improved esterase activity up to three fold. When another mutation was added to it, i.e., Glu79His, the new variant enhanced esterase activity more than 10-fold.

In 2016, Devamani et al. used divergent evolution to study the HNL promiscuity towards many reactions 108 . They have reconstructed the ancestral enzymes at four branch points in the divergence HNL's from esterases ~ 100 million years ago. The ancestral enzyme sequences were inferred from the sequences of the modern descendant enzymes using either neighbor joining, maximum

parsimony, maximum likelihood, or a combination of maximum parsimony and maximum likelihood. They were investigated towards Henry reaction to synthesize 2-nitro-1-phenylethanol. MeHNL gave 76% conversion and 5% ee of (S)-enantiomer, HNL1-ML (construct originmaximum likelihood) gave 85% conversion and 83% ee of (S)-enantiomer, HNL 1-NJ (construct origin- neighbour joining) gave 98% conversion and 95% ee of (S)-enantiomer, HNL 1 gave 91% conversion and 96% ee of (S)-enantiomer and Arabidopsis thaliana esterase (AtEST) gave 96% conversion and 88% ee of (R)-enantiomer. Among the other promiscuous activities, HNL 1-NJ catalyzed Michael addition that resulted in 19% conversion and 56% ee of (S)-enantiomer of 3-(2nitro-1-phenyl ethyl) pentane-2, 4-dione. It also showed lactonase activity giving 66% conversion and 99% ee of (S)-enantiomer of 5-phenyldihydrofuran-2(3H)¹⁰⁸. Esterase 2 (EST 2) showed 34% conversion and 55% ee of (R)-methyl mandelate, Esterase 1 (EST 1) showed 24% conversion and 34% ee of (R)- methyl mandelate and Rauvolfia serpentine esterase (RsEST) showed 68% conversion and 99% ee of (R)- methyl mandelate. Few of them also showed Lactamase activity to synthesize 2-Azabicyclo-[2.2.1]-hept-5-en-3-one as the product. Towards this reaction, Esterase 3-NJ (construct origin-neighbor joining) showed 47% conversion and 78% ee for (1R,4S)-product, EST 2 produced the (1R,4S)-product in 37% conversion and 59% ee, EST 1 resulted in 52% conversion and 96% ee of the (1R,4S)-product and SABP2 showed 51% conversion and 92% ee of the (1R,4S)-product.

In 2017 Jones et al. uncovered how the identical active sites show opposite enantioselectivities in case of HbHNL and AtHNL¹⁰⁹. They reconstructed the last common ancestor of HbHNL and AtHNL called EST3 mL which could catalyze both cyanohydrin cleavage and ester hydrolysis. EST3 mL has Asn11 and Met236, similar to AtHNL while the corresponding residues in HbHNL

are Thr11 and Lys236. Using SDM, they exchanged key active site amino acids in both *At*HNL and *Hb*HNL, and studied the library to address the opposite enantioselectivity of them.

In 2020, the same group reconstructed a catalytically active ancestral HNL, i.e., HNL1 in the α/β -hydrolase fold superfamily¹¹⁰. They replaced HbHNL with three residues corresponding to HNL1 (Leu121Phe, Leu146Met and Leu178Phe) that expanded its binding site and resulted in increased esterase activity by 125-fold. This replacement also improved HNL activity by 3-fold. Subsequently, they altered the active site of HNL1 by replacing its three residues with the corresponding residues of HbHNL (HNL1 w/o binding) and noticed that the esterase activity of HNL1 w/o binding decreased 15-fold as compared to HNL1 and the HNL activity decreased 2-fold. The promiscuity (= 1/selectivity) of HNL1 w/o binding decreased 7 fold as compared to HNL1, mainly due to the decline in the esterase activity. Further, they made replacement in HNL1 (Thr11Gly/Lys236Gly/Glu79His) aiming to gain esterase catalysis. They observed 10-fold decreased HNL catalytic efficiency and 22-fold increased esterase catalytic efficiency by the triple variant 110. This HNL1 + esterase catalysis variant was equally effective as an esterase, but retained more HNL activity. The esterase activities of HbHNL + esterase catalysis variant and HNL1 + esterase catalysis variant were ~10-fold lower than that for a related esterase (SABP2).

1.8. Requirement of HNL engineering for promiscuous synthesis of enantiopure β nitroalcohols

HNLs play a significant role as green catalysts in the sustainable chemistry and offer an alternative to the existing methods of using hazardous metals and toxic chemicals for several stereoselective C-C bond-formation reactions. They have emerged as potential biocatalysts for the synthesis of various optically pure cyanohydrins and β -nitroalcohols, which can be applied in pharmaceutical,

agrochemical, chemical and cosmetic industries. HNL catalyzed stereoselective synthesis of chiral β -nitroalcohols has a predominant role in fulfilling the need for synthesizing diverse industrially significant products. Further, using a single HNL, one could access to enantiocomplementary β -nitroalcohols using nitroaldol and retro-nitroaldol reactions. Undoubtedly, the synthetic scope of the HNL catalyzed promiscuous nitroaldol reaction is high compared to the chiral cyanohydrin synthesis because the later reaction involves the use of hydrogen cyanide and hence is not preferred by the industries. So far, AtHNL is the only HNL reported in both enantioselective cleavage (retro-nitroaldol) and synthesis (nitroaldol) of chiral β -nitroalcohols. Unlike (R)-selective GtHNL and AcHNL, the AtHNL doesn't require any cofactor for its catalysis. However, AtHNL's promiscuous nitroaldolase activity is limited by low enantioselectivity, poor yield, and narrow substrate scope in the enantioselective synthesis of β -nitroalcohols. While the design and engineering of AtHNL could improve the promiscuous catalytic activity, which subsequently opens the opportunities for synthetic applications of the engineered enzymes, lack of mechanistic understanding remains a constraint in this approach.

Thus, the goal of the thesis is to engineer AtHNL, to improve its catalytic properties for nitroaldolase and retro-nitroaldolase activity. We also aimed to investigate the mechanism of the enzyme by choosing the simple retro-nitroaldol reaction. We further envisioned to develop a new chemo-enzymatic method to synthesize a chiral intermediate of (R)-Tembamide, i.e., (R)-1-(4-methoxyphenyl)-2-nitroethanol using engineered AtHNL catalyzed nitroaldol reaction.

1.9. Objectives

The major objectives of the thesis are framed as follows:

- ❖ To investigate the binding site of *At*HNL, identify and alter residues, for increased catalytic efficiency and enantioselectivity towards the promiscuous retro-nitroaldol reaction.
- * To improve nitroaldolase activity of AtHNL and synthesize diverse (R)-β-nitroalcohols using engineered enzymes.
- ❖ To develop a new chemo-enzymatic method for synthesis of a chiral intermediate of (*R*)Tembamide, a natural product drug, using engineered *AtHNL*.

1.10. References

- (1) Patrick C. Cirino and Lianhong Sun*, ‡. Advancing Biocatalysis through Enzyme, Cellular, and Platform Engineering. *Biotechnol*. *Prog.* **2008**, *24*, 515–519.
- (2) Bornscheuer, U. T.; Huisman, G. W.; Kazlauskas, R. J.; Lutz, S.; Moore, J. C.; Robins, K. Engineering the Third Wave of Biocatalysis. *Nature* **2012**, *485* (7397), 185–194. https://doi.org/10.1038/nature11117.
- (3) Dadashipour, M.; Asano, Y. Hydroxynitrile Lyases: Insights into Biochemistry, Discovery, and Engineering. *ACS Catal.* **2011**, *1* (9), 1121–1149. https://doi.org/10.1021/cs200325q.
- (4) Padhi, S. K. Modern Approaches to Discovering New Hydroxynitrile Lyases for Biocatalysis. *ChemBioChem* **2017**, *18* (2), 152–160. https://doi.org/10.1002/cbic.201600495.
- (5) Gregory, R. J. H. Cyanohydrins in Nature and the Laboratory : Biology, Preparations, and Synthetic Applications. *Chem. Rev.* **1999**, *99* (0), 3649–3682.
- (6) Bracco, P.; Busch, H.; von Langermann, J.; Hanefeld, U. Enantioselective Synthesis of Cyanohydrins Catalysed by Hydroxynitrile Lyases a Review. *Org. Biomol. Chem.* **2016**,

- 14 (27), 6375–6389. https://doi.org/10.1039/C6OB00934D.
- (7) Jangir, N.; Padhi, S. K. Immobilized Baliospermum Montanum Hydroxynitrile Lyase Catalyzed Synthesis of Chiral Cyanohydrins. *Bioorg. Chem.* **2019**, *84* (August 2018), 32–40. https://doi.org/10.1016/j.bioorg.2018.11.017.
- (8) Jangir, N.; Sangoji, D.; Padhi, S. K. Baliospermum Montanum Hydroxynitrile Lyase Catalyzed Synthesis of Chiral Cyanohydrins in a Biphasic Solvent. *Biocatal. Agric. Biotechnol.* 2018, 16 (May), 229–236. https://doi.org/10.1016/j.bcab.2018.08.008.
- (9) Andexer, J.; Langermann, J. Von; Mell, A.; Bocola, M.; Kragl, U.; Eggert, T.; Pohl, M. An R-Selective Hydroxynitrile Lyase from Arabidopsis thaliana with an a / b -Hydrolase Fold. Angew. Chemie - Int. Ed. 2007, 46, 8679–8681. https://doi.org/10.1002/anie.200701455.
- (10) Dreveny, I.; Gruber, K.; Glieder, A.; Thompson, A.; Kratky, C. The Hydroxynitrile Lyase from Almond: A Lyase That Looks like an Oxidoreductase. *Structure* **2001**, *9* (9), 803–815. https://doi.org/10.1016/S0969-2126(01)00639-6.
- (11) Trummler, K.; Fo, S.; Pfizenmaier, K.; Wajant, H. Expression of the Zn 2 + -Containing Hydroxynitrile Lyase from Flax (Linum Usitatissimum) in Pichia Pastoris Utilization of the Recombinant Enzyme for Enzymatic Analysis and Site-Directed Mutagenesis. *Plant Sci.* **1998**, *139*, 19–27.
- (12) Dadashipour, M.; Ishida, Y.; Yamamoto, K.; Asano, Y. Discovery and Molecular and Biocatalytic Properties of Hydroxynitrile Lyase from an Invasive Millipede, Chamberlinius Hualienensis . *Proc. Natl. Acad. Sci.* 2015, 112 (34), 10605–10610. https://doi.org/10.1073/pnas.1508311112.

- (13) Yamaguchi, T.; Nuylert, A.; Ina, A.; Tanabe, T.; Asano, Y. Hydroxynitrile Lyases from Cyanogenic Millipedes: Molecular Cloning, Heterologous Expression, and Whole-Cell Biocatalysis for the Production of (R)-Mandelonitrile. *Sci. Rep.* **2018**, 8 (1), 1–10. https://doi.org/10.1038/s41598-018-20190-x.
- (14) Cheng, I. P.; Poulton, J. E. Cloning of CDNA of Prunus Serotina (R)-(+)-Mandelonitrile Lyase and Identification of a Putative Fad-Binding Site. *Plant Cell Physiol.* **1993**, *34* (7), 1139–1143.
- (15) Alagöz, D.; Tükel, S. S.; Yildirim, D. Purification, Immobilization and Characterization of (R)-Hydroxynitrile Lyase from Prunus Amygdalus Turcomanica Seeds and Their Applicability for Synthesis of Enantiopure Cyanohydrins. *J. Mol. Catal. B Enzym.* 2014, 101, 40–46. https://doi.org/10.1016/j.molcatb.2013.12.019.
- (16) Nanda, S.; Kato, Y.; Asano, Y. A New (R)-Hydroxynitrile Lyase from Prunus Mume: Asymmetric Synthesis of Cyanohydrins. *Tetrahedron* **2005**, *61* (46), 10908–10916. https://doi.org/10.1016/j.tet.2005.08.105.
- (17) Nanda, S.; Kato, Y.; Asano, Y. PmHNL -Catalyzed Synthesis of Aliphatic(R)-Cyanohydrins. *Tetrahedron: Asymmetry* **2006**, *17*, 735–741. https://doi.org/10.1055/s-2006-941778.
- (18) Yao, L.; Li, H.; Yang, J.; Li, C.; Shen, Y. Purification and Characterization of a Hydroxynitrile Lyase from Amygdalus Pedunculata Pall. *Int. J. Biol. Macromol.* **2018**, *118*, 189–194. https://doi.org/10.1016/j.ijbiomac.2018.06.037.
- (19) Nuylert, A.; Ishida, Y.; Asano, Y. Effect of Glycosylation on the Biocatalytic Properties of Hydroxynitrile Lyase from the Passion Fruit, Passiflora Edulis: A Comparison of Natural

- and Recombinant Enzymes. *ChemBioChem* **2017**, *18* (3), 257–265. https://doi.org/10.1002/cbic.201600447.
- (20) Ueatrongchit, T.; Tamura, K.; Ohmiya, T.; H-Kittikun, A.; Asano, Y. Hydroxynitrile Lyase from Passiflora Edulis: Purification, Characteristics and Application in Asymmetric Synthesis of (R)-Mandelonitrile. *Enzyme Microb. Technol.* 2010, 46 (6), 456–465. https://doi.org/10.1016/j.enzmictec.2010.02.008.
- (21) Zheng, Y. C.; Xu, J. H.; Wang, H.; Lin, G. Q.; Hong, R.; Yu, H. L. Hydroxynitrile Lyase Isozymes from Prunus Communis: Identification, Characterization and Synthetic Applications. *Adv. Synth. Catal.* 2017, 359 (7), 1185–1193. https://doi.org/10.1002/adsc.201601332.
- (22) Asif, M.; Bhalla, T. C. Enantiopure Synthesis of (R)-Mandelonitrile Using Hydroxynitrile Lyase of Wild Apricot (Prunus Armeniaca L.) [ParsHNL] in Aqueous/Organic Biphasic System. *Catal. Letters* **2017**, *147* (6), 1592–1597. https://doi.org/10.1007/s10562-017-2025-5.
- (23) Asif, M.; Bhalla, T. C. Hydroxynitrile Lyase of Wild Apricot (Prunus Armeniaca L.): Purification, Characterization and Application in Synthesis of Enantiopure Mandelonitrile. *Catal. Letters* **2016**, *146* (6), 1118–1127. https://doi.org/10.1007/s10562-016-1725-6.
- (24) Bhunya, R.; Mahapatra, T.; Nanda, S. Prunus Armeniaca Hydroxynitrile Lyase (ParsHNL)-Catalyzed Asymmetric Synthesis of Cyanohydrins from Sterically Demanding Aromatic Aldehydes. *Tetrahedron Asymmetry* 2009, 20 (13), 1526–1530. https://doi.org/10.1016/j.tetasy.2009.05.022.

- (25) Wiedner, R.; Gruber-Khadjawi, M.; Schwab, H.; Steiner, K. Discovery of a Novel (R)-Selective Bacterial Hydroxynitrile Lyase from Acidobacterium Capsulatum. *Comput. Struct. Biotechnol. J.* **2014**, *10* (16), 58–62. https://doi.org/10.1016/j.csbj.2014.07.002.
- (26) Hajnal, I.; Łyskowski, A.; Hanefeld, U.; Gruber, K.; Schwab, H.; Steiner, K. Biochemical and Structural Characterization of a Novel Bacterial Manganese-Dependent Hydroxynitrile Lyase. *FEBS J.* **2013**, 280 (22), 5815–5828. https://doi.org/10.1111/febs.12501.
- (27) Dadashipour, M.; Yamazaki, M.; Momonoi, K.; Fuhshuku, K.; Kanase, Y.; Uchimura, E.; Kaiyun, G.; Asano, Y. S -Selective Hydroxynitrile Lyase from a Plant Baliospermum Montanum: Molecular Characterization of Recombinant Enzyme. *J. Biotechnol.* **2011**, *153* (3–4), 100–110. https://doi.org/10.1016/j.jbiotec.2011.02.004.
- (28) Purkarthofer, T.; Gruber, K.; Gruber-Khadjawi, M.; Waich, K.; Skranc, W.; Mink, D.; Griengl, H. A Biocatalytic Henry Reaction The Hydroxynitrile Lyase from Hevea Brasiliensis Also Catalyzes Nitroaldol Reactions. *Angew. Chemie Int. Ed.* **2006**, *45* (21), 3454–3456. https://doi.org/10.1002/anie.200504230.
- (29) Wajant, H.; Pfizenmaier, K. Identification of Potential Active-Site Residues in the Hydroxynitrile Lyase from Manihot Esculenta by Site-Directed Mutagenesis. *J. Biol. Chem.* 1996, 271 (42), 25830–25834. https://doi.org/10.1074/jbc.271.42.25830.
- (30) Wajant, H.; Mundry, K. W.; Pfizenmaier, K. Molecular Cloning of Hydroxynitrile Lyase from Sorghum Bicolor (L.). Homologies to Serine Carboxypeptidases. *Plant Mol. Biol.* 1994, 26 (2), 735–746. https://doi.org/10.1007/BF00013758.
- (31) Wajant, H.; Förster, S.; Selmar, D.; Effenberger, F.; Pfizenmaier, K. Purification and Characterization of a Novel (R)-Mandelonitrile Lyase from the Fern Phlebodium Aureum.

- Plant Physiol. 1995, 109 (4), 1231–1238. https://doi.org/10.1104/pp.109.4.1231.
- (32) Torrelo, G.; Ribeiro De Souza, F. Z.; Carrilho, E.; Hanefeld, U. Xylella Fastidiosa Esterase Rather than Hydroxynitrile Lyase. *ChemBioChem* **2015**, *16* (4), 625–630. https://doi.org/10.1002/cbic.201402685.
- (33) Caruso, C. S.; de Fátima Travensolo, R.; de Campus Bicudo, R.; de Macedo Lemos, E. G.; Ulian de Araújo, A. P.; Carrilho, E. α-Hydroxynitrile Lyase Protein from Xylella Fastidiosa: Cloning, Expression, and Characterization. *Microb. Pathog.* 2009, 47 (3), 118–127. https://doi.org/10.1016/j.micpath.2009.06.007.
- (34) Kuroki, G. W.; Conn, E. E. Mandelonitrile Lyase from Ximenia Americana L.: Stereospecificity and Lack of Flavin Prosthetic Group. *Proc. Natl. Acad. Sci. U. S. A.* **1989**, 86 (18), 6978–6981. https://doi.org/10.1073/pnas.86.18.6978.
- (35) Hussain, Z.; Wiedner, R.; Steiner, K.; Hajek, T.; Avi, M.; Hecher, B.; Sessitsch, A.; Schwab, H. Characterization of Two Bacterial Hydroxynitrile Lyases with High Similarity to Cupin Superfamily Proteins. *Appl. Environ. Microbiol.* 2012, 78 (6), 2053–2055. https://doi.org/10.1128/aem.06899-11.
- (36) Lanfranchi, E.; Pavkov-Keller, T.; Koehler, E. M.; Diepold, M.; Steiner, K.; Darnhofer, B.; Hartler, J.; Bergh, T. Van Den; Joosten, H. J.; Gruber-Khadjawi, M.; Thallinger, G. G.; Birner-Gruenberger, R.; Gruber, K.; Winkler, M.; Glieder, A. Erratum: Enzyme Discovery beyond Homology: A Unique Hydroxynitrile Lyase in the Bet v1 Superfamily. *Sci. Rep.* 2017, 7, 46834. https://doi.org/10.1038/srep46834.
- (37) Nuylert, A.; Nakabayashi, M.; Yamaguchi, T.; Asano, Y. Discovery and Structural Analysis to Improve the Enantioselectivity of Hydroxynitrile Lyase from Parafontaria Laminata

- Millipedes for (R)-2-Chloromandelonitrile Synthesis. *ACS Omega* **2020**, *5* (43), 27896–27908. https://doi.org/10.1021/acsomega.0c03070.
- (38) Isobe, K.; Kitagawa, A.; Kanamori, K.; Kashiwagi, N.; Matsui, D.; Yamaguchi, T.; Fuhshuku, K. I.; Semba, H.; Asano, Y. Characterization of a Novel Hydroxynitrile Lyase from Nandina Domestica Thunb. *Biosci. Biotechnol. Biochem.* 2018, 82 (10), 1760–1769. https://doi.org/10.1080/09168451.2018.1490171.
- (39) Andexer, J. N.; Staunig, N.; Eggert, T.; Kratky, C.; Pohl, M. Hydroxynitrile Lyases with a / b -Hydrolase Fold: Two Enzymes with Almost Identical 3D Structures but Opposite Enantioselectivities and Different Reaction Mechanisms. *ChemBioChem* **2012**, *13*, 1932–1939. https://doi.org/10.1002/cbic.201200239.
- (40) Zhu, W.; Liu, Y.; Zhang, R. A QM/MM Study of the Reaction Mechanism of (R)-Hydroxynitrile Lyases from Arabidopsis Thaliana (AtHNL). *Proteins Struct. Funct. Bioinforma.* **2015**, *83* (1), 66–77. https://doi.org/10.1002/prot.24648.
- (41) Okrob, D.; Metzner, J.; Wiechert, W.; Gruber, K.; Pohl, M. Tailoring a Stabilized Variant of Hydroxynitrile Lyase from Arabidopsis Thaliana. *ChemBioChem* **2012**, *13* (6), 797–802. https://doi.org/10.1002/cbic.201100619.
- (42) Scholz, K. E.; Kopka, B.; Wirtz, A.; Pohl, M.; Jaeger, K. Fusion of a Flavin-Based Fluorescent Protein to Hydroxynitrile Lyase from Arabidopsis Thaliana Improves Enzyme Stability. *Appl. Environ. Microbiol.* **2013**, *79* (15), 4727–4733. https://doi.org/10.1128/AEM.00795-13.
- (43) Diener, M.; Kopka, B.; Pohl, M.; Jaeger, K. E.; Krauss, U. Fusion of a Coiled-Coil Domain Facilitates the High-Level Production of Catalytically Active Enzyme Inclusion Bodies.

- ChemCatChem **2016**, 8 (1), 142–152. https://doi.org/10.1002/cctc.201501001.
- (44) Wiedner, R.; Schwab, H.; Steiner, K. Hydroxynitrile Lyases for Biocatalytic Synthesis of Chiral Cyanohydrins. *Green Biocatal*. **2016**, 603–628. https://doi.org/10.1002/9781118828083.ch25.
- (45) Gupta, R. D. Recent Advances in Enzyme Promiscuity. *Sustain. Chem. Process.* **2016**, *4* (1), 1–7. https://doi.org/10.1186/s40508-016-0046-9.
- (46) Kazlauskas, R. J. Enhancing Catalytic Promiscuity for Biocatalysis. *Curr. Opin. Chem. Biol.* **2005**, *9* (2), 195–201. https://doi.org/10.1016/j.cbpa.2005.02.008.
- (47) O'Brien, P. J.; Herschlag, D. Catalytic Promiscuity and the Evolution of New Enzymatic Activities. *Chem. Biol.* **1999**, *6* (4). https://doi.org/10.1016/S1074-5521(99)80033-7.
- (48) Leveson-Gower, R. B.; Mayer, C.; Roelfes, G. The Importance of Catalytic Promiscuity for Enzyme Design and Evolution. *Nat. Rev. Chem.* **2019**, *3* (12), 687–705. https://doi.org/10.1038/s41570-019-0143-x.
- (49) Otte, K. B.; Hauer, B. Enzyme Engineering in the Context of Novel Pathways and Products.

 Curr. Opin. Biotechnol. 2015, 35 (December 2015), 16–22.

 https://doi.org/10.1016/j.copbio.2014.12.011.
- (50) Chen, K.; Arnold, F. H. Engineering New Catalytic Activities in Enzymes. *Nat. Catal.* 2020, 3 (3), 203–213. https://doi.org/10.1038/s41929-019-0385-5.
- (51) Hiroaki Sasai, Takeyuki Suzuki, Shigeru Arai, Takayoshi Arai, and M. S. Basic Character of Rare Earth Metal Alkoxides. Utilization in Catalytic C-C Bond-Forming Reactions and Catalytic Asymmetric Nitroaldol Reactions. *J. Am. Chem. SO* **1992**, *114* (11), 4418–4420.

- (52) Chandrasekhar, S.; Shrinidhi, A. Useful Extensions of the Henry Reaction: Expeditious Routes to Nitroalkanes and Nitroalkenes in Aqueous Media. *Synth. Commun.* **2014**, *44* (20), 3008–3018. https://doi.org/10.1080/00397911.2014.926373.
- (53) Luzzio, F. A. The Henry Reaction: Recent Examples. *Tetrahedron* 2001, 57 (6), 915–945.
 https://doi.org/10.1016/s0040-4020(00)00965-0.
- (54) Filippova, L.; Stenstrøm, Y.; Hansen, T. V. Cu (II)-Catalyzed Asymmetric Henry Reaction with a Novel C<inf>1</Inf>-Symmetric Aminopinane-Derived Ligand. *Molecules* **2015**, 20 (4), 6224–6236. https://doi.org/10.3390/molecules20046224.
- (55) White, J. D.; Shaw, S. A New Catalyst for the Asymmetric Henry Reaction: Synthesis of β-Nitroethanols in High Enantiomeric Excess. *Org. Lett.* **2012**, *14* (24), 6270–6273. https://doi.org/10.1021/ol3030023.
- (56) Phukan, M.; Borah, K. J.; Borah, R. Henry Reaction in Environmentally Benign Methods Using Imidazole as Catalyst. *Green Chem. Lett. Rev.* **2009**, *2* (4), 249–253. https://doi.org/10.1080/17518250903410074.
- (57) Gao, N.; Chen, Y. L.; He, Y. H.; Guan, Z. Highly Efficient and Large-Scalable Glucoamylase-Catalyzed Henry Reactions. *RSC Adv.* **2013**, *3* (37), 16850–16856. https://doi.org/10.1039/c3ra41287c.
- (58) Sasai, H.; Suzuki, T.; Itoh, N.; Shibasaki, M. Catalytic Asymmetric Synthesis of Propranolol and Metoprolol Using a La–Li–BINOL Complex. *Appl. Organomet. Chem.* **1995**, 9 (5–6), 421–426. https://doi.org/10.1002/aoc.590090508.
- (59) Shi, Y.; Li, Y.; Sun, J.; Lai, Q.; Wei, C.; Gong, Z.; Gu, Q.; Song, Z. Synthesis and

- Applications in Henry Reactions of Novel Chiral Thiazoline Tridentate Ligands. *Appl. Organomet. Chem.* **2015**, 29 (10), 661–667. https://doi.org/10.1002/aoc.3347.
- (60) Sohtome, Y.; Hashimoto, Y.; Nagasawa, K. Guanidine-Thiourea Bifunctional Organocatalyst for the Asymmetric Henry (Nitroaldol) Reaction. *Adv. Synth. Catal.* **2005**, 347 (11–13), 1643–1648. https://doi.org/10.1002/adsc.200505148.
- (61) Alvarez-Casao, Y.; Marques-Lopez, E.; Herrera, R. P. Organocatalytic Enantioselective Henry Reactions. *Symmetry* (*Basel*). **2011**, *3* (2), 220–245. https://doi.org/10.3390/sym3020220.
- (62) Xu, D. Q.; Wang, Y. F.; Luo, S. P.; Zhang, S.; Zhong, A. G.; Chen, H.; Xu, Z. Y. A Novel Enantioselective Catalytic Tandem Oxa-Michael-Henry Reaction: One-Pot Organocatalytic Asymmetric Synthesis of 3-Nitro-2H-Chromenes. *Adv. Synth. Catal.* **2008**, *350* (16), 2610–2616. https://doi.org/10.1002/adsc.200800535.
- (63) Bosica, G.; Polidano, K. Solvent-Free Henry and Michael Reactions with Nitroalkanes Promoted by Potassium Carbonate as a Versatile Heterogeneous Catalyst. *J. Chem.* **2017**, 2017 (Scheme 1), 1–10. https://doi.org/10.1155/2017/6267036.
- (64) Marcelli, T.; Van Der Haas, R. N. S.; Van Maarseveen, J. H.; Hiemstra, H. Asymmetric Organocatalytic Henry Reaction. *Angew. Chemie - Int. Ed.* 2006, 45 (6), 929–931. https://doi.org/10.1002/anie.200503724.
- (65) Arai, T.; Watanabe, M.; Fujiwara, A.; Yokoyama, N.; Yanagisawa, A. Direct Monitoring of the Asymmetric Induction of Solid-Phase Catalysis Using Circular Dichroism: Diamine-CuI-Catalyzed Asymmetric Henry Reaction. *Angew. Chemie Int. Ed.* 2006, 45 (36), 5978–5981. https://doi.org/10.1002/anie.200602255.

- (66) Xu, X.; Furukawa, T.; Okino, T.; Miyabe, H.; Takemoto, Y. Bifunctional-Thiourea-Catalyzed Diastereo- And Enantioselective Aza-Henry Reaction. *Chem. - A Eur. J.* 2005, 12 (2), 466–476. https://doi.org/10.1002/chem.200500735.
- (67) Xiong, Y.; Wang, F.; Huang, X.; Wen, Y.; Feng, X. A New Copper (I)-Tetrahydrosalen-Catab Zed Asymmetric Henry Reaction and Its Extension to the Synthesis of (S)-Norphenylephrine. *Chem. A Eur. J.* **2007**, *13* (3), 829–833. https://doi.org/10.1002/chem.200601262.
- (68) Blay, G.; Domingo, L. R.; Hernández-Olmos, V.; Pedro, J. R. New Highly Asymmetric Henry Reaction Catalyzed by CuII and a C1-Symmetric Aminopyridine Ligand, and Its Application to the Synthesis of Miconazole. *Chem. - A Eur. J.* 2008, 14 (15), 4725–4730. https://doi.org/10.1002/chem.200800069.
- (69) Xu, K.; Lai, G.; Zha, Z.; Pan, S.; Chen, H.; Wang, Z. A Highly Anti-Selective Asymmetric Henry Reaction Catalyzed by a Chiral Copper Complex: Applications to the Syntheses of (+)-Spisulosine and a Pyrroloisoquinoline Derivative. *Chem. A Eur. J.* **2012**, *18* (39), 12357–12362. https://doi.org/10.1002/chem.201201775.
- (70) Ballini, R.; Bosica, G. Nitroaldol Reaction in Aqueous Media: An Important Improvement of the Henry Reaction. *J. Org. Chem.* **1997**, 62 (2), 425–427. https://doi.org/10.1021/jo961201h.
- (71) Bekerle-Bogner, M.; Gruber-Khadjawi, M.; Wiltsche, H.; Wiedner, R.; Schwab, H.; Steiner, K. (R)-Selective Nitroaldol Reaction Catalyzed by Metal-Dependent Bacterial Hydroxynitrile Lyases. *ChemCatChem* **2016**, 8 (13), 2214–2216. https://doi.org/10.1002/cctc.201600150.

- (72) Fuhshuku, K. I.; Asano, Y. Synthesis of (R)-Beta-Nitro Alcohols Catalyzed by R-Selective Hydroxynitrile Lyase from Arabidopsis Thaliana in the Aqueous-Organic Biphasic System. *J. Biotechnol.* **2011**, *153* (3–4), 153–159. https://doi.org/10.1016/j.jbiotec.2011.03.011.
- (73) Ayon Chatterjee, D.H. Sreenivasa Rao, and S. K. P. One-Pot Enzyme Cascade Catalyzed Asymmetrization of Primary Alcohols: Synthesis of Enantiocomplementary Chiral β-Nitroalcohols. *Adv. Synth. Catal.* **2021**, *363* (23), 5310–5318. https://doi.org/10.1002/adsc.202100803.
- (74) Yuryev, R.; Briechle, S.; Gruber-Khadjawi, M.; Griengl, H.; Liese, A. Asymmetric Retro-Henry Reaction Catalyzed by Hydroxynitrile Lyase from Hevea Brasiliensis. *ChemCatChem* **2010**, 2 (8), 981–986. https://doi.org/10.1002/cctc.201000147.
- (75) Yuryev, R.; Purkarthofer, T.; Gruber, M.; Griengl, H.; Liese, A. Kinetic Studies of the Asymmetric Henry Reaction Catalyzed by Hydroxynitrile Lyase from Hevea Brasiliensis.

 *Biocatal.** Biotransformation** 2010, 28 (May), 348–356.

 https://doi.org/10.3109/10242422.2010.530661.
- (76) Rao, D. H. S.; Padhi, S. K. Production of (S)-β-Nitro Alcohols by Enantioselective C–C Bond Cleavage with an R-Selective Hydroxynitrile Lyase. *ChemBioChem* **2019**, *20* (3), 371–378. https://doi.org/10.1002/cbic.201800416.
- (77) Rao, D. H. S.; Shivani, K.; Padhi, S. K. Immobilized Arabidopsis Thaliana Hydroxynitrile Lyase-Catalyzed Retro-Henry Reaction in the Synthesis of (S)-β-Nitroalcohols. *Appl. Biochem. Biotechnol.* **2021**,*193* (2), 560–576. https://doi.org/10.1007/s12010-020-03442-3.
- (78) Heaney, F. *The Nitro Group in Organic Synthesis*; 2004; Vol. 2001. https://doi.org/10.1055/s-2001-18700.

- (79) Milner, S. E.; Moody, T. S.; Maguire, A. R. Biocatalytic Approaches to the Henry (Nitroaldol) Reaction. *European J. Org. Chem.* 2012, 3059–3067. https://doi.org/10.1002/ejoc.201101840.
- (80) Noland, W. E. The Nef Reaktion. Chem. Revs. 1955, 1899 (55), 137–155.
- (81) Ballini, R.; Petrini, M. Nitroalkanes as Key Building Blocks for the Synthesis of Heterocyclic Derivatives. *Arkivoc* **2009**, *2009* (9), 195–223. https://doi.org/10.3998/ark.5550190.0010.912.
- (82) Lednicer, D. *The Organic Chemistry of Drug Synthesis, Volume 7*; 2007. https://doi.org/10.1002/9780470180679.
- (83) Ager, D. J.; Prakash, I.; Schaad, D. R. 1,2-Amino Alcohols and Their Heterocyclic Derivatives as Chiral Auxiliaries in Asymmetric Synthesis. *Chem. Rev.* **1996**, *96* (2), 835–875. https://doi.org/10.1021/cr9500038.
- (84) Gupta, P.; Mahajan, N. Biocatalytic Approaches towards the Stereoselective Synthesis of Vicinal Amino Alcohols. *New J. Chem.* **2018**, *42* (15), 12296–12327. https://doi.org/10.1039/c8nj00485d.
- (85) Bobzin, S. C.; Faulkner, D. J. Diterpenes from the Pohnpeian Marine Sponge Chelonaplysilla Sp. J. Nat. Prod. 1991, 54 (1), 225–232. https://doi.org/10.1021/np50073a023.
- (86) Cheng, M. J.; Lee, K. H.; Tsai, I. L.; Chen, I. S. Two New Sesquiterpenoids and Anti-HIV Principles from the Root Bark of Zanthoxylum Ailanthoides. *Bioorganic Med. Chem.* **2005**, *13* (21), 5915–5920. https://doi.org/10.1016/j.bmc.2005.07.050.

- (87) Porciatti F, Cerbai E, Masini I, M. A. Electrophysiological Evaluation of the Beta-Blocking Properties and Direct Membrane Effects of l-Moprolol and Its Enantiomer d-Moprolol. *Arch. Int. Pharmacodyn. Ther* **1989**, 299, 200–209.
- (88) Dukes, M.; Smith, L. H. β-Adrenergic Blocking Agents. 9. Absolute Configuration of Propranolol and of a Number of Related Aryloxypropanolamines and Arylethanolamines. *J. Med. Chem.* 1971, 14 (4), 326–328. https://doi.org/10.1021/jm00286a013.
- (89) Nyrönen, T.; Pihlavisto, M.; Peltonen, J. M.; Hoffrén, A. M.; Varis, M.; Salminen, T.; Wurster, S.; Marjamäki, A.; Kanerva, L.; Katainen, E.; Laaksonen, L.; Savola, J. M.; Scheinin, M.; Johnson, M. S. Molecular Mechanism for Agonist-Promoted A2A-Adrenoceptor Activation by Norepinephrine and Epinephrine. *Mol. Pharmacol.* 2001, 59 (5), 1343–1354. https://doi.org/10.1124/mol.59.5.1343.
- (90) Refsum, P. M. T. and H. Class III Antiarrhythrnic Action Linked with Positive Inotropy: Effects of the d- and I-Isomer of Sotalol on Isolated Rat Atria at Threshold and Suprathreshold Stimulation. *Pharmacol. Toxicol.* **1988**, 62, 272–277.
- (91) Yadav, J. S.; Reddy, P. T.; Nanda, S.; Bhaskar Rao, A. Stereoselective Synthesis of (R)-(-)-Denopamine, (R)-(-)-Tembamide and (R)-(-)-Aegeline via Asymmetric Reduction of Azidoketones by Daucus Carota in Aqueous Medium. *Tetrahedron Asymmetry* 2002, 12 (24), 3381–3385. https://doi.org/10.1016/S0957-4166(02)00024-1.
- (92) Pessin, J. E.; Gitomer, W.; Oka, Y.; Oppenheimer, C. L.; Czech, M. P. β-Adrenergic Regulation of Insulin and Epidermal Growth Factor Receptors in Rat Adipocytes. *J. Biol. Chem.* **1983**, 258 (12), 7386–7394. https://doi.org/10.1016/s0021-9258(18)32191-4.
- (93) Procopiou, P. A.; Barrett, V. J.; Bevan, N. J.; Biggadike, K.; Box, P. C.; Butchers, P. R.;

- Coe, D. M.; Conroy, R.; Emmons, A.; Ford, A. J.; Holmes, D. S.; Horsley, H.; Kerr, F.; Li-Kwai-Cheung, A. M.; Looker, B. E.; Mann, I. S.; McLay, I. M.; Morrison, V. S.; Mutch, P. J.; Smith, C. E.; Tomlin, P. Synthesis and Structure-Activity Relationships of Long-Acting B2 Adrenergic Receptor Agonists Incorporating Metabolic Inactivation: An Antedrug Approach. *J. Med. Chem.* **2010**, *53* (11), 4522–4530. https://doi.org/10.1021/jm100326d.
- (94) Yuan, M. L.; Xie, J. H.; Yang, X. H.; Zhou, Q. L. Enantioselective Synthesis of Chiral 1,2-Amino Alcohols via Asymmetric Hydrogenation of α-Amino Ketones with Chiral Spiro Iridium Catalysts. *Synth.* 2014, 46 (21), 2910–2916. https://doi.org/10.1055/s-0034-1378891.
- (95) Yokoyama H, Yanagisawa T, T. N. Details of Mode and Mechanism of Action of Denopamine, a New Orally Active Cardiotonic Agent with Affinity for Beta 1-Receptors. *J. Cardiovasc. Pharmacol.* 1988, 12 (3), 323–331.
- (96) Cuadros, R.; Montejo De Garcini, E.; Wandosell, F.; Faircloth, G.; Fernández-Sousa, J. M.; Avila, J. The Marine Compound Spisulosine, an Inhibitor of Cell Proliferation, Promotes the Disassembly of Actin Stress Fibers. *Cancer Lett.* **2000**, *152* (1), 23–29. https://doi.org/10.1016/S0304-3835(99)00428-0.
- (97) Ma, G.; Bavadekar, S. A.; Davis, Y. M.; Lalchandani, S. G.; Nagmani, R.; Schaneberg, B. T.; Khan, I. A.; Feller, D. R. Pharmacological Effects of Ephedrine Alkaloids on Human A1- and A2-Adrenergic Receptor Subtypes. *J. Pharmacol. Exp. Ther.* 2007, 322 (1), 214–221. https://doi.org/10.1124/jpet.107.120709.
- (98) Optical, T.; Arnold, A.; Albertson, N. F.; McKay, F. C.; Lape, H. E.; Hoppe, J. O.; Selberts, W. H.; Arnold, A. Isomers of Metaraminol. Synthesis and Biological. *J. Med. Chem* **1970**,

- 951 (18), 132–134.
- (99) Jones, O. M.; Thompson, J. M.; Brading, A. F.; Mortensen, N. J. M. C. L-Erythro-Methoxamine Is More Potent than Phenylephrine in Effecting Contraction of Internal Anal Sphincter in Vitro. *Br. J. Surg.* **2003**, *90* (7), 872–876. https://doi.org/10.1002/bjs.4120.
- (100) Yunis, A. A. Chloramphenicol: Relation of Structure to Activity and Toxicity. *Annu. Rev. Pharmacol. Toxicol.* **1988**, 28, 83–100. https://doi.org/10.1146/annurev.pa.28.040188.000503.
- (101) Hashimoto, K.; Kumagai, N.; Shibasaki, M. Self-Assembled Asymmetric Catalyst Engaged in a Continuous-Flow Platform: An Anti -Selective Catalytic Asymmetric Nitroaldol Reaction. *Org. Lett.* **2014**, *16* (13), 3496–3499. https://doi.org/10.1021/ol501432h.
- (102) Rao, D. H. S.; Chatterjee, A.; Padhi, S. K. Biocatalytic Approaches for Enantio and Diastereoselective Synthesis of Chiral β-Nitroalcohols. *Org. Biomol. Chem.* **2021**, *19* (2), 322–337. https://doi.org/10.1039/d0ob02019b.
- (103) Mandana Gruber-Khadjawi, Thomas Purkarthofer, Wolfgang Skranc, and H. G. Hydroxynitrile Lyase-Catalyzed Enzymatic Nitroaldol (Henry) Reaction. Adv. Synth. Catal. 2007, 349, 1445–1450. https://doi.org/10.1002/adsc.200700064.
- (104) Bekerle-Bogner, M.; Gruber-Khadjawi, M.; Wiltsche, H.; Wiedner, R.; Schwab, H.; Steiner, K. (R)-Selective Nitroaldol Reaction Catalyzed by Metal-Dependent Bacterial Hydroxynitrile Lyases. *ChemCatChem* **2016**, 8 (13), 2214–2216. https://doi.org/10.1002/cctc.201600150.
- (105) Langermann, J. Von; Nedrud, D. M.; Kazlauskas, R. J. Increasing the Reaction Rate of

- Hydroxynitrile Lyase from Hevea Brasiliensis toward Mandelonitrile by Copying Active Site Residues from an Esterase That Accepts Aromatic Esters. *ChemBioChem* **2014**, *15*, 1931–1938. https://doi.org/10.1002/cbic.201402081.
- (106) Vishnu Priya, B.; Sreenivasa Rao, D. H.; Gilani, R.; Lata, S.; Rai, N.; Akif, M.; Kumar Padhi, S. Enzyme Engineering Improves Catalytic Efficiency and Enantioselectivity of Hydroxynitrile Lyase for Promiscuous Retro-Nitroaldolase Activity. *Bioorg. Chem.* **2022**, *120* (January), 105594. https://doi.org/10.1016/j.bioorg.2021.105594.
- (107) Nedrud, D. M.; Lin, H.; Lopez, G.; Padhi, S. K.; Legatt, G. A.; Kazlauskas, R. J. Uncovering Divergent Evolution of α/β-Hydrolases: A Surprising Residue Substitution Needed to Convert Hevea Brasiliensis Hydroxynitrile Lyase into an Esterase. *Chem. Sci.* **2014**, *5* (11), 4265–4277. https://doi.org/10.1039/c4sc01544d.
- (108) Devamani, T.; Rauwerdink, A. M.; Lunzer, M.; Jones, B. J.; Mooney, J. L.; Tan, M. A. O.; Zhang, Z. J.; Xu, J. H.; Dean, A. M.; Kazlauskas, R. J. Catalytic Promiscuity of Ancestral Esterases and Hydroxynitrile Lyases. *J. Am. Chem. Soc.* **2016**, *138* (3), 1046–1056. https://doi.org/10.1021/jacs.5b12209.
- (109) Jones, B. J.; Bata, Z.; Kazlauskas, R. J. Identical Active Sites in Hydroxynitrile Lyases Show Opposite Enantioselectivity and Reveal Possible Ancestral Mechanism. *ACS Catal.* 2017, 7 (6), 4221–4229. https://doi.org/10.1021/acscatal.7b01108.
- (110) Jones, B. J.; Evans, R. L.; Mylrea, N. J.; Chaudhury, D.; Luo, C.; Guan, B.; Pierce, C. T.; Gordon, W. R.; Wilmot, C. M.; Kazlauskas, R. J. Larger Active Site in an Ancestral Hydroxynitrile Lyase Increases Catalytically Promiscuous Esterase Activity. *PLoS One* **2020**, *15* (6), e0235341. https://doi.org/10.1371/journal.pone.0235341.

Chapter 2: AtHNL engineering to increase catalytic efficiency and enantioselectivity towards the promiscuous retro-nitroaldol reaction

2.1. Introduction

In recent years enzymes have been increasingly exploited in the green synthesis of non-natural molecules and for different abiological reactions, by virtue of their substrate and catalytic promiscuity¹. However, the catalytic efficiency of natural enzymes for promiscuous reactions are often found to be low. This has triggered the research for laboratory evolution of enzymes with improved catalytic properties. While design and engineering of enzymes for improved promiscuous catalytic activity can be facilitated with mechanistic understanding, in several cases, the mechanism of promiscuous catalytic activity is not well understood. Here we have tried to address a similar case of improvement of promiscuous retro-nitroaldolase activity of a hydroxynitrile lyase (HNL) by protein engineering and predicted its plausible catalytic mechanism.

HNLs in nature catalyze cyanogenesis of cyanohydrins^{2,3}. In vitro they carry out the reverse transformation of nucleophilic addition of cyanide to the carbonyl center in the synthesis of enantiopure cyanohydrins^{4,5}. A few of them show promiscuity in addition of nucleophiles other than cyanides, e.g., nitromethane leading to the stereoselective synthesis of nitroaldol reaction products, i.e., β -nitroalcohols⁶⁻¹⁰. Both the enantiopure cyanohydrins and β -nitroalcohols are important chiral synthons used in the preparation of pharmaceuticals, agrochemicals, and biologically active molecules. The reverse transformation of the above two synthetic reactions are cyanogenesis and retro-nitroaldol or retro-Henry reaction (**Scheme 2.1**). The latter is a synthetically important biotransformation, because a HNL catalyzed retro-nitroaldol reaction produces enantioenriched β -nitroalcohols having absolute configuration opposite to that of the stereopreference of the HNL¹¹⁻¹³. This approach enables the enzyme to produce opposite stereopreference products as compared to that it produces in the nitroaldol reaction and hence we

became interested on this reaction. Kinetic resolution, dynamic kinetic resolution are other biocatalytic approaches for synthesis of chiral β -nitroalcohols^{14–16}. As the retro-nitroaldol reaction is emerging as a new synthetic route to prepare enantiopure β -nitroalcohols, we aimed to improve the catalytic efficiency of AtHNL's retro-nitroaldolase activity by protein enginering.

Scheme 2.1: Retro-nitroaldol reaction (top), and conventional cyanogenesis (bottom) by AtHNL.

The catalytic efficiency of *At*HNL's promiscuous retro-nitroaldolase activity is reported to be 2571 min⁻¹.mM⁻¹¹¹. To improve it further, we engineered *At*HNL by altering residues in its binding site. In order to accomplish our objective, we docked both (*R*)-mandelonitrile (MN) and (*R*)-2-nitro-1-phenylethanol (NPE) into the active site of *At*HNL separately and identified three residues in the binding site (Phe82, Phe179, and Tyr14). Site saturation mutagenesis (SSM) was performed at positions Phe179, and Tyr14; while a smart library was created for Phe82 by replacing it with polar amino acids. The resulting variants were quantified in a spectrophotometer for the retro-nitroaldol reaction using cleavage of racemic NPE to benzaldehyde. The NPE cleavage study uncovered nearly a dozen of variants in the Phe179 and Tyr14 series that exhibited more than a two-fold increase in the promiscuous retro-nitroaldolase activity than the wild type (WT). The variants showing higher retro-nitroaldolase activity than the WT were kinetically characterized. Selected

variants were explored for enantioselective preparation of (S)-NPE. Overall, this study has produced variants with higher catalytic efficiency for retro-nitroaldol reaction, and higher enantioselectivity (E value) in (S)-NPE production compared to the WT. It also resulted in more than half a dozen of synthetically useful variants showing >99% ee in the preparation of (S)-NPE. Additionally, molecular docking and molecular dynamics simulations investigations showed a better binding and orientation of the substrate in the active site of F179N mutant, which may attribute towards the higher catalytic efficiency observed in F179N.

2.2. Objectives

- 1. To investigate, identify binding site residues and carry out protein engineering.
- 2. To screen AtHNL variants towards retro-nitroaldolase activity.
- 3. To prepare (S)- β nitroalcohol using engineered AtHNL variants.
- 4. To study and understand the binding site of AtHNL towards the retro-nitroaldolase activity using in-silico studies.
- 5. To carry out preparative scale synthesis of (S)- β nitroalcohol by retro-nitroaldol reaction using engineered AtHNL.

2.3. Materials and methods

2.3.1. Chemicals and materials

AtHNL (UniProt accession ID: Q9LFT6) synthetic gene cloned in pET28a was procured from Abgenex Pvt. Ltd, India. Culture media and kanamycin were purchased from HiMedia laboratory Pvt. Ltd, India. Isopropyl-β-D-1-thiogalactopyranoside (IPTG) was obtained from BR-BIOCHEM Pvt. Ltd, India. Aldehydes, nitromethane and mandelonitrile were procured from Sigma Aldrich,

AVRA, SRL and Alfa-Aesar. HPLC grade solvents were obtained from RANKEM, Molychem, FINAR, and SRL.

2.3.2. Primers employed in this work

Primers were synthesized by Eurofins Genomics India Pvt. Ltd., Hyderabad, India (Table 2.1).

Table 2.1: List of Primers used in this study. Italicized nucleotides are the site of mutation.

Name	Sequence
F82A- FP	GTTGGTTTCAGC GCG GGTGGCATCAAC
F82A- RP	GTTGATGCCACC <i>CGC</i> GCTGAAACCAAC
F179A- FP	GTCAAGGCAGC GCG TTTACCGAGGAT
F179A- RP	ATCCTCGGTAAA <i>CGC</i> GCTGCCTTGAC
F179N-FP	GTCAAGGCAGC <i>AAC</i> TTTACCGAGGAT
F179N-RP	ATCCTCGGTAAA <i>GTT</i> GCTGCCTTGAC
F82MVK-FP	GTTGGTTTCAGC <i>MVK</i> GGTGGCATCAAC
F82MBK-RP	GTTGATGCCACC <i>MBK</i> GCTGAAACCAAC
Y14NNK-FP	TTCATAATGCG <i>NNK</i> CACGGTGCGTG
Y14MNN-RP	CACGCACCGTG <i>MNN</i> CGCATTATGAA
F179NNK-FP	GTCAAGGCAGC <i>NNK</i> TTTACCGAGGAT
F179MNN-RP	ATCCTCGGTAAA <i>MNN</i> GCTGCCTTGAC

2.3.3. Mutagenesis

Site directed (SDM) and site saturation mutagenesis (SSM) was done by PCR using mutagenic primers (**Table 2.1**) and pET28a-*At*HNL plasmid as the template.

2.3.3.1. Creation of *At*HNL variants (F82A, F179A)

A 25 μ L PCR mixture typically contained ~100 ng DNA template, 0.5 μ M of each of forward and reverse primers (**Table 2.1**), 5× PCR buffer (1x final concentration), 200 μ M dNTPs, 3% v/v of

DMSO, 0.25 μL *Pfu* polymerase, and PCR grade nuclease free water. The thermocycling program for plasmid amplification was 98 °C for 1 min, 20 cycles of 98 °C for 30 s, 60 °C for 30 s and 72 °C for 3 min, with a final extension at 72 °C for 10 min. After the reaction, a 5 μL of PCR product was run on an 1% agarose gel to check for the amplification and remaining 20 μL product was digested with DpnI (0.5 μL) along with 2 μL of CutSmart buffer to remove the methylated parental strand. Subsequently, transformed into *E. coli* DH5α competent cells and spread on an LB-media-plate containing 50 μg/mL kanamycin, incubated at 37 °C overnight. Colonies from the LB+ kanamycin plate were grown; plasmids were extracted and sent for DNA sequencing until all the mutants were confirmed. The mutant plasmids were successively transformed in *E. coli* BL21 (DE3) for protein expression.

2.3.3.2. Creation of SSM library at F82, F179, and Y14

The PCR composition and conditions are same as described in **2.3.3.1** section above. For SSM, degenerate codons were kept in the sequence whose details are mentioned in **Table 2.1**. After the reaction, the remaining protocols for DpnI digestion, transformation, plasmid purification and sequencing are same as described in **2.3.3.1** section.

2.3.3.3. Creation of *At*HNL double variants

To prepare F82A-F179N, PCR composition and conditions were maintained similar to that described in **2.3.3.1** section, except F82A plasmid was taken as template and forward and reverse primers for F179N (**Table 2.1**) were used in the PCR. To prepare F82A-F179W, and F82A-F179V, we used F179W and F179V plasmids respectively as templates along with F82A forward and reverse primers in the PCR.

2.3.4. Enzyme purification

Firstly, E. coli BL21 (DE3) cells carrying the recombinant plasmid were cultivated in 20 mL of LB medium containing kanamycin (50 µg mL⁻¹) at 37 °C and 180 rpm for 12 h. The overnight culture was inoculated into 2 L LB medium and grown at 37 °C until the culture's optical density (OD_{600}) reached 0.5 - 0.8 which was then induced with 0.5 mM IPTG and grown at 30 °C for an additional 6 h. The cells were harvested by centrifugation (8000 rpm, 10 min) at 4 °C and the pellet was suspended in 20 mM potassium phosphate buffer (KPB), pH 7.0. The cells were lysed by ultrasonication in an ice bath, and the supernatant was collected by centrifugation at 10,000 rpm for 45 min at 4 °C. Further, all the protein purification steps were done at 4°C. The supernatant was loaded onto a standard Ni-NTA affinity column. The column was sequentially washed and equilibrated with binding buffer [20 mM imidazole, 300 mM sodium chloride, 20 mM KPB (pH 7.0)] and wash buffer [50 mM imidazole, 300 mM sodium chloride, 20 mM KPB (pH 7.0)] and subsequently eluted with 500 mM imidazole, 300 mM sodium chloride, 20 mM KPB (pH 7.0)]. The eluted protein was dialyzed in 20 mM KPB for 3 h thrice and then concentrated using Amicon® Ultra-0.5 centrifugal filters with a molecular weight cut-off (MWCO) of 10 kDa. The protein fraction thus obtained were analysed by SDS-PAGE and the protein concentration was measured using nanodrop.

2.3.5. CD spectroscopy measurements

The secondary structure and conformational changes of the *At*HNL variants were compared with that of the wild type by Circular Dichroism (CD) spectrometry. CD measurements were carried out on a Jasco J-810 spectropolarimeter (JAPAN) using a quartz cell with a path length of 0.2 cm in a nitrogen atmosphere. A concentration of 1 mg/mL of each protein dissolved in 20 mM KPB, pH 7.0 was used for the analysis in a final volume of 500 μL. The spectra were recorded at 25°C

in the range of 190 to 300 nm with an accumulation of three scans and the scan speed is 50 nm per minute. For all spectra, 20 mM KPB buffer was used as the control and the baseline was subtracted using it. Finally, the CD spectra data collected were deconvoluted using CDNN 2.1 software to get the percentages of secondary structural elements.

2.3.6. Cyanogenesis and retro-nitroaldolase activity of AtHNL and its variants

The assay was performed in a 96 well microtiter plate and was monitored using a Multiskan GO UV–Visible spectrophotometer at 25°C. Each well of it contained reaction mixture of 160 μ L 50 mM citrate phosphate buffer (pH 5.5), 20 μ L purified enzyme (1 mg/mL) and 20 μ L substrate [racemic mandelonitrile (MN), 67 mM / racemic 2-nitro-1-phenylethanol (NPE), 20 mM] predissolved in 1 mL of 5 mM citrate buffer pH 3.15 making a total volume of 200 μ L. Control experiment was carried out in an identical manner except the enzyme replaced with 20 mM KPB, pH 7.0. The assay was done in triplicates and the absorbance of the control resulted due to spontaneous reaction was subtracted from the enzymatic reaction. The assay measured the formation of benzaldehyde resulted by enzymatic cleavage of MN or NPE at 280 nm. The activity was calculated using molar extinction coefficient of benzaldehyde (1376 M⁻¹ cm⁻¹). We did not check F82H and F82N due to continuous negative results from the F82 series.

2.3.7. Determination of kinetic parameters of AtHNL variants for cyanogenesis and retronitroaldol reaction

The kinetic parameters were determined by measuring the initial rate of enzymatic reaction at different substrate (racemic MN/ NPE) concentrations (0.0125 – 12 mM) using 1 mg/mL of enzyme. The reaction mixture contained 160 μ L of 50 mM citrate phosphate buffer (pH 5.5), 20 μ L purified enzyme (1 mg/mL) and 20 μ L of racemic MN/NPE (0.0125 – 12 mM) pre-dissolved in 1 mL of 5 mM citrate buffer (pH 3.15) making a total volume of 200 μ L. The reaction rate was

measured at 280 nm in a UV-Visible spectrophotometer. Each reaction was done in triplicates and activity was measured every 10 seconds till 1 minute and the activity at one minute was used to plot the kinetic curve. Solver function in Microsoft excel was used to best fit the data to Michaelis – Menten equation.

2.3.8. Synthesis of racemic NPE

Racemic NPE was synthesized by a protocol already used in our laboratory¹¹.

2.3.9. At HNL variant catalyzed preparation of (S)- β -nitroalcohol using retro-nitroaldol reaction

A reaction mixture of 3 mg of purified AtHNL variant in 20 mM KPB pH 7, 2 µmol of racemic NPE, 17.5% v/v of 50 mM citrate phosphate buffer pH 5.5, and 65% v/v of toluene was taken in a 1.5 mL microcentrifuge tube. The reaction mixture was shaken at 1200 rpm, 30 °C in an incubator shaker up to 3 h. A 50 µL of aliquot was taken from the reaction mixture (after vigorous shaking) and added to 150 μL of hexane:2-propanol = 9:1, centrifuged at 15,000×g, 4 °C for 5 min. From the upper organic layer, a 20 µL was taken in a syringe and analyzed in a HPLC (Agilent) using Chiralpak® IB chiral column. HPLC conditions: n-hexane: 2-propanol = 90:10 (v/v); flow rate: 1 mL/min; absorbance: 210 nm. The retention times of benzaldehyde, (R)-NPE, and (S)-NPE are 4.6, 10.5, and 11.4 min respectively. The % conversion representing the absolute amount of (S)-NPE was calculated by the equation $^{[a]}c = [\frac{S-NPE}{S-NPE+R-NPE+benzaldehyde}]$. Sih's equation $E = \frac{\ln [(1-c)(1-ee)]}{\ln [(1-c)(1+ee)]}$ was used to calculate the E values¹⁷. The c, and ee used in the Sih's equation were determined as follows: % $c = [1 - \frac{R+S}{R0+S0}]*100$. R: % area of (R)-NPE after reaction, S: % area of (S)-NPE after reaction; Ro: % area of (R)-NPE before reaction, So: % area of (S)-NPE before reaction. % $ee = [\frac{(S-R)}{(S+R)}]*100$.

2.3.10. Computational details

2.3.10.1. Molecular docking studies

Molecular docking of wildtype AtHNL with (R)-MN and (R)-NPE was performed. Also, molecular docking was done between the substrate (R)-NPE and AtHNL mutants: F82A, F179A, F82A-F179N using MGL tool Autodock 4.2 tools¹⁸. Briefly, we removed the crystal water molecules from the native AtHNL coordinate (PDB ID 3DQZ). The polar hydrogen atoms and Kollman charges were added to proteins and Gasteiger charges were assigned to the substrate, NPE. The grid box of size 40 Å × 40 Å ×54 Å in X, Y, Z coordinates was selected to cover the protein-substrate active area. Lamarckian Genetic Algorithm was used for protein-substrate flexible docking, which was set to 10 LGA runs with a population size of 150 and total 27000 generations. After successful completion of runs, the lowest binding free energy complex having best docking conformation were analyzed for further interaction studies.

2.3.10.2. Molecular dynamic simulations

To analyze the structural stability of the complex, Molecular Dynamics Simulations was performed using GROMACS 5.1.4^{19,20}. PRODRG2 server was used for generating the topology files of substrate, which uses GROMOS96 45a3 force field^{19,21}. The SPC water model was implemented for water molecules. The protein- substrate complex was capped with cubic box incorporating water molecules which was placed at 1.0 nm to the box of the wall from the surface of the protein. Further counter ions were added to neutralize the system. Then the whole system was minimized using steepest descent algorithm for 20, 000 steps until the largest force acting in the system was smaller than 1,000 kJ/mol/nm. Then the system was equilibrated for two phases of equilibration, namely NVT and NPT ensemble. NVT ensemble was used at 300 K for 50 ps using a modified V-rescale Berendsen thermostat with a time constant of 0.1 ps, followed by NPT

ensemble to 1 atm using Parinello Rahman coupling method with a time constant of 2 ps for 50 ps. Then the equilibrated complex was kept for production run for 50 ns at 300 K. The long range electrostatics was controlled using Particle Mesh Ewald method with a space cut off of 10 Å. Constraints were implemented for hydrogen bonds using P-LINCS algorithm²². Whole analysis was done using the frames from the production run (10000 for 300 K). g_rms, and g_rmsf, function of GROMACS were used for trajectory analysis. Figures were generated using XMGRACE and GNUPLOT.

2.3.10.3. Binding free energy calculations

Molecular Mechanics Poisson Boltzmann Surface Area (MMPBSA) was used to calculate the binding free energy of substrate complex with WT and mutant proteins from the snapshots of MD trajectories using g_mmpbsa tool of GROMACS²³. Particularly, the binding free energy of ligand-protein complex in the solvent was expressed as:

$$\Delta G_{binding} = G_{complex} - (G_{protein} + G_{ligand})$$

where $G_{complex}$ is the total free energy of the protein-ligand complex, $G_{protein}$ and G_{ligand} are total energy of separated protein and ligand in solvent, respectively. The free energy for each individual $G_{complex}$, $G_{protein}$ and G_{ligand} were estimated by:

$$G_X = E_{mm} + G_{solvation}$$

where x is the protein, ligand, or complex. E_{mm} is the average molecular mechanics potential energy in vacuum and $G_{solvation}$ is free energy of solvation. The molecular mechanics potential energy was calculated in vacuum as following:

$$E_{mm} = E_{bonded} + E_{non-bonded} = E_{bonded} + (E_{vdw} + E_{elec})$$

where E_{bonded} is bonded interaction including of bond, angle, dihedral and improper interactions and $E_{non-bonded}$ is non-bonded interactions consisting of van der Waals (E_{vdw}) and electrostatic (E_{elec}) interactions. ΔE_{bonded} is always taken as zero.

The solvation free energy ($G_{solvation}$) was estimated as the sum of electrostatic solvation free energy (G_{polar}) and apolar solvation free energy ($G_{non-polar}$):

$$G_{solvation} = G_{polar} + G_{non-polar}$$

where G_{polar} was computed using the Poisson-Boltzmann (PB) equation and $G_{non-polar}$ estimated from the solvent-accessible surface area (SASA) as equation following:

$$G_{nonpolar} = \gamma SASA + b$$

where γ is a coefficient related to surface tension of the solvent and b is fitting parameter. The values of the constant are as follows:

$$\gamma = 0.02267 \text{ kJ/mol/Å}^2 \text{ or } 0.0054 \text{ kcal/mol/Å}^2$$

b = 3.849 kJ/mol or 0.916 kcal/mol.

2.3.11. Preparative scale synthesis of (S)-NPE

AtHNL-F179N catalyzed preparative scale synthesis of (S)-NPE was carried out using crude cell lysates.

2.3.11.1. Optimization of biocatalytic parameters for preparative scale synthesis of (S)-NPE

In a first set of experiments, the enzyme amount and time of biotransformation was optimized. Four reaction mixtures, each containing 4 µmol of racemic NPE, 50 mM citrate phosphate buffer pH 5.5, 65% v/v of toluene and F179N cell lysate (133 U, 200 U, 266 U and 400 U), were taken in a 5 mL microcentrifuge tube. Each reaction mixture was shaken at 1200 rpm, 30 °C in an incubator shaker and aliquots were taken at different time points i.e., 3, 6, 9, 12 and 24 h. In a second set of experiments, the above reaction conditions were maintained using 200 U of F179N

cell lysate, while the % v/v of toluene was varied as 65, 60, and 50; and aliquots were taken at different time points, i.e., 3, 4, 5, and 6 h. In a subsequent set of experiments, the % v/v of toluene was varied as 65, 70, and 75; and aliquots were taken at different time points i.e., 2, 3, and 4 h. Extraction and HPLC analysis of the product was done similar to the protocol that was described in section 2.3.9.

2.3.11.2. Preparative scale synthesis

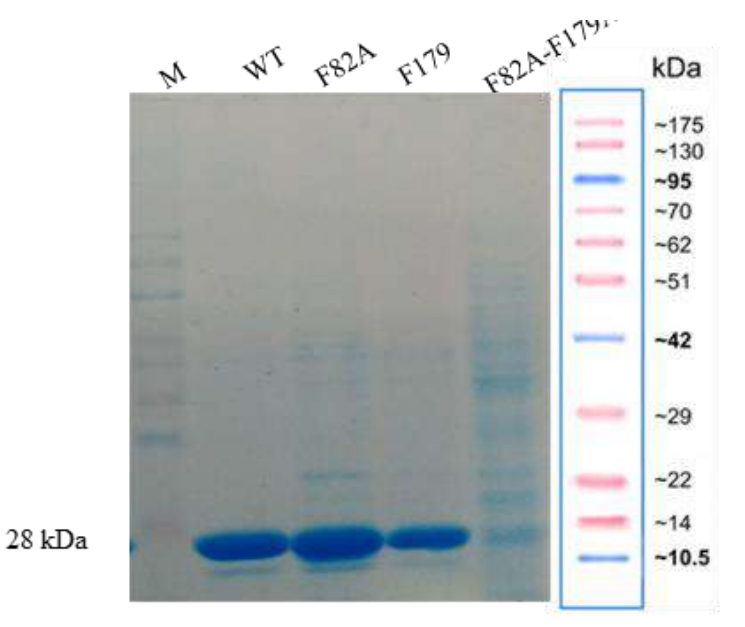
Ten mini preparative scale reactions each containing 1000 U (1.1 mL) of *At*HNL-F179N cell lysate, 1.1 mL of 50 mM citrate phosphate buffer pH 5.5, 20 µmol of racemic NPE, and 65% v/v of toluene (4.1 mL) were taken in a 50 mL round bottom flask, stirred in a magnetic stirrer at 1200 rpm, 30 °C. At the end of 3 h, each reaction mixture was extracted with 100 mL of diethyl ether, the organic layers collected were combined, dried over anhydrous sodium sulphate and solvents were evaporated in a rotary evaporator. The product was analyzed by chiral HPLC as per 2.3.9 section. Column purification of the crude product was done using hexane: ethyl acetate (90:10) to get pure NPE.

2.4. Results

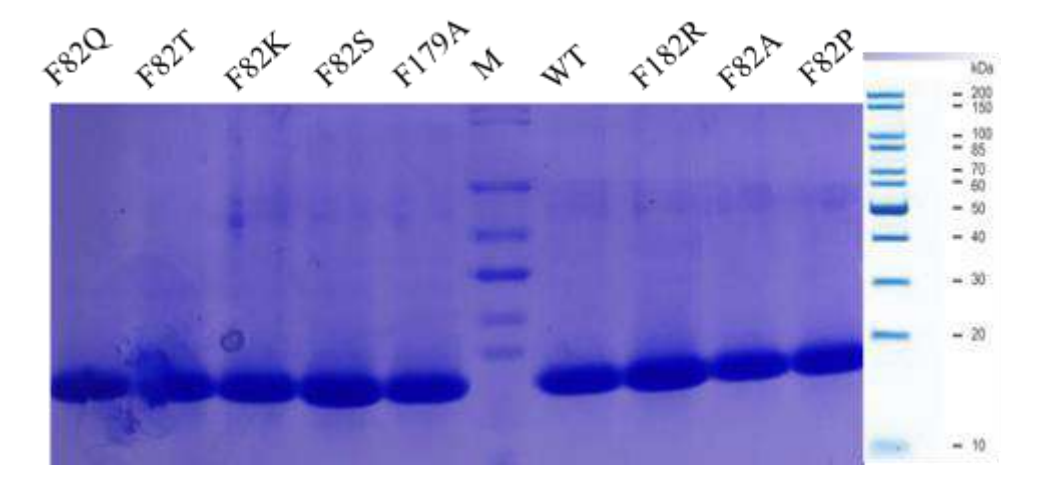
2.4.1. SDS-PAGE of purified AtHNL and its variants

The wild type *At*HNL and its variants generated using SDM and SSM were purified as described in section **2.3.4** above and were characterized by SDS-PAGE (**Figure 2.1**). All the pure proteins were analyzed by 12% SDS-PAGE using medium range pre-stained protein marker (BR-BIOCHEM) and stained by Coomassie Brilliant Blue R-250. A clear band at ~28 kDa indicated the good expression and purity of the purified *At*HNL and its variants.

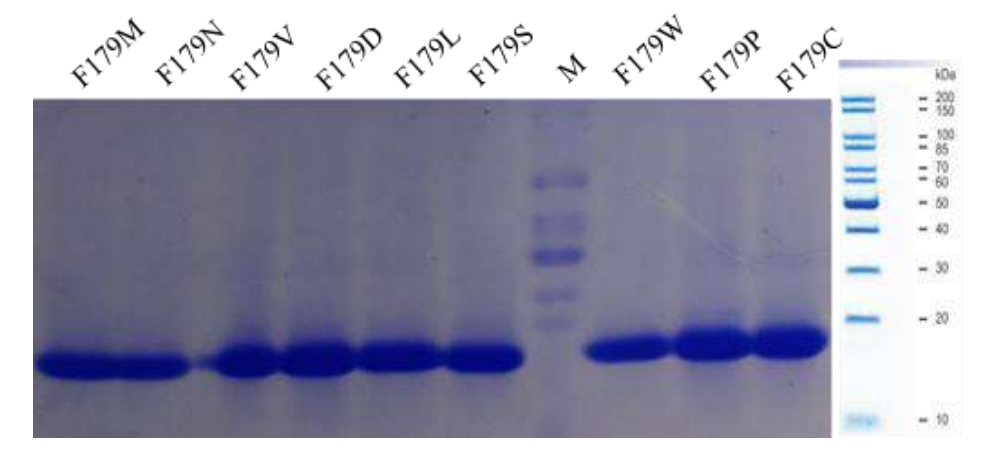


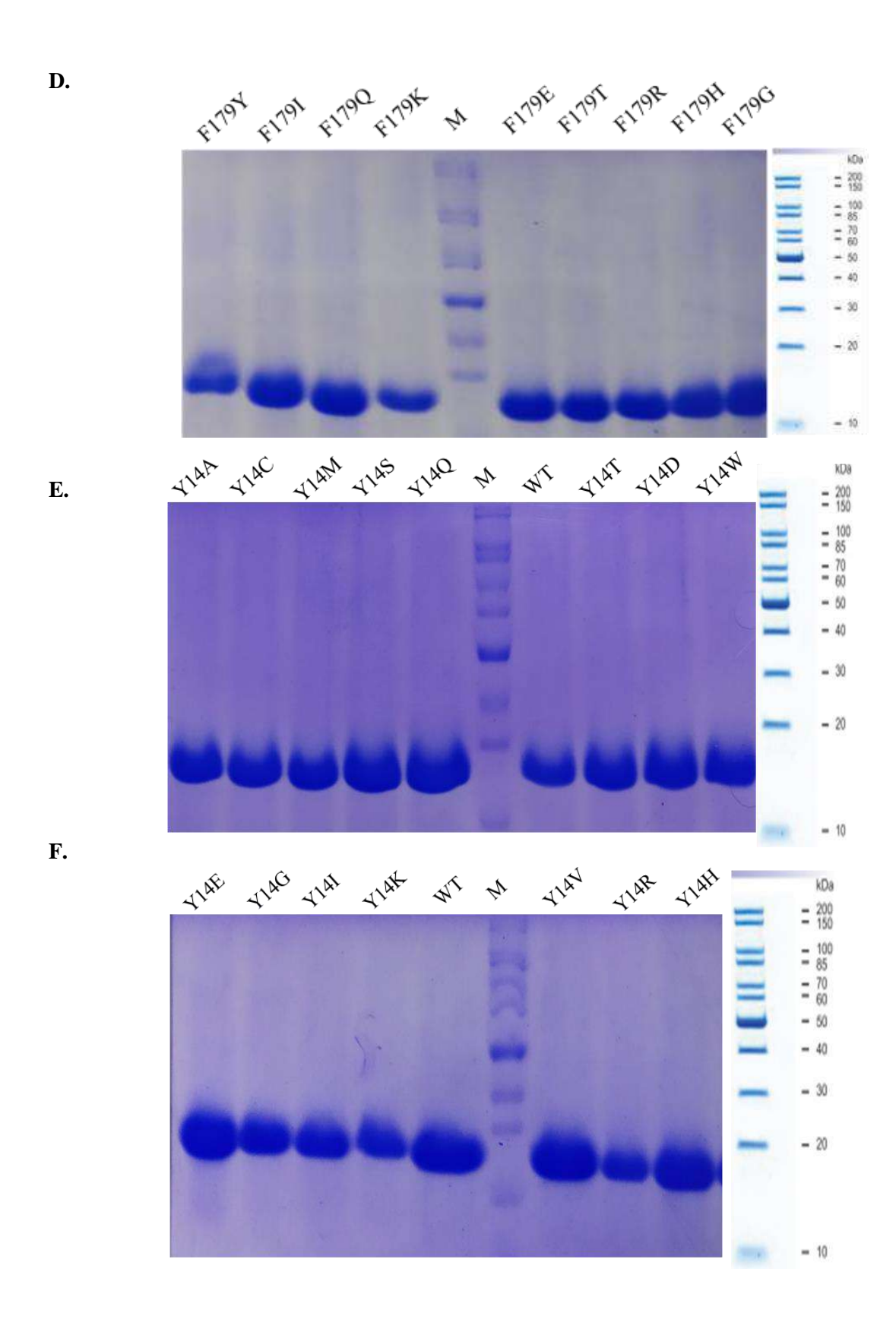


B.



C.





G.

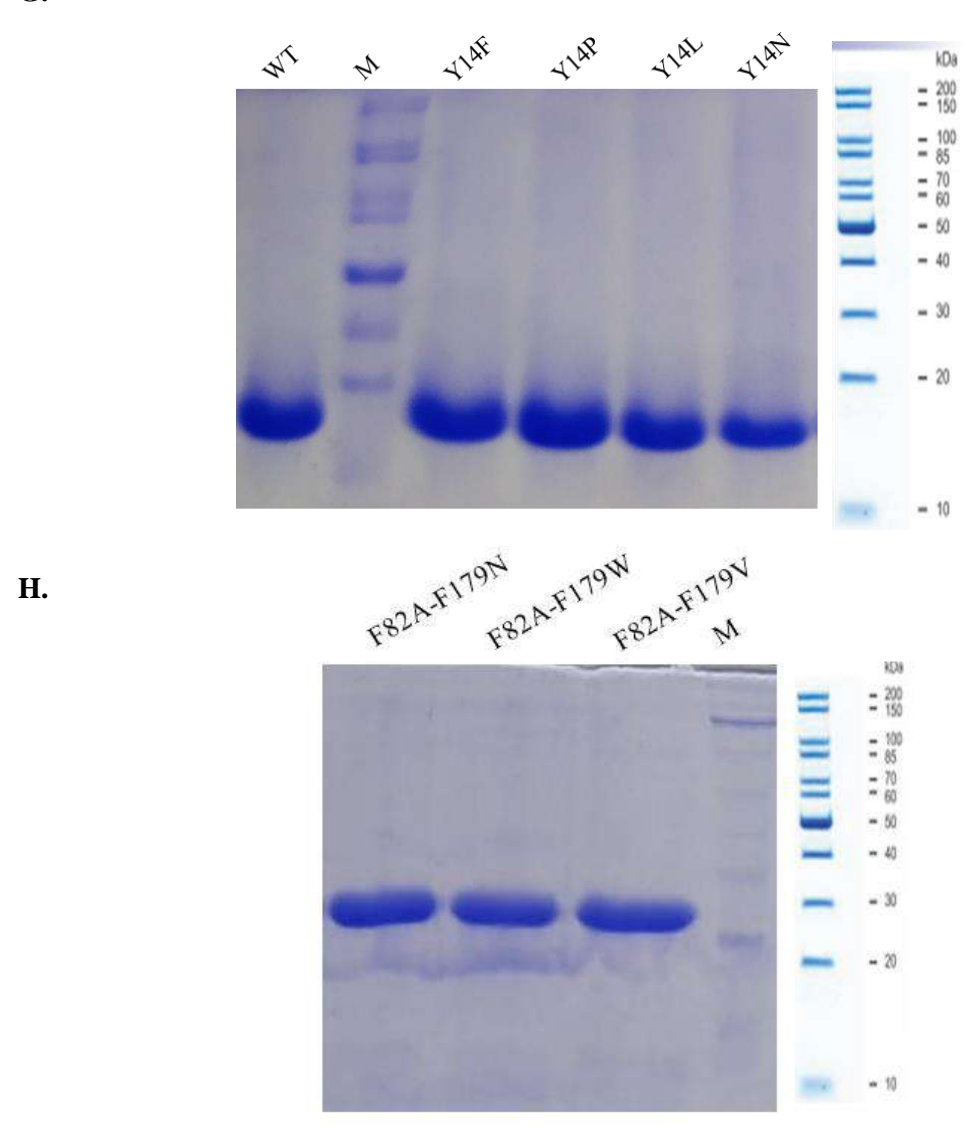


Figure 2.1 (A-H): SDS-PAGE analysis of Ni-NTA purified *At*HNL and its variants. Lane M: standard protein marker.

2.4.2. Steady state kinetics of AtHNL toward cyanogenesis and retro-nitroaldol reaction

The kinetic parameters of AtHNL were determined using rac-MN cleavage assay. From the Michaelis-Menten plot (**Figure 2.2**) the kinetic parameters towards cyanogenesis were found to be, $K_{\rm M}$: 1.66 ± 0.34 mM, $k_{\rm cat}$: 3797.92 ± 556.20 min⁻¹, $k_{\rm cat}$ / $K_{\rm M}$: 2772.20 ± 217.40 min⁻¹ mM⁻¹ and

 V_{max} : 149.90 ±19.86 U/mg (**Table 2.3**). Similarly, kinetic parameters of AtHNL were determined for the promiscuous retro-nitroaldol reaction using substrate rac-NPE. The Michaelis-Menten plot (**Figure 2.3**) was prepared by using NPE cleavage. The kinetic parameters were found to be K_{M} : 0.015±0.01 mM, k_{cat} : 49.0± 0.56 min⁻¹, k_{cat} / K_{M} : 3614.10± 1762.03 min⁻¹ mM⁻¹ and V_{max} : 1.75± 0.02 U/mg (**Table 2.3**).

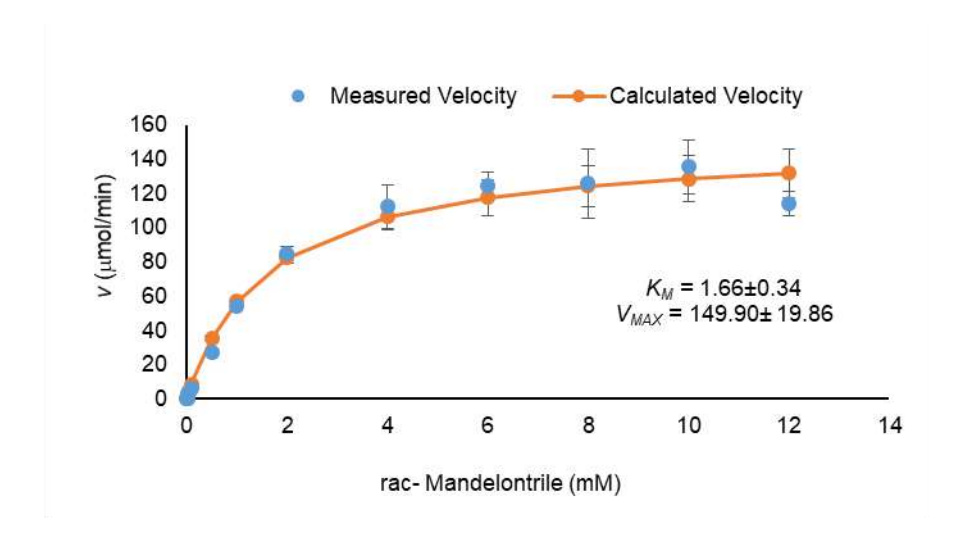


Figure 2.2: Michaelis-Menten curve for wild type AtHNL with rac-MN as substrate.

The reaction mixture contained 160 μ L of 50 mM citrate phosphate buffer (pH 5.5), 20 μ L purified enzyme (1 mg/mL) and 20 μ L substrate (0.0125 – 12 mM) pre-dissolved in 1 mL of 5 mM citrate buffer (pH 3.15) making a total volume of 200 μ L. The reaction rate was measured at 280 nm using a Multiskan GO UV–Visible spectrophotometer. Solver function in Microsoft excel was used to best fit the data to Michaelis – Menten equation.

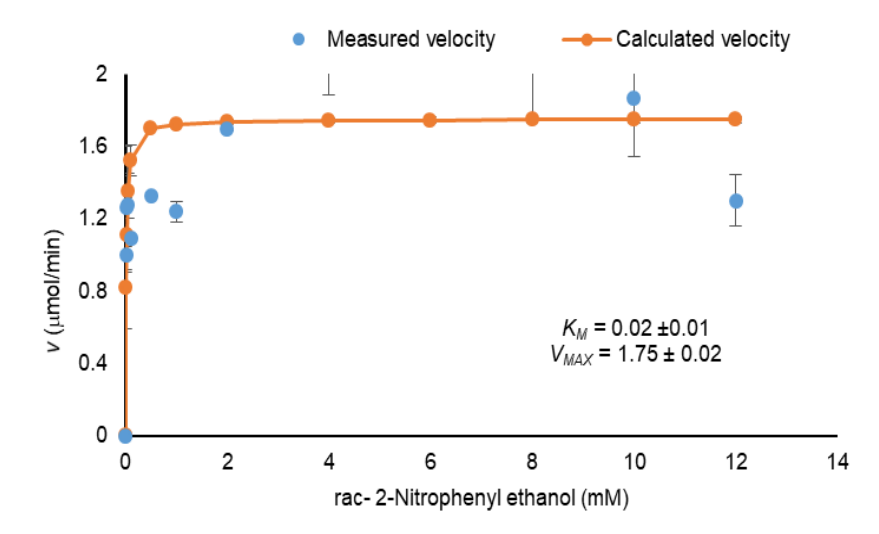


Figure 2.3: Michaelis-Menten curve for wild type AtHNL with rac- NPE as substrate.

The reaction composition and conditions are same as mentioned in **Figure 2.2** caption, except the substrate MN is replaced by NPE.

2.4.3. CD spectroscopy measurements of AtHNL and its variants (F82A, F179A and F179A - F179A)

The structural integrity of F82A, F179A, and F82A-F179A in comparison with the wild type was studied using circular dichroism (CD) spectroscopy. It was observed that the CD spectra of F82A and F179A are similar to that of WT (**Figure 2.4**). In the case of F82A-F179A, there was a gradual decrease in its CD signal (**Figure 2.4**). Using CDNN software, the percentage of secondary structures of the wild type and the variants was quantified (**Table 2.2**).

Table 2.2: The percentage of α-helix of WT, F82A, F179A and, F82A-F179A.

Enzyme	α-Helix (%)	β-Sheets (%)	Random coils (%)
WT	34.97±1.21	12.90±1.50	52.13±2.70
F82A	24.50±3.10	23.83±2.81	51.67±3.43
F179A	29.72±2.20	17.47±0.38	49.73±4.25
F82A-F179A	18.05±3.60	35.40±6.10	46.55±2.50

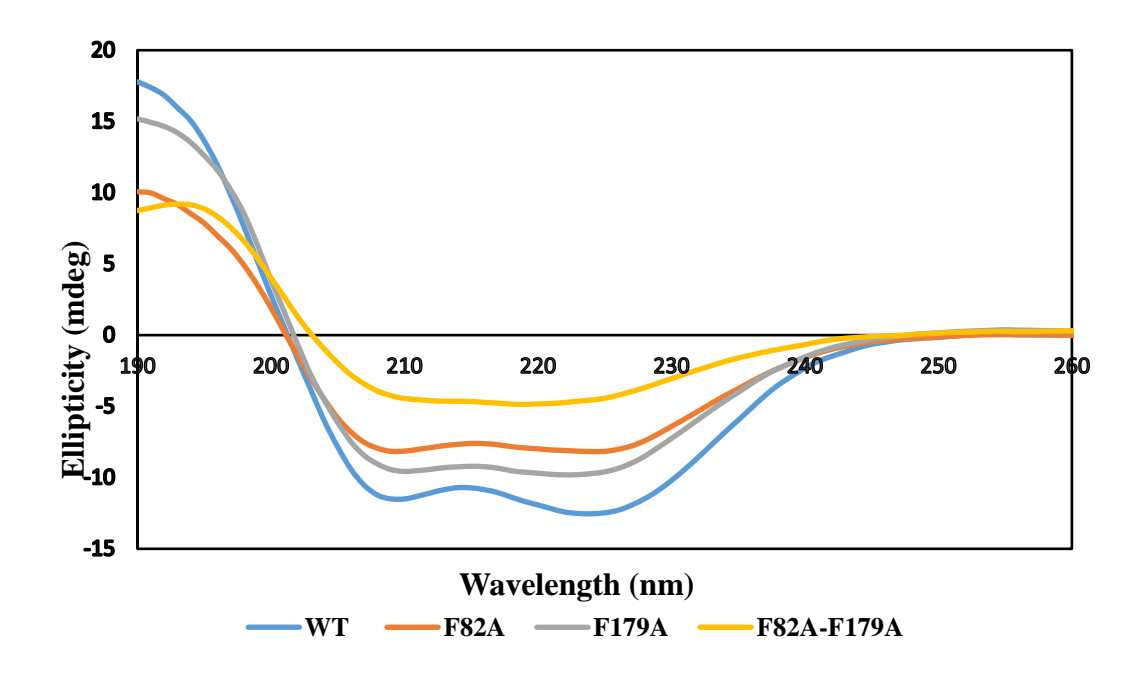


Figure 2.4: Comparison of CD spectra of wild type *At*HNL with variants F82A, F179A and F82A-F179A.

2.4.4. Steady state kinetics of AtHNL-F82A and AtHNL-F179A variants towards cyanogenesis and retro-nitroaldol reaction

Kinetic studies of F82A and F179A variants were performed using cleavage of racemic MN (**Figure 2.5** and **Figure 2.6**) and NPE (**Figure 2.7** and **Figure 2.8**) separately in comparison with the wild type which are shown in **Table 2.3**.

Table 2.3: Kinetic parameters of wild type *At*HNL and variants using MN and NPE in cyanogenesis and retro-nitroaldol reaction, respectively.

Enz	MN			NPE			Selectivity ^[a]		
	K_m (mM)	V_{max}	$k_{\rm cat}$	k_{cat}/K_m	K_m (mM)	V_{max}	$k_{\rm cat}$	k_{cat}/K_m	
		(U/mg)	(\min^{-1})	$(min^{-1}mM^{-1})$		(U/mg)	(\min^{-1})	$(min^{-1}mM^{-1})$	
WT	1.66 ± 0.34	149.90	$3797.92 \pm$	$2772.20\pm$	0.015 ± 0.01	$1.75\pm$	$49.0 \pm$	3614.10±	1.3
		± 19.86	556.20	217.40		0.02	0.56	1762.03	
F82A	1.84 ± 0.10	120.98	$3488.52 \pm$	$1732.14\pm$	$0.01\pm3\times10^{-4}$	$0.97 \pm$	$27.10 \pm$	$2925.80\pm$	1.69
		± 0.98	27.32	79.01		0.03	0.79	1.41	
F179A	10.10 ± 5.51	36.48	$1021.38 \pm$	$101.22\pm$	0.03 ± 0.01	$1.30 \pm$	$36.44 \pm$	$1250.92 \pm$	12.36
		± 11.60	325.00	18.28		0.04	1.13	208.10	

[a]Selectivity=[$(k_{cat}/K_m)_{NPE}$ / $(k_{cat}/K_m)_{MN}$], i.e., retro-nitroaldol /cyanogenesis. The kinetic parameters were determined as per **section 2.3.7**. The data are mean \pm standard deviation.

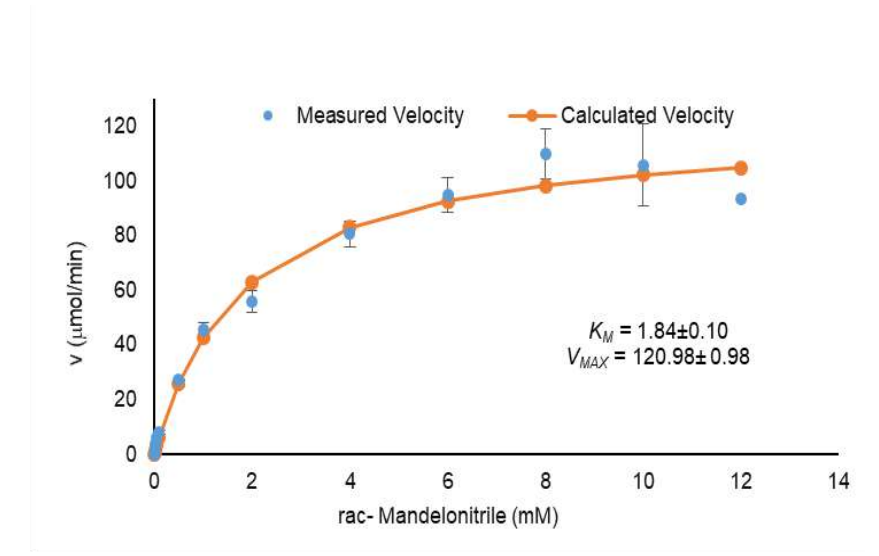


Figure 2.5: Michaelis-Menten curve for F82A variant with rac-MN as substrate.

The reaction composition and conditions are same as mentioned in **Figure 2.2** caption, except the wild type AtHNL is replaced by its variant F82A.

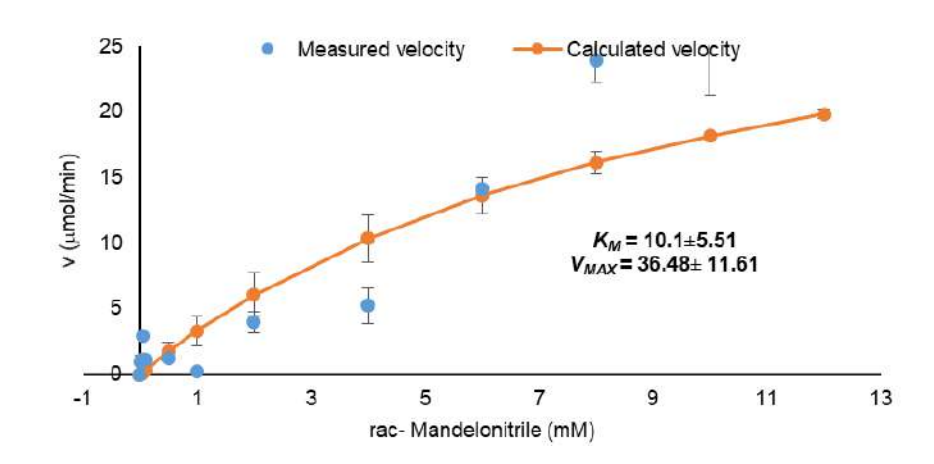


Figure 2.6: Michaelis-Menten curve for F179A variant with rac-MN as substrate.

The reaction composition and conditions are same as mentioned in **Figure 2.2** caption, except the wild type *At*HNL is replaced by its variant F179A.

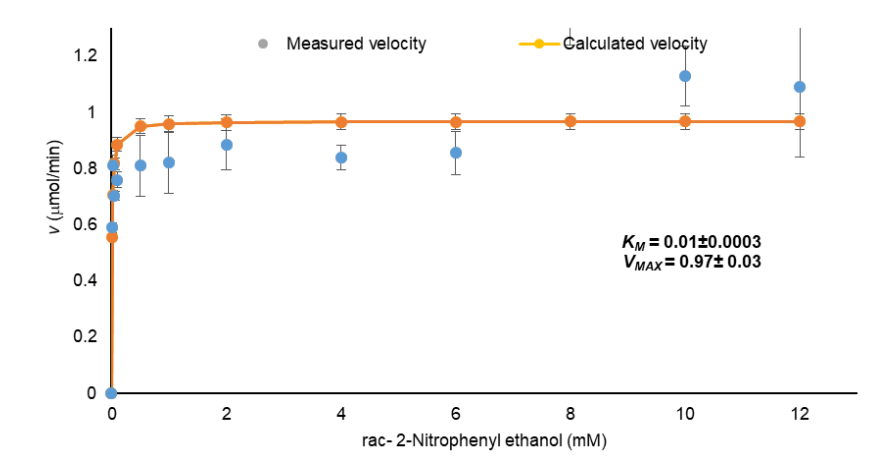


Figure 2.7: Michaelis-Menten curve for F82A variant with rac-NPE as substrate.

The reaction composition and conditions are same as mentioned in **Figure 2.2** caption, except the wild type AtHNL is replaced by its variant F82A and the substrate MN is replaced by NPE.

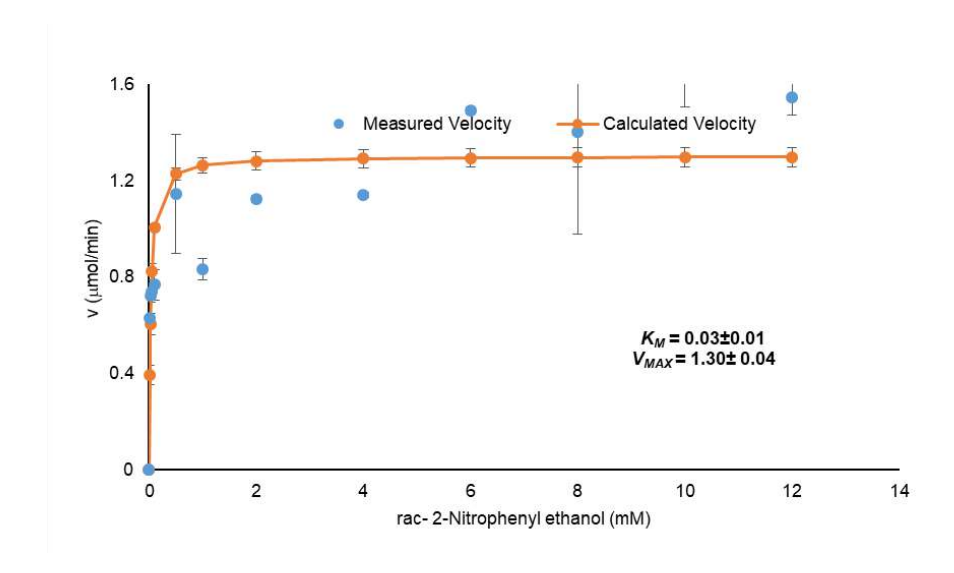


Figure 2.8: Michaelis-Menten curve for F179A variant with rac-NPE as substrate.

The reaction composition and conditions are same as mentioned in **Figure 2.2** caption, except the wild type AtHNL is replaced by its variant F179A and the substrate MN is replaced by NPE.

2.4.5. Cyanogenesis and retro-nitroaldolase activity of AtHNL library of variants

The purified proteins (**Figure 2.1: A-G, Table 2.4**) from all the three libraries were used in a microtiter plate assay to measure cyanogenesis and retro-nitroaldolase activity (**Figure 2.9**).

Table 2.4: Production of *At*HNL mutant proteins in U per liter from purification.

S.	<i>At</i> HNL	Total activity U/L of culture	S.	<i>At</i> HNL	Total activity U/L of
No			No		culture
1	WT	1281.84	24	F179T	223.8
2	F82A	11.4	25	F179Y	306.16
3	F82K	10.4	26	F179K	5.46
4	F82T	151.24	27	F179N	353.34
5	F82S	170.48	28	Y14A	732.46
6	F82P	8.74	29	Y14C	277.25
7	F82R	3.5	30	Y14Q	128.94
8	F82Q	11.92	31	Y14H	86.2
9	F179A	46.24	32	Y14N	31.54
10	F179D	59.84	33	Y14P	1.52
11	F179G	22.4	34	Y14S	94.64
12	F179L	451.88	35	Y14D	162.24
13	F179S	47.32	36	Y14F	916.96
14	F179C	956.88	37	Y14M	818
15	F179H	238.2	38	Y14V	906.2
16	F179P	69.36	39	Y14W	283.54
17	F179Q	20.42	40	Y14L	1324.24
18	F179R	9.3	41	Y14E	209.3
19	F179W	1098.22	42	Y14T	334.42
20	F179V	955.12	43	Y14K	56.5
21	F179M	548.2	44	Y14G	442.2
22	F179I	238.8	45	Y14I	37.46
23	F179E	49.14	46	Y14R	6.2

The activity is based on cyanogenesis as described in 2.6.

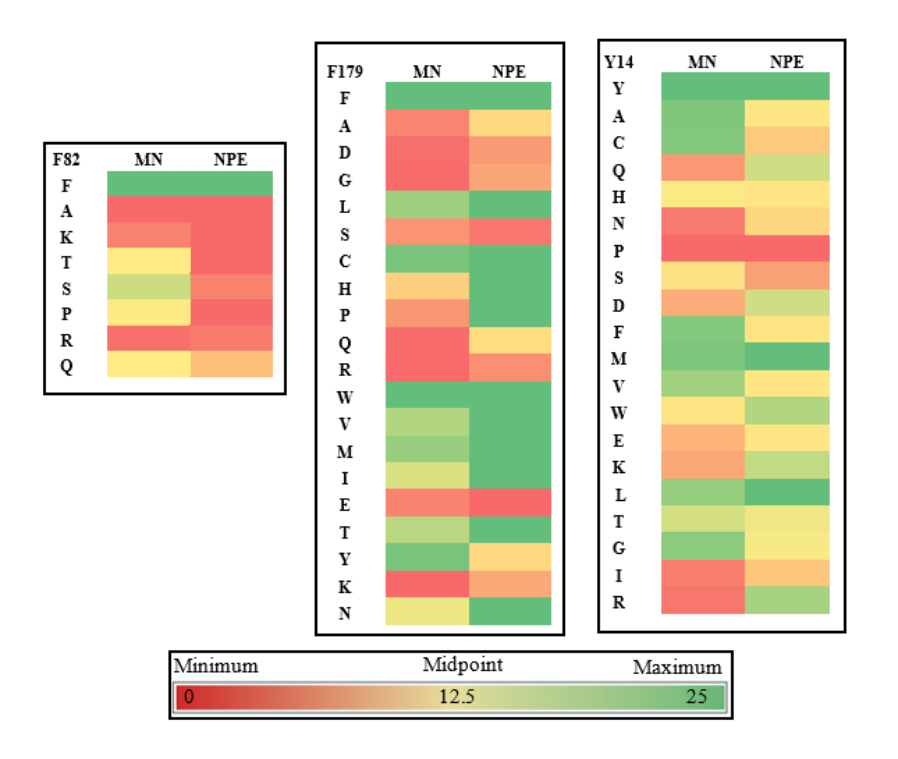


Figure 2.9: Cyanogenesis and retro-nitroaldolase activity of AtHNL variants modified at position F82 (left), F179 (middle), and Y14 (right). The reactions were performed in 50 mM citrate phosphate buffer (pH 5.5) at 25 °C with a final reaction volume of 200 μ L. The data are mean \pm standard deviation.

2.4.6. Kinetics analysis of AtHNL variants for retro-nitroaldolase activity

A dozen of variants from the F179 and Y14 series showing greater retro-nitroaldolase activity than the WT (**Figure 2.9**) were selected. The corresponding purified enzymes were used to measure their steady-state kinetic parameters (**Figure 2.10-2.21**). **Table 2.5**, represents the data along with WT, F82A and F179A, mentioned earlier.

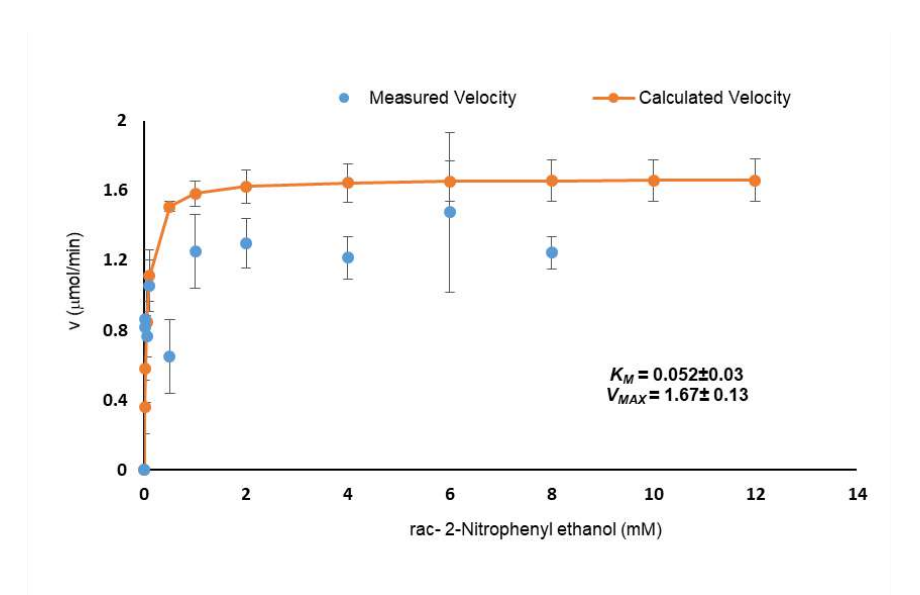


Figure 2.10: Michaelis-Menten curve for F179C variant with rac-NPE as substrate.

The reaction composition and conditions are same as mentioned in **Figure 2.2** caption, except the wild type AtHNL is replaced by its variant F179C and the substrate MN is replaced by NPE.

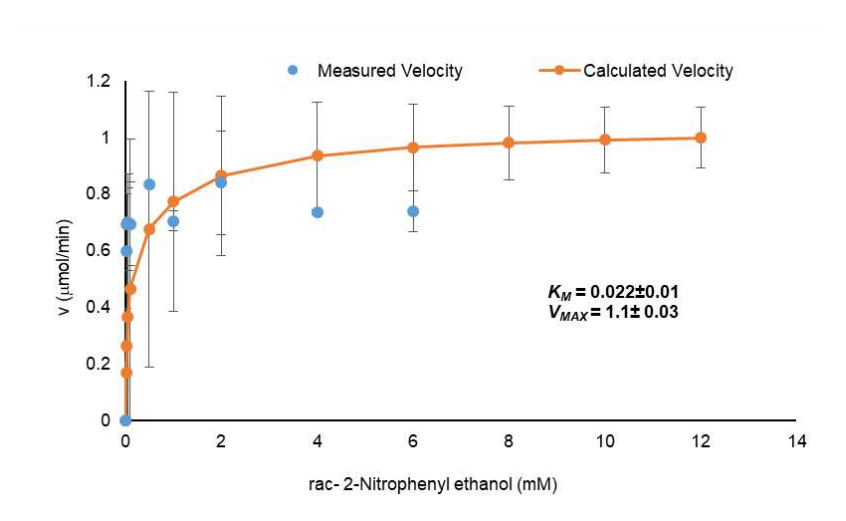


Figure 2.11: Michaelis-Menten curve for F179H variant with rac-NPE as substrate.

The reaction composition and conditions are same as mentioned in **Figure 2.2** caption, except the wild type AtHNL is replaced by its variant F179H and the substrate MN is replaced by NPE.

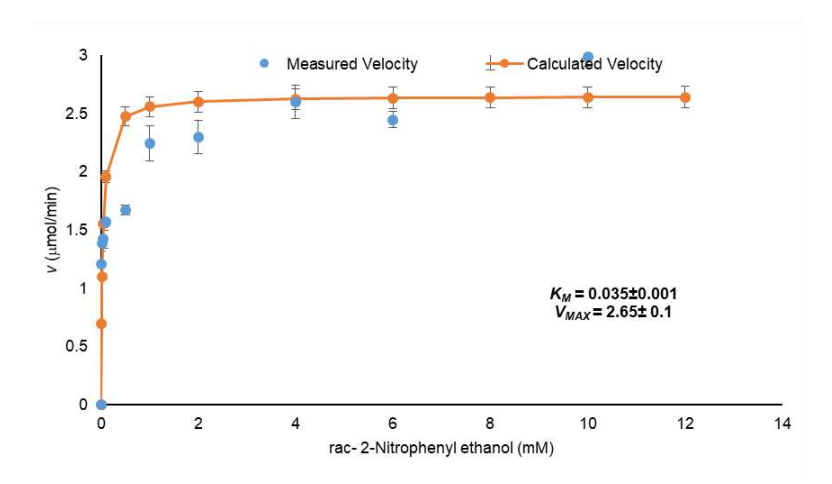


Figure 2.12: Michaelis-Menten curve for F179I variant with rac-NPE as substrate.

The reaction composition and conditions are same as mentioned in **Figure 2.2** caption, except the wild type AtHNL is replaced by its variant F179I and the substrate MN is replaced by NPE.

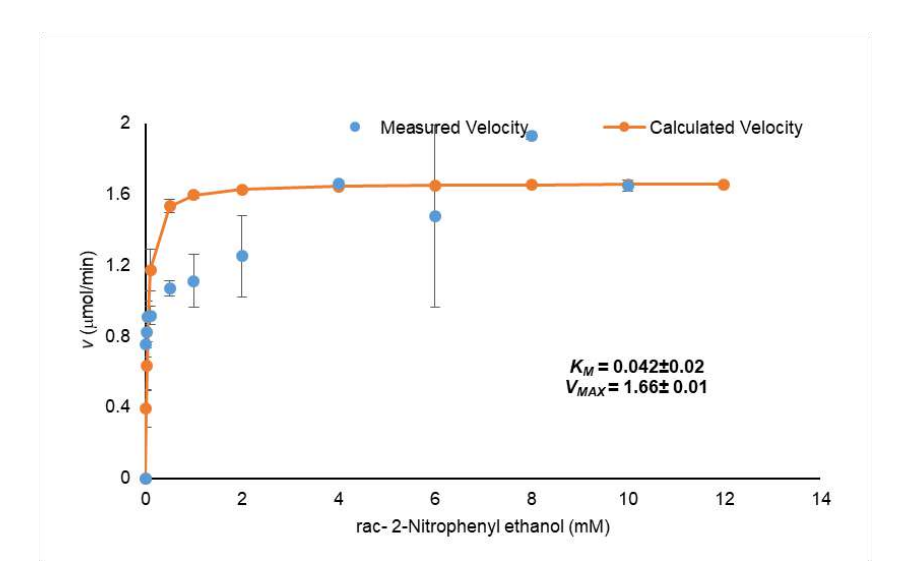


Figure 2.13: Michaelis-Menten curve for F179L variant with rac-NPE as substrate.

The reaction composition and conditions are same as mentioned in **Figure 2.2** caption, except the wild type *At*HNL is replaced by its variant F179L and the substrate MN is replaced by NPE.

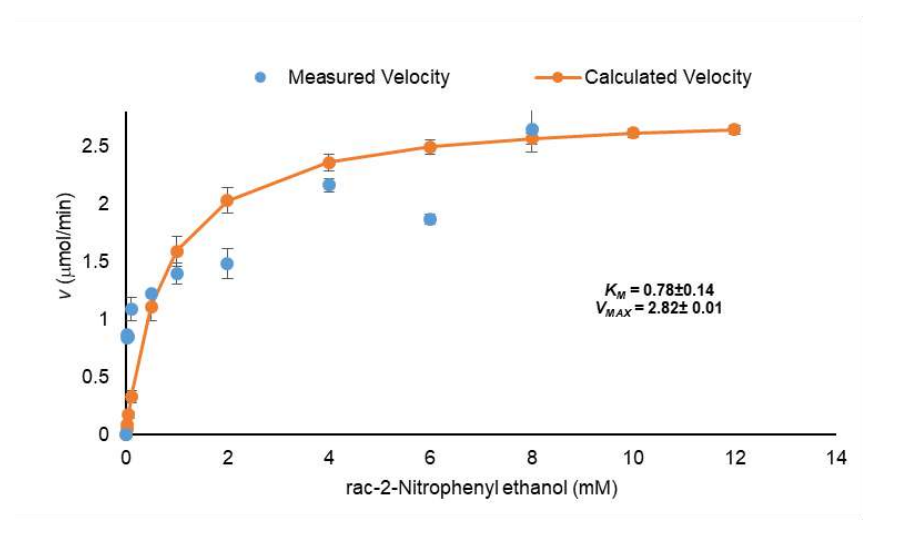


Figure 2.14:. Michaelis-Menten curve for F179M variant with rac-NPE as substrate.

The reaction composition and conditions are same as mentioned in **Figure 2.2** caption, except the wild type AtHNL is replaced by its variant F179M and the substrate MN is replaced by NPE.

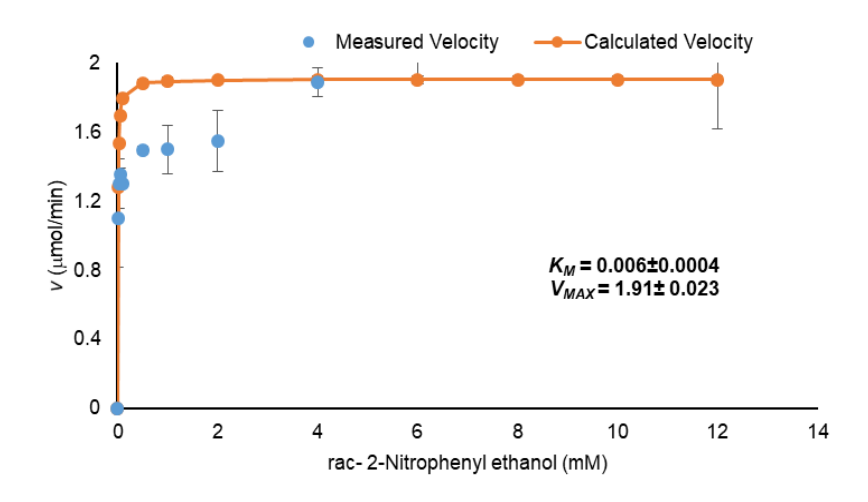


Figure 2.15: Michaelis-Menten curve for F179N variant with rac-NPE as substrate.

The reaction composition and conditions are same as mentioned in **Figure 2.2** caption, except the wild type AtHNL is replaced by its variant F179N and the substrate MN is replaced by NPE.

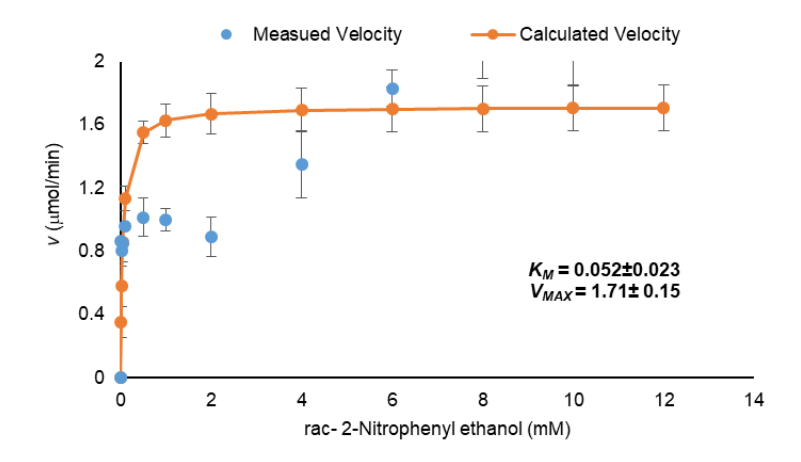


Figure 2.16: Michaelis-Menten curve for F179P variant with rac-NPE as substrate.

The reaction composition and conditions are same as mentioned in **Figure 2.2** caption, except the wild type AtHNL is replaced by its variant F179P and the substrate MN is replaced by NPE.

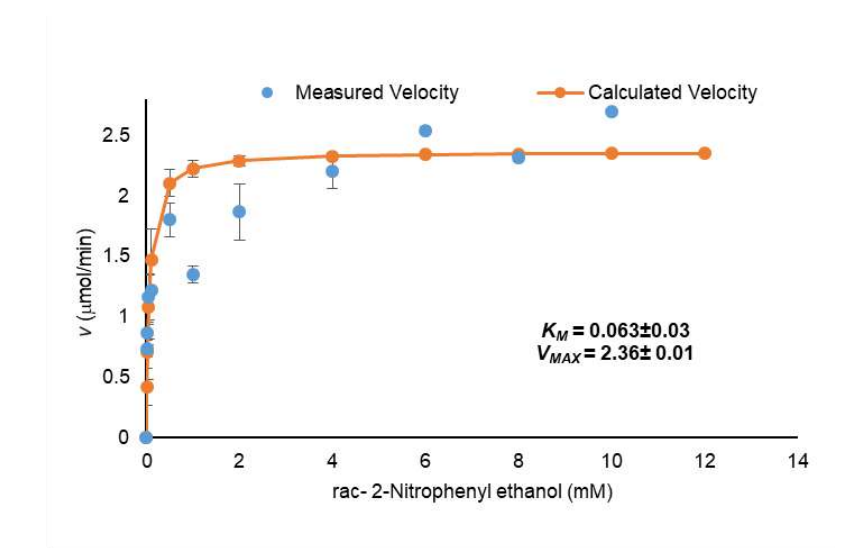


Figure 2.17: Michaelis-Menten curve for F179T variant with rac-NPE as substrate.

The reaction composition and conditions are same as mentioned in **Figure 2.2** caption, except the wild type *At*HNL is replaced by its variant F179T and the substrate MN is replaced by NPE.

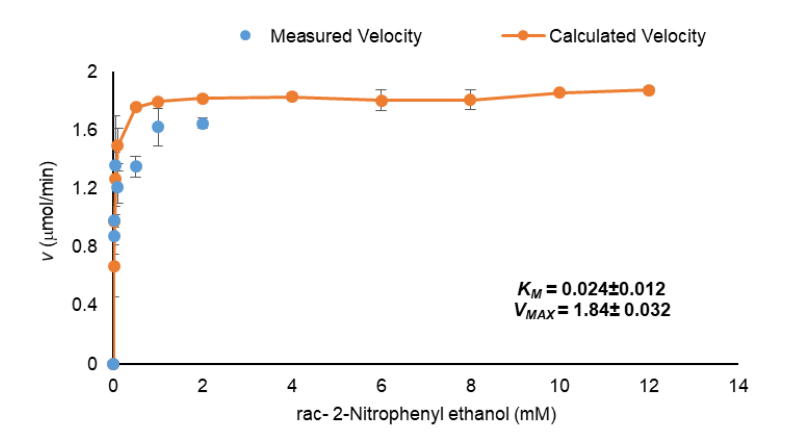


Figure 2.18: Michaelis-Menten curve for F179V variant with rac-NPE as substrate.

The reaction composition and conditions are same as mentioned in **Figure 2.2** caption, except the wild type *At*HNL is replaced by its variant F179V and the substrate MN is replaced by NPE.

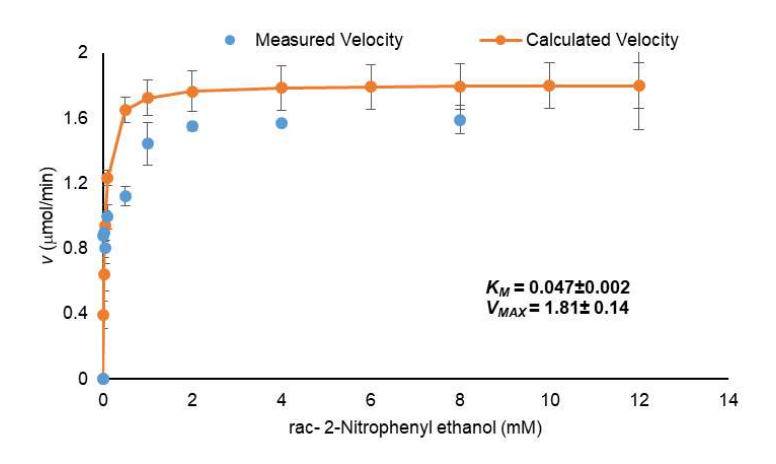


Figure 2.19: Michaelis-Menten curve for F179W variant with rac-NPE as substrate.

The reaction composition and conditions are same as mentioned in **Figure 2.2** caption, except the wild type *At*HNL is replaced by its variant F179W and the substrate MN is replaced by NPE.

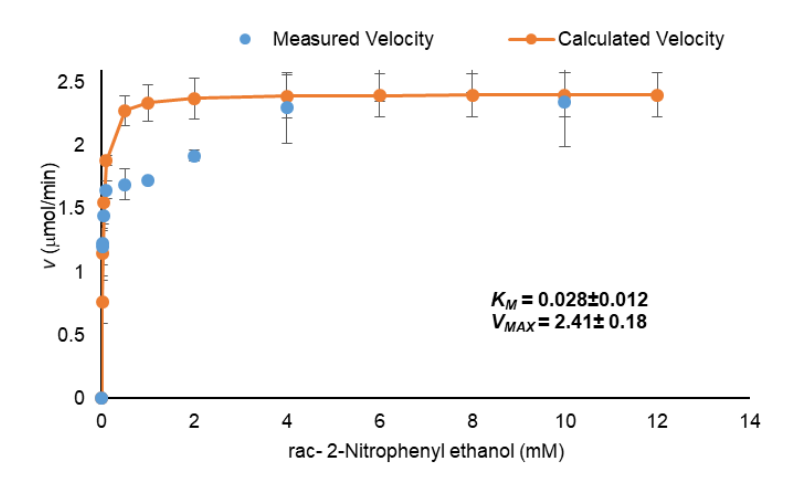


Figure 2.20: Michaelis-Menten curve for Y14L variant with rac-NPE as substrate.

The reaction composition and conditions are same as mentioned in **Figure 2.2** caption, except the wild type AtHNL is replaced by its variant Y14L and the substrate MN is replaced by NPE.

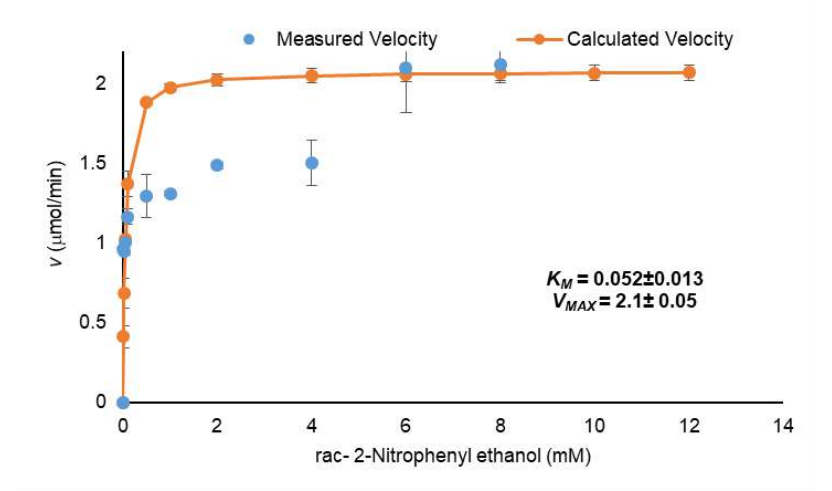


Figure 2.21: Michaelis-Menten curve for Y14M variant with rac-NPE as substrate.

The reaction composition and conditions are same as mentioned in **Figure 2.2** caption, except the wild type AtHNL is replaced by its variant Y14M and the substrate MN is replaced by NPE.

Table 2.5: Steady-state kinetic parameters of purified AtHNL WT and variant libraries for the retro-nitroaldol reaction.

Enz	$K_{\rm m}$ (mM)	V _{max} (U/mg)	$k_{\rm cat}({\rm min}^{-1})$	$k_{\text{cat}}/K_{\text{m}} (\text{mM}^{-1} \text{min}^{-1})$
WT	0.015±0.010	1.75±0.020	49.00 ± 0.56	3614.10± 1762.03
F82A	0.010±0.003	0.97±0.030	27.10±0.79	2925.80±1.41
F179A	0.029±0.010	1.30±0.040	36.44±1.13	1250.92± 208.05
F179C	0.052±0.030	1.66±0.130	46.67±3.49	1076.31±584.70
F179M	0.780±0.140	2.82±0.010	78.83±0.28	102.84±18.34
F179N	0.006±0.0004	1.91±0.020	53.34±0.65	8775.60±482.58
F179L	0.042±0.017	1.66±0.005	46.54±0.13	1098.30±8.66
F179W	0.047±0.020	1.81±0.140	50.60±4.04	1079.50±236.60
F179H	0.020±0.010	1.10±0.030	30.80±0.90	1400.76±650.08
F179T	0.063±0.027	2.36±0.012	66.15±0.33	1169.22±512.92
F179P	0.052±0.024	1.71±0.150	47.96±4.20	1012.04±381.89
F179V	0.024±0.012	1.84±0.030	51.50±0.89	2493.36±1237.43
F179I	0.035±0.001	2.65±0.009	74.19±2.57	2118.40±0.57
Y14L	0.028±0.012	2.41±0.180	67.44±4.97	2582.43±931.30
Y14M	0.052±0.013	2.08±0.051	58.12±1.43	1156.59±255.28

The reaction mixture contained 160 μ L of 50 mM citrate phosphate buffer (pH 5.5), 20 μ L purified enzyme (1 mg/mL) and 20 μ L of racemic NPE (0.0125 – 12 mM) pre-dissolved in 1 mL of 5 mM citrate buffer (pH 3.15) making a total volume of 200 μ L. The reaction rate was measured at 280 nm in a UV–Visible spectrophotometer. The data are mean \pm standard deviation.

2.4.7. At HNL variants catalyzed preparation of (S)-β-nitroalcohol

The fourteen variants of **Table 2.5** were evaluated for the retro-nitroaldol reaction using purified enzymes for the production of (S)- β -nitroalcohol. The products were analyzed by chiral HPLC to calculate the % enantiomeric excess (ee) and % conversion of (S)-NPE (**Figure 2.22**). **Figure 2.23-2.39** represent their HPLC chromatograms.

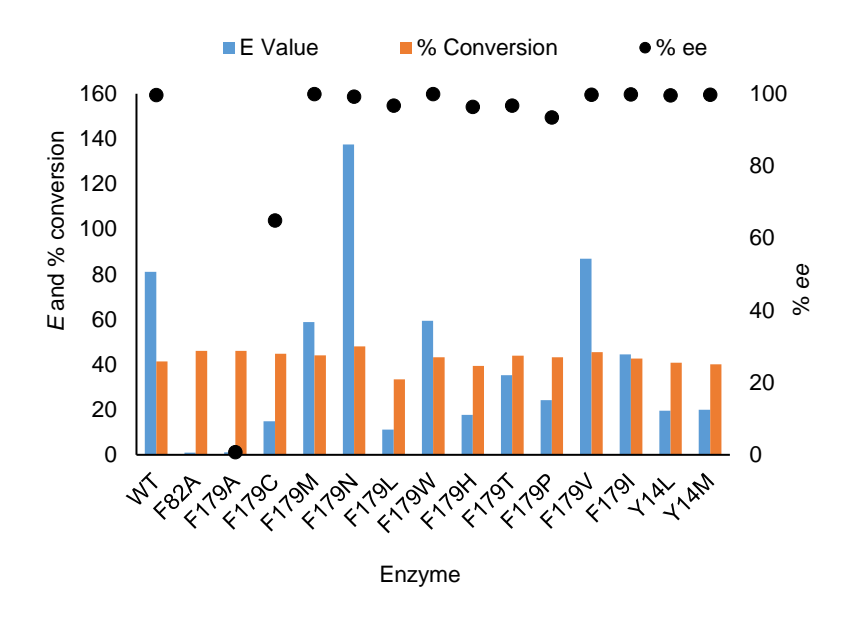


Figure 2.22: Retro- nitroaldol reaction of *At*HNL variants in the preparation of (*S*)-NPE.

A reaction mixture of 3 mg of purified *At*HNL variant in 20 mM KPB pH 7, 2 μmol of racemic NPE, 17.5% v/v of 50 mM CPB pH 5.5, and 65% v/v of toluene was shaken at 1200 rpm, 30 °C up to 3 h. The % conversion (red bar) represents the absolute amount of (*S*)-NPE.

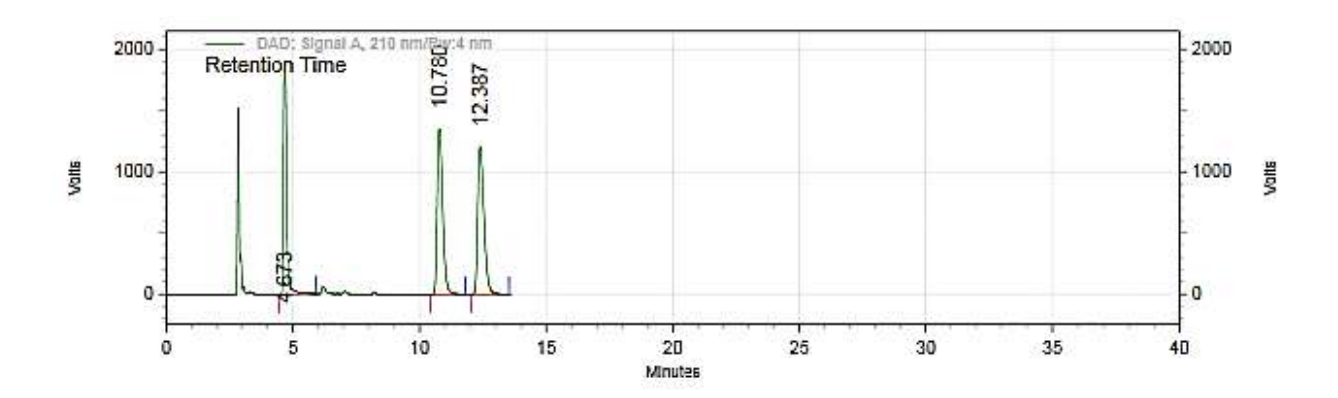


Figure 2.23: HPLC spectrum of the standards: benzaldehyde, (*R*)- and (*S*)-NPE.

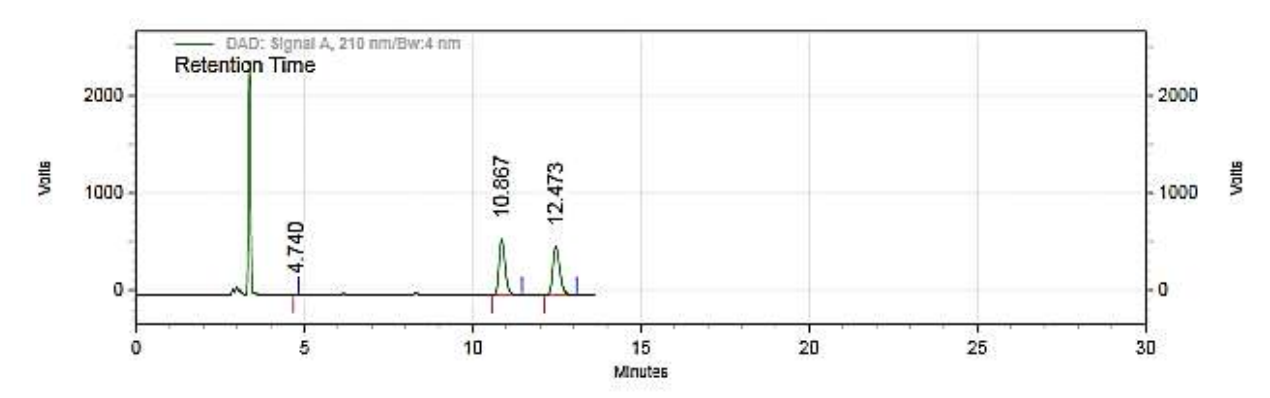


Figure 2.24: HPLC spectrum of the control reaction where enzyme was replaced by 20 mM KPB buffer shows no enantioselective cleavage of rac-NPE.

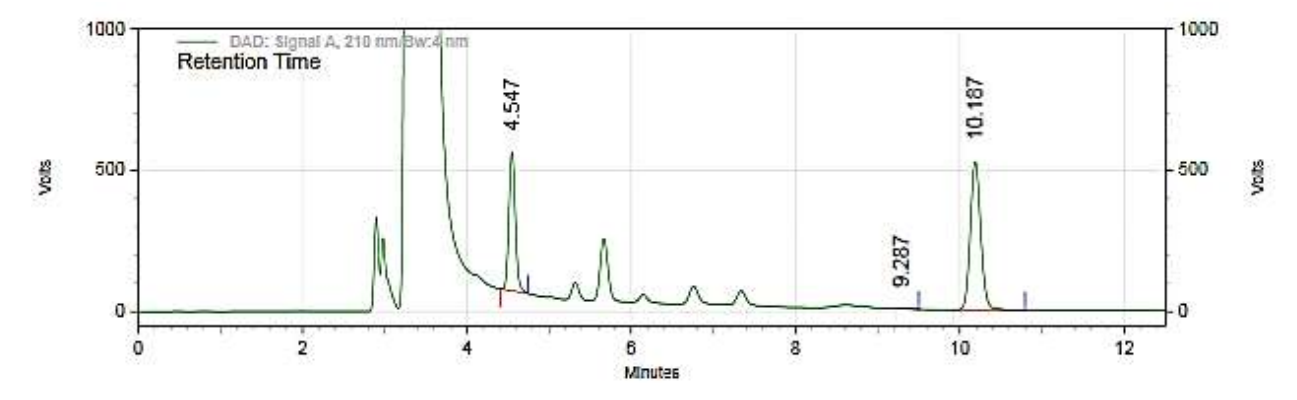


Figure 2.25: HPLC spectrum of wild type *At*HNL showing enantioselective cleavage of rac-NPE.

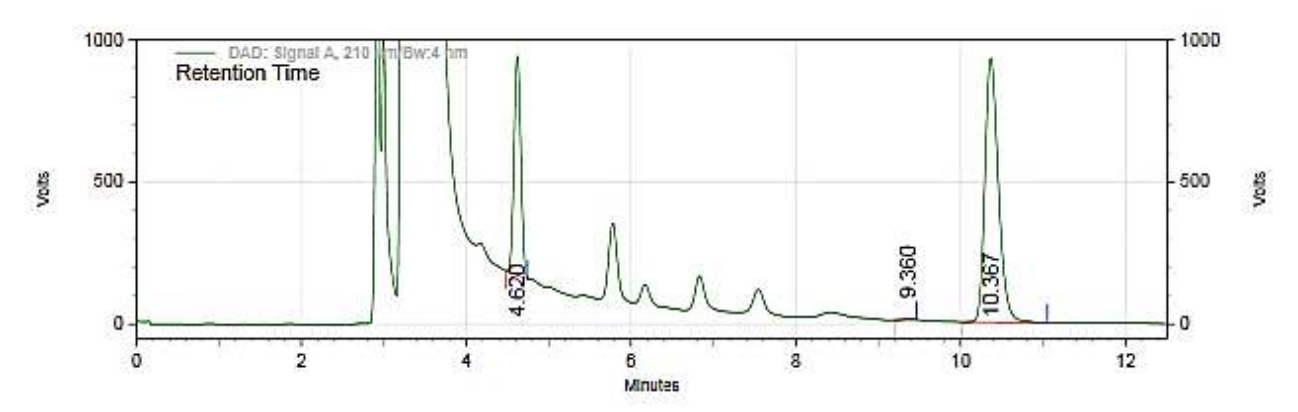


Figure 2.26: HPLC spectrum of the variant F179N showing enantioselective cleavage of rac-NPE.

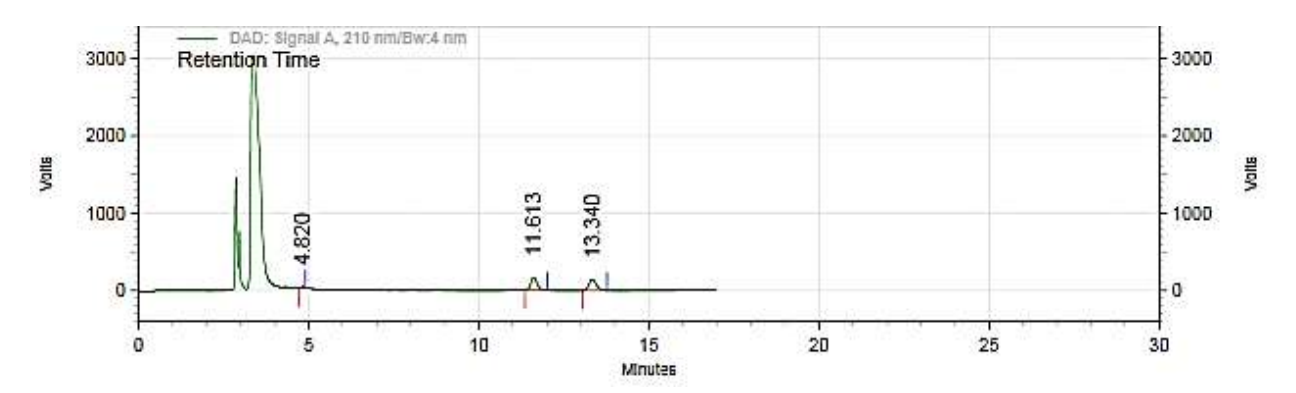


Figure 2.27: HPLC spectrum of the variant F82A showing enantioselective cleavage of rac-NPE.

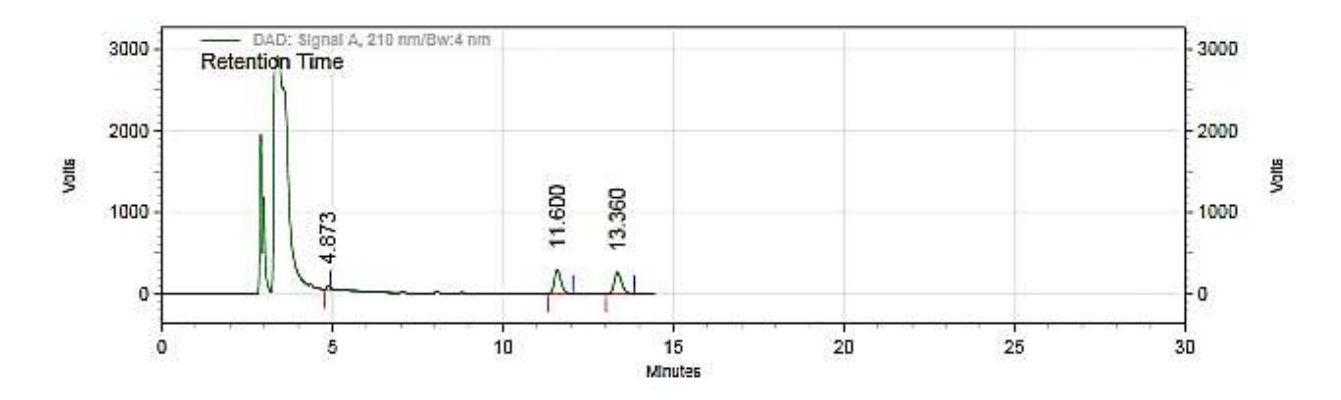


Figure 2.28: HPLC spectrum of the variant F179A showing enantioselective cleavage of rac-NPE.

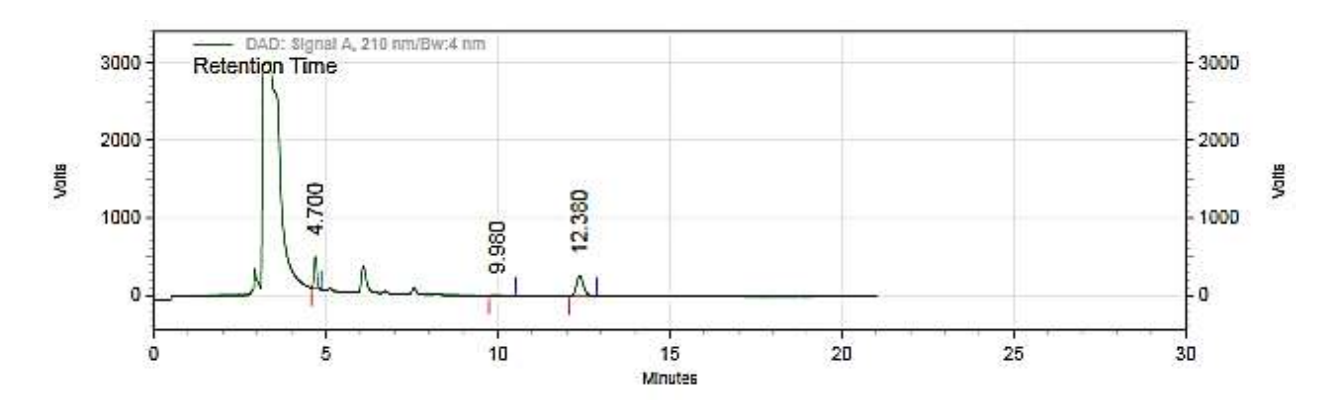


Figure 2.29: HPLC spectrum of the variant F179L showing enantioselective cleavage of rac-NPE.

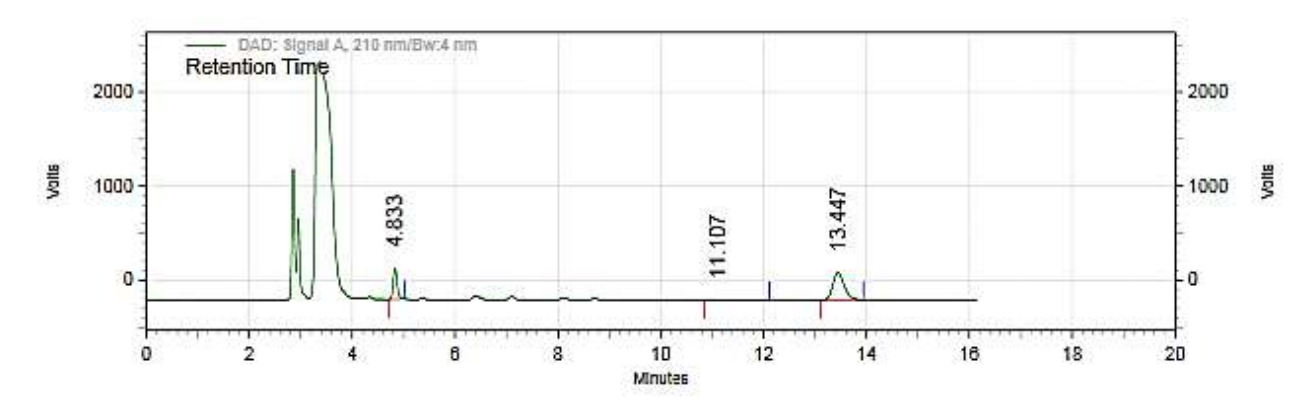


Figure 2.30: HPLC spectrum of the variant F179T showing enantioselective cleavage of rac-NPE.

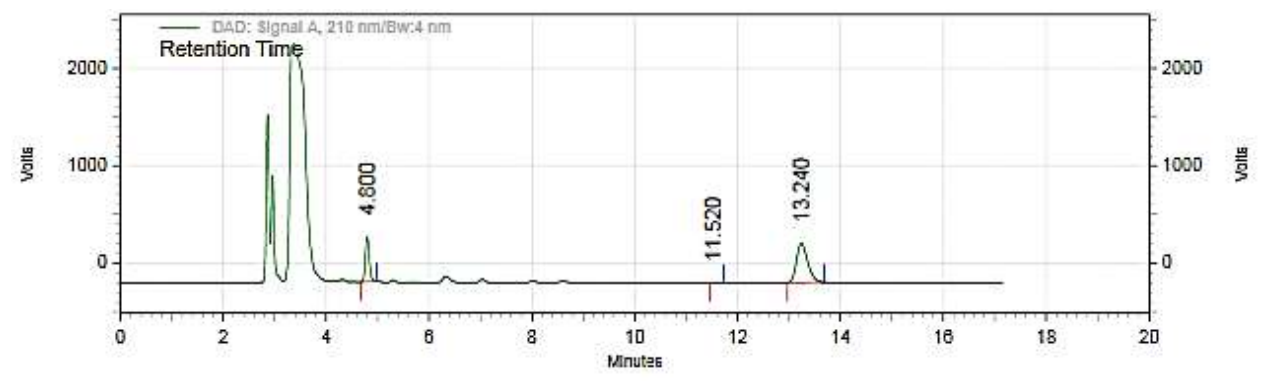


Figure 2.31: HPLC spectrum of the variant F179W showing enantioselective cleavage of rac-NPE.

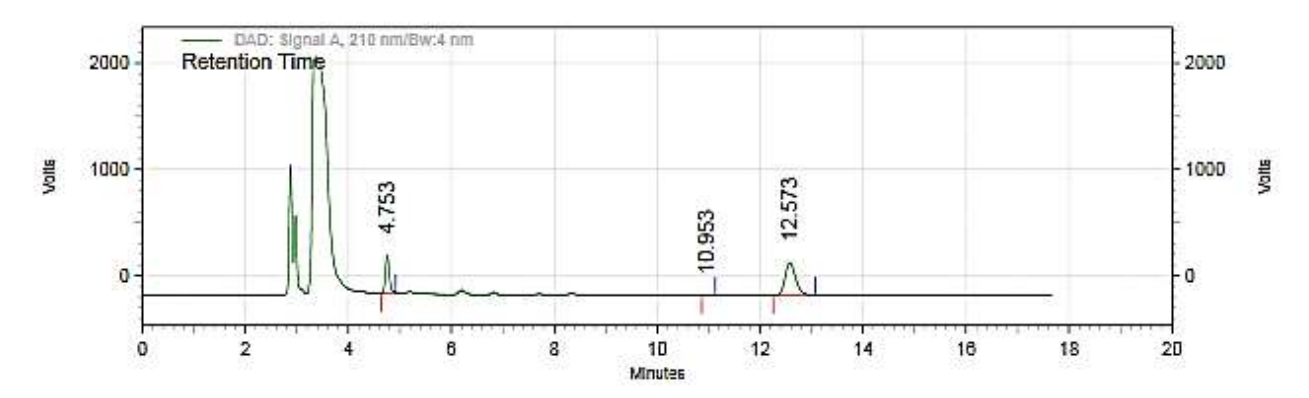


Figure 2.32: HPLC spectrum of the variant F179I showing enantioselective cleavage of rac-NPE.

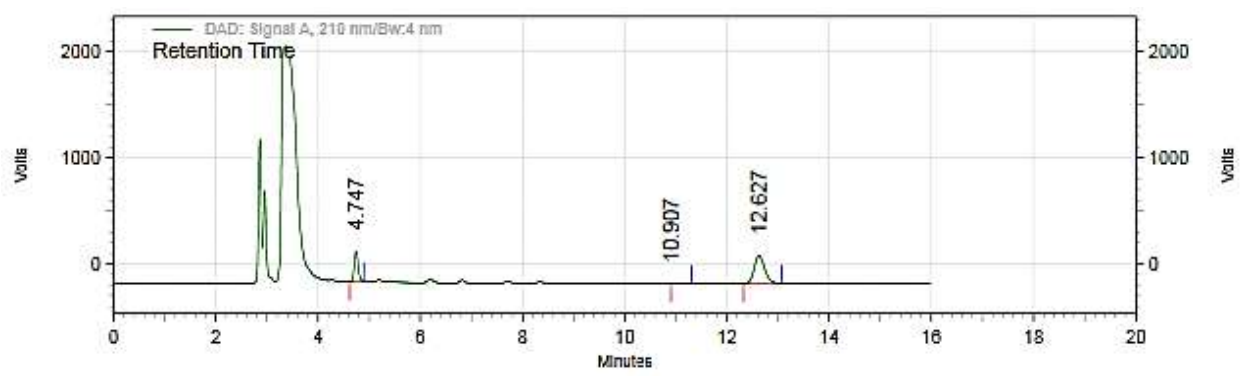


Figure 2.33: HPLC spectrum of the variant F179M showing enantioselective cleavage of rac-NPE.

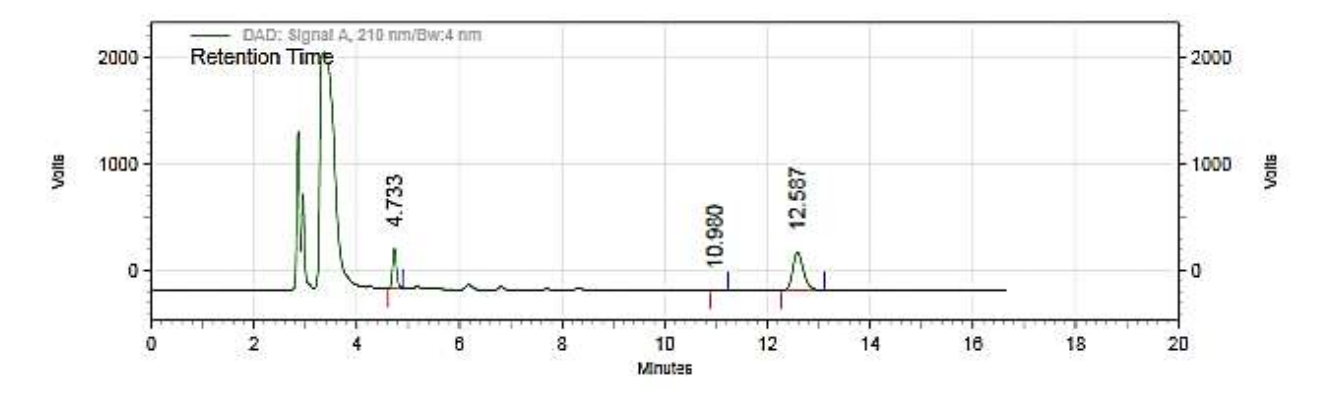


Figure 2.34: HPLC spectrum of the variant F179V showing enantioselective cleavage of rac-NPE.

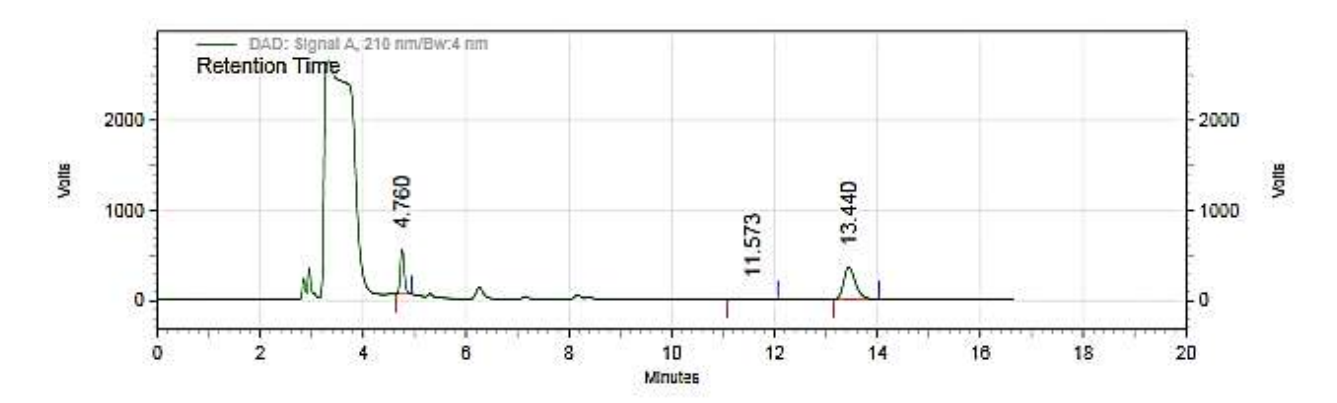


Figure 2.35: HPLC spectrum of the variant F179H showing enantioselective cleavage of rac-NPE.

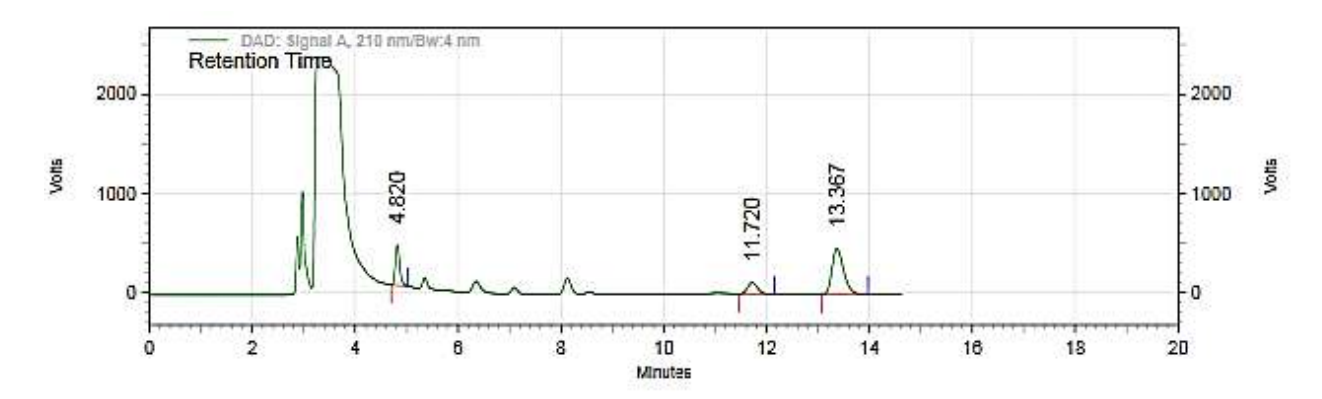


Figure 2.36: HPLC spectrum of the variant F179C showing enantioselective cleavage of rac-NPE.

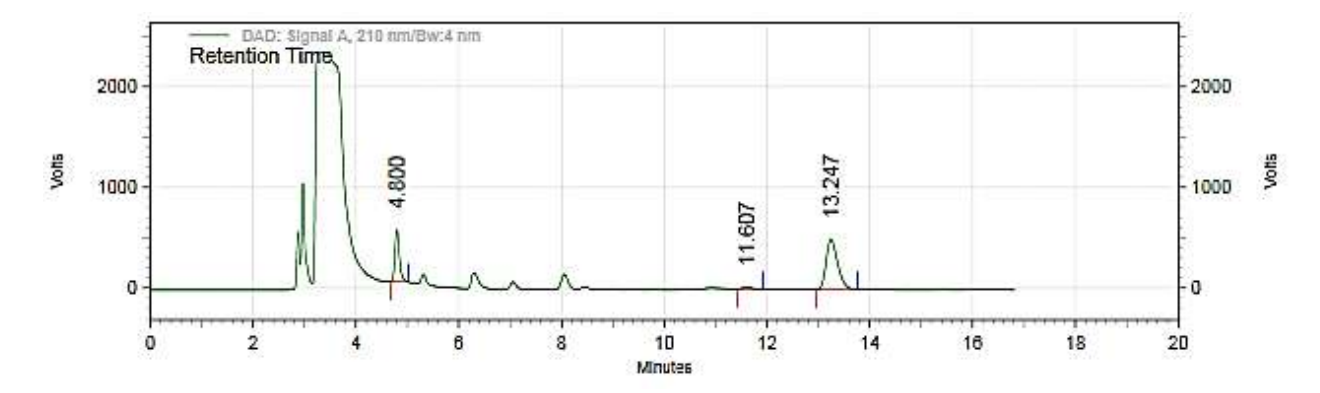


Figure 2.37: HPLC spectrum of the variant F179P showing enantioselective cleavage of rac-NPE.

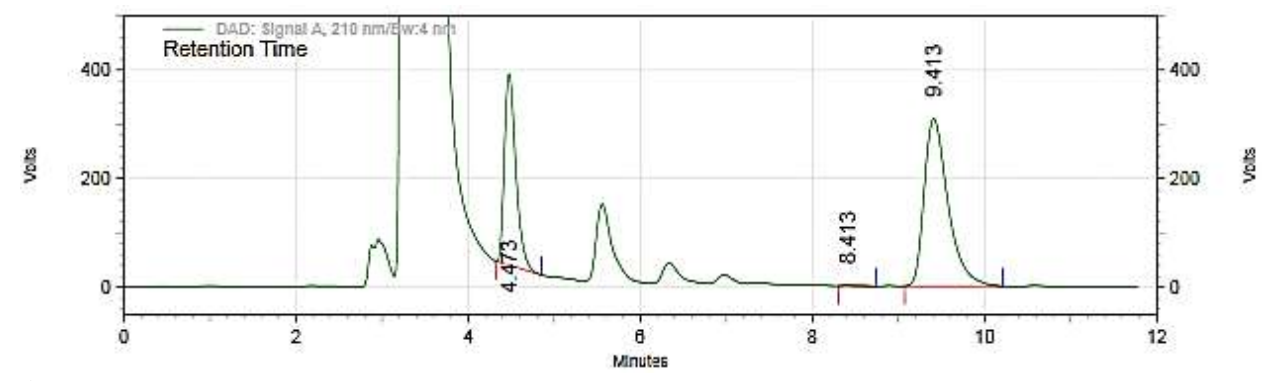


Figure 2.38: HPLC spectrum of the variant Y14L showing enantioselective cleavage of rac-NPE.

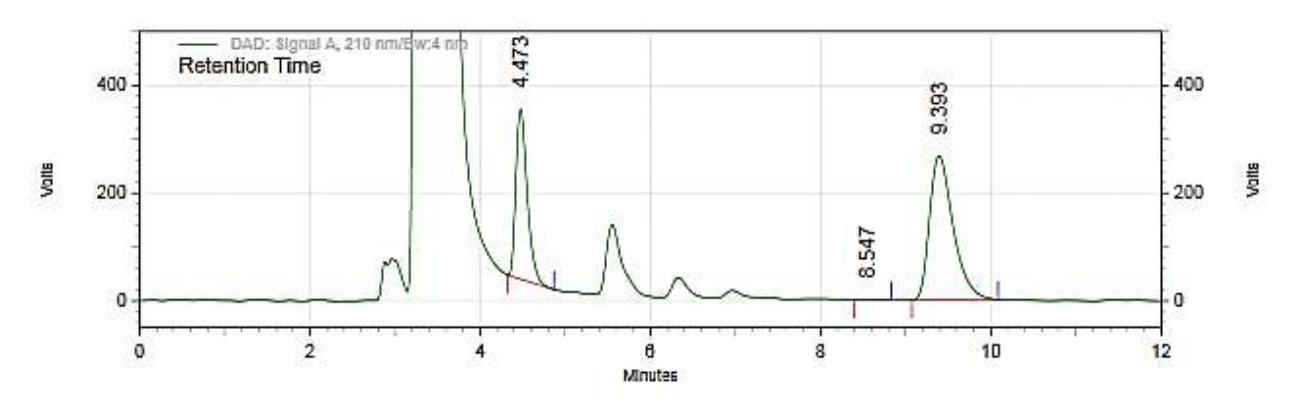


Figure 2.39: HPLC spectrum of the variant Y14M showing enantioselective cleavage of rac-NPE.

2.4.8. Study of AtHNL double variants towards the retro-nitroaldol reaction

Futher to enhance the enantioselectivity and catalytic efficiency, we have created three double variants, F82A-F179N, F82A-F179V and F82A-F179W using appropriate primers (**Table 2.1**) and each variant was confirmed by DNA sequencing. The double variants were purified (**Figure 2.1**: **H**), and used to measure their steady-state kinetic parameters (**Table 2.6**, **Figure 2.40-2.42**). They were also evaluated for the retro-nitroaldol reaction in the production of (*S*)-β-nitroalcohol (**Figure 2.43**). **Figure 2.44-2.46** represent their HPLC chromatograms.

Table 2.6: Steady-state kinetic parameters of purified *At*HNL double variants for the retronitroaldol reaction.

Enz	NPE			
	$K_{\rm m}$ (mM)	V _{max} (U/mg)	$k_{\rm cat}({\rm min}^{-1})$	$k_{\text{cat}}/K_{\text{m}} (\text{min}^{-1}\text{mM}^{-1})$
WT	0.015±0.010	1.75±0.020	49.00 ± 0.56	3614.10 ± 1762.03
F179N	0.006 ± 0.0004	1.91±0.020	53.34±0.65	8775.60±482.58
F82A-F179N	0.015±0.003	0.72 ± 0.012	20.08±0.330	1351.31±230.840
F82A-F179W	0.018±0.010	1.20±0.250	33.60±6.870	2166.95±1001.520
F82A-F179V	0.048±0.020	1.20±0.100	33.67±2.910	741.67 ± 212.880

The reaction mixture contained 160 μ L of 50 mM citrate phosphate buffer (CPB) (pH 5.5), 20 μ L purified enzyme (1 mg/mL) and 20 μ L of racemic NPE (0.0125 – 12 mM) pre-dissolved in 1 mL of 5 mM citrate buffer (pH 3.15) making a total volume of 200 μ L. The reaction rate was measured at 280 nm in a UV–Visible spectrophotometer. The data are mean \pm standard deviation.

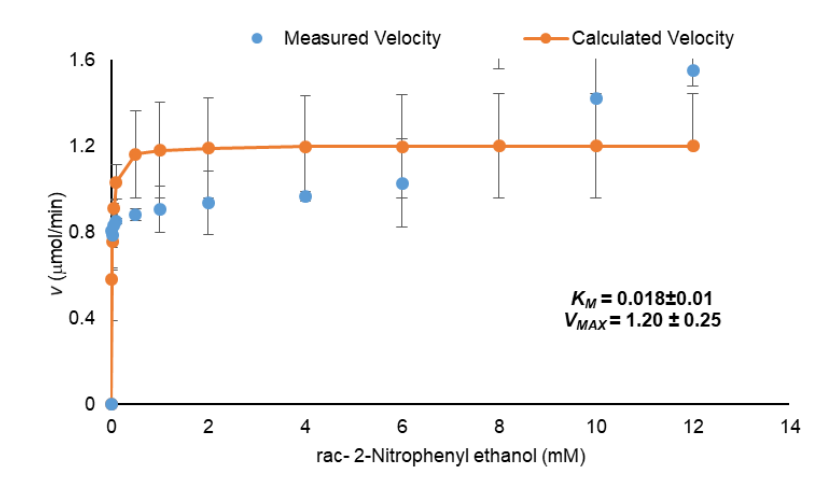


Figure 2.40: Michaelis-Menten curve for F82A-F179W variant with rac-NPE as substrate.

The reaction composition and conditions are same as mentioned in **Figure 2.2** caption, except the wild type *At*HNL is replaced by its variant F82A-F179W and the substrate MN is replaced by NPE.

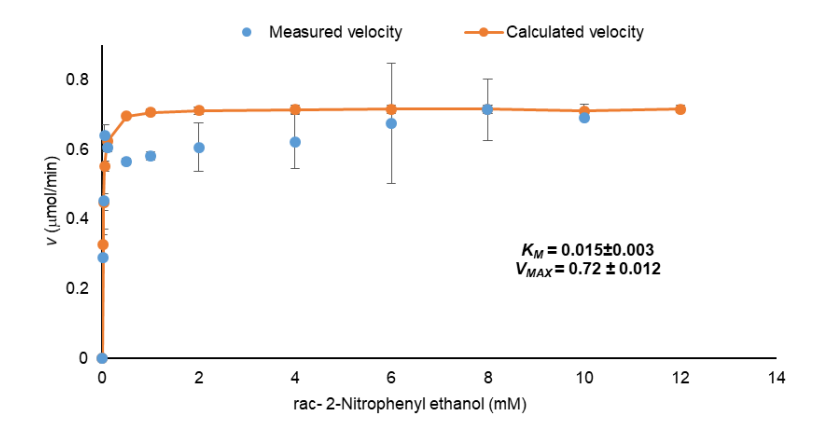


Figure 2.41: Michaelis-Menten curve for F82A-F179N variant with rac-NPE as substrate.

The reaction composition and conditions are same as mentioned in **Figure 2.2** caption, except the wild type *At*HNL is replaced by its variant F82A-F179N and the substrate MN is replaced by NPE.

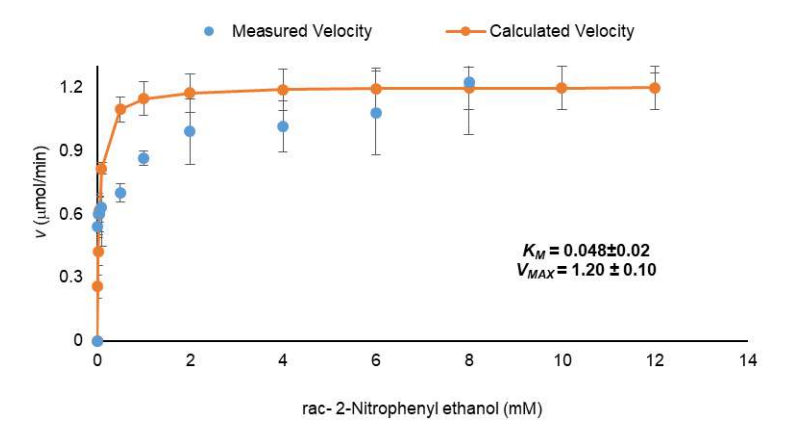


Figure 2.42: Michaelis-Menten curve for F82A-F179V variant with rac-NPE as substrate.

The reaction composition and conditions are same as mentioned in **Figure 2.2** caption, except the wild type *At*HNL is replaced by its variant F82A-F179V and the substrate MN is replaced by NPE.

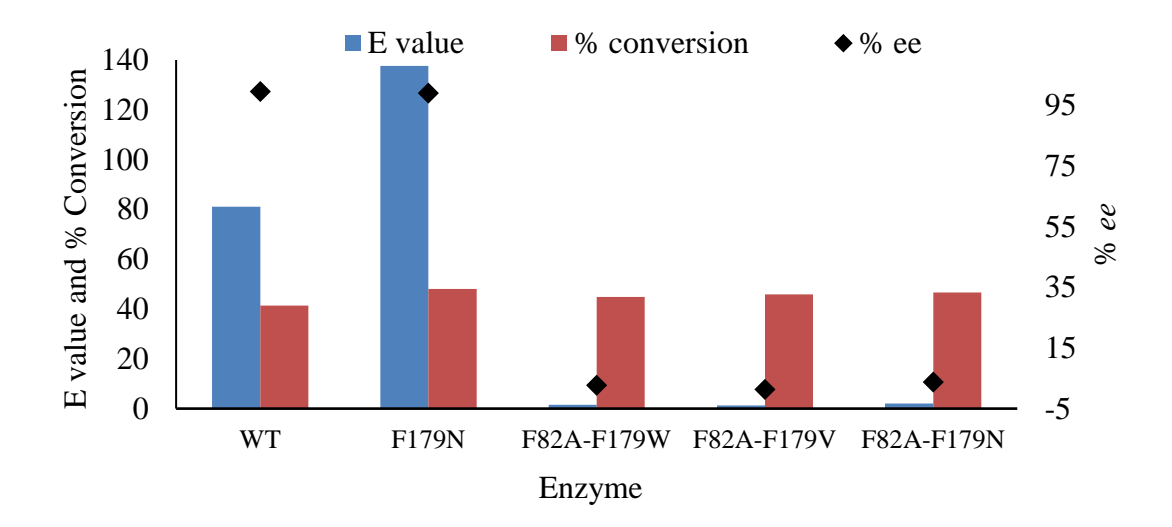


Figure 2.43: Retro-nitroaldol reaction of *At*HNL variants in the preparation of (*S*)-NPE.

A reaction mixture of 3 mg of purified AtHNL variant in 20 mM KPB pH 7, 2 μ mol of racemic NPE, 17.5% v/v of 50 mM CPB pH 5.5, and 65% v/v of toluene was shaken at 1200 rpm, 30 °C up to 3 h.

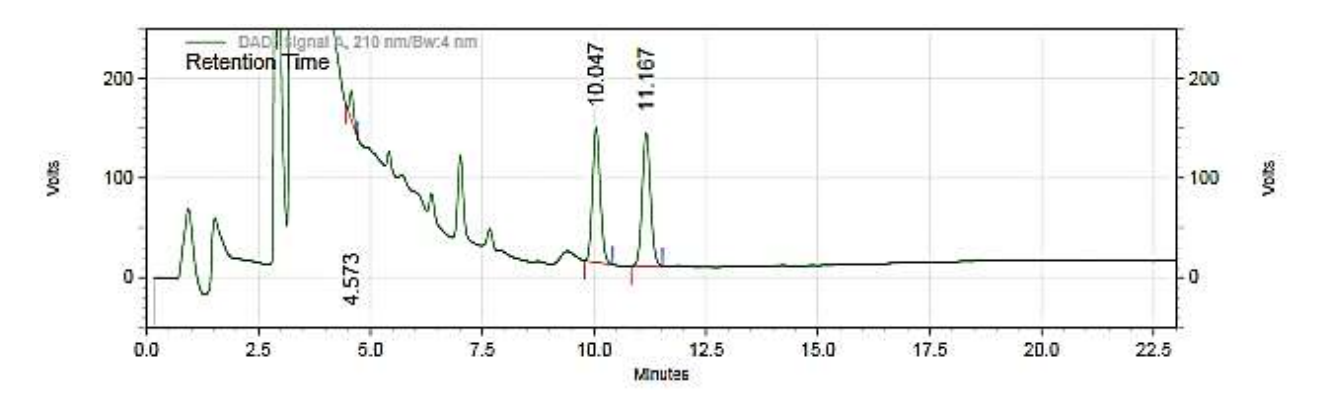


Figure 2.44: HPLC spectrum of the double variant F82A-F179W in the enantioselective cleavage of rac-NPE.

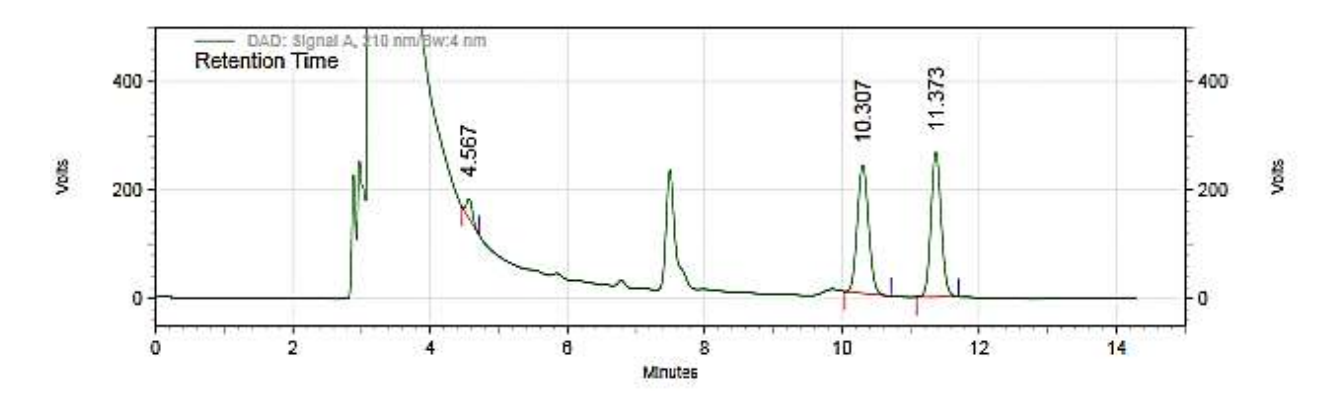


Figure 2.45: HPLC spectrum of the double variant F82A-F179V in the enantioselective cleavage of rac-NPE.

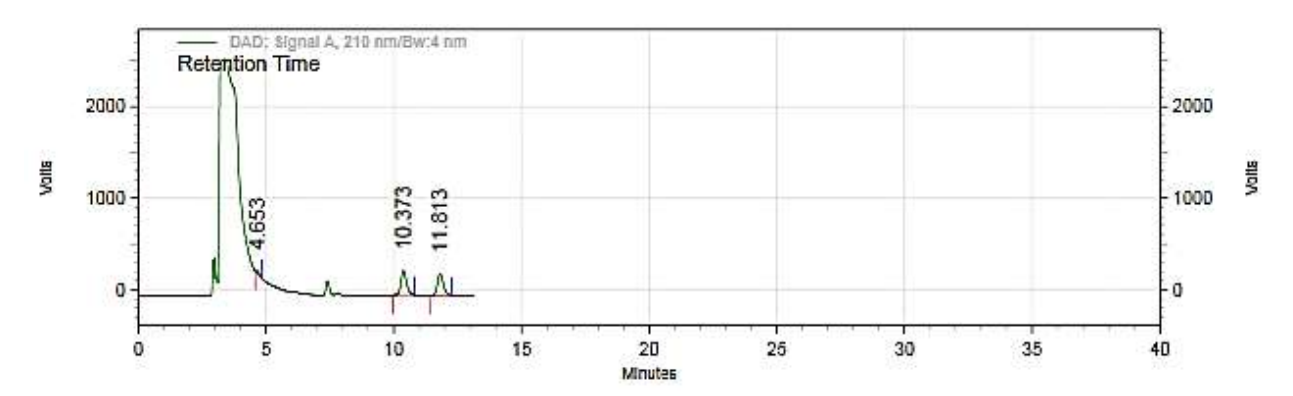
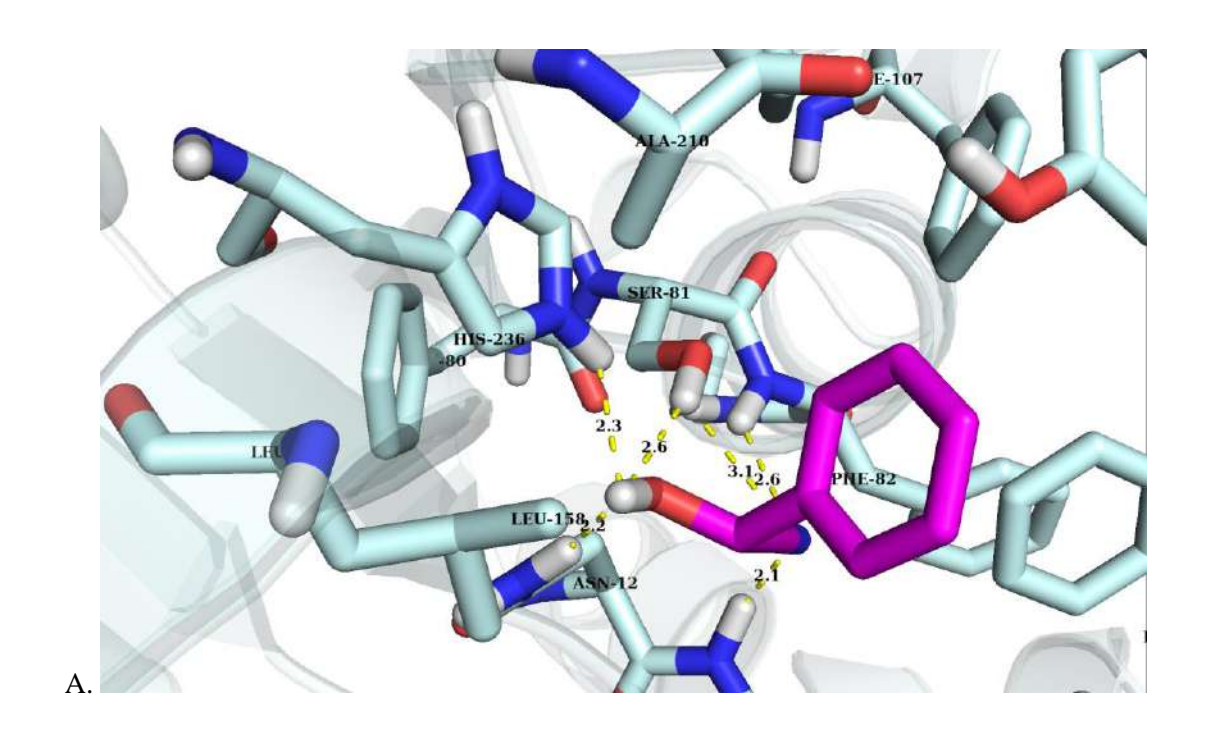


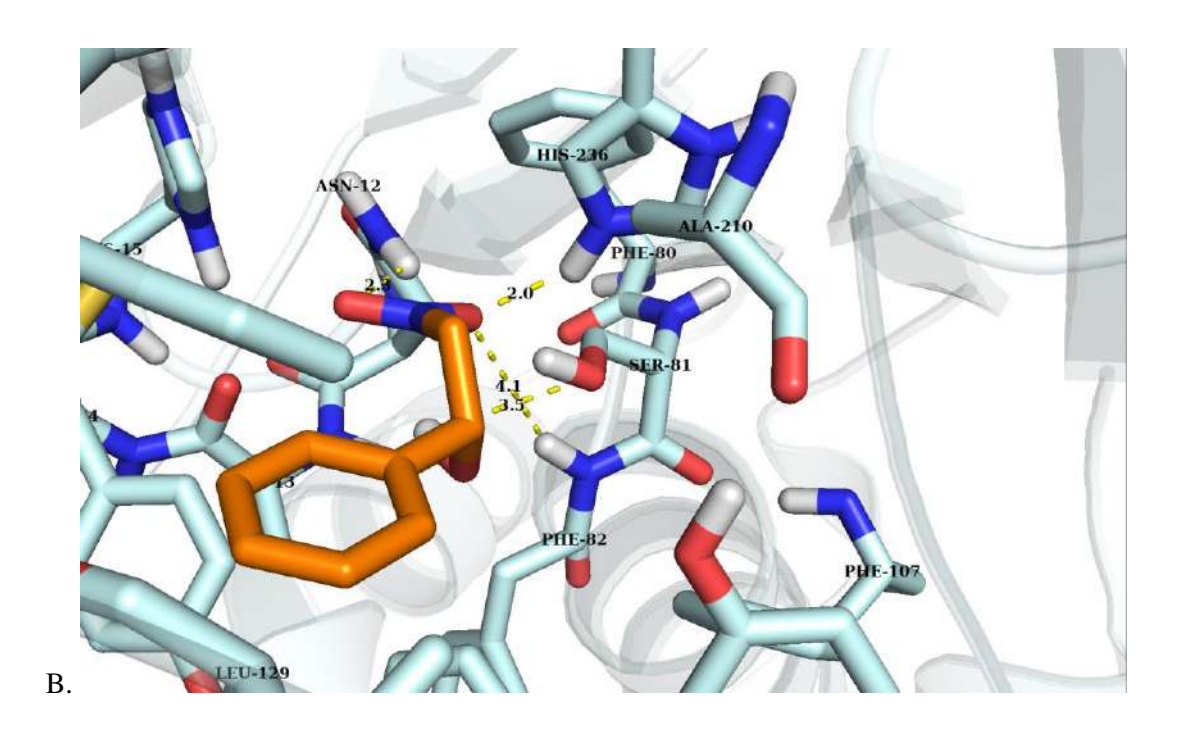
Figure 2.46: HPLC spectrum of the double variant F82A-F179N in the enantioselective cleavage of rac-NPE.

2.4.9. Computational studies

2.4.9.1. Docking studies to identify hot spots in AtHNL binding site

Docking of (R)-MN and (R)-NPE was performed into the catalytic site of AtHNL and the modeled complexes of AtHNL-(R)-MN and AtHNL-(R)-NPE were superimposed to find out the differential binding of these two substrates (**Table 2.7**, **Figure 2.47**).





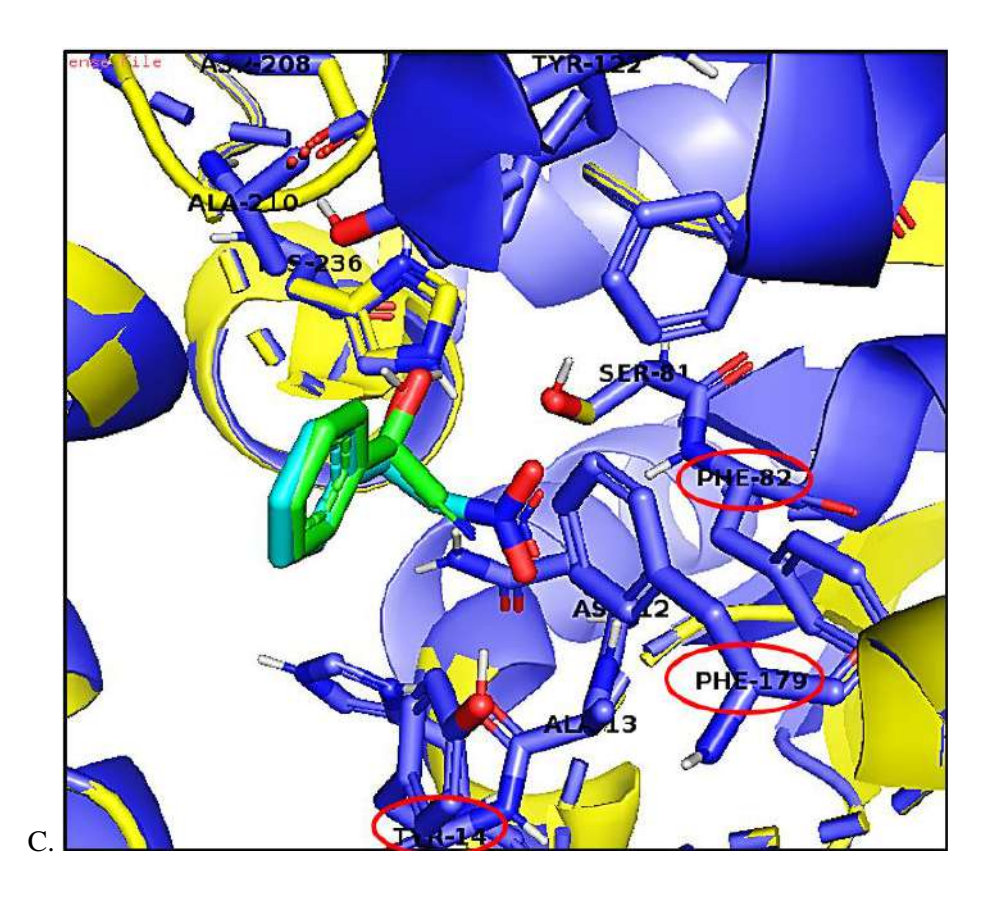


Figure 2.47: Modelled AtHNL complex shows interaction of the enzyme with substrate as seen in **Table 2.7**, A. with (R)-MN, B. with (R)-NPE, C. superimposed model complexes of AtHNL-(R)-MN and AtHNL-(R)-NPE (The amino acids 5Å around the active site interacting with the substrates are shown.

Table 2.7: Docking results of MN and NPE with *At*HNL.

Functional group of substrate in H-bonding	Enz-sub H-bonding distance, this study	Enz-sub H-bonding, earlier studies ¹⁻²
OH group of (R)-NPE	Oγ of Ser81 : 3.5 A°	Not reported
NO_2 group of (R)-NPE	His236-Nε2: 2.0 A°	
	Asn12-δ-NH: 1.8, 2.3 A°	
	NH of main chain of Phe82: 4.1 A°	
OH group of (R) -MN	Nε of His236 : 2.3 A°	Nε of His236
	NH of δ-amide of Asn12 : 2.2 A°	NH of δ-amide of Asn12
	Oγ of Ser81 : 2.6 A°	Oγ of Ser81
CN group of (R)-MN	NH of main chain of Ser81: 3.1 A°	NH (main chain) of Ser81
	NH of main chain of Ala13: 2.1 A°	NH (main chain) of Ala13
	NH of main chain of Phe82 : 2.6 A°	NH (main chain) of Phe82

2.4.9.2. Study of the binding pocket of *At*HNL

From the modeled *At*HNL-(*R*)-NPE structure, we identified residues present within 5 Å from the substrate. The residues selected are: Asn12, Ala13, Tyr14, His15, Phe80, Ser81, Phe82, Phe107, Tyr122, Leu129, Cys132, Leu147, Met149, Phe153, Leu158, Phe179, Ala210, and His236 (**Figure 2.48**).

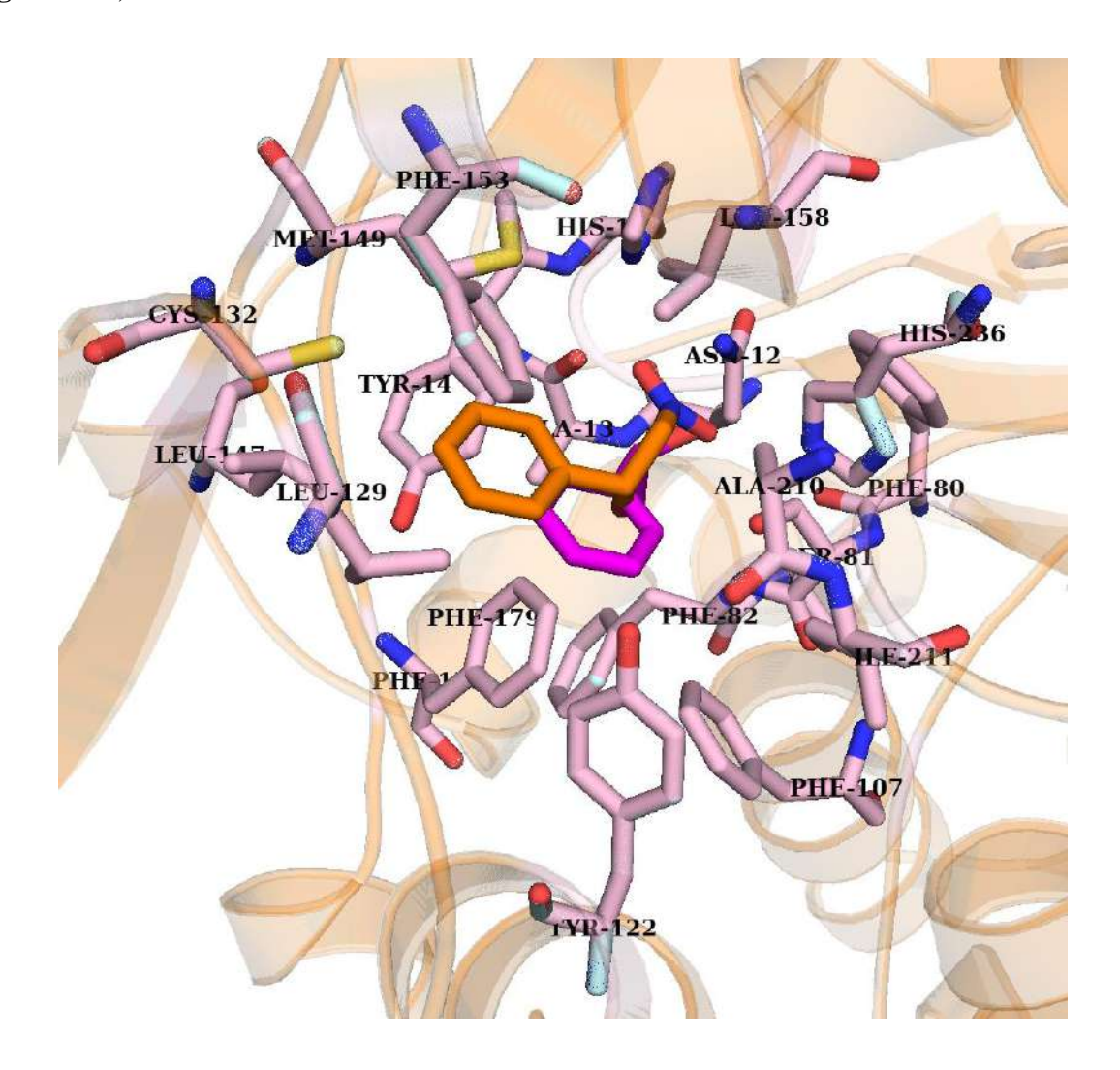


Figure 2.48: Superimposed model complexes of AtHNL-(R)-MN and AtHNL-(R)-NPE (The amino acids 5Å around the active site interacting with the substrates are shown comprising of the AtHNL binding pocket.

2.4.9.3. Molecular docking and interaction studies to understand the substrate binding and enantioselectivity of the variants

Molecular docking of (*R*)-NPE and (*S*)-NPE were performed into the catalytic site of *At*HNL mutants F82A, F179N and F82A-F179N, along with the wild type and found their binding efficiency and interactions with these substrates (**Table 2.8**). The substrate interactions in case of both the WT and F179N, which showed enantioselectivity, are illustrated in **Figure 2.49**.

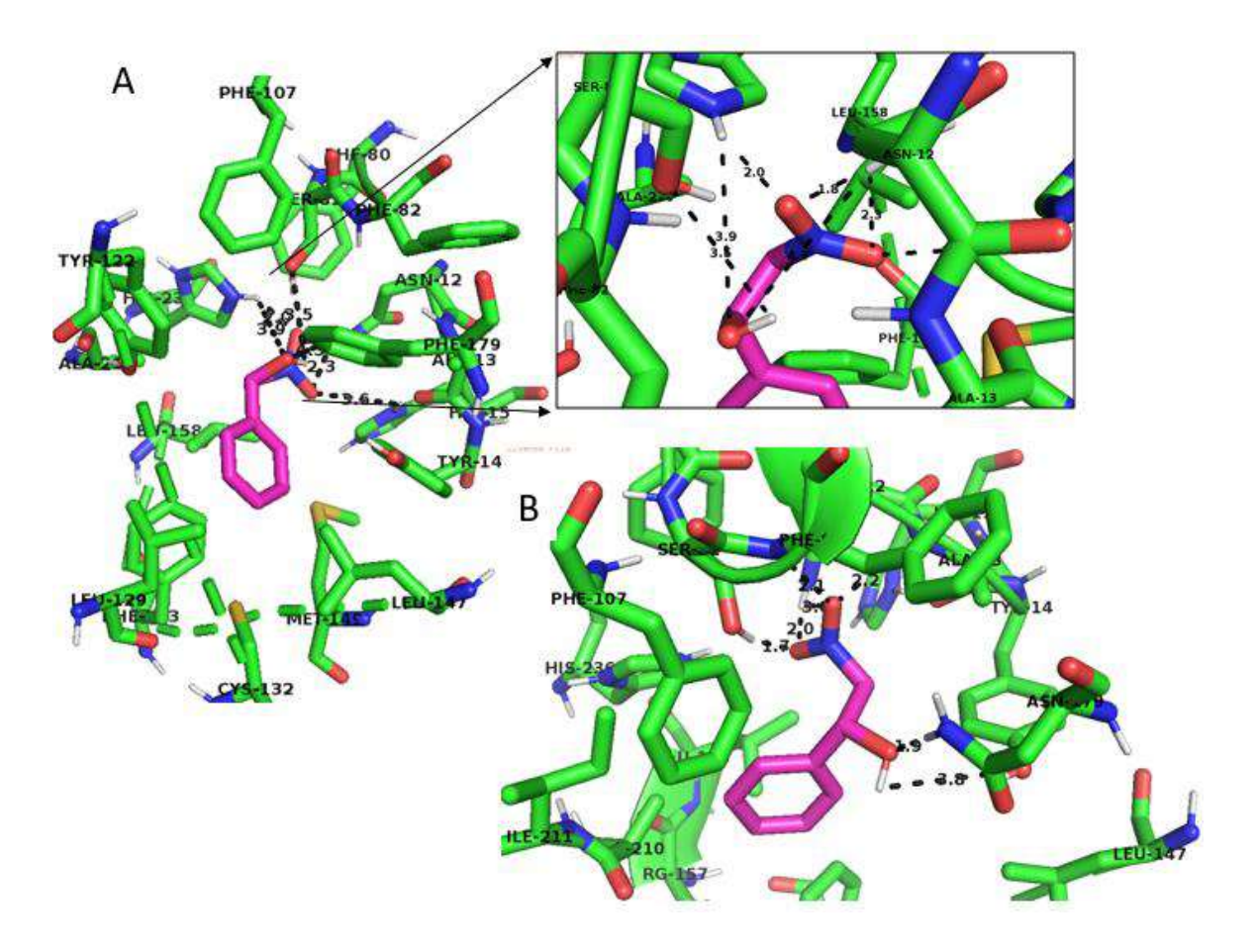


Figure 2.49: Important interactions between the enzyme and (R)-NPE in A) WT+(R)-NPE (enlarged active site shows H-bonds), B) F179N+(R)-NPE.

Table 2.8: Binding energy and active site distance to substrate calculation results for (R)-NPE and (S)-NPE in WT and modelled mutant proteins docking.

Enzyme	Substrate	Nitro group		Hydroxyl group		Binding energy
		Interacting atom	Distance (A°)	Interacting atom	Distance (A°)	(kcal.mol ⁻¹)
WT	(R)-NPE	H236-Nε2 N12-δ-NH H15-Nδ1	2.0 1.8, 2.3 3.6	S81-Ογ H236-Nε2 N12-δ-NH	3.5 3.9 4.3	-6.11
WT	(S)-NPE	S81-Oγ H236-Nε2 N12-δ-NH A13 main chain NH F82 main chain NH	1.7, 2.4 2.3 1.7, 2.8 2.4 2.6	S81-Ογ H236-Nε2 H15-Nδ1 N12-δ-NH	5.6 4.9 4.7 4.0	-6.29
F82A	(R)-NPE	S81-Oγ N12-δ-NH A13 main chain NH F82 main chain NH	2.6 3.5 1.9, 3.7 2.6, 1.8 (O2, O3)	S81-Ογ H236-Nε2 N12-δ-NH	1.8 2.4 1.8	-6.33
F82A	(S)-NPE	S81-Ογ H236-Νε2 N12-δ-NH	1.6 1.7 1.9, 3.2	S81-Ογ Υ122-Οη	4.5 2.1	-6.36
F179N	(R)-NPE	S81-Oγ N12-δ-NH F82 main chain NH A13 main chain NH	1.7 2.0, 3.0 (O2, O3) 2.1 2.2	N179-δ-NH Y14-Oη	1.9 3.8	-6.24
F179N	(S)-NPE	S81-Oγ N12-δ-NH H236-Nε2 N179-δ-NH	1.8 1.9 1.9 4.6	S81-Oγ N179-δ-NH F82 main chain CO	5.2 6.4 3.1	-5.57
F82A- F179N	(R)-NPE	N12-δ-NH H236-Nε2 A13 main chain NH H15-Nδ1	1.7, 2.4 2.0 2.8 4.1	S81-Oγ H236-Nε2 F82 main chain NH	2.1 3.8 3.7	-5.5
F82A- F179N	(S)-NPE	S81-Oγ H236-Nε2 N12-δ-NH A13 main chain NH	1.7 1.8 2.0, 3.2 4.1	S81-Ογ H236-Νε2 Y122-Οη A210 main chain CO	4.6 4.3 2.9 3.0	-5.7

2.4.9.4. RMSD and RMSF analysis

Molecular dynamic simulations (50 ns) of substrate in complex with WT and F179N was performed and analyzed their Root Mean Square deviations (RMSD) and Root Mean Square Fluctuations (RMSF) values (**Figure 2.50**). This flexibility in the catalytically relevant region was

further investigated by measuring the inter-atomic positions of C_{α} atoms of the catalytic triads (S81_D208, D208_H236 and S81_H236) (**Table 2.9**).

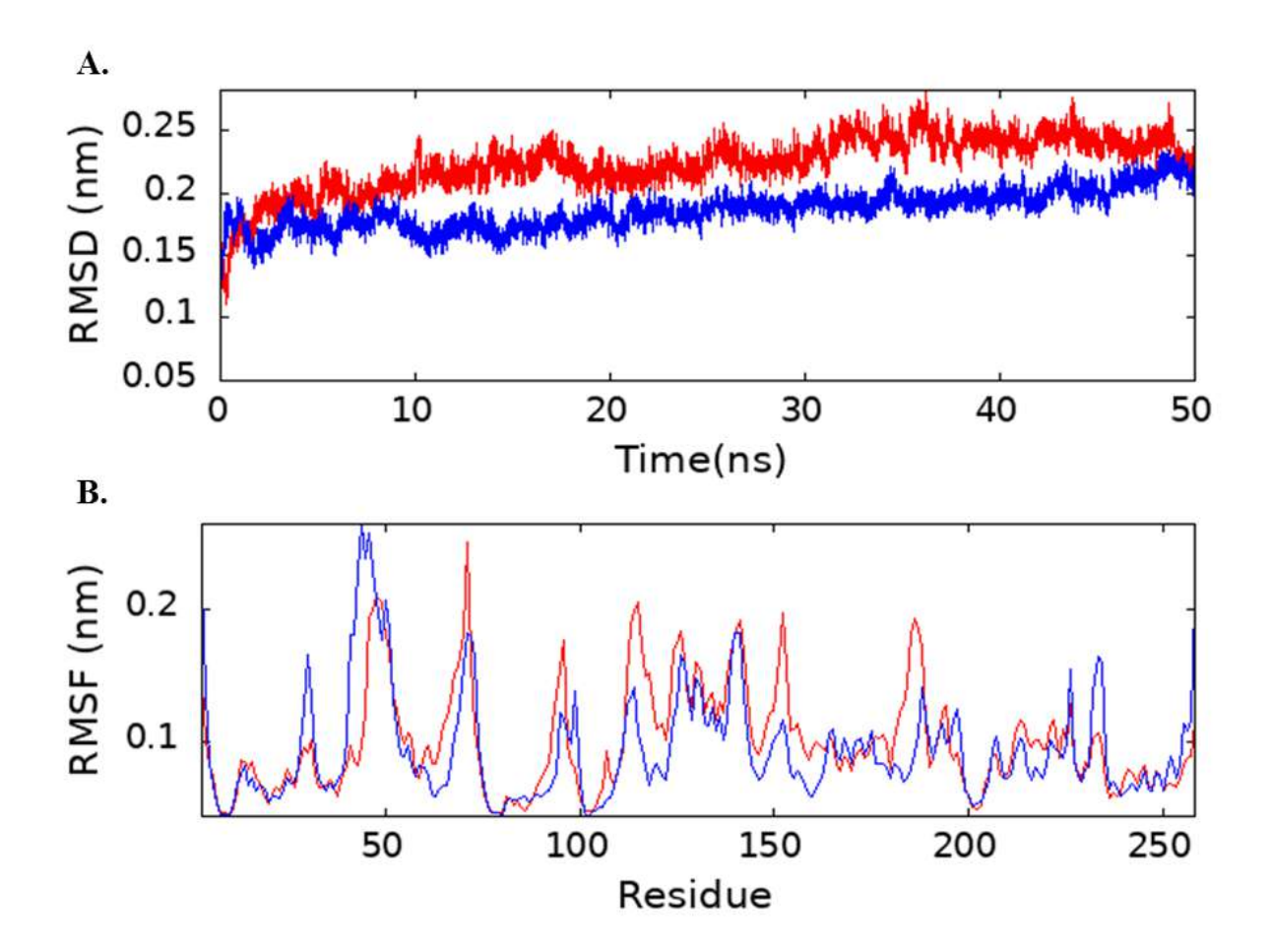


Figure 2.50: A) Backbone RMSD vs. Time B) RMSF vs. Residue Number for WT+ NPE (red), F179N +NPE (blue).

Table 2.9: Catalytic triad distance in nm between C_{α} atoms of proteins in WT and its mutant.

	WT + R-NPE	F179N+ <i>R</i> -NPE
Ser81_Asp208	1.15 ± 0.04	1.22 ± 0.06
Asp208 His236	0.5 ± 0.03	0.56 ± 0.05
Ser81 His236	0.8 ± 0.04	0.8 ± 0.04
_		

.

2.4.9.5. Evaluation of binding free energy of substrate complex with WT and mutant proteins

The MMPBSA calculations of substrate complexed with WT and F179N are given in **Table 2.10**. The mutant F179N possessed higher negative binding free energy value of –106 kJ/mol compared to the WT.

Table 2.10: Average MMPBSA free energy of substrate complex with WT and its mutant.

System	Energy (kJmol ⁻¹)								
	Van der Waals	Van der Waals Electrostatic Polar solvation SASA Total							
WT + R-NPE	-115.83	-25.84	56.98	-9.46	-94.15				
F179N + <i>R</i> -NPE	-128.46	-23.20	57.39	-11.75	-106.03				

2.4.9.6. Plausible retro-nitroaldol mechanism based on MDS study of substrate interaction

From the simulation studies, snapshots of interactions of (R)-NPE with the active site residues of WT at different time intervals, 10 to 50 ns, were collected. Based on the analysis of the results (**Figure 2.51, Table 2.11**), a plausible retro-nitroaldol mechanism by AtHNL is proposed as below (**Scheme 2.2**).

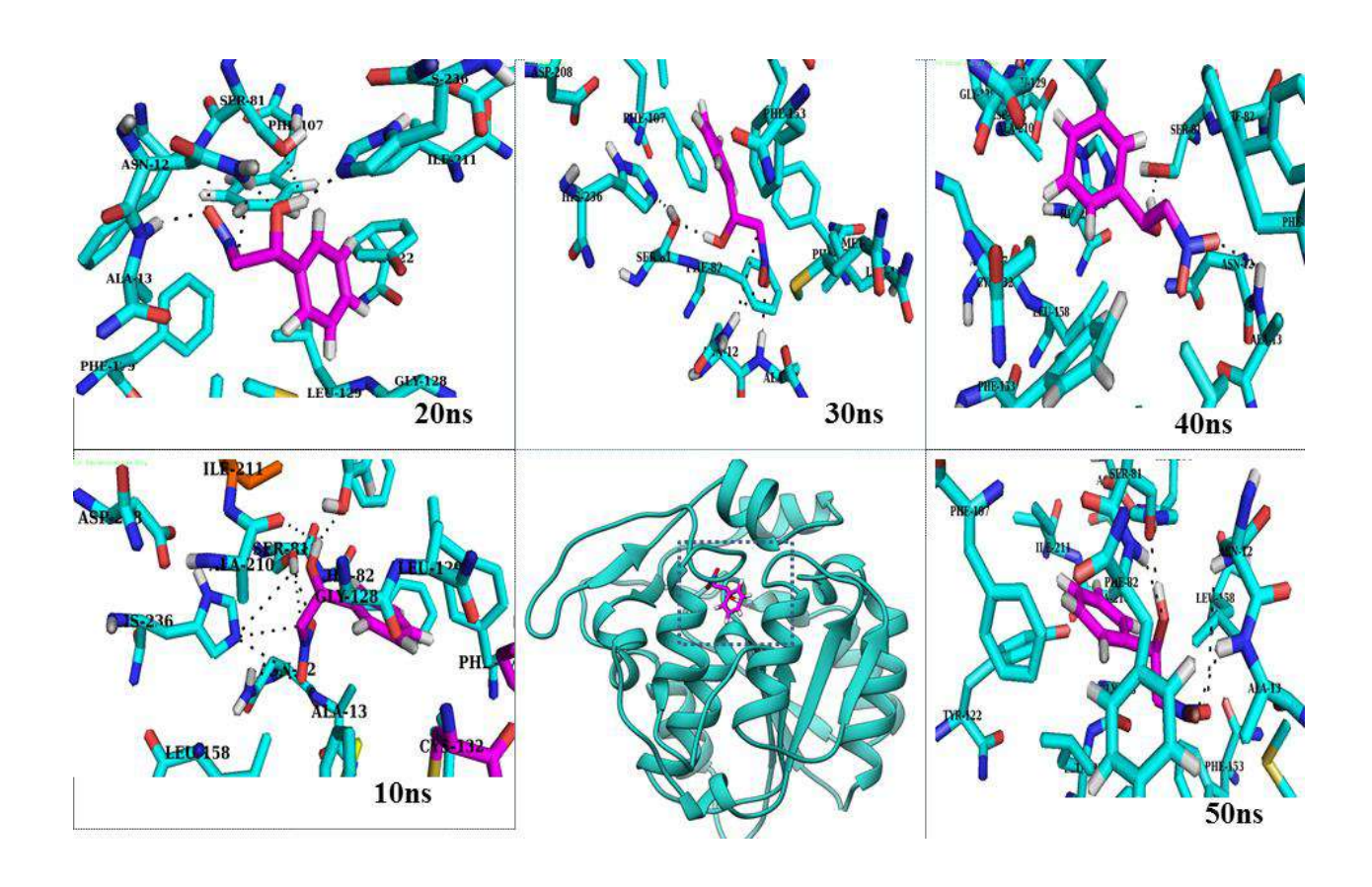


Figure 2.51: Active site interacting residues for WT complex with (*R*)-NPE at interval of 10-50 ns MDS.

Table 2.11: Active site distance to substrate at different time points from MDS study.

Time scale (ns)	Residue-atom	Residue-atom	Substrate-atom	Distance (A°)
0	D208-Oδ1	H236-Nδ1		1.7
	Η236-Νε2	S81-Oγ		2.8
		S81-Oγ	01	3.5
		Η236-Νε2	O2	2.0
		N12-δ-NH	O2	1.8
		N12-δ-NH	O3	2.3
		H15-Nδ1	O3	3.6
		S81-Oγ	C1	3.4
10	D208-Oδ1	H236-Nδ1		2.2
	Η236-Νε2	S81-Oγ		4.0
		S81-Oγ	01	3.3
		Υ122-Οη	01	2.6
		A210 main chain CO	01	3.4
		A13 main chain NH	O2	3.3
		S81-Oγ	O2	2.3

		A13 main chain NH	O3	3.2
		Ν12-δ-ΝΗ	O3	3.2
		Η236-Νε2	O3	3.6
		Η236-Νε2	C1	3.6
		S81-Oγ	C1	3.4
20	D208-Oδ1	Η236-Νδ1		2.1
	Η236-Νε2	S81-Oγ		4.5
		S81-Oγ	O1	3.9
		Η236-Νε2	O1	1.7
		Ν12-δ-ΝΗ	O1	2.1
		A13 main chain NH	O2	2.2
		F82 main chain NH	O2	2.1
		Ν12-δ-ΝΗ	C1	3.4
30	D208-Oδ1	Η236-Νδ1		2.5
	Η236-Νε2	S81-Oγ		2.1
		S81-Oγ	O1	1.9
		A13 main chain NH	O2	2.1
		Ν12-δ-ΝΗ	O3	2.1
		Ν12-δ-ΝΗ	C1	4.3
40	D208-Oδ1	Η236-Νδ1		2.1
	Η236-Νε2	S81-Ογ		1.9
		S81-Oγ	O1	2.0
		Ν12-δ-ΝΗ	01	2.1
		A13 main chain NH	O2	2.6
50	D208-Oδ1	Η236-Νδ1		2.1
	Η236-Νε2	S81-Ογ		1.8
		S81-Oγ	O1	1.7
		F82 main chain NH	O1	2.5
		A13 main chain NH	O2	2.8
		N12-δ-NH	O3	4.4

Atom numbering of the substrate used in the above table

Scheme 2.2: Proposed mechanism of retro-nitroaldolase activity by AtHNL based on MDS study of (R)-NPE interaction (not based on X-ray structure).

2.4.10. Preparative scale synthesis of (S)-NPE using AtHNL-F179N

To achieve maximum conversion and enantioselectivity, different optimization experiments were performed that include with (a) different units of enzyme at different time points (**Table 2.12**), (b) decreased % v/v of toluene (**Table 2.13**) and (c) increased % v/v of toluene (**Table 2.14**). The HPLC spectrum are given in **Figure 2.52-2.54**. The best condition was with 200 U of F179N with 65% v/v of toluene at 3h. Further, this was scaled up to 1000 U and ten mini preparative scale reactions each containing 1000 U of F179N was kept and the organic layers collected were combined, dried over anhydrous sodium sulphate and solvents were evaporated in a rotary evaporator. The product was analyzed by chiral HPLC as per **2.3.9** section. Column purification

of the crude product was done using hexane: ethyl acetate (90:10) to get pure NPE and confirmed by ¹H and ¹³C NMR (**Figure 2.55, 2.56**). Preparative scale synthesis of the retro-nitroaldol reaction has produced (*S*)-NPE in 92.88 % ee, and 48.6% isolated yield including ~20% ethyl acetate impurity (**Figure 2.57**).

Table 2.12: Optimization of retro-nitroaldolase activity of cell lysates of F179N at different enzyme units and time points.

	133 U		200 U		266 U		400 U	
Time (h)	% conv	% ee	%	% ee	% conv	% ee	%	% ee
			conv				conv	
3	45.85	46.97	48.12	80.61	46.51	85.32	46.98	82.94
6	44.87	62.97	46.07	85.65	43.14	80.93	43.61	77.61
9	45.55	81.86	42.39	84.67	43.65	74.25	40.99	71.76
12	43.09	86.83	42.62	83.49	38.59	71.18	39.95	70.36
24	35.04	91.15	35.38	71.97	29.08	55.46	38.16	63.00

Table 2.13: Optimization of retro-nitroaldolase activity of cell lysates of F179N (200 U) using different % v/v of toluene.

% v/v of toluene	65		6	0	50	
Time (h)	%	% ee	%	% ee	%	% ee
	conv		conv		conv	
3	48.12	88.30	42.64	87.76	37.22	80.34
4	46.39	91.05	43.45	86.72	39.05	81.08
5	45.79	90.82	43.10	85.40	33.94	73.81
6	44.74	88.79	40.67	81.80	38.06	75.91

Table 2.14: Optimization of retro-nitroaldolase activity of cell lysates of F179N (200 U) using higher contents of toluene

% v/v of toluene	65		7	0	75	
Time (h)	% ee		%	% ee	%	% ee
	conv		conv		conv	
2	44.76	75.99	45.51	74.46	45.27	72.87
3	44.12	88.74	46.46	85.99	44.53	80.40
4	43.79	89.55	45.49	87.62	44.24	85.79

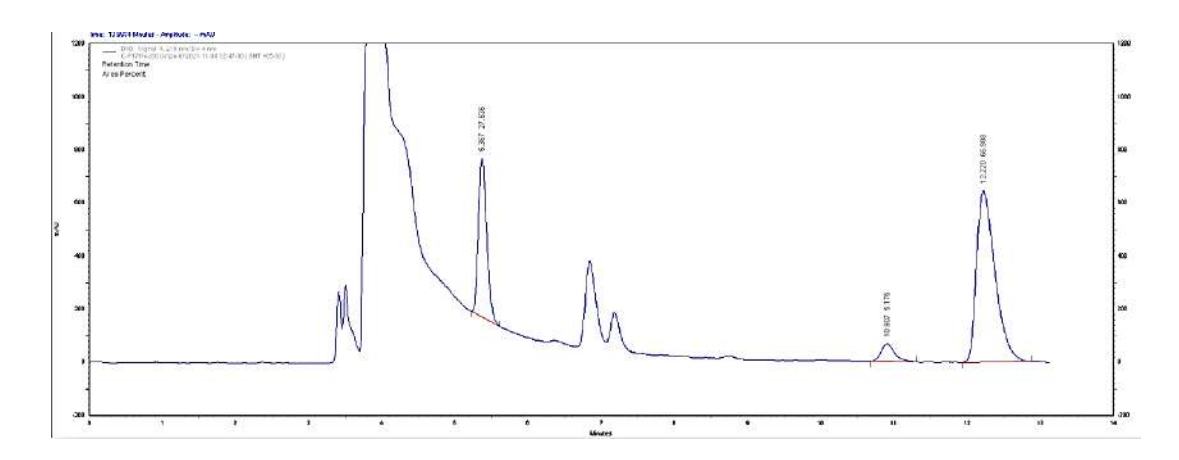


Figure 2.52: HPLC spectrum of F179N cell lysate catalyzed (200 U) enantioselective cleavage of rac-NPE at 6 h.

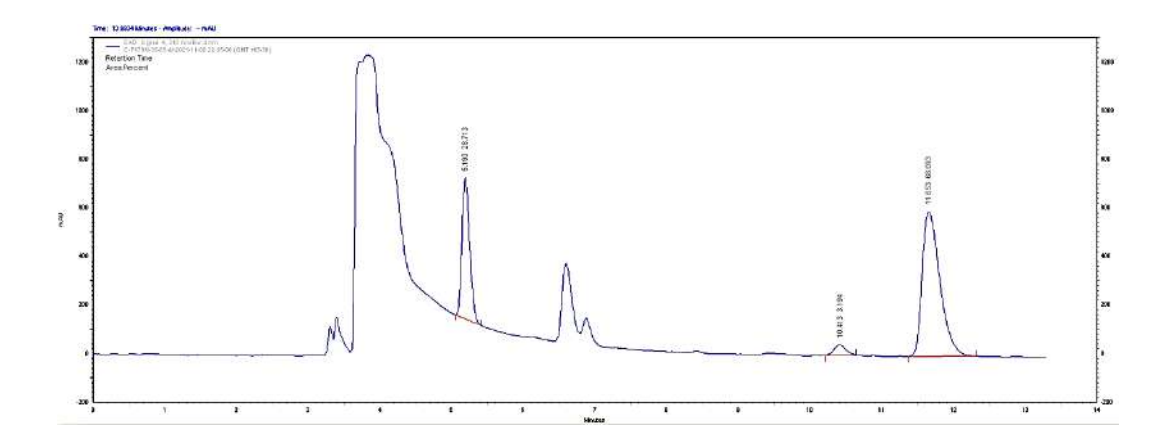


Figure 2.53: HPLC spectrum of F179N cell lysate catalyzed (200 U) enantioselective cleavage of rac-NPE in 65% v/v of toluene at 4 h.

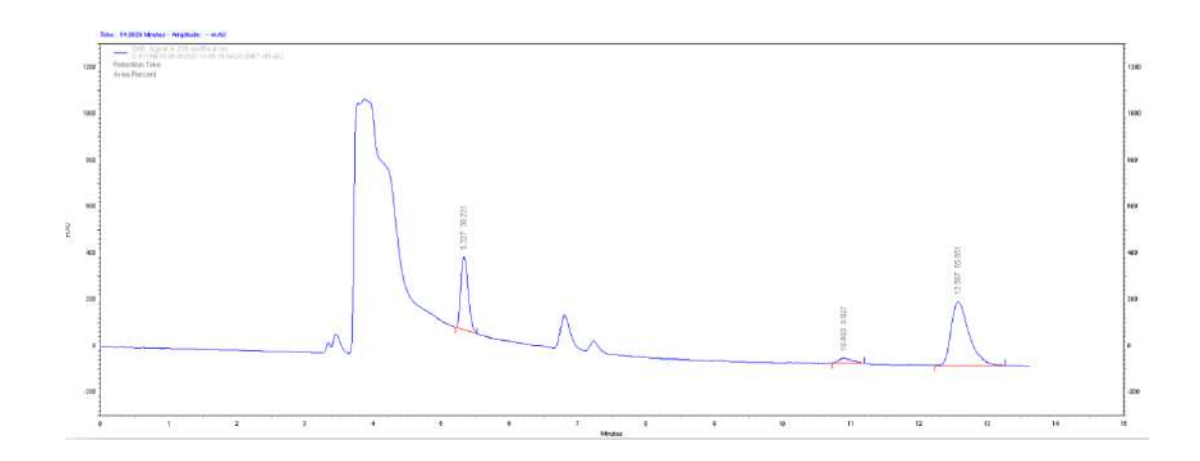


Figure 2.54: HPLC spectrum of F179N cell lysate catalyzed (200 U) enantioselective cleavage of rac-NPE in 65% v/v of toluene at 3 h.

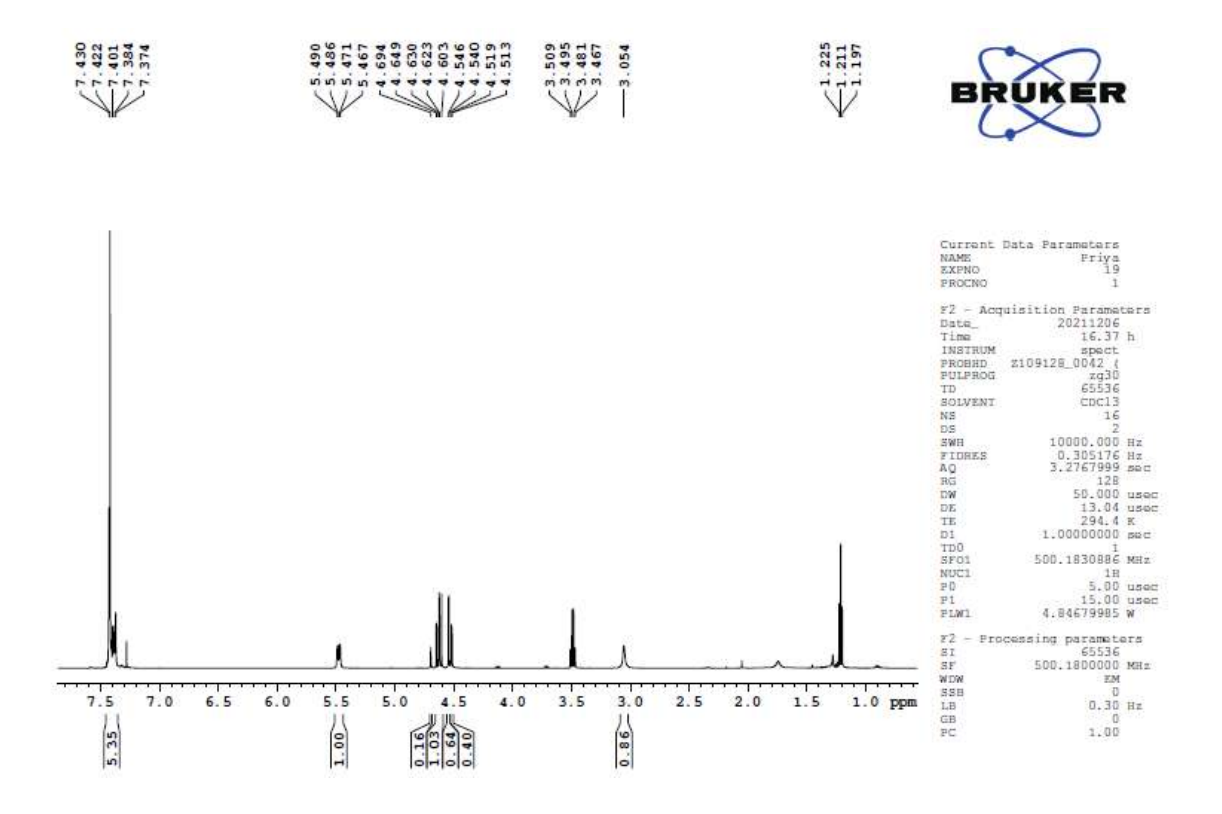


Figure 2.55: ¹H NMR of NPE obtained by of F179N cell lysate catalyzed enantioselective cleavage followed by column purification.

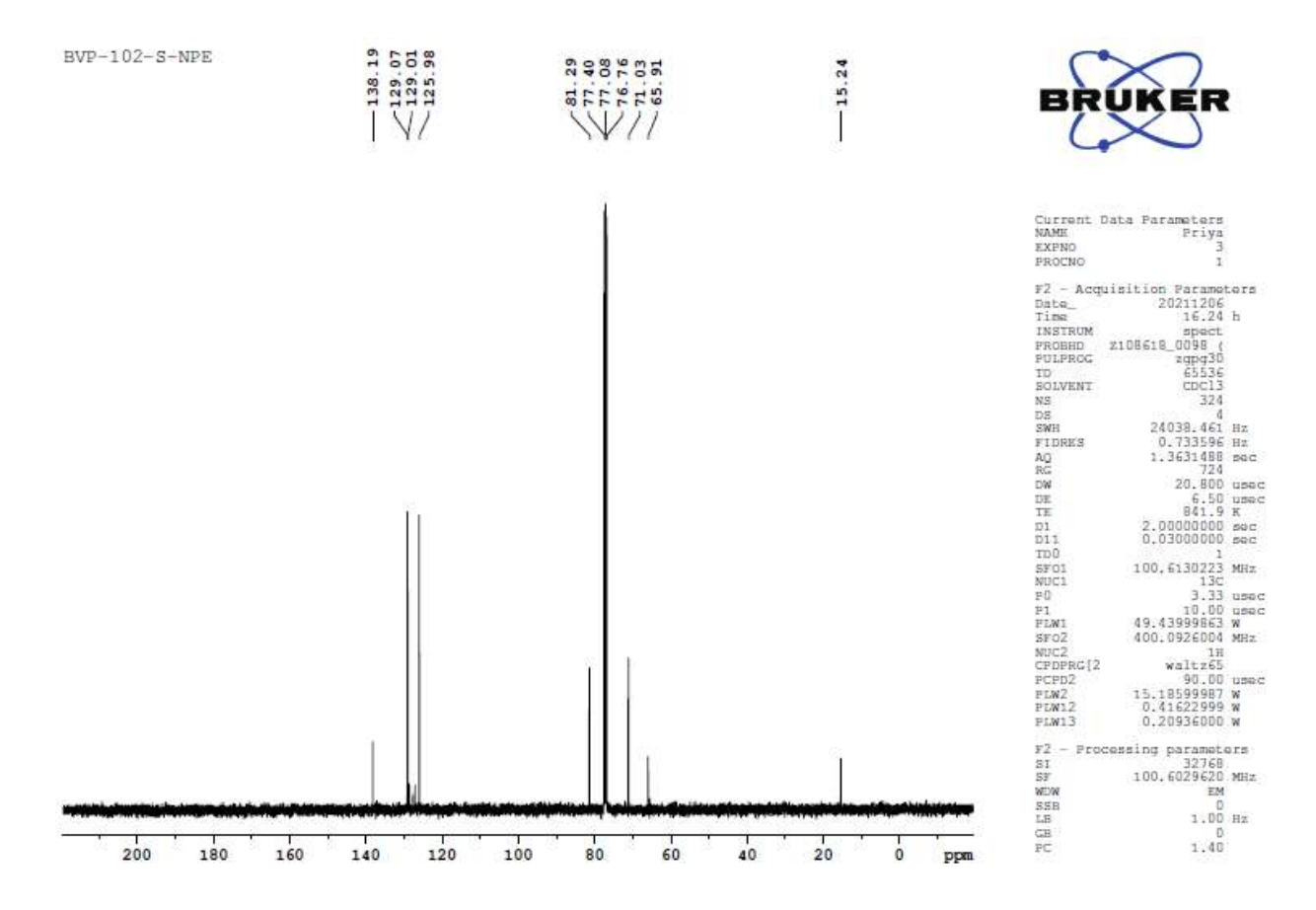


Figure 2.56: ¹³C NMR of NPE obtained by of F179N cell lysate catalyzed enantioselective cleavage followed by column purification.

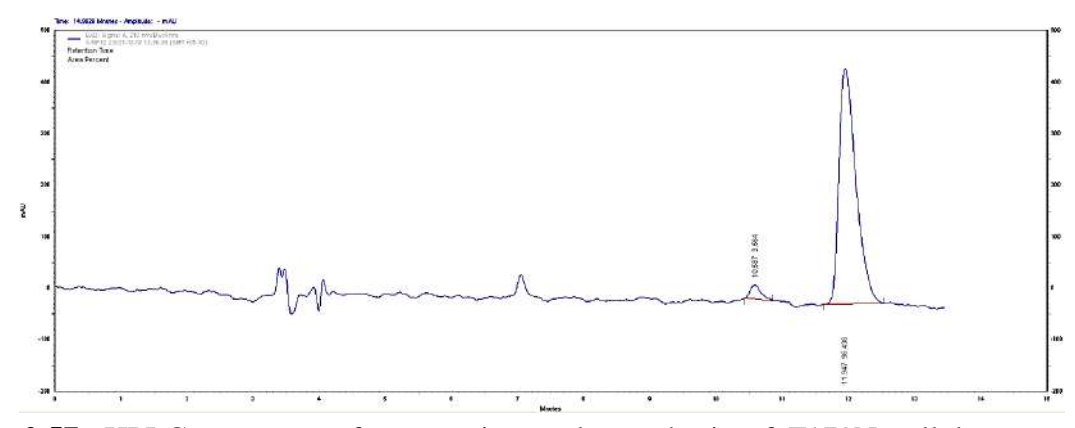


Figure 2.57: HPLC spectrum of preparative scale synthesis of F179N cell lysate catalyzed enantioselective cleavage of rac-NPE at 3 h after column purification, 92.88% *ee*.

2.5. Discussion

2.5.1. Kinetic studies of AtHNL toward cyanogenesis and retro-nitroaldol reaction

Our initial study aimed at understanding the kinetic properties of AtHNL towards cyanogenesis and retro-nitroaldol reaction. We have selected racemic MN and NPE as substrates due to the difficulty in getting their pure (R)-forms, to investigate the cyanogenesis and retro-nitroaldol kinetics respectively. Kinetic parameters of AtHNL for both the reactions were calculated from the Michaelis-Menten plot (**Table 2.3**, **Figure 2.2-2.3**). At HNL has shown V_{max} of 149.9 U/mg for MN cleavage, which is comparable with the earlier reports of 133.6²⁴ and 90 U/mg²⁵. We found $k_{\rm cat}$ 3797 min⁻¹ compared to 2530 min⁻¹ by Devamani et al. for MN cleavage²⁶. Its $V_{\rm max}$ for retronitroaldolase activity was found to be 1.75 U/mg, vs. 1.1 U/mg reported by us earlier¹¹. Comparison of the kinetics data between the two reactions revealed that AtHNL has nearly equal catalytic efficiency for both of these reactions. The $k_{\text{cat}}/K_{\text{m}}$ for MN cleavage was found to be $2772.20 \pm 217.4 \text{ vs } 3614.1 \pm 1762.03 \text{ min}^{-1}.\text{mM}^{-1}$ for NPE cleavage. Importantly, a comparison of the $K_{\rm m}$ values of AtHNL for both these reactions showed that the enzyme has ~110 times lower $K_{\rm m}$ for NPE cleavage than MN. This implies that NPE has a good binding affinity than MN with the WT-AtHNL. However, an assessment of the turnover number (k_{cat}) of AtHNL for these two different reactions showed that NPE cleavage is ~ 77 fold less efficient than MN cleavage. This result has inspired us to carry out the current study. We expected that AtHNL's promiscuous retronitroaldolase activity has the potential to be improved, and it could be explored for various synthetic applications. We hypothesized that engineering of AtHNL binding pocket may provide new variants with higher k_{cat} than the WT.

2.5.2. Docking studies to identify hot spots in AtHNL binding site

Docking of (R)-MN and (R)-NPE was performed into the catalytic site of AtHNL, to find out the differential binding of these two substrates. The aim was to identify residues in the binding site to be altered to enhance the retro-nitroaldolase activity of the enzyme. Structurally both (R)-MN and (R)-NPE share high degree of similarity, except the -CN is replaced by $-CH_2$ -NO₂ in the latter. Logically both the molecules should have a common binding site because the aromatic benzene ring and the secondary hydroxyl group are common in both the molecules. Even if the synthetic reactions were considered, the same enzyme uses benzaldehyde as a common substrate, while nitrile anion is used in the cyanation, for β -nitroalcohol synthesis the enzyme uses nitromethane as the nucleophile. Therefore, in principle, products of both the synthesis reactions, i.e., (R)-MN and (R)-NPE should be niched in the same binding pocket. We hoped that a comparison of both the Michaelis complex would reveal the difference in the binding of AtHNL with the two substrates. Such molecular insights will significantly help to understand and improve the catalytic potential of AtHNL for enantioselective retro-nitroaldol reaction.

To test the validity of our method, we first docked (R)-MN into the active site of AtHNL (**Table 2.7**, **Figure 2.47A**). The resulted model showed H bond donation from the –OH of (R)-MN to the enzyme. The H-bond acceptor could be Nɛ of His236, NH of δ -amide of Asn12, and –O γ of Ser81. H-bond donation by the oxyanion hole (Ala13 and Phe82 main chain NH) to the nitrile group of (R)-MN was also observed. These essential H-bond transfers constitutes the catalytically active conformation (CAC) and are in accordance with the AtHNL's cyanogenesis mechanism^{27,28}. In the case of the docking of (R)-NPE into AtHNL (**Figure 2.47B**), the Michaelis complex has established H-bonding between the –OH of the substrate with O γ of Ser81. The NO₂ group of (R)-NPE has made H- bonding with NH of δ -amide of Asn12 and Nɛ of His236. A H-bond between the main chain NH of Phe82 and the -NO₂ group of substrate could be possible. These results

suggests that His236, Ser81, Asn12, and Phe82 are important for the retro-nitroaldolase activity of *At*HNL. Subsequently, the modeled complexes of *At*HNL-(*R*)-MN and *At*HNL-(*R*)-NPE were superimposed (**Figure 2.47C**). We examined the overlaid structural models and compared the differential binding of the two substrates in the *At*HNL binding pocket. His236, Ser81, Asn12, Ala13, and Phe82 are believed to be important for cyanogenesis and retro-nitroaldolase activity (**Table 2.7**). Besides Phe82, another aromatic amino acid Phe179 was predicted to be important for substrate binding. A possible hydrophobic interaction was predicted between the substrate aromatic ring and the phenyl ring of Phe179 (4.5 Å). Both Phe82 and Phe179 are present within 5 Å from the active site Ser81.

2.5.3. Alanine mutants (Phe82 and Phe179) of AtHNL show higher selectivity for retronitroaldolase activity over cyanogenesis

We prepared alanine mutation of Phe82 and Phe179 to find out the role of these two residues in the catalysis of cyanogenesis and retro-nitroaldol reaction. Accordingly, three variants, F82A, F179A, and F82A-F179A were prepared (**Figure 2.1A**), and their structural integrity was studied using circular dichroism (CD) spectroscopy. It was observed that the CD spectra of F82A and F179A are similar to that of WT (**Figure 2.4**). In the case of F82A-F179A, there was a gradual decrease in its CD signal. The decrease of the CD signal indicates a decrease in helical secondary structure content. Using CDNN software, the percentage of secondary structures of the WT and the variants was quantified (**Table 2.2**). The percentage of α -helix of F82A and F179A was similar to that of WT whereas the percentage of α -helix of F82A-F179A drastically decreased which implies its instability and improper folding.

Kinetic studies of F82A and F179A were performed using cleavage of racemic MN and NPE separately (**Table 2.3**, **Figure 2.5-2.8**). F82A has shown a little increase in K_m , and decrease in k_{cat}

compared to the WT in the cyanogenesis reaction. Overall, the catalytic efficiency of F82A was decreased to ~62% of the WT for cyanogenesis. Jones et al. also observed decreased (R)-MN cleavage activity in the case of F82 and F179 variants of AtHNL²⁹. In the case of the retronitroaldol reaction, both F82A and F179A have shown low $K_{\rm m}$ similar to that of WT. This suggests that NPE has a good binding affinity than MN towards both these mutants, similar to the WT. However, the $V_{\rm max}$ of F82A, and F179A were decreased 1.8 and 1.35 fold respectively. The $k_{\rm cat}$ and $k_{\text{cat}}/K_{\text{m}}$ of both the variants also decreased for retro-nitroaldol reaction as compared to the WT. This result is in favor of our objective to find engineered AtHNL variants with higher binding affinity; although both of them showed lower catalytic efficiency than the WT. Further, we determined the selectivity of these variants as the ratio of catalytic efficiency of retro-nitroaldolase vs cyanogenesis activity. To our delight, F82A has shown almost similar selectivity to that of WT, while F179A showed 12 fold increased selectivity for retro-nitroaldolase activity over cyanogenesis. The importance of both of the positions is thus clear from the study for retronitroaldolase activity of AtHNL, especially the significance of Phe179. Additionally, the results suggest that alanine may not be the best substitute for the corresponding positions as none of them could show higher catalytic efficiency. This necessitates investigating the role of other residues at these positions.

2.5.4. Study of the binding pocket of AtHNL

We further attempted to identify residues in the *At*HNL binding site that could impact the promiscuous retro-nitroaldolase activity. From the modeled *At*HNL-(*R*)-NPE structure, we identified residues present within 5 Å from the substrate. The residues selected are: Asn12, Ala13, Tyr14, His15, Phe80, Ser81, Phe82, Phe107, Tyr122, Leu129, Cys132, Leu147, Met149, Phe153, Leu158, Phe179, Ala210, and His236 (**Figure 2.48**). As the nitroaldolase mechanism by any HNL

has not been established so far, we believed the participation of Asn12, Ser81, Phe82, and His236 in the retro-nitroaldolase mechanism based on the docking studies (**Table 2.7**). It was difficult to evaluate the possible role of the remaining dozen of positions that may impact on the retro-nitroaldolase activity of *AtHNL*. We have selected Tyr14 for protein engineering due to its close proximity with the two mechanistically important residues Asn12 and Ala13.

2.5.5. Semi-rational engineering: creating saturation libraries at positions Y14, F82 and F179

Based on the predicted role of the main chain NH of Phe82 in H-bond formation (**Table 2.7**), we hypothesized to replace it with polar residues, assuming possible polar interaction between substrate (nitro) and the replaced residue might stabilize the formation of Michaelis complex. Hence, instead of substituting Phe82 with any other amino acid, we have selected to use the MVK codon, which uses only 12 codons for eight polar amino acids (Asn, Gln, Pro, Ser, His, Thr, Arg, and Lys). In case of the other two positions, i.e., Phe179, and Tyr14, SSM was performed using the codon NNK. The library of variants was created using appropriate degenerate primers (**Table 2.1**), and each variant was confirmed by DNA sequencing.

2.5.6. Cyanogenesis and retro-nitroaldolase activity of AtHNL library of variants

The purified protein (**Figure 2.1: A-G, Table 2.4**) of each mutein from all the three libraries was used in a microtiter plate assay to measure cyanogenesis and retro-nitroaldolase activity. None of the Phe82 variants tested have shown higher retro-nitroaldolase activity than the WT (**Figure 2.9**). The activity data suggests that Phe82 is not only a critical position but a crucial residue for the retro-nitroaldolase activity of *At*HNL. These variants also produced lower cyanogenesis activity than the WT, emphasizing the importance of the residue in the catalysis of cleavage of cyanohydrin. Analysis of the retro-nitroaldolase activity of Phe179 series variants revealed that

ten of them have nearly the same or higher activity than the WT. In those variants, the Phe was substituted by Leu, Cys, His, Pro, Trp, Val, Ile, Thr, Asn, and Met (Figure 2.9). As these amino acid list includes polar, non-polar, aromatic, and aliphatic, so it is believed that Phe179 is a binding residue whose alteration with different amino acids provides a varied degree of NPE binding with the enzyme, which helps to increase the retro-nitroaldolase activity. However, it is hard to explain how other residues (A, D, G, S, R, E, Q, Y, and K) in place of Phe179 produced poor substrate binding. Interestingly, a few variants showed similar cyanogenesis activity to that of the WT, while most of them had lower than it. Screening of the Tyr14 SSM library also did not result in improved cyanogenesis activity. We found higher retro-nitroaldolase activity by two variants, Y14M and Y14L, as compared to the WT (Figure 2.9). To understand the role of the F179 and Y14 series of variants with higher retro-nitroaldolase activity, we have carried out kinetic studies of them.

2.5.7. Kinetics analysis of AtHNL variants for retro-nitroaldolase activity

A dozen of variants from the F179 and Y14 series showing greater retro-nitroaldolase activity than the WT (**Figure 2.9**) were selected. The corresponding purified enzymes were used to measure their steady-state kinetic parameters (**Figure 2.10-2.21**). **Table 2.5**, represents the data along with WT, F82A and F179A, discussed earlier. Analysis of the kinetic parameters of variants in the retro-aldolase activity revealed greater V_{max} and k_{cat} by eight of them than the WT. They are, F179M, F179N, F179W, F179T, F179V, and F179I in the F179 series, and Y14L and Y14M in the Y14 series. However, most of these variants have shown increased K_{m} values than the WT towards retro-nitroaldolase activity. F179N is the only one that showed a lower K_{m} value (0.006±0.0004) apart from greater V_{max} (1.91±0.02) and k_{cat} (53.34±0.65). The catalytic efficiency ($k_{\text{cat}}/K_{\text{m}}$) of the F179N was found to be ~2.4 fold greater than the WT. This result emphasizes the importance of F179 for retro-nitroaldolase activity.

2.5.8. At HNL variants catalyzed preparation of (S)-β-nitroalcohol

The fourteen variants of **Table 2.5** were evaluated for the retro-nitroaldol reaction using purified enzymes for the production of (S)- β -nitroalcohol. The products were analyzed by chiral HPLC to calculate the % ee and % conversion of (S)-NPE (Figure 2.22). Figure 2.23-2.39 represent their HPLC chromatograms. Analysis of the HPLC data revealed that except F82A, F179A and F179C, other variants have shown very good % ee of product. Loss of enantioselectivity was observed in the case of both F82A and F179A. This suggests that probably both the variants have lost the selectivity for binding to the (R)-NPE. Unselective binding to both the enantiomers can lead to poor catalytic activity (Figure 2.9). and enantioselectivity. In the case of F179L, F179H, F179T and F179P, % ee of the product was found to be in the range of 93-96, while the remaining variants showed excellent, (>99%) ee of (S)-NPE. The biocatalytic production of (S)-NPE in the retronitroaldol reaction by F179L, F179H, Y14L and Y14M was found to be less than the WT, (33-41%). The remaining variants showed higher % conversion than the WT. Further, to check the enantioselectivity of the variants and compare them with the WT, we have calculated their E values or the enantiomeric ratio (E) towards the preparation of (S)- β -nitroalcohol (**Figure 2.22**). The E value is commonly used to characterize the enantioselectivity in enzyme-catalyzed kinetic resolution. Two variants, F179V, and F179N, have shown greater E than the WT. The enantiomeric ratio of F179V was 86.9 vs. 81 for the WT. However, in the case of F179N, the E value was found to be 137.6, which is ~1.7 fold more than the WT. This confirms that F179N is a potent variant with higher enantioselectivity towards the production of (S)- β -nitroalcohol than the native enzyme.

2.5.9. Study of AtHNL double variants towards the retro-nitroaldol reaction

To further enhance the enantioselectivity and catalytic efficiency, we aimed to create double variants by adding mutations based on the successful results. Apart from F179N and F179V, we have selected F179W and F82A for this study. We did not consider F179M even though it showed an E value 58.85 as its $K_{\rm m}$ value is 52 folds more than WT. F82A was selected because it is the only other variant that had lower $K_{\rm m}$ than the WT towards the retro-nitroaldol reaction. We have created three double variants, F82A-F179N, F82A-F179V and F82A-F179W using appropriate primers (Table 2.1) and each variant was confirmed by DNA sequencing. The double variants were purified (Figure 2.1: H), and used to measure their steady-state kinetic parameters (Table **2.6**, Figure 2.40-2.42). Analysis of the kinetic parameters of these variants in the retro-aldolase activity revealed that F82A-F179N has the same $K_{\rm m}$ as that of the WT. Addition of F82A into F179N has not showed synergistic effect. The $K_{\rm m}$ of this double variant has increased compared to F179N, and k_{cat} was found to be lower than either of the WT and F179N. F82A-F179W and F82A-F179V have shown 1.2 and 3.2 fold increased $K_{\rm m}$ than the WT, while both showed similar $V_{\rm max}$ values i.e., 1.20 U/mg and k_{cat} values i.e., 33.6 min⁻¹ with only minimal deviation between them. In the case of F82A-F179W, both $K_{\rm m}$ and $k_{\rm cat}$ were found to be in between the single variants. Unfortunately, the catalytic efficiency of all the three double variants were found to be less than the WT. The enantioselectivity and conversion of the double variants towards retro-nitroaldol reaction were determined using the purified enzymes. We observed a very poor enantioselectivity (<4% ee) in the case of all the three double variants (**Figure 2.43**). **Figure 2.44-2.46** represent their HPLC chromatograms. The loss of enantioselectivity by the double variants is similar to the F82A. Although F82A was added with the hope to achieve lower K_m, its possible selectivity for both the enantiomers of NPE could have consequenced in the loss of enantioselectivity by all the three double variants.

2.5.10. Molecular docking and interaction studies to understand the substrate binding and enantioselectivity of the variants

Docking of (R)-NPE and (S)-NPE were performed into the catalytic site of AtHNL mutants F82A, F179N and F82A-F179N, along with the WT, to find out their binding efficiency and interactions with the substrate. The F82A-(S)-NPE has shown highest negative binding energy of -6.36 kcal/mol followed by -6.33 kcal/mol by F82A-(R)-NPE (**Table 2.8**). This suggests tight binding of both the substrate enantiomers with F82A than either WT or the double variant. This result resembles with our kinetics data, (lower $K_{\rm m}$ by F82A than the WT), in (**Table 2.6**). The active site distance to substrate calculations indicate that in case of both the enantiomers, essential H-bond transfers for catalytically active conformation (CAC) is satisfied. We speculate that, Y122 accepts a H-bond from the substrate –OH in the case of F82A-(S)-NPE, the role commonly played by S81. The loss of enantioselectivity in case of F82A is probably due to the preference to both substrate enantiomers by its active site. The double variant F82A-F179N, also showed a similar substrate preference to both the enantiomers of NPE, along with the lowest negative binding energy among the other proteins. Consequently, F82A-F179N also showed poor enantioselectivity towards retronitroaldol reaction. In case of WT, higher negative binding energy was observed with (S)-NPE binding than the (R)-enantiomer. However, based on the active site distance to substrate calculations, only WT-(R)-NPE complex could satisfy the required CAC. In the case of WT-(S)-NPE, crucial H-bond between the enzyme (Ser81 Oy) and substrate –OH group could not be established. This justifies the enantioselectivity by WT for the retro-nitroaldol reaction. Interestingly, the binding energy calculations clearly revealed the high preference of F179N for the (R)-NPE, over the (S)-enantiomer. Required H-bonds could establish CAC in the F179N-(R)-NPE complex, while the Ser81 conformation hinders the same in the case of F179N-(S)-NPE. We believe that both, the low binding energy and CAC in the case of F179N-(R)-NPE as compared to F179N-(S)-NPE, could explain the higher E value obtained by the F179N in the retro-nitroaldol reaction. The substrate interactions in case of both the WT and F179N, which showed enantioselectivity, are illustrated in **Figure 2.49**. It reveals important interactions between the enzyme and (R)-NPE. In the case of WT-(R)-NPE, catalytic residues His236, Ser81, Asn12, and main chain NH of the binding residue Phe82 are seen making H-bond with the substrate (**Figure 2.49A**). Significant differences in the interactions are noticed between F179N-(R)-NPE and WT-(R)-NPE. The former has His236-(R)-NPE H-bond missing. The anticipated key H-bond transfer between the substrate –OH group and Ser81 is replaced by NH of δ -amide of Asn179. Ser81 has made H-bonding the –NO2 of the substrate. Stabilization by Asn179 is not observed in the case of F179N-(S)-NPE complex (**Table 2.8**).

2.5.11. RMSD and RMSF analysis

In order to study the structural stability of docked complex and dynamics behavior of substrate in complex with WT and mutant, MDS was performed for 50 ns. The RMSD of backbone atoms of the two complexes (WT + R-NPE and F179N + R-NPE) against the 50 ns of simulations were found to be <2.5 Å. **Figure 2.50A** shows that the mutant complex has sustained the overall stability after 5 ns but WT tends to have slightly higher RMSD after 25 ns which were maintained till the end of the simulations. This suggests that substarte is better stabilized in the case of the mutant. Position and relative flexibility of each amino acid residue of WT AtHNL and F179N in complex with substrate (R)-NPE were analyzed. WT complex has shown relatively higher RMSF compared to the mutant. Moreover, the flexibility of residues around mutation site has not changed

significantly (**Figure 2.50B**). However, the mutant F179N showed a higher flexibility in catalytic relevant region. This flexibility in the catalytically relevant region was further investigated by measuring the inter-atomic positions of C_{α} atoms of the catalytic triads (S81_D208, D208_H236 and S81_H236). In the case of F179N, the inter-atomic positions of C_{α} atoms between S81_D208 was found to be deviated from its original positions compared to the WT (**Table 2.9**). Such higher inter-atomic distance probably suggests better adjustability with the substrate leading to efficient catalysis.

2.5.12. Evaluation of binding free energy of substrate complex with WT and mutant proteins

The MMPBSA calculations of substrate complexed with WT and mutant proteins are given in **Table 2.10.** The mutant F179N possessed higher negative binding free energy value of -106 kJ/mol compared to the WT. These binding energies suggest a significant potential for the formation of stable molecular interactions between amino acid residues of F179N and NPE. Interestingly, Van der Waals, electrostatic interactions and non-polar solvation energy negatively contributed to the total interaction energy for the mutant F179N, while for WT only polar solvation energy positively contributing to the total free-binding energy. The negative binding free energy supports our experimental low K_m by the F179N for NPE (**Table 2.6**).

2.5.13. Plausible retro-nitroaldol mechanism based on MDS study of substrate interaction

From the MDS study, snapshots of interactions of (R)-NPE with the active site residues of WT at different time intervals, 10 to 50 ns, were collected. Based on the analysis of the results (**Figure 2.51, Table 2.11**), we propose here a plausible retro-nitroaldol mechanism by AtHNL (**Scheme 2.2**). In addition to the catalytic triad, Asp208-His236-Ser81, the NH of δ -amide of Asn12, and main chain NH of Ala13 and Phe82 are believed to play crucial role in the catalysis. The substrate

bound complex is stabilized by H-bonds between His236, NH of δ -amide of Asn12 and the two oxygen atoms of the nitro group of the substrate (**II of Scheme 2.2**). The catalytic His236 accepts a proton from the Ser81, which initiates the deprotonation of the substrate hydroxyl group. The next important step is the elimination of nitromethane carbanion that results in the formation of benzaldehyde. The carbonyl oxygen interacts with His236 and NH of δ -amide of Asn12. While the carbanion center is stabilized by a H-bond with the NH of δ -amide of Asn12, its nitro group makes H-bond with the main chain NH of Ala13 and Phe82 (they are believed to be cyanide anion stabilizers in mandelonitrile cleavage mechanism) (**III of Scheme 2.2**)³⁰. A proton transfer from His236 to the nitromethane carbanion via Ser81 produces nitromethane. This mechanism resembles to the cyanogenesis mechanism by AtHNL²⁴.

Our mutagenesis study supports this mechanism. Phe82 is a crucial residue for the intermediate nitromethane carbanion stabilization and hence important for the retro-nitroaldol mechanism. Although its main chain NH is involved in the H-bond interaction, any modification at Phe82 has failed to retain both the retro-nitroaldolase and cyanogenesis activity.

2.5.14. Preparative scale synthesis of (S)-NPE using AtHNL-F179N

Optimization of cell lysates of F179N catalyzed retro-nitroaldol reaction with different units of enzyme has produced (*S*)-NPE in 86% ee and 46% conversion in case of 200 U of the enzyme at 6 h (**Figure 2.52, Table 2.12**). Subsequent optimization of the biotransformation using varied % v/v of toluene from 50 to 65, with 200 U of F179N has resulted in 91% ee of (*S*)-NPE with 43.5% conversion in case of 65% v/v of toluene in 4 h (**Figure 2.53, Table 2.13**). Further investigation of the optimization with increased contents of toluene from 65 to 75% v/v, showed similar results with maximum 46.5% conversion and 89% ee of product at 3 h (**Figure 2.54, Table 2.14**). The best condition was with 200 U of F179N with 65% v/v of toluene at 3h. Further, this was scaled

up to 1000 U and ten mini preparative scale reactions each containing 1000 U of F179N was kept and the organic layers collected were combined, dried over anhydrous sodium sulphate and solvents were evaporated in a rotary evaporator. The product was analyzed by chiral HPLC as per 2.3.9 section. Column purification of the crude product was done using hexane: ethyl acetate (90:10) to get pure NPE and confirmed by ¹H and ¹³C NMR (**Figure 2.55, 2.56**). Preparative scale synthesis of the retro-nitroaldol reaction has produced (*S*)-NPE in 92.88 % ee, and 48.6% isolated yield including ~20% ethyl acetate impurity (**Figure 2.57**).

2.6. Conclusions

The catalytic efficiency of AtHNL was enhanced by protein engineering towards promiscuous retro-nitroaldol reaction, which is emerging as an important route to prepare enantiopure βnitroalcohols. Our preliminary kinetic studies suggested that AtHNL has a higher binding affinity for NPE than MN. Based on docking and binding site analysis, we identified Phe82, Phe179, and Tyr14 of AtHNL to investigate and improve the retro-nitroaldolase activity. Alanine substitution at Phe179 has resulted in ~12 fold increased retro-nitroaldolase selectivity over cyanogenesis. Replacing Phe82 by polar residues has resulted in loss of retro-nitroaldolase activity, which indicates that Phe82 is crucial for the concerned catalysis. Analysis of the retro-nitroaldolase activity of variants of two SSM libraries of Phe179 and Tyr14 series has uncovered a dozen of them having nearly the same or higher activity than the WT. Kinetics study of fourteen selected variants has revealed that eight (F179M, F179N, F179W, F179T, F179V, F179I, Y14L and Y14M) of them have greater V_{max} and k_{cat} than the WT, while F179N is the only one that showed a lower $K_{\rm m}(0.006\pm0.0004~{\rm mM})$ apart from greater $V_{\rm max}(1.91\pm0.02~{\rm U/mg})$ and $k_{\rm cat}(53.34\pm0.65~{\rm min^{-1}})$. The catalytic efficiency (k_{cat}/K_m) of the F179N was found to be ~2.4 fold greater than the WT. Two variants, F179V, and F179N, have shown greater E than the WT. In the case of F179N, the E value

was found to be 137.6, which is ~1.7 fold more than the WT. This is the first study that revealed the importance of Phe179 for retro-nitroaldolase activity of AtHNL. Preparative scale synthesis of (S)-NPE using crude cell lysates of F179N under optimized conditions produced 93% ee, and 48.6% isolated yield of the product including ~20% ethyl acetate impurity. Three double variants, F82A-F179N, F82A-F179V and F82A-F179W, created by addition of mutations based on lower $K_{\rm m}$ and higher $k_{\rm cat}$ for retro-nitroaldolase activity, showed poor catalytic efficiency than the WT. Complete loss of enantioselectivity was observed in the case of all the three double variants. Docking of both enantiomers of NPE with the WT and mutants illustrated higher negative binding energy in the case of F179N with the (R)-NPE than the (S). CAC could not be achieved in the case of WT and F179N with (S)-NPE, which explains the higher enantioselectivity of F179N towards retro-nitroaldol reaction. The enzyme-substrate interaction plots (PyMol) have supported the strong substrate binding by the F179N, as observed from kinetics studies. Molecular dynamics simulation study on structural stability of the docked complexes on a 50 ns time scale has revealed higher stability by the F179N complex than the WT beyond 25 ns. The RMSF calculations along with inter-atomic positions of C_{α} atoms of the catalytic triads has suggested higher flexibility in the case of F179N, which supports its efficient catalysis. MMPBSA calculations showed the higher negative binding free energy in the case of F179N-(R)-NPE complex compared to WT. This observation further supports our experimental low K_m by the F179N for NPE. Based on the interaction between (R)-NPE and AtHNL WT at different time intervals from the MDS study, a plausible retro-nitroaldol mechanism was proposed.

2.7. References

(1) Leveson-Gower, R. B.; Mayer, C.; Roelfes, G. The Importance of Catalytic Promiscuity for Enzyme Design and Evolution. *Nat. Rev. Chem.* **2019**, *3* (12), 687–705.

- https://doi.org/10.1038/s41570-019-0143-x.
- (2) Dadashipour, M.; Asano, Y. Hydroxynitrile Lyases: Insights into Biochemistry, Discovery, and Engineering. *ACS Catal.* **2011**, *1* (9), 1121–1149. https://doi.org/10.1021/cs200325q.
- (3) Padhi, S. K. Modern Approaches to Discovering New Hydroxynitrile Lyases for Biocatalysis. *ChemBioChem* **2017**, *18*, 152–160. https://doi.org/10.1002/cbic.201600495.
- (4) Jangir, N.; Padhi, S. K. Immobilized *Baliospermum Montanum* Hydroxynitrile Lyase Catalyzed Synthesis of Chiral Cyanohydrins. *Bioorg. Chem.* **2019**, 84 (November 2018), 32–40. https://doi.org/10.1016/j.bioorg.2018.11.017.
- (5) Bracco, P.; Busch, H.; Von Langermann, J.; Hanefeld, U. Enantioselective Synthesis of Cyanohydrins Catalysed by Hydroxynitrile Lyases-a Review. *Org. Biomol. Chem.* **2016**, *14* (27), 6375–6389. https://doi.org/10.1039/c6ob00934d.
- (6) Purkarthofer, T.; Gruber, K.; Gruber-Khadjawi, M.; Waich, K.; Skranc, W.; Mink, D.; Griengl, H. A Biocatalytic Henry Reaction The Hydroxynitrile Lyase from Hevea Brasiliensis Also Catalyzes Nitroaldol Reactions. *Angew. Chemie Int. Ed.* 2006, 45 (21), 3454–3456. https://doi.org/10.1002/anie.200504230.
- (7) Fuhshuku, K. I.; Asano, Y. Synthesis of (R)-Beta-Nitro Alcohols Catalyzed by R-Selective Hydroxynitrile Lyase from Arabidopsis Thaliana in the Aqueous-Organic Biphasic System. *J. Biotechnol.* **2011**, *153* (3–4), 153–159. https://doi.org/10.1016/j.jbiotec.2011.03.011.
- (8) Bekerle-Bogner, M.; Gruber-Khadjawi, M.; Wiltsche, H.; Wiedner, R.; Schwab, H.; Steiner, K. (R)-Selective Nitroaldol Reaction Catalyzed by Metal-Dependent Bacterial Hydroxynitrile Lyases. *ChemCatChem* 2016, 8 (13), 2214–2216. https://doi.org/10.1002/cctc.201600150.
- (9) Rao, D. H. S.; Chatterjee, A.; Padhi, S. K. Biocatalytic Approaches for Enantio and

- Diastereoselective Synthesis of Chiral β-Nitroalcohols. *Org. Biomol. Chem.* **2021**, *19* (2), 322–337. https://doi.org/10.1039/d0ob02019b.
- (10) Ayon Chatterjee, D.H. Sreenivasa Rao, and S. K. P. One-Pot Enzyme Cascade Catalyzed Asymmetrization of Primary Alcohols: Synthesis of Enantiocomplementary Chiral β-Nitroalcohols. *Adv. Synth. Catal.* **2021**, *363* (23), 5310–5318. https://doi.org/10.1002/adsc.202100803.
- (11) Rao, D. H. S.; Padhi, S. K. Production of (S)-β-Nitro Alcohols by Enantioselective C–C Bond Cleavage with an R-Selective Hydroxynitrile Lyase. *ChemBioChem* **2019**, *20* (3), 371–378. https://doi.org/10.1002/cbic.201800416.
- (12) Yuryev, R.; Briechle, S.; Gruber-Khadjawi, M.; Griengl, H.; Liese, A. Asymmetric Retro-Henry Reaction Catalyzed by Hydroxynitrile Lyase from Hevea Brasiliensis. *ChemCatChem* **2010**, 2 (8), 981–986. https://doi.org/10.1002/cctc.201000147.
- (13) Rao, D. H. S.; Shivani, K.; Padhi, S. K. Immobilized Arabidopsis Thaliana Hydroxynitrile Lyase-Catalyzed Retro-Henry Reaction in the Synthesis of (S)-β-Nitroalcohols. *Appl. Biochem. Biotechnol.* **2021**,*193* (2), 560–576. https://doi.org/10.1007/s12010-020-03442-3.
- (14) Vongvilai, P.; Angelin, M.; Larsson, R.; Ramström, O. Dynamic Combinatorial Resolution: Direct Asymmetric Lipase-Mediated Screening of a Dynamic Nitroaldol Library. *Angew. Chemie - Int. Ed.* 2007, 46 (6), 948–950. https://doi.org/10.1002/anie.200603740.
- (15) Sorgedrager, M. J.; Malpique, R.; Van Rantwijk, F.; Sheldon, R. A. Lipase Catalysed Resolution of Nitro Aldol Adducts. *Tetrahedron Asymmetry* **2004**, *15* (8), 1295–1299. https://doi.org/10.1016/j.tetasy.2004.02.025.
- (16) Vongvilai, P.; Larsson, R.; Ramström, O. Direct Asymmetric Dynamic Kinetic Resolution by Combined Lipase Catalysis and Nitroaldol (Henry) Reaction. *Adv. Synth. Catal.* **2008**,

- 350 (3), 448–452. https://doi.org/10.1002/adsc.200700432.
- (17) Chen, C.; Fujimoto, Y.; Girdaukas, G.; Sih, C. J. Quantitative Analyses of Biochemical Kinetic Resolutions of Enantiomers' 1. *J. Am. Chem. Soc.* **1982**, *104*, 7294–7299.
- (18) Garrett M. Morris, Ruth Huey, William Lindstrom, Michel F. Sanner, Richard K. Belew, David S. Goodsell, A. J. O. AutoDock4 and AutoDockTools4: Automated Docking with Selective Receptor Flexibility GARRETT. *J. Comput. Chem.* 2009, 30, 2785–2791. https://doi.org/10.1002/jcc.
- (19) Pronk, S.; Páll, S.; Schulz, R.; Larsson, P.; Bjelkmar, P.; Apostolov, R.; Shirts, M. R.; Smith, J. C.; Kasson, P. M.; Van Der Spoel, D.; Hess, B.; Lindahl, E. GROMACS 4.5: A High-Throughput and Highly Parallel Open Source Molecular Simulation Toolkit. *Bioinformatics* 2013, 29 (7), 845–854. https://doi.org/10.1093/bioinformatics/btt055.
- (20) Hess, B.; Kutzner, C.; Van Der Spoel, D.; Lindahl, E. GRGMACS 4: Algorithms for Highly Efficient, Load-Balanced, and Scalable Molecular Simulation. *J. Chem. Theory Comput.* **2008**, *4* (3), 435–447. https://doi.org/10.1021/ct700301q.
- (21) Schüttelkopf, A. W.; Van Aalten, D. M. F. PRODRG: A Tool for High-Throughput Crystallography of Protein-Ligand Complexes. *Acta Crystallogr. Sect. D Biol. Crystallogr.* **2004**, *60* (8), 1355–1363. https://doi.org/10.1107/S0907444904011679.
- (22) Hess, B. P-LINCS: A Parallel Linear Constraint Solver for Molecular Simulation. *J. Chem. Theory Comput.* **2008**, *4* (1), 116–122. https://doi.org/10.1021/ct700200b.
- (23) Kumari, R.; Kumar, R.; Lynn, A. G-Mmpbsa -A GROMACS Tool for High-Throughput MM-PBSA Calculations. *J. Chem. Inf. Model.* **2014**, *54* (7), 1951–1962. https://doi.org/10.1021/ci500020m.
- (24) Okrob, D.; Metzner, J.; Wiechert, W.; Gruber, K.; Pohl, M. Tailoring a Stabilized Variant

- of Hydroxynitrile Lyase from Arabidopsis Thaliana. *ChemBioChem* **2012**, *13* (6), 797–802. https://doi.org/10.1002/cbic.201100619.
- (25) Guterl, J. K.; Andexer, J. N.; Sehl, T.; von Langermann, J.; Frindi-Wosch, I.; Rosenkranz, T.; Fitter, J.; Gruber, K.; Kragl, U.; Eggert, T.; Pohl, M. Uneven Twins: Comparison of Two Enantiocomplementary Hydroxynitrile Lyases with α/β-Hydrolase Fold. *J. Biotechnol.* 2009, 141 (3–4), 166–173. https://doi.org/10.1016/j.jbiotec.2009.03.010.
- (26) Kazlauskas, R. J.; Devamani, T.; Rauwerdink, A. M.; Lunzer, M.; Jones, B. J.; Mooney, J. L.; Tan, M. A. O.; Zhang, Z. J.; Xu, J. H.; Dean, A. M. Catalytic Promiscuity of Ancestral Esterases and Hydroxynitrile Lyases. *J. Am. Chem. Soc.* 2016, *138* (3), 1046–1056. https://doi.org/10.1021/jacs.5b12209.
- (27) Andexer, J. N.; Staunig, N.; Eggert, T.; Kratky, C.; Pohl, M.; Gruber, K. Hydroxynitrile Lyases with α/β-Hydrolase Fold: Two Enzymes with Almost Identical 3D Structures but Opposite Enantioselectivities and Different Reaction Mechanisms. *ChemBioChem* **2012**, *13* (13), 1932–1939. https://doi.org/10.1002/cbic.201200239.
- (28) Zhu, W.; Liu, Y.; Zhang, R. A QM/MM Study of the Reaction Mechanism of (R)-Hydroxynitrile Lyases from Arabidopsis Thaliana (AtHNL). *Proteins Struct. Funct. Bioinforma*. **2015**, *83* (1), 66–77. https://doi.org/10.1002/prot.24648.
- (29) Jones, B. J.; Bata, Z.; Kazlauskas, R. J. Identical Active Sites in Hydroxynitrile Lyases Show Opposite Enantioselectivity and Reveal Possible Ancestral Mechanism. ACS Catal. 2017, 7 (6), 4221–4229. https://doi.org/10.1021/acscatal.7b01108.
- (30) Rauwerdink, A.; Kazlauskas, R. J. How the Same Core Catalytic Machinery Catalyzes 17 Different Reactions: The Serine-Histidine-Aspartate Catalytic Triad of α/β-Hydrolase Fold Enzymes. *ACS Catal.* **2015**, *5* (10), 6153–6176. https://doi.org/10.1021/acscatal.5b01539.

Chapter 3: Enantioselective synthesis of diverse (R)- β -nitroalcohols by engineered AtHNL using promiscuous nitroaldol reaction

3.1. Introduction

A huge demand has grown in the global market towards the synthesis of enantiopure drugs due to their inherent therapeutic behavior in the biological system. Optically pure compounds are very important to synthesize these enantiomerically pure drugs. Chiral β-nitroalcohols are one such important optically pure synthons for the synthesis of various enantiopure drugs that have gained much attention in the recent times and several routes have been reported for their synthesis $^{1-3}$. One such method is Henry reaction or nitroaldol reaction which is an important and classic transformation in organic synthesis⁴. It involves a carbon-carbon bond formation usually a coupling between a nucleophilic nitro alkane with an electrophilic aldehyde (or ketone) to form βnitroalcohol (Scheme 1.5). The different functional groups present in the β -nitroalcohol structure can easily be transformed into other chiral building blocks. The nitro group of β-nitroalcohol moiety can easily be transformed into other chiral building blocks by oxidation, reduction, Nef reaction and nucleophilic displacement (**Scheme 1.4**). Chiral β -nitroalcohols are the precursors for different drugs, biologically active molecules and natural products (Figure 1.3). In organic chemistry, several metals and non-metal-based catalysts have been reported in the asymmetric synthesis β-nitroalcohols^{5–23}. Currently, synthesis of chiral molecules using green and ecofriendly catalysis is being chosen to avoid the complications formed in the reactions catalyzed by chemical catalysts. Due to their environment friendly and high selectivity enzyme-based catalysis or biocatalysis is the best alternative unlike chemical catalysis for green and sustainable organic transformations.

There exist several biocatalytic routes in the synthesis of enantiopure β -nitroalcohols such as Henry reaction, kinetic resolution, retro-Henry reaction, dynamic kinetic resolution, and asymmetric reduction^{24–39}. Among all the above mentioned, the most important biocatalytic route

to synthesize chiral β-nitroalcohols is using Henry reaction catalyzed by HNLs. In addition to their natural enantioselective hydrocyanation activity, a few HNLs catalyze promiscuous stereoselective Henry reaction. Among HNLs, (S)-selective HNLs from Hevea brasiliensis (HbHNL)³⁹, Baliospermum montanum (BmHNL)⁴⁰ and (R)-selective HNLs from Arabidopsis thaliana (AtHNL), Granulicella tundricola (GtHNL) and Acidobacterium capsulatum (AcHNL)³⁵ are reported to catalyze the stereoselective Henry reaction. Both (R)-selective GtHNL and AcHNL, are metal dependent cupin fold HNLs that require metal cofactor in the catalysis of enantioselective Henry reaction and their substrate scope is limited to only four substrates. Yu et al. reported an acyl-peptide releasing enzyme from Sulfolobus tokodaii (ST0779) catalyzing promiscuous Henry reaction, which took long reaction time for its catalysis and did not show uniform enantiopreference, as its enantioselectivity varied with the electronic effects of the substituents on the benzaldehyde ring⁴¹. So far, AtHNL is the only (R)-selective HNL reported to catalyse promiscuous Henry reaction without any cofactor requirement for its catalysis. However, AtHNL's promiscuous nitroaldolase activity is limited to poor yield (2-34%) and low enantioselectivity²⁹. In a recent study, AtHNL was employed in a cascade reaction to synthesize (R)- β -nitroalcohols and observed poor enantioselectivity in case of several of aromatic aldehydes as substrates⁴⁰.

To make the nitroaldol reaction an efficient biocatalytic method, the efficiency of the biocatalytic reaction needs to be improved. Recently, engineered AtHNLs have been used in the synthesis of (S)-β-nitroalcohol via retro-Henry reaction⁴². Several AtHNL variants were employed to synthesize (S)-β-nitroalcohol for a better enantioselectivity. In the present chapter, we aimed to investigate those AtHNL variants towards promiscuous nitroaldol reaction (**Scheme 3.1**). Variants of all the three saturation libraries used in the previous study were explored in the enantioselective synthesis of (R)-β-nitroalcohols using Henry reaction. The primary screening of the variants using

benzaldehyde and nitromethane as substrates has identified several of them showing >96% *ee* (F179A, F179H, F179C, F179N, F179L, F179M, F179V, F179K, F179W, Y14K, Y14R), >95% *ee* (Y14F, F179S), >93% *ee* (Y14C and Y14M), while the conversion reached up to >33% in case of Y14C, Y14F, and Y14A. Subsequently selected variants, i.e., F179H, F179N, F179L, and F179W from the F179 saturation library and Y14A, Y14C, Y14F, Y14M, Y14G, Y14L and Y14T from the Y14 saturation library were employed in the synthesis of diverse (*R*)-β-nitroalcohols. The experimental results revealed that the *At*HNL variants have overcome several existing limitations and provided improve yield, enhanced enantioselectivity and expanded substrate scope towards the promiscuous niroaldol reaction (**Scheme 3.1**).

Scheme 3.1: Biocatalytic asymmetric Henry reaction in synthesis of (R)- β -nitroalcohols using engineered AtHNLs.

3.2. Objectives

- 1. To screen all the three saturation library variants towards enantioselective nitroaldol synthesis using benzaldehyde and nitromethane as substrates.
- 2. To develop analytical methods for chiral resolution of all racemic β -nitroalcohols using HPLC chiral column.
- 3. To synthesize diverse (R)- β -nitroalcohols using selected AtHNL variants.

- 4. To create the multiple variants to be used for the enantioselective nitroaldol reaction.
- 5. To study the AtHNL multiple variants in the synthesis of various (R)- β -nitroalcohols.

3.3. Materials and methods

3.3.1. Chemicals and materials

AtHNL (UniProt accession ID: Q9LFT6) synthetic gene cloned in pET28a was obtained from Abgenex Pvt. Ltd, India. Culture media and kanamycin were procured from HiMedia laboratory Pvt. Ltd, India. Isopropyl-β-D-1-thiogalactopyranoside (IPTG) was purchased from BR-BIOCHEM Pvt. Ltd, India. Chemicals such as aldehydes, nitromethane and mandelonitrile were purchased from Sigma Aldrich, AVRA, SRL and Alfa-Aesar. HPLC grade solvents were obtained from RANKEM, Molychem, FINAR, and SRL.

3.3.2. Mutagenesis

3.3.2.1. Creation of SSM library at F82, F179, and Y14

Site saturation and site directed mutagenesis was done as per the procedure described in **section**2.3.3.1 in **chapter 2**. The primers employed in this work are mentioned **Table 2.1**.

3.3.2.2. Creation of *At*HNL double variants

To prepare Y14F-F179N, and Y14F-F179W, PCR composition and conditions were maintained similar to that described in **2.3.3.1** in **chapter 2**, F179N and F179W plasmids were taken as templates and forward and reverse primers for Y14F (**Table 2.1**) were used in the PCR. To prepare Y14M-F179N and Y14M-F179W, we used Y14M plasmid as a template with F179N (**Table 2.1**) and F179W (**Table 3.1**) forward and reverse primers with same PCR conditions as described in **2.3.3.1** of **chapter 2**.

Table 3.1: Primers used to prepare Y14M-F179W double variant in this study. Italicized nucleotides are the site of mutation.

Name	Sequence
F179W - FP	GTCAAGGCAGC <i>TGG</i> TTTACCGAGGAT
F179W - RP	ATCCTCGGTAAA <i>CCA</i> GCTGCCTTGAC

3.3.3. Enzyme expression and purification

Expression and purification of *At*HNL and its variants was performed as described in section **2.3.4** of **Chapter 2**.

3.3.4. HNL assay

The assay was performed in a 96 well microtiter plate and was monitored using a Multiskan GO UV–Visible spectrophotometer at 25°C. Each well contained reaction mixture of 160 μ L of 50 mM citrate phosphate buffer (pH 5.5), 20 μ L purified enzyme (1 mg/mL), and 20 μ L substrate (racemic MN, 67 mM) pre-dissolved in 1 mL of 5 mM citrate buffer (pH 3.15) making a total volume of 200 μ L. The control experiment was carried out identically except the enzyme is replaced with 20 mM KPB, pH 7.0. The assay was done in triplicates and the absorbance of the control resulting due to the spontaneous reaction was subtracted from the enzymatic reaction. The assay measured the formation of benzaldehyde resulting from enzymatic cleavage of MN at 280 mm. The activity was calculated using the molar extinction coefficient of benzaldehyde (1376 M⁻¹ cm⁻¹).

3.3.5. Synthesis of racemic β-nitroalcohols

Synthesis of various racemic β -nitroalcohols was carried out by addition of aldehydes to nitromethane in 1:10 molar ratio in the presence of 5 mol% of Ba(OH)₂ as a catalyst as per the procedure described in the paper previously published from our lab⁴³.

3.3.6. Screening of AtHNL and its variants for (R)-NPE synthesis

A reaction mixture of 1 mL containing 125 units of purified variant enzyme and n-butyl acetate in equal v/v ratio along with 25 μ L of nitromethane and 12.5 μ mol of the benzaldehyde was taken in a 2 mL glass vial. In the control, the enzyme was replaced by an equal volume of 20 mM potassium phosphate buffer (KPB). The reaction mixture was placed on a thermomixer at 1,200 rpm for 3 h at 30 °C. After every hour, 100 μ L of aliquot was taken and extracted with 150 μ L of diethyl ether. To this, a pinch of sodium sulfate was added and vortexed. After centrifugation at 10,000 rpm for 2 min at 4°C, the upper layer was taken and this step was repeated one more time. Finally, 20 μ L of the upper organic layer was taken and analyzed in an HPLC (Agilent) using Chiralpak® IB chiral column using 1 mL/min flow rate and 90:10 of hexane: isopropanol. The % conversion represents the absolute amount of (R)-NPE, and was calculated by the equation % C= $\left[\frac{S-NPE+R-NPE}{S-NPE+R-NPE+benzaldehyde*conversion factor}\right]$ and % $ee = \left[\frac{(R-S)}{(S+R)}\right]*100$.

3.3.7. At HNL variant catalyzed preparation of various (R)- β -nitroalcohols using nitroaldol reaction

A reaction mixture consisting of 62.5-125 units of purified variant enzyme and *n*-butyl acetate in equal v/v ratio along with 1.75 M of nitromethane and 20 mM of aldehyde was taken in a 2 mL glass vial. After the reaction, the remaining protocols for extraction and HPLC analysis are the same as mentioned in **section 3.3.6**.

3.4. Results

3.4.1. SDS-PAGE of purified *At*HNL and its variants

The wild type *At*HNL and its variants generated using SDM and SSM were purified as described in section **2.3.4** above and were characterized by SDS-PAGE (**Figure 2.1: A-H; Figure 3.1**). All the pure proteins were analyzed by 12% SDS-PAGE using medium range pre-stained protein marker (BR-BIOCHEM) and stained by Coomassie Brilliant Blue R-250. A clear band at ~28 kDa indicated the good expression and purity of the purified *At*HNL and its variants.

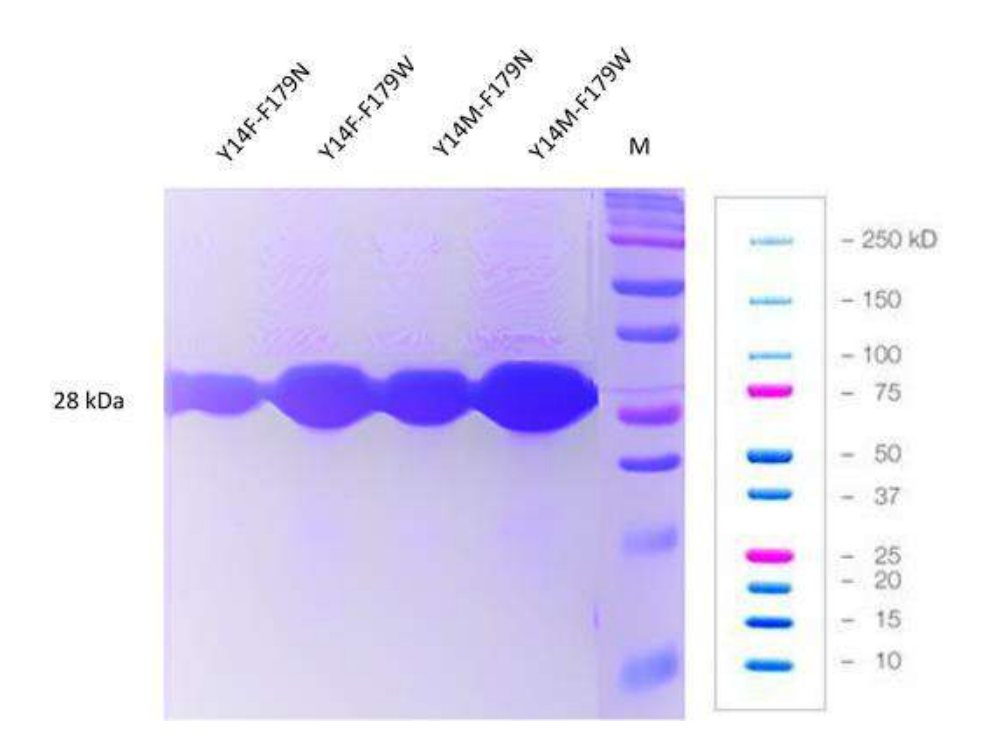


Figure 3.1: SDS-PAGE analysis of Ni-NTA purified *At*HNL double variants. Lane M: standard protein marker.

3.4.2. Screening of AtHNL and its variants for (R)-NPE synthesis

A primary screening of all the saturation library variants was carried out towards the synthesis of (*R*)-2-nitro-1-phenylethanol (NPE) using promiscuous nitroaldol reaction (**Figure 3.2**). The purified

variantsts from the three libraries were used in the nitroaldol reaction and were analyzed by chiral HPLC (Scheme 3.2, Table 3.2; Figure 3.3-3.48).

$$H$$
 + CH_3NO_2 AtHNL eng variants NO_2 R)-2-nitro-1-phenylethanol or R)-NPE

Scheme 3.2: Screening of *At*HNL variants towards enantioselective synthesis of (*R*)-NPE.

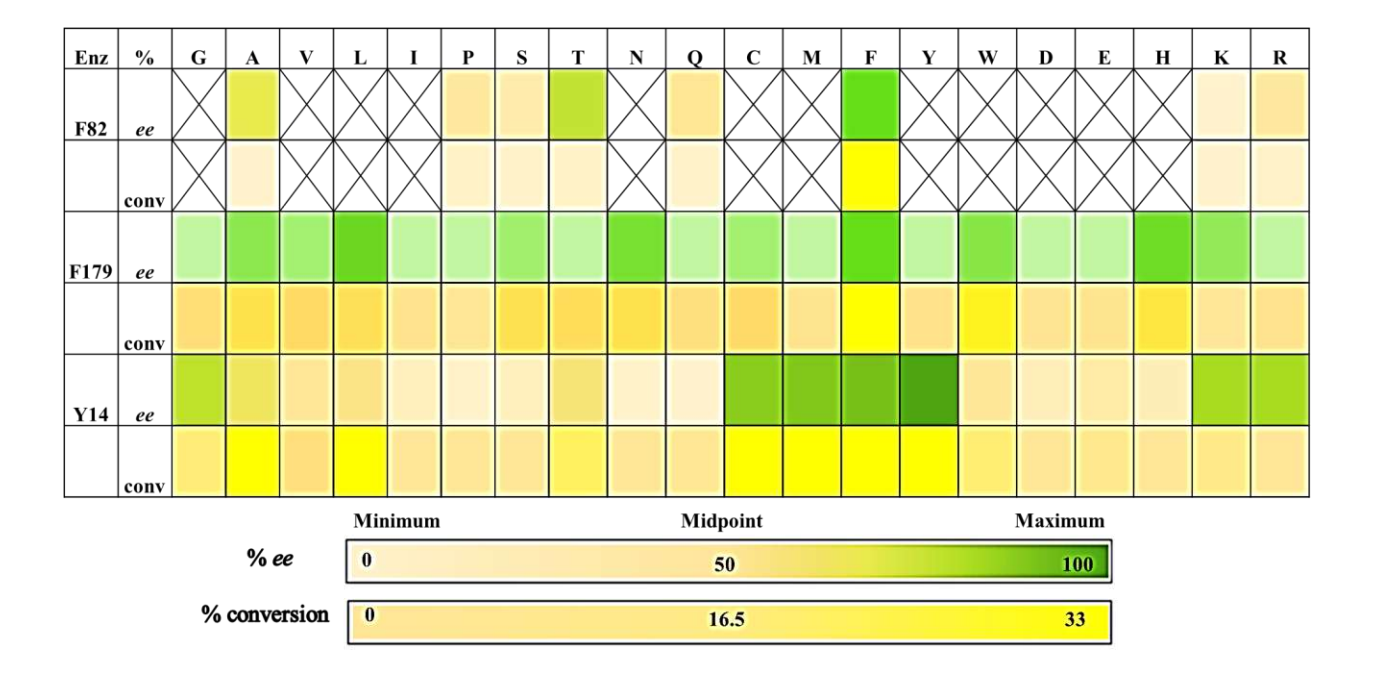


Figure 3.2: Primary screening of *At*HNL variants altered at positions F82, F179 and Y14 in the synthesis of (*R*)-NPE. The 2 h analysis data is considered and used here to draw the heat map.

Table 3.2a: Enantioselective synthesis of (*R*)-NPE catalysed by F82 saturation library variants.

S. No	Variants	1 h		2 h		3 h	
		% conv	% ee	% conv	% ee	% conv	% ee
1	WT	17.45	97.5	23.31	96.32	24.45	96.24
2	F82A	0.22	66.67	0.14	33.33	0.8	48.35

3	F82K	0.15	-11.11	0.16	-28	0.42	-28.87
4	F82T	0.23	62.96	1.03	50.85	0.87	60.40
5	F82R	0.48	-9.41	0.68	-6.07	0.99	-4.68
6	F82S	0.15	-21.12	0.26	-12.19	0.35	-6.67
7	F82P	0.69	-13.29	0.87	-6.57	1.18	-3.0
8	F82Q	0.24	-1.79	0.46	-0.46	0.62	0.7

Table 3.2b: Enantioselective synthesis of (R)-2-nitrophenyl ethanol catalysed by F179 saturation library variants.

S. No	Variants	1 h		2 h		3 h	
		% conv	% ee	% conv	% ee	% conv	% ee
1	WT	17.45	97.5	23.31	96.32	24.45	96.24
2	F179A	3.09	98.77	8.97	98.10	13.01	98.11
3	F179H	6.3	98.3	11.01	97.29	12.09	95.9
4	F179S	5.5	94.32	7.94	95.1	8.19	96.39
5	F179C	2.68	96.97	3.78	97.74	3.78	97.96
6	F179P	0.15	7.04	0.25	3.33	0.60	2.86
7	F179R	0.39	1.64	0.96	6.94	1.00	3.83
8	F179N	6.26	97.34	8.47	96.87	10.13	94.39
9	F179Q	4.91	94.43	2.14	67.89	0.34	86.25
10	F179G	1.57	79.06	2.72	78.23	3.11	77.44
11	F179I	0.50	10.64	1.00	32.62	1.84	5.10
12	F179E	0.25	4.35	0.78	0.81	1.27	7.56
13	F179L	6.52	98.62	7.32	97.49	7.82	96.72
14	F179M	0.34	97.52	0.72	94.64	0.99	96.99
15	F179T	2.56	77.35	4.19	83.59	6.1	81.21
16	F179V	1.85	96.89	4.18	96.95	3.79	97.18
17	F179K	4.82	95.30	7.22	95.74	9.19	94.1
18	F179Y	0.85	83.8	1.3	84.42	2.16	91.3

19	F179W	16.58	97.1	17.37	96.20	17.9	91.11
20	F179D	0.25	5.17	0.59	1.45	1.13	3.98

Table 3.2c: Enantioselective synthesis of (R)-2-nitrophenyl ethanol catalysed by Y14 saturation library variants

S. No	Variants	1 h		2 h		3 h	
		% conv	% ee	% conv	% ee	% conv	% ee
1	WT	17.45	97.5	23.31	96.32	24.45	96.24
2	Y14A	28.61	87.91	33.2	89.37	34.61	86.79
3	Y14C	29.84	95.32	32.53	93.96	34.05	91.95
4	Y14Q	22.01	88.35	3.33	-0.13	3.05	-38.35
5	Y14H	0.30	28.21	0.73	36.56	1.55	53.65
6	Y14N	0.77	4.11	0.98	9.84	1.3	2.8
7	Y14P	0.8	25	1.36	33.13	1.95	2.40
8	Y14S	0.23	11.86	0.65	28.14	1.06	37.5
9	Y14D	7.42	88.20	1.55	33.90	1.64	30.99
10	Y14F	30.65	97.00	32.89	94.68	33.95	92.60
11	Y14M	22.90	96.04	28.16	94.26	30.38	91.23
12	Y14V	11.79	77.89	18.58	76.92	24.83	70.50
13	Y14W	10.31	88.53	13.21	85.88	15.01	82.92
14	Y14L	22.81	93.54	23.01	87.43	23.47	83.84
15	Y14E	5.31	70.44	6.2	64.88	6.86	62.7
16	Y14T	14.57	87.82	15.1	88.17	15.4	86.09
17	Y14K	5.46	97.50	10.72	96.57	10.63	95.62
18	Y14G	8.52	94.16	12.94	92.18	13.02	73.73
19	Y14I	0.52	-5.82	0.08	28.57	0.01	100
20	Y14R	0.19	88.41	0.13	95.74	0.01	-100

Based on the above results (**Table 3.2; Figure 3.3-3.48**), eleven different *At*HNL variants, i.e., F179H, F179N, F179L, and F179W from the F179 saturation library and Y14A, Y14C, Y14F, Y14M, Y14G, Y14L and Y14T from the Y14 saturation library were selected for further study to explore their potential in the synthesis of diverse (*R*)-β-nitroalcohols.

3.4.2.1. HPLC chromatograms of AtHNL and its variants catalyzed synthesis of (R)-NPE

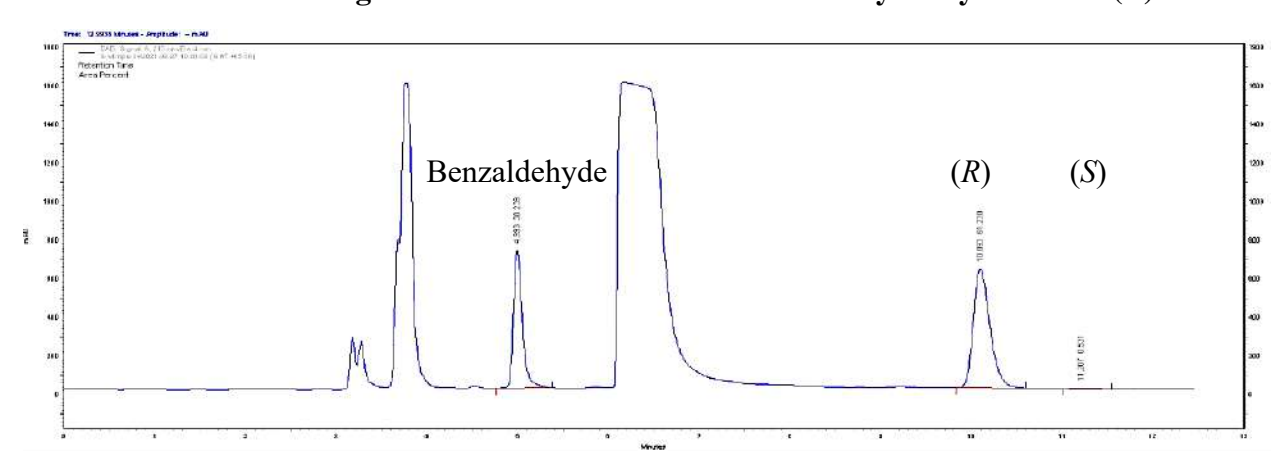


Figure 3.3: HPLC spectrum of wild type *At*HNL showing enantioselective synthesis of (*R*)-NPE at 2 h.

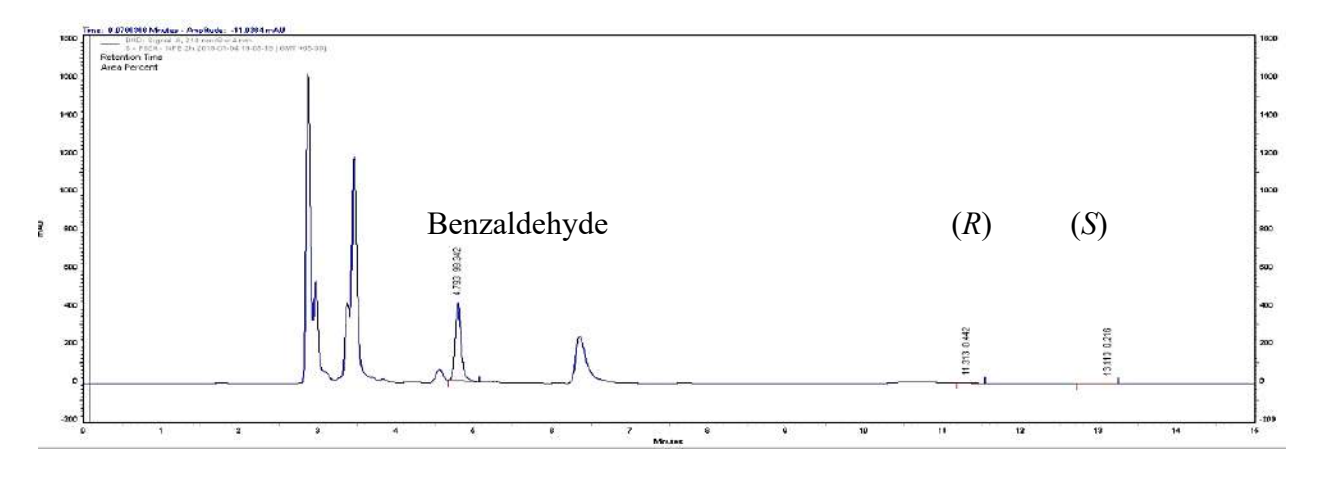


Figure 3.4: HPLC spectrum of F82A showing enantioselective synthesis of (*R*)-NPE at 2 h.

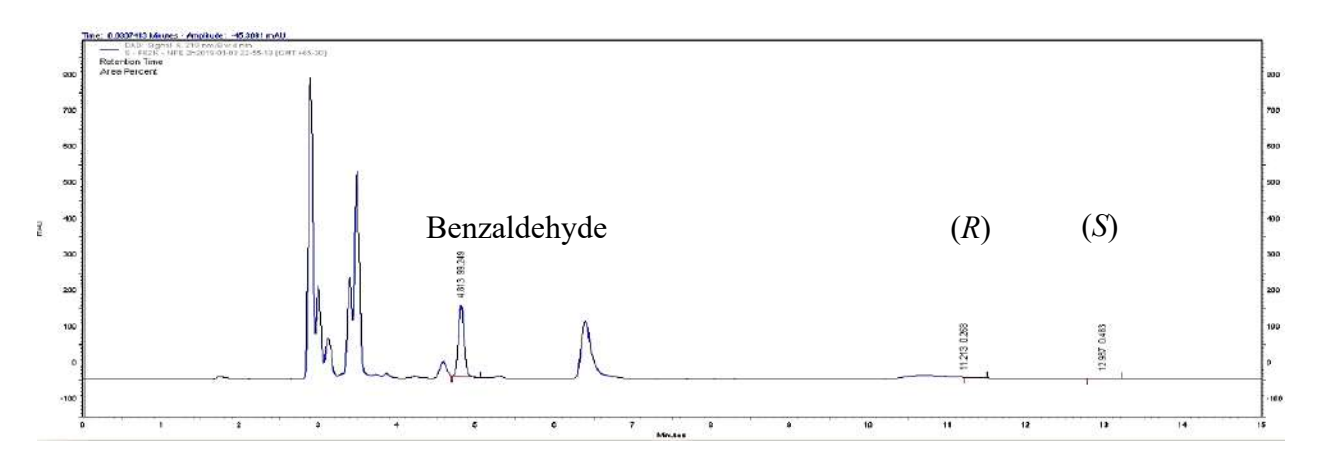


Figure 3.5: HPLC spectrum of F82K showing enantioselective synthesis of (*R*)-NPE at 2 h.

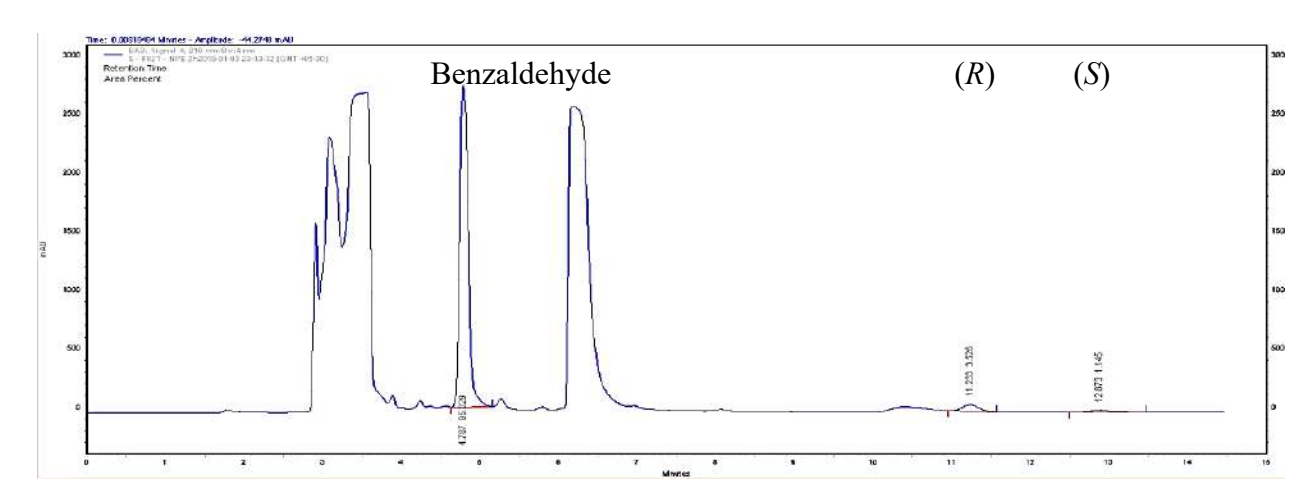


Figure 3.6: HPLC spectrum of F82T showing enantioselective synthesis of (*R*)-NPE at 2 h.

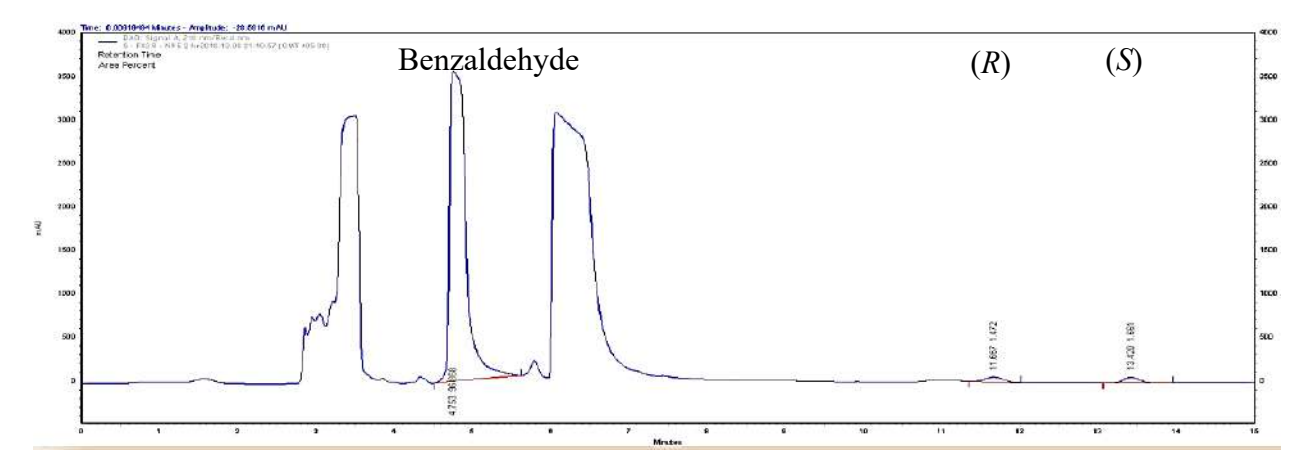


Figure 3.7: HPLC spectrum of F82R showing enantioselective synthesis of (*R*)-NPE at 2 h.

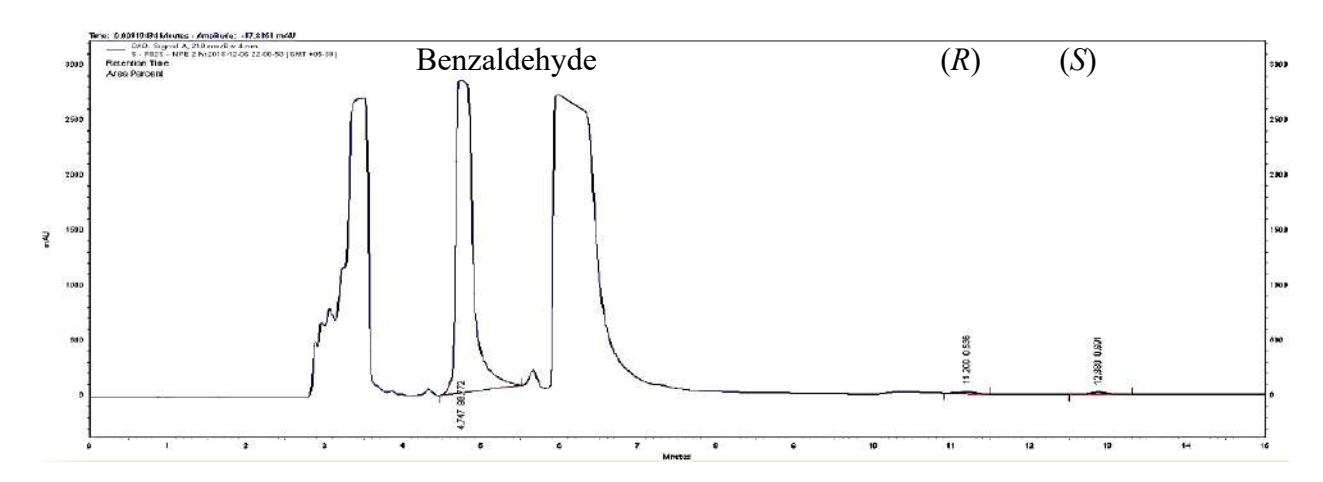


Figure 3.8: HPLC spectrum of F82S showing enantioselective synthesis of (*R*)-NPE at 2 h.

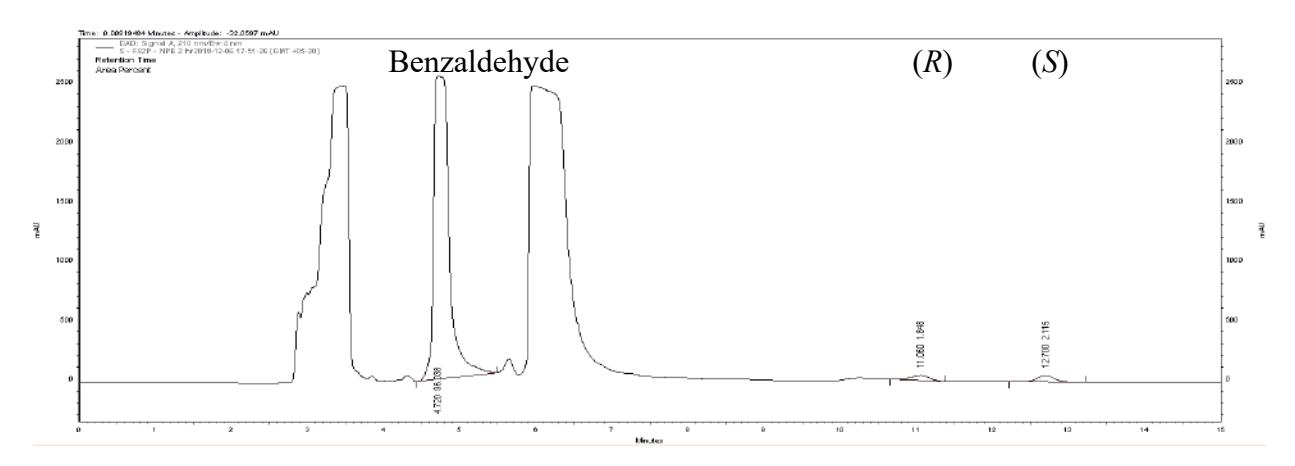


Figure 3.9: HPLC spectrum of F82P showing enantioselective synthesis of (R)-NPE at 2 h.

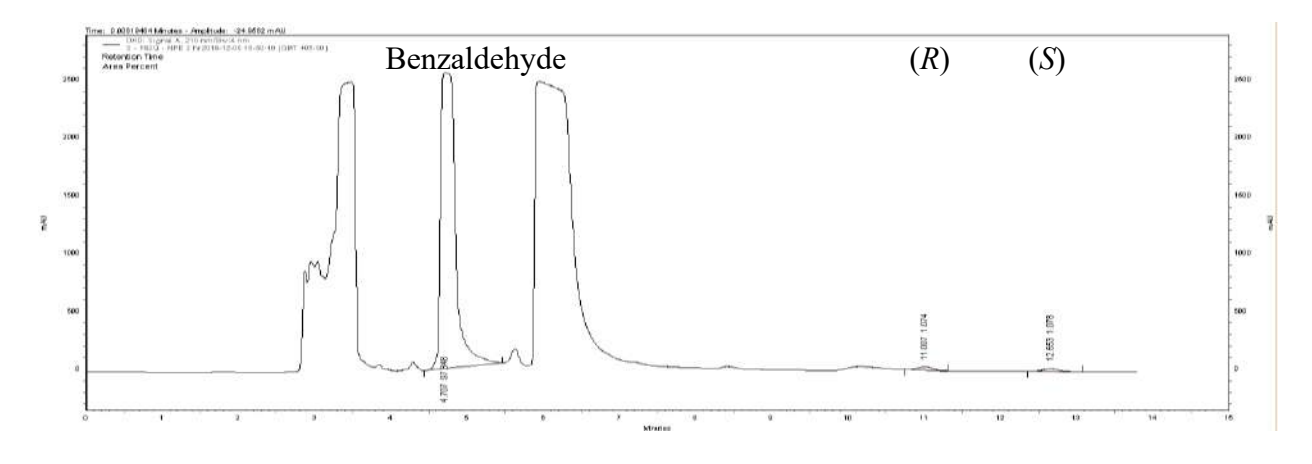


Figure 3.10: HPLC spectrum of F82Q showing enantioselective synthesis of (*R*)-NPE at 2 h.

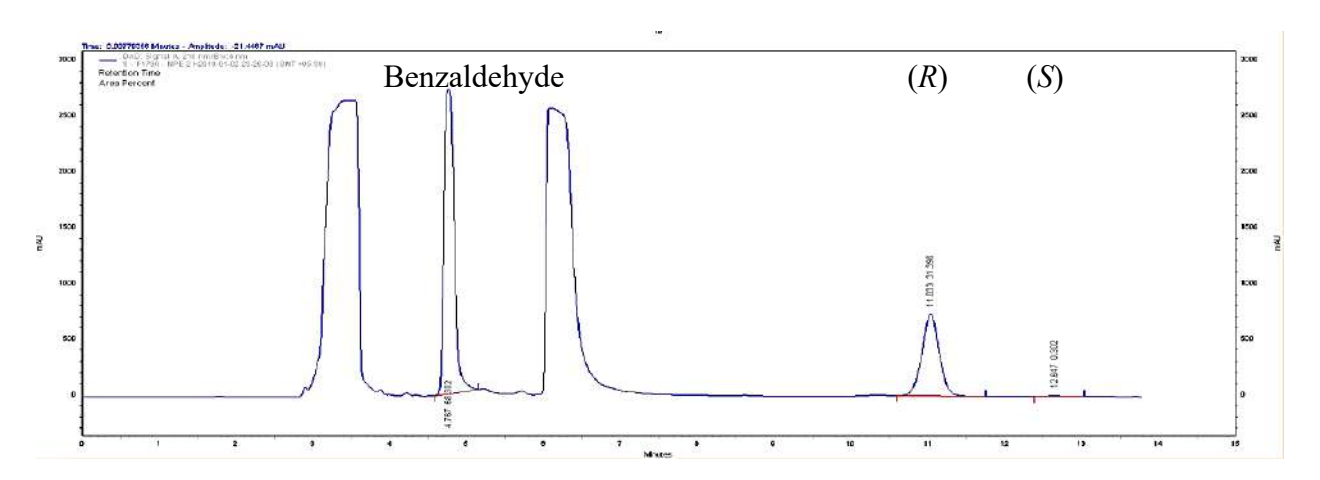


Figure 3.11: HPLC spectrum of F179A showing enantioselective synthesis of (*R*)-NPE at 2 h.

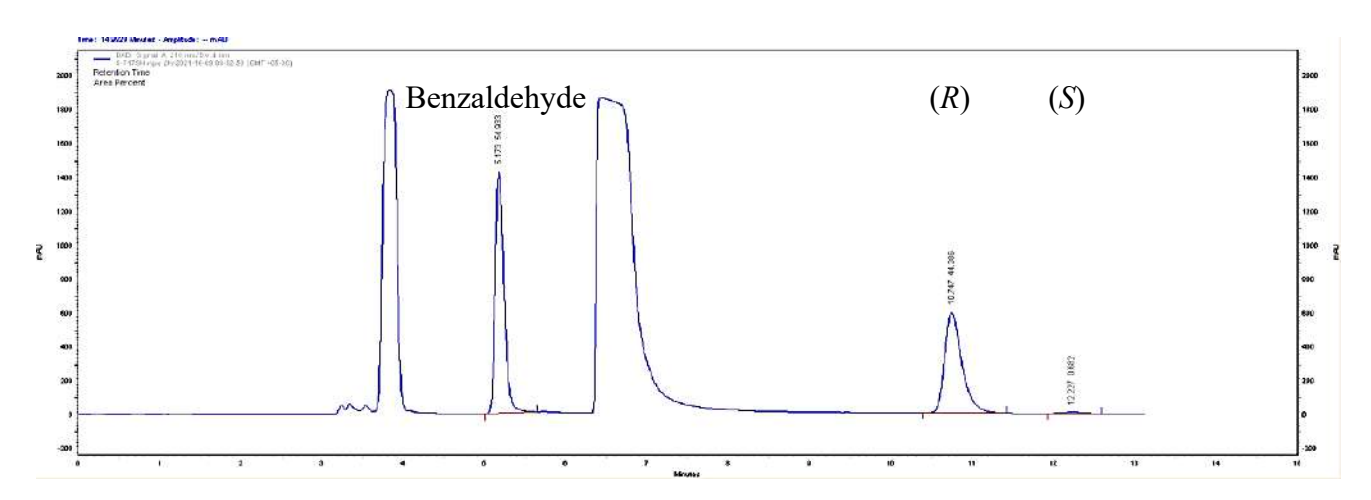


Figure 3.12: HPLC spectrum of F179H showing enantioselective synthesis of (*R*)-NPE at 2 h.

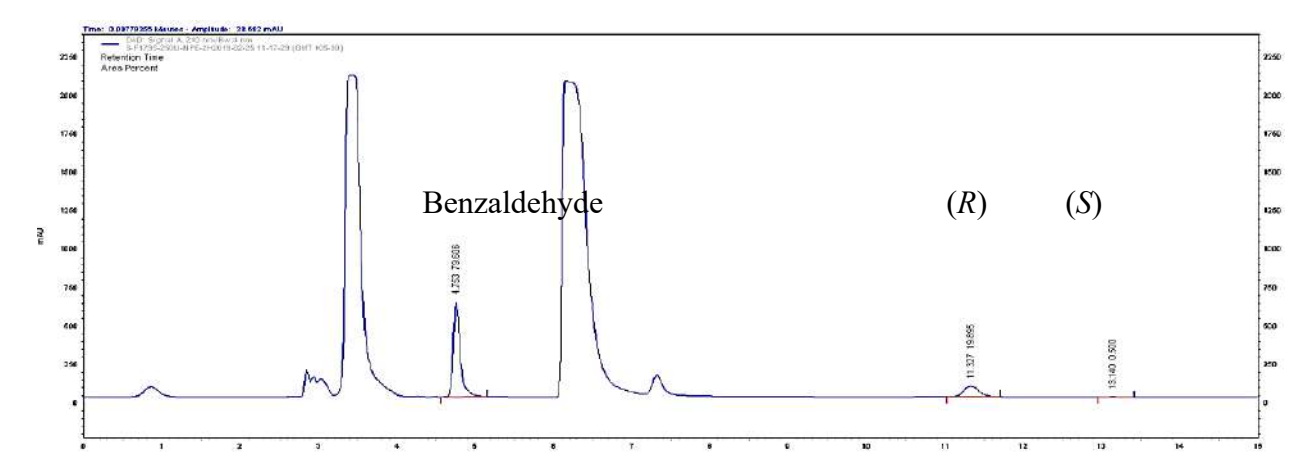


Figure 3.13: HPLC spectrum of F179S showing enantioselective synthesis of (*R*)-NPE at 2 h.

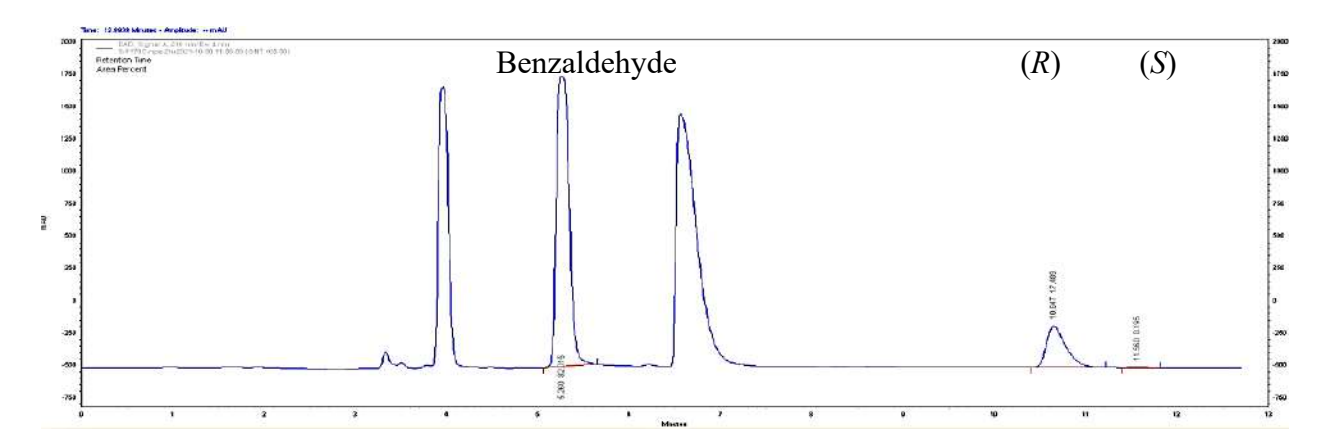


Figure 3.14: HPLC spectrum of F179C showing enantioselective synthesis of (R)-NPE at 2 h.

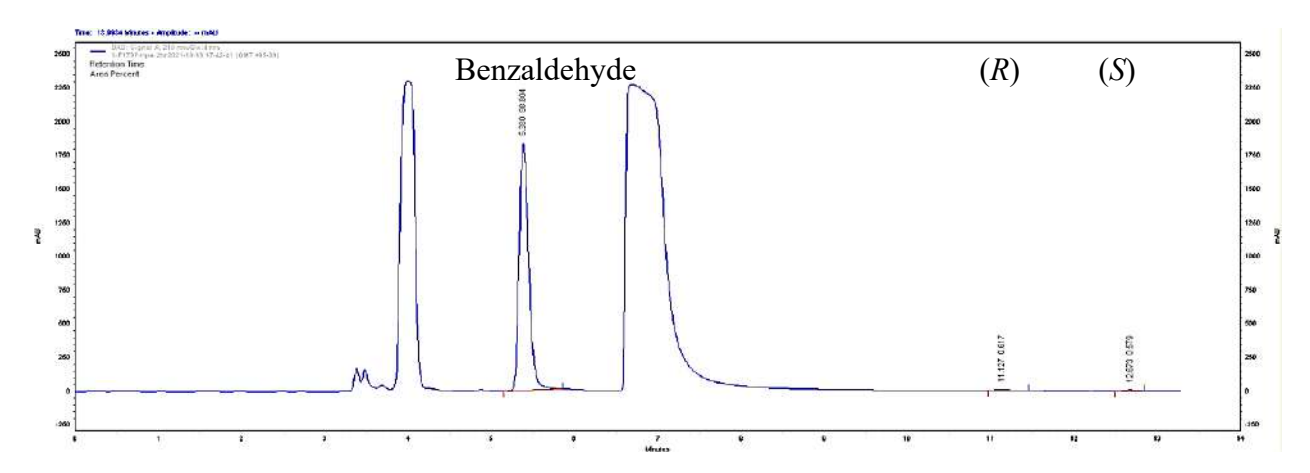


Figure 3.15: HPLC spectrum of F179P showing enantioselective synthesis of (*R*)-NPE at 2 h.

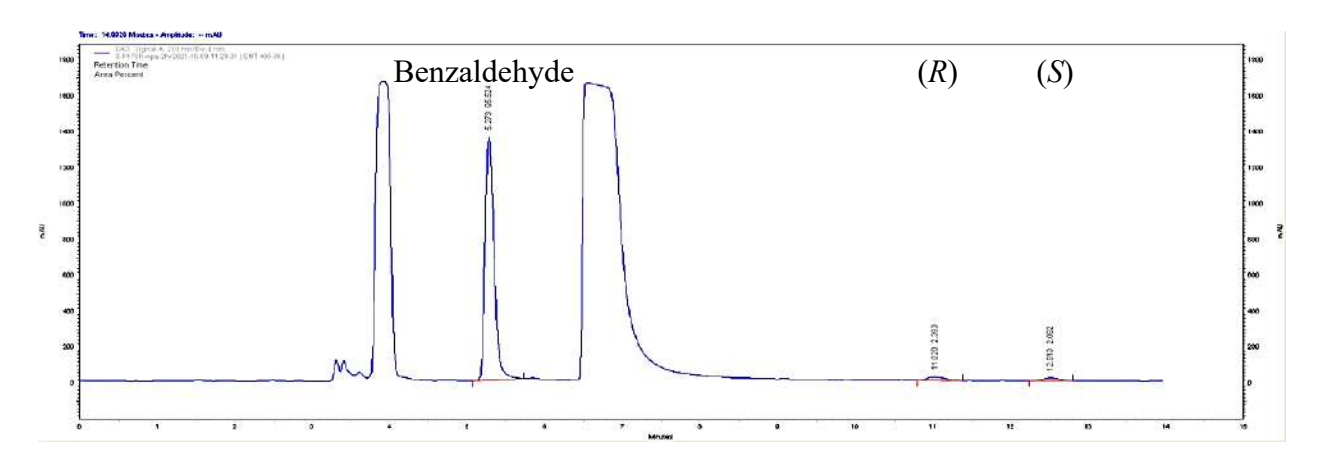


Figure 3.16: HPLC spectrum of F179R showing enantioselective synthesis of (*R*)-NPE at 2 h.

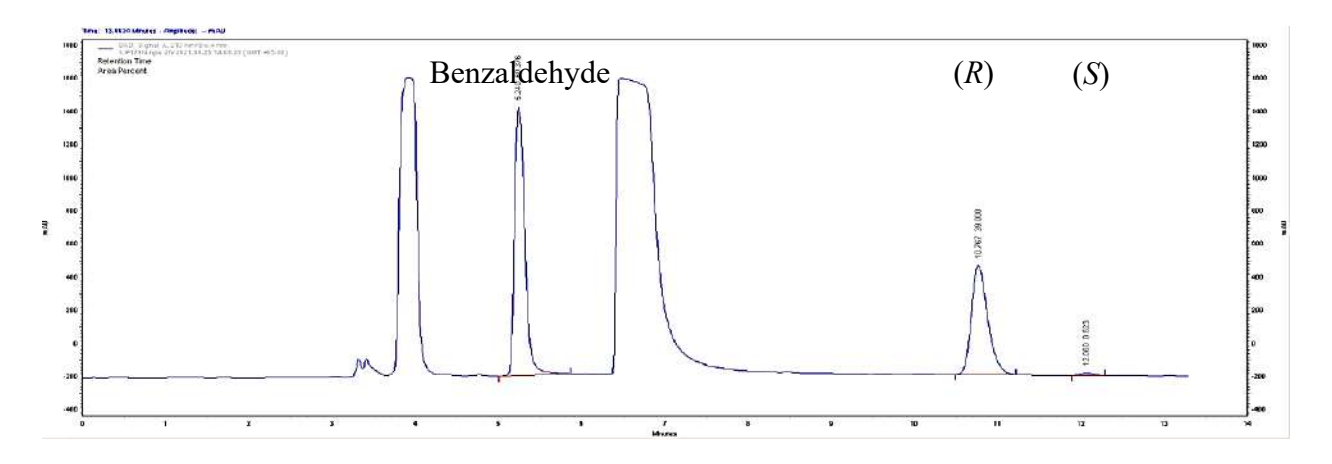


Figure 3.17: HPLC spectrum of F179N showing enantioselective synthesis of (*R*)-NPE at 2 h.

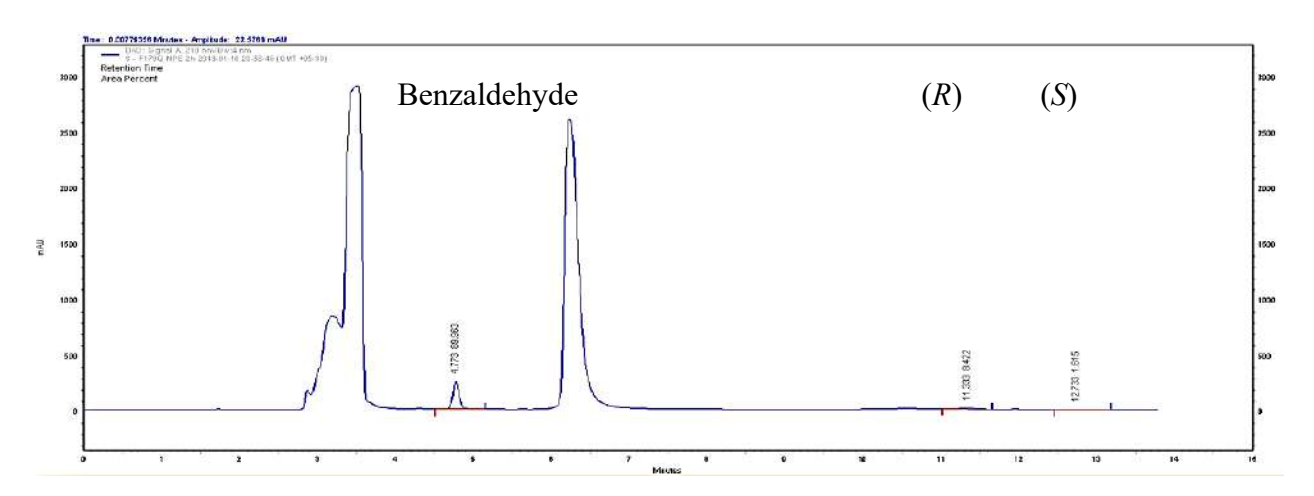


Figure 3.18: HPLC spectrum of F179Q showing enantioselective synthesis of (*R*)-NPE at 2 h.

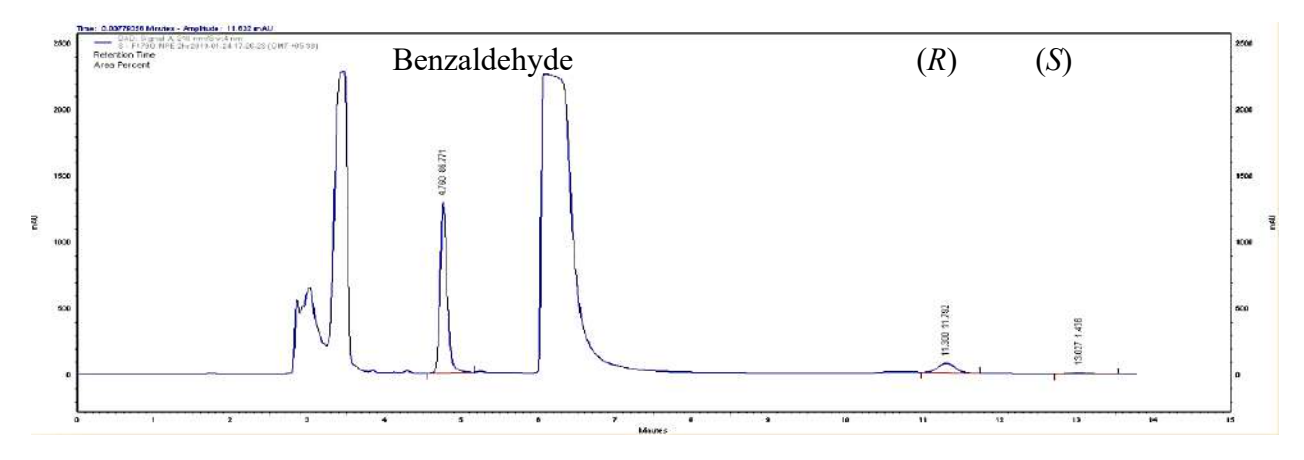


Figure 3.19: HPLC spectrum of F179G showing enantioselective synthesis of (*R*)-NPE at 2 h.

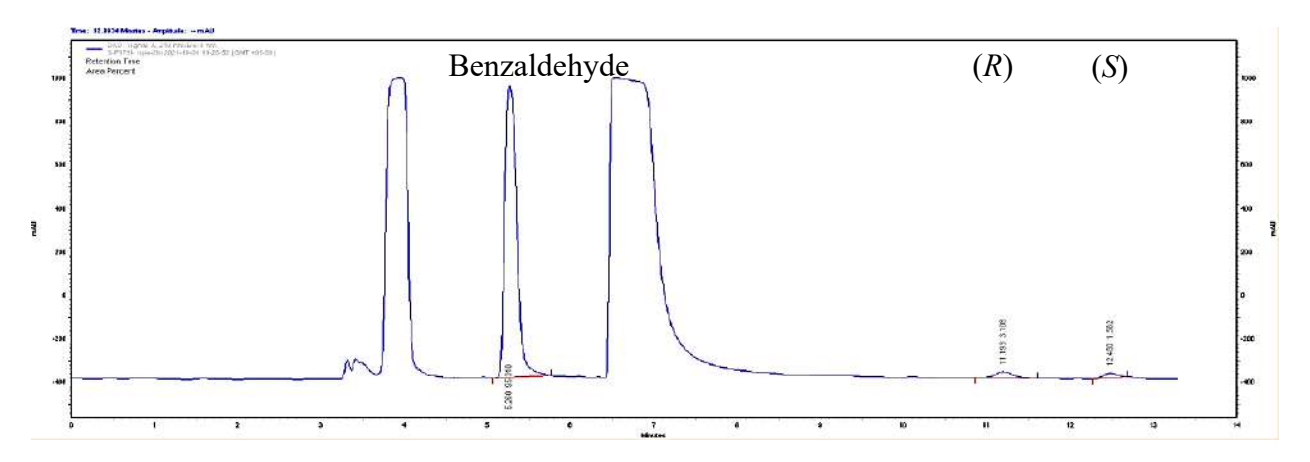


Figure 3.20: HPLC spectrum of F179I showing enantioselective synthesis of (*R*)-NPE at 2 h.

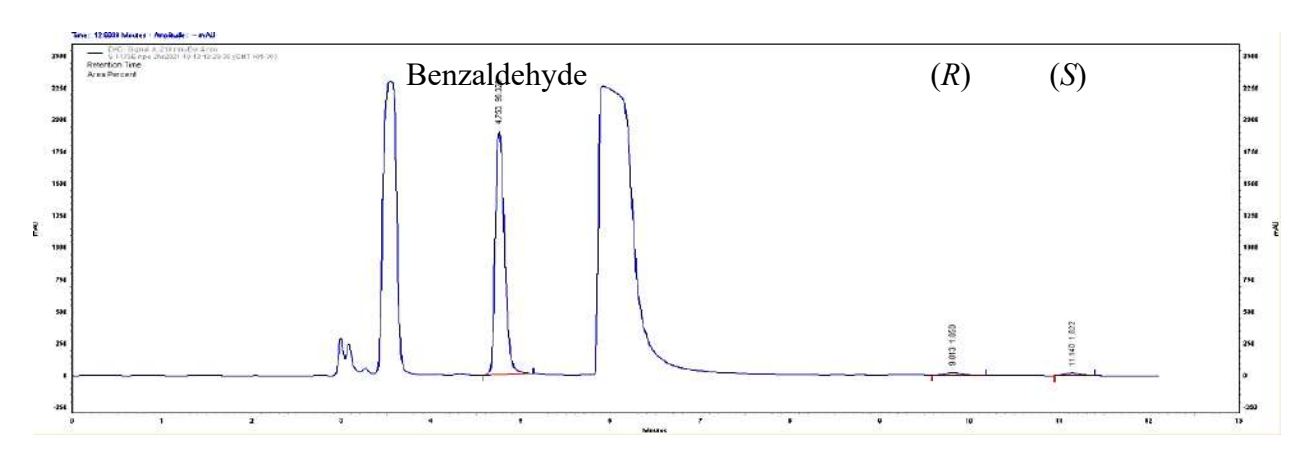


Figure 3.21: HPLC spectrum of F179E showing enantioselective synthesis of (*R*)-NPE at 2 h.

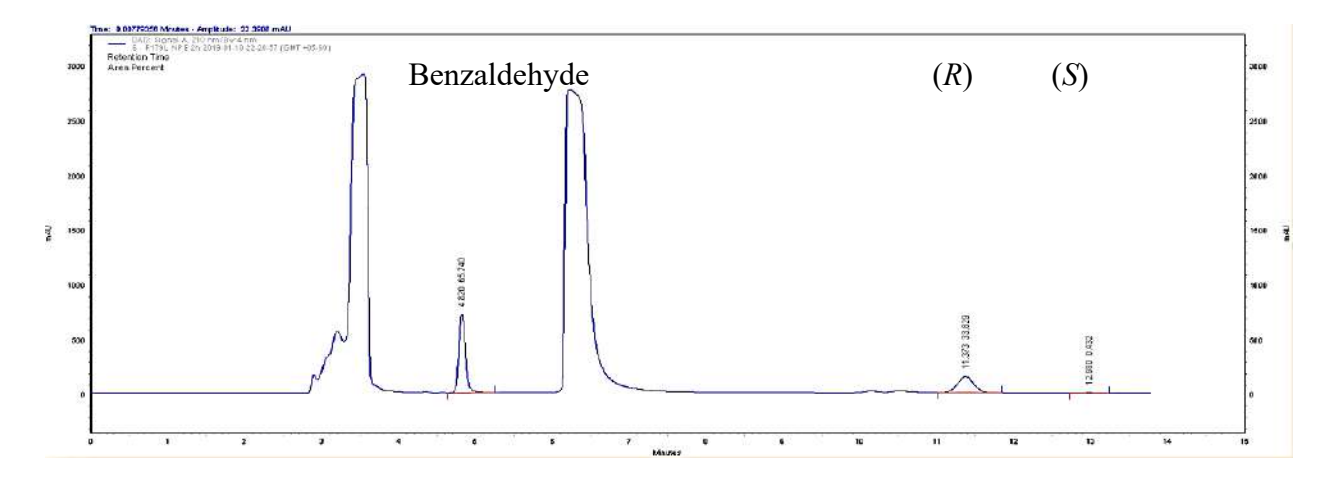


Figure 3.22: HPLC spectrum of F179L showing enantioselective synthesis of (R)-NPE at 2 h.

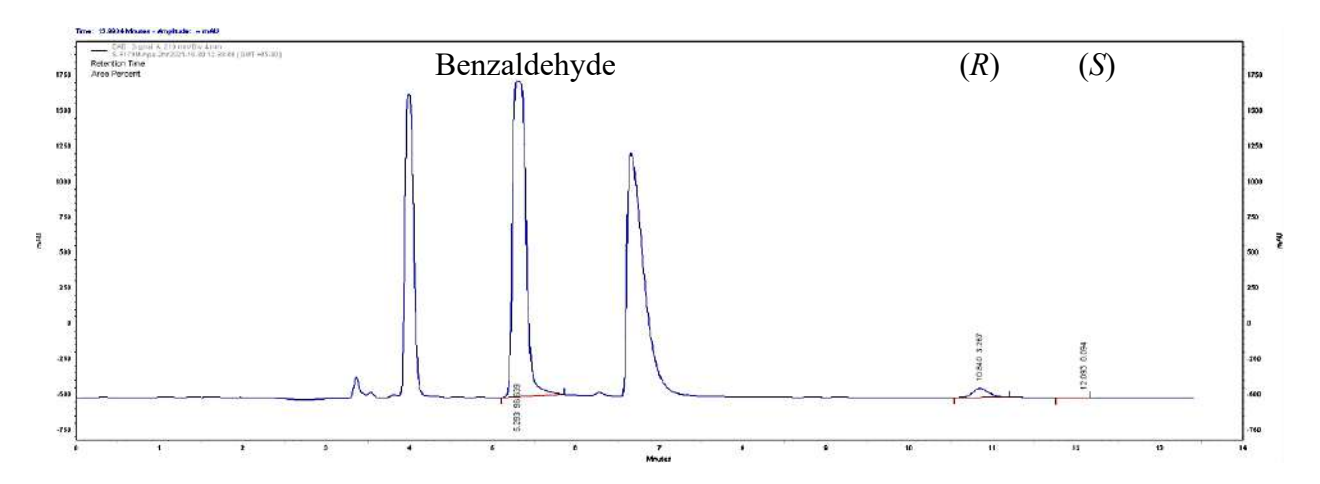


Figure 3.23: HPLC spectrum of F179M showing enantioselective synthesis of (*R*)-NPE at 2 h.

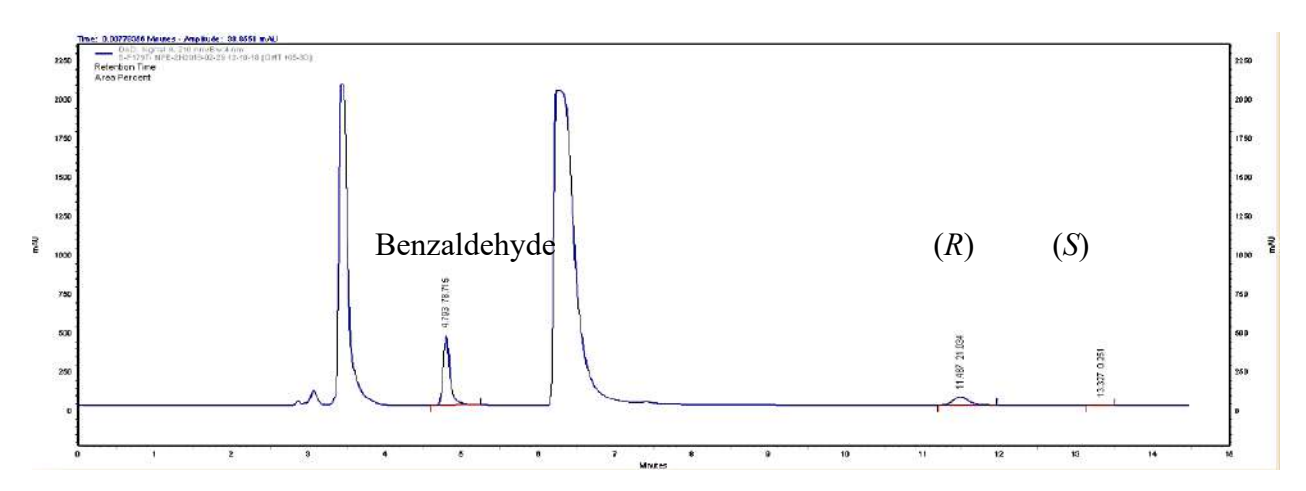


Figure 3.24: HPLC spectrum of F179T showing enantioselective synthesis of (*R*)-NPE at 2 h.

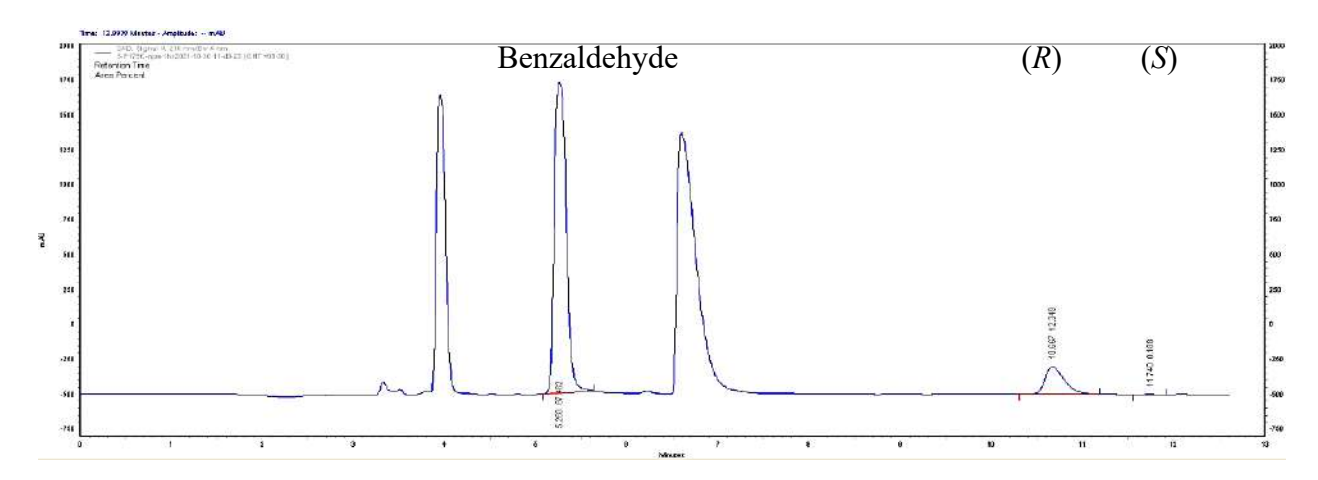


Figure 3.25: HPLC spectrum of F179V showing enantioselective synthesis of (*R*)-NPE at 2 h.

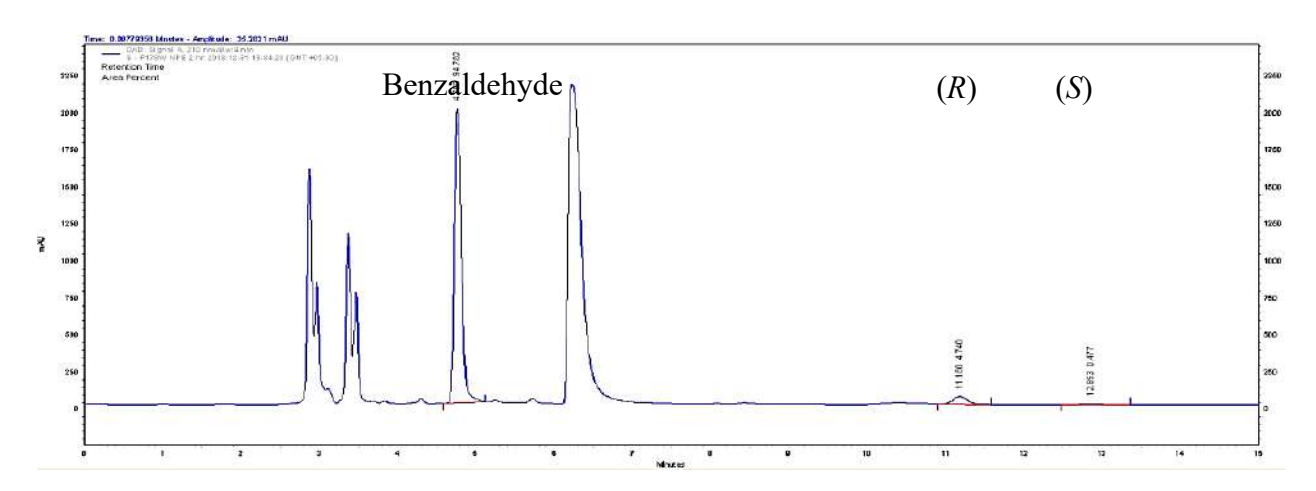


Figure 3.26: HPLC spectrum of F179K showing enantioselective synthesis of (R)-NPE at 2 h.

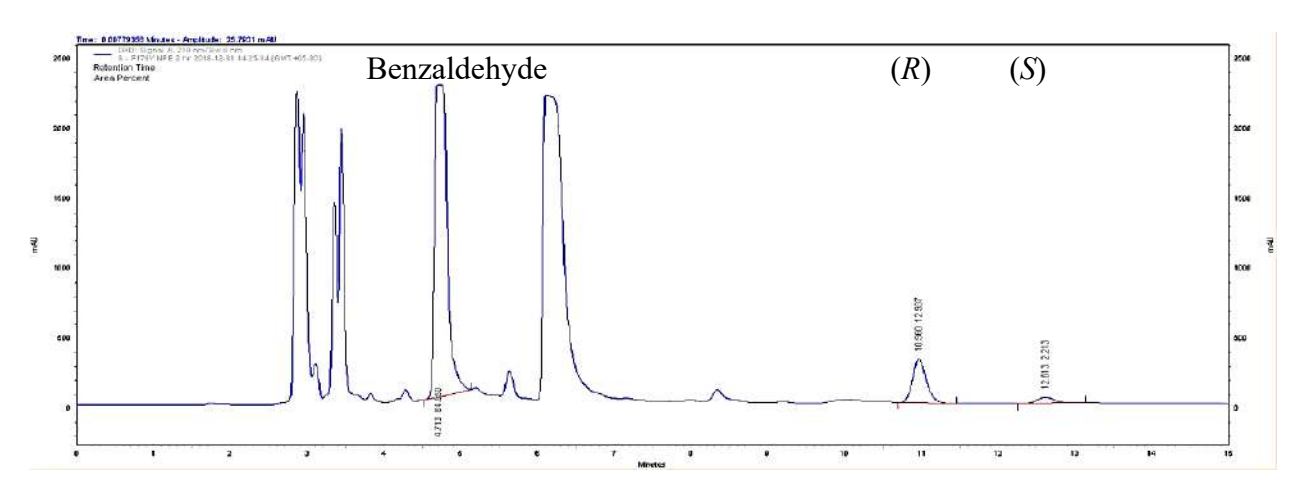


Figure 3.27: HPLC spectrum of F179Y showing enantioselective synthesis of (*R*)-NPE at 2 h.

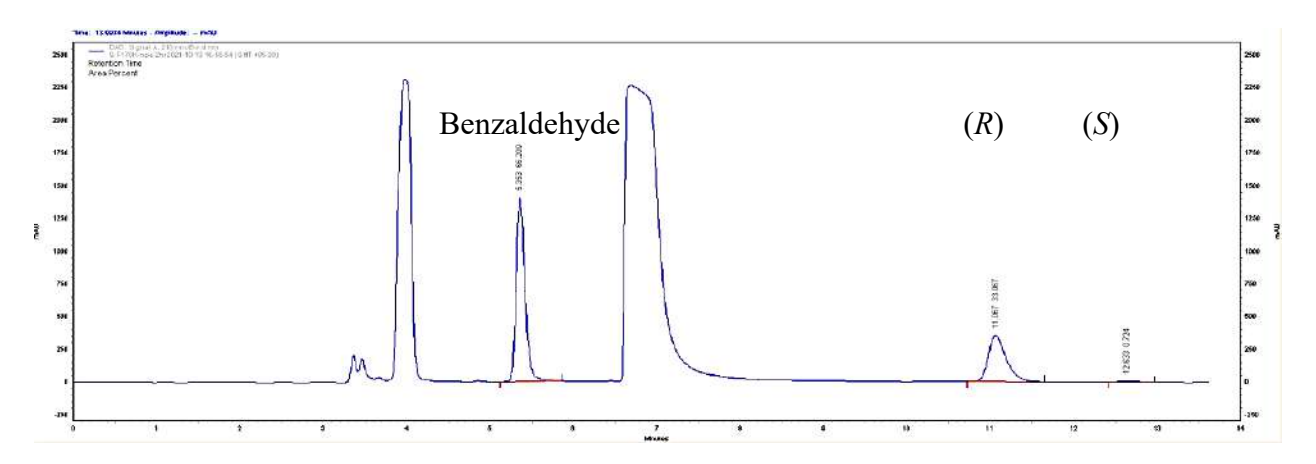


Figure 3.28: HPLC spectrum of F179W showing enantioselective synthesis of (*R*)-NPE at 2 h.

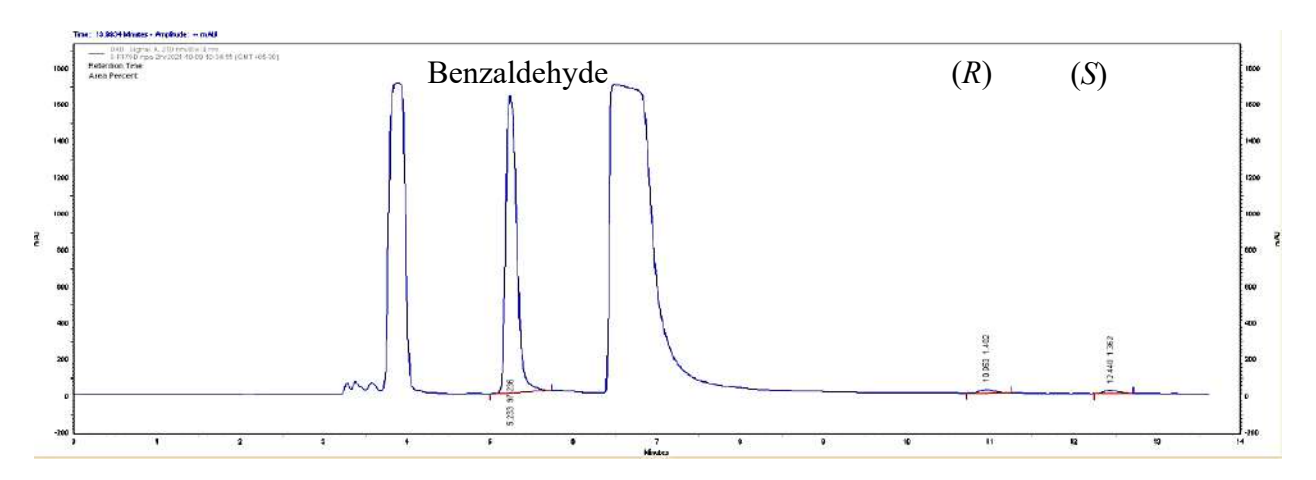


Figure 3.29: HPLC spectrum of F179D showing enantioselective synthesis of (*R*)-NPE at 2 h.

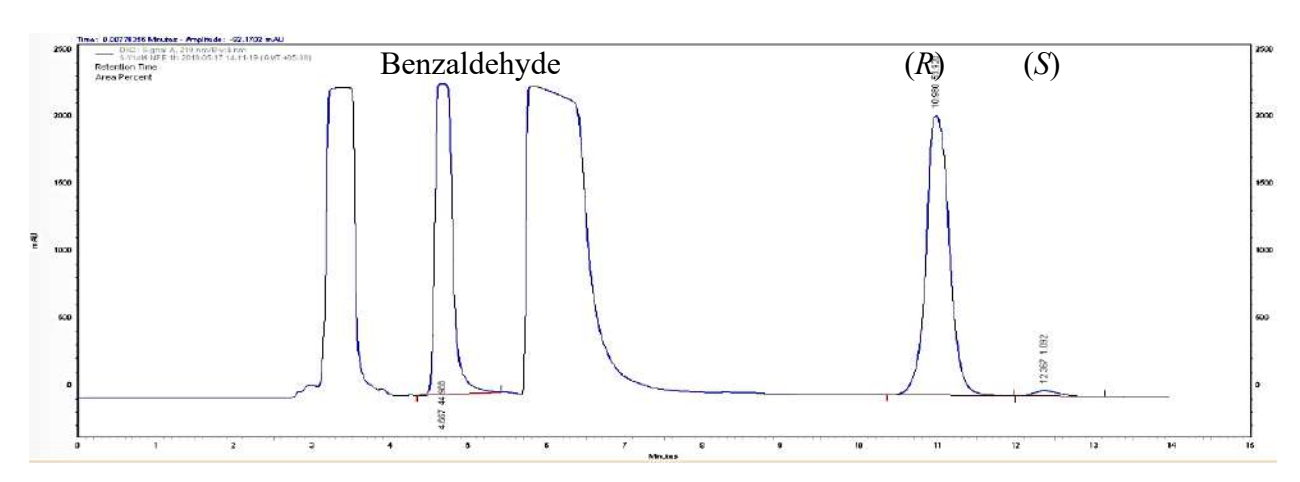


Figure 3.30: HPLC spectrum of Y14A showing enantioselective synthesis of (*R*)-NPE at 2 h.

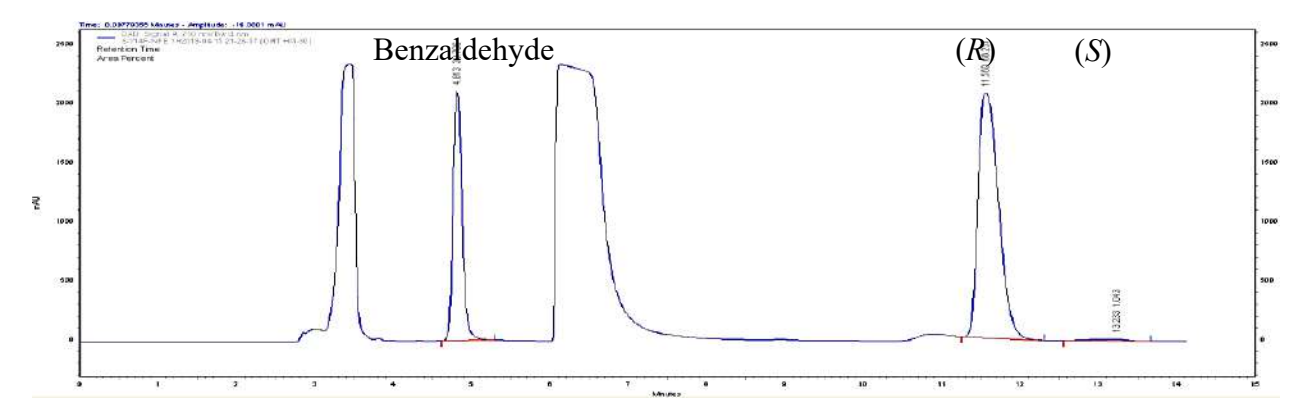


Figure 3.31: HPLC spectrum of Y14C showing enantioselective synthesis of (R)-NPE at 2 h.

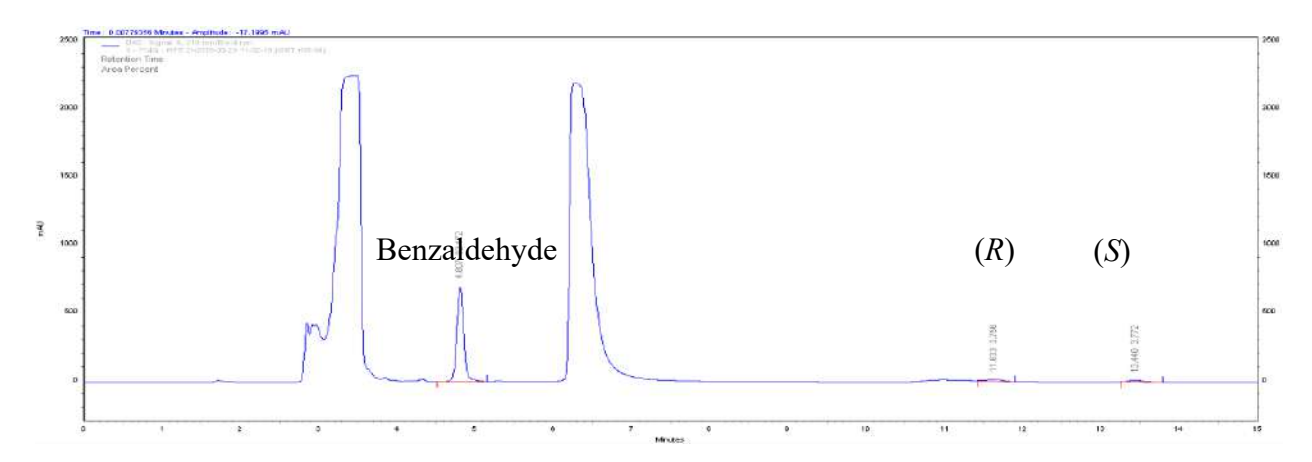


Figure 3.32: HPLC spectrum of Y14Q showing enantioselective synthesis of (R)-NPE at 2 h.

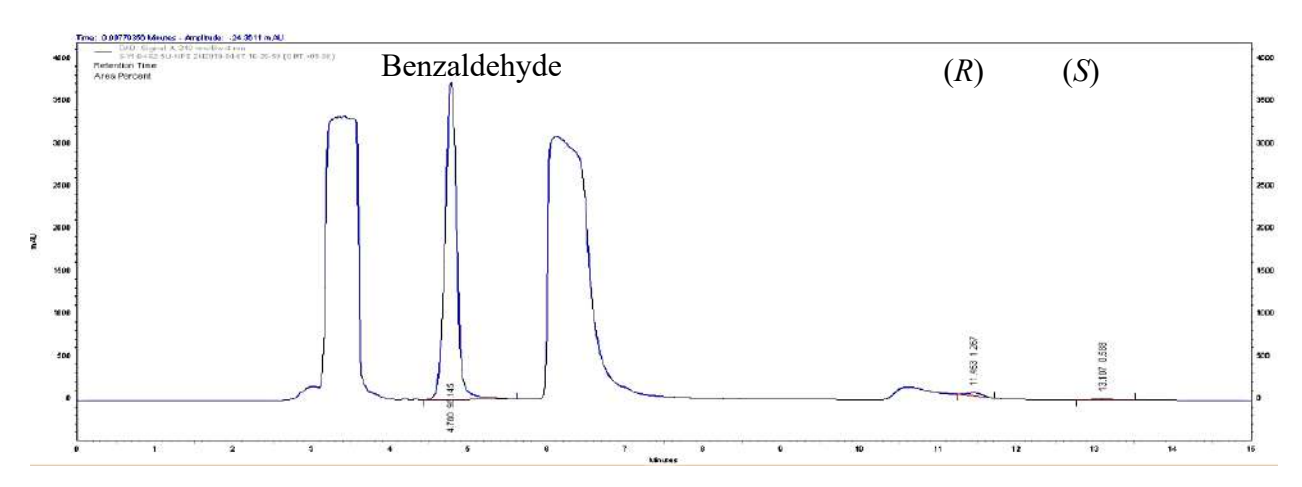


Figure 3.33: HPLC spectrum of Y14H showing enantioselective synthesis of (R)-NPE at 2 h.

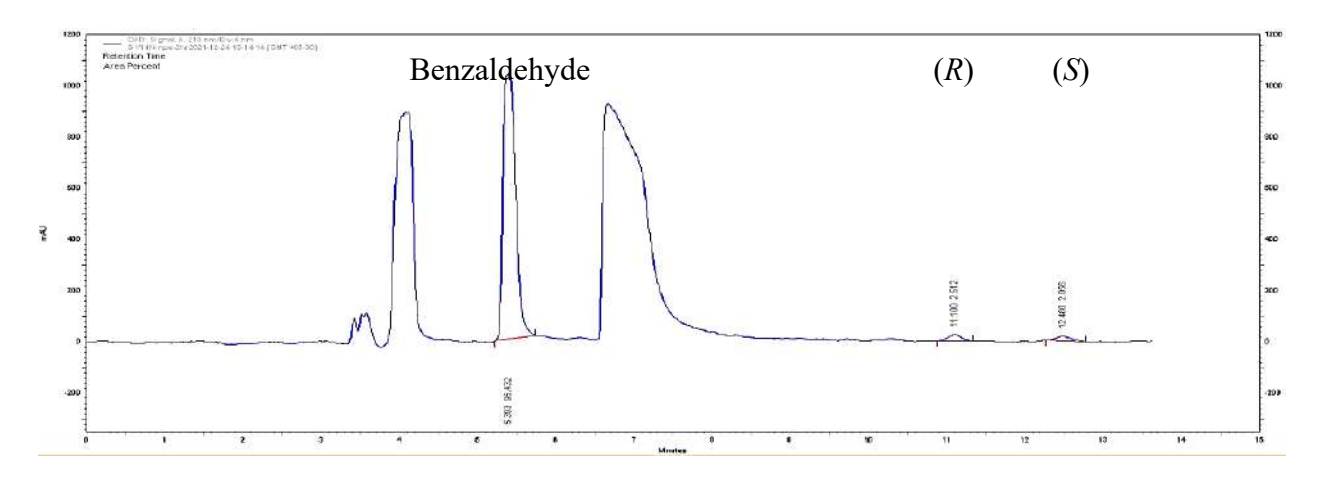


Figure 3.34: HPLC spectrum of Y14N showing enantioselective synthesis of (R)-NPE at 2 h.

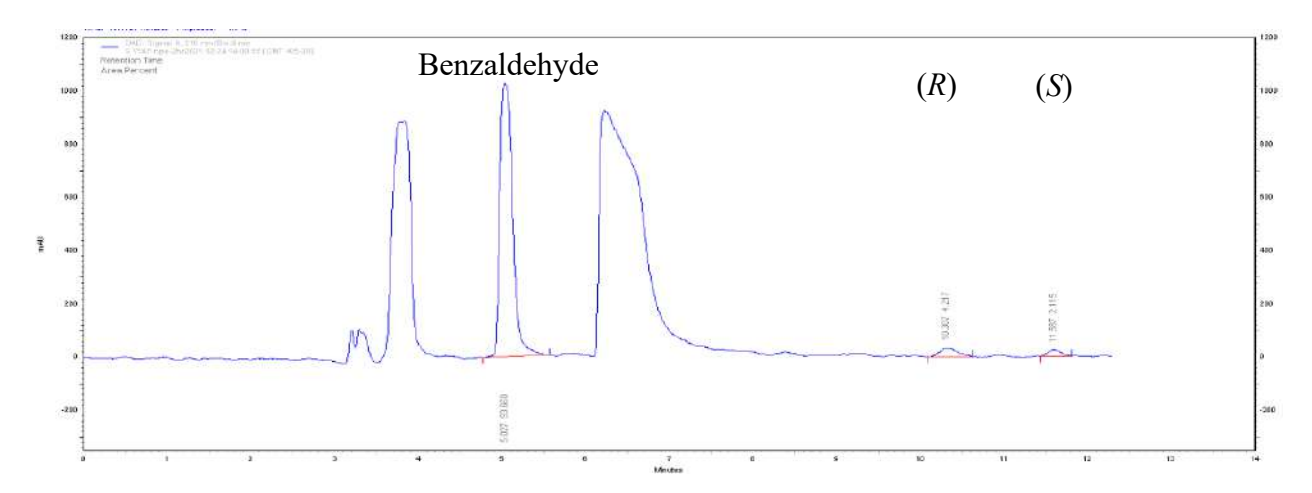


Figure 3.35: HPLC spectrum of Y14P showing enantioselective synthesis of (R)-NPE at 2 h.

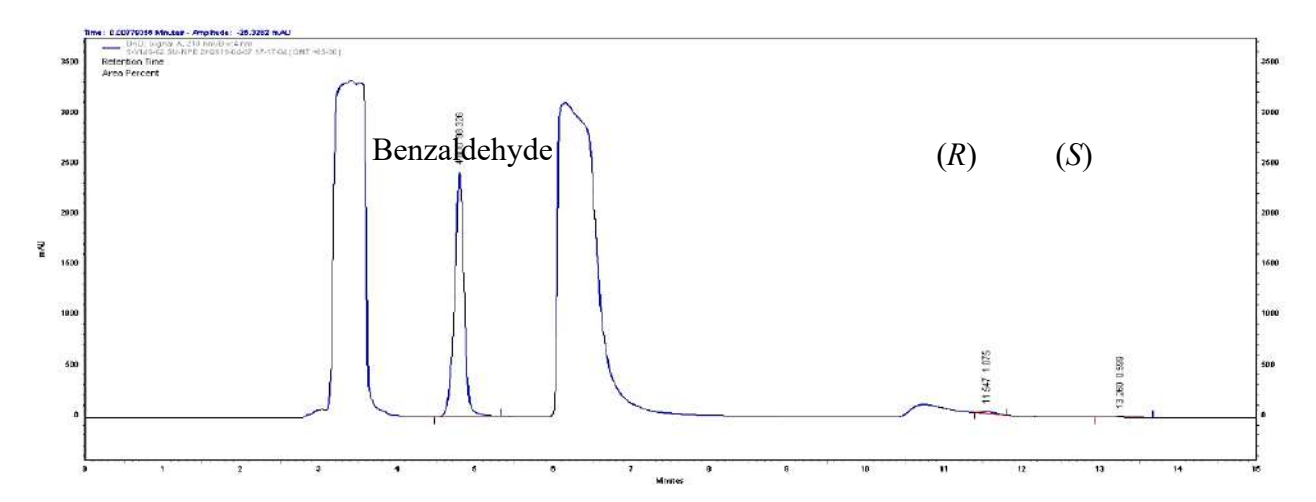


Figure 3.36: HPLC spectrum of Y14S showing enantioselective synthesis of (*R*)-NPE at 2 h.

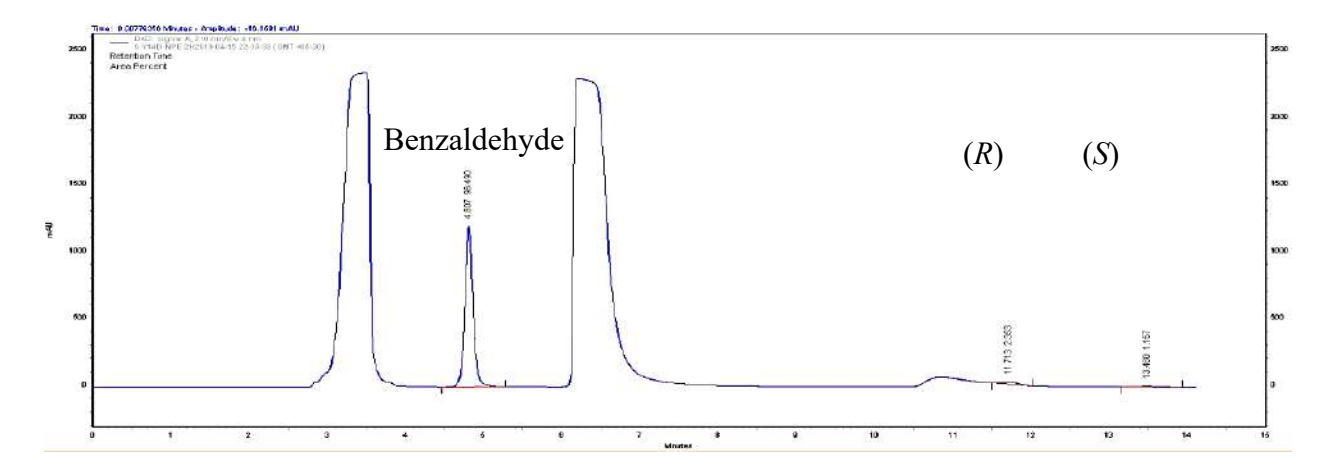


Figure 3.37: HPLC spectrum of Y14D showing enantioselective synthesis of (R)-NPE at 2 h.

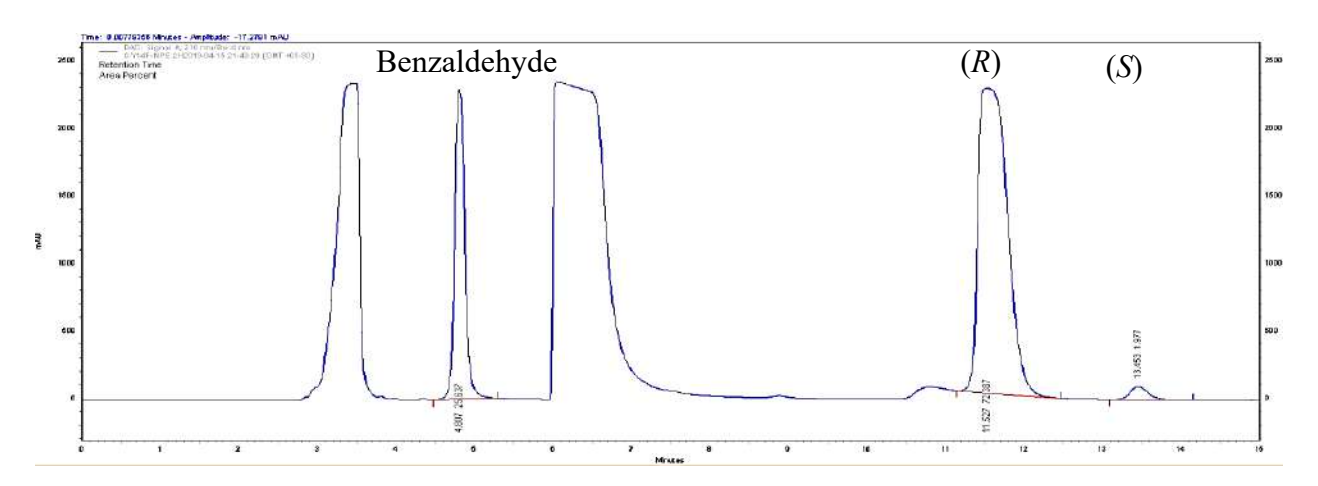


Figure 3.38: HPLC spectrum of Y14F showing enantioselective synthesis of (*R*)-NPE at 2 h.

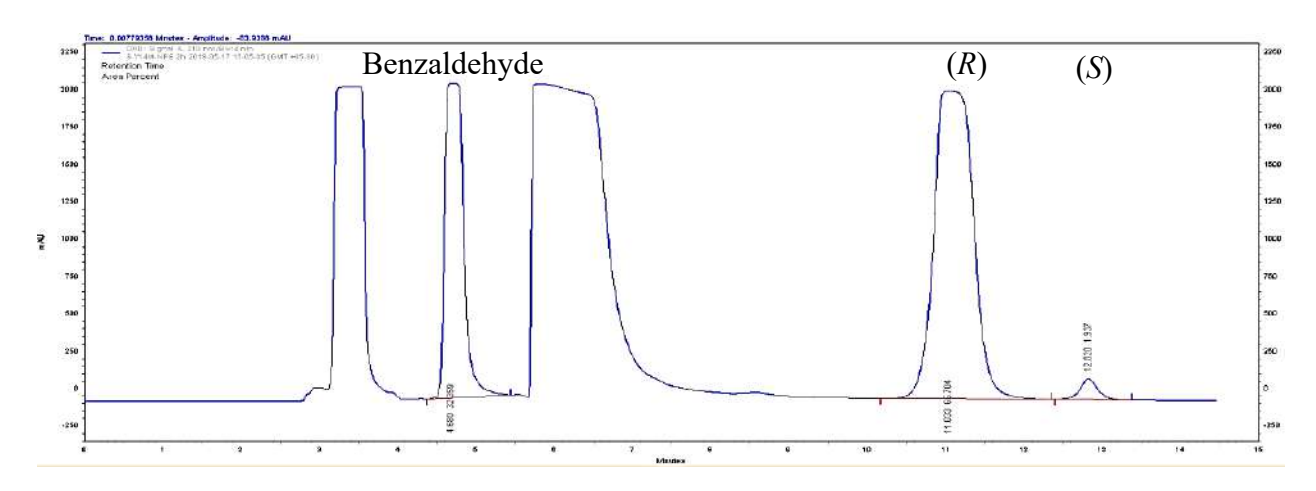


Figure 3.39: HPLC spectrum of Y14M showing enantioselective synthesis of (R)-NPE at 2 h.

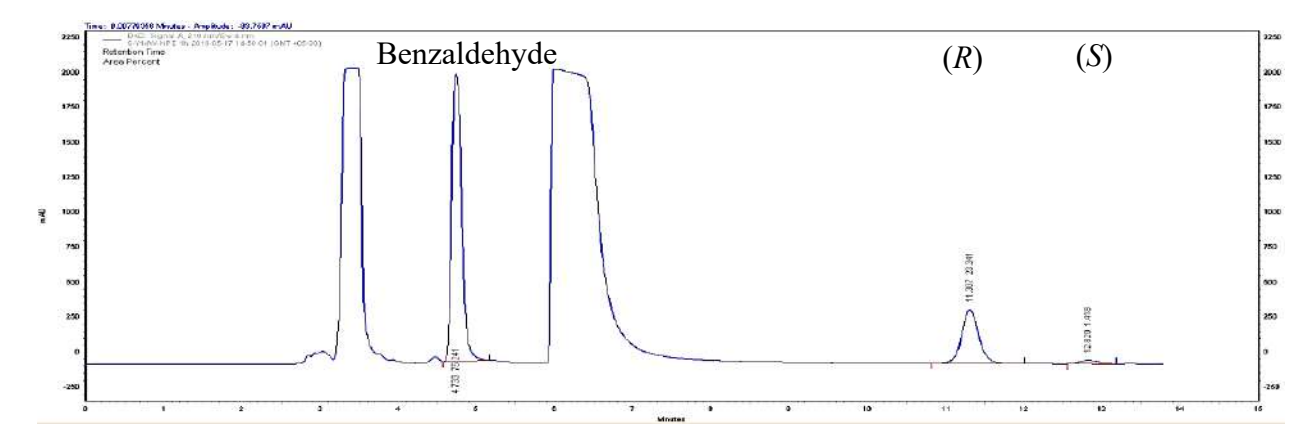


Figure 3.40: HPLC spectrum of Y14V showing enantioselective synthesis of (R)-NPE at 2 h.

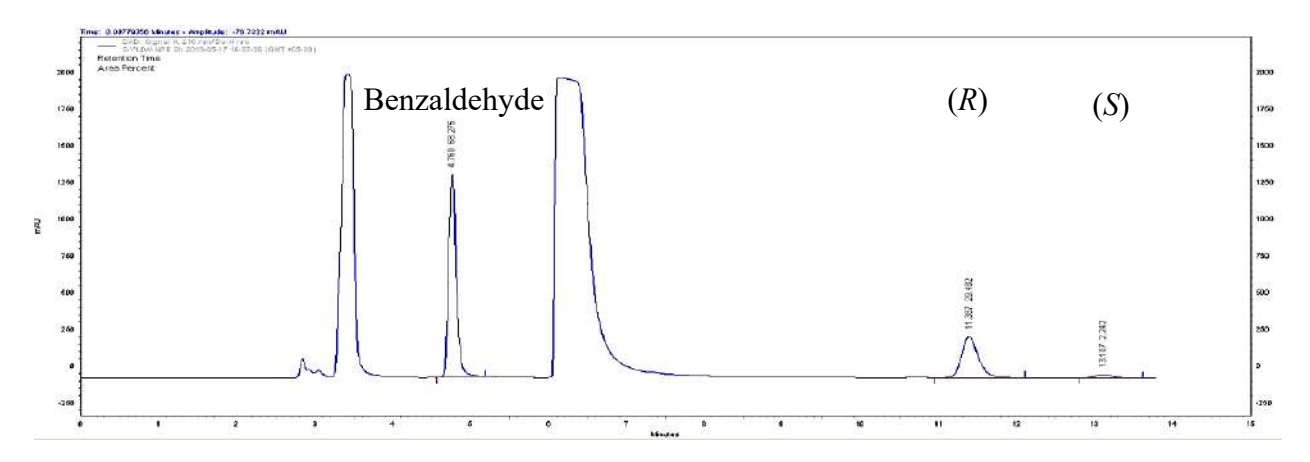


Figure 3.41: HPLC spectrum of Y14W showing enantioselective synthesis of (*R*)-NPE at 2 h.

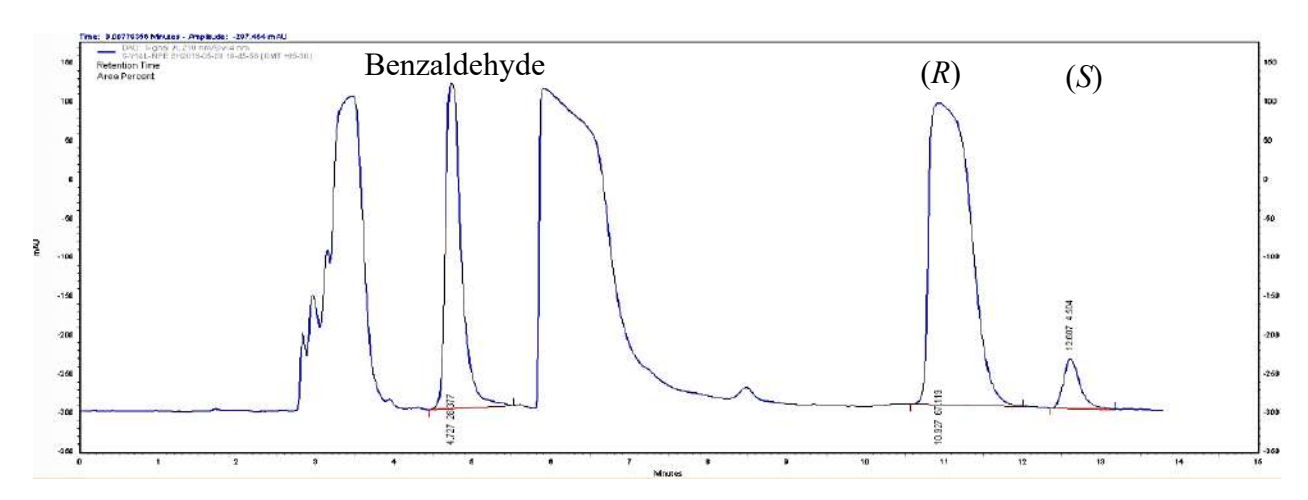


Figure 3.42: HPLC spectrum of Y14L showing enantioselective synthesis of (R)-NPE at 2 h.

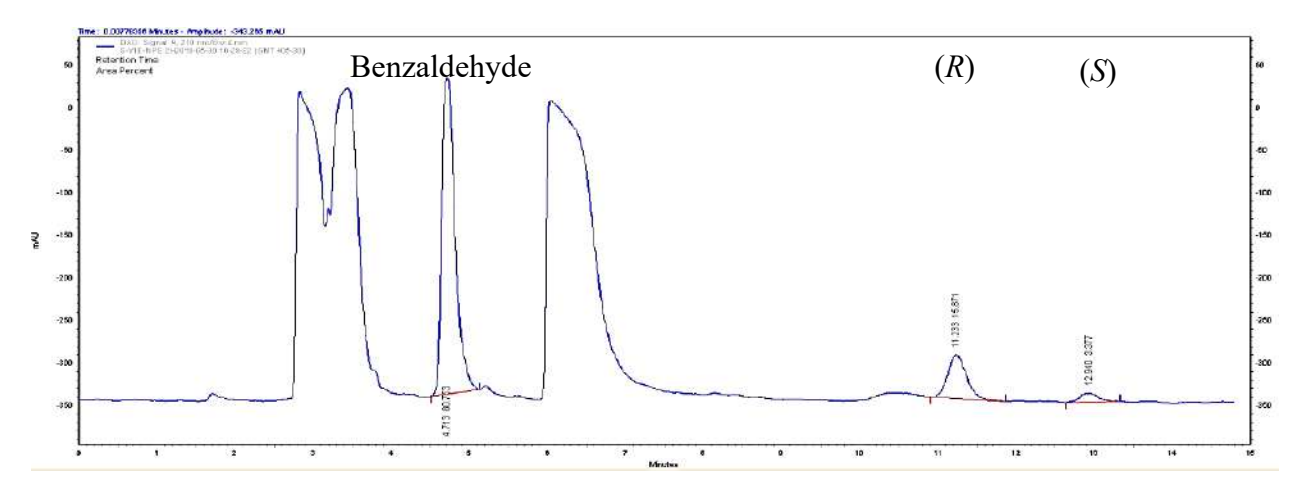


Figure 3.43: HPLC spectrum of Y14E showing enantioselective synthesis of (R)-NPE at 2 h.

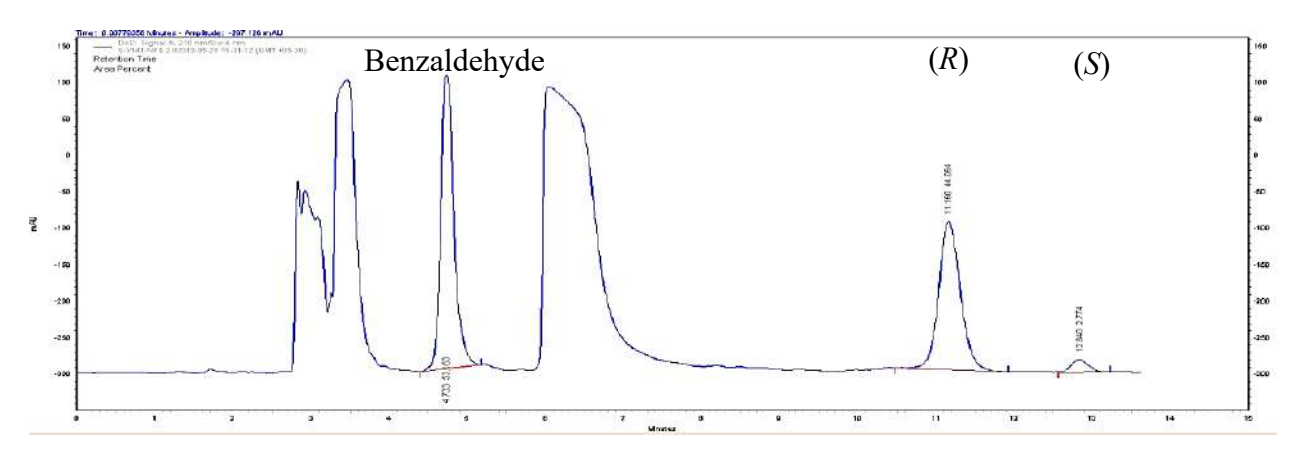


Figure 3.44: HPLC spectrum of Y14T showing enantioselective synthesis of (*R*)-NPE at 2 h.

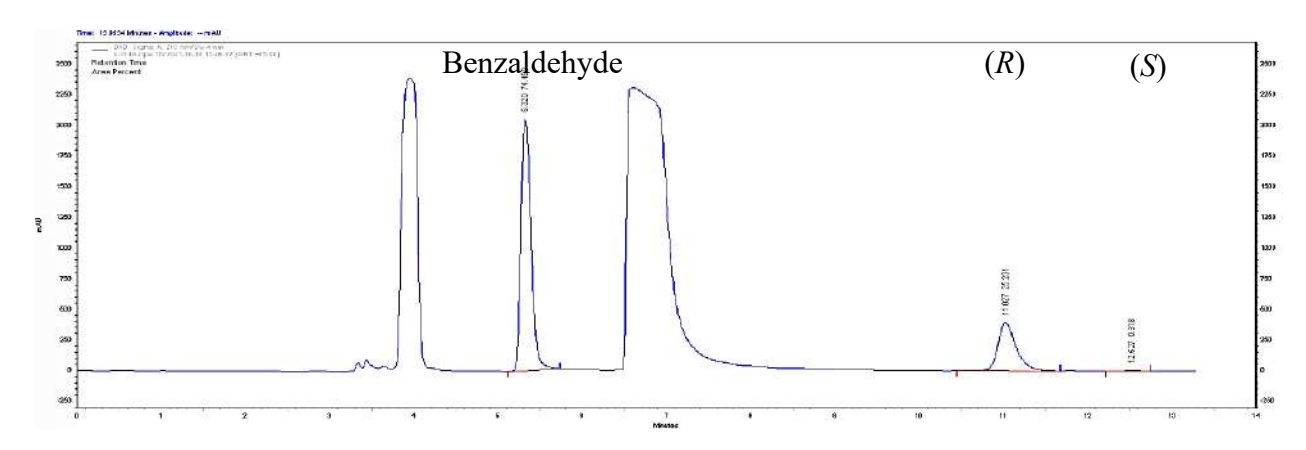


Figure 3.45: HPLC spectrum of Y14K showing enantioselective synthesis of (*R*)-NPE at 2 h.

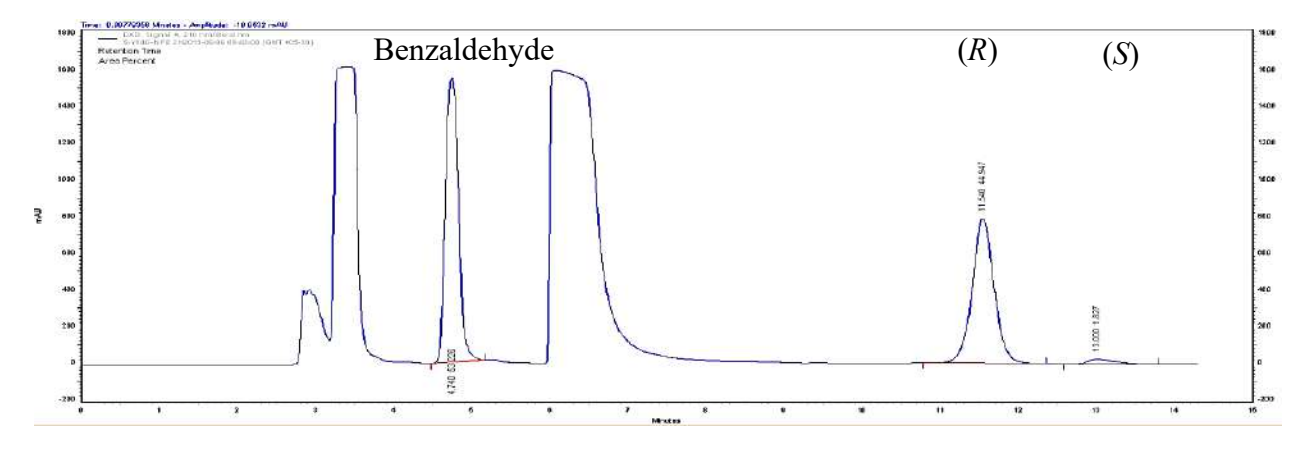


Figure 3.46: HPLC spectrum of Y14G showing enantioselective synthesis of (*R*)-NPE at 2 h.

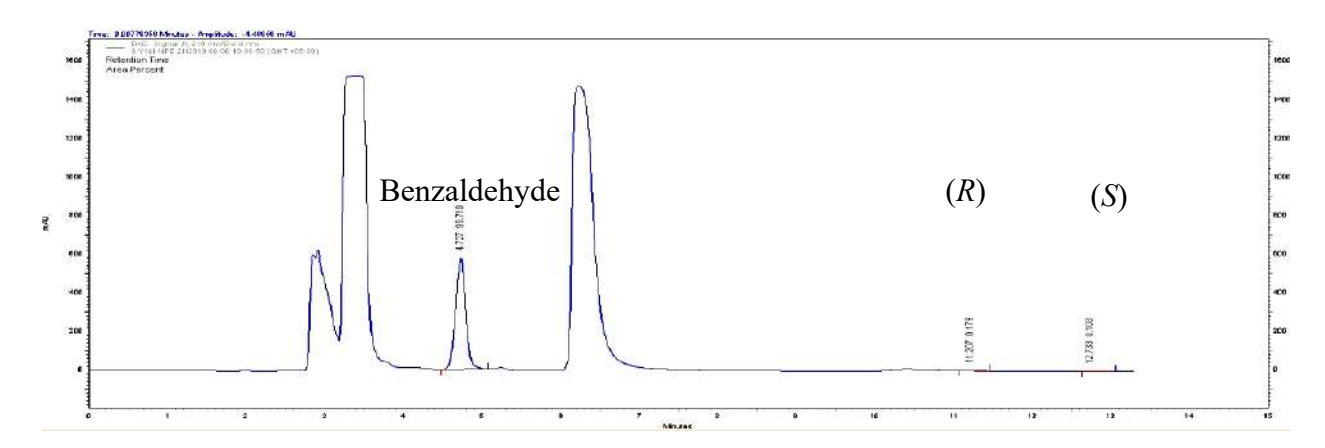


Figure 3.47: HPLC spectrum of Y14I showing enantioselective synthesis of (*R*)-NPE at 2 h.

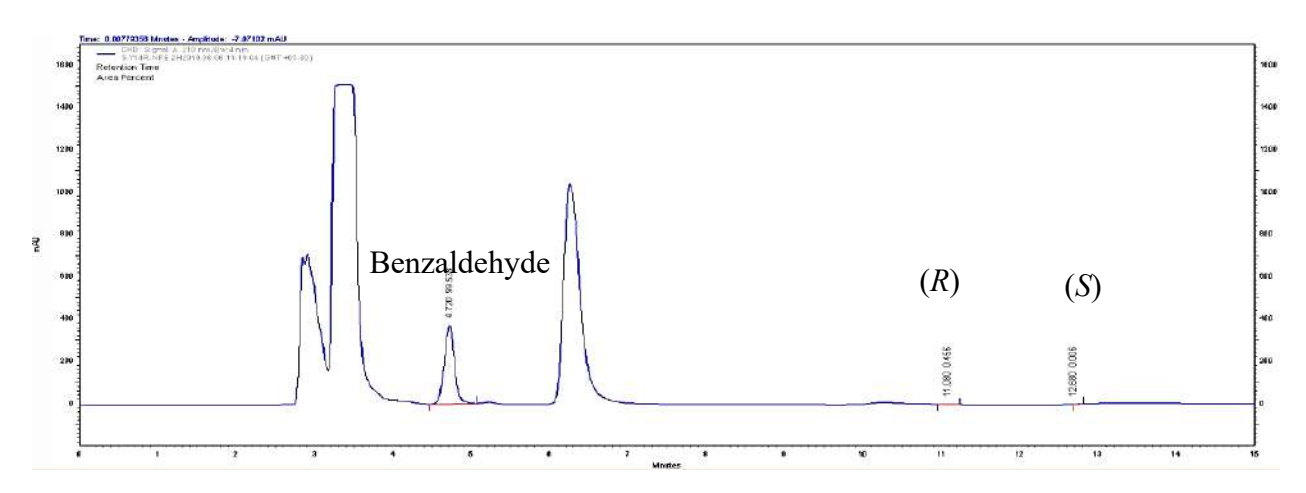


Figure 3.48: HPLC spectrum of Y14R showing enantioselective synthesis of (*R*)-NPE at 2 h.

3.4.3. NMR characterization of the racemic β-nitro alcohols

Racemic synthesis of twelve racemic β -nitroalcohols (**Table 3.3**) was carried out by addition of different aldehydes to nitromethane in 1:10 molar ratio in the presence of 5 mol% of Ba(OH)₂ as a catalyst and their NMR characterization was confirmed as per the previous literature^{29,40,44,45}.

3.4.4. Chiral resolution of racemic β-nitroalcohols by HPLC

All the twelve racemic β-nitroalcohols were resolved using Chiralpak® IB chiral column using 1 mL/min flow rate at a wavelength of 210 nm (**Table 3.3; Figure 3.49-3.60**).

Table 3.3: HPLC conditions and retention times of aldehydes and racemic β -nitroalcohols.

	HPLC condit	ions	Retention time	Retention time
ОН	<i>n</i> -hexane:		of aldehyde (min)	of
$R \longrightarrow NO_2$	2-propanol (v/v)		(R) and (S)-BNAs
	A			(min)
Ph	Î		4.7	10.9, 12.4
trans-cinnamyl Ph			6.9	24.2, 22.8
3-chloro Ph			5.3	10.4 11.8
4-chloro Ph	90:10		5.4	10.8, 12.5
4-fluoro Ph			5.2	9.7, 10.8
3-methyl Ph			4.9	9.1, 9.7
4-methyl Ph			4.9	9.9, 11.5
4-nitro Ph	\		10.4	22.1, 25.6
3-methoxy Ph	97:3 for 6 min followed by 9		6.1	19.2, 21.7
2,4-dimethoxy Ph	90:10 80:20 90:10		8.3	12.3, 16.5
3,4,5-tri methoxy Ph			7.2	13.6, 15.7
4-benzyloxy Ph			8.1	18.2, 20.4

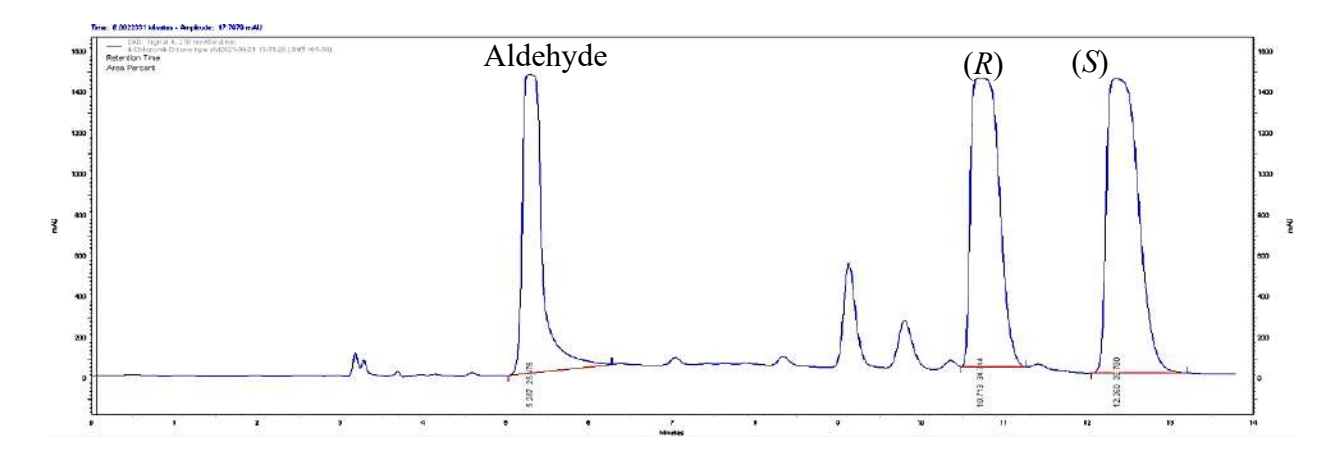


Figure 3.49: HPLC spectrum of the standards: benzaldehyde, (*R*)- and (*S*)-NPE.

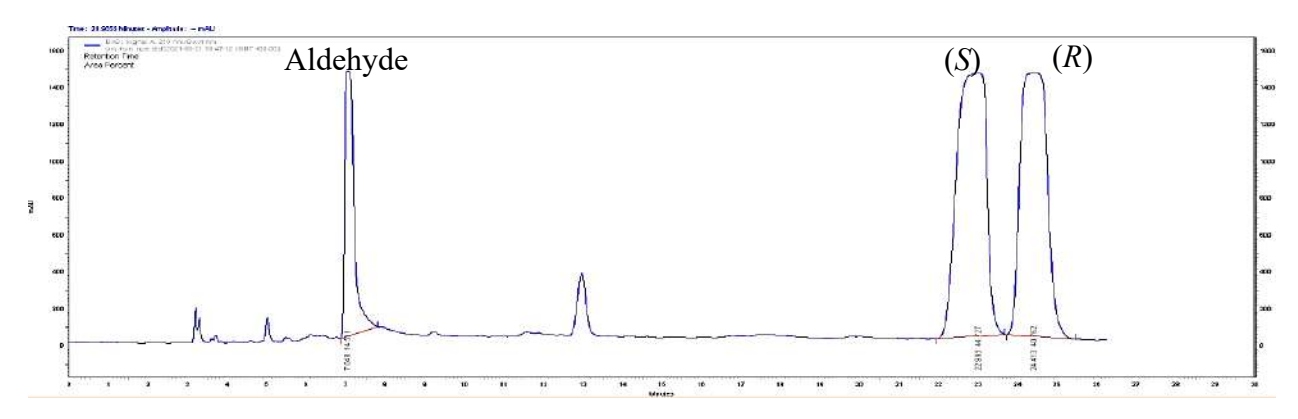


Figure 3.50: HPLC spectrum of the standards: *trans* cinnamaldehyde, and corresponding (S)- and (R)- β -nitroalcohols.

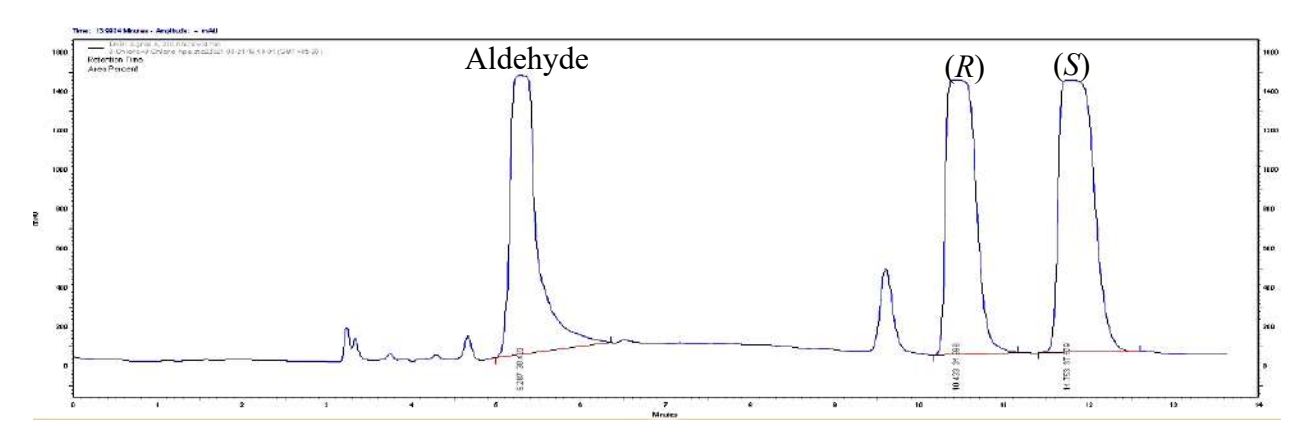


Figure 3.51: HPLC spectrum of the standards: 3-chlorobenzaldehdye, and corresponding (R)-and (S)- β -nitroalcohols.

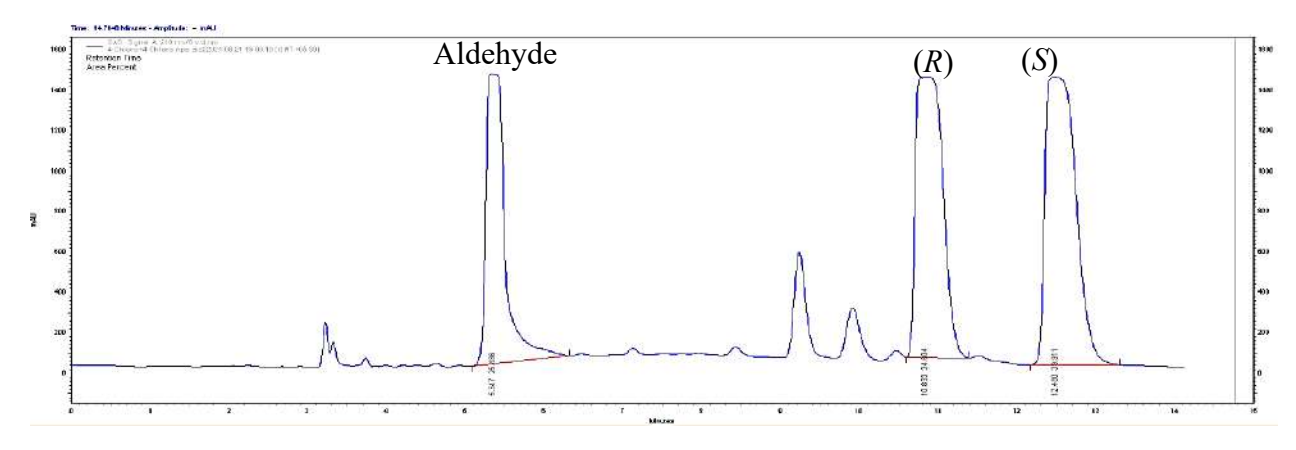


Figure 3.52: HPLC spectrum of the standards: 4-chlorobenzaldehdye, and corresponding (R)-and (S)- β -nitroalcohols.

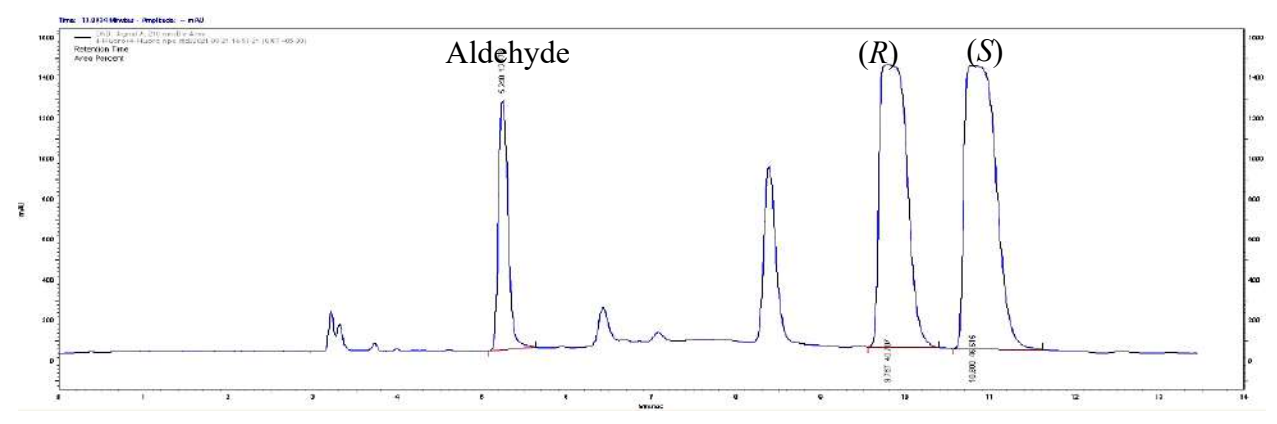


Figure 3.53: HPLC spectrum of the standards: 4-fluorobenzaldehdye, and corresponding (R)- and (S)- β -nitroalcohols.

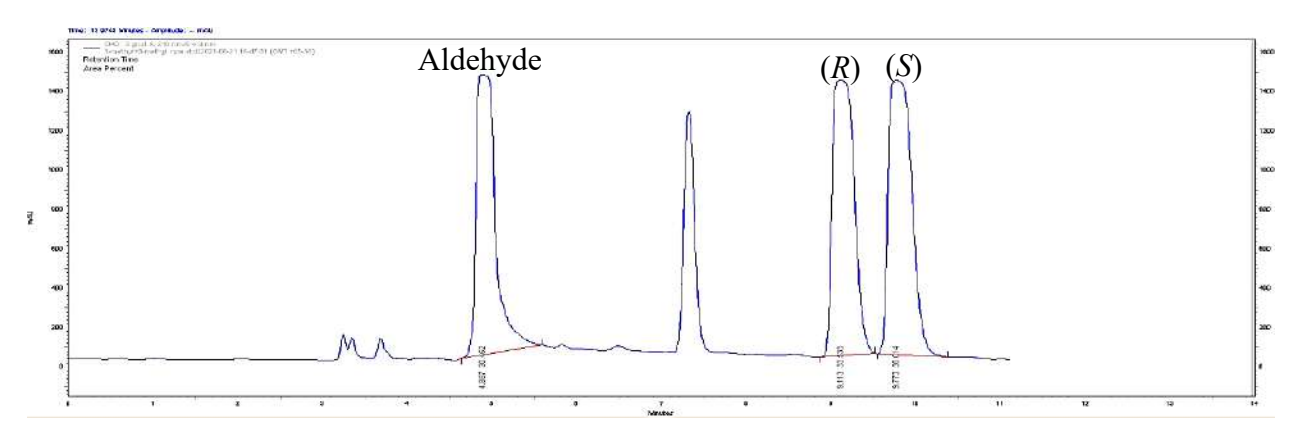


Figure 3.54: HPLC spectrum of the standards: 3-methylbenzaldehdye, and corresponding (R)-and (S)- β -nitroalcohols.

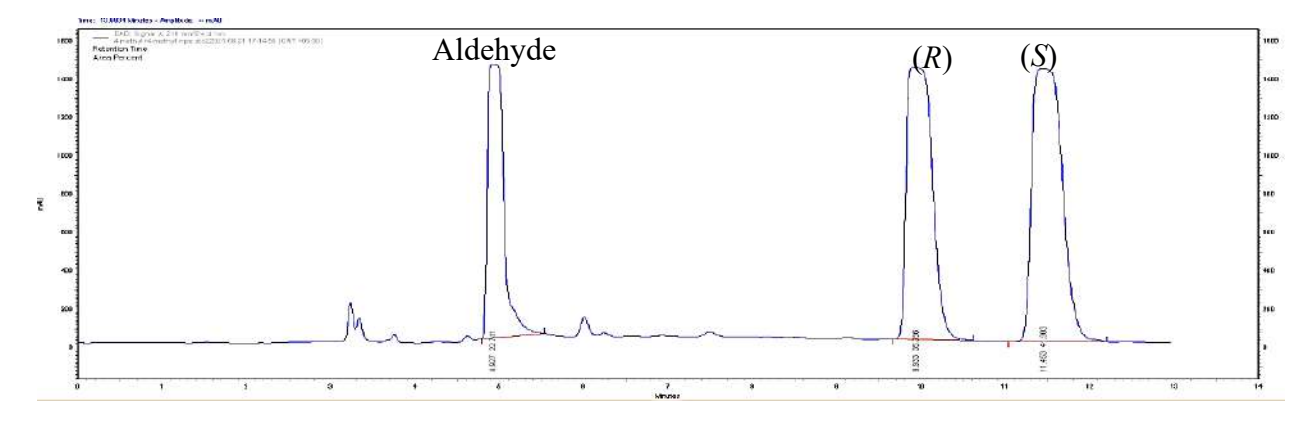


Figure 3.55: HPLC spectrum of the standards: 4-methylbenzaldehdye, and corresponding (R)-and (S)- β -nitroalcohols.

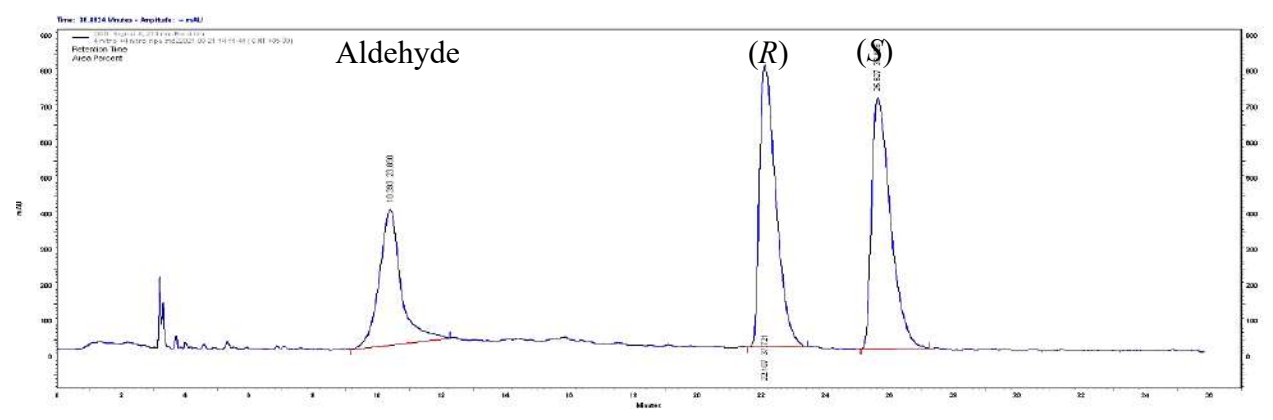


Figure 3.56: HPLC spectrum of the standards: 4-nitrobenzaldehdye, and corresponding (R)- and (S)- β -nitroalcohols.

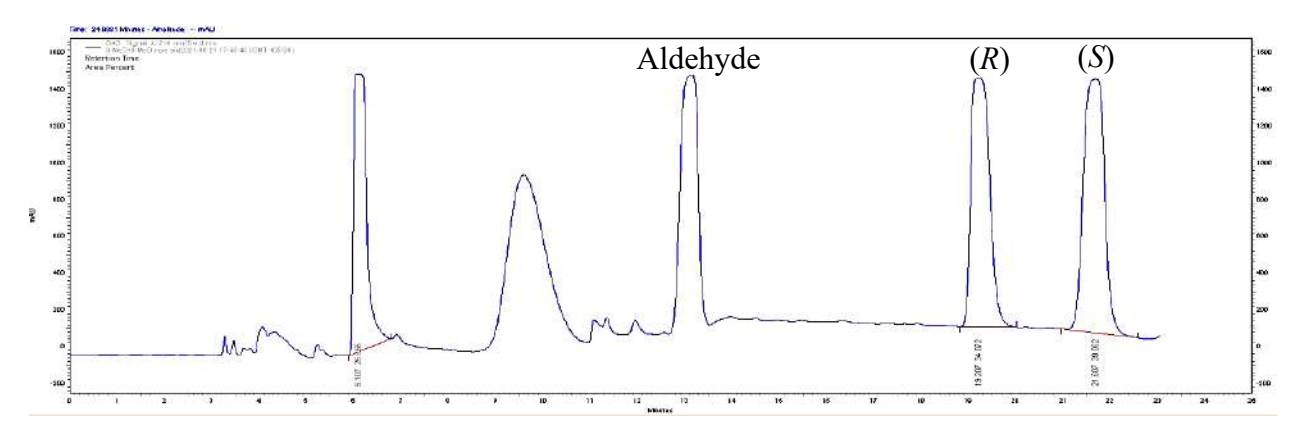


Figure 3.57: HPLC spectrum of the standards: 3-methoxybenzaldehdye, and corresponding (R)-and (S)- β -nitroalcohols.

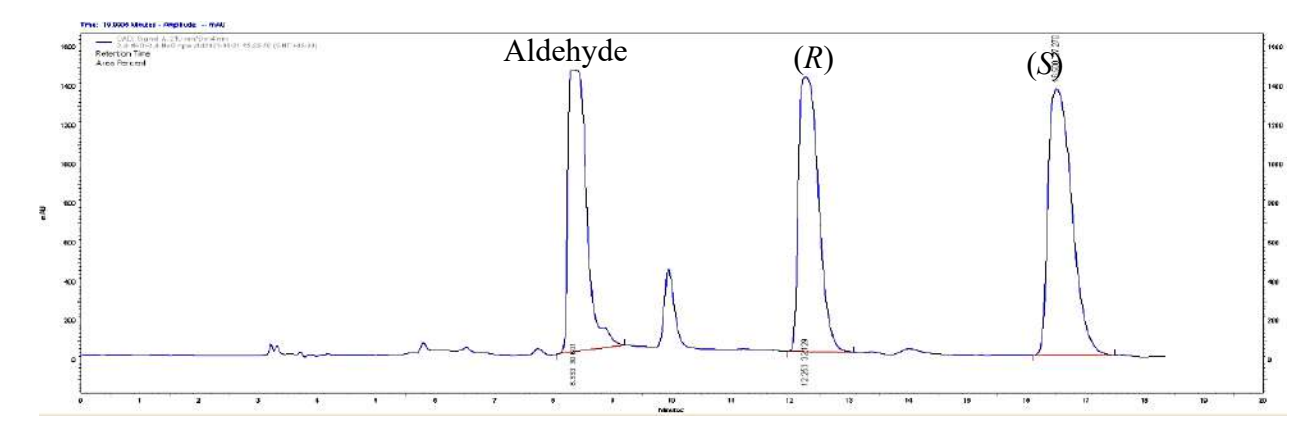


Figure 3.58: HPLC spectrum of the standards: 2,4-dimethoxybenzaldehdye, and corresponding (R)- and (S)- β -nitroalcohols.

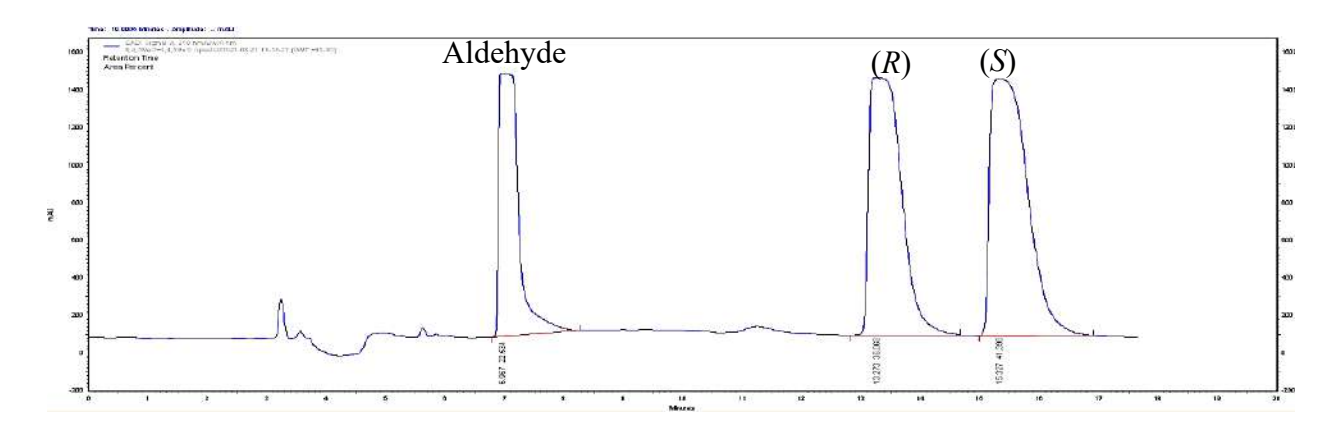


Figure 3.59: HPLC spectrum of the standards: 3,4,5-trimethoxybenzaldehdye, corresponding (R)-and (S)- β -nitroalcohols.

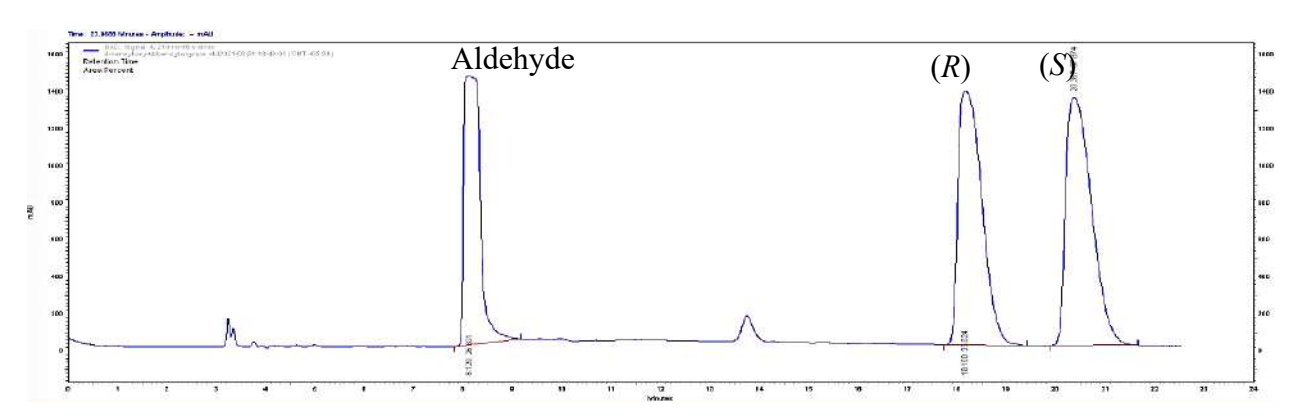


Figure 3.60: HPLC spectrum of the standards: 4-benzyloxybenzaldehdye, corresponding (R)- and (S)- β -nitroalcohols.

3.4.5. At HNL variant (62.5 U) catalyzed synthesis of various (R)- β -nitroalcohols using nitroaldol reaction

Twelve aromatic aldehydes (20 mM) including benzaldehyde were used as substrates along with 1.75 M of nitromethane in the enantioselective nitroaldol reaction. Twelve different enzymes, i.e., *At*HNL wild type and its variants (F179H, F179N, F179L, and F179W from the F179 saturation library and Y14A, Y14C, Y14F, Y14M, Y14G, Y14L and Y14T from the Y14 saturation library), 62.5 U of each were used as a catalyst, which resulted into a total of 144 biotransformations towards the synthesis of the (*R*)-β-nitroalcohols (**Scheme 3.3, Table 3.4, Figure 3.61-132**). The

variants Y14F, Y14M, F179W and F179N have exhibited better % conversion and % ee than the wild type (**Table 3.4**). We observed that F179N has shown better results than the wild type AtHNL, i.e., 96% ee and 76% conversion with benzaldehyde, 64% ee and 95% conversion with 3chlorobenzaldehyde and 98% ee and 58% conversion with 3-methylbenzaldehyde in the synthesis of their corresponding (R)- β -nitroalcohols. The F179W has shown better results than the wild type At HNL in the synthesis of (R)- β -nitroalcohol of trans cinnamaldehyde, i.e., 91% ee and 13% conversion. Y14M produced (R)-NPE in 95% ee and 75% conversion. The Y14F variant gave better results in the synthesis of (R)-β-nitroalcohols of 4-chlorobenzaldehyde with 95% ee and 33% 4-nitrobenzaldehyde with 26% conversion, 44% and conversion, 2,4dimethoxybenzaldehyde with 93% ee and 12% conversion, 4-methylbenzaldehyde with 98% ee and 51% conversion, 3-methoxybenzaldehyde with 93% ee and 61% conversion, 3,4,5trimethoxybenzaldehyde with 80% ee and 52% conversion and 4-benzyloxybenzaldehyde with 89% *ee* and 2% conversion (**Table 3.4**).

$$O$$
 R
+ CH₃NO₂

AtHNL eng variants
 OH
 R
NO₂

(R)-β-nitroalcohols

Scheme 3.3: AtHNL variants in the enantioselective synthesis of diverse (R)- β -nitroalcohols.

Table 3.4: AtHNL variants (62.5 U) catalysed enantioselective synthesis of (R)-β-nitroalcohols.

R	WT	F179H	F179N	F179L	F179W	Y14A	Y14M	Y14F	Y14C	Y14G	Y14L	Y14T
Ph	61	53	76	44	47	57	75	68	49	39	69	39
	98	97	96	85	97	91	97	98	98	87	96	90
trans cinnamyl	7 82	5 24	8 91	8 50	13 91	ND	8 77	13 88	1 83	ND	9 88	ND
4-Fluoro Ph	4 77	ND	3 35	ND	ND	ND	ND	0.4 86	ND	ND	ND	ND
4-Chloro Ph	18	12	44	15	11	10	24	33	7	5	22	7
	86	5	92	43	80	44	91	95	84	15	77	25
4-Nitro Ph	48	45	50	43	39	41	45	44	30	40	44	45
	7	0.3	33	4	11	11	13	26	11	7	11	2
2,4-Dimethoxy Ph	12 87	1 57	5 82	3 68	10 89	ND	5 98	12 93	2 83	1 56	3 73	1 70
3-Chloro Ph	54	13	64	39	41	40	59	62	45	38	51	41
	97	13	95	82	95	87	97	98	96	85	96	86
3-Methyl Ph	8	4	58	44	30	39	55	51	33	16	53	19
	90	26	98	96	99	94	92	94	99	85	98	83
4-Methyl Ph	31	4	49	37	19	13	46	51	10	5	38	6
	98	20	98	93	99	96	97	98	94	64	92	61
3-Methoxy Ph	55	7	58	39	40	28	55	61	41	11	39	11
	95	74	96	98	99	94	99	93	98	97	99	88
3,4,5-Trimethoxy Ph	46	17	24	30	33	24	39	52	11	27	29	28
	70	9	52	7	66	14	65	80	19	3	49	2
4-Benzyloxy Ph	ND	ND	ND	ND	ND	ND	ND	2 89	ND	ND	ND	ND

ND: not determined; % ee is highlighted in bold and % conversion is in plain.

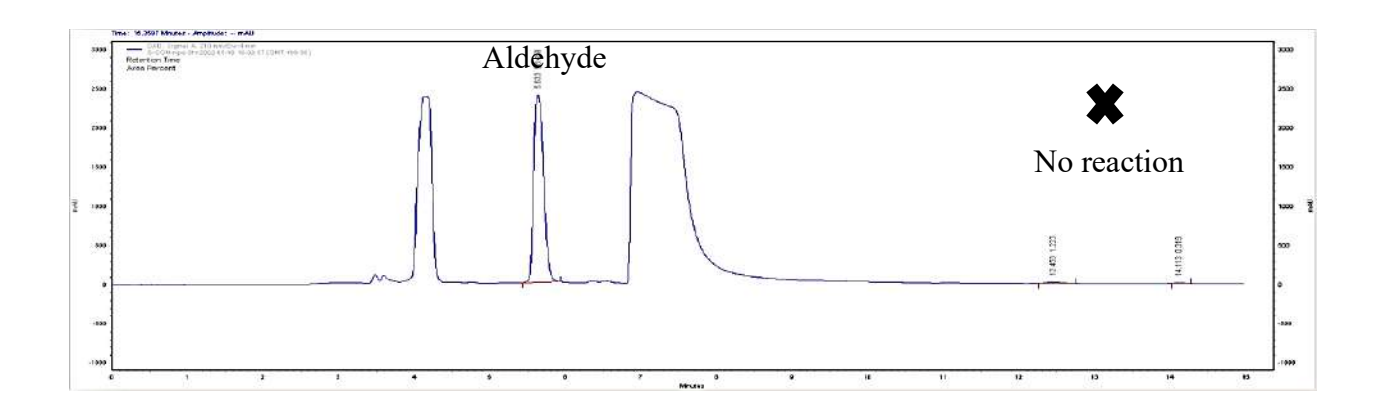


Figure 3.61: HPLC spectrum of control reaction at 3 h where enzyme is replaced by 20 mM KPB and benzaldehyde used as the substrate.

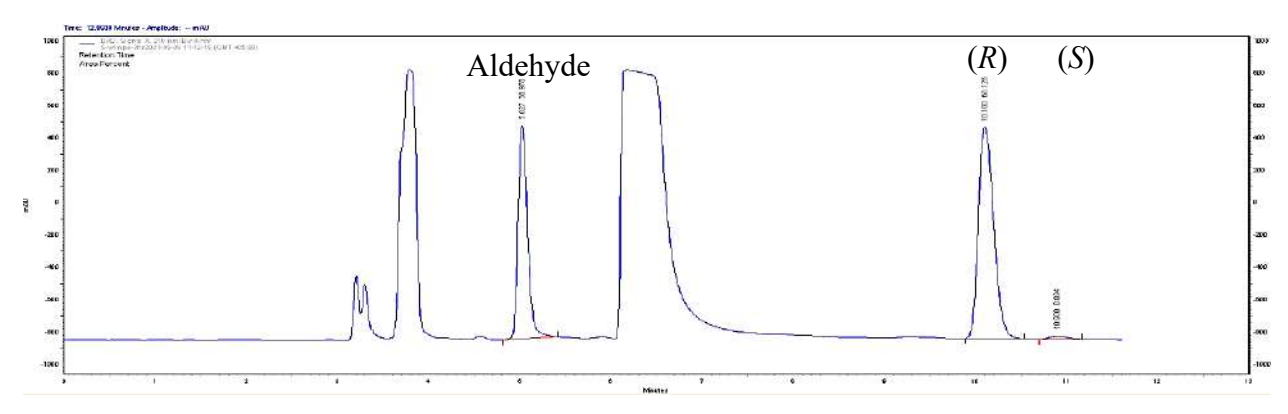


Figure 3.62: HPLC spectrum of wild type AtHNL showing enantioselective synthesis of (R)-2-nitro-1-phenylethanol at 3 h using benzaldehyde as the substrate.

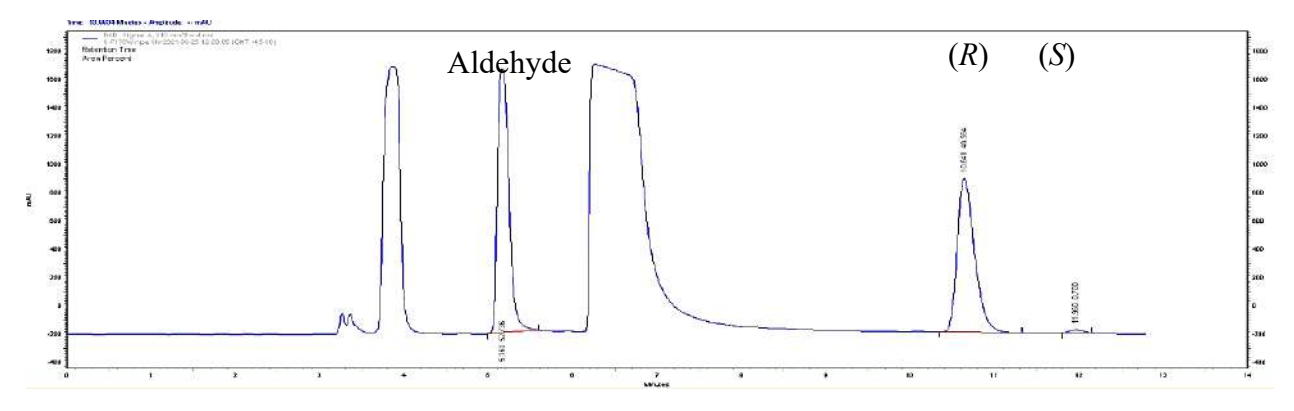


Figure 3.63: HPLC spectrum of the F179W variant showing enantioselective synthesis of (*R*)- 2-nitro-1-phenylethanol at 3 h using benzaldehyde as the substrate.

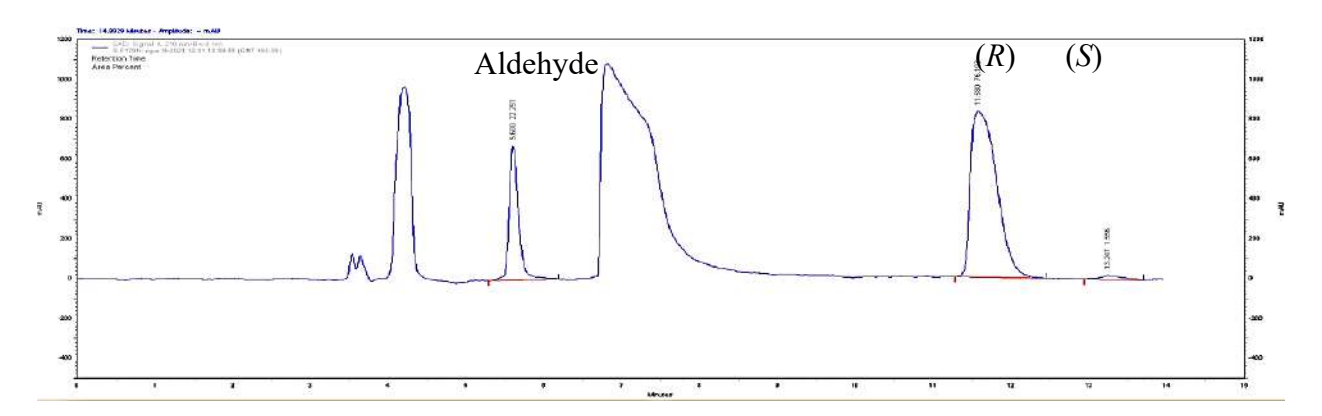


Figure 3.64: HPLC spectrum of the F179N variant showing enantioselective synthesis of (R)- 2-nitro-1-phenylethanol at 3 h using benzaldehyde as the substrate.

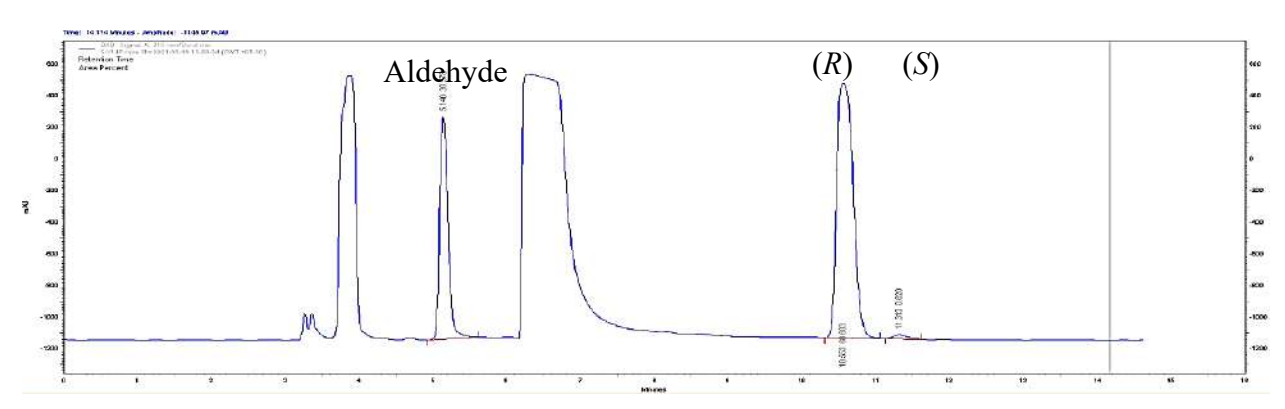


Figure 3.65: HPLC spectrum of the Y14F variant showing enantioselective synthesis of (R)- 2-nitro-1-phenylethanol at 3 h using benzaldehyde as the substrate.

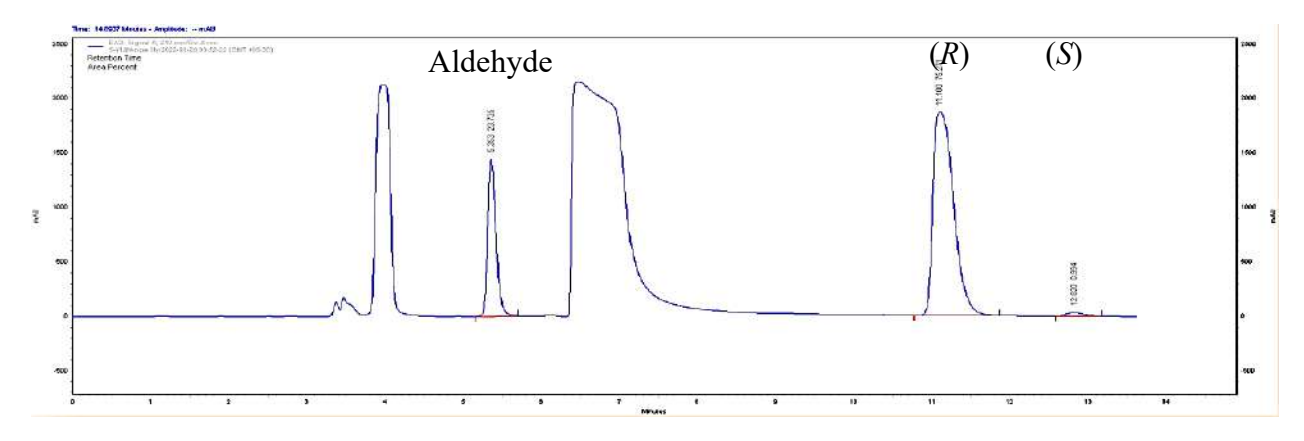


Figure 3.66: HPLC spectrum of the Y14M variant showing enantioselective synthesis of (R)- 2-nitro-1-phenylethanol at 3 h using benzaldehyde as the substrate.

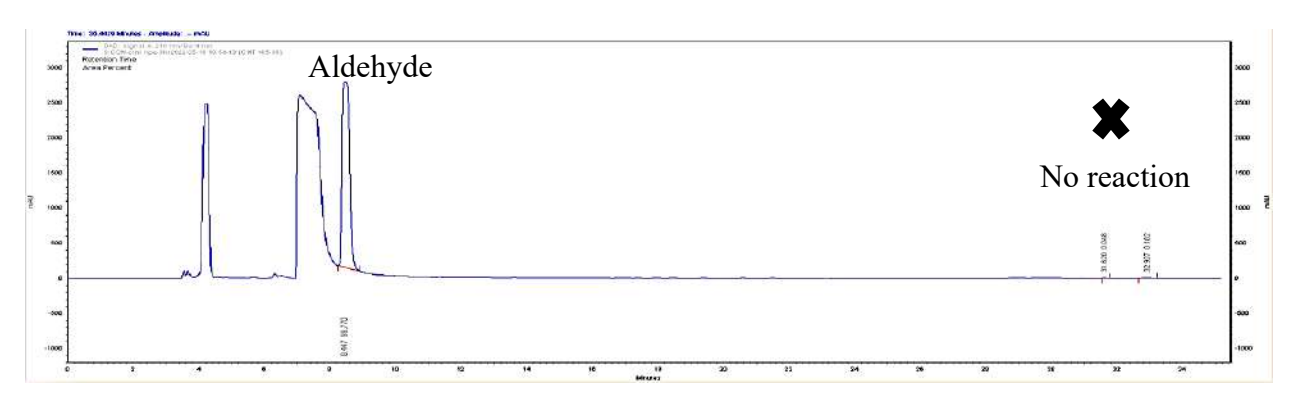


Figure 3.67: HPLC spectrum of control reaction at 3 h where enzyme is replaced by 20 mM KPB and *trans* cinnamaldehyde used as the substrate.

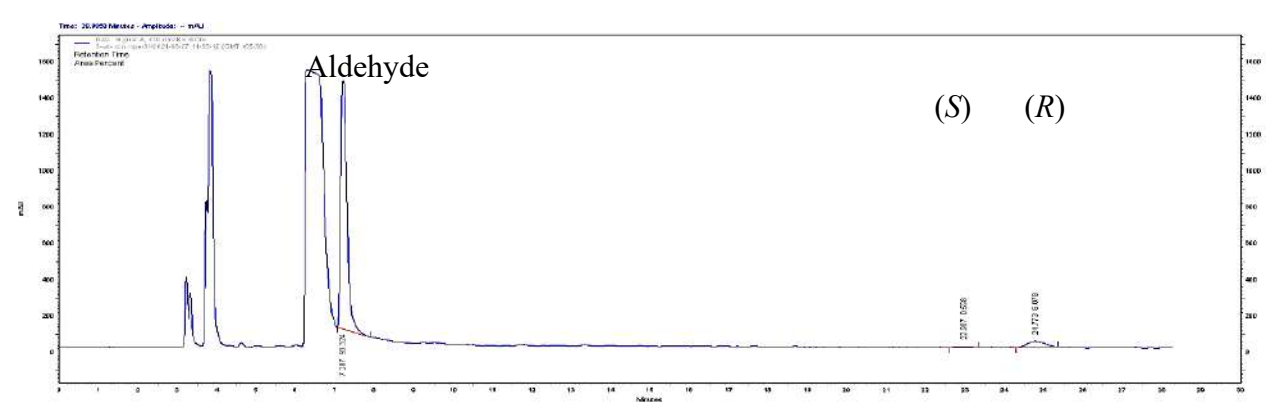


Figure 3.68: HPLC spectrum of wild type AtHNL showing enantioselective synthesis of (R)-(E)-1-nitro-4-phenylbut-3-en-2-ol at 3 h using trans cinnamaldehyde as the substrate.

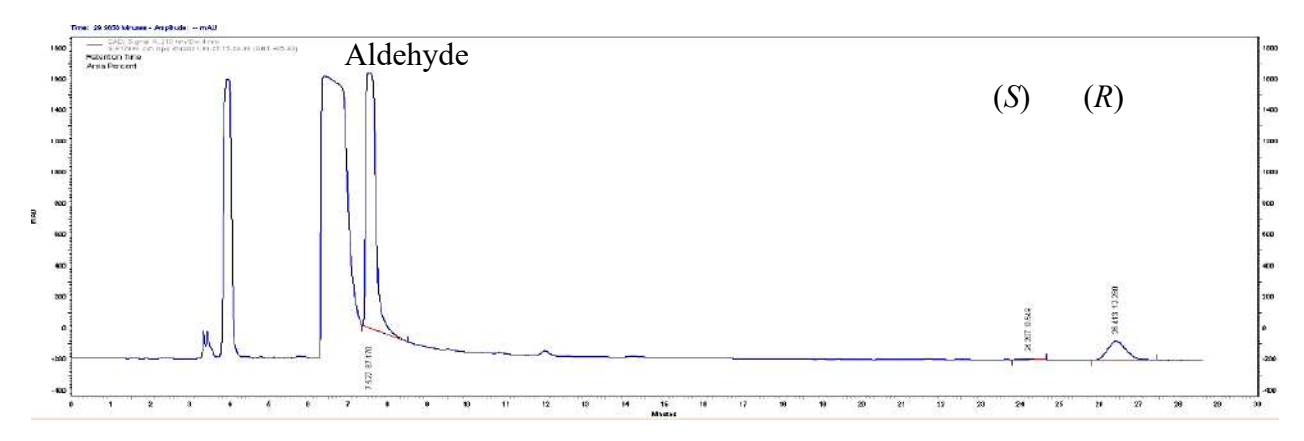


Figure 3.69: HPLC spectrum of the F179W variant showing enantioselective synthesis of (R)-(E)-1-nitro-4-phenylbut-3-en-2-ol at 3 h using *trans* cinnamaldehyde as the substrate.

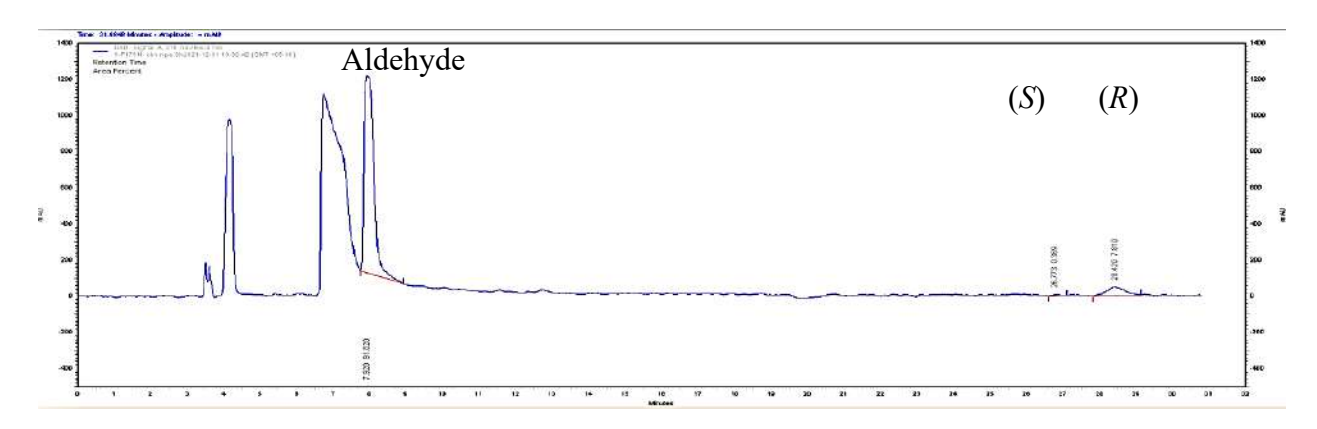


Figure 3.70: HPLC spectrum of the F179N variant showing enantioselective synthesis of (R)-(E)-1-nitro-4-phenylbut-3-en-2-ol at 3 h using *trans* cinnamaldehyde as the substrate.

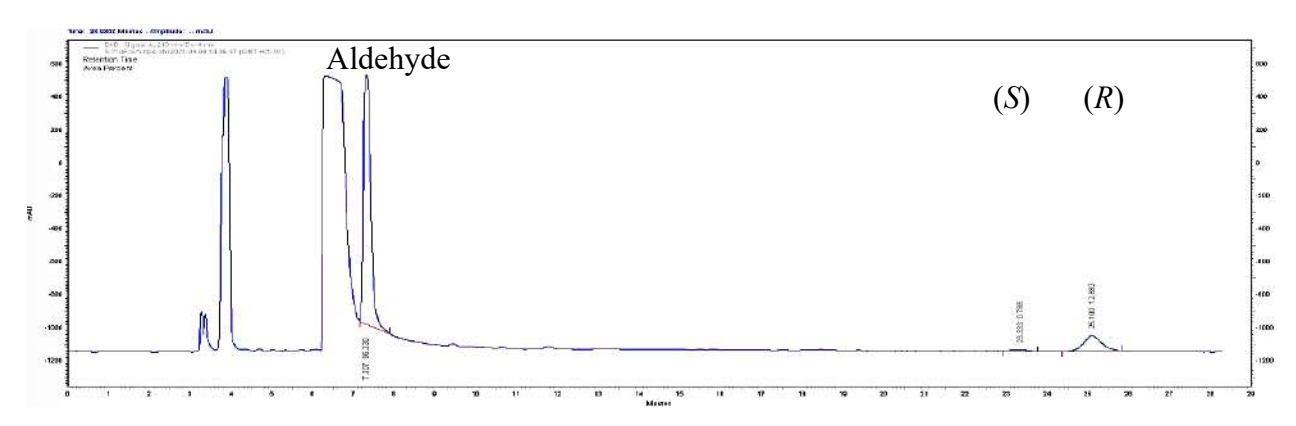


Figure 3.71: HPLC spectrum of the Y14F variant showing enantioselective synthesis of (R)-(E)-1-nitro-4-phenylbut-3-en-2-ol at 3 h using *trans* cinnamaldehyde as the substrate.

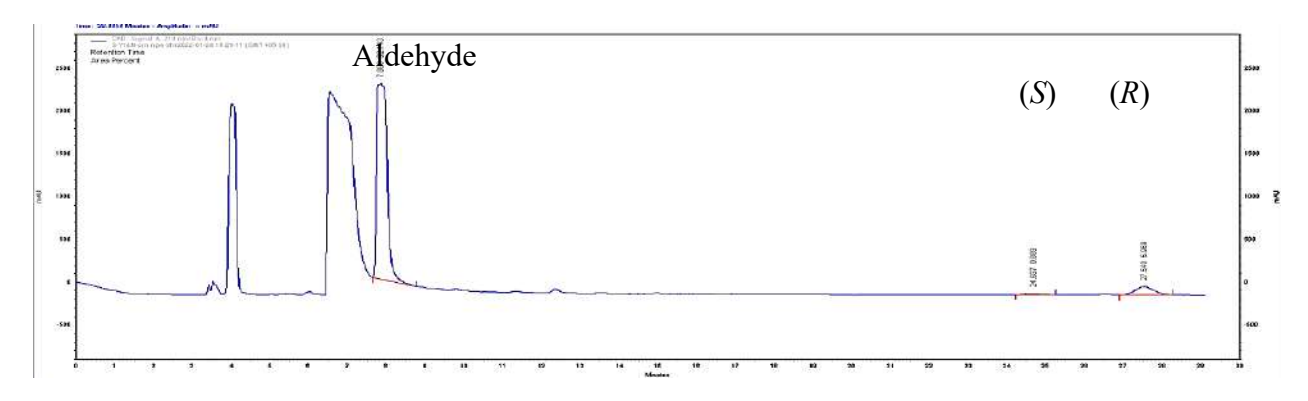


Figure 3.72: HPLC spectrum of the Y14M variant showing enantioselective synthesis of (R)-(E)-1-nitro-4-phenylbut-3-en-2-ol at 3 h using *trans* cinnamaldehyde as the substrate.

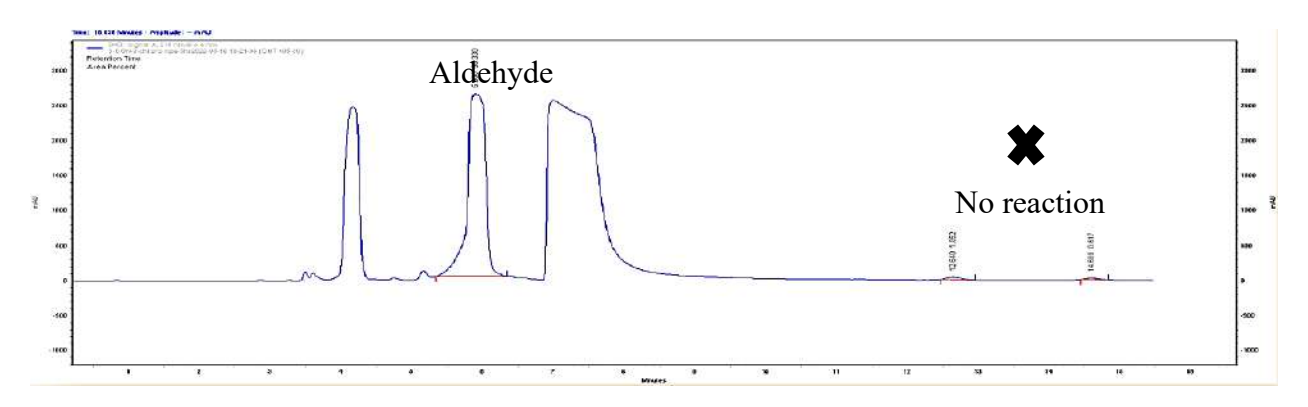


Figure 3.73: HPLC spectrum of control reaction at 3 h where enzyme is replaced by 20 mM KPB and 3-chlorobenzaldehyde used as the substrate.

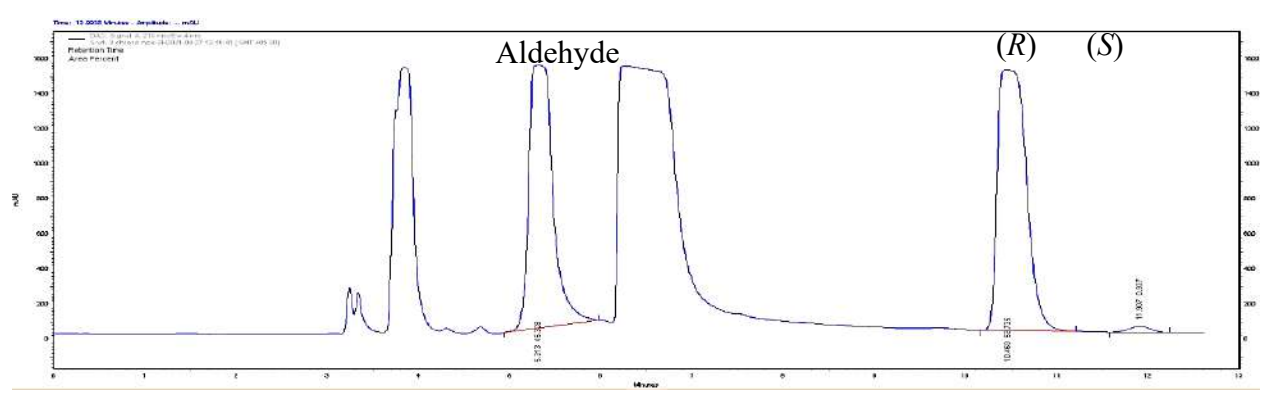


Figure 3.74: HPLC spectrum of wild type AtHNL showing enantioselective synthesis of (R)-1-(3-chlorophenyl)-2-nitroethanol at 3 h using 3-chlorobenzaldehyde as the substrate.

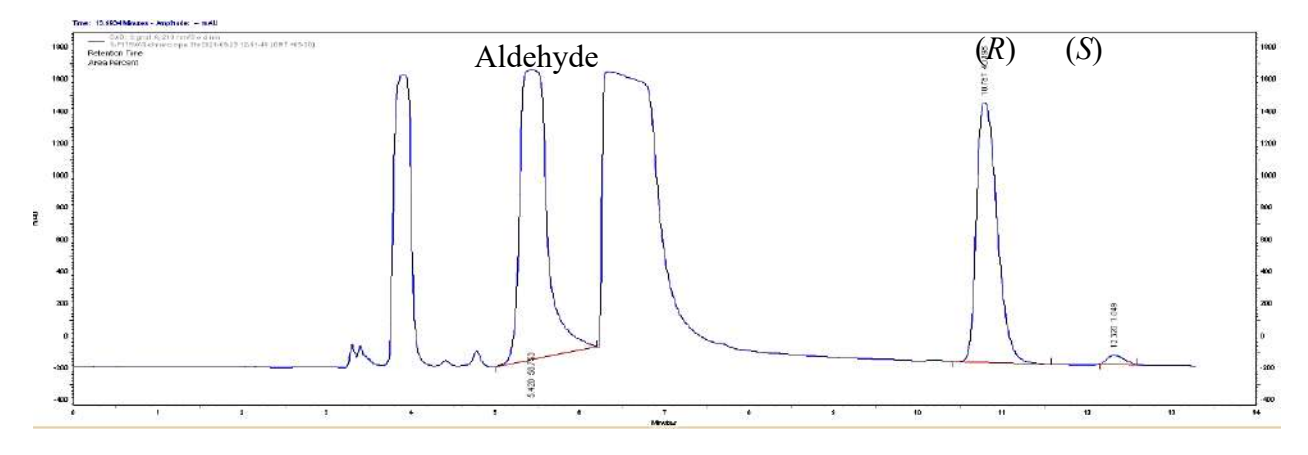


Figure 3.75: HPLC spectrum of the F179W variant showing enantioselective synthesis of (R)-1-(3-chlorophenyl)-2-nitroethanol at 3 h using 3-chlorobenzaldehyde as the substrate.

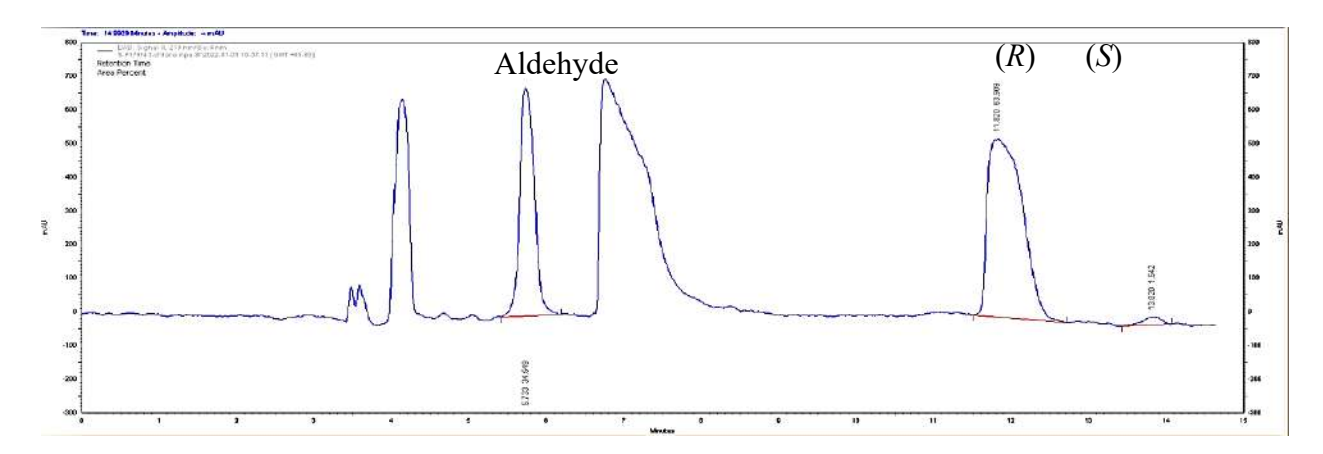


Figure 3.76: HPLC spectrum of the F179N variant showing enantioselective synthesis of (R)-1-(3-chlorophenyl)-2-nitroethanol at 3 h using 3-chlorobenzaldehyde as the substrate.

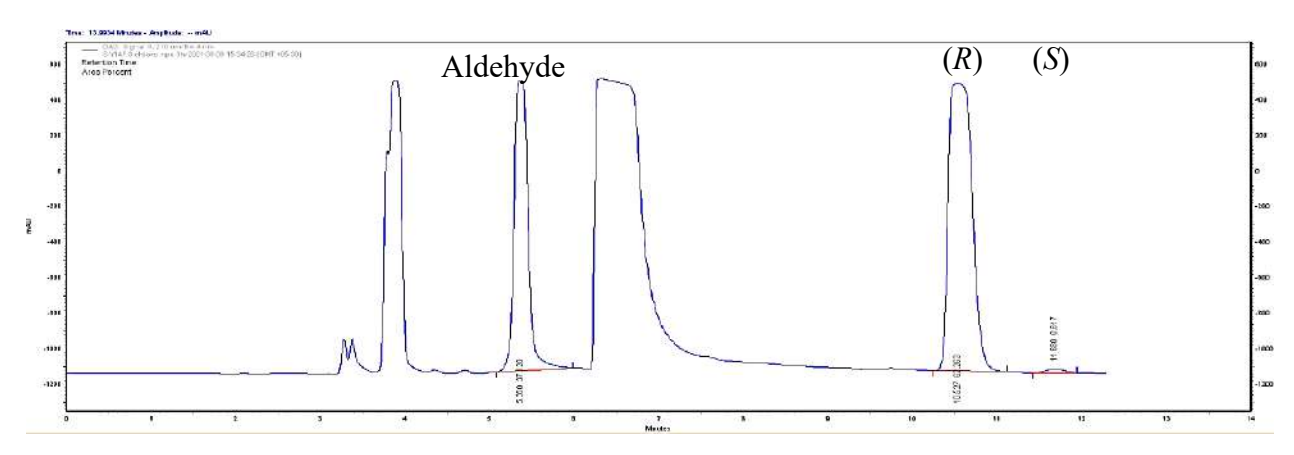


Figure 3.77: HPLC spectrum of the Y14F variant showing enantioselective synthesis of (R)-1-(3-chlorophenyl)-2-nitroethanol at 3 h using 3-chlorobenzaldehyde as the substrate.

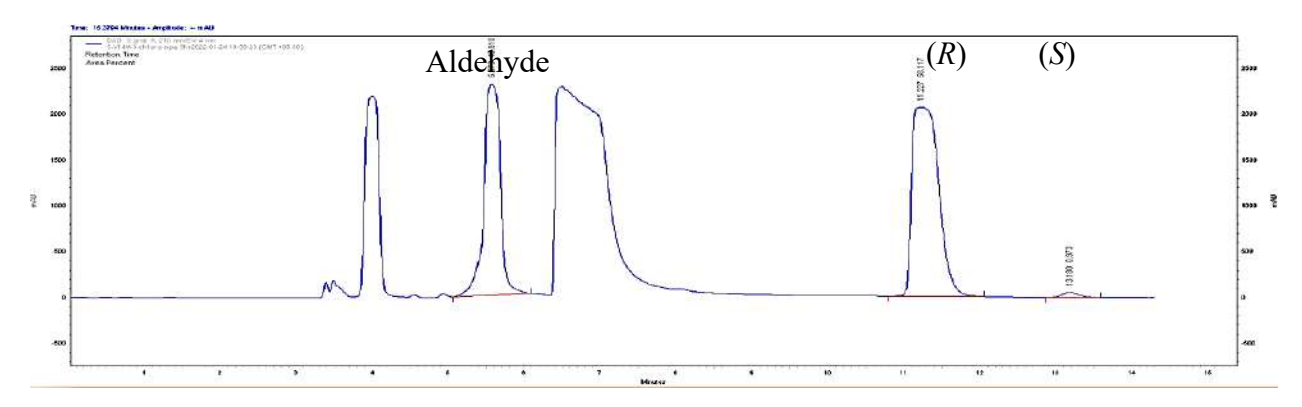


Figure 3.78: HPLC spectrum of the Y14M variant showing enantioselective synthesis of (*R*)-1-(3-chlorophenyl)-2-nitroethanol at 3 h using 3-chlorobenzaldehyde as the substrate.

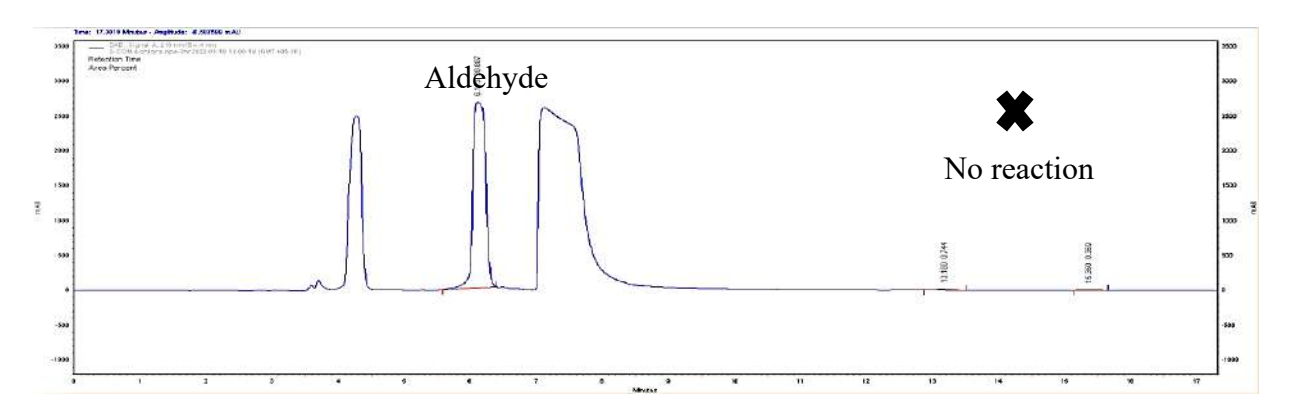


Figure 3.79: HPLC spectrum of control reaction at 3 h where enzyme is replaced by 20 mM KPB and 4-chlorobenzaldehyde used as the substrate.

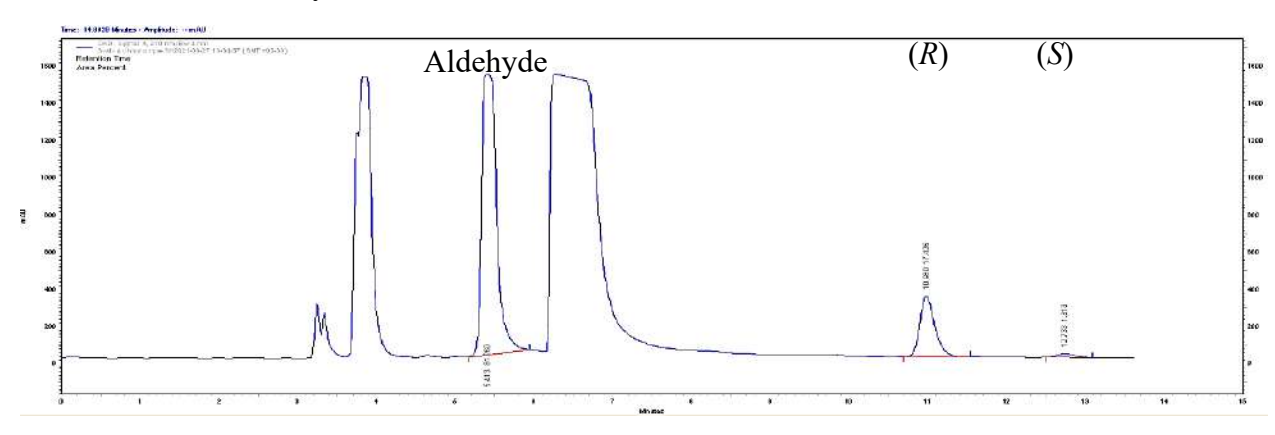


Figure 3.80: HPLC spectrum of wild type AtHNL showing enantioselective synthesis of (R)-1-(4-chlorophenyl)-2-nitroethanol at 3 h using 4-chlorobenzaldehyde as the substrate.

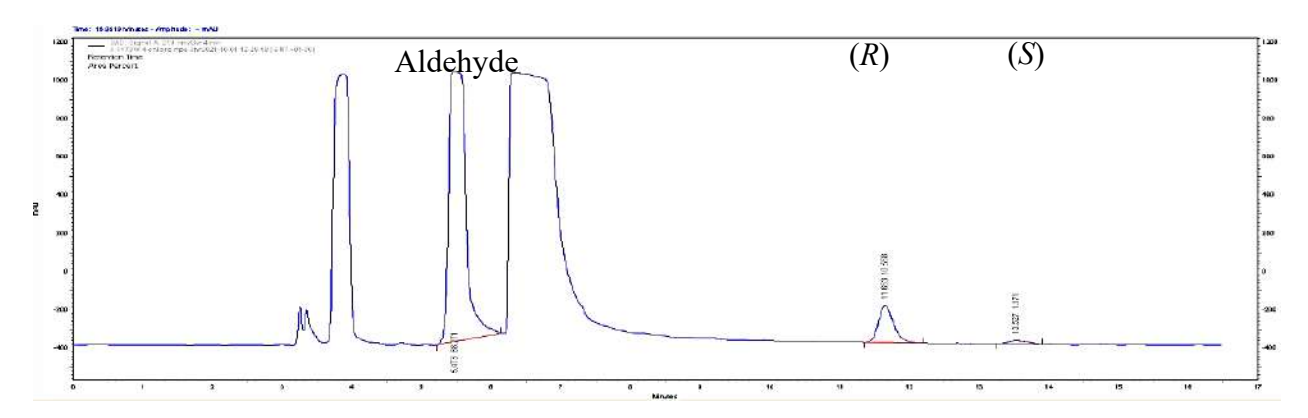


Figure 3.81: HPLC spectrum of the F179W variant showing enantioselective synthesis of (R)-1-(4-chlorophenyl)-2-nitroethanol at 3 h using 4-chlorobenzaldehyde as the substrate.

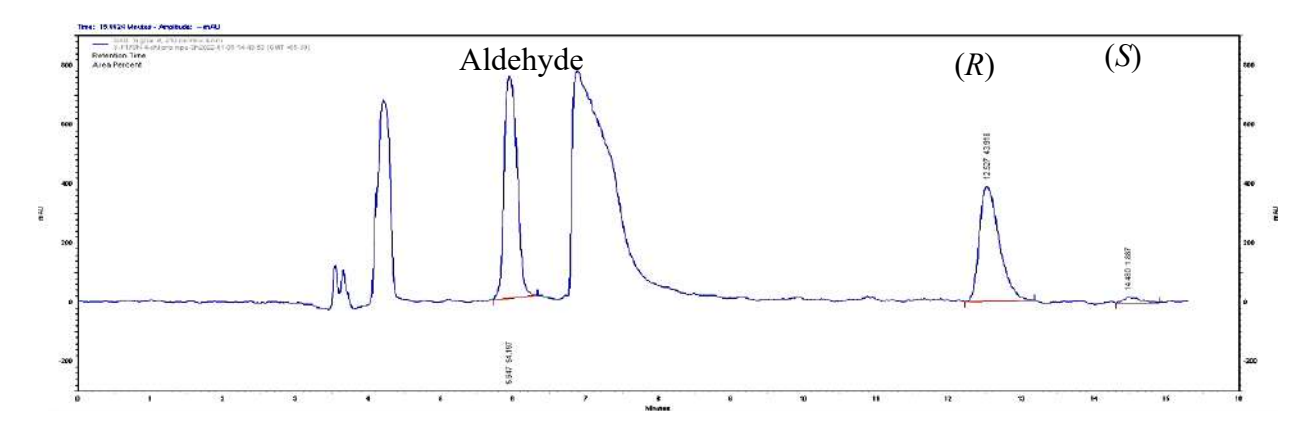


Figure 3.82: HPLC spectrum of the F179N variant showing enantioselective synthesis of (R)-1-(4-chlorophenyl)-2-nitroethanol at 3 h using 4-chlorobenzaldehyde as the substrate.

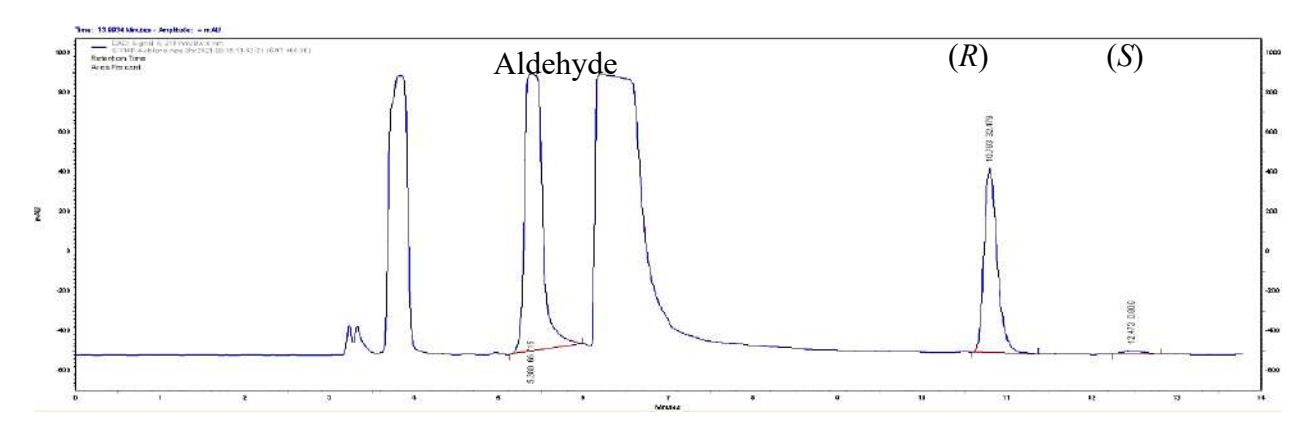


Figure 3.83: HPLC spectrum of the Y14F variant showing enantioselective synthesis of (R)-1-(4-chlorophenyl)-2-nitroethanol at 3 h using 4-chlorobenzaldehyde as the substrate.

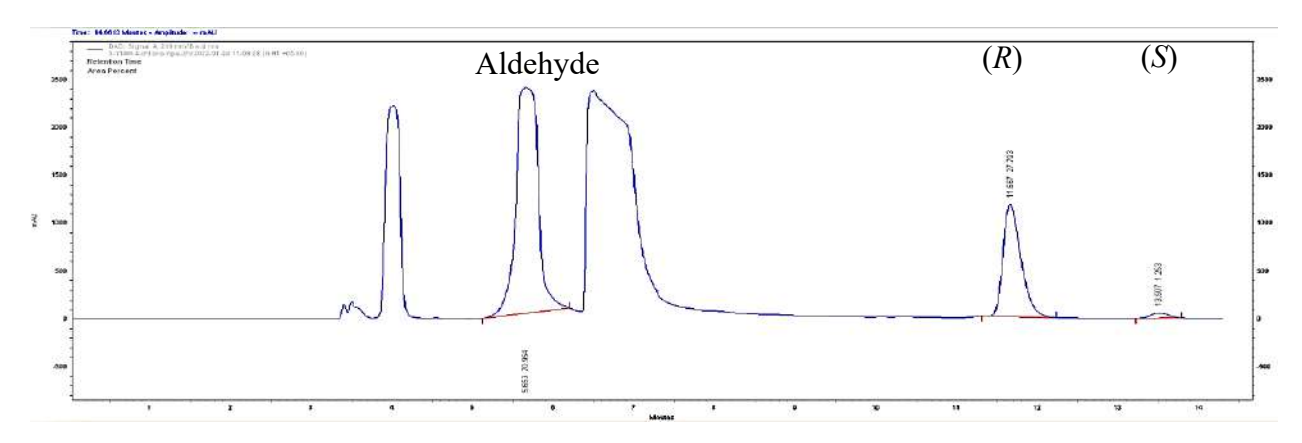


Figure 3.84: HPLC spectrum of the Y14M variant showing enantioselective synthesis of (R)-1-(4-chlorophenyl)-2-nitroethanol at 3 h using 4-chlorobenzaldehyde as the substrate.

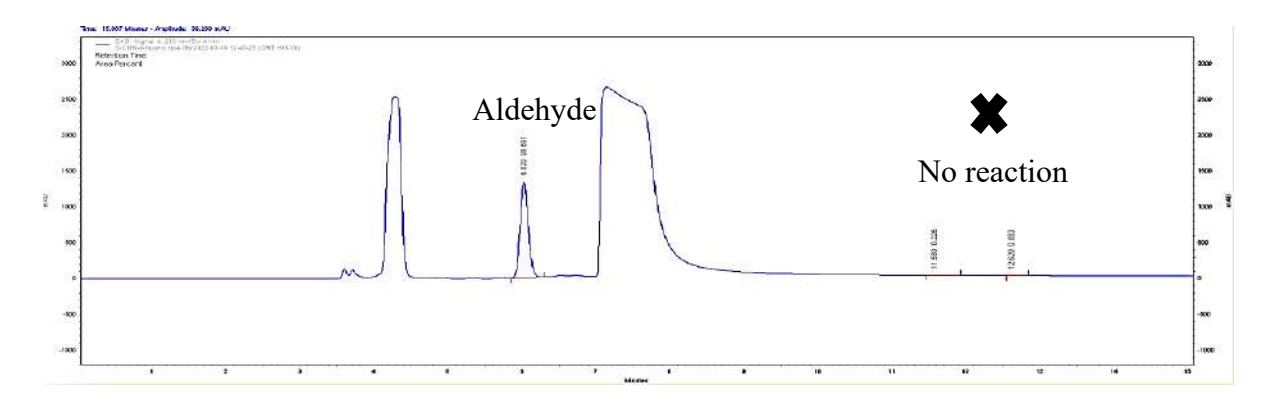


Figure 3.85: HPLC spectrum of control reaction at 3 h where enzyme is replaced by 20 mM KPB and 4-fluorobenzaldehyde used as the substrate.

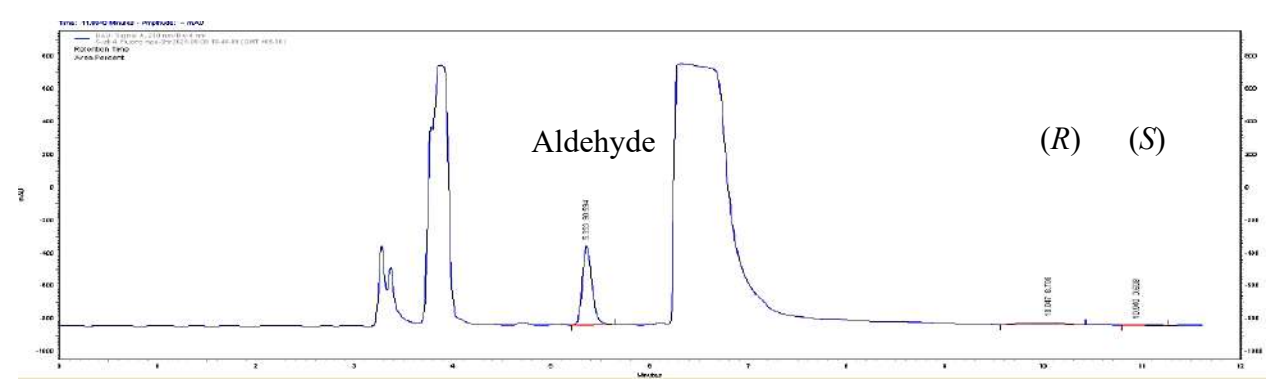


Figure 3.86: HPLC spectrum of wild type AtHNL showing enantioselective synthesis of (R)-1-(4-fluorophenyl)-2-nitroethanol at 3 h using 4-fluorobenzaldehyde as the substrate.

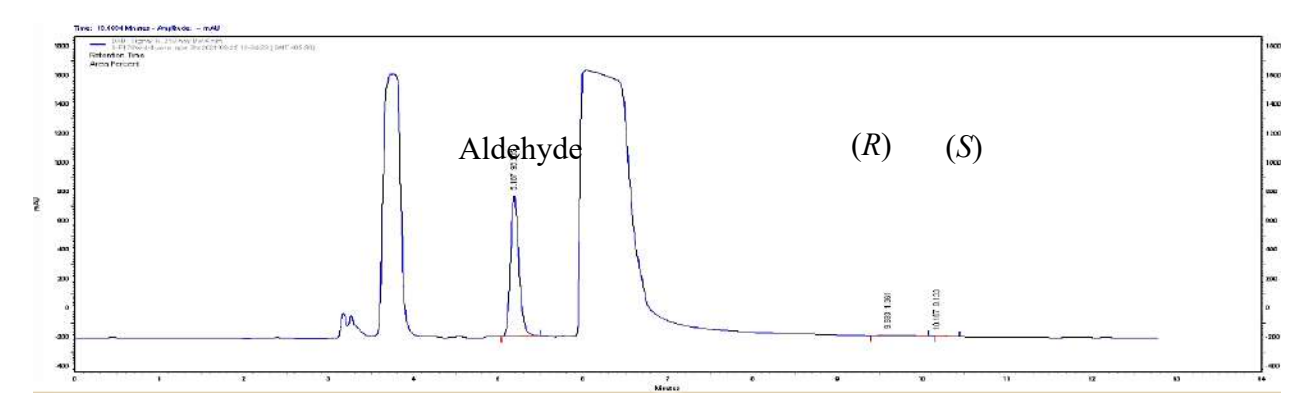


Figure 3.87: HPLC spectrum of the F179W variant showing enantioselective synthesis of (R)-1-(4-fluorophenyl)-2-nitroethanol at 3 h using 4-fluorobenzaldehyde as the substrate.

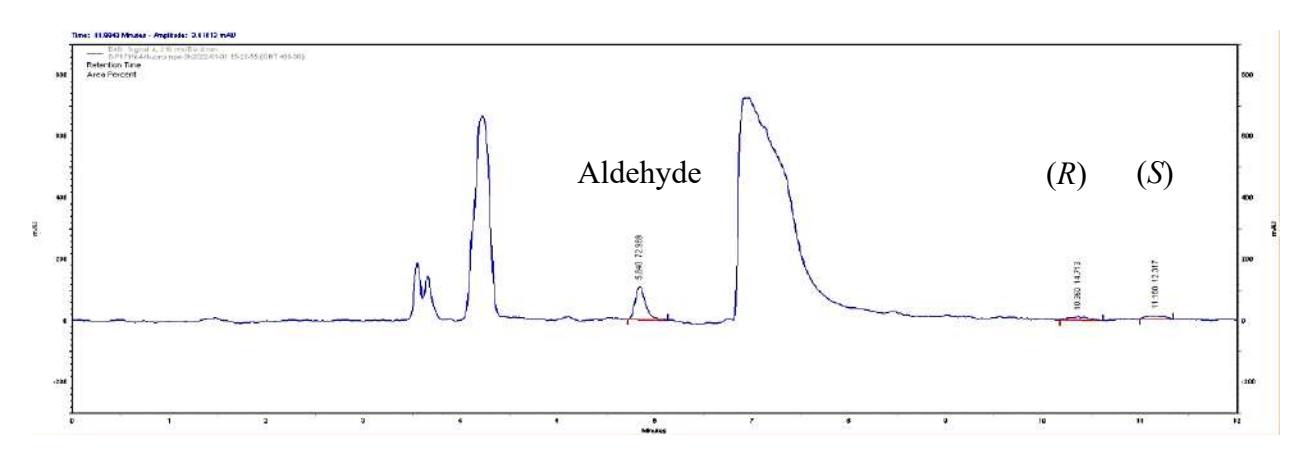


Figure 3.88: HPLC spectrum of the F179N variant showing enantioselective synthesis of (R)-1-(4-fluorophenyl)-2-nitroethanol at 3 h using 4-fluorobenzaldehyde as the substrate.

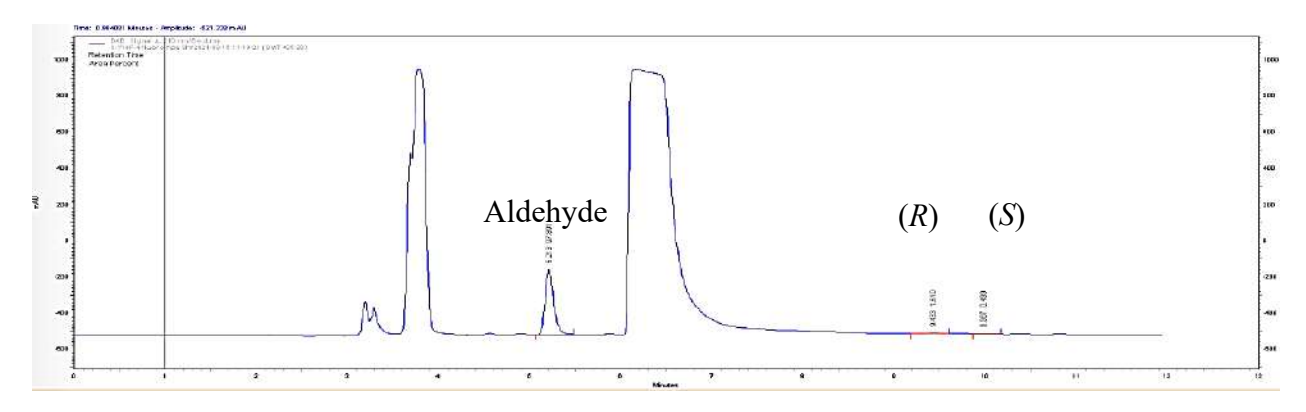


Figure 3.89: HPLC spectrum of the Y14F variant showing enantioselective synthesis of (R)-1-(4-fluorophenyl)-2-nitroethanol at 3 h using 4-fluorobenzaldehyde as the substrate.

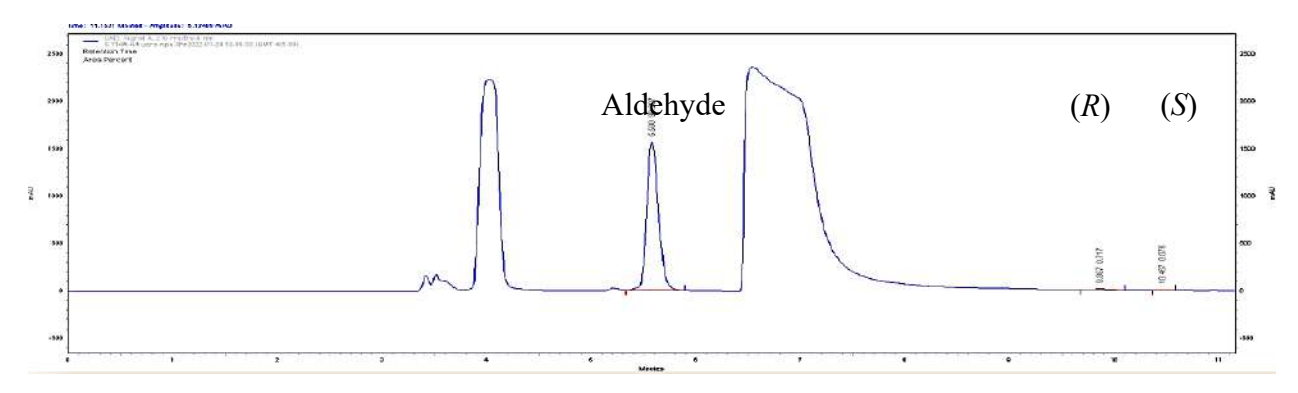


Figure 3.90: HPLC spectrum of the Y14M variant showing enantioselective synthesis of (R)-1-(4-fluorophenyl)-2-nitroethanol at 3 h using 4-fluorobenzaldehyde as the substrate.

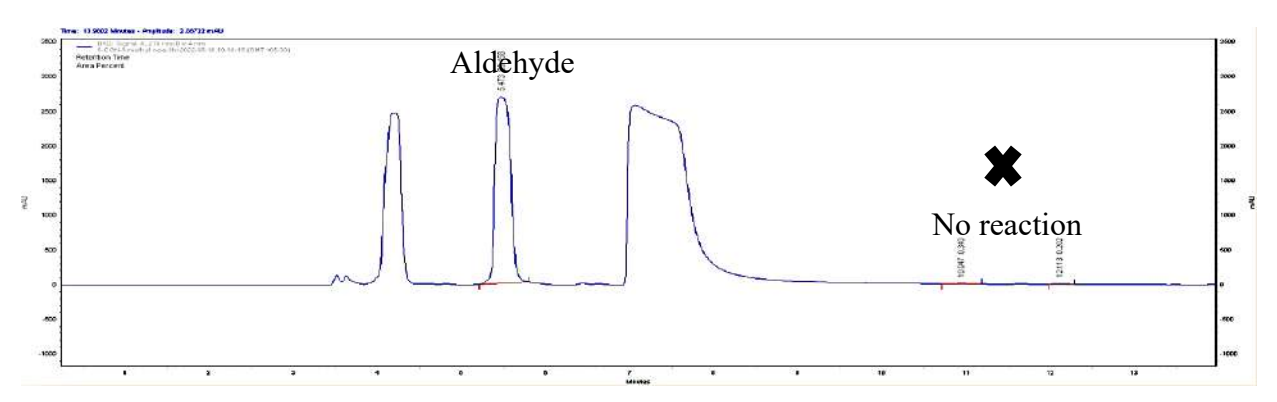


Figure 3.91: HPLC spectrum of control reaction at 3 h where enzyme is replaced by 20 mM KPB and 3-methylbenzaldehyde used as the substrate.

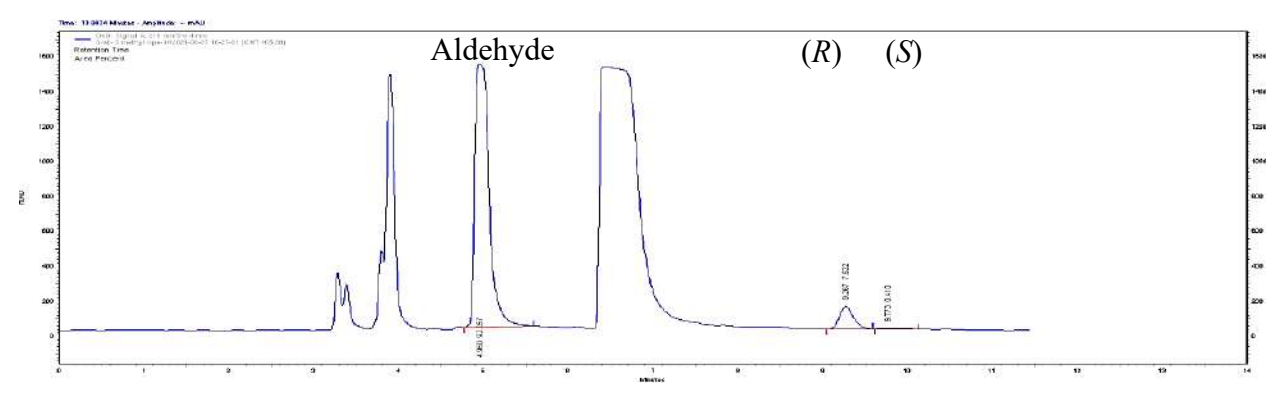


Figure 3.92: HPLC spectrum of wild type AtHNL showing enantioselective synthesis of (R)-1-(3-methylphenyl)-2-nitroethanol at 3 h using 3-methylbenzaldehyde as the substrate.

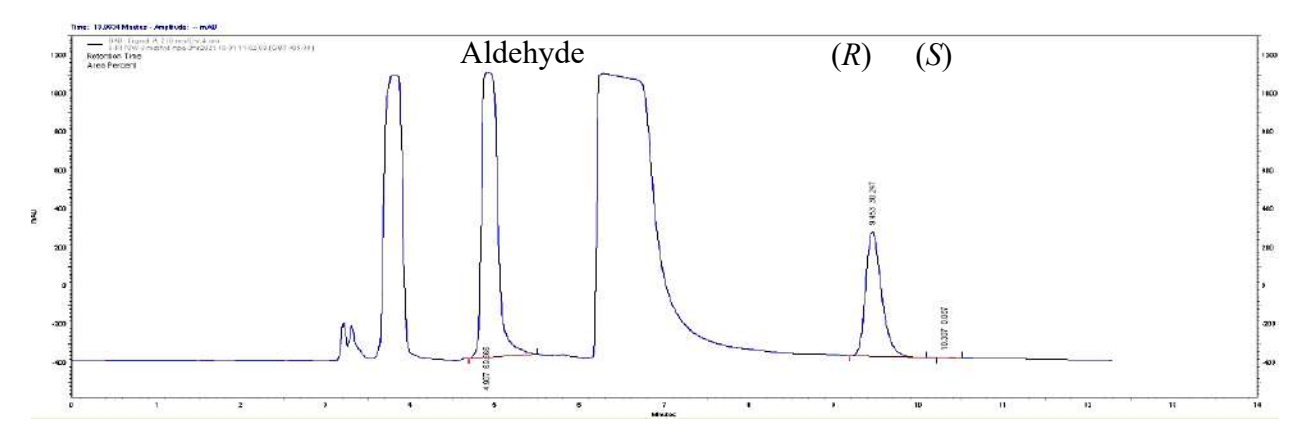


Figure 3.93: HPLC spectrum of the F179W variant showing enantioselective synthesis of (R)-1-(3-methylphenyl)-2-nitroethanol at 3 h using 3-methylbenzaldehyde as the substrate.

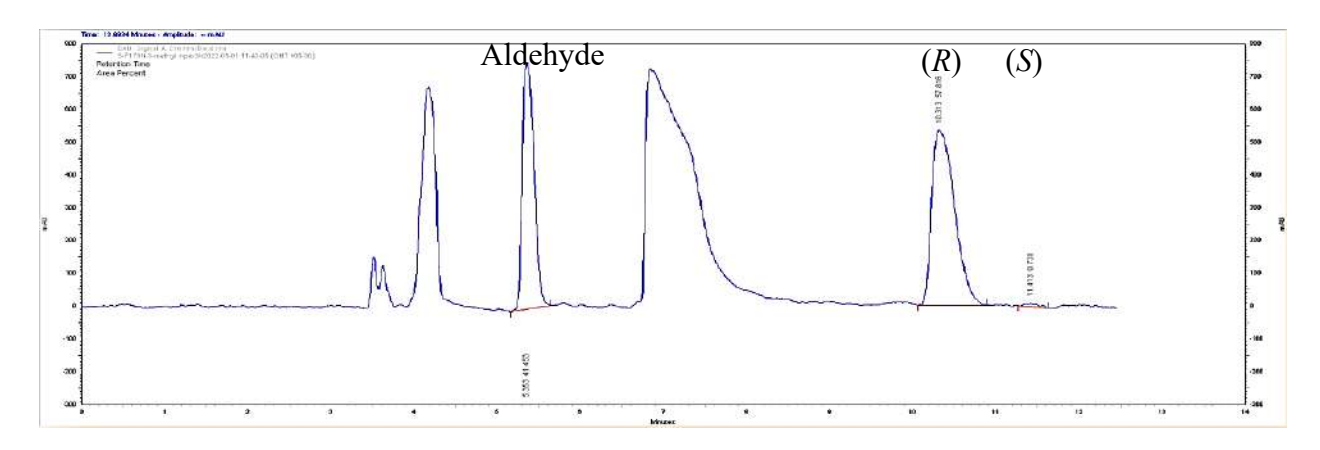


Figure 3.94: HPLC spectrum of the F179N variant showing enantioselective synthesis of (R)-1-(3-methylphenyl)-2-nitroethanol at 3 h using 3-methylbenzaldehyde as the substrate.

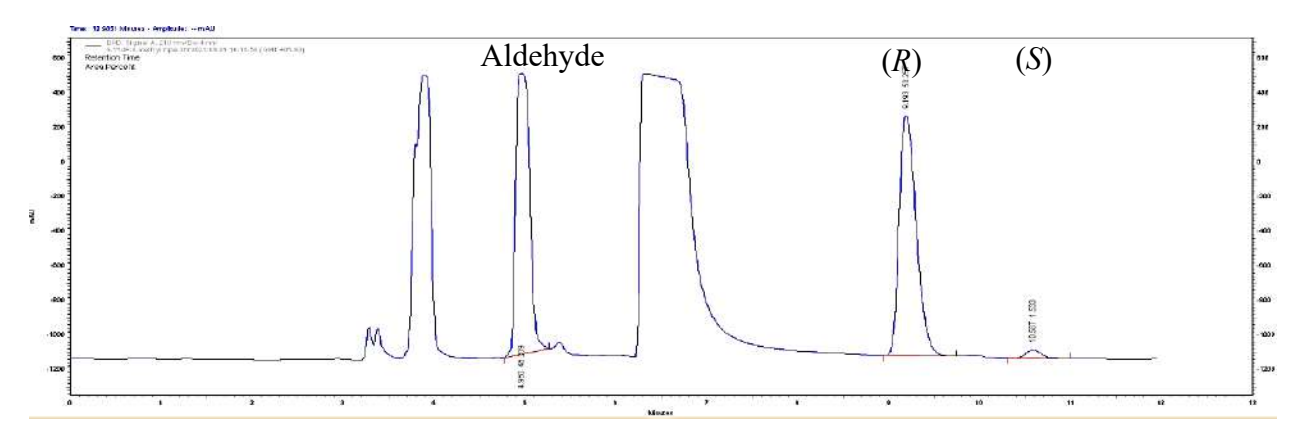


Figure 3.95: HPLC spectrum of the Y14F variant showing enantioselective synthesis of (R)-1-(3-methylphenyl)-2-nitroethanol at 3 h using 3-methylbenzaldehyde as the substrate.

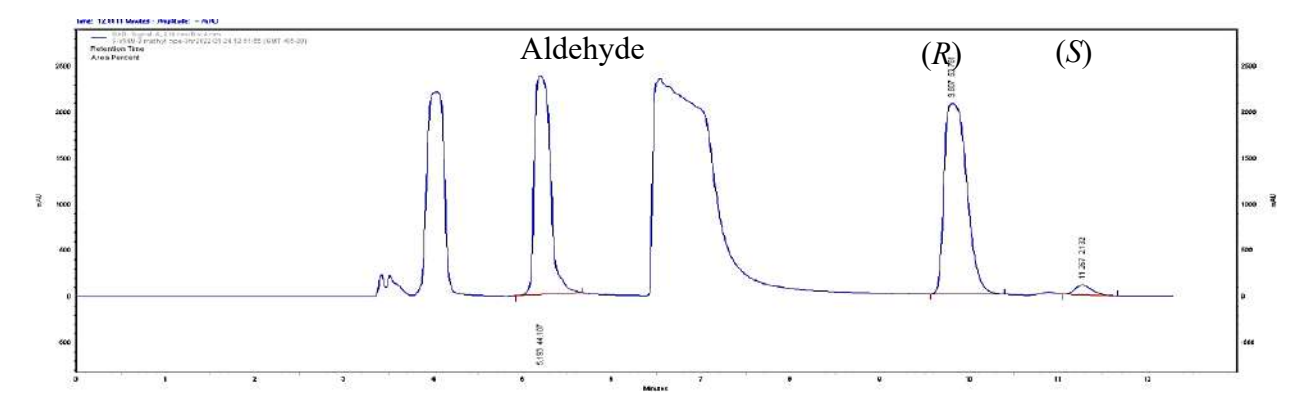


Figure 3.96: HPLC spectrum of the Y14M variant showing enantioselective synthesis of (R)-1-(3-methylphenyl)-2-nitroethanol at 3 h using 3-methylbenzaldehyde as the substrate.

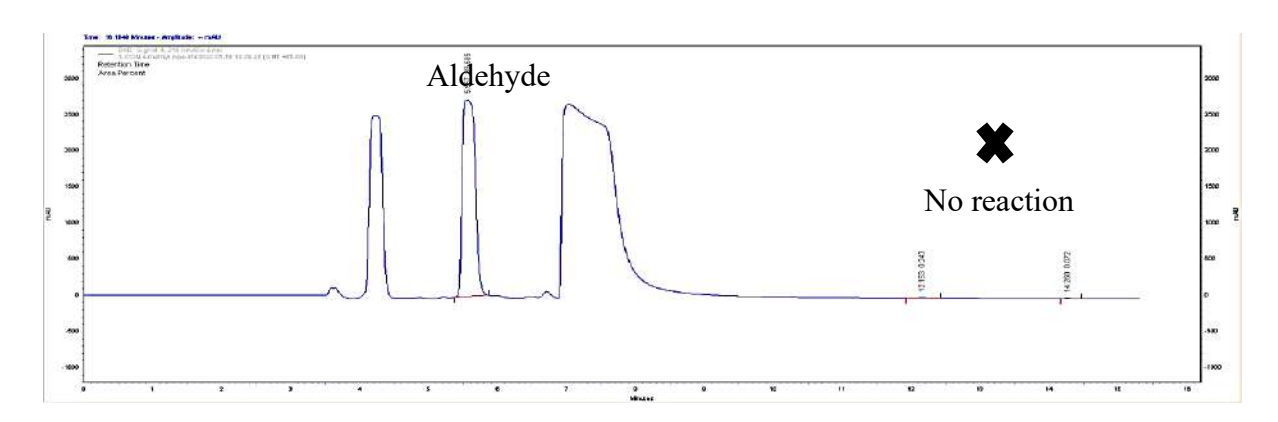


Figure 3.97: HPLC spectrum of control reaction at 3 h where enzyme is replaced by 20 mM KPB and 4-methylbenzaldehyde used as the substrate.

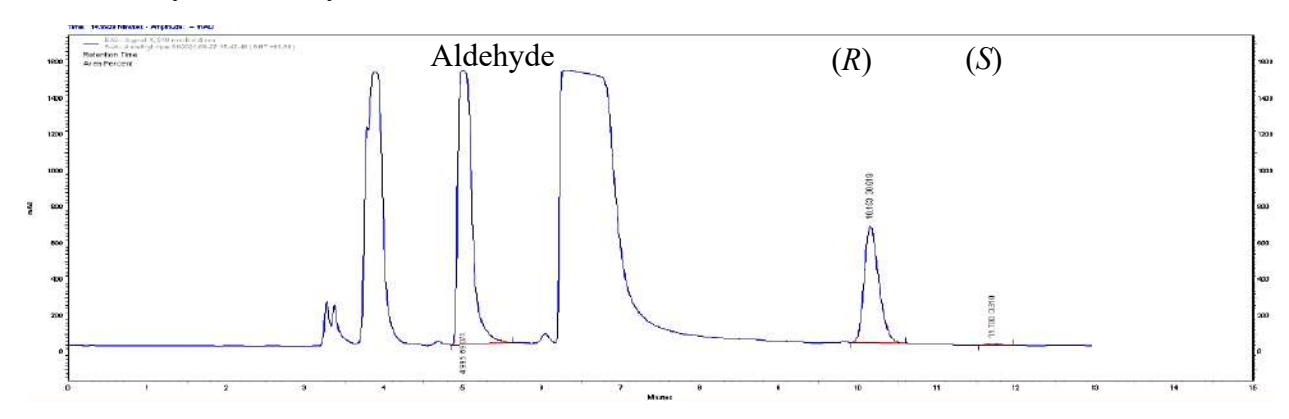


Figure 3.98: HPLC spectrum of wild type AtHNL showing enantioselective synthesis of (R)-1-(4-methylphenyl)-2-nitroethanol at 3 h using 4-methylbenzaldehyde as the substrate.

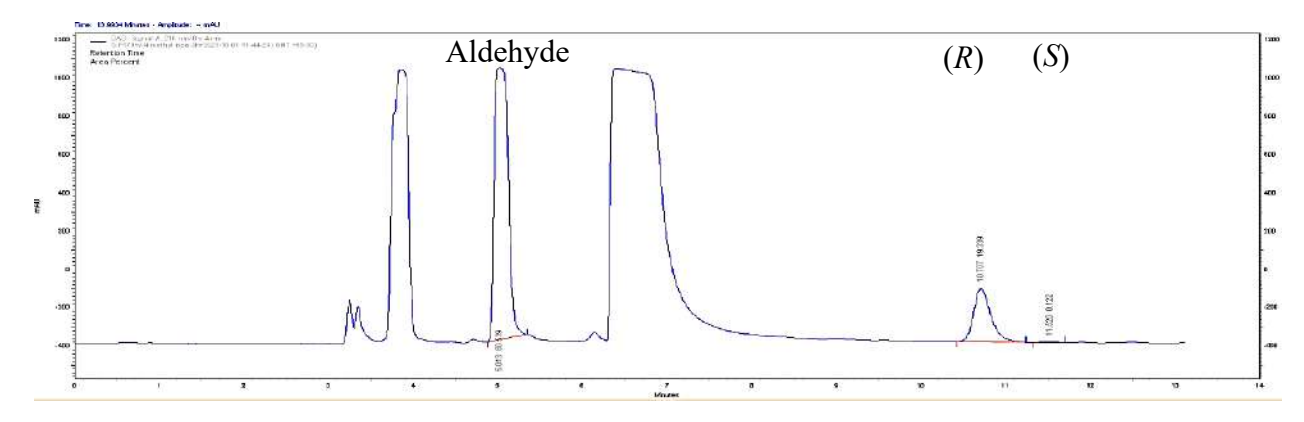


Figure 3.99: HPLC spectrum of the F179W variant showing enantioselective synthesis of (R)-1-(4-methylphenyl)-2-nitroethanol at 3 h using 4-methylbenzaldehyde as the substrate.

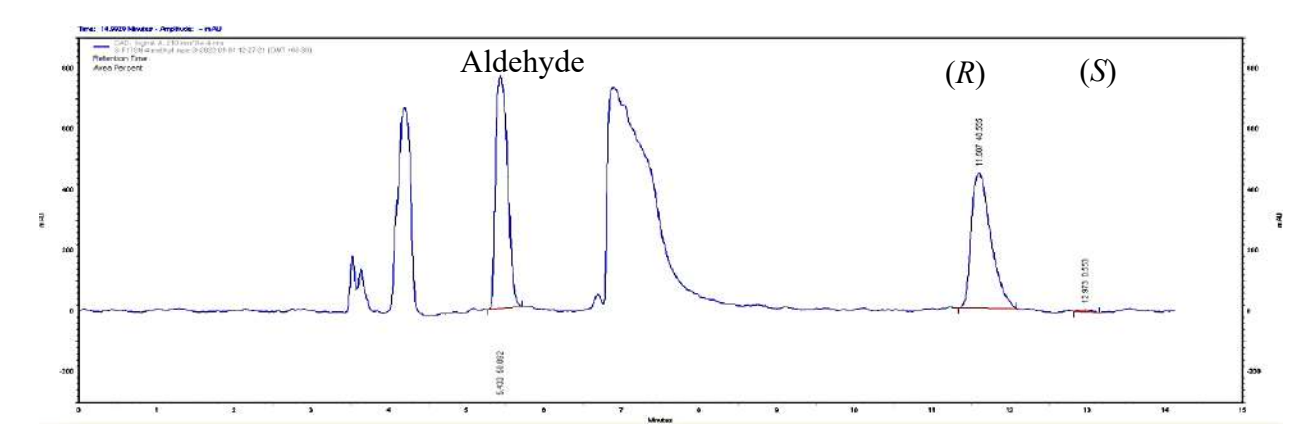


Figure 3.100: HPLC spectrum of the F179N variant showing enantioselective synthesis of (*R*)-1-(4-methylphenyl)-2-nitroethanol at 3 h using 4-methylbenzaldehyde as the substrate.

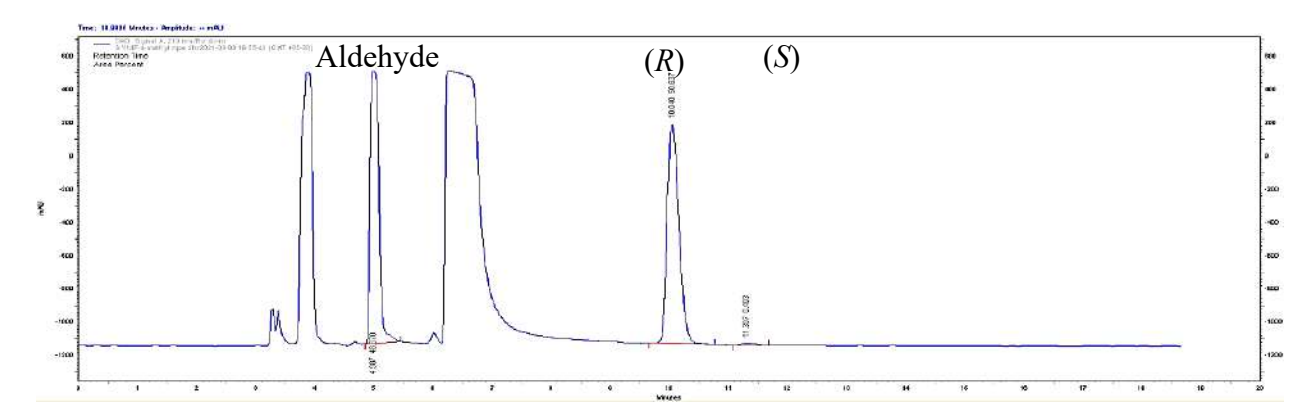


Figure 3.101: HPLC spectrum of the Y14F variant showing enantioselective synthesis of (R)-1-(4-methylphenyl)-2-nitroethanol at 3 h using 4-methylbenzaldehyde as the substrate.

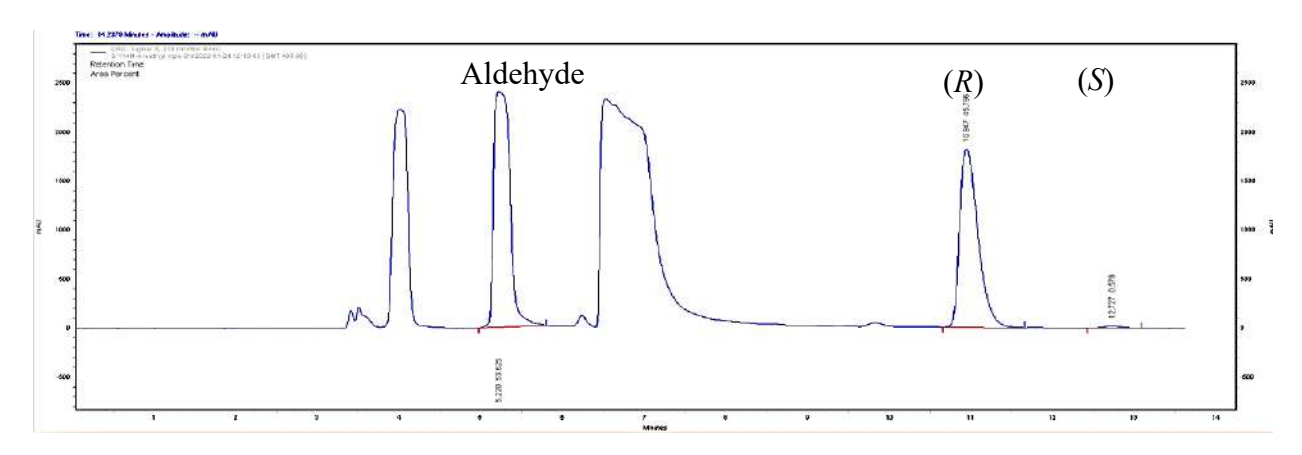


Figure 3.102: HPLC spectrum of the Y14M variant showing enantioselective synthesis of (R)-1-(4-methylphenyl)-2-nitroethanol at 3 h using 4-methylbenzaldehyde as the substrate.

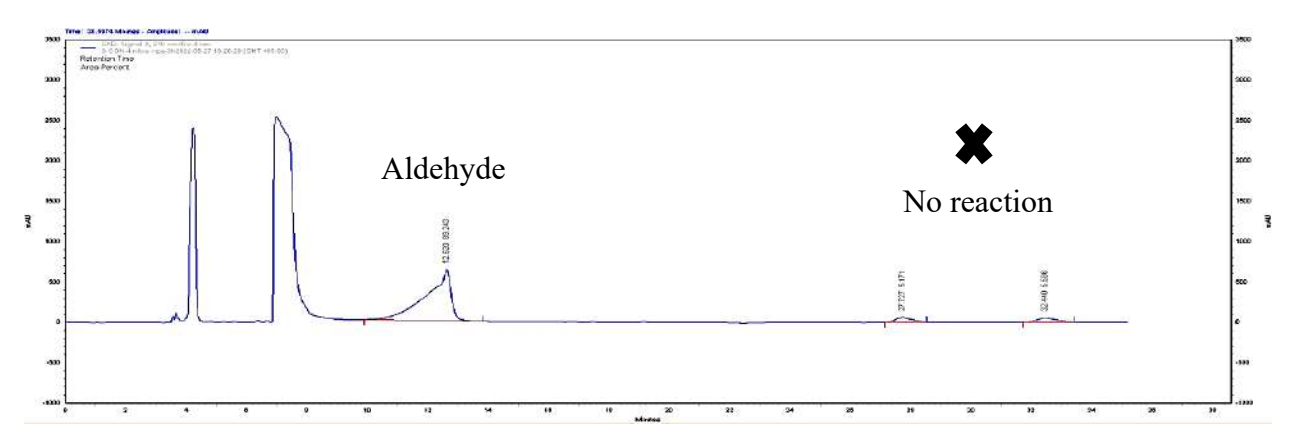


Figure 3.103: HPLC spectrum of control reaction at 3 h where enzyme is replaced by 20 mM KPB and 4-nitrobenzaldehyde used as the substrate.

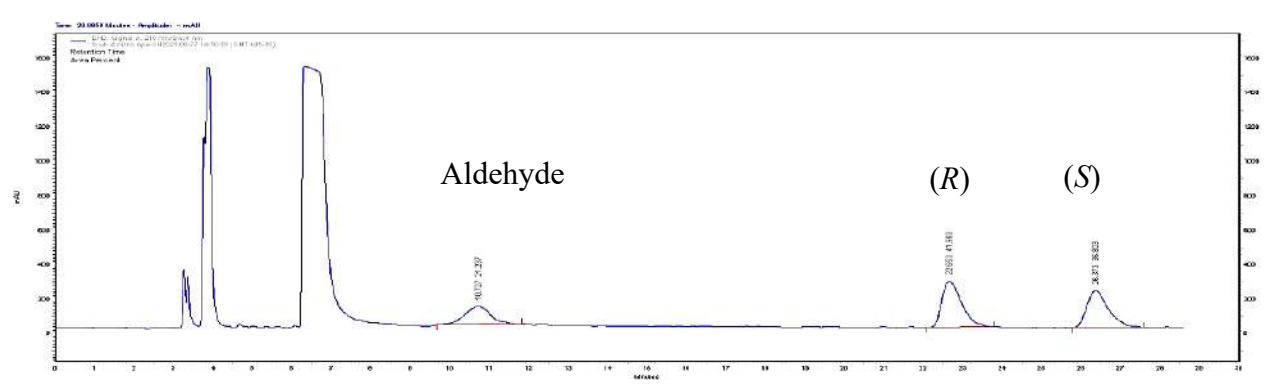


Figure 3.104: HPLC spectrum of wild type AtHNL showing enantioselective synthesis of (R)-1-(4-nitrophenyl)-2-nitroethanol at 3 h using 4-nitrobenzaldehyde as the substrate.

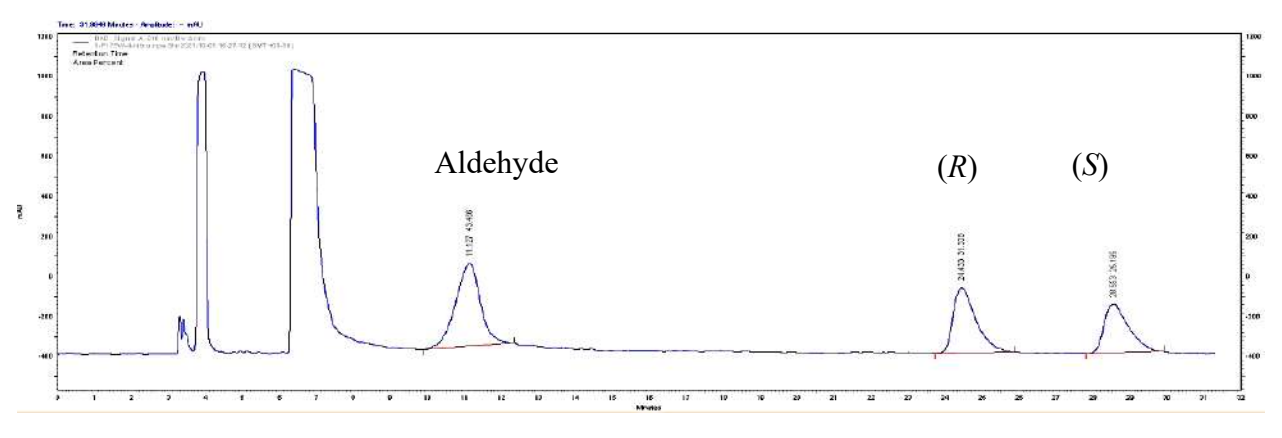


Figure 3.105: HPLC spectrum of the F179W variant showing enantioselective synthesis of (*R*)-1-(4-nitrophenyl)-2-nitroethanol at 3 h using 4-nitrobenzaldehyde as the substrate.

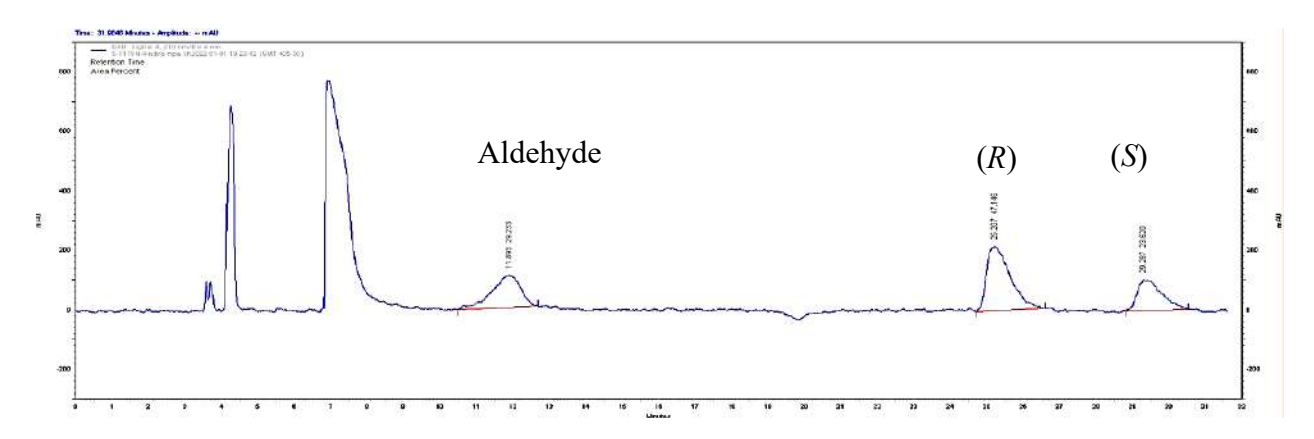


Figure 3.106: HPLC spectrum of the F179N variant showing enantioselective synthesis of (R)-1-(4-nitrophenyl)-2-nitroethanol at 3 h using 4-nitrobenzaldehyde as the substrate.

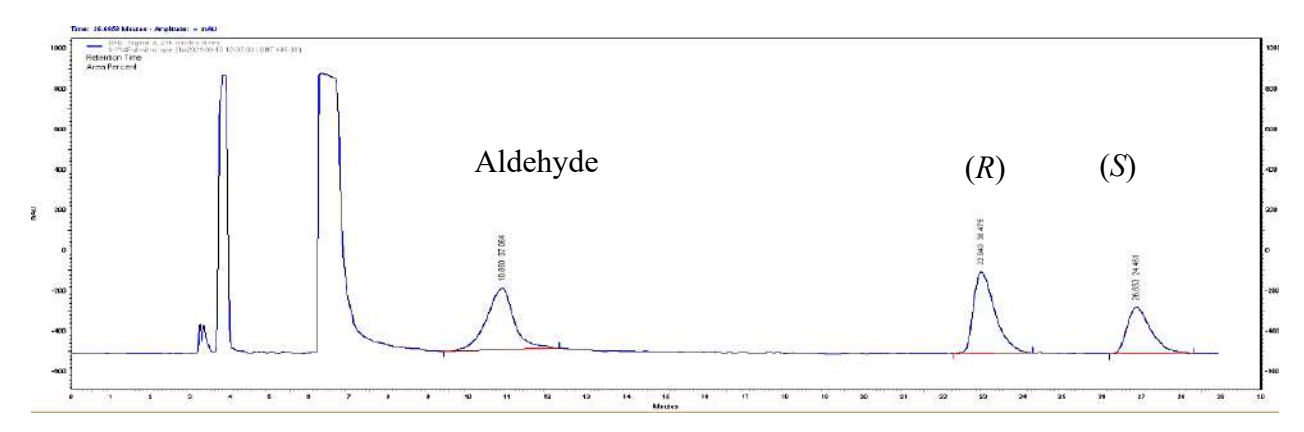


Figure 3.107: HPLC spectrum of the Y14F variant showing enantioselective synthesis of (R)-1-(4-nitrophenyl)-2-nitroethanol at 3 h using 4-nitrobenzaldehyde as the substrate.

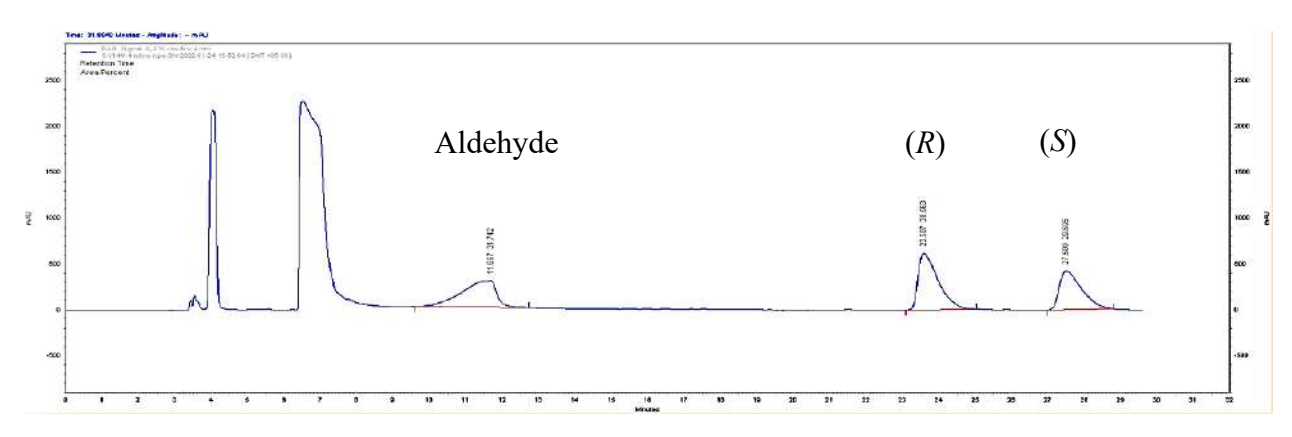


Figure 3.108: HPLC spectrum of the Y14M variant showing enantioselective synthesis of (R)-1-(4-nitrophenyl)-2-nitroethanol at 3 h using 4-nitrobenzaldehyde as the substrate.

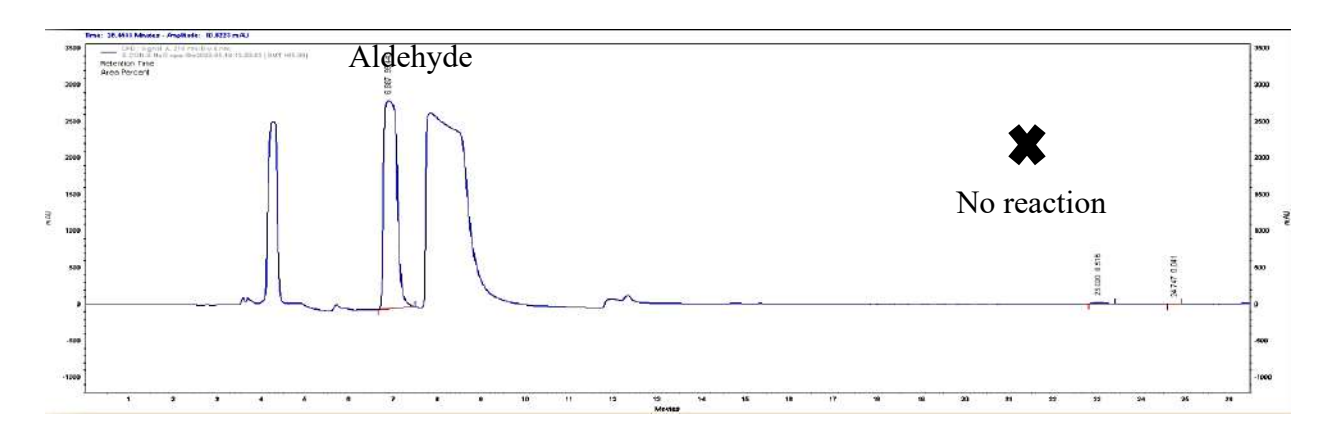


Figure 3.109: HPLC spectrum of control reaction at 3 h where enzyme is replaced by 20 mM KPB and 3-methoxybenzaldehyde used as the substrate.

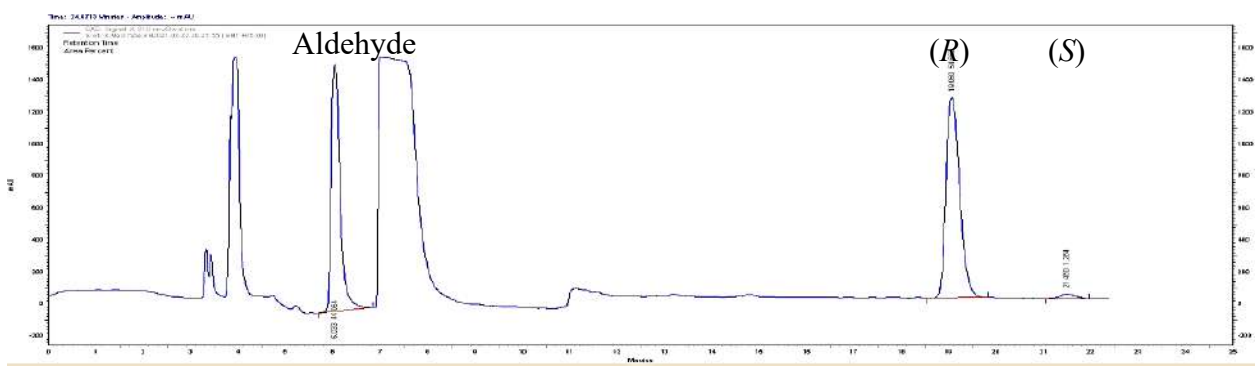


Figure 3.110: HPLC spectrum of wild type AtHNL showing enantioselective synthesis of (R)-1-(3-methoxyphenyl)-2-nitroethanol at 3 h using 3-methoxybenzaldehyde as the substrate.

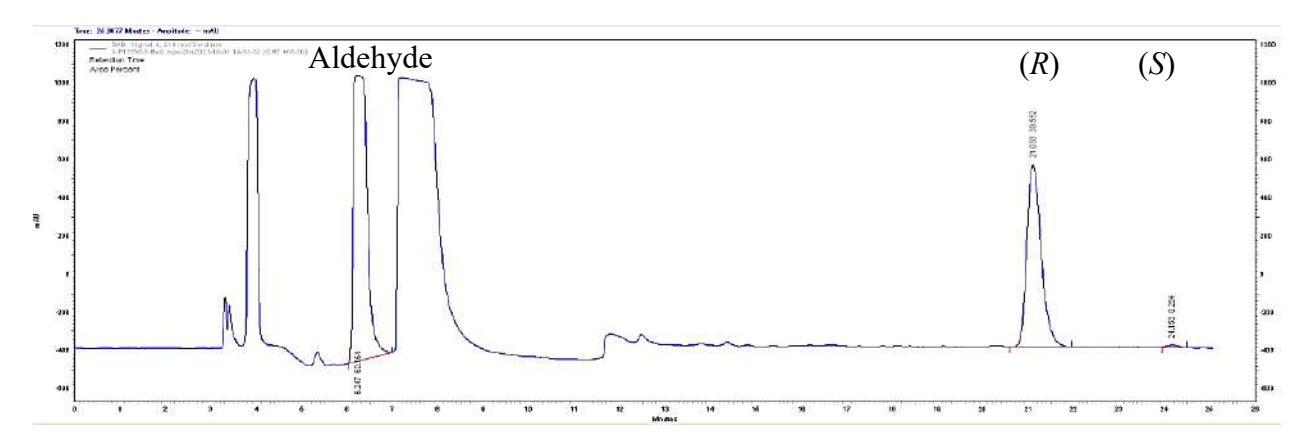


Figure 3.111: HPLC spectrum of the F179W variant showing enantioselective synthesis of (*R*)-1-(3-methoxyphenyl)-2-nitroethanol at 3 h using 3-methoxybenzaldehyde as the substrate.

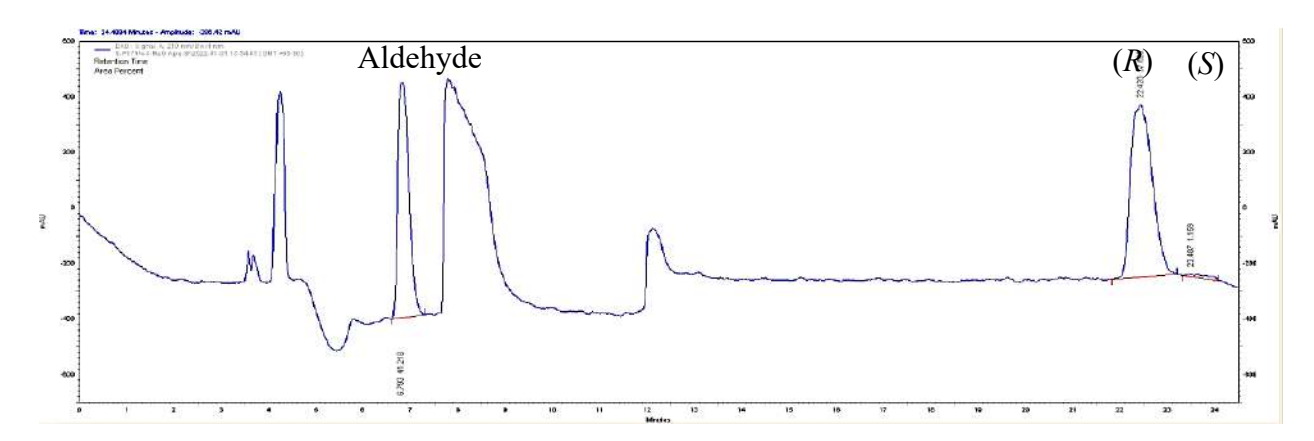


Figure 3.112: HPLC spectrum of the F179N variant showing enantioselective synthesis of (R)-1-(3-methoxyphenyl)-2-nitroethanol at 3 h using 3- methoxybenzaldehyde as the substrate.

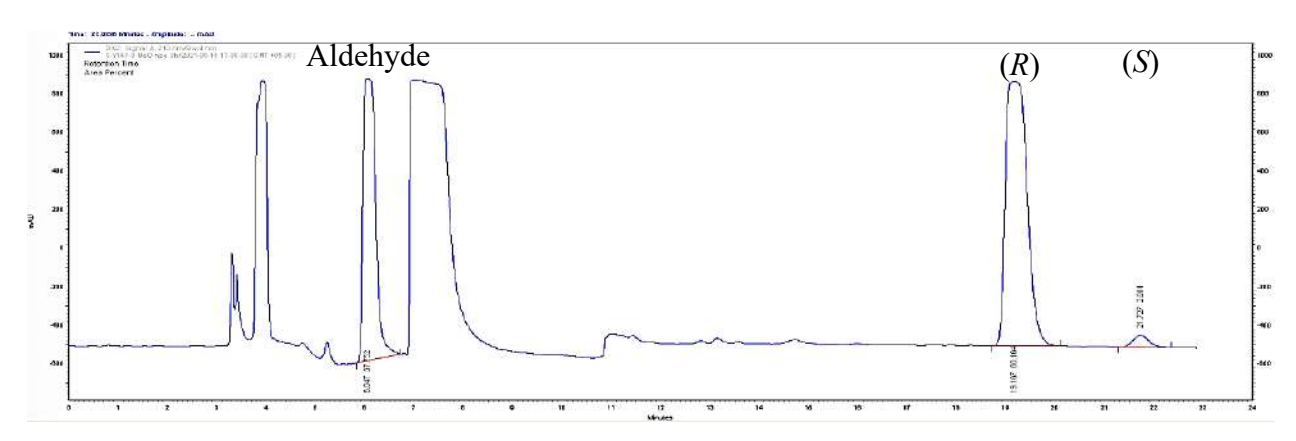


Figure 3.113: HPLC spectrum of the Y14F variant showing enantioselective synthesis of (R)-1-(3-methoxyphenyl)-2-nitroethanol at 3 h using 3-methoxybenzaldehyde as the substrate.

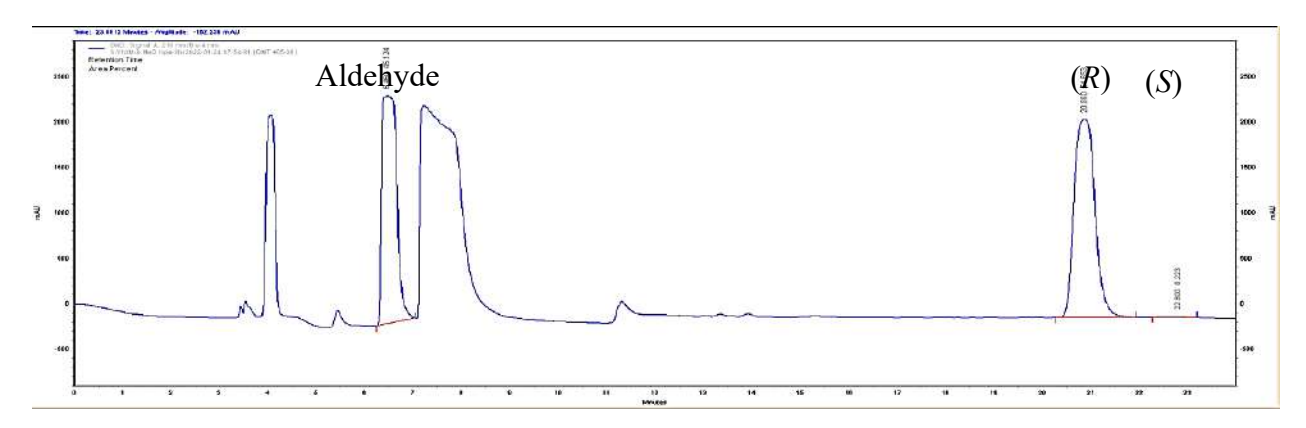


Figure 3.114: HPLC spectrum of the Y14M variant showing enantioselective synthesis of (R)-1-(3-methoxyphenyl)-2-nitroethanol at 3 h using 3-methoxybenzaldehyde as the substrate.

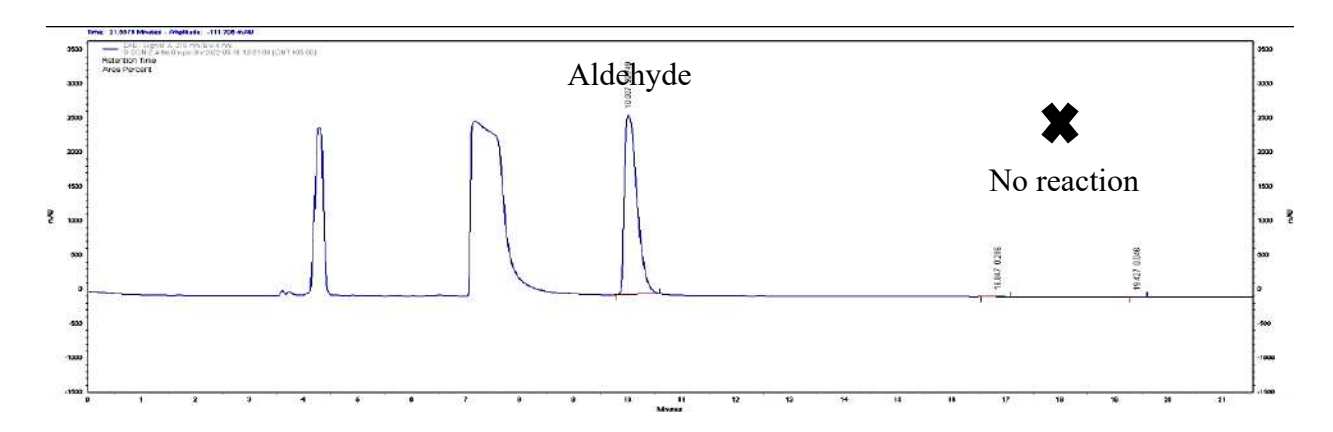


Figure 3.115: HPLC spectrum of control reaction at 3 h where enzyme is replaced by 20 mM KPB and 2,4-dimethoxybenzaldehyde used as the substrate.

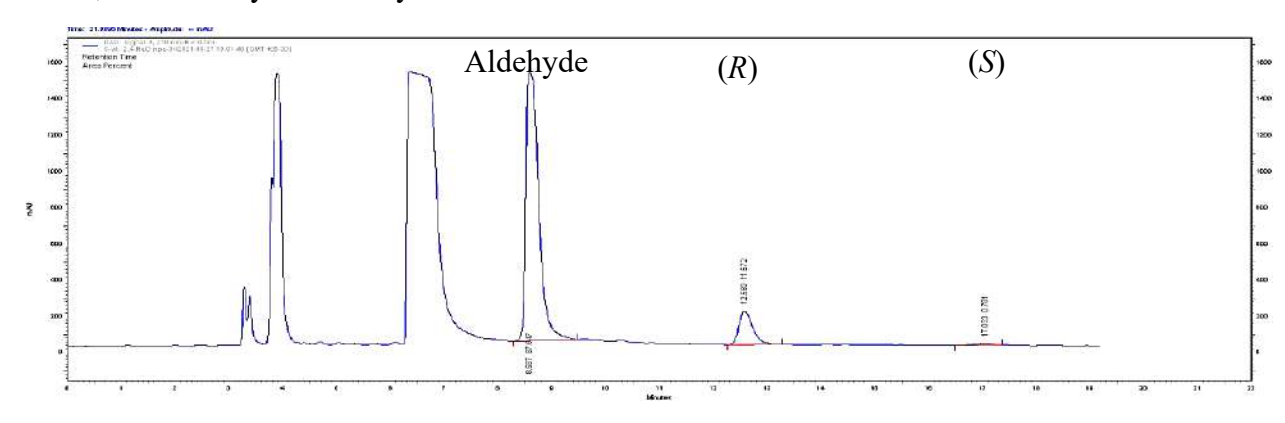


Figure 3.116: HPLC spectrum of wild type AtHNL showing enantioselective synthesis of (R)-1-(2, 4-dimethoxyphenyl)-2-nitroethanol at 3 h using 2,4-dimethoxybenzaldehyde as the substrate.

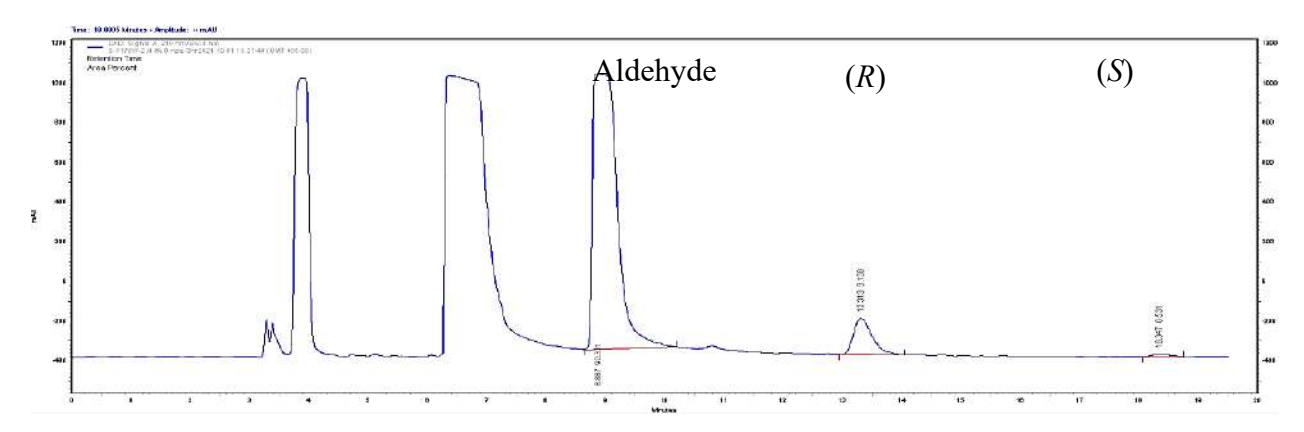


Figure 3.117: HPLC spectrum of the F179W variant showing enantioselective synthesis of (R)-1-(2, 4-dimethoxyphenyl)-2-nitroethanol at 3 h using 2,4-dimethoxybenzaldehyde as the substrate.

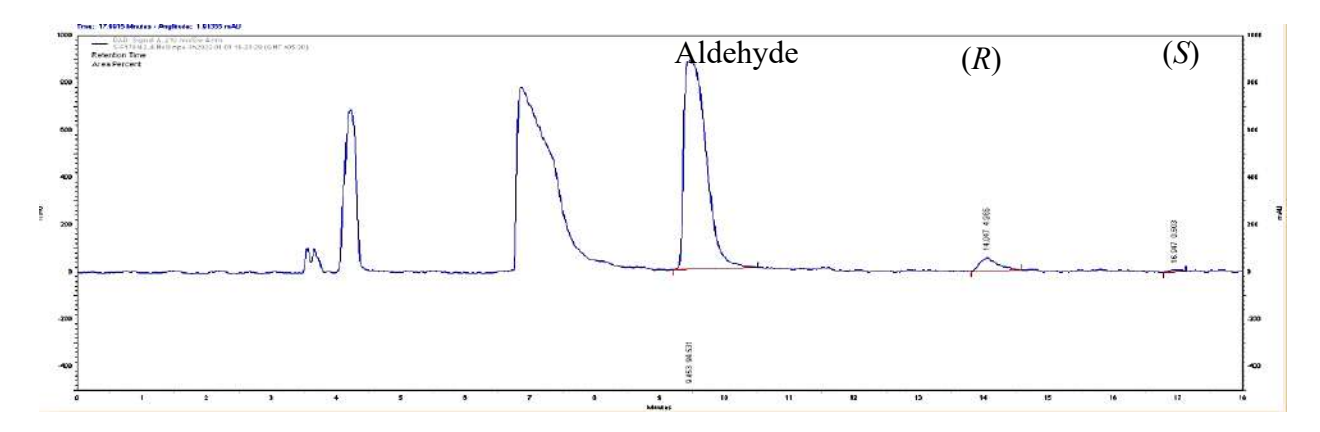


Figure 3.118: HPLC spectrum of the F179N variant showing enantioselective synthesis of (R)-1-(2, 4-dimethoxyphenyl)-2-nitroethanol at 3 h using 2,4-dimethoxybenzaldehyde as the substrate.

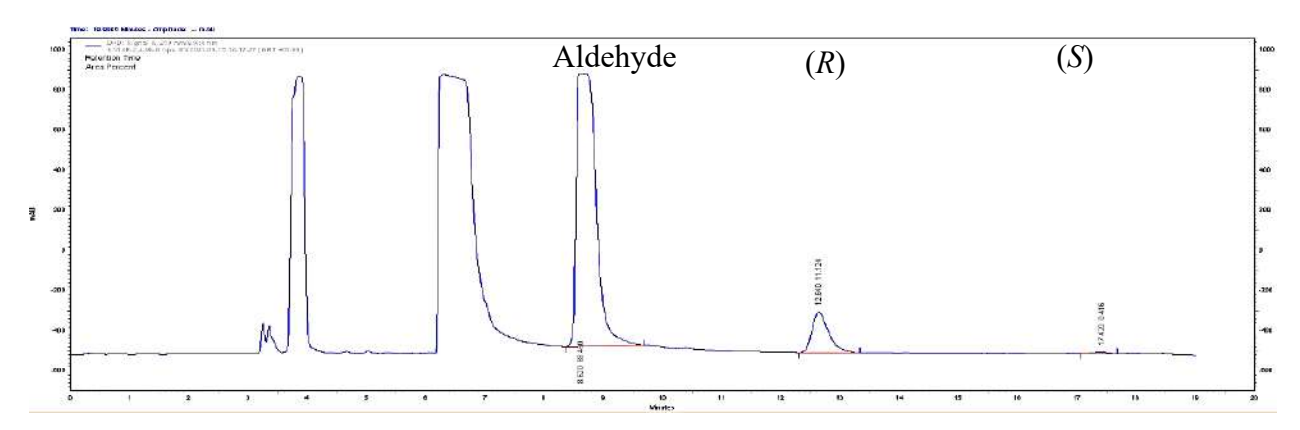


Figure 3.119: HPLC spectrum of the Y14F variant showing enantioselective synthesis of (R)-1-(2, 4-dimethoxyphenyl)-2-nitroethanol at 3 h using 2,4-dimethoxybenzaldehyde as the substrate.

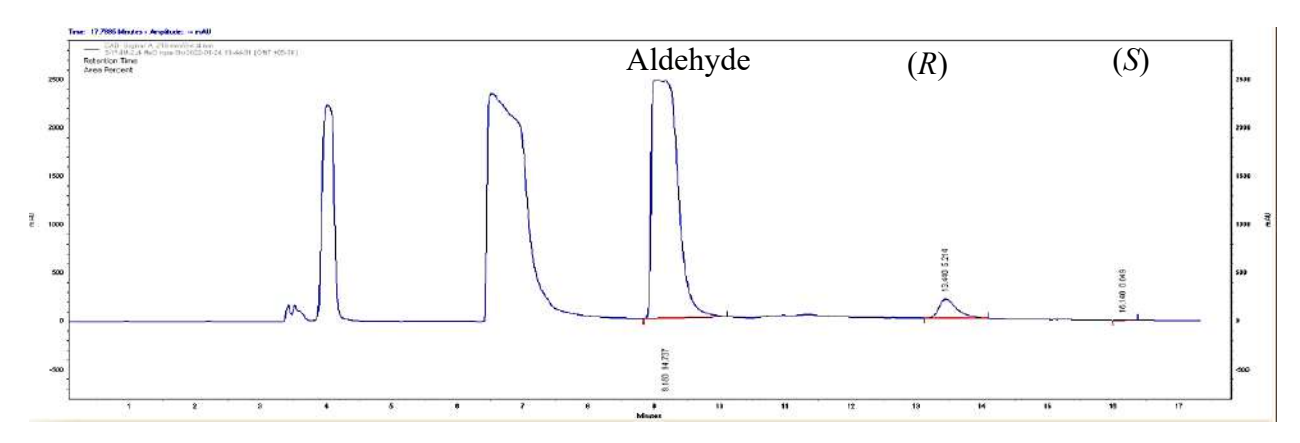


Figure 3.120: HPLC spectrum of the Y14M variant showing enantioselective synthesis of (R)-1-(2, 4-dimethoxyphenyl)-2-nitroethanol at 3 h using 2,4-dimethoxybenzaldehyde as the substrate.

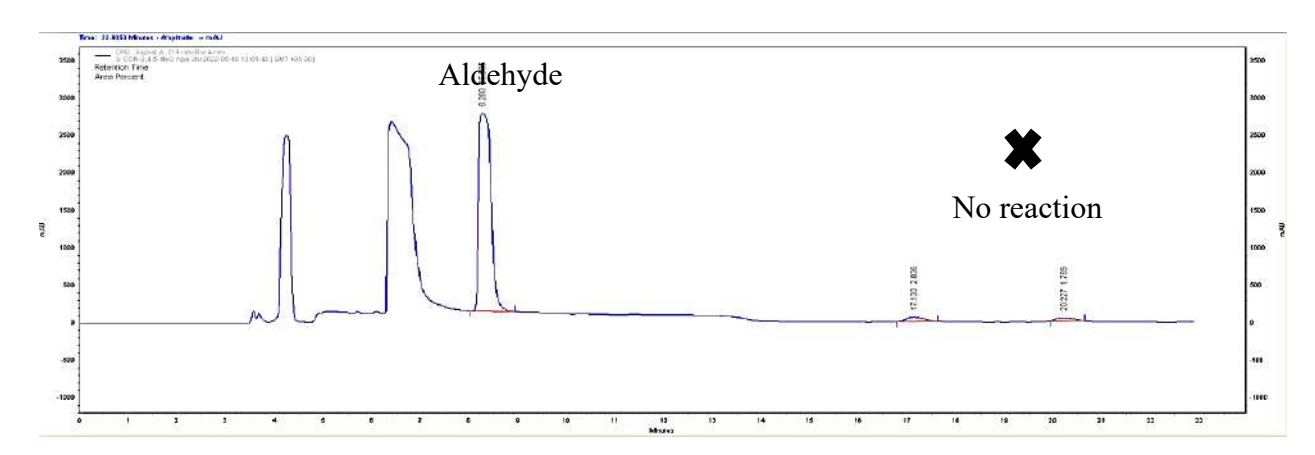


Figure 3.121: HPLC spectrum of control reaction at 3 h where enzyme is replaced by 20 mM KPB and 3,4,5-trimethoxybenzaldehyde used as the substrate.

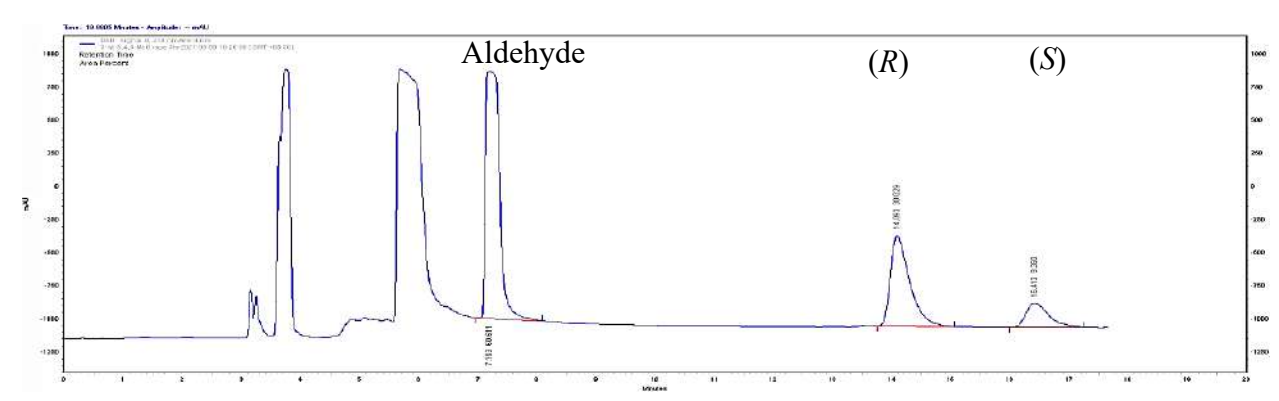


Figure 3.122: HPLC spectrum of wild type AtHNL showing enantioselective synthesis of (R)-1-(3,4,5-trimethoxyphenyl)-2-nitroethanol at 3 h using 3,4,5-trimethoxybenzaldehyde as the substrate.

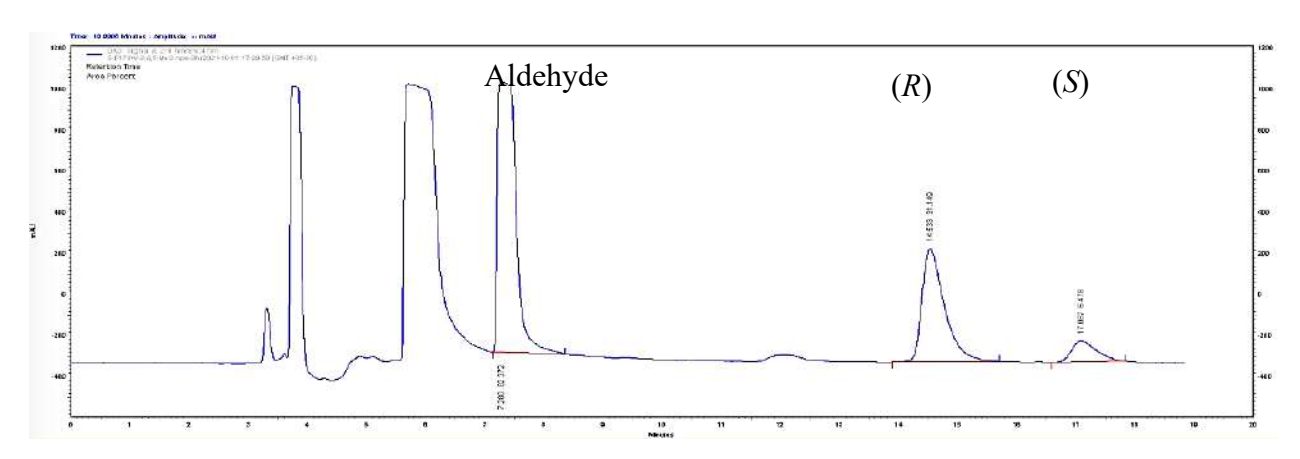


Figure 3.123: HPLC spectrum of the F179W variant showing enantioselective synthesis of (R)-1-(3,4,5-trimethoxyphenyl)-2-nitroethanol at 3 h using 3,4,5-trimethoxybenzaldehyde as the substrate.

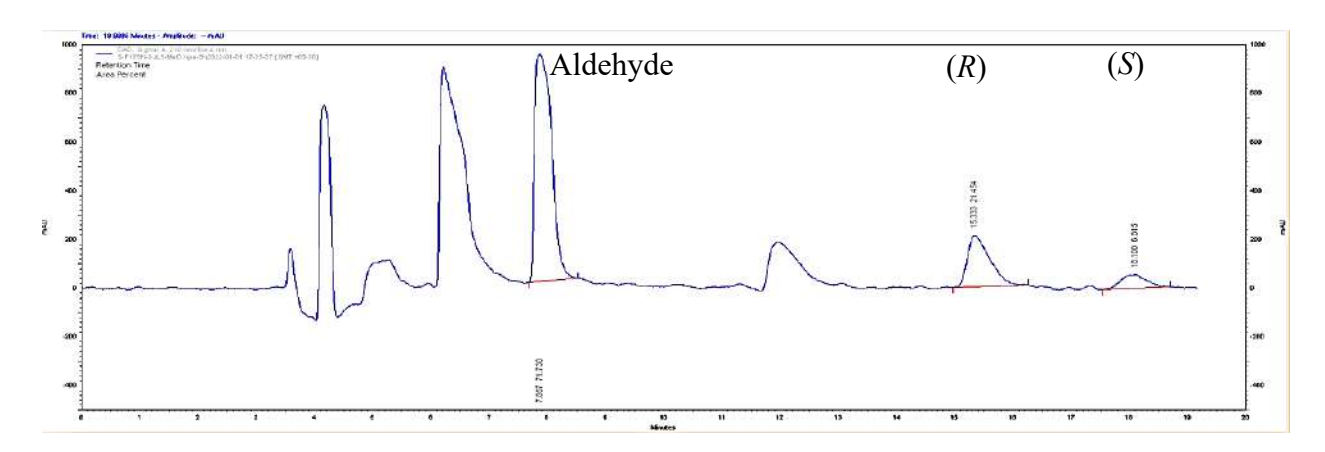


Figure 3.124: HPLC spectrum of the F179N variant showing enantioselective synthesis of (R)-1-(3,4,5-trimethoxyphenyl)-2-nitroethanol at 3 h using 3,4,5-trimethoxybenzaldehyde as the substrate.

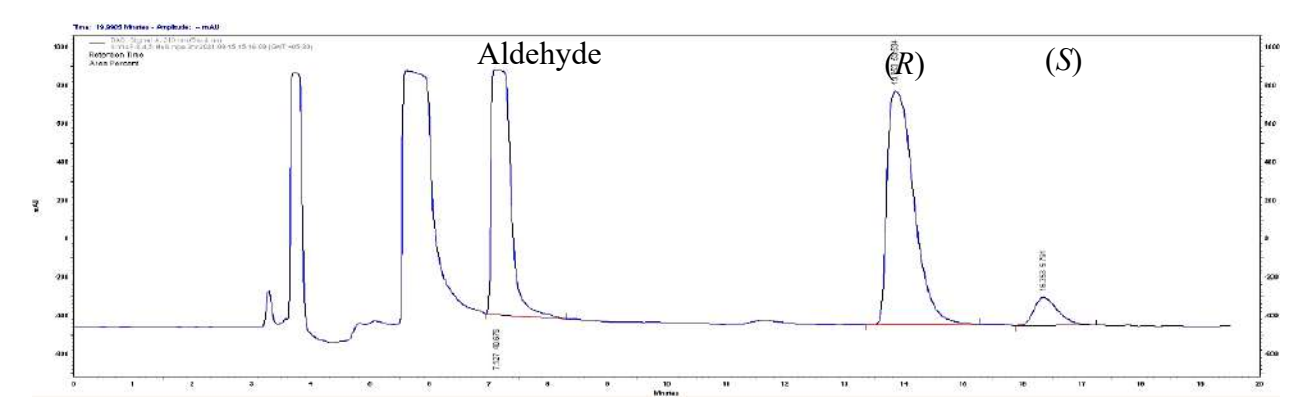


Figure 3.125: HPLC spectrum of the Y14F variant showing enantioselective synthesis of (R)-1-(3,4,5-trimethoxyphenyl)-2-nitroethanol at 3 h using 3,4,5-trimethoxybenzaldehyde as the substrate.

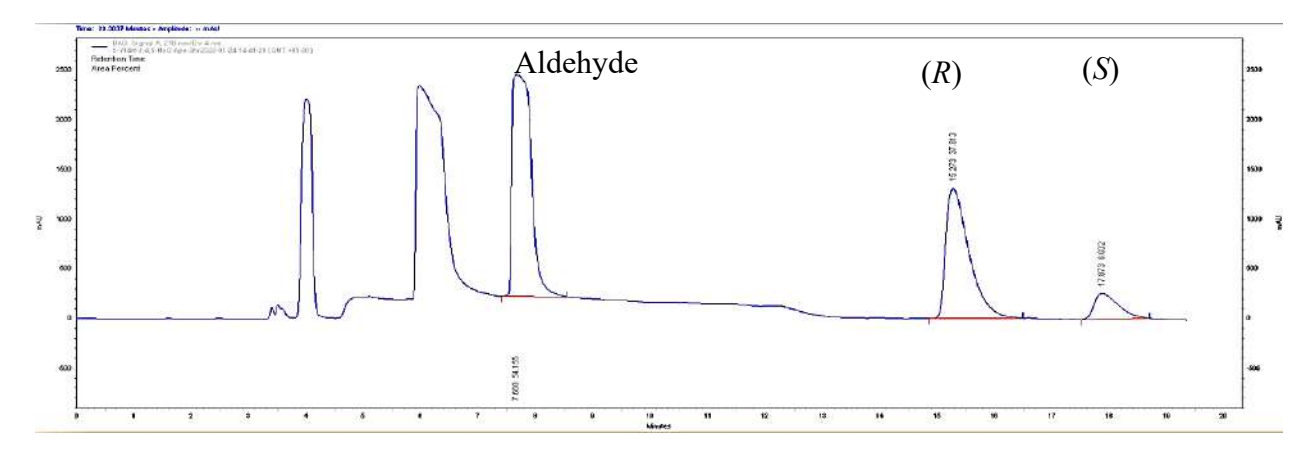


Figure 3.126: HPLC spectrum of the Y14M variant showing enantioselective synthesis of (R)-1-(3,4,5-trimethoxyphenyl)-2-nitroethanol at 3 h using 3,4,5-trimethoxybenzaldehyde as the substrate.

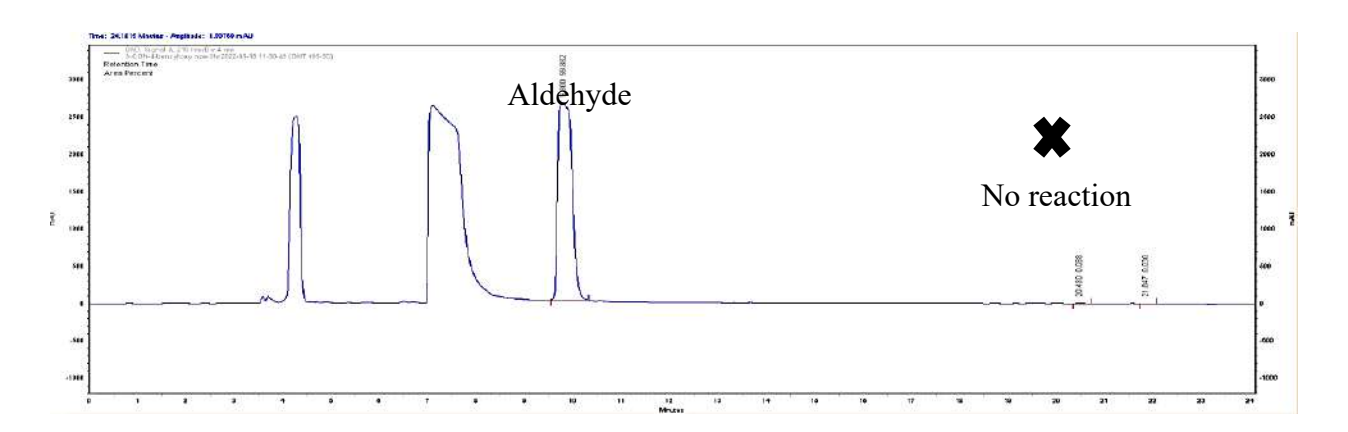


Figure 3.127: HPLC spectrum of control reaction at 3 h where enzyme is replaced by 20 mM KPB and 4-bezyloxybenzaldehyde used as the substrate.

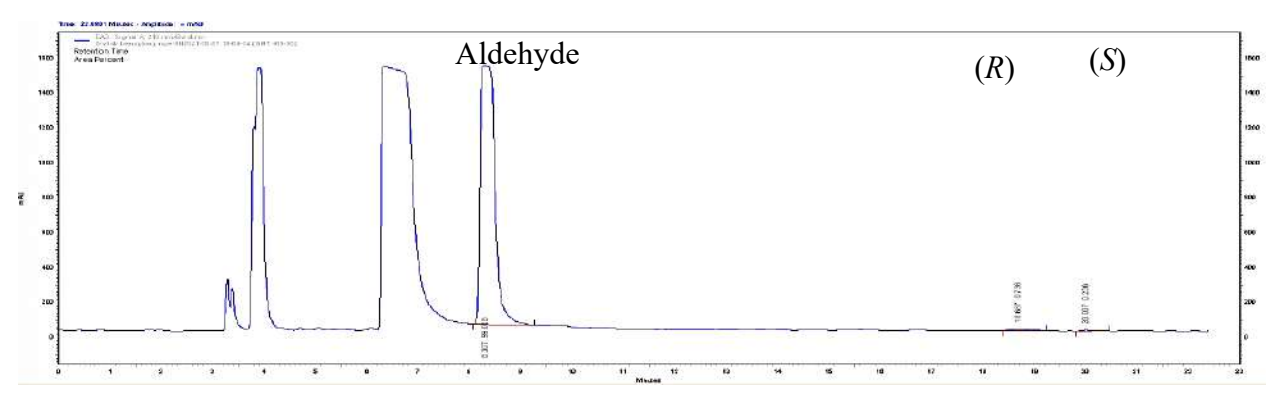


Figure 3.128: HPLC spectrum of wild type AtHNL showing enantioselective synthesis of (R)-1-(4-benzyloxyphenyl)-2-nitroethanol at 3 h using 4-benzyloxybenzaldehyde as the substrate.

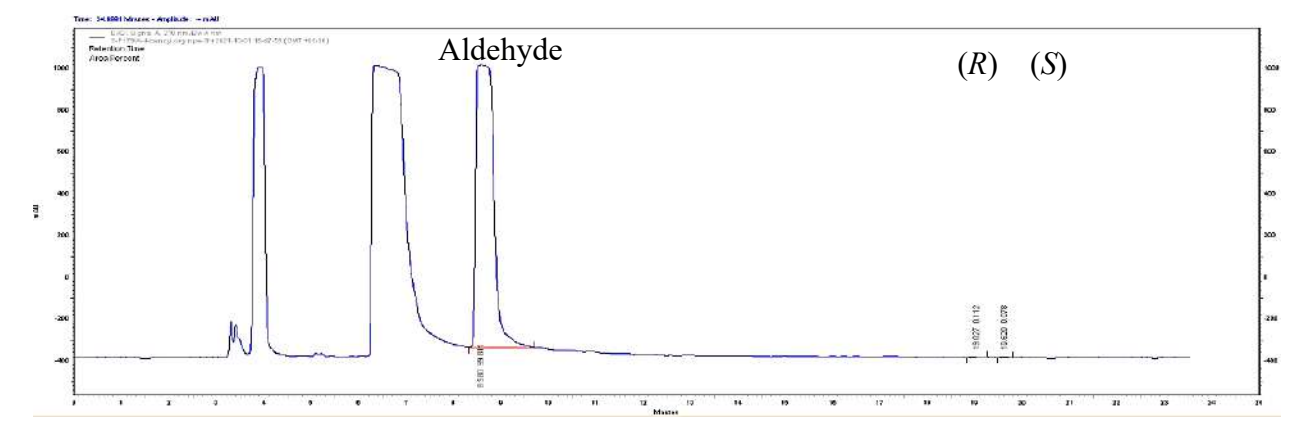


Figure 3.129: HPLC spectrum of the F179W variant showing enantioselective synthesis of (*R*)-1-(4-benzyloxyphenyl)-2-nitroethanol at 3 h using 4-benzyloxybenzaldehyde as the substrate.

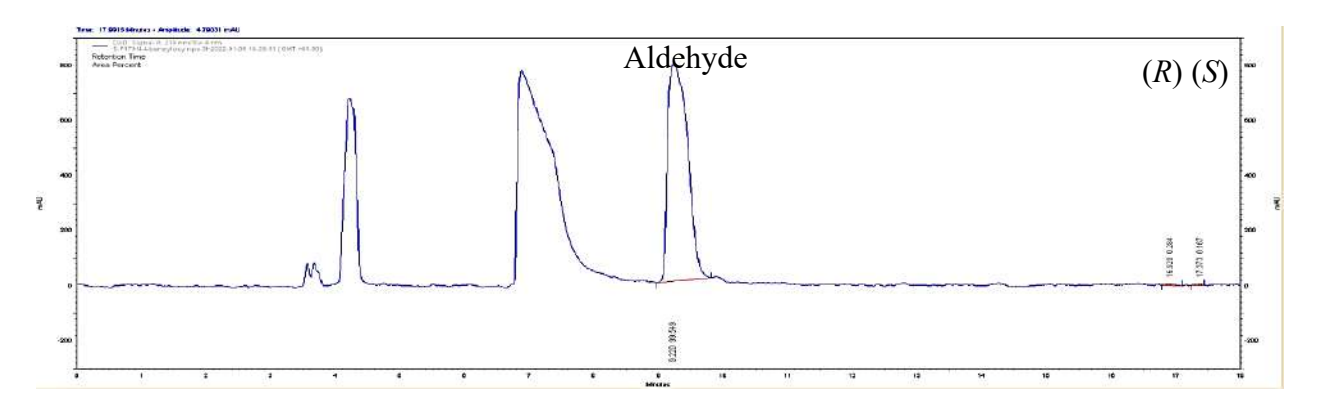


Figure 3.130: HPLC spectrum of the F179N variant showing enantioselective synthesis of (*R*)-1-(4-benzyloxyphenyl)-2-nitroethanol at 3 h using 4-benzyloxybenzaldehyde as the substrate.

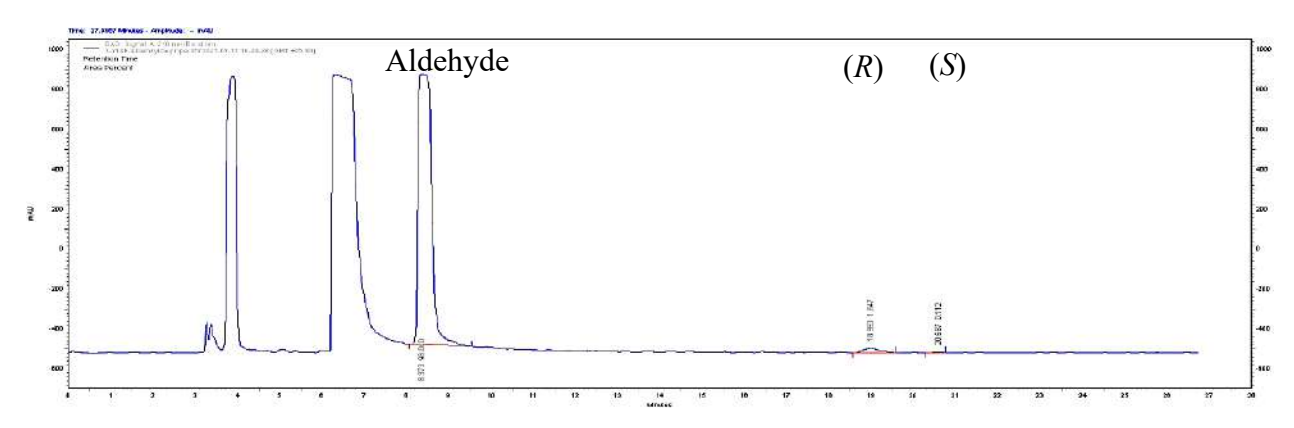


Figure 3.131: HPLC spectrum of the Y14F variant showing enantioselective synthesis of (R)-1-(4-benzyloxyphenyl)-2-nitroethanol at 3 h using 4-benzyloxybenzaldehyde as the substrate.

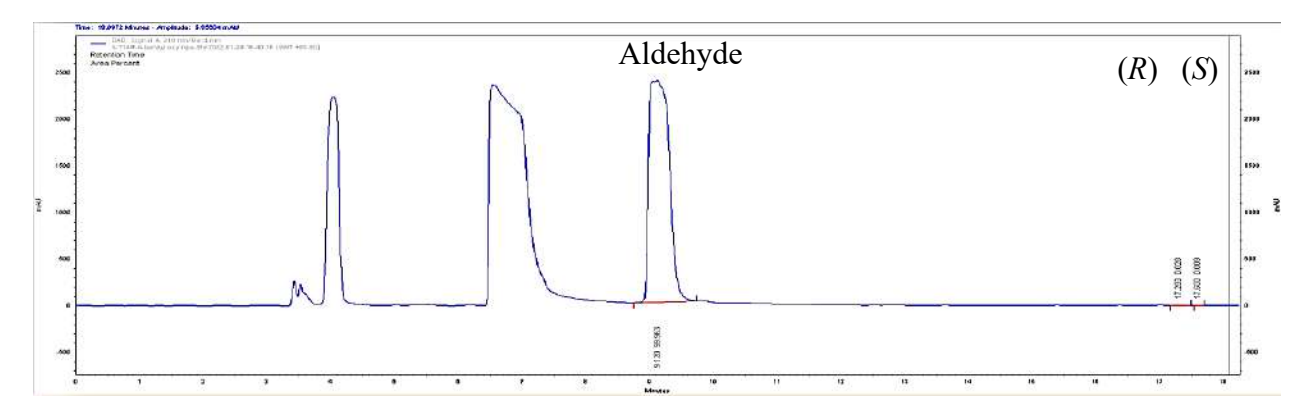


Figure 3.132: HPLC spectrum of the Y14M variant showing enantioselective synthesis of (R)-1-(4-benzyloxyphenyl)-2-nitroethanol at 3 h using 4-benzyloxybenzaldehyde as the substrate.

3.4.6. Enantioselective synthesis of various (R)- β -nitroalcohols by nitroaldol reaction using higher amount of AtHNL variants (125 U)

We assumed that an increase in the enzyme amount would improve the conversion and enantioselectivity in the AtHNL variants catalyzed synthesis of (R)- β -nitroalcohols. Accordingly, we have carried out biocatalysis of all the twelve substrates with 125 U of AtHNL variants, Y14F, Y14M, F179W and F179N, which were performed better with most of the substrates (**Table.3.4**). The detailed improvement in terms of % conversion and % ee found are shown in **Table.3.5** (**Figure 3.133–146**).

The variants Y14F, Y14M, F179W and F179N have exhibited better % conversion and % ee than the wild type after increasing the amount of enzyme (**Table 3.5**). We have observed that F179N has shown better results than the wild type AtHNL, i.e., 97% ee and 82% conversion with benzaldehyde, 98% ee and 72% conversion with 3- chlorobenzaldehyde and 98% ee and 59% conversion with 3-methylbenzaldehyde. The F179W variant did not show better results than the previous one with respect to trans cinnamaldehyde, i.e., 81% ee and 8% conversion. Y14M has shown 93% ee and 84% conversion with benzaldehyde, 91% ee and 5% conversion with 4fluorobenzaldehyde and 95% ee and 7% conversion with 4-benzyloxybenzaldehyde. Y14F also gave better results i.e., 91% ee and 53% conversion with 4-chlorobenzaldehyde, 16% ee and 53% 27% conversion with 4-nitrobenzaldehyde, 98% and conversion with 2,4eedimethoxybenzladehyde, 99% ee and 61% conversion with 4-methylbenzaldehyde, 99% ee and 65% conversion with 3-methoxybenzaldehyde, 91% ee and 67% conversion with 3,4,5trimethoxybenzaldehyde and 95% ee and 5% conversion with 4-benzyloxybenzaldehyde (**Table 3.5**).

Table 3.5: At HNL variants (125 U) catalysed enantioselective synthesis of (R)- β -nitroalcohols.

R	WT	WT	F179N	F179N	F179W	F179W	Y14M	Y14M	Y14F	Y14F
	(62.5U)	(125U)								
Ph	61	-	76	82	47	58	75	84	68	75
	98		96	97	97	99	97	93	98	99
trans cinnamyl	7	-	8	-	13	8	8	-	13	-
	82		91		91	81	77		88	
4-Fluoro Ph	ND	4	ND	3	ND	3	ND	5	ND	0.4
		77		35		56		91		86
4-Chloro Ph	18	-	44	-	11	-	24	-	33	53
	86		92		80		91		95	91
4-Nitro Ph	48	-	50	-	39	-	45	-	44	53
	7		33		11		13		22	16
2,4-Dimethoxy	12	-	5	-	10	-	5	-	12	27
Ph	87		82		89		98		93	98
3-Chloro Ph	54	-	64	72	41	-	59	-	62	-
	97		95	98	95		97		98	
3-Methyl Ph	8	-	58	59	30	-	55	-	51	-
	90		98	98	99		92		94	
4-Methyl Ph	31	-	49	-	19	-	46	-	51	61
	98		98		99		97		98	99
3-Methoxy Ph	55	-	58	-	40	-	55	-	61	65
	95		96		99		99		93	99
3,4,5-Tri	46	-	24	-	33	-	39	-	52	67
methoxy Ph	70		52		66		65		80	91
4-Benzyloxy	ND	2	ND	3	ND	0.2	ND	7	2	5
Ph		70		88		38		95	89	95

ND: not determined; – mark: not done; % ee is highlighted in bold and % conversion is in plain.

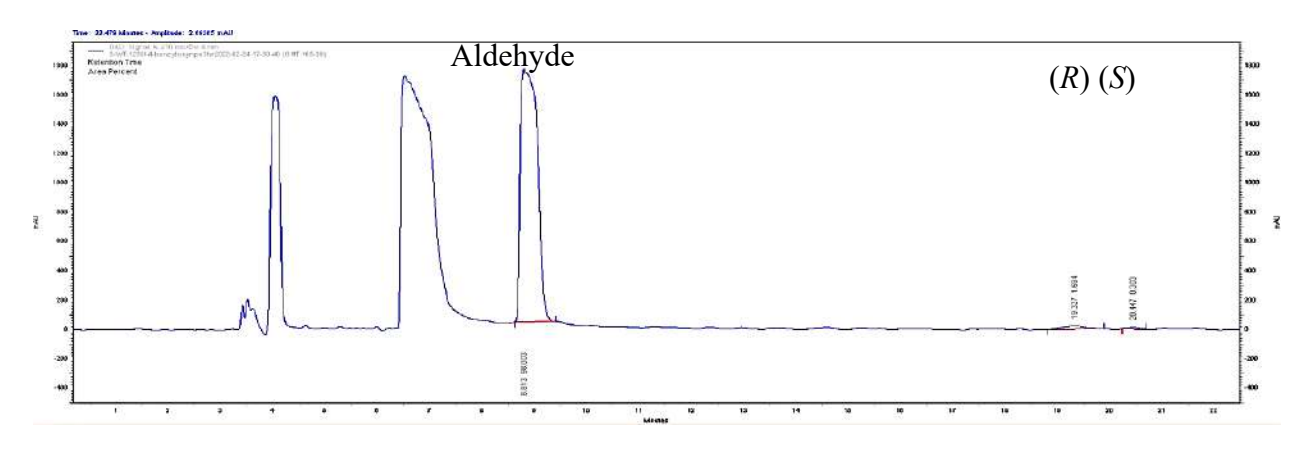


Figure 3.133: HPLC spectrum of AtHNL WT (125 U) catalyzed synthesis of (R)- β -nitroalcohol of 4-benzyloxybenzaldehyde at 3 h.

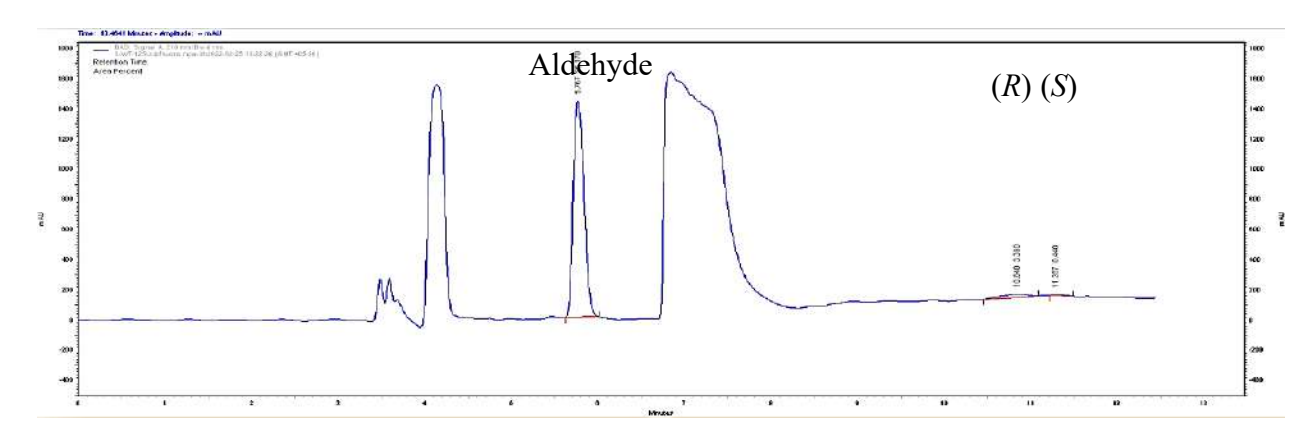


Figure 3.134: HPLC spectrum of AtHNL WT (125 U) catalyzed synthesis of (R)- β -nitroalcohol of 4-fluorobenzaldehyde at 3 h.

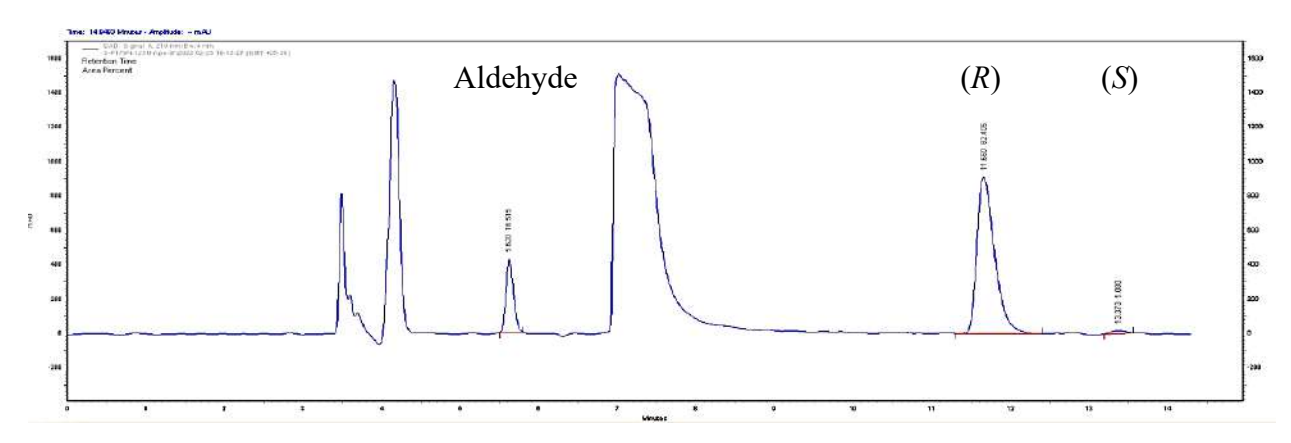


Figure 3.135: HPLC spectrum of the F179N variant (125 U) catalyzed synthesis of (R)- β -nitroalcohol of benzaldehyde at 3 h.

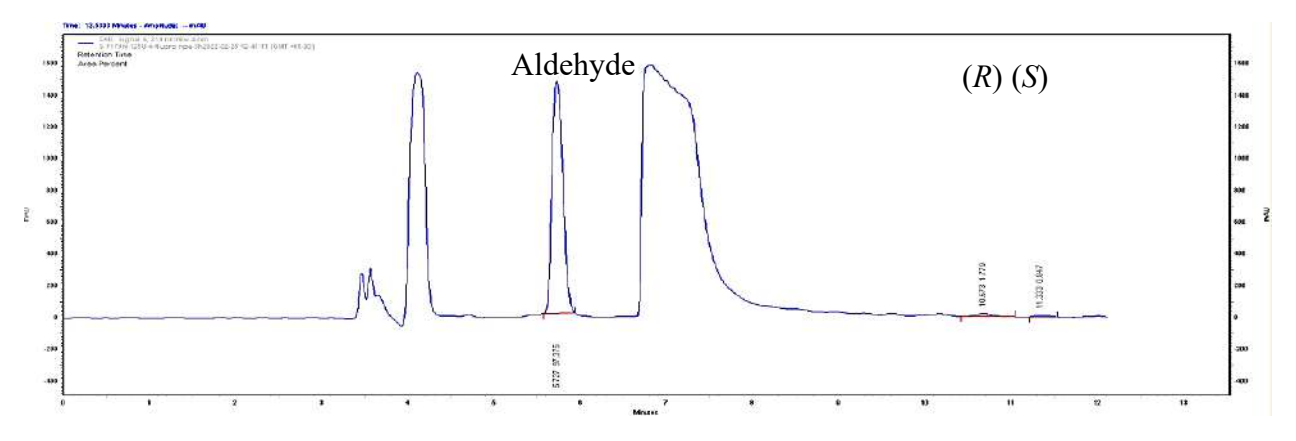


Figure 3.136: HPLC spectrum of the F179N variant (125 U) catalyzed synthesis of (R)- β -nitroalcohol of 4-fluorobenzaldehyde at 3 h.

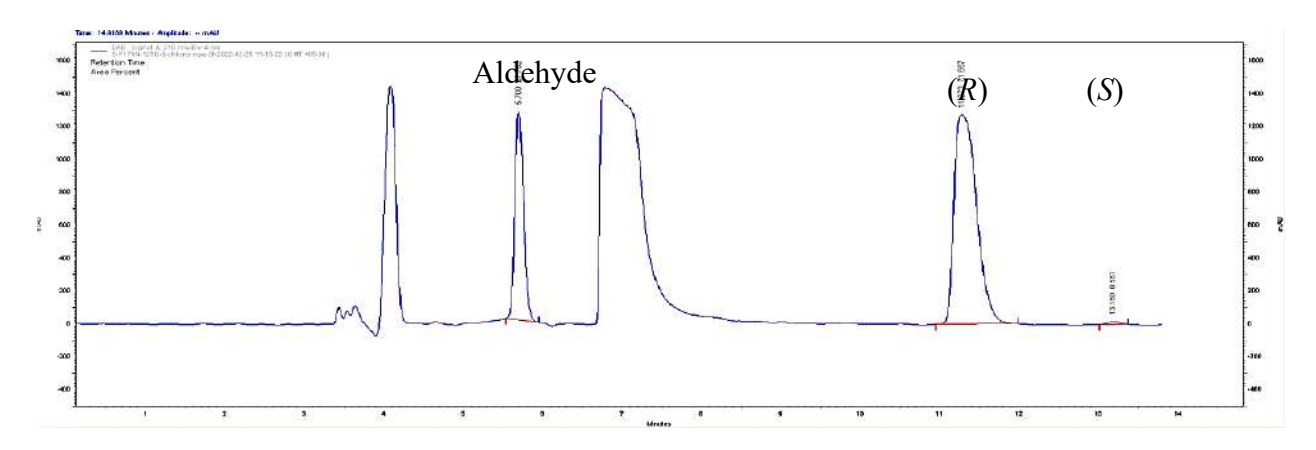


Figure 3.137: HPLC spectrum of the F179N variant (125 U) catalyzed synthesis of (R)- β -nitroalcohol of 3-chlororobenzaldehyde at 3 h.

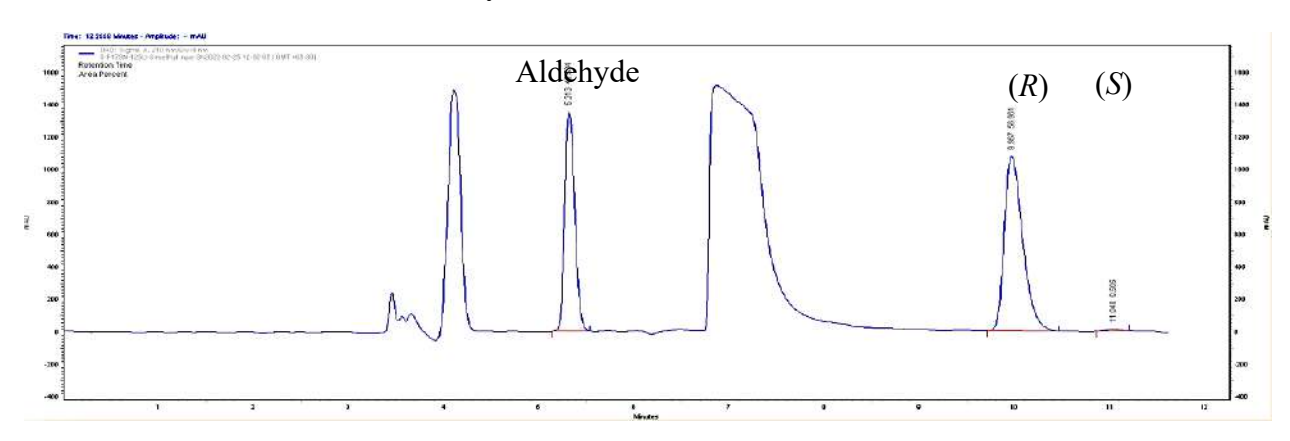


Figure 3.138: HPLC spectrum of the F179N variant (125 U) catalyzed synthesis of (R)- β -nitroalcohol of 3-methylbenzaldehyde at 3 h.

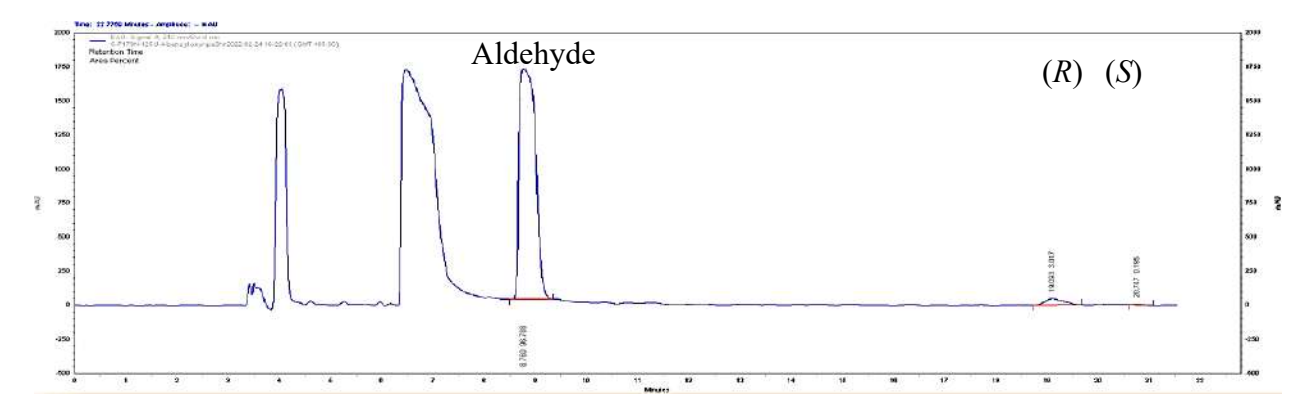


Figure 3.139: HPLC spectrum of the F179N variant (125 U) catalyzed synthesis of (R)- β -nitroalcohol of 4-benzyloxybenzaldehyde at 3 h.

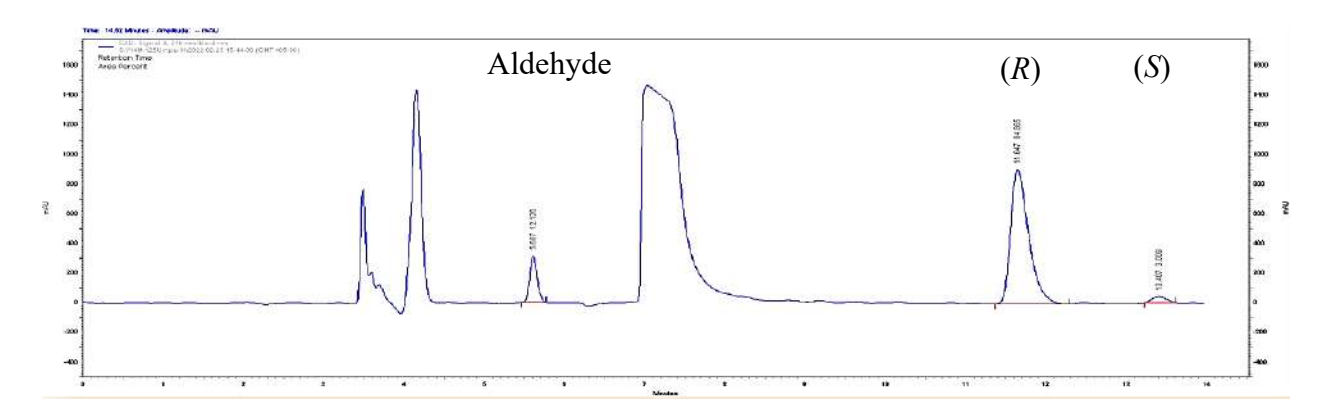


Figure 3.140: HPLC spectrum of the Y14M variant (125 U) catalyzed synthesis of (R)- β -nitroalcohol of benzaldehyde at 3 h.

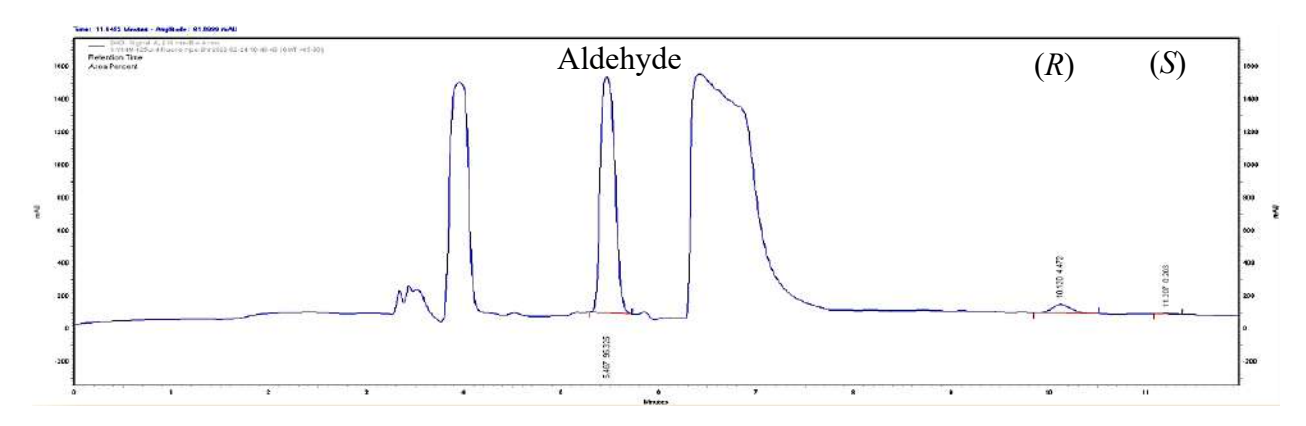


Figure 3.141: HPLC spectrum of the Y14M variant (125 U) catalyzed synthesis of (R)- β -nitroalcohol of 4-fluorobenzaldehyde at 3 h.

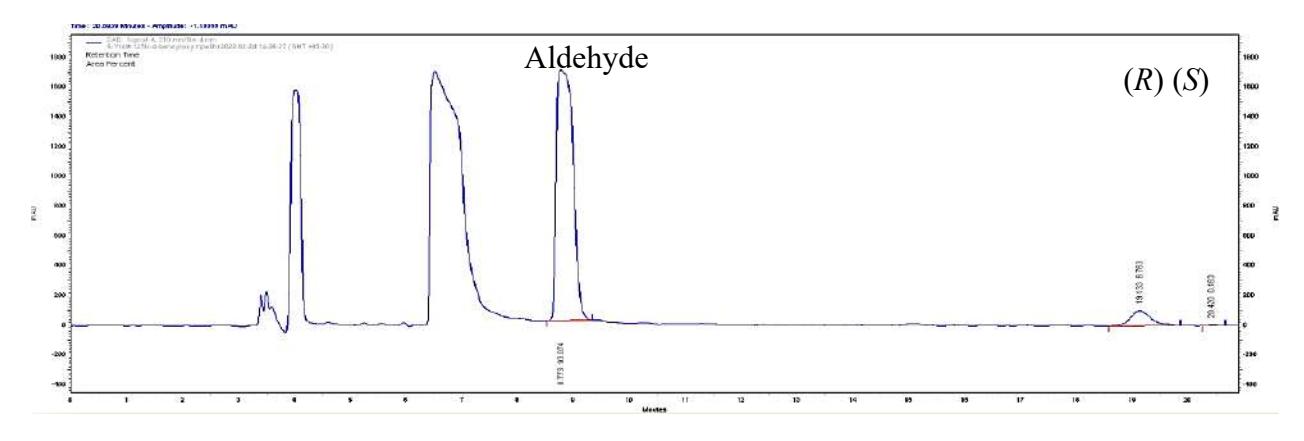


Figure 3.142: HPLC spectrum of the Y14M variant (125 U) catalyzed synthesis of (R)- β -nitroalcohol of 4-benzyloxybenzaldehyde at 3 h.

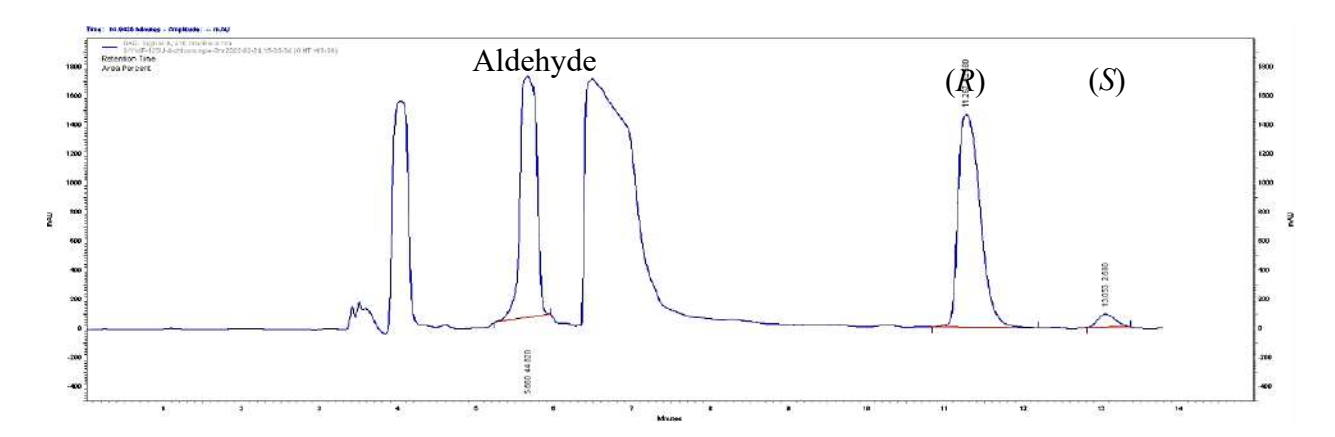


Figure 3.143: HPLC spectrum of the Y14F variant (125 U) catalyzed synthesis of (R)- β -nitroalcohol of 4-chlorobenzaldehyde at 3 h.

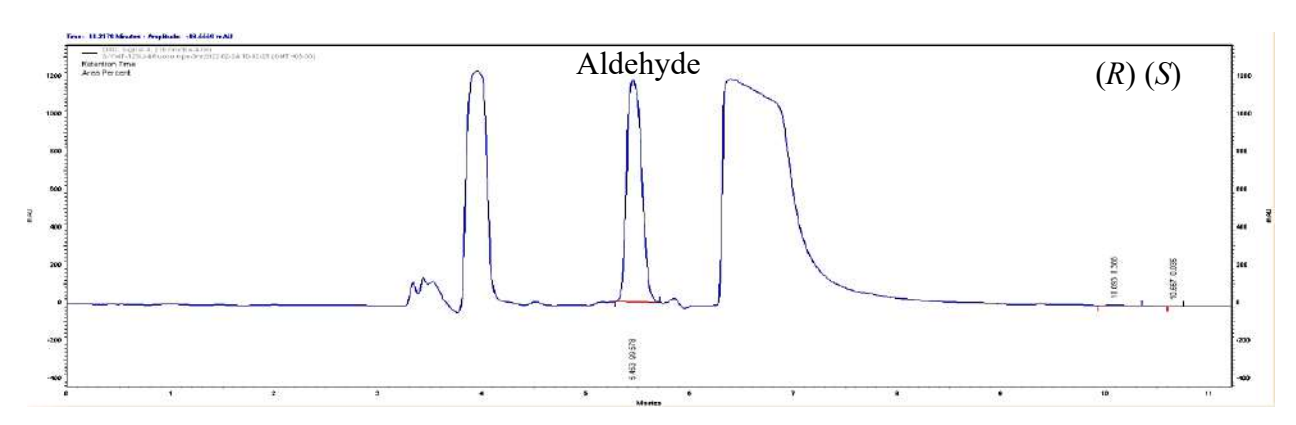


Figure 3.144: HPLC spectrum of the Y14F variant (125 U) catalyzed synthesis of (R)- β -nitroalcohol of 4-fluorobenzaldehyde at 3 h.

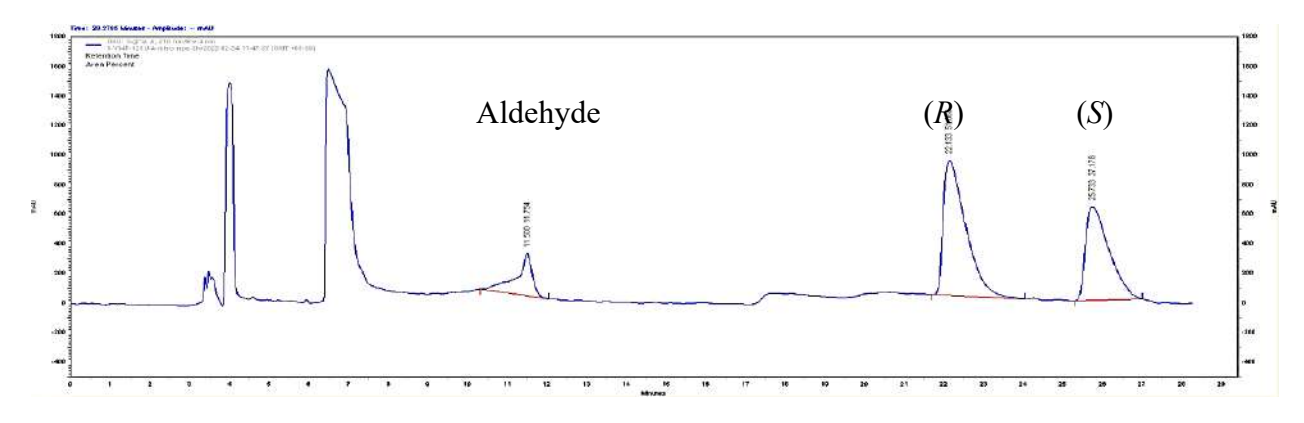


Figure 3.145: HPLC spectrum of the Y14F variant (125 U) catalyzed synthesis of (R)- β -nitroalcohol of 4-nitrobenzaldehyde at 3 h.

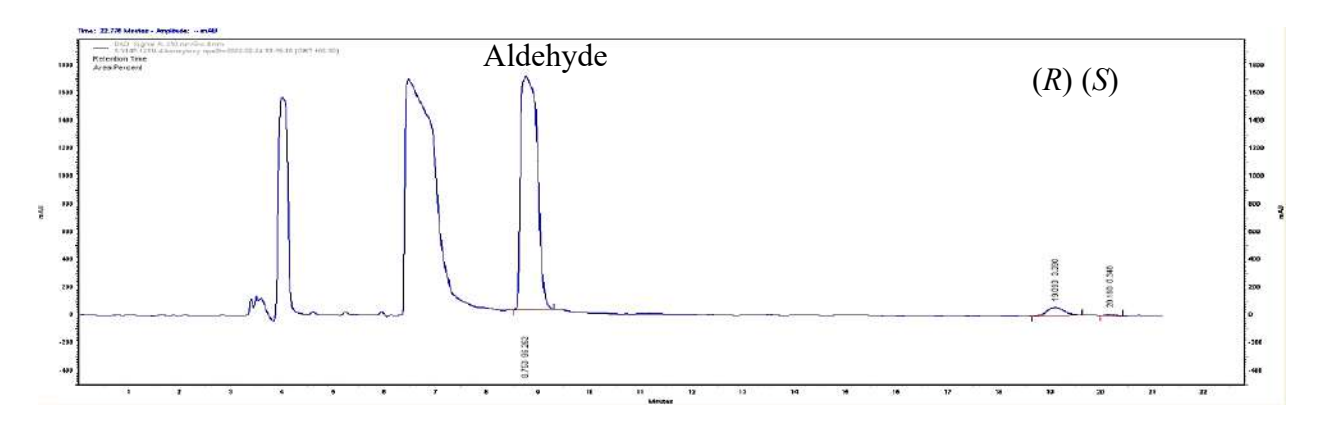


Figure 3.146: HPLC spectrum of the Y14F variant (125 U) catalyzed synthesis of (R)-β-nitroalcohol of 4-benzyloxybenzaldehyde at 3 h.

3.4.7. At HNL double variants catalyzed synthesis of various (R)- β -nitroalcohols using nitroaldol reaction

Two *At*HNL double variants, i.e., Y14M-F179W and Y14M-F179N were evaluated in the biocatalytic synthesis of all the twelve (*R*)-β-nitroalcohols as studied in **3.4.5** and **3.4.6**. Initially 62.5 U of the enzyme was used in the biocatalysis of *At*HNL-Y14M-F179W and was compared with the data of corresponding wide type catalyzed reaction (**Table.3.6**, **Figure 3.147–158**). With the aim to further improve the conversion and enantioselectivity we investigated the biocatalysis of all the twelve substrates using 125 U of purified *At*HNL-Y14M-F179W (**Table.3.6**, **Figure 3.159–164**). This double variant showed improved results than the wild type *At*HNL, i.e., 99% *ee* and 76% conversion with benzaldehyde, 93% *ee* and 24% conversion with *trans* cinnamaldehyde and 82% *ee* and 3% conversion with 4-fluorobenzaldehyde, 97% *ee* and 56% conversion with 4-chlorobenzaldehyde, 56% *ee* and 53% conversion with 4-nitrobenzaldehyde and 98% *ee* and 4% conversion with 4-benzyloxybenzaldehyde in the synthesis of their corresponding (*R*)-β-nitroalcohols.

Our attempt to study the biocatalysis of three other double variants Y14F-F179N, Y14F-F179W and Y14M-F179N was hampered by their poor protein expression. Therefore, we have decided to study them using corresponding crude cell lysates. Unfortunately, we found low specific activity in case of all three of them. Expecting to get comparable results, we did biocatalysis with 200 U of crude cell lysate of these enzymes and studied the enantioselective nitroaldol synthesis with all the tweleve substrates. Disappointingly, most of them did not show any improvement in enantioselectivity in the nitroaldol reaction of most of the substrates (**Table 3.6**), except Y14F-F179W in case of 3,4,5-trimethoxybenzaldehyde (86% *ee* and 11% conversion).

Table 3.6: At HNL double variants catalyzed enantioselective synthesis of (R)- β -nitroalcohols.

R	WT	Y14M-	Y14M-	Y14M-	Y14F-	Y14F-
K	(62.5U)	F179W	F179W	F179N	F179W	F179N
	(02.30)			(200U-	(200U-	(200U-
		(62.5U)	(125U)	`	`	`
DI	61	60	7.6	crude)	crude)	crude)
Ph	61	60	76	4	10	5
	98	98	99	74	18	57
trans cinnamyl	7	21	24	ND	ND	ND
·	82	95	93			
4-Fluoro Ph	ND	ND	3	ND	ND	2
			82			65
4-Chloro Ph	18	45	56	1	2	2
	86	96	97	43	24	56
4-Nitro Ph	48	49	53	24	34	23
	7	37	56	7	10	15
2,4-Dimethoxy Ph	12	17	-	ND	ND	ND
	87	97				
3-Chloro Ph	54	52	-	4	6	6
	97	96		16	13	56
3-Methyl Ph	8	56	-	1	2	2
-	90	99		71	50	85
4-Methyl Ph	31	56	-	1	2	1
-	98	98		48	11	67
3-Methoxy Ph	55	54	-	2	3	3
	95	99		61	58	60
3,4,5-Trimethoxy	46	48	-	ND	11	6
Ph	70	84			86	16
4-Benzyloxy Ph	ND	4	4	ND	ND	ND
		78	98			

ND: not determined; – mark: not done; % ee is highlighted in bold and % conversion is in plain.

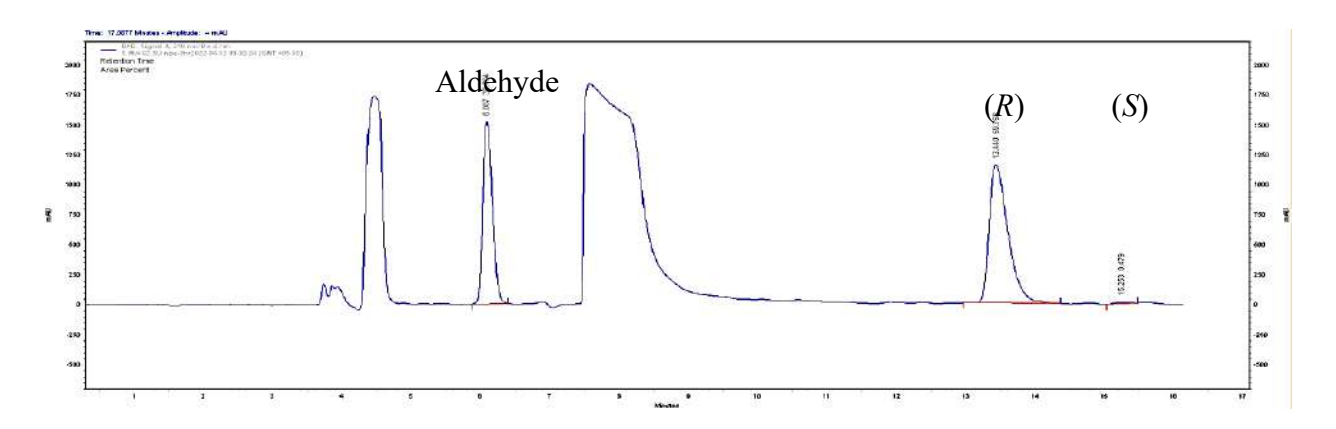


Figure 3.147: HPLC spectrum of the Y14M-F179W catalyzed enantioselective synthesis of (R)-nitroalcohol of benzaldehyde at 3 h.

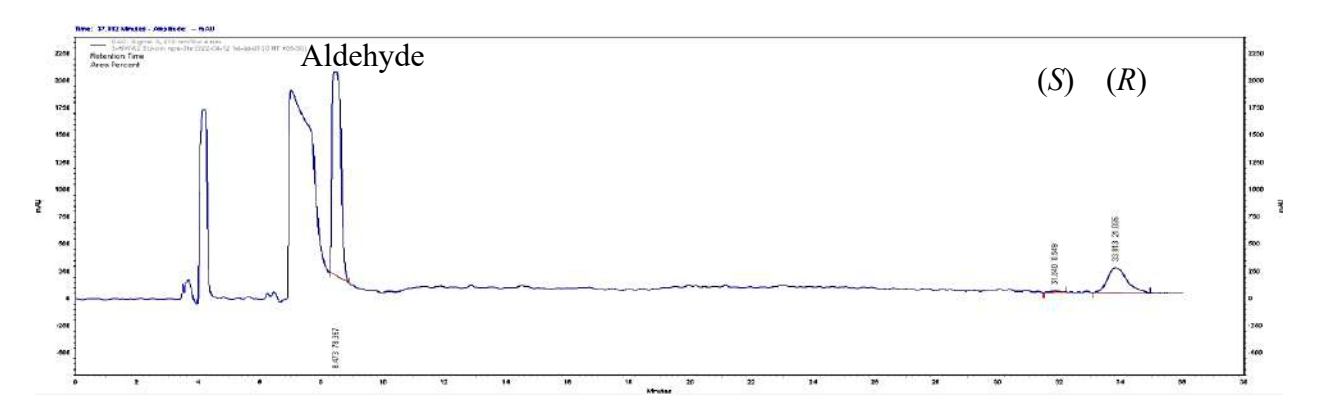


Figure 3.148: HPLC spectrum of the Y14M-F179W catalyzed enantioselective synthesis of (R)-nitroalcohol of *trans* cinnamaldehyde at 3 h.

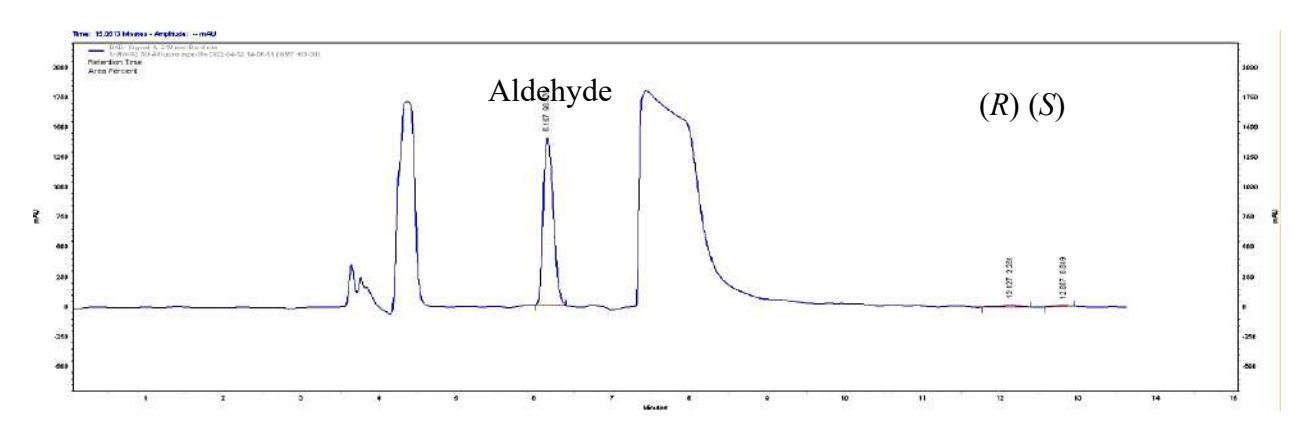


Figure 3.149: HPLC spectrum of the Y14M-F179W catalyzed enantioselective synthesis of (R)-nitroalcohol of 4-fluorobenzaldehyde at 3 h.

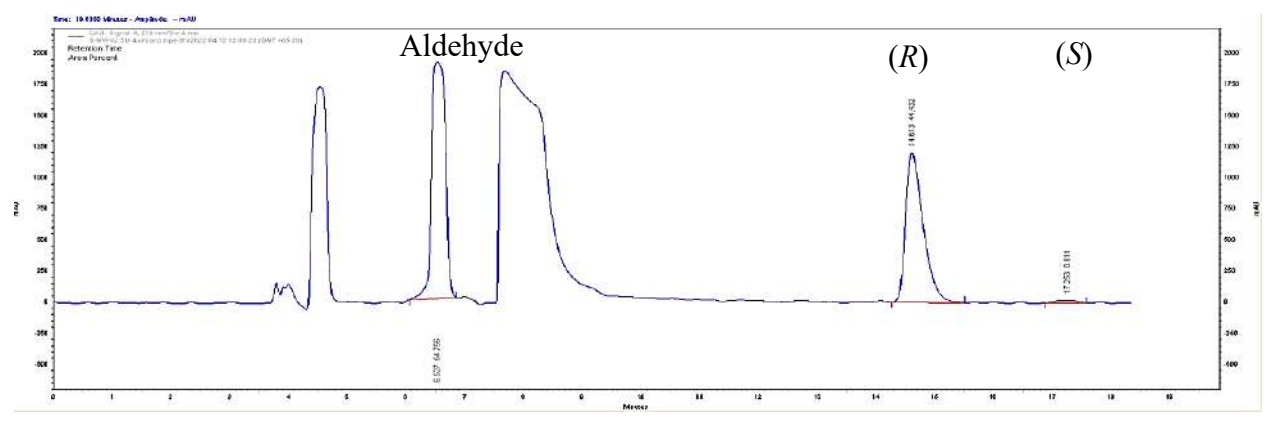


Figure 3.150: HPLC spectrum of the Y14M-F179W catalyzed enantioselective synthesis of (R)-nitroalcohol of 4-chlorobenzaldehyde at 3 h.

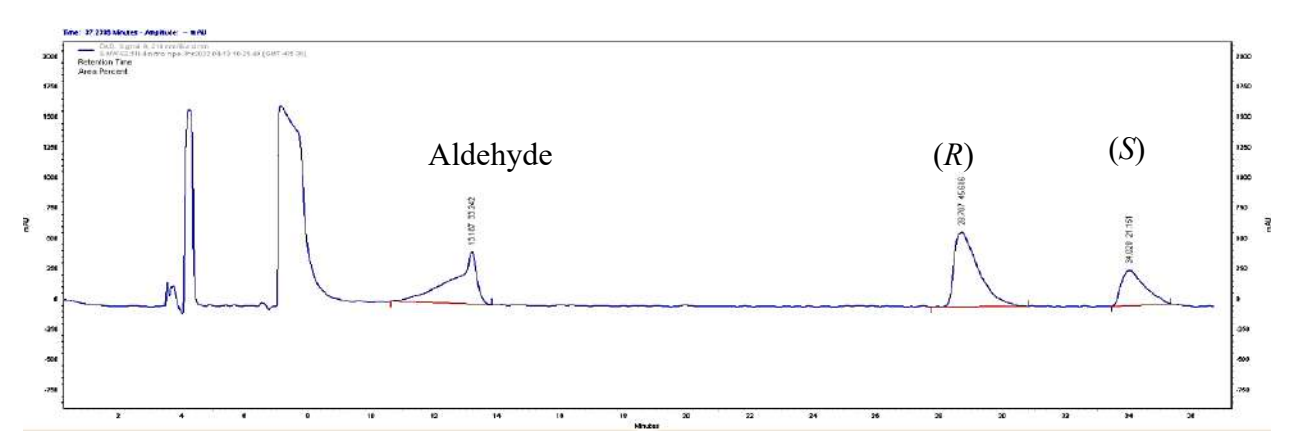


Figure 3.151: HPLC spectrum of the Y14M-F179W catalyzed enantioselective synthesis of (R)-nitroalcohol of 4-nitrobenzaldehyde at 3 h.

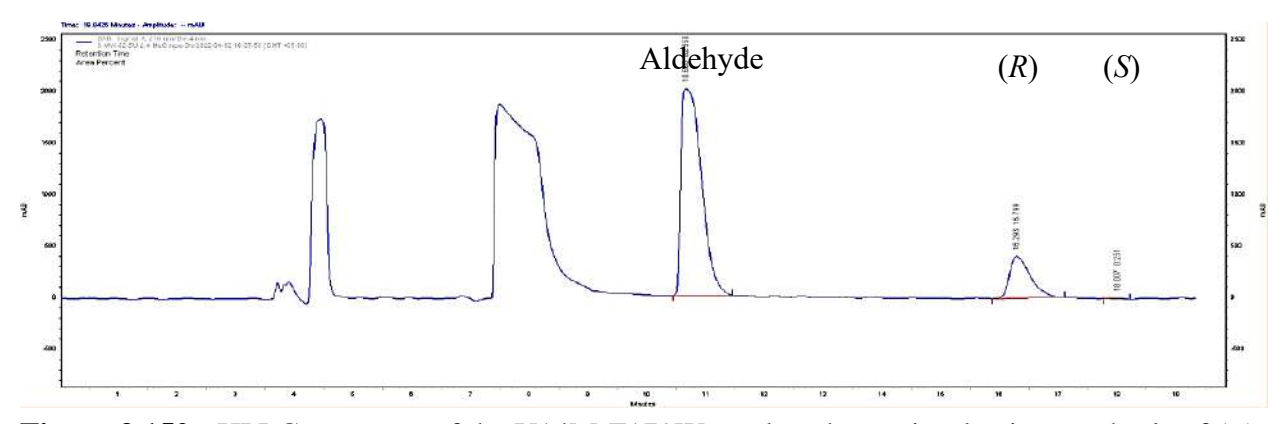


Figure 3.152: HPLC spectrum of the Y14M-F179W catalyzed enantioselective synthesis of (R)-nitroalcohol of 2,4-dimethoxybenzaldehyde at 3 h.

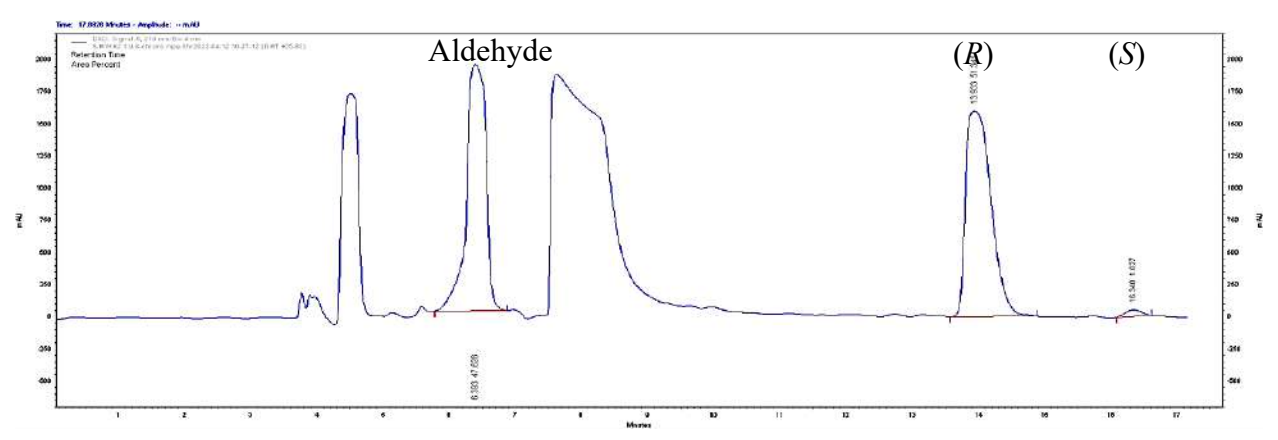


Figure 3.153: HPLC spectrum of the Y14M-F179W catalyzed enantioselective synthesis of (R)-nitroalcohol of 3-chlorobenzaldehyde at 3 h.

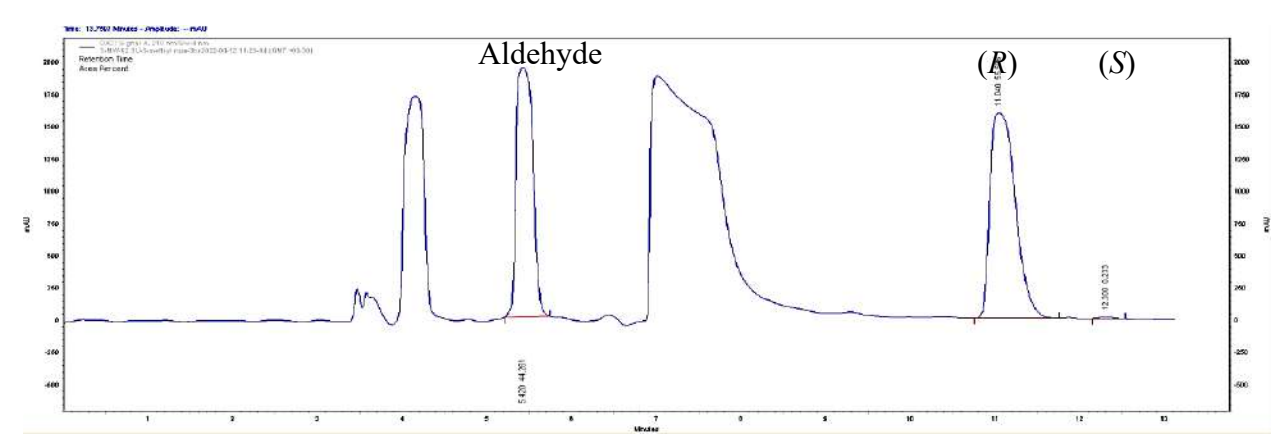


Figure 3.154: HPLC spectrum of the Y14M-F179W catalyzed enantioselective synthesis of (R)-nitroalcohol of 3-methylbenzaldehyde at 3 h.

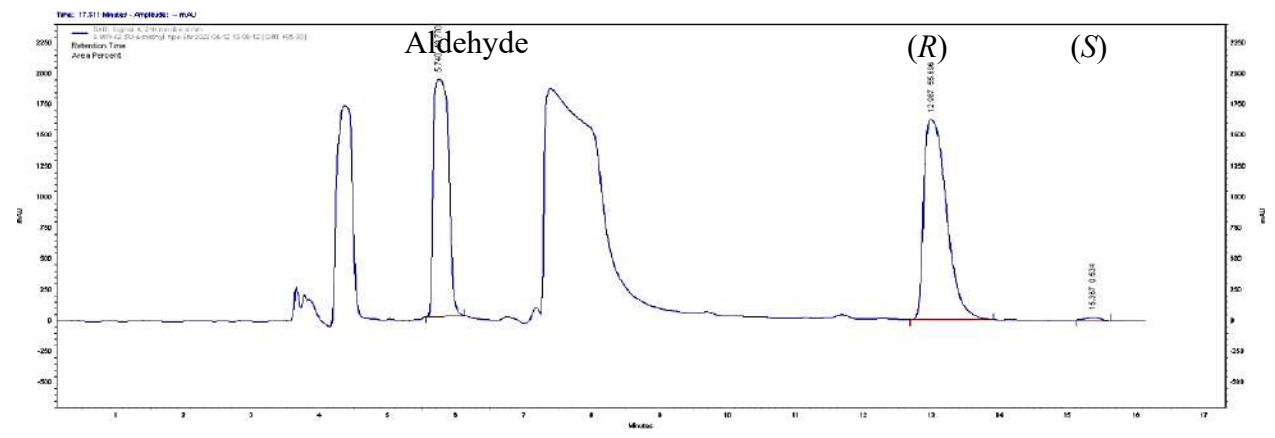


Figure 3.155: HPLC spectrum of the Y14M-F179W catalyzed enantioselective synthesis of (R)-nitroalcohol of 4-methylbenzaldehyde at 3 h.

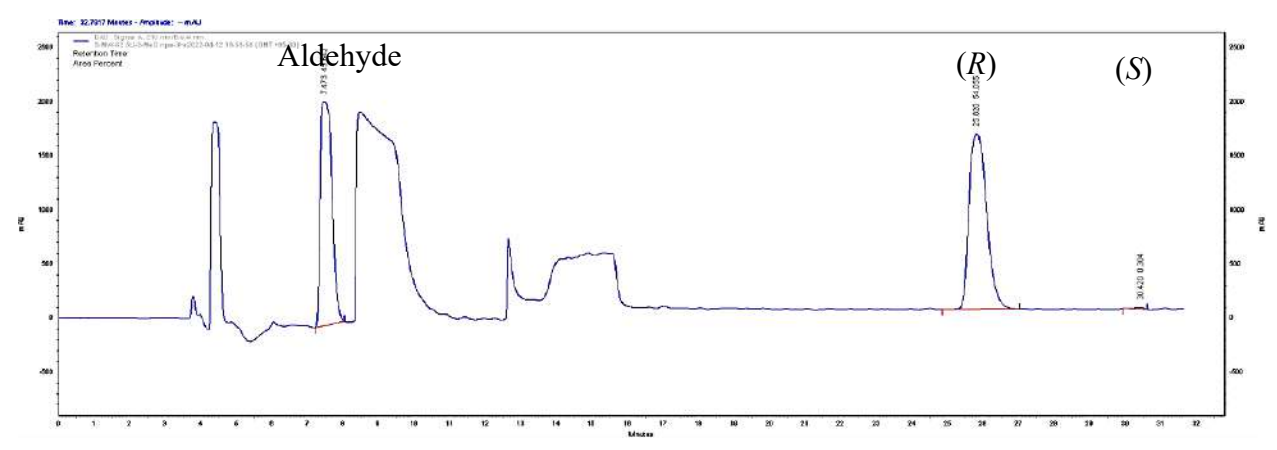


Figure 3.156: HPLC spectrum of the Y14M-F179W catalyzed enantioselective synthesis of (R)-nitroalcohol of 3-methoxybenzaldehyde at 3 h.

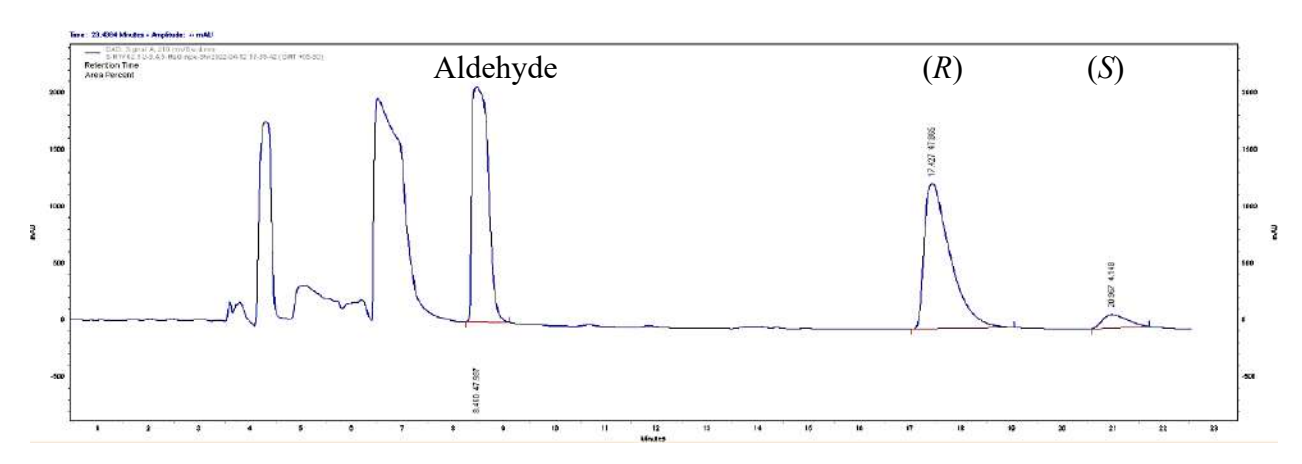


Figure 3.157: HPLC spectrum of the Y14M-F179W catalyzed enantioselective synthesis of (R)- β -nitroalcohol of 3,4,5-trimethoxybenzaldehyde at 3 h.

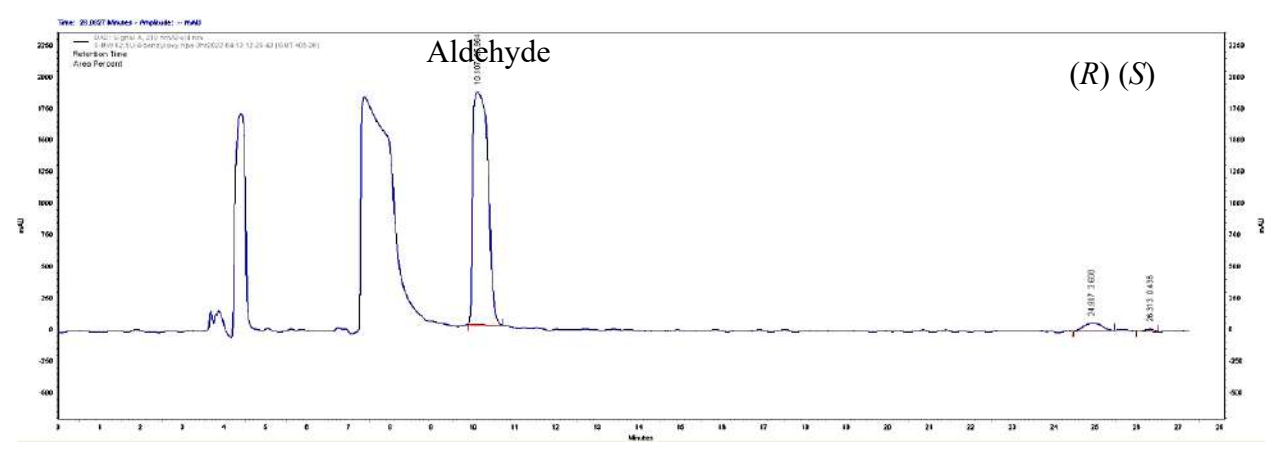


Figure 3.158: HPLC spectrum of the Y14M-F179W catalyzed enantioselective synthesis of (R)-nitroalcohol of 4-benzyloxybenzaldehyde at 3 h.

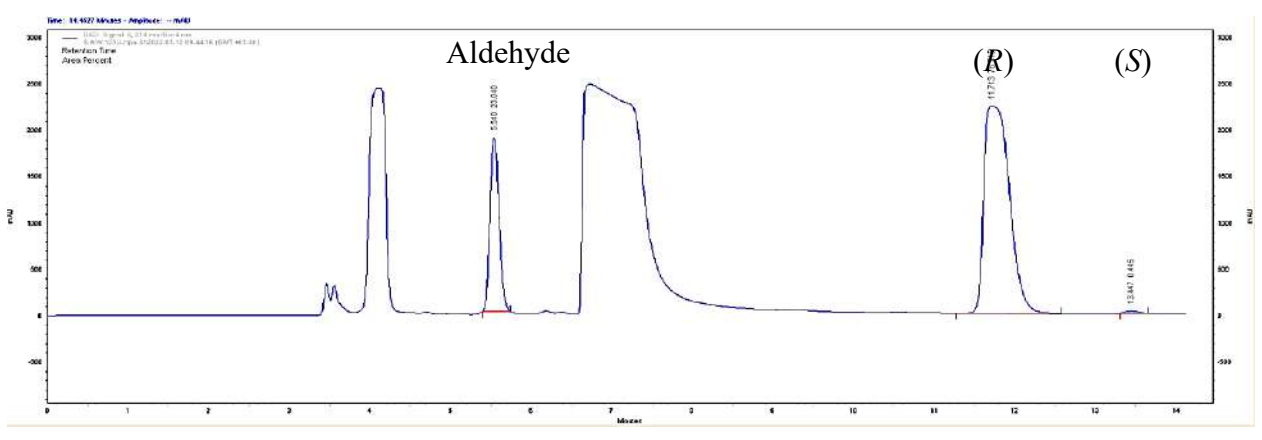


Figure 3.159: HPLC spectrum of the Y14M-F179W (125 U) catalyzed enantioselective synthesis of (R)-β-nitroalcohol of benzaldehyde at 3 h.

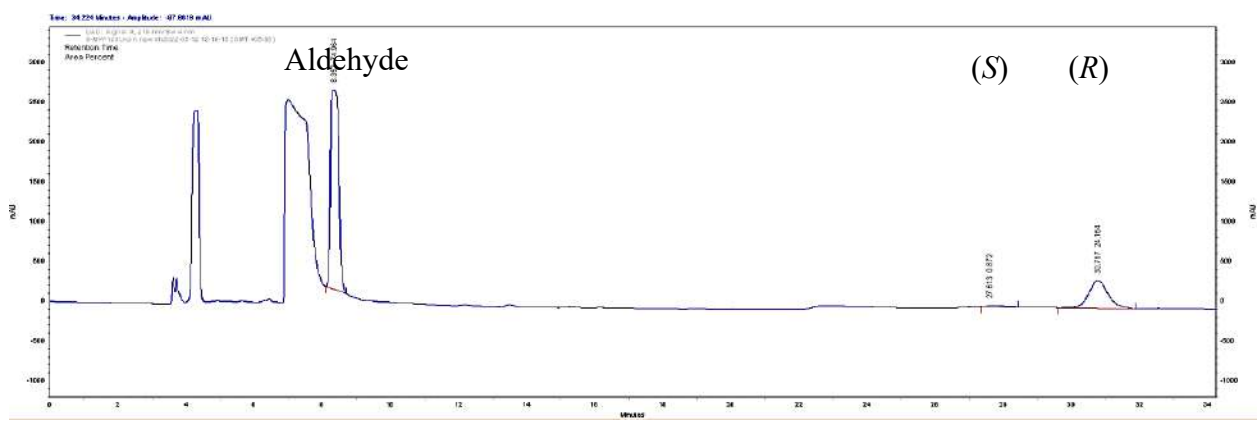


Figure 3.160: HPLC spectrum of the Y14M-F179W (125 U) catalyzed enantioselective synthesis of (R)- β -nitroalcohol of *trans* cinnamaldehyde at 3 h.

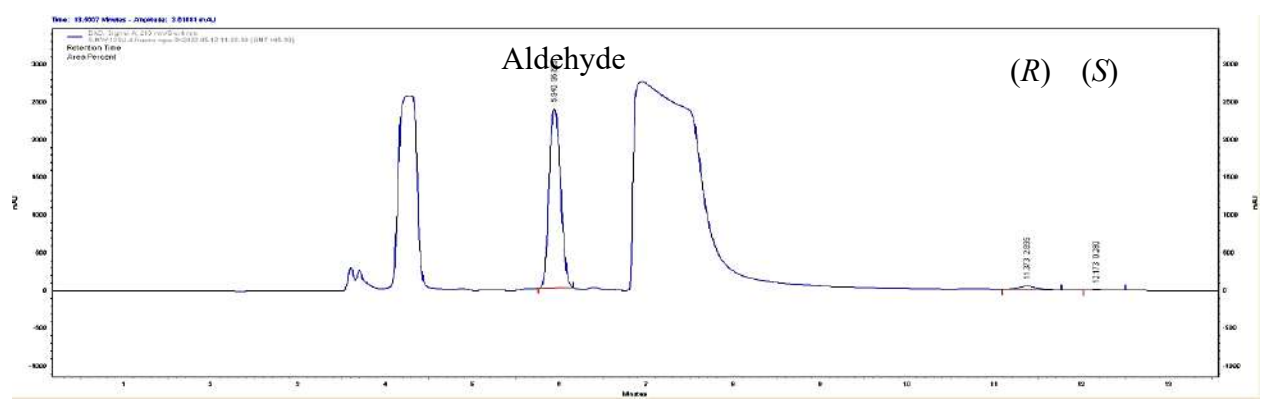


Figure 3.161: HPLC spectrum of the Y14M-F179W (125 U) catalyzed enantioselective synthesis of (*R*)-β-nitroalcohol of 4-fluorobenzaldehyde at 3 h.

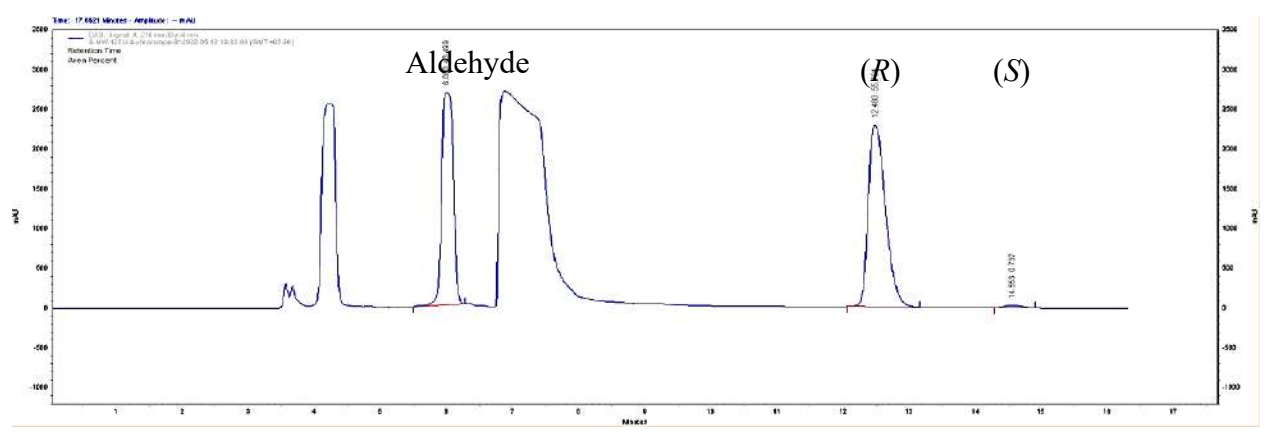


Figure 3.162: HPLC spectrum of the Y14M-F179W (125 U) catalyzed enantioselective synthesis of (R)- β -nitroalcohol of 4-chlorobenzaldehyde at 3 h.

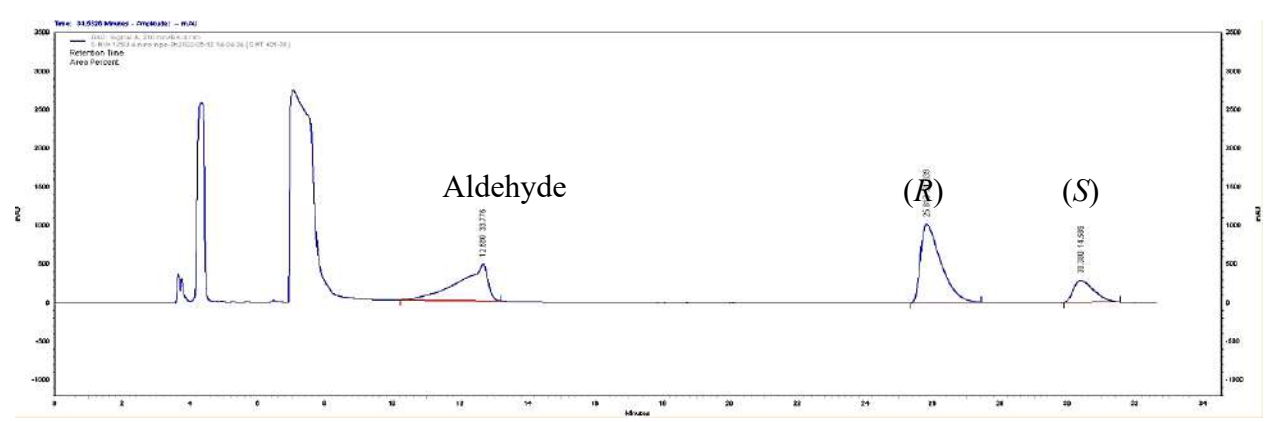


Figure 3.163: HPLC spectrum of the Y14M-F179W (125 U) catalyzed enantioselective synthesis of (*R*)-β-nitroalcohol of 4-nitrobenzaldehyde at 3 h.

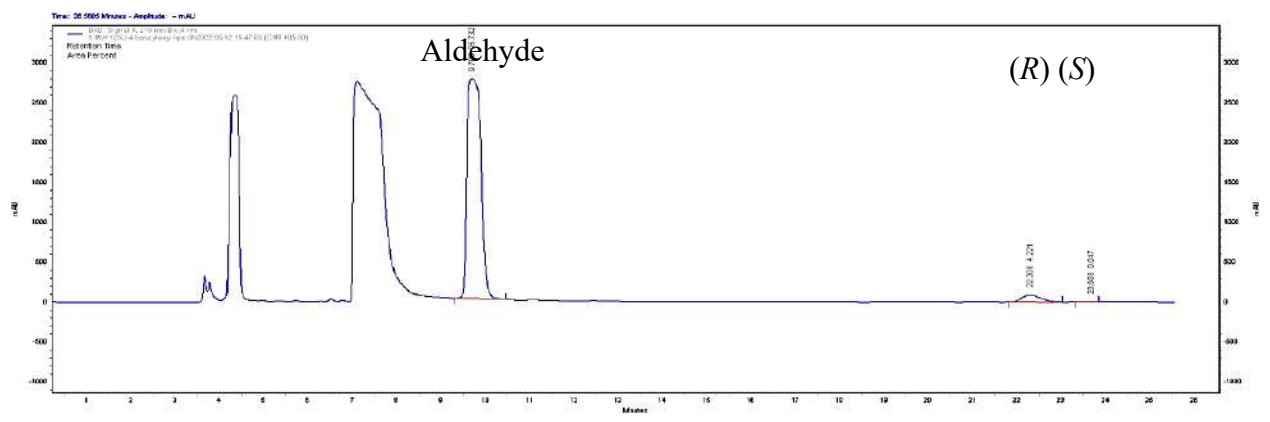


Figure 3.164: HPLC spectrum of the Y14M-F179W (125 U) catalyzed enantioselective synthesis of (R)- β -nitroalcohol of 4-benzyloxybenzaldehyde at 3 h.

3.5. Discussion

3.5.1. Screening of AtHNL and its variants for (R)-NPE synthesis

We began this study aiming to uncover an engineered AtHNL variant that could efficiently catalyze the enantioselective synthesis of (R)- β -nitroalcohols using promiscuous Henry reaction. To accomplish this objective, in our first step we performed a preliminary screening of all the saturation library variants that were discussed in the previous chapter (Scheme 3.2) to synthesize (R)-NPE. The variants of F82A library did not show any higher nitroaldolase activity than the WT (Table 3.2a, Figure 3.2-3.10). Even in our previous study, F82 variants have shown lower retronitroaldolase activity. This screening data suggests that Phe82 is a very crucial residue for not only retro-nitroaldolase activity but also for nitroaldolase activity of AtHNL, although its exact role is yet to be discovered. Nearly a dozen of variants in the F179 saturation library have shown good % ee but the % conversion was moderate in a few of them. The variants F179A, F179H, F179C, F179N, F179L, F179M, F179V, F179K, and F179W have shown >96% ee and F179S has shown >95% ee of (R)-NPE at 2 h. However, among these variants, F179C, F179M and F179V have shown very minimal % conversion, unlike others which have moderate % conversion ranging from 10-17% (Table 3.2b, Figure 3.2, 3.11-3.29). Among the Y14 saturation library variants, Y14K and Y14R have shown ~96% ee, Y14F has shown >95% ee, Y14C and Y14M shown >93% ee, Y14G showed ~92% ee and Y14A, Y14T, and Y14L have shown ~90% ee of (R)-NPE (Table 3.2c, Figure 3.2, 3.30-3.48). Highest conversion of ~33% was observed in case of Y14A, Y14C and Y14F as compared to 23% by the wild type. Y14M and Y14L have shown ~28% conversion, Y14G and Y14K have shown ~12% conversion, however, a very minimal % conversion was found in case of Y14R. Even though F179C, F179M, F179V, F179S and Y14R showed good enantioselectivity, as their conversion in the asymmetric synthesis of (R)-NPE was poor, they were not selected for further studies. Similarly, the F179A, F179K and Y14K variants are also not selected due to their poor protein expression and very low specific activity. Finally, the single variants F179H, F179N, F179L, and F179W from the F179 saturation library and Y14A, Y14C, Y14F, Y14M, Y14G, Y14L and Y14T from the Y14 saturation library were shortlisted for further investigations. Analysis to understand and draw an analogy between the natures of the selected amino acids that are being replaced to their role at molecular level towards the enantioselective synthesis of (*R*)-NPE has become difficult.

3.5.2. Chiral resolution of racemic β-nitroalcohols by HPLC

Chiral resolution of racemic β -nitroalcohols was performed using Chiralpak® IB chiral column in a HPLC with a flow rate of 1 mL/min (**Table 3.3; Figure 3.49-3.60**). The analysis was performed at wavelength of 210 nm using different ratio of *n*-hexane and 2-propanol as the mobile phase. For sample preparation, 4 µmol of the respective the racemic β -nitroalcohol was dissolved in the mobile phase (*n*-hexane and 2-propanol) and was used for chiral analysis.

The compounds 2-nitro-1-phenylethanol, (*E*)-1-nitro-4-phenylbut-3-en-2-ol, 1-(3-chlorophenyl)-2-nitroethanol, 1-(4-chlorophenyl)-2-nitroethanol, 1-(4-fluorophenyl)-2-nitroethanol, 1-(3-methylphenyl)-2-nitroethanol, 1-(4-methylphenyl)-2-nitroethanol, 1-(4-nitrophenyl)-2-nitroethanol, 1-(2, 4-dimethoxyphenyl)-2-nitroethanol and 1-(4-benzyloxyphenyl)-2-nitroethanol were resolved using 90:10 *n*-hexane and 2-propanol ratio. The compound 1-(3-methoxyphenyl)-2-nitroethanol was initially run on 97:3 of *n*-hexane and 2-propanol for 6 minutes to separate aldehyde and nitromethane peaks followed by 90:10 ratio to resolve both the enantiomers. Finally, 1-(3, 4, 5-trimethoxyphenyl)-2-nitroethanol was resolved at 80:20 *n*-hexane and 2-propanol ratio. **Table 3.3** represents the retention times of these compounds and their respective aldehydes.

3.5.3. At HNL variants catalyzed synthesis of various (R)- β -nitroalcohols using nitroaldol reaction

Purified enzymes of the single variants F179H, F179N, F179L, and F179W from the F179 saturation library and Y14A, Y14C, Y14F, Y14M, Y14G, Y14L and Y14T from the Y14 saturation library, were used in the biocatalytic study in enantioselective synthesis of (R)-βnitroalcohols by nitroaldol reaction. To explore the substrate scope of these variants, a dozen of diverse aldehydes were carefully chosen. The set of substrates included 4-benzyloxy benzaldehyde, an aromatic aldehyde with a bulky benzyloxy group at the para position, trans cinnamaldehyde that has a longer carbon skeleton, and ten aromatic aldehydes. The versatile substrate set of aromatic aldehydes contained single, double and triple substitutions of different functional groups (-CH₃, -OCH₃, -NO₂, -F, -Cl₂) in the aromatic ring, substituents at different positions (ortho, meta, and para) of the aromatic ring, and both electron-donating and withdrawing groups. Our initial set of biocatalysis consisted of 144 (12 enzymes × 12 aldehydes) diverse enantioselective Henry reactions (Table 3.4; Figure 3.61-3.132). Here we adopted modified biocatalytic conditions for these transformations, i.e., 62.5 U of AtHNL variants, 20 mM aldehyde and 1.75 M nitromethane were used. These conditions are different than that used for screening study. Subsequently, we have selected four single variants Y14F, Y14M, F179W and F179N, which performed better with most of the substrates, and tested them again in biocatalysis with 125 U of the enzyme to check for any improvement in enantioselectivity and/or conversion (**Table 3.5**; Figure 3.133-3.146). Later four double variants, i.e., Y14F-F179N, Y14F-F179W, Y14M-F179W and Y14M-F179N were created and investigated against the above twelve substrates in synthesis of corresponding (R)-β-nitroalcohols. Unfortunately, three of them, Y14F-F179N, Y14F-F179W and Y14M-F179N showed very poor expression and low specific activity. So, 200 U of crude

enzyme of each of them were employed in the biocatalysis to check if they show any selectivity towards any of the substrates. But none of them showed any positive results for any of the substrates (**Table 3.6**). *At*HNL-Y14M-F179W unlike the other double variants displayed better expression and good specific activity, hence, biocatalysis was performed using 62.5 U of its purified enzyme, with all substrates (**Table 3.6**; **Figure 3.147-3.158**). Later biocatalysis was carried out using 125 U of this enzyme with selected susbtrates to obtain further improvement in enantioselectivity and conversion (**Table 3.6**; **Figure 3.159-3.164**). The improved biocatalytic features for each substrate using engineered *At*HNL is discussed below.

First HNL catalyzed nitroaldol reaction to synthesize (R)-NPE was reported by Asano et al. using wild type AtHNL, which showed only 30% conversion with 91% ee in 2 h²⁹. Yu et al. used an acyl-peptide releasing enzyme from Sulfolobus tokodaii (ST0779) to synthesize (R)-NPE from benzaldehyde using promiscuous Henry reaction, which took long reaction time (90 h) for its catalysis to obtain only 34% conversion with just 17% ee^{41} . This enzyme did not show uniform enantiopreference, as its enantioselectivity varied with the electronic effects of the substituents on the benzaldehyde ring. Two other (R)-selective HNLs, GtHNL, AcHNL have also been reported in the synthesis of (R)-NPE from benzaldehyde but they require metal cofactor in their catalysis unlike AtHNL³⁵. While wild type AcHNL and GtHNL gave low conversions and % ee in (R)-NPE synthesis, in case of AcHNL-A40H, 74% conversion with 97% ee and GtHNL-A40R, 75% conversion with 94% ee of (R)-NPE was reported at 24 h. Both the variants used 20 mM benzaldehyde and hence the product obtained is equivalent to 14.8-15 mM. In our study, we achieved 84% conversion with Y14M and 82% conversion with F179N using 20 mM benzaldehyde, hence the product concentration calculated to be 16.4 & 16.8 mM respectively in 3 h. Compared to the 24 h reaction time by AcHNL and GtHNL variants, our AtHNL variants (Y14M

& F179N) produced (*R*)-NPE in just 3 h with comparable or better yield. Horse liver alcohol dehydrogenase (HLADH)-*At*HNL cascade was another approach to produce (*R*)-NPE from benzylalcohol. The nitroaldol step of this cascade used 800 U of *At*HNL in the benzaldehyde to (*R*)-NPE synthesis and gave 64% conversion with good enantioselectivity at 6 h⁴⁰. In our study, with 62.5 U of *At*HNL we achieved 61% conversion and 98% *ee* of (*R*)-NPE from benzaldehyde. With 125 U of F179N and Y14M, the % conversions were increased to 82 and 84 while high % *ee* of 97 and 93 were observed respectively at 3 h (**Table 3.5**). Y14M-F179W showed 76% conversion with 99% *ee* at 3 h (**Table 3.6**). Compared to the previous studies, we improved the synthesis of (*R*)-NPE from benzaldehyde in terms of % conversion and enantiopurity in less time and less amount of enzyme using *At*HNL variants.

We reported here for the first time the engineered *At*HNL catalyzed enantioselective synthesis of (*R*)-(*E*)-1-nitro-4-phenylbut-3-en-2-ol from *trans* cinnamaldehyde. Earlier, immobilized *At*HNL was reported with racemic *trans* cinnamaldehyde as substrate in the retro-Henry reaction but it showed only 5% *ee* and 47% conversion of the corresponding (*S*)- product at 9 h indicating very poor selectivity²⁷. In the current study, wild type *At*HNL showed 7% conversion and 82% *ee* while F179W showed 13% conversion and 91% *ee* in 3 h (**Table 3.5**). The double variant Y14M-F1799W showed 24% conversion and 93% *ee* at 3 h (**Table 3.6**). Clearly, *At*HNL engineering has enhanced both the substrate preference and enantioselectivity in the synthesis of (*R*)-(*E*)-1-nitro-4-phenylbut-3-en-2-ol.

In case of enantioselective synthesis of (*R*)-1-(4-fluorophenyl)-2-nitroethanol, with 125 U of Y14M we could achieve 91% *ee* with 5% conversion at 3 h (**Table 3.5**), while the wild type *At*HNL showed only 4% conversion with 77% *ee*. Earlier, Asano et al. reported 80% *ee* using 250 U of

wild type $AtHNL^{29}$. The Y14M has improved the % ee to 91 using half of the enzyme amount used in the earlier report.

Wild type AtHNL was reported to synthesize (R)-1-(4-chlorophenyl)-2-nitroethanol in 9% conversion with 87% ee^{29} . The ST0779 catayzed conversion of 4-chlorobenzaldehyde by Henry reaction produced 45% conversion with 78% ee of (R)-1-(4-chlorophenyl)-2-nitroethanol using 20 mg of enzyme, while the reaction took long time (60 h)⁴¹. HLADH-AtHNL cascade mediated synthesis of (R)-1-(4-chlorophenyl)-2-nitroethanol was also reported where 800 U of AtHNL was used in the nitroaldol reaction step to give only 38% conversion with 98% ee at 4 h⁴⁰. We observed 18% and 86% by the wild type AtHNL, 53% and 91% by the Y14F (**Table 3.5**) and 56% and 95% conversion and ee respectively by 125 U of Y14M-F1799W in 3 h (**Table 3.6**). Both high conversion and % ee were achieved in less time and amount of enzyme compared to previous reports using AtHNL variants.

The only enzymatic nitroaldol to synthesize (*R*)-1-(4-nitrophenyl)-2-nitroethanol from its corresponding aldehyde using ST0779 reported 92% conversion with 94% *ee* of product. However, the reaction required 20 mg of enzyme and took long reaction time of 18 h⁴¹. In case of HLADH-*At*HNL cascade, 800 U of *At*HNL was used in the nitroaldol reaction, which gave 89% conversion and 69% *ee* at 8 h⁴⁰. We found 48% conversion and only 7% *ee* at 3 h by the wild type *At*HNL, while, Y14F has shown 53% conversion and 16% *ee* and F179N has shown 50% conversion with 33% *ee* at 3 h (**Table 3.5**). The % *ee* of (*R*)-1-(4-nitrophenyl)-2-nitroethanol was improved to 56 by Y14M-F1799W and 53% conversion was found at 3h using 125 U of the enzyme (**Table 3.6**).

We reported here for the first time the biocatalytic enantioselective synthesis of (R)-1-(2, 4 - d)-dimethoxyphenyl)-2-nitroethanol by nitroaldol reaction. The WT could produce it in only 12%

conversion with 87% *ee*. To our delight, Y14F has improved the conversion of the product to almost double, where 27% conversion and enantioselectivity also increased to 98% (**Table 3.5**).

Earlier report of WT AtHNL catalysed nitroaldol reaction produced (R)-1-(3-chlorophenyl)-2-nitroethanol using in 17% conversion with 91% ee^{29} . Lipase PS catalyzed kinetic resolution has produced unreacted (R)-1-(3-chlorophenyl)-2-nitroethanol in 52% conversion and 99% ee^{46} . Asymmetric reduction of corresponding α -nitroketone by RasADH has demonstrated in the synthesis of (R)-1-(3-chlorophenyl)-2-nitroethanol in 72% conversion and 96% ee^{26} . In the HLADH-AtHNL cascade to produce (R)-1-(3-chlorophenyl)-2-nitroethanol from 3-chlorobenzylalcohol, the nitroaldol step resulted in 75.8% conv, and 99% ee at 4 h⁴⁰. We observed 54% conv and 97% ee of product by the WT AtHNL catalyzed nitroaldol synthesis. Three variants, Y14F, Y14M, and F179N have appeared to be better the WT in the asymmetric nitroaldol reaction. In case of F179N, (R)-1-(3-chlorophenyl)-2-nitroethanol was obtained in 72% conversion with 98% ee while Y14M and Y14F showed 59% and 62% conversions and 97% and 98% ee, respectively at 3 h (**Table 3.5**).

Previously, AtHNL WT catalyzed nitroaldol synthesis of (R)-1-(3-methylphenyl)-2-nitroethanol resulted in 12% conversion with 96% ee^{29} . The ketoreductase RasADH catalyzed asymmetric reduction of corresponding α -nitroketone was neither efficient nor shown high enantioselectivity (38% conv, 91% ee)²⁶. Kinetic resolution of racemic 1-(3-methylphenyl)-2-nitroethanol by lipase PS catalyzed gave the unreacted (R)-1-(3-methylphenyl)-2-nitroethanol in 54% conversion and 99% ee^{46} . Our study revealed five AtHNL variants for synthesis of (R)-1-(3-methylphenyl)-2-nitroethanol by asymmetric Henry reaction. While the WT produced in 8% conversion and 90% ee, the five variants, Y14F, Y14M, F179N, F179W and Y14M-F179W, have shown significant increase in both conversion and enantioselectivity. They produced (R)-1-(3-methylphenyl)-2-

nitroethanol in 30-59% conversion with 92-99% *ee* (**Table 3.5 and 3.6**). Both F179N (59% conv, 98% *ee*) and Y14M-F179W (56% conv, 99% *ee*) have proved to be the best biocatalysts so far to synthesize (*R*)-1-(3-methylphenyl)-2-nitroethanol.

The first attempt for the enantioselective synthesis of (R)-1-(4-methylphenyl)-2-nitroethanol was by Asano et al²⁹. They used wild type AtHNL for catalyzing the nitroaldol reaction that resulted in only 11% conversion and 94% ee in 2 h. This promiscuous reaction in the presence of high amount (50 mg) of human serum albumin in water when carried out for 168 h, the % conversion to (R)-1-(4-methylphenyl)-2-nitroethanol was found to be 53, however the % ee was just limited to 60^{47} . In case of lipase PS catalyzed kinetic resolution of racemic 1-(4-methylphenyl)-2-nitroethanol, a 51% conversion with 99% ee was reported⁴⁶. Biocatalytic asymmetric reduction of the corresponding α -nitroketone by RasADH, a ketoreductase from Ralstonia species exhibited excellent conversion of >99%, however the ee was $86\%^{26}$. Our nitroaldol synthesis by the wild type AtHNL gave 31% conversion and 98% ee of (R)-1-(4-methylphenyl)-2-nitroethanol. Among the variants, four of them, i.e., Y14F, Y14M, F179N and Y14M-F179W exhibited higher conversion (46-61%) with 97-99% ee (Table 3.5 and 3.6). Y14F gave the highest enantioselectivity (99% ee) and 61% conversion towards the synthesis of (R)-1-(4-methylphenyl)-2-nitroethanol.

The first study on WT AtHNL catalyzed nitroaldol reaction in enantioselective synthesis of (R)-1-(3-methoxyphenyl)-2-nitroethanol resulted in 13% conversion and 91% ee^{29} . The ketoreductase RasADH catalyzed asymmetric reduction of corresponding α -nitroketone produced the β -nitroalcohol in 59% conversion and 79% ee^{26} . We found 55% conversion and 95% ee of (R)-1-(3-methoxyphenyl)-2-nitroethanol by the wild type AtHNL, while Y14F, Y14M, F179N and Y14M-F179W have shown 54-65% conversion and 95-99% ee (**Table 3.5 and 3.6**). Among them the

Y14F synthesized (*R*)-1-(3-methoxyphenyl)-2-nitroethanol in 65% conversion, with 95% *ee* and still remains the best biocatalyst so far to produce this product.

We reported here for the first time the biocatalytic enantioselective synthesis of (*R*)-1-(3,4,5 - trimethoxyphenyl)-2-nitroethanol using engineered *At*HNL. The wild type *At*HNL displayed 46% conversion and 70% *ee* in the synthesis of this product. To our delight, two variants, Y14F, and Y14M-F179W have shown higher conversion and enantioselectivity than the WT. While Y14F has produced (*R*)-1-(3,4,5 -trimethoxyphenyl)-2-nitroethanol in 67% conversion and 91% *ee* (**Table 3.5**), the double variant Y14M-F179W could produce it in 48% conversion and 84% *ee* (**Table 3.6**).

The only biocatalytic asymmetric synthesis of (*R*)-1-(4-benzyloxyphenyl)-2-nitroethanol was reported using HLADH-*At*HNL cascade reaction. In that study, the nitroaldol reaction provided only 2.6% conversion to (*R*)-1-(4-benzyloxyphenyl)-2-nitroethanol in 8 h⁴⁰. We observed that four variants, Y14F, Y14M, F179N and Y14M-F179W displayed higher % conversion and % *ee* of the product than the wild type *At*HNL (2% conversion and 70% *ee*). The F179N showed 3% conversion and 88% *ee*, while Y14M, Y14F and Y14M-F179W showed 4-7% conversions and 95-97% *ee*, of (*R*)-1-(4-benzyloxyphenyl)-2-nitroethanol respectively (**Table 3.5 and 3.6**).

Overall, the engineered AtHNL variants have demonstrated enhanced conversion and enantioselectivity along with broad substrate scope in the synthesis of a broad range of (R)- β -nitroalcohols. Therefore, While the two enzyme cascade produced only 1.5% conversion to (R)-1-(4-benzyloxyphenyl)-2-nitroethanol, more than fourfold increased conversion was exhibited by the Y14M.

3.6. Conclusions

In this chapter, we aimed to uncover AtHNL variants that would efficiently catalyze enantioselective nitroaldol reaction in the synthesis of (R)- β -nitroalcohols. We envisioned to find variants with increased enantioselectivity, conversion and broad substrate selectivity than the wild type AtHNL. Three AtHNL library of variants (F179, Y14 and F82 series) were investigated towards promiscuous nitroaldol reaction in the synthesis of (R)-NPE.

The primary screening has highlighted several variants with >96% ee (F179A, F179H, F179C, F179N, F179L, F179M, F179V, F179K, F179W, Y14K, Y14R), >95% ee (Y14F, F179S), >94% ee (Y14C and Y14M) and a few with >33% conversion (Y14C, Y14F, and Y14A) as compared to 23% by the wild type AtHNL. From the screening study we could also observe that Phe82 is a very crucial residue for not only retro-nitroaldolase activity but also for nitroaldolase activity of AtHNL. The selected single variants were employed in the synthesis of various (R)- β -nitroalcohols by nitroaldol reaction. For the first time engineered AtHNLs were used in exploring their selectivity for a wide range of substrates by means of stereoselective Henry reaction. We have tested engineered AtHNLs for five new substrates (trans cinnamaldehyde, 4-nitrobenzaldehyde, 2,4-dimethoxybenzaldehyde, 3,4,5-trimethoxybenzaldehyde and 4-benzyloxybenzaldehyde) towards the promiscuous Henry reaction. Our investigation on the substrate scope of a dozen of selected AtHNL variants to synthesize diverse (R)- β -nitroalcohols revealed that the substitution of Phe 179 with Trp and Asn, and Tyr 14 with Phe and Met has improved the enzyme's activity very significantly. F179N variant has shown highest % ee and % conversion for the substrates: benzaldehyde, 3-chlorobenzaldehyde and 3-methylbenzaldehyde in the synthesis of their corresponding (R)-β-nitroalcohols. Similarly, F179W for trans cinnamaldehyde, Y14M for benzaldehyde, 4-fluorobenzaldehyde and 4-benzyloxybenzaldehyde, and Y14F for 4chlorobenzaldehyde, 4-nitrobenzaldehyde, 2,4-dimethoxy benzaldehyde, 4-methylbenzaldehyde, 3-methoxybenzaldehyde and 3,4,5-trimethoxybenzaldehyde as substrates in corresponding nitroaldol synthesis. Y14M and F179N have shown >80% conversion along with >90% ee when benzaldehyde was used as substrate. The double variant Y14M-F179W showed improved % ee and % conversion for benzaldehyde, trans cinnamaldehyde, 4-chlorobenzaldehyde, 4nitrobenzaldehyde and 4-benzyloxybenzaldehyde. With AtHNL engineering, we efficiently improved not only the substrate selectivity but also enantioselectivity for bulky substrates such as trans cinnamaldehyde and 4-benzyloxybenzaldehyde towards stereoselective Henry reaction. AtHNL engineering was also proven productive with other aromatic aldehydes containing single, double and triple substitutions in the aromatic ring, substituents at different positions of aromatic ring, and towards both electron-donating and withdrawing groups. Finally, in the present chapter we successfully improved the efficiency of promiscuous Henry reaction using modified reaction conditions as well as engineered AtHNLs. Our study uncovered AtHNL variants with expanded substrate scope, improved the yield and enantioselectivity, which can be considered as better biocatalysts towards stereoselective Henry reaction. Further investigations using molecular docking and simulation studies on how the engineered enzymes improved the substrate, and enantioselectivity towards Henry reaction may help us to understand the molecular basis of it and may unravel the mechanism. This would provide even better scope to develop AtHNL variants as a potent chiral catalysts to gain high enantioselectivity, yield in asymmetric synthesis of several chiral β -nitroalcohols.

3.7. References

Luzzio, F. A. The Henry Reaction: Recent Examples. *Tetrahedron* 2001, 57 (6), 915–945.
 https://doi.org/10.1016/s0040-4020(00)00965-0.

- (2) Milner, S. E.; Moody, T. S.; Maguire, A. R. Biocatalytic Approaches to the Henry (Nitroaldol) Reaction. *Eur. J. Org. Chem.* **2012**, 3059–3067. https://doi.org/10.1002/ejoc.201101840.
- (3) Rao, D. H. S.; Chatterjee, A.; Padhi, S. K. Biocatalytic Approaches for Enantio and Diastereoselective Synthesis of Chiral β-Nitroalcohols. *Org. Biomol. Chem.* **2021**, *19* (2), 322–337. https://doi.org/10.1039/d0ob02019b.
- (4) Henry, L. C. R. Formation Synthétique d'alcools Nitrés. Comptes rendus académie des Sci.
 1895, No. 120, 1265–1268.
- (5) Marcelli, T.; Van Der Haas, R. N. S.; Van Maarseveen, J. H.; Hiemstra, H. Asymmetric Organocatalytic Henry Reaction. *Angew. Chemie - Int. Ed.* 2006, 45 (6), 929–931. https://doi.org/10.1002/anie.200503724.
- (6) Arai, T.; Watanabe, M.; Fujiwara, A.; Yokoyama, N.; Yanagisawa, A. Direct Monitoring of the Asymmetric Induction of Solid-Phase Catalysis Using Circular Dichroism: Diamine-CuI-Catalyzed Asymmetric Henry Reaction. *Angew. Chemie Int. Ed.* 2006, 45 (36), 5978–5981. https://doi.org/10.1002/anie.200602255.
- (7) Filippova, L.; Stenstrøm, Y.; Hansen, T. V. Cu (II)-Catalyzed Asymmetric Henry Reaction with a Novel C<inf>1</Inf>-Symmetric Aminopinane-Derived Ligand. *Molecules* **2015**, 20 (4), 6224–6236. https://doi.org/10.3390/molecules20046224.
- (8) Phukan, M.; Borah, K. J.; Borah, R. Henry Reaction in Environmentally Benign Methods
 Using Imidazole as Catalyst. *Green Chem. Lett. Rev.* **2009**, *2* (4), 249–253.
 https://doi.org/10.1080/17518250903410074.

- (9) Shi, Y.; Li, Y.; Sun, J.; Lai, Q.; Wei, C.; Gong, Z.; Gu, Q.; Song, Z. Synthesis and Applications in Henry Reactions of Novel Chiral Thiazoline Tridentate Ligands. *Appl. Organomet. Chem.* **2015**, *29* (10), 661–667. https://doi.org/10.1002/aoc.3347.
- (10) Gao, N.; Chen, Y. L.; He, Y. H.; Guan, Z. Highly Efficient and Large-Scalable Glucoamylase-Catalyzed Henry Reactions. *RSC Adv.* **2013**, *3* (37), 16850–16856. https://doi.org/10.1039/c3ra41287c.
- (11) Sasai, H.; Suzuki, T.; Itoh, N.; Shibasaki, M. Catalytic Asymmetric Synthesis of Propranolol and Metoprolol Using a La–Li–BINOL Complex. *Appl. Organomet. Chem.* **1995**, *9* (5–6), 421–426. https://doi.org/10.1002/aoc.590090508.
- (12) Sohtome, Y.; Hashimoto, Y.; Nagasawa, K. Guanidine-Thiourea Bifunctional Organocatalyst for the Asymmetric Henry (Nitroaldol) Reaction. *Adv. Synth. Catal.* **2005**, 347 (11–13), 1643–1648. https://doi.org/10.1002/adsc.200505148.
- (13) Alvarez-Casao, Y.; Marques-Lopez, E.; Herrera, R. P. Organocatalytic Enantioselective Henry Reactions. *Symmetry* (*Basel*). **2011**, *3* (2), 220–245. https://doi.org/10.3390/sym3020220.
- (14) Xu, D. Q.; Wang, Y. F.; Luo, S. P.; Zhang, S.; Zhong, A. G.; Chen, H.; Xu, Z. Y. A Novel Enantioselective Catalytic Tandem Oxa-Michael-Henry Reaction: One-Pot Organocatalytic Asymmetric Synthesis of 3-Nitro-2H-Chromenes. *Adv. Synth. Catal.* **2008**, *350* (16), 2610–2616. https://doi.org/10.1002/adsc.200800535.
- (15) Hiroaki Sasai, Takeyuki Suzuki, Shigeru Arai, Takayoshi Arai, and M. S. Basic Character of Rare Earth Metal Alkoxides. Utilization in Catalytic C-C Bond-Forming Reactions and

- Catalytic Asymmetric Nitroaldol Reactions. J. Am. Chem. SO 1992, 114 (11), 4418–4420.
- (16) Chandrasekhar, S.; Shrinidhi, A. Useful Extensions of the Henry Reaction: Expeditious Routes to Nitroalkanes and Nitroalkenes in Aqueous Media. *Synth. Commun.* **2014**, *44* (20), 3008–3018. https://doi.org/10.1080/00397911.2014.926373.
- (17) Xu, X.; Furukawa, T.; Okino, T.; Miyabe, H.; Takemoto, Y. Bifunctional-Thiourea-Catalyzed Diastereo- And Enantioselective Aza-Henry Reaction. *Chem. A Eur. J.* **2005**, 12 (2), 466–476. https://doi.org/10.1002/chem.200500735.
- (18) Bosica, G.; Polidano, K. Solvent-Free Henry and Michael Reactions with Nitroalkanes Promoted by Potassium Carbonate as a Versatile Heterogeneous Catalyst. *J. Chem.* **2017**, 2017 (Scheme 1), 1–10. https://doi.org/10.1155/2017/6267036.
- (19) Xiong, Y.; Wang, F.; Huang, X.; Wen, Y.; Feng, X. A New Copper (I)-Tetrahydrosalen-Catab Zed Asymmetric Henry Reaction and Its Extension to the Synthesis of (S)-Norphenylephrine. *Chem. A Eur. J.* 2007, 13 (3), 829–833. https://doi.org/10.1002/chem.200601262.
- (20) Ballini, R.; Bosica, G. Nitroaldol Reaction in Aqueous Media: An Important Improvement of the Henry Reaction. *J. Org. Chem.* **1997**, 62 (2), 425–427. https://doi.org/10.1021/jo961201h.
- (21) Xu, K.; Lai, G.; Zha, Z.; Pan, S.; Chen, H.; Wang, Z. A Highly Anti-Selective Asymmetric Henry Reaction Catalyzed by a Chiral Copper Complex: Applications to the Syntheses of (+)-Spisulosine and a Pyrroloisoquinoline Derivative. *Chem. A Eur. J.* **2012**, *18* (39), 12357–12362. https://doi.org/10.1002/chem.201201775.

- (22) Blay, G.; Domingo, L. R.; Hernández-Olmos, V.; Pedro, J. R. New Highly Asymmetric Henry Reaction Catalyzed by CuII and a C1-Symmetric Aminopyridine Ligand, and Its Application to the Synthesis of Miconazole. *Chem. - A Eur. J.* 2008, 14 (15), 4725–4730. https://doi.org/10.1002/chem.200800069.
- (23) White, J. D.; Shaw, S. A New Catalyst for the Asymmetric Henry Reaction: Synthesis of β-Nitroethanols in High Enantiomeric Excess. *Org. Lett.* **2012**, *14* (24), 6270–6273. https://doi.org/10.1021/ol3030023.
- (24) Chadha, A.; Venkataraman, S.; Preetha, R.; Padhi, S. K. Candida Parapsilosis: A Versatile Biocatalyst for Organic Oxidation-Reduction Reactions. *Bioorg. Chem.* **2016**, *68*, 187–213. https://doi.org/10.1016/j.bioorg.2016.08.007.
- (25) Hasnaoui, G.; Lutje Spelberg, J. H.; De Vries, E.; Tang, L.; Hauer, B.; Janssen, D. B. Nitrite-Mediated Hydrolysis of Epoxides Catalyzed by Halohydrin Dehalogenase from Agrobacterium Radiobacter AD1: A New Tool for the Kinetic Resolution of Epoxides.
 Tetrahedron Asymmetry 2005, 16 (9), 1685–1692.
 https://doi.org/10.1016/j.tetasy.2005.03.021.
- (26) Wang, Z.; Wu, X.; Li, Z.; Huang, Z.; Chen, F. Ketoreductase Catalyzed Stereoselective Bioreduction of α-Nitro Ketones. *Org. Biomol. Chem.* 2019, 17 (14), 3575–3580. https://doi.org/10.1039/c9ob00051h.
- (27) Rao, D. H. S.; Shivani, K.; Padhi, S. K. Immobilized Arabidopsis Thaliana Hydroxynitrile Lyase-Catalyzed Retro-Henry Reaction in the Synthesis of (S)-β-Nitroalcohols. *Appl. Biochem. Biotechnol.* **2021**, *193* (2), 560–576. https://doi.org/10.1007/s12010-020-03442-

- (28) Venkataraman, S.; Chadha, A. Enantio- & Chemo-Selective Preparation of Enantiomerically Enriched Aliphatic Nitro Alcohols Using Candida Parapsilosis ATCC 7330. RSC Adv. 2015, 5 (90), 73807–73813. https://doi.org/10.1039/c5ra13593a.
- (29) Fuhshuku, K. I.; Asano, Y. Synthesis of (R)-Beta-Nitro Alcohols Catalyzed by R-Selective Hydroxynitrile Lyase from Arabidopsis Thaliana in the Aqueous-Organic Biphasic System. *J. Biotechnol.* **2011**, *153* (3–4), 153–159. https://doi.org/10.1016/j.jbiotec.2011.03.011.
- (30) Mandana Gruber-Khadjawi, Thomas Purkarthofer, Wolfgang Skranc, and H. G. Hydroxynitrile Lyase-Catalyzed Enzymatic Nitroaldol (Henry) Reaction. *Adv. Synth. Catal.* 2007, 349, 1445–1450. https://doi.org/10.1002/adsc.200700064.
- (31) Rao, D. H. S.; Padhi, S. K. Production of (S)-β-Nitro Alcohols by Enantioselective C–C Bond Cleavage with an R-Selective Hydroxynitrile Lyase. *ChemBioChem* **2019**, *20* (3), 371–378. https://doi.org/10.1002/cbic.201800416.
- (32) Milner, S. E.; Brossat, M.; Moody, T. S.; Elcoate, C. J.; Lawrence, S. E.; Maguire, A. R. Efficient Kinetic Bioresolution of 2-Nitrocyclohexanol. *Tetrahedron Asymmetry* 2010, 21 (8), 1011–1016. https://doi.org/10.1016/j.tetasy.2010.05.006.
- (33) Vongvilai, P.; Angelin, M.; Larsson, R.; Ramström, O. Dynamic Combinatorial Resolution: Direct Asymmetric Lipase-Mediated Screening of a Dynamic Nitroaldol Library. *Angew. Chemie Int. Ed.* **2007**, *46* (6), 948–950. https://doi.org/10.1002/anie.200603740.
- (34) Soumen Dutta, Nitee Kumari, Sateesh Dubbu, Sun Woo Jang, Amit Kumar, Hiroyoshi

- Ohtsu, Junghoon Kim, Seung Hwan Cho, Masaki Kawano, and I. S. L. Highly Mesoporous Metal-Organic Frameworks as Synergistic Multimodal Catalytic Platforms for Divergent Cascade Reactions. *Angew. Chemie Int. Ed.* **2020**, *132*, 3444–3450.
- (35) Bekerle-Bogner, M.; Gruber-Khadjawi, M.; Wiltsche, H.; Wiedner, R.; Schwab, H.; Steiner, K. (R)-Selective Nitroaldol Reaction Catalyzed by Metal-Dependent Bacterial Hydroxynitrile Lyases. *ChemCatChem* **2016**, 8 (13), 2214–2216. https://doi.org/10.1002/cctc.201600150.
- (36) Tentori, F.; Brenna, E.; Colombo, D.; Crotti, M.; Gatti, F. G.; Chiara, M. G.; Pedrocchi-Fantoni, G. Biocatalytic Approach to Chiral β-Nitroalcohols by Enantioselective Alcohol Dehydrogenase-Mediated Reduction of α-Nitroketones. *Catalysts* **2018**, 8 (8). https://doi.org/10.3390/catal8080308.
- (37) Zhang, Y.; Hu, L.; Ramström, O. Double Parallel Dynamic Resolution through Lipase-Catalyzed Asymmetric Transformation. *Chem. Commun.* 2013, 49 (18), 1805–1807. https://doi.org/10.1039/c3cc38203f.
- (38) Xu, F.; Wang, J.; Liu, B.; Wu, Q.; Lin, X. Enzymatic Synthesis of Optical Pure β-Nitroalcohols by Combining D-Aminoacylase-Catalyzed Nitroaldol Reaction and Immobilized Lipase PS-Catalyzed Kinetic Resolution. *Green Chem.* **2011**, *13* (9), 2359–2361. https://doi.org/10.1039/c1gc15417f.
- (39) Purkarthofer, T.; Gruber, K.; Gruber-Khadjawi, M.; Waich, K.; Skranc, W.; Mink, D.; Griengl, H. A Biocatalytic Henry Reaction The Hydroxynitrile Lyase from Hevea Brasiliensis Also Catalyzes Nitroaldol Reactions. *Angew. Chemie Int. Ed.* **2006**, *45* (21),

- 3454–3456. https://doi.org/10.1002/anie.200504230.
- (40) Ayon Chatterjee, D.H. Sreenivasa Rao, and S. K. P. One-Pot Enzyme Cascade Catalyzed Asymmetrization of Primary Alcohols: Synthesis of Enantiocomplementary Chiral β-Nitroalcohols. *Adv. Synth. Catal.* **2021**, *363* (23), 5310–5318. https://doi.org/10.1002/adsc.202100803.
- (41) Yu, X.; Pérez, B.; Zhang, Z.; Gao, R.; Guo, Z. Mining Catalytic Promiscuity from: Thermophilic Archaea: An Acyl-Peptide Releasing Enzyme from Sulfolobus Tokodaii (ST0779) for Nitroaldol Reactions. *Green Chem.* 2016, 18 (9), 2753–2761. https://doi.org/10.1039/c5gc02674a.
- (42) Vishnu Priya, B.; Sreenivasa Rao, D. H.; Gilani, R.; Lata, S.; Rai, N.; Akif, M.; Kumar Padhi, S. Enzyme Engineering Improves Catalytic Efficiency and Enantioselectivity of Hydroxynitrile Lyase for Promiscuous Retro-Nitroaldolase Activity. *Bioorg. Chem.* **2022**, *120* (January), 105594. https://doi.org/10.1016/j.bioorg.2021.105594.
- (43) Rao, D. H. S.; Padhi, S. K. Production of (S)-β-Nitro Alcohols by Enantioselective C–C Bond Cleavage with an R-Selective Hydroxynitrile Lyase. *ChemBioChem* **2019**, *20* (3), 371–378. https://doi.org/10.1002/cbic.201800416.
- (44) Zhang, L.; Wu, H.; Yang, Z.; Xu, X.; Zhao, H.; Huang, Y.; Wang, Y. Synthesis and Computation of Diastereomeric Phenanthroline-Quinine Ligands and Their Application in Asymmetric Henry Reaction. *Tetrahedron* 2013, 69 (49), 10644–10652. https://doi.org/10.1016/j.tet.2013.10.010.
- (45) Ginotra, S. K.; Singh, V. K. Enantioselective Henry Reaction Catalyzed by a C2-Symmetric

- Bis(Oxazoline)-Cu(OAc)2·H2O Complex. *Org. Biomol. Chem.* **2007**, *5* (24), 3932–3937. https://doi.org/10.1039/b714153j.
- (46) Li, N.; Hu, S. Bin; Feng, G. Y. Resolution of 2-Nitroalcohols by Burkholderia Cepacia Lipase-Catalyzed Enantioselective Acylation. *Biotechnol. Lett.* **2012**, *34* (1), 153–158. https://doi.org/10.1007/s10529-011-0754-x.
- (47) Matsumoto, K.; Asakura, S. Albumin-Mediated Asymmetric Nitroaldol Reaction of Aromatic Aldehydes with Nitromethane in Water. *Tetrahedron Lett.* **2014**, *55* (50), 6919–6921. https://doi.org/10.1016/j.tetlet.2014.10.109.

Chapter 4: Development of a chemoenzymatic method for synthesis of a chiral intermediate of (R)-Tembamide, using engineered AtHNL

4.1. Introduction

The chiral β-amino alcohols are an important class of compounds widely used in the synthesis of several natural and synthetic biologically active molecules such as antibiotics, alkaloids, enzyme inhibitors, and β -blockers^{1,2}. One of the most common methods to synthesize β -amino alcohols is the reduction of β-nitroalcohols³. A few examples of different drug molecules and natural products, which have this moiety in their structural backbone are discussed in section 1.5.2 of chapter 1 (Figure 1.3). These enantiopure drugs and biologically active molecules are very important in health and medicinal arena due to their inherent therapeutic behavior of the individual enantiomers of the drug that acts in the biological system. Among many potential drug intermediates, panisaldehyde or 4-methoxybenzaldehyde is a widely used molecule in the pharmaceutical and food industry. The optically pure β -nitroalcohol obtained from 4-methoxybenzaldehyde, i.e., (R)- 1-(4methoxyphenyl)-2-nitroethanol is an extensively used structural element seen in various drugs, flavors and perfumes, making it more industrially significant and commercially important chiral drug intermediate. One such drug is (R)-Tembamide, a naturally occurring β -hydroxyamide, which is isolated from Fagara hyemalis (St. Hill) Engler, belongs to Rutaceae family⁴. This drug is used in traditional Indian medications as a good control for hypoglycemia^{5,6}. Considering the importance of (R)-Tembamide, we aimed to develop a simple and efficient chemo-enzymatic route to synthesize the (R)-Tembamide drug intermediate i.e., (R)-2-amino-1-(4-methoxyphenyl)-2ethanol, which is an industrially significant active pharmaceutical ingredient (API)⁷. For the first time, we synthesized the (R)-2-amino-1-(4-methoxyphenyl)-2-ethanol using nitroaldol reaction (Scheme 4.1).

Scheme 4.1: Chemo-enzymatic synthesis of (R)-Tembamide drug intermediate i.e., (R)-2-amino-1-(4-methoxyphenyl)-2-ethanol using engineered AtHNL.

To achieve this objective, we used five successful AtHNL variants, i.e., F179W, F179N, Y14F, Y14M and Y14M-F179W, selected based on their catalytic performance in the enantioselective synthesis of diverse (R)- β -nitroalcohols from the previous chapter. For the first part of the reaction of **Scheme 4.1**, i.e., towards the synthesis of (R)-1-(4-methoxyphenyl)-2-nitroethanol, we used 125 U of each of the purified enzymes of F179W, F179N, Y14F, Y14M and Y14M-F179W along with the wild type, to catalyze the coupling of 4-methoxybenzaldehyde with nitromethane. The double variant, Y14M-F179W showed the highest % conversion (70) than others with > 99% ee in the synthesis of (R)-1-(4-methoxyphenyl)-2-nitroethanol. Subsequently, Y14M-F179W was used in the preparative scale synthesis of (R)- 1-(4-methoxyphenyl)-2-nitroethanol, which was further reduced to (R)-2-amino-1-(4-methoxyphenyl)-2-ethanol by HCOOH/Zn in methanol at room temperature. Using a new, simple and efficient chemo-enzymatic route involving engineered

AtHNL catalyzed nitroaldol reaction we have successfully synthesized the (R)-Tembamide drug intermediate, i.e., (R)-2-amino-1-(4-methoxyphenyl)-2-ethanol, an industrially significant API with high enantioselectivity and conversion.

4.2. Objectives

- 6. To develop analytical methods for chiral resolution of racemic 1-(4-methoxyphenyl)-2-nitroethanol using HPLC chiral column.
- 7. To screen the selected variants of Y14 and F179 series in the enantioselective synthesis of (*R*)-1-(4-methoxyphenyl)-2-nitroethanol.
- 8. To synthesize the (*R*)-Tembamide drug intermediate from (*R*)-1-(4-methoxyphenyl)-2-nitroethanol.

4.3. Materials and methods

4.3.1. Chemicals and materials

AtHNL (UniProt accession ID: Q9LFT6) synthetic gene cloned in pET28a was obtained from Abgenex Pvt. Ltd, India. Culture media and kanamycin were procured from HiMedia laboratory Pvt. Ltd, India. Isopropyl-β-D-1-thiogalactopyranoside (IPTG) was purchased from BR-BIOCHEM Pvt. Ltd, India. Chemicals such as aldehydes, nitromethane and mandelonitrile were purchased from Sigma Aldrich, AVRA, SRL and Alfa-Aesar. HPLC grade solvents were obtained from RANKEM, Molychem, FINAR, and SRL.

4.3.2. Mutagenesis

4.3.2.1. Creation of SSM library at F179, and Y14

Site saturation and site directed mutagenesis was done as per the procedure described in **section**2.3.3.1 in **chapter** 2⁸. The primers employed in this work are mentioned **Table** 2.1.

4.3.2.2. Creation of AtHNL double variants

To prepare Y14M-F179W, PCR composition and conditions were maintained similar to that described in **2.3.3.1** in **chapter 2**, Y14M plasmid was taken as template and forward and reverse primers for F179W (**Table 3.1**) were used in the PCR.

4.3.3. Enzyme expression and purification

Expression and purification of *At*HNL and its variants was performed as described in section **2.3.4** of **Chapter 2**.

4.3.4. HNL assay

The HNL assay of *At*HNL and its variants was performed as described in section **3.3.4** of **Chapter 3**.

4.3.5. Synthesis of racemic 1-(4-methoxyphenyl)-2-nitroethanol

Racemic synthesis of 1-(4-methoxyphenyl)-2-nitroethanol was carried out by addition of 4-methoxybenzaldehyde to nitromethane in 1:10 molar ratio in the presence of 5 mol% of Ba(OH)₂ as a catalyst as per the procedure described in the paper previously published from our lab⁹. Chiral resolution of racemic 1-(4-methoxyphenyl)-2-nitroethanol was performed using Chiralpak® IB at 1 mL/min flow rate (**Table 4.1; Figure 4.5**). The analysis was performed at wavelength of 210 nm using n-hexane and 2-propanol as the mobile phase.

4.3.6. AtHNL variant catalyzed synthesis of various (R)-1-(4-methoxyphenyl)-2-nitroethanol using nitroaldol reaction

A reaction mixture of 125 units of purified variant enzymes with *n*-butyl acetate in equal v/v ratio along with 1.75 M of nitromethane and 20 mM of 4-methoxybenzaladehdye were taken in a 2 mL glass vial. The reaction conditions, protocols of aliquot taking, extraction and analysis are the same as mentioned in **section 3.3.6**.

4.3.7. Preparative scale synthesis of (R)-1-(4-methoxyphenyl)-2-nitroethanol

AtHNL-Y14M-F179W catalyzed preparative scale synthesis of (*R*)-1-(4-methoxyphenyl)-2-nitroethanol was carried out using crude cell lysates. Ten mini preparative scale reactions each containing 1000 U of Y14M-F179W cell lysate along with equal v/v of *n*-butyl acetate, 8.75 M of nitromethane and 100 mM of 4-methoxybenzaladehdye were taken in a 50 mL round bottom flask, stirred in a magnetic stirrer at 1200 rpm, 30 °C. At the end of 2 h, each reaction mixture was extracted with 100 mL of diethyl ether, the organic layers collected were combined, dried over anhydrous Na₂SO₄ and solvents were evaporated in a rotary evaporator. The product was analyzed by chiral HPLC as per **section 3.3.6**. Column purification of the crude product was done using hexane: ethyl acetate (90:10) to get pure (*R*)-1-(4-methoxyphenyl)-2-nitroethanol. The purified product was confirmed by ¹H and ¹³C NMR.

4.3.8. Preparative scale synthesis of (R)-Tembamide drug intermediate, i.e., (R)-2-amino-1-(4-methoxyphenyl)-2-ethanol

A suspension of (*R*)-1-(4-methoxyphenyl)-2-nitroethanol (1 mmol) and activated zinc dust (2 mmol) in methanol (5 mL) was stirred with 90% formic acid at room temperature for overnight. The catalyst was removed by filtration and the filtrate was extracted with diethyl ether¹⁰. Further,

it was washed with saturated sodium chloride and the organic layer was separated. This extraction was done thrice and the combined organic layer subjected to acid-base extraction with 5% HCl and 2M NaOH to remove side compounds other than amines. Finally, the obtained organic layer was dried over anhydrous Na₂SO₄ and concentrated to give the crude (*R*)-2-amino-1-(4-methoxyphenyl) ethanol which was further confirmed by ¹H and ¹³C NMR.

4.4. Results

4.4.1. NMR characterization of racemic 1-(4-methoxyphenyl)-2-nitroethanol

1-(4-methoxyphenyl)-2-nitroethanol⁹

¹H NMR (500 MHz, CDCl₃) δ 7.29 (dt, J = 8.6, 1.8 Hz, 2H), 6.89 (dt, J = 8.7, 1.6 Hz, 2H), 5.45 – 5.27 (m, 1H), 4.57 (ddt, J = 13.1, 9.7, 1.7 Hz, 1H), 4.45 (ddt, J = 13.2, 3.4, 1.7 Hz, 1H), 3.79 (t, J = 1.4 Hz, 3H); ¹³C NMR (101 MHz, CDCl₃) δ 160.04, 130.47, 127.38, 114.42, 81.40, 70.73, 55.42.

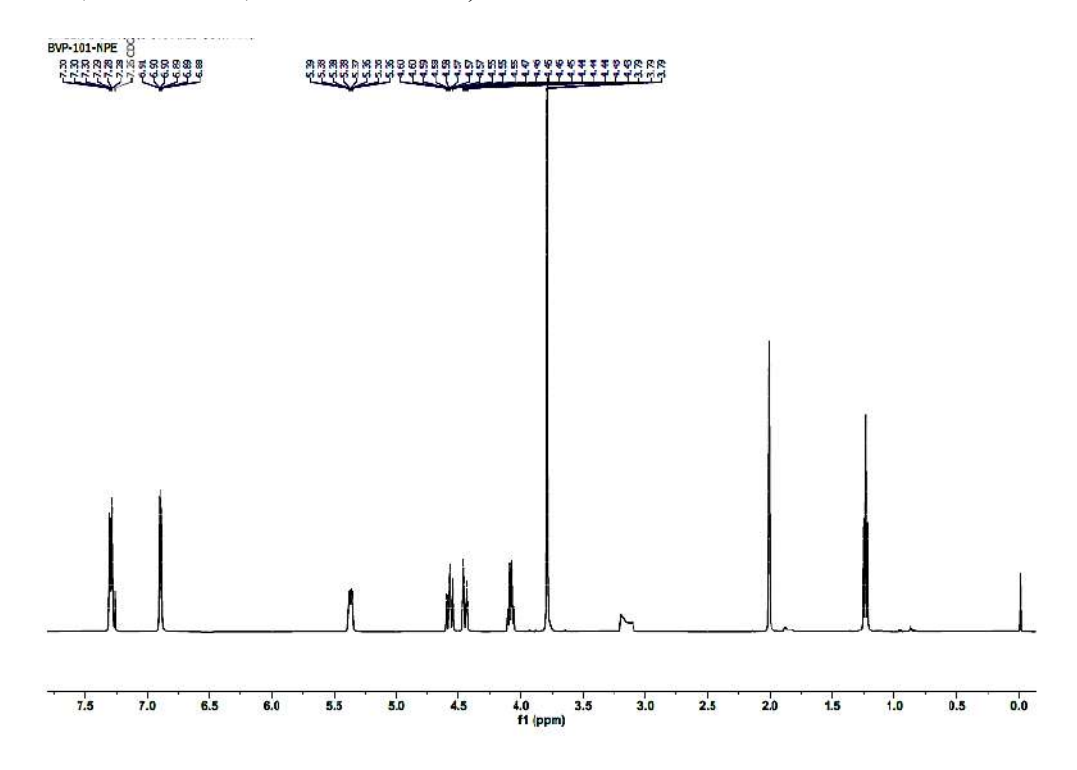


Figure 4.1: ¹H NMR spectrum of 1-(4-methoxyphenyl)-2-nitroethanol.

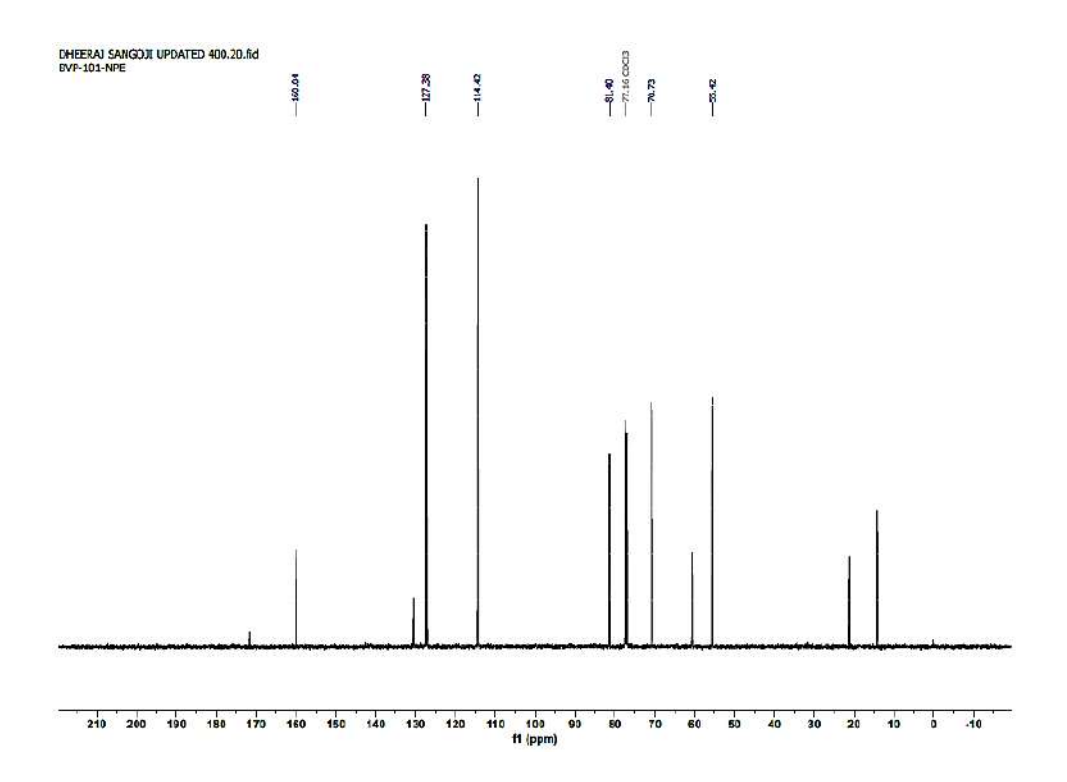


Figure 4.2: ¹³C NMR spectrum of 1-(4-methoxyphenyl)-2-nitroethanol.

4.4.2. Chiral resolution of racemic 1-(4-methoxyphenyl)-2-nitroethanol by HPLC

The racemic 1-(4-methoxyphenyl)-2-nitroethanol was resolved using Chiralpak® IB chiral column using 1 mL/min flow rate at a wavelength of 210 nm (**Table 4.1**; **Figure 4.5**). For sample preparation, 4 µmol of the respective the racemic 1-(4-methoxyphenyl)-2-nitroethanol was dissolved in the mobile phase (*n*-hexane and 2-propanol) and was used for chiral analysis. The compound 1-(4-methoxyphenyl)-2-nitroethanol was initially run on 99:1 mobile phase ratio for 8 minutes to separate aldehyde and nitromethane peaks followed by 90:10 ratio to resolve both the enantiomers.

Table 4.1: HPLC conditions and retention time of 4-methoxybenzaldehyde and racemic 1-(4-methoxyphenyl)-2-nitroethanol.

	HPLC condition		RT of
ОН	<i>n</i> -hexane:	RT of aldehyde (min)	(R) and (S) BNAs
NO_2	2-propanol (v/v)		(min)
R °			
4-methoxy Ph	99:1 for 8 minutes followed by 90:10	12.1	19.7, 21.1

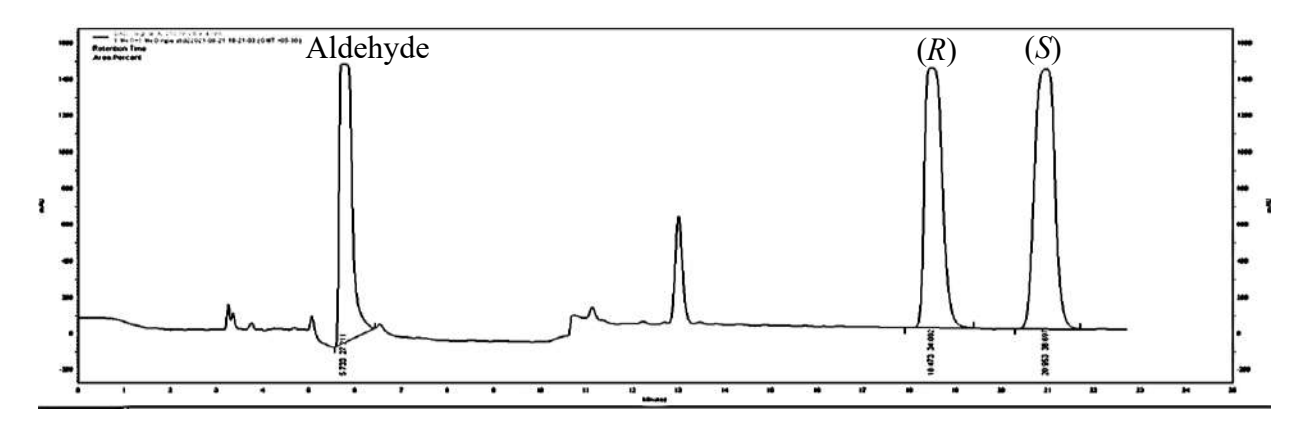


Figure 4.3: HPLC spectrum of the standards: 4-methoxybenzaldehdye, (*R*)- and (*S*)- enantiomers of 1-(4-methoxyphenyl)-2-nitroethanol.

4.4.3. AtHNL variant (125 U) catalyzed synthesis of (R)-1-(4-methoxyphenyl)-2-nitroethanol using nitroaldol reaction

The purified variants Y14F, Y14M, F179W, F179N and Y14M- F179W (125 U) along with the wild type *At*HNL were employed in the synthesis of (*R*)-1-(4-methoxyphenyl)-2-nitroethanol where 20 mM of 4-methoxybenzaldehyde and 1.75 M of nitromethane were used as the substrates.

The % conversion and % *ee* obtained in each case is given in **Figure 4.6**, while, the HPLC chromatograms are represented in **Figure 4.7-4.13**.

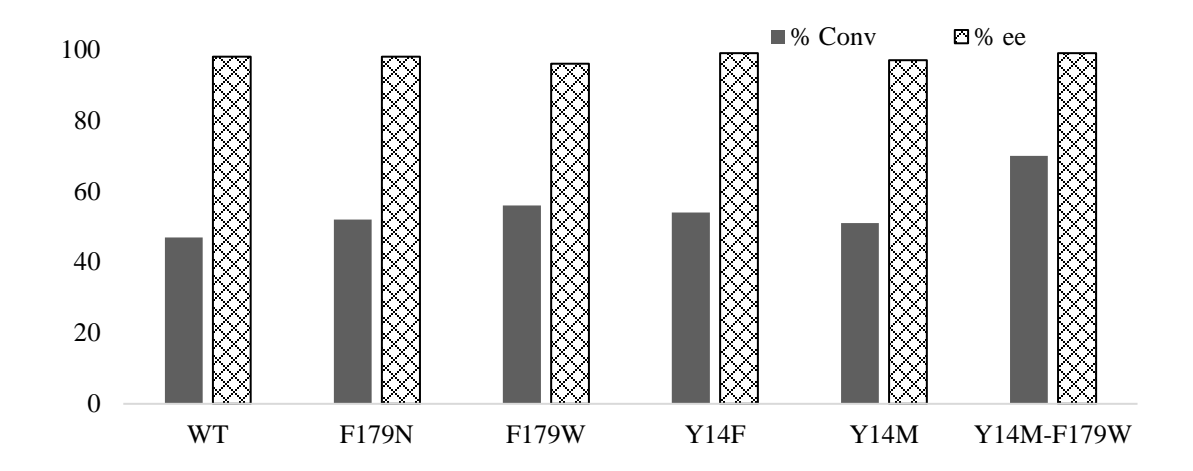


Figure 4.4: *At*HNL variants catalysed enantioselective synthesis of (*R*)-1-(4-methoxyphenyl)-2-nitroethanol.

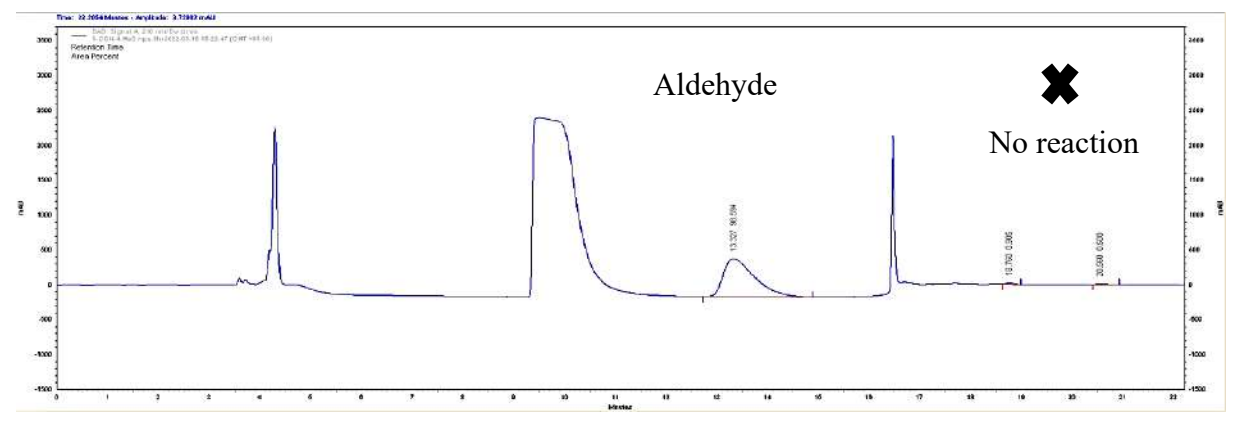


Figure 4.5: HPLC spectrum of control reaction at 3 h where enzyme is replaced by 20 mM KPB and 4-methoxybenzaldehyde was used as the substrate.

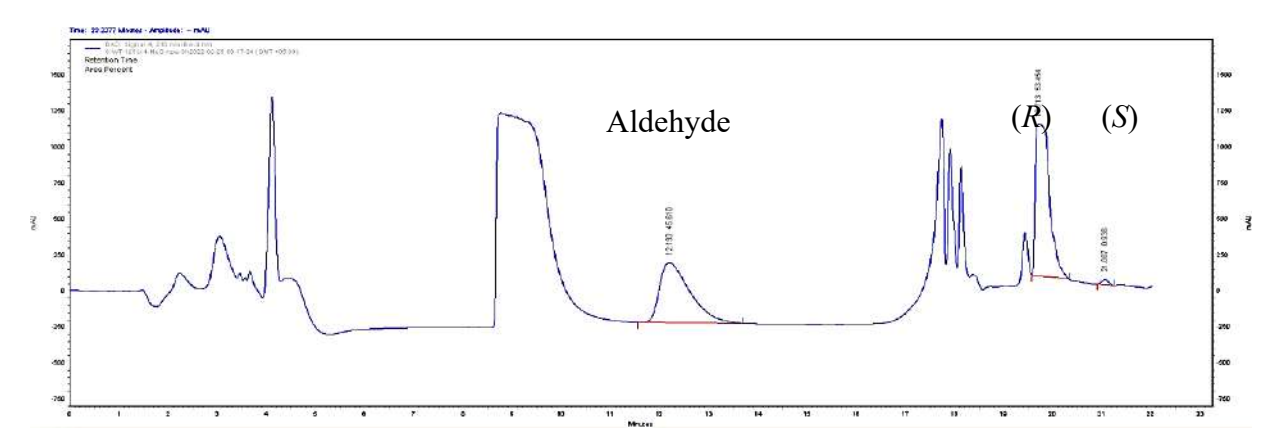


Figure 4.6: HPLC spectrum of wild type AtHNL (125 U) catalyzed nitroaldol reaction showing enantioselective synthesis of (R)-1-(4-methoxyphenyl)-2-nitroethanol at 3 h.

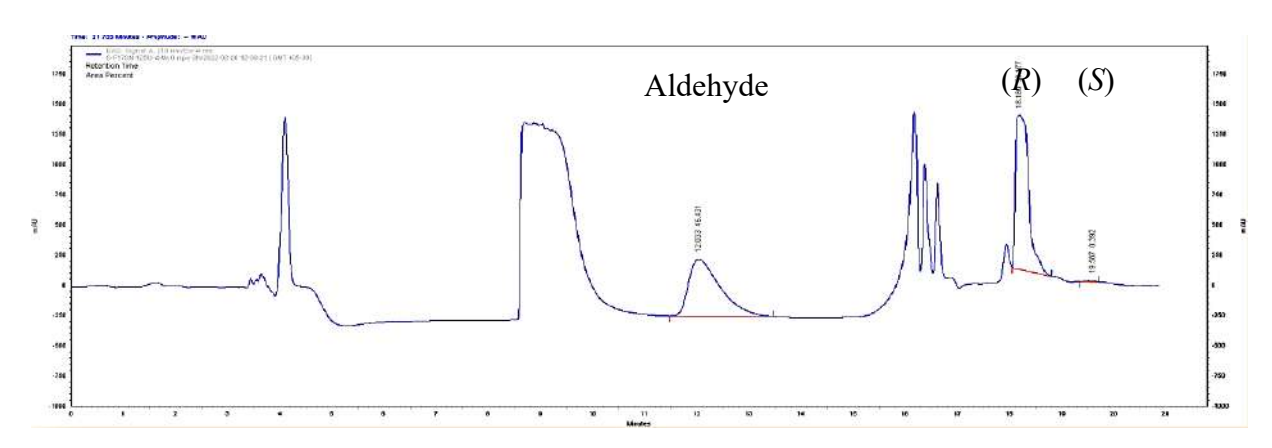


Figure 4.7: HPLC spectrum of F179N (125 U) catalyzed nitroaldol reaction showing enantioselective synthesis of (R)-1-(4-methoxyphenyl)-2-nitroethanol at 3 h.

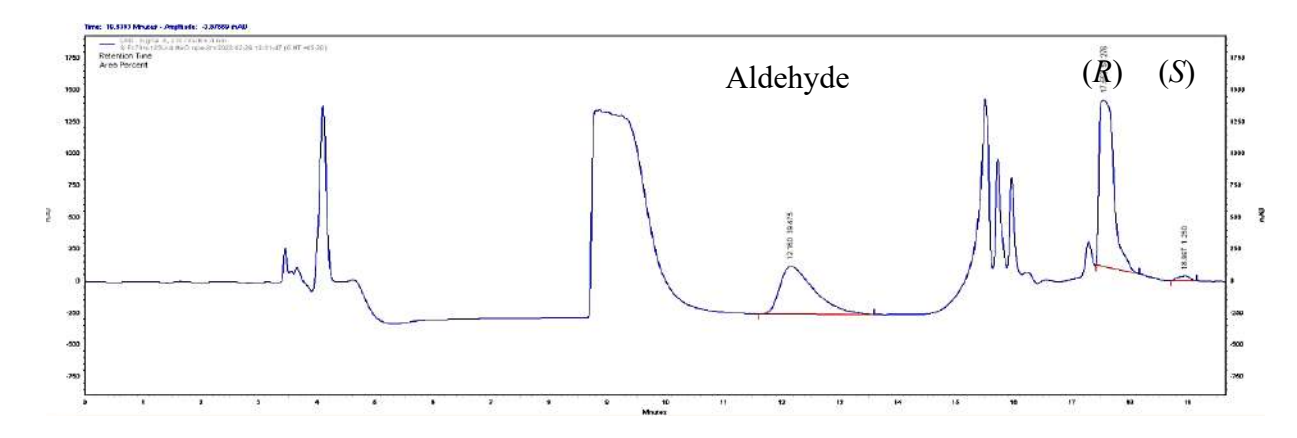


Figure 4.8: HPLC spectrum of F179W (125 U) catalyzed nitroaldol reaction showing enantioselective synthesis of (R)-1-(4-methoxyphenyl)-2-nitroethanol at 3 h.

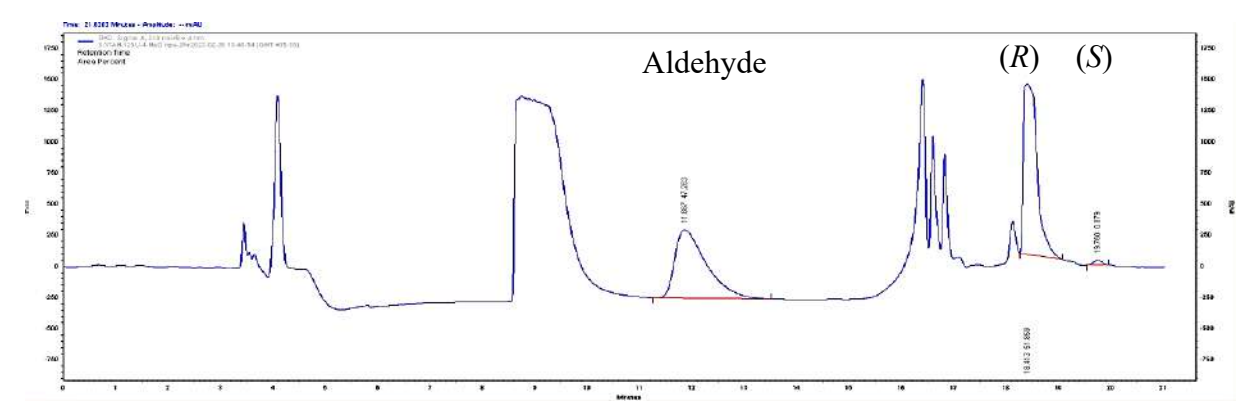


Figure 4.9: HPLC spectrum of Y14M (125 U) catalyzed nitroaldol reaction showing enantioselective synthesis of (R)-1-(4-methoxyphenyl)-2-nitroethanol at 3 h.

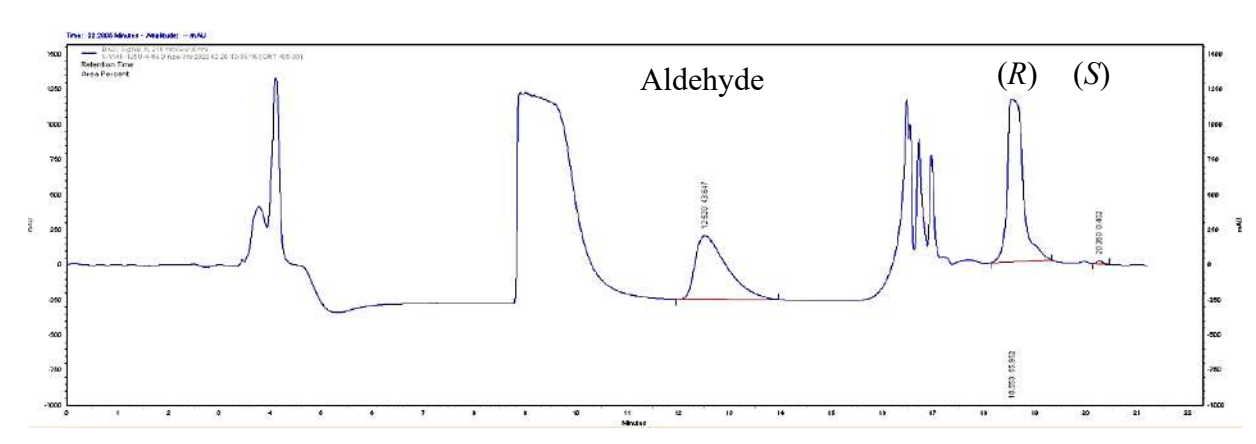


Figure 4.10: HPLC spectrum of Y14F (125 U) catalyzed nitroaldol reaction showing enantioselective synthesis of (R)-1-(4-methoxyphenyl)-2-nitroethanol at 3 h.

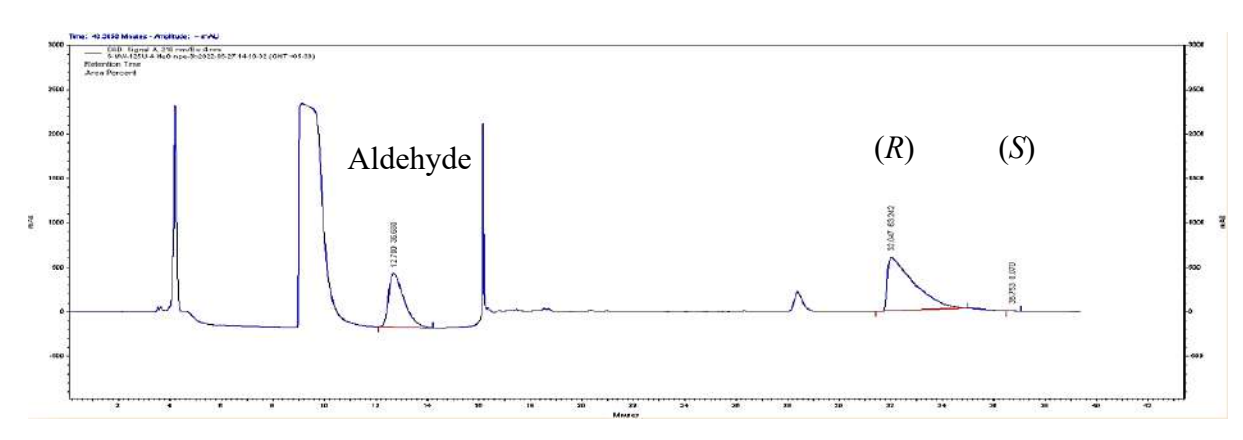


Figure 4.11: HPLC spectrum of Y14M-F179W (125 U) catalyzed nitroaldol reaction showing enantioselective synthesis of (*R*)-1-(4-methoxyphenyl)-2-nitroethanol at 3 h.

4.4.4. Preparative scale synthesis of (R)-1-(4-methoxyphenyl)-2-nitroethanol using Y14M-F179W crude cell lysate

AtHNL-Y14M-F179W crude cell lysate (200 U) was employed to catalyze preparative scale synthesis of (R)-1-(4-methoxyphenyl)-2-nitroethanol (**Figure 4.14**), which subsequently scaled up using 1000 U of the enzyme. Ten mini preparative scale reactions each containing 1000 U of Y14M-F179W cell lysate were carried out and the product was analyzed by chiral HPLC is represented in **Figure 4.15**. Column purification of the crude product was done using hexane: ethyl acetate (90:10) to get pure (R)-1-(4-methoxyphenyl)-2-nitroethanol, which was further confirmed by 1 H and 13 C NMR (**Figure 4.16 – 4.18**).

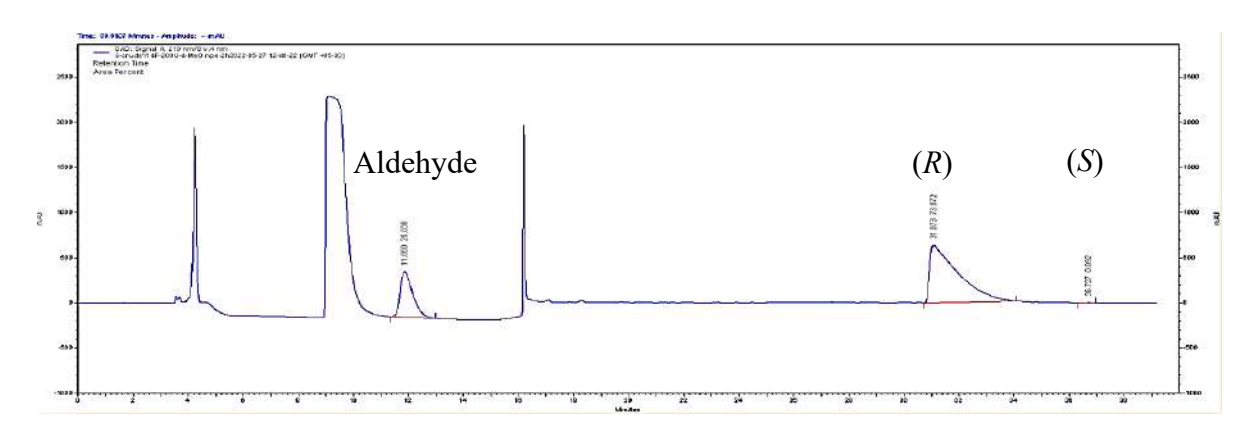


Figure 4.12: HPLC spectrum of Y14M-F179W cell lysate (200 U) catalyzed nitroaldol reaction showing enantioselective synthesis of (R)-1-(4-methoxyphenyl)-2-nitroethanol at 2 h.

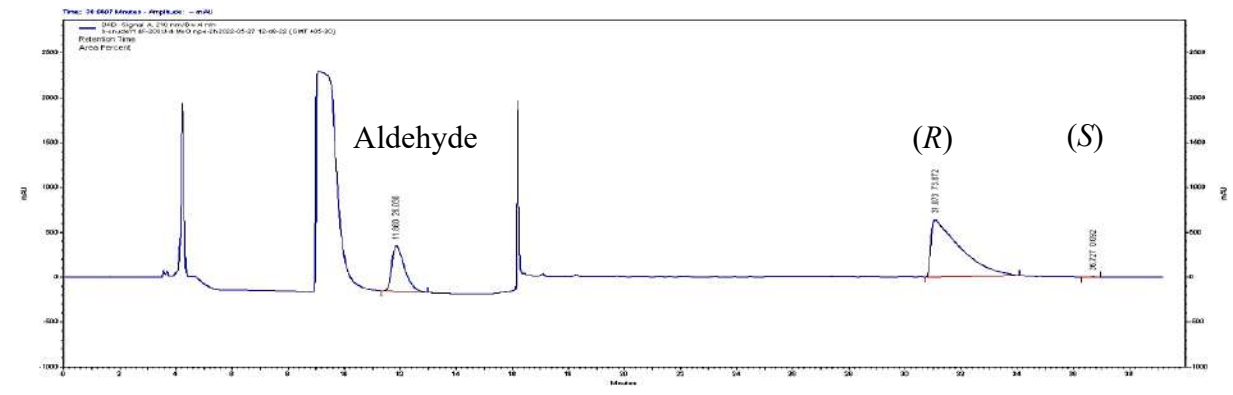


Figure 4.13: HPLC spectrum of Y14M-F179W cell lysate (1000 U) catalyzed nitroaldol reaction showing enantioselective synthesis of (R)-1-(4-methoxyphenyl)-2-nitroethanol at 2 h.

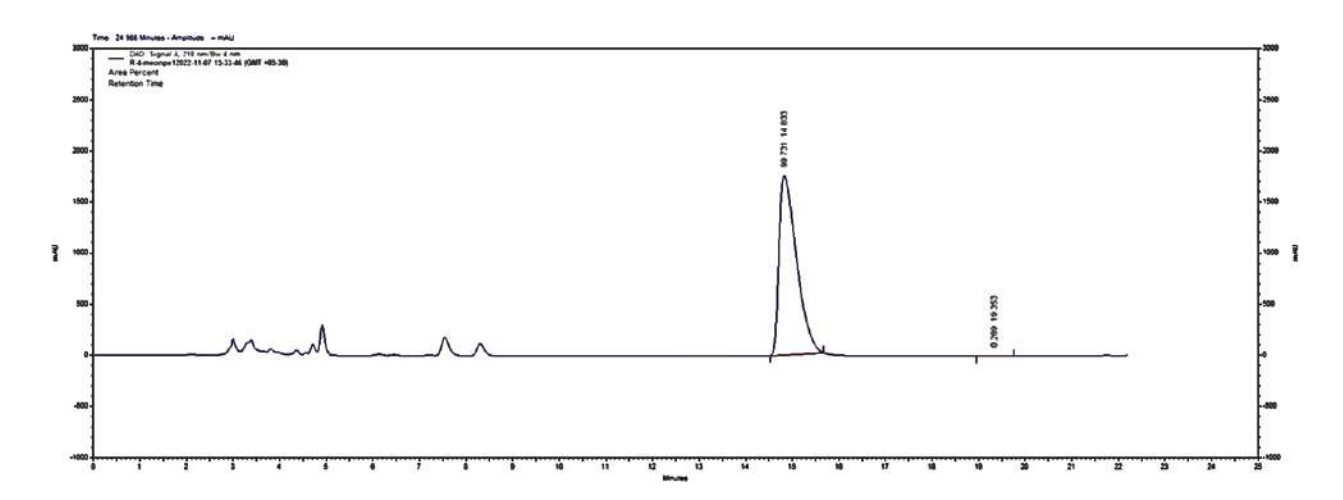


Figure 4.14: HPLC spectrum of Y14M-F179W cell lysate catalyzed preparative scale enantioselective synthesis of (R)-1-(4-methoxy nitro phenyl) ethanol at 2 h after column purification, >99 % ee.

NMR characterization of Y14M-F179W catalyzed synthesis of (R)-1-(4-methoxyphenyl)-2-nitroethanol

¹H NMR (500 MHz, CDCl₃) δ 7.34 (dt, J = 8.6, 1.8 Hz, 2H), 6.91 (dt, J = 8.7, 1.6 Hz, 2H), 5.42 – 5.38 (m, 1H), 4.62 (ddt, J = 13.1, 9.7, 1.7 Hz, 1H), 4.49 (ddt, J = 13.2, 3.4, 1.7 Hz, 1H), 3.81 (t, J = 1.4 Hz, 3H); ¹³C NMR (101 MHz, CDCl₃) δ 160.55, 130.81, 127.43, 114.84, 81.56, 70.97, 55.56.

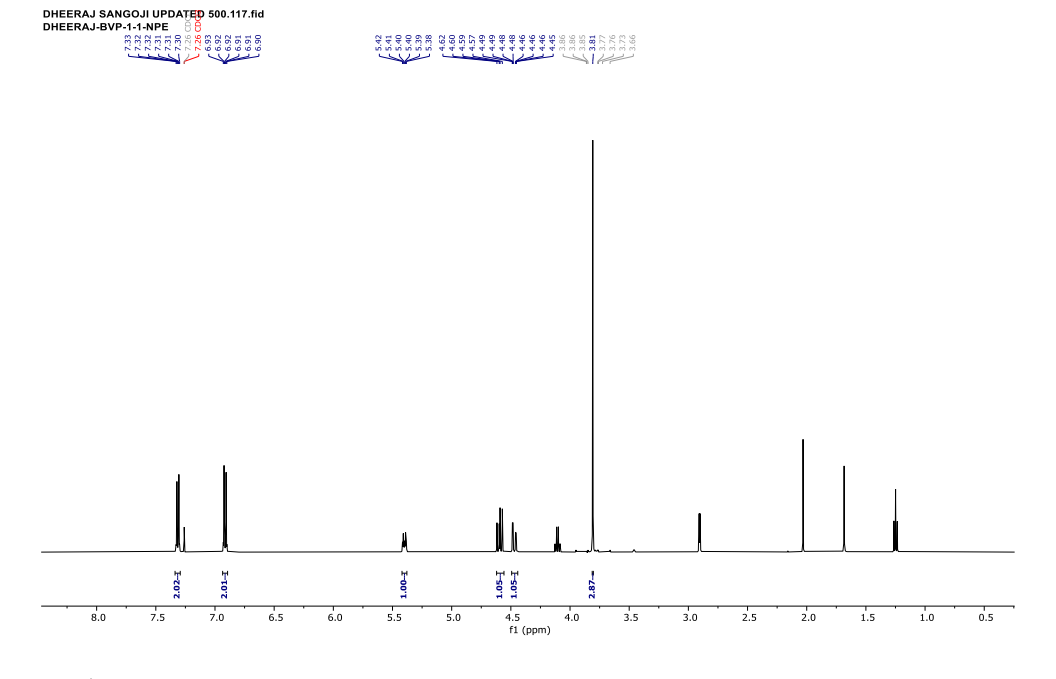


Figure 4.15: ¹H NMR spectrum of (*R*)-1-(4-methoxyphenyl)-2-nitroethanol.

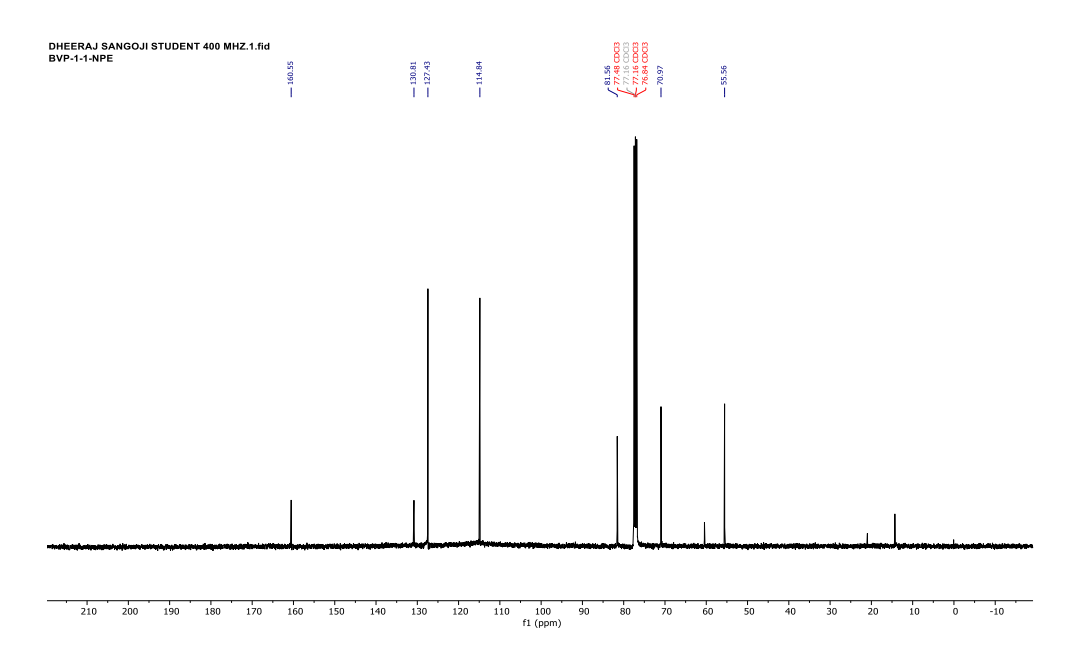


Figure 4.16: 13 C NMR spectrum of (R)-1-(4-methoxyphenyl)-2-nitroethanol.

4.4.5. Preparative scale synthesis of (R)-Tembamide drug intermediate, i.e., (R)-2-amino-1-(4-methoxyphenyl)-2-ethanol

The reduction of the nitro functionality of (R)-1-(4-methoxyphenyl)-2-nitroethanol by activated zinc dust in methanol along with 90% formic acid has produced its corresponding amino product, i.e., (R)-2-amino-1-(4-methoxyphenyl) ethanol which was confirmed with previous NMR reports⁷. **Figure 4.19** – **4.20** represents the crude 1 H and 13 C NMR of the reduced product.

NMR characterization of (R)-2-amino-1-(4-methoxyphenyl) ethanol synthesized by our chemo-enzymatic method

 1 H NMR (500 MHz, DMSO) δ 7.25 (d, 2H), 6.90 (d, 2H), 5.75 (s, 1H), 4.42 (s, 1H), 3.73 (s, 3H),3.37-3.44 (m,2H),1.21-125 (s,2H); 13 C NMR (101 MHz, DMSO) δ 49.24, 55.01, 72.50, 113.40, 127.03, 130.02, 158.15.

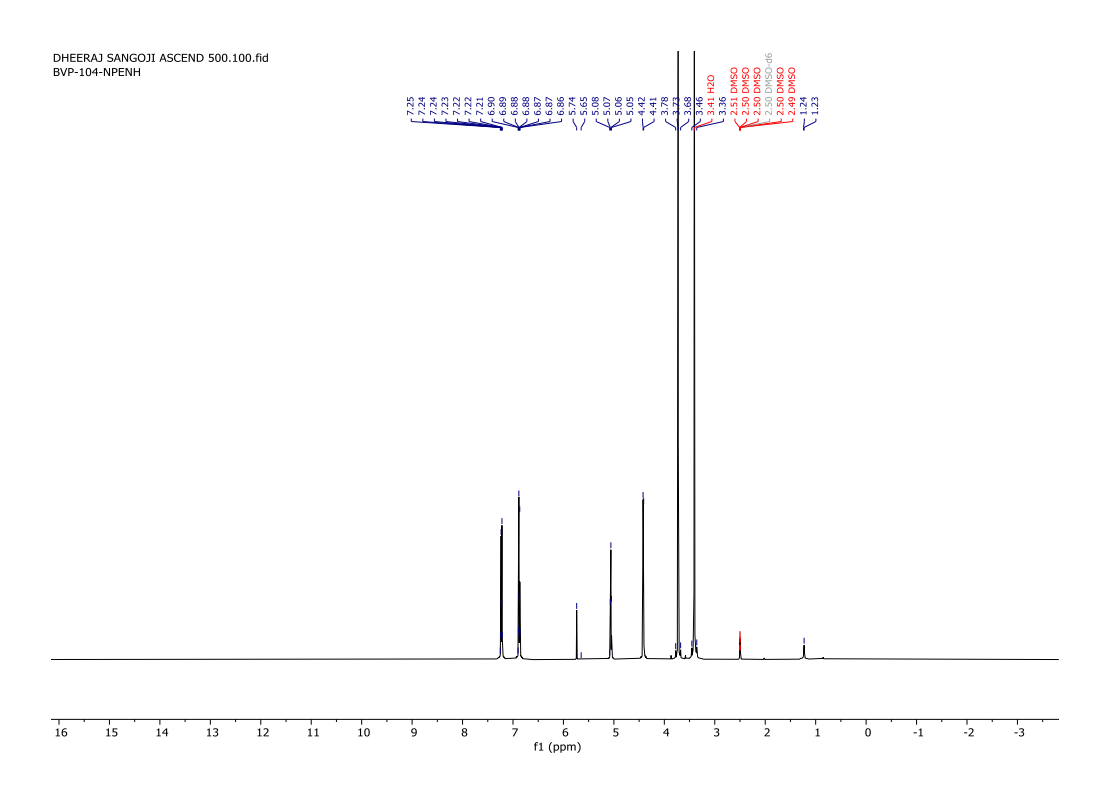


Figure 4.17: Crude ¹H NMR spectrum of (*R*)-2-amino-1-(4-methoxyphenyl) ethanol.

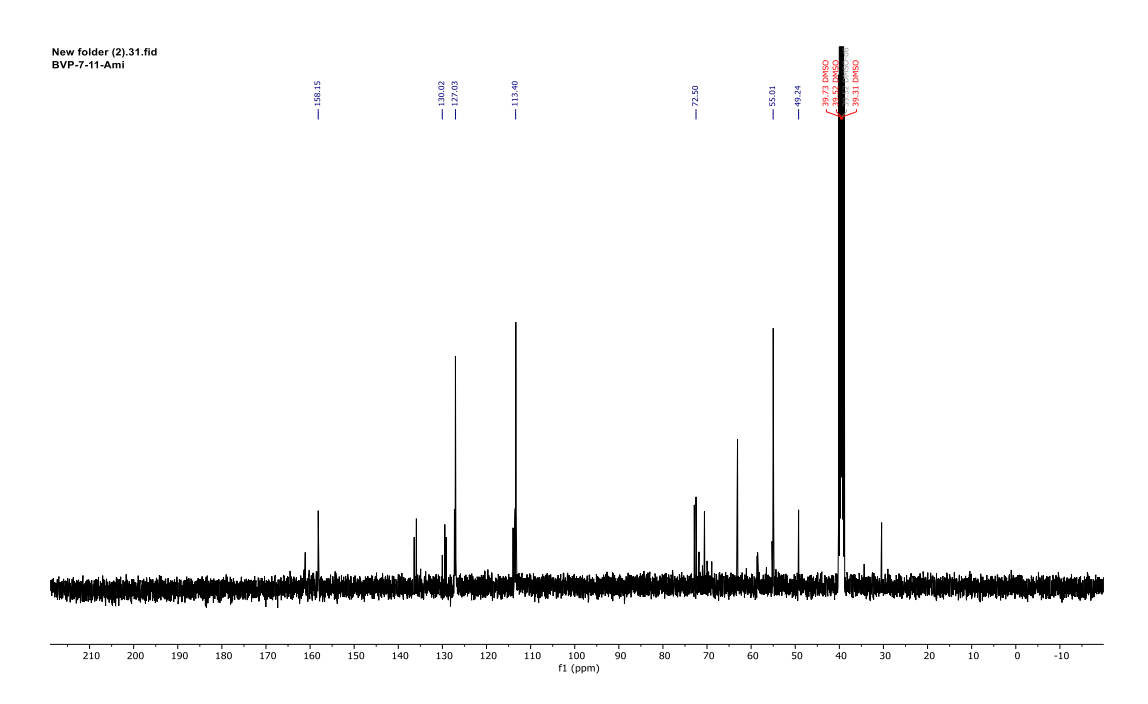


Figure 4.18: Crude ¹³C NMR spectrum of (*R*)-2-amino-1-(4-methoxyphenyl) ethanol.

4.5. Discussion

4.5.1. AtHNL variants (125 U) catalyzed synthesis of (R)-1-(4-methoxyphenyl)-2-nitroethanol using nitroaldol reaction

Purified AtHNL variants, F179W, F179N, Y14F, Y14M and Y14M-F179W, selected based on our previous study were employed in the enantioselective synthesis of (R)-1-(4-methoxyphenyl)-2-nitroethanol aiming to achieve high conversion and enantioselectivity. Earlier, Asano et al. synthesized (R)-1-(4-methoxyphenyl)-2-nitroethanol using wild type AtHNL, however, the conversion was only 2% with 79% ee at 2 h¹¹. Yu et al. explored ST0779 in the synthesis of (R)-1-(4-methoxyphenyl)-2-nitroethanol from 4-methoxybenzaldehyde using promiscuous Henry reaction which took long reaction time (72 h) for its catalysis to obtain 32% conversion with 86% ee using 20 mg of enzyme¹². Asymmetric reduction of corresponding α -nitroketone by RasADH has demonstrated in the synthesis of (R)-1-(4-methoxyphenyl)-2-nitroethanol in 99% conversion and 99% ee^{13} . The starting material α -nitroketone however requires additional steps to synthesize. Wild type AtHNL catalyzed retro-Henry reaction using racemic 1-(4-methoxyphenyl)-2-nitroethanol as substrate was reported to show only 44% ee and 41% conversion of the corresponding (S)- product at 6 h indicating very poor selectivity⁹.

In our study to synthesize (R)-1-(4-methoxyphenyl)-2-nitroethanol using promiscuous Henry reaction, wild type AtHNL showed 47% conversion and 98% ee, while other single variants (F179N, F179W, Y14M and Y14F) showed 51-56% conversions with 96-99% ee in 3 h. The double variant, Y14M-F179W showed the highest, 70% conversion among others with > 99% ee in the synthesis of (R)-1-(4-methoxyphenyl)-2-nitroethanol (**Figure 4.6-4.13**). Finally, the double variant Y14M-F179W was chosen for further experimental studies.

4.5.2. Preparative scale synthesis of (R)-1-(4-methoxyphenyl)-2-nitroethanol using Y14M-F179W crude cell lysate followed by synthesis of (R)- Tembamide drug intermediate, i.e., (R)-2-amino-1-(4-methoxyphenyl)-2-ethanol

Use of crude cell lysates in biocatalysis is often preferred, especially for preparative as well as industrial scale synthesis. This is because use of crude cell lysates in biocatalysis is economical than the purified enzymes. *At*HNL-Y14M-F179W crude cell lysate (200 U) catalyzed preparative scale synthesis of (*R*)-1-(4-methoxyphenyl)-2-nitroethanol has resulted in 70 % conversion and 99% *ee* (**Figure 4.14**). Further, the biotransformation was carried out with 1000 U of crude cell lysate, before using higher scale of enzyme. Subsequently, ten mini preparative scale reactions each containing 1000 U of Y14M-F179W cell lysate were carried out. The final product after column purification was found to have 99% *ee*, and 65.4% isolated yield (**Figure 4.15**). The product was confirmed by ¹H and ¹³C NMR (**Figure 4.16 – 4.18**).

From the literature analysis, it is very evident that there exists many approaches to synthesize various β -amino alcohols, which are the main precursors of β -hydroxyamides^{7,14,15}. These β -amino alcohols have been prepared through microbial reduction of α -azido and α -bromoketones or α -tosyloxyketones or lipase-mediated resolution of α -azidoalcohols^{15–21}. Few are reported with a multi-step syntheses using optically active cyanohydrins as starting materials⁵. For the first time, we explored the promiscuous nitroaldol reaction in the chemoenzymatic synthesis of a β -amino alcohol, where 4-methoxybenzladehyde was used as the starting material. A direct coupling of 4-methoxybenzladehyde with nitromethane in the presence of engineered *At*HNL produced the corresponding, β -nitroalcohol in an atom economy approach. A simple reduction of the nitro group of the β -nitroalcohol was exploited to give β -amino alcohol as the final product. The current study has identified the double variant *At*HNL- Y14M-F179W, which produced (*R*)-1-(4-

methoxyphenyl)-2-nitroethanol in 99% *ee*, and 65.4% isolated yield and its reduced product (*R*)-2-amino-1-(4-methoxyphenyl) ethanol, an intermediate of (*R*)-Tembamide in 99% *ee*, and 58% isolated yield.

4.6. Conclusions

A new, simple and efficient chemo-enzymatic route involving nitroaldol reaction was applied in the synthesis of (R)-Tembamide intermediate, i.e., (R)-2-amino-1-(4-methoxyphenyl)-2-ethanol, which is an industrially significant active pharmaceutical ingredient. This involved a two-step process, first an enzymatic synthesis of (R)-1-(4-methoxyphenyl)-2-nitroethanol by AtHNL double variant Y14M-F179W, followed by a chemical reduction of the product. Among the different enzymes studied that includes the wild type, single variants, and the double variant, the latter has shown the highest conversion (70%) with >99% ee. This biocatalytic reaction involved enantioselecive C-C bond formation between 4-methoxybenzaldehdye and nitromethane catalyzed by an engineered enzyme. This approach besides using an atom efficient process, also uses substrates that are readily available, and hence avoids additional chemical synthesis steps as required by other approaches. The biocatalytic reaction product, i.e., (R)-1-(4-methoxyphenyl)-2nitroethanol was simply reduced to (R)-2-amino-1-(4-methoxyphenyl)-2-ethanol using HCOOH/Zn in methanol at room temperature. In our study, we have successfully combined an engineered AtHNL along with chemical catalyst to efficiently synthesize the (R)-Tembamide drug intermediate, i.e., (R)-2-amino-1-(4-methoxyphenyl)-2-ethanol in a preparative scale with > 99%ee and 58% isolated yield of the product. This chiral intermediate is the precursor, which can be used to synthesize (R)-Tembamide in a large scale with subsequent organic synthesis approaches.

4.7. References

(1) Gupta, P.; Mahajan, N. Biocatalytic Approaches towards the Stereoselective Synthesis of

- Vicinal Amino Alcohols. *New J. Chem.* **2018**, *42* (15), 12296–12327. https://doi.org/10.1039/c8nj00485d.
- (2) Ager, D. J.; Prakash, I.; Schaad, D. R. 1,2-Amino Alcohols and Their Heterocyclic Derivatives as Chiral Auxiliaries in Asymmetric Synthesis. *Chem. Rev.* **1996**, *96* (2), 835–875. https://doi.org/10.1021/cr9500038.
- (3) Milner, S. E.; Moody, T. S.; Maguire, A. R. Biocatalytic Approaches to the Henry (Nitroaldol) Reaction. *European J. Org. Chem.* 2012, 3059–3067. https://doi.org/10.1002/ejoc.201101840.
- (4) S. M. Albónico, A. M. K. and V. D. Tembamide from Fagara Hyema/Is (St. Hill.) Engler. *J. Chem. Soc. C Org.* **1967**, 1327–1328.
- (5) Brown, R. F. C.; Donohue, A. C.; Jackson, W. R.; McCarthy, T. D. Synthetic Applications of Optically Active Cyanohydrins. Enantioselective Syntheses of the Hydroxyamides Tembamide and Aegeline, the Cardiac Drug Denopamine, and Some Analogues of the Bronchodilator Salbutamol. *Tetrahedron* 1994, 50 (48), 13739–13752. https://doi.org/10.1016/S0040-4020(01)85686-6.
- (6) Brown, R. F. C.; Jackson, W. R.; McCarthy, T. D. The Synthesis of Homochiral Naturally Occurring Hydroxy Amides. *Tetrahedron: Asymmetry* **1993**, *4* (2), 205–206. https://doi.org/10.1016/S0957-4166(00)82338-1.
- (7) Tae Cho, B.; Kyu Kang, S.; Hye Shin, S. Application of Optically Active 1,2-Diol Monotosylates for Synthesis of β-Azido and β-Amino Alcohols with Very High Enantiomeric Purity. Synthesis of Enantiopure (R)-Octopamine, (R)-Tembamide and (R)-Aegeline. *Tetrahedron Asymmetry* 2002, 13 (11), 1209–1217.

- https://doi.org/10.1016/S0957-4166(02)00322-1.
- (8) Vishnu Priya, B.; Sreenivasa Rao, D. H.; Gilani, R.; Lata, S.; Rai, N.; Akif, M.; Kumar Padhi, S. Enzyme Engineering Improves Catalytic Efficiency and Enantioselectivity of Hydroxynitrile Lyase for Promiscuous Retro-Nitroaldolase Activity. *Bioorg. Chem.* 2022, 120 (January), 105594. https://doi.org/10.1016/j.bioorg.2021.105594.
- (9) Rao, D. H. S.; Padhi, S. K. Production of (S)-β-Nitro Alcohols by Enantioselective C–C Bond Cleavage with an R-Selective Hydroxynitrile Lyase. *ChemBioChem* 2019, 20 (3), 371–378. https://doi.org/10.1002/cbic.201800416.
- (10) Channe Gowda, D.; Mahesh, B.; Gowda, S. Zinc-Catalyzed Ammonium Formate Reductions: Rapid and Selective Reduction of Aliphatic and Aromatic Nitro Compounds. *Indian J. Chem. - Sect. B Org. Med. Chem.* 2001, 40 (1), 75–77.
- (11) Fuhshuku, K. I.; Asano, Y. Synthesis of (R)-Beta-Nitro Alcohols Catalyzed by R-Selective Hydroxynitrile Lyase from Arabidopsis Thaliana in the Aqueous-Organic Biphasic System. *J. Biotechnol.* **2011**, *153* (3–4), 153–159.
- (12) Yu, X.; Pérez, B.; Zhang, Z.; Gao, R.; Guo, Z. Mining Catalytic Promiscuity from: Thermophilic Archaea: An Acyl-Peptide Releasing Enzyme from Sulfolobus Tokodaii (ST0779) for Nitroaldol Reactions. *Green Chem.* 2016, 18 (9), 2753–2761.
- (13) Wang, Z.; Wu, X.; Li, Z.; Huang, Z.; Chen, F. Ketoreductase Catalyzed Stereoselective Bioreduction of α-Nitro Ketones. *Org. Biomol. Chem.* **2019**, *17* (14), 3575–3580.
- (14) Sadyandy, R.; Fernandes, R. A.; Kumar, P. An Asymmetric Dihydroxylation Route to (R) (-) -Octopamine, (R) (-) -Tembamide and (R) (-) -Aegeline. 2005, 2005 (iii), 36-43.

- (15) Kamal, A.; Shaik, A. A.; Sandbhor, M.; Malik, M. S. Chemoenzymatic Synthesis of (R) and (S) -Tembamide, Aegeline and Denopamine by a One-Pot Lipase Resolution Protocol. **2004**, *15*, 3939–3944. https://doi.org/10.1016/j.tetasy.2004.11.013.
- (16) Arnold, W. A Catalytic Enantioselective Synthesis of Denopamine, a Useful Drug for Congestive Heart. **1991**, No. 5, 442–444.
- (17) Cho, B. T.; Yang, W. K.; Choi, O. K. Convenient Synthesis of Optically Active 1,2-Diol Monosulfonates and Terminal Epoxides. **2001**, No. Scheme 1.
- (18) Corey, E. J.; Helal, C. J. Remarkable Advances in Catalytic Methods for Enantio-Selective Synthesis of Chiral Organic Molecules Have Chemistry. Great Progress Has Been Made Not Only in Reduction of Carbonyl Compounds with Chiral Oxazaborolidine Catalysts: A New Paradigm for Enantioselective Catalysis and a Powerful New Synthetic Method **.
- (19) Yadav, J. S.; Reddy, P. T.; Nanda, S.; Bhaskar Rao, A. Stereoselective Synthesis of (R)-(-)-Denopamine, (R)-(-)-Tembamide and (R)-(-)-Aegeline via Asymmetric Reduction of Azidoketones by Daucus Carota in Aqueous Medium. *Tetrahedron Asymmetry* 2002, 12 (24), 3381–3385. https://doi.org/10.1016/S0957-4166(02)00024-1.
- (20) Goswami, J.; Bezbaruah, R. L.; Goswami, A.; Borthakur, N. A Convenient Stereoselective Synthesis of (R) (-) -Denopamine and (R) (-) -Salmeterol. **2001**, *12*, 3343–3348.
- (21) Fardelone, C.; Rodrigues, J. A. R.; Moran, P. J. S. Bioreduction of 2-Azido-1-Arylethanones Mediated by Geotrichum Candidum and Rhodotorula Glutinis. **2006**, *39*, 9–12. https://doi.org/10.1016/j.molcatb.2006.01.015.

<u>Chapter 5</u>: Conclusions and future prospects

The increasing applications of protein engineering in the recent times has established it as an inevitable tool in the field of biocatalysis. It has gained huge importance in industries, where it is employed as a crucial technique to tailor natural enzyme. Altering wild type enzymes often produces potential biocatalysts with a wide range of desirable properties, suitable for industrial application. In the current study, protein engineering was utilized as the key tool on a hydroxynitrile lyase (HNL) to achieve desired biocatalytic properties, such as increased enantioselectivity, conversions, stability, selectivity and tolerance of broad substrate while catalyzing a promiscuous reaction. HNL catalyzed biocatalysis is known to produce a wide range of enantiopure chiral products, which are highly valuable in the global market. They are diverse enzymes with respect to their source, sequence, structural fold and catalytic site. Despite of such natural diversity, their application in biotechnology industry is restricted due to several limitations such as poor enantioselectivity, limited yield and not being evolved to accept unnatural substrates. HNL engineering is the best solution to overcome such limitations and to evolve as an efficient biocatalyst in the synthesis of several enantiopure chiral molecules. Here, we have tried to synthesize enantiopure β-nitroalcohols using the promiscuous Henry (nitroaldol) and retro-Henry (retro-nitroaldol) reactions using engineered HNL. These enantiopure β-nitroalcohols are chiral drug intermediates, which have diverse applications in pharmaceutical, agrochemical, and cosmetic industries. HNL catalyzed stereoselective synthesis of chiral β-nitroalcohols is considered to be one of the most predominant methods among other biocatalytic approaches. It is because, Henry reaction involves a direct C-C bond formation reaction, an atom economy approach, and does not require addition steps of substrate synthesis. Further, one could access to enantiocomplementary β-nitroalcohols using HNL catalysed Henry and retro-Henry reactions. To date, AtHNL is the only (R)-selective HNL reported in both enantioselective cleavage (retronitroaldol) and synthesis (nitroaldol) of chiral β -nitroalcohols. It doesn't require any cofactor for its catalysis unlike other (R)-selective HNLs, GtHNL and AcHNL. The aim of the thesis was to engineer AtHNL in order to overcome the limitations associated with the promiscuous nitroaldolase and retro-nitroaldolase activity of the wild type enzyme. We observed enhanced promiscuous retro- nitroaldolase activity of AtHNL by protein engineering. The limitations such as low enantioselectivity, poor yield, and narrow substrate scope in the enantioselective synthesis of β -nitroalcohols are resolved using AtHNL engineering. Using engineered AtHNL catalyzed nitroaldol reaction, we developed a new chemo-enzymatic method to synthesize a chiral intermediate of (R)-Tembamide, i.e., (R)-1-(4-methoxyphenyl)-2-nitroethanol.

In order to to improve the catalytic efficiency of *At*HNL's retro-nitroaldolase activity, we engineered *At*HNL by altering residues in its binding site. Separate kinetic studies of the wild type *At*HNL with the promiscuous substrate 2-nitro-1-phenylethanol (NPE) and mandelonitrile (MN) revealed that former has higher binding affinity than MN. To explore this differential binding affinity of the two substrates, we docked both (*R*)-MN and (*R*)-NPE into the active site of *At*HNL separately and identified three residues in the binding site (Phe82, Phe179, and Tyr14). Site saturation mutagenesis (SSM) was performed at positions Phe179, and Tyr14; while a smart library was created at Phe82 by replacing it with polar amino acids. In case of F179A, we observed ~12 fold increased retro-nitroaldolase selectivity over cyanogenesis. Further, replacing Phe82 by polar residues has resulted in drastic decrease of the retro-nitroaldolase activity, which indicates that Phe82 is crucial for the concerned catalysis.

Study of retro-nitroaldolase activity using NPE as substrate has disclosed nearly a dozen of variants in the Phe179 and Tyr14 series that exhibited more than a two-fold increased activity than the wild type (WT). The variants showing higher retro-nitroaldolase activity than the WT were

kinetically characterized. Kinetics analysis of fourteen selected variants has revealed that eight (F179M, F179N, F179W, F179T, F179V, F179I, Y14L and Y14M) of them have greater V_{max} and k_{cat} than the WT, while F179N is the only one that showed a lower K_{M} (0.006±0.0004 mM) apart from greater V_{max} (1.91±0.02 U/mg) and k_{cat} (53.34±0.65 min⁻¹). The catalytic efficiency ($k_{\text{cat}}/K_{\text{M}}$) of the F179N was found to be ~2.4 fold greater than the WT. Selected variants from NPE cleavage study were also explored for enantioselective preparation of (S)-NPE. Two variants, F179V, and F179N, have shown greater E than the WT. In the case of F179N, the E value was found to be 137.6, which is ~1.7 fold more than the WT. Three double variants, F82A-F179N, F82A-F179V and F82A-F179W, created by addition of mutations based on lower $K_{\rm M}$ and higher $k_{\rm cat}$ for retronitroaldolase activity, showed poor catalytic efficiency than the WT. Docking of both enantiomers of NPE with the WT and mutants illustrated higher negative binding energy in the case of F179N with the (R)-NPE than the (S). Catalytic active site conformation could not be achieved in the case of WT and F179N with (S)-NPE, which explains the higher enantioselectivity of F179N towards retro-nitroaldol reaction. The enzyme-substrate interaction plots (PyMol) have supported the strong substrate binding by the F179N and a better orientation of the substrate in the active site of F179N, which is similar with the data observed from kinetics. These results from the computation studies may attribute towards its higher catalytic efficiency of F179N.

Molecular dynamics simulation study on structural stability of the docked complexes on a 50 ns time scale has revealed higher stability by the F179N complex than the WT beyond 25 ns. The RMSF calculations along with inter-atomic positions of C_{α} atoms of the catalytic triads have suggested higher flexibility in the case of F179N, which supports its efficient catalysis. MMPBSA calculations showed the higher negative binding free energy in the case of F179N-(R)-NPE complex compared to the WT. This observation further supports our experimental low $K_{\rm M}$ by the

F179N for NPE. Based on the interactions between (*R*)-NPE and *At*HNL wild type at different time intervals from the MDS study, a plausible retro-nitroaldol mechanism was proposed. Finally, a preparative scale synthesis of (*S*)-NPE using crude cell lysates of F179N under optimized conditions was performed where the (*S*)-NPE was produced in 93% *ee*, and 48.6% isolated yield including ~20% ethyl acetate impurity.

To address the second objective where we intended to improve the biocatalytic properties of AtHNL towards its promiscuous nitroaldolase activity, we initially explored the three saturation libraries that were exploited in our previous study. In this study our main focus was to overcome several of AtHNL's limitations, i.e., improve its yield, enhance its enantioselectivity and also to expand its substrate scope for diverse aromatic aldehydes using engineered AtHNLs. As a part of it, the primary screening of the three saturation libraries revealed several variants with >96% ee (F179A, F179H, F179C, F179N, F179L, F179M, F179V, F179K, F179W, Y14K, Y14R), >95% ee (Y14F, F179S), >93% ee (Y14C and Y14M) and a few with >33% conversion (Y14C, Y14F, and Y14A) as compared to the WT, in the nitroaldol reaction. We could also observe from this screening study that Phe82 is a very crucial residue for not only retro-nitroaldolase activity but also for nitroaldolase activity of AtHNL. Based on the screening outcome, F179H, F179N, F179L, and F179W from the F179 saturation library and Y14A, Y14C, Y14F, Y14M, Y14G, Y14L and Y14T from the Y14 saturation library were employed in the synthesis of various (R)-βnitroalcohols. For the first time engineered AtHNLs were exploited in exploring their selectivity for a wide range of substrates towards stereoselective Henry reaction. The engineered AtHNLs showed high enantioselectivity towards the synthesis of (R)- β -nitroalcohols of five aldehydes, trans cinnamaldehyde, 4-nitro benzaldehyde, 2,4-dimethoxy benzaldehyde, 3,4,5-trimethoxy benzaldehyde and 4-benzyloxy benzaldehyde. Our study of the substrate scope of dozen of

selected AtHNL variants in the synthesis of diverse (R)- β -nitroalcohols revealed that the variants F179N, F179W, Y14M and Y14F have improved the enzyme's activity very significantly. F179N variant has shown highest % ee and % conversion in the (R)-β-nitroalcohol synthesis for the substrates: benzaldehyde, 3-chlorobenzaldehyde and 3-methylbenzaldehyde, F179W for trans cinnamaldehyde, Y14M for benzaldehyde, 4-fluorobenzaldehyde and 4-benzyloxybenzaldehyde and Y14F for 4-chlorobenzaldehyde, 4-nitrobenzaldehyde, 2,4-dimethoxy benzaldehyde, 4methylbenzaldehyde, 3-methoxybenzaldehyde and 3,4,5-trimethoxybenzaldehyde. Y14M and F179N have shown > 80% conversion along with 93-97% ee in the synthesis of (R)-NPE. The double variant Y14M-F179W showed improved % ee and % conversion in synthesis of (R)-βnitroalcohol of benzaldehyde, trans cinnamaldehyde, 4-chlorobenzaldehyde, 4-nitrobenzaldehyde and 4-benzyloxybenzaldehyde. We found AtHNL variants that improved the selectivity towards bulky substrates such as trans cinnamaldehyde and 4-benzyloxybenzaldehyde. The AtHNL engineering was also proven productive with several aromatic aldehydes containing single, double and triple substitutions in the aromatic ring, substituents at different positions of aromatic ring, and both electron-donating and withdrawing groups, as substrates in the chiral β-nitroalcohol synthesis. Finally, in this objective we successfully improved the promiscuous Henry reaction activity by several engineered AtHNLs using modified biocatalytic conditions. We have uncovered AtHNL variants that broadened the substrate scope, effectively improved the yield and enantioselectivity towards stereoselective Henry reaction.

To achieve the final objective of the thesis, a new, simple and efficient chemo-enzymatic route involving nitroaldol reaction was developed to synthesize a chiral intermediate of (R)-Tembamide, i.e., (R)-2-amino-1-(4-methoxyphenyl)-2-ethanol, which is an industrially significant active pharmaceutical ingredient. We envisioned to achieve this in a two-step process, first an enzymatic

synthesis of (*R*)-1-(4-methoxyphenyl)-2-nitroethanol, followed by a chemical reduction of the product. For the first reaction, we exploited engineered *At*HNL variants (F179W, F179N, Y14F, Y14M and Y14M-F179W) selected from the previous study, where they were employed in the enantioselective synthesis of diverse (*R*)-β-nitroalcohols. The double variant Y14M-F179W showed the highest % conversion (70%) than others with 99% *ee* in the synthesis of (*R*)-1-(4-methoxyphenyl)-2-nitroethanol. Further, this product was reduced to (*R*)-2-amino-1-(4-methoxyphenyl)-2-ethanol using a simple HCOOH/Zn in methanol at room temperature. We successfully made a cleaner and greener combination of an engineered *At*HNL along with a chemical catalyst to efficiently synthesize the (*R*)-Tembamide drug intermediate, i.e., (*R*)-2-amino-1-(4-methoxyphenyl)-2-ethanol in a preparative scale with 99% *ee* and 58% isolated yield of the product.

Future prospects:

- In the present study, we have demonstrated the AtHNL variants catalyzed retro-Henry reaction in the preparation of (S)-NPE using benzaldehyde as the substrate. The engineered AtHNLs can be exploited to prepare diverse (S)- β -nitroalcohols, which extends the application of the method and the biocatalysts.
- We investigated AtHNL variants in the efficient synthesis of a number of (R)-β-nitroalcohols using Henry reaction. A computation study involving molecular docking and simulations and crystallographic studies of engineered enzymes with different substrates, would reveal the molecular binding and interactions involved and may unravel the mechanism too.
- In this study, AtHNL engineering was done to improve both Henry and retro-Henry reactions, which are promiscuous in nature. These AtHNL saturation library variants can

also be explored in the synthesis of a wide range of enantiocomplementary synthesis of chiral cyanohydrins using their natural cyanogenesis and synthesis reactions. They could also be investigated towards other promiscuous reactions using carbon nucleophiles other than nitroalkanes.

- The engineered *At*HNLs can be exploited in related cascades and chemo-enzymatic syntheses to produce chiral molecules of chemical diversity.
- Our chemo-enzymatic method of synthesis of (*R*)-Tembamide drug intermediate, i.e., (*R*)-2-amino-1-(4-methoxyphenyl)-2-ethanol can be scaled up and extended to large-scale preparation of (*R*)-Tembamide, which is reported as a good control for hypoglycemia.
- Another future prospect of this study is to synthesize (*S*)-Tembamide, which is known for its anti-HIV activity. It can be synthesized by replacing *At*HNL variant catalyzed nitroaldol reaction with retro-nitroaldol reaction in the first step of the chemo-enzymatic process, while the subsequent steps can be similar to that used in the synthesis of (*R*)-Tembamide.

LIST OF PUBLICATIONS

a) In refereed international journals

■ Badipatla Vishnu Priya ^a, D.H. Sreenivasa Rao ^{a,1}, Rubina Gilani ^{a,1}, Surabhi Lata ^{b,1}, Nivedita Rai ^a, Mohd. Akif ^b, Santosh Kumar Padhi ^{a*}. Enzyme engineering improves catalytic efficiency and enantioselectivity of hydroxynitrile lyase for promiscuous retro-nitroaldolase activity. *Bioorganic Chemistry*, 120 (2022) 105594. Impact factor: 5.4.

b) Presentations at conferences

- Badipatla Vishnu Priya*, D.H. Sreenivasa Rao, Rubina Gilani, Surabhi Lata, Nivedita Rai, Mohd. Akif, Santosh Kumar Padhi "Improvement of catalytic efficiency and enantioselectivity of an engineered Hydroxynitrile lyase towards promiscuous retro nitroaldolase activity"-poster presented at International Symposium "Chemical Wisdom by Her" organized by Department of Chemistry, Deshbandhu College (DU) held on 31st January, 2022.
- Badipatla Vishnu Priya*, Rubina Gilani, Nivedita Rai, Santosh Kumar Padhi "The promiscuous nitroaldolase activity of a plant hydroxynitrile lyase vs. its natural activity of cyanogenesis"- poster presented at National Seminar on "Biomolecular interactions in development and diseases" organized by Department of Biochemistry, UoH held on 26-28th September, 2019.
- Badipatla Vishnu Priya*, Rubina Gilani, Nivedita Rai, Santosh Kumar Padhi "Understanding the promiscuous nitroaldolase activity of a hydroxynitrile lyase vs. its natural cyanohydrin cleavage activity" poster presented at BioQuest-2019 organized by School of Life Sciences, UoH held on 11th March 2019.
- Nivedita Rai*, **Badipatla Vishnu Priya**, D. H. Sreenivasa Rao, Lipika Pattanayak, Surya Narayan Rath, and Santosh Kumar Padhi, "A theoretical and experimental study on two different reactions catalyzed by the same catalytic site of a α/β-hydrolase fold hydroxynitrile lyase" poster presented at **BioQuest-2017** organized by School of Life Sciences, UoH held on 12th −13th October 2017.



University of Hyderabad Hyderabad- 500 046, India

PLAGIARISM FREE CERTIFICATE

This is to certify that the similarity index of this thesis as checked by the Library of the University of Hyderabad is 36%. Out of this, 25% similarity has been found from the candidate's (Badipatla Vishnu Priya) own publication, which form the adequate part of the thesis. Another 4% is from the M. Sc. theses of my laboratory, where the corresponding students were worked with Vishnu Priya for their M. Sc. thesis and used the same protocols that were used by her. This brings to overall plagiarism of the thesis to 36% - 29% = 7%.

The details the of student's publication is as follows:

Paper

% Similarity

1. Badipatla Vishnu Priya a, D.H. Sreenivasa Rao a,1, Rubina Gilani a,1, Surabhi Lata b,1, Nivedita Rai a, Mohd. Akif b, Santosh Kumar Padhi a*. Enzyme engineering improves catalytic efficiency and enantioselectivity of hydroxynitrile lyase for promiscuous retro-nitroaldolase activity. *Bioorganic Chemistry*, 120 (2022) 105594.

25% (Source No. 1)

About 7% similarity was identified from external sources in the present thesis, which is in accordance with the regulations of the University. All the publications related to this thesis have been appended at the end of the thesis. Hence the present thesis may be considered to be plagiarism free.

Dr. Santosh Kumar Padhi Supervisor

Dr. Santosh Kumar Padhi Assistant Professor Department of Biochemistry School of Life Sciences University of Hyderabad Hyderabad-500 046. India

Protein engineering of Arabidopsis thaliana hydroxynitrile lyase (AtHNL) improves promiscuous nitroaldolase and retronitroaldolase activity

by Badipatla Vishnu Priya

Submission date: 14-Nov-2022 04:55PM (UTC+0530)

Submission ID: 1953543609

File name: Badipatla Vishnu Priya.pdf (5.56M)

Word count: 35497

Character count: 183354

Protein engineering of Arabidopsis thaliana hydroxynitrile lyase (AtHNL) improves promiscuous nitroaldolase and retronitroaldolase activity

ORIGINALITY REPORT

36_%

7%
INTERNET SOURCES

34%

8% STUDENT PAPERS

PRIMARY SOURCES

Badipatla Vishnu Priya, D.H. Sreenivasa Rao, Rubina Gilani, Surabhi Lata, Nivedita Rai, Mohd. Akif, Santosh Kumar Padhi. "Enzyme Santosh Kumar Padhi engineering improves catalytic efficiency enantioselectivity of hydroxynitrile lyase for Iniversity of Hyderabad Hyderabad-500 046. India promiscuous retro-nitroaldolase activity",

Bioorganic Chemistry, 2022

Submitted to University of Hyderabad pr. Santosh Kumar Parnia Assistant Professor Department of Biochemistry School of Life Sciences University of Hyderabad Hyderabad-500 046. India

Ken-ichi Fuhshuku, Yasuhisa Asano.
"Synthesis of (R)-β-nitro alcohols catalyzed by R-selective hydroxynitrile lyase from

Arabidopsis thaliana in the aqueous-organic biphasic system", Journal of Biotechnology, 2011

Publication

1%

4	Ayon Chatterjee, D.H. Sreenivasa Rao, Santosh Padhi. "One - Pot Enzyme Cascade Catalyzed Asymmetrization of Primary Alcohols: Synthesis of Enantiocomplement Asymmetrical Chiral β - Nitroalcohols", Advanced Synthesis of Enantiocomplement Asymmetrical Chiral β - Nitroalcohols", Advanced Synthesis of Enantiocomplement Asymmetrical Chiral β - Nitroalcohols (Advanced Synthesis) **Catalysis**, 2021	h Kumar Padhi ant Professor it of Biochemistry Life Sciences of Hyderabad 1-500 046. India
5	docksci.com Internet Source	<1%
6	D. H. Sreenivasa Rao, Santosh Kumar Padhi. " Production of ()-β-Nitro Alcohols by Enantioselective C–C Bond Cleavage with an - Selective Hydroxynitrile Lyase ", ChemBioChem, 2019 Publication	<1%
7	www.ncbi.nlm.nih.gov Internet Source	<1%
8	pubs.rsc.org Internet Source	<1%
9	D. H. Sreenivasa Rao, Ayon Chatterjee, Santosh Kumar Padhi. "Biocatalytic approaches for enantio and diastereoselective synthesis of chiral β-nitroalcohols", Organic & Biomolecular Chemistry, 2020	<1%



15	Eko Adi Prasetyanto, Hailian Jin, Sang-Eon Park. "Chiral enhancement in the confined space of zeolites for the asymmetric synthesis of β-hydroxy nitroalkanes", Tetrahedron: Asymmetry, 2011 Publication	<\!\\
16	Ewa Wolińska. "Asymmetric Henry reactions catalyzed by copper(II) complexes of chiral 1,2,4-triazine-oxazoline ligands: the impact of substitution in the oxazoline ring on ligand activity", Tetrahedron: Asymmetry, 2014 Publication	<1%
17	hdl.handle.net Internet Source	<1%
18	Pankaj Gupta, Neha Mahajan. "Biocatalytic Approaches Towards Stereoselective Synthesis of Vicinal Amino Alcohols", New Journal of Chemistry, 2018	<1%
19	Sinéad E. Milner. "Biocatalytic Approaches to the Henry (Nitroaldol) Reaction", European Journal of Organic Chemistry, 04/12/2012	<1%
20	Santosh Kumar Padhi. "Modern Approaches to Discovering New Hydroxynitrile Lyases for	<1%

Biocatalysis", ChemBioChem, 2017

Publication



26	"Enantioselective nitroaldol reaction catalyzed by chiral C1-tetrahydro-1,1'-bisisoquinoline-copper(I) complexes", Tetrahedron: Asymmetry, 2011 Publication	<1%
27	pubs.acs.org Internet Source	<1%
28	Mita Halder, Piyali Bhanja, Md. Mominul Islam, Asim Bhaumik, Sk. Manirul Islam. "Chiral copper-salen complex grafted over functionalized mesoporous silica as an efficient catalyst for asymmetric Henry reactions and synthesis of the potent drug ()-isoproterenol ", New Journal of Chemistry, 2018 Publication	<1%
29	Jin-Liang Li, Li Liu, Yu-Ning Pei, Hua-Jie Zhu. "Copper(II)-containing C2-symmetric bistetracarboline amides in enantioselective Henry reactions", Tetrahedron, 2014 Publication	<1%
30	Lee, D.M "Asymmetric transfer hydrogenation of 2-tosyloxy-1-(4-hydroxyphenyl)ethanone derivatives: synthesis of (R)-tembamide, (R)-aegeline, (R)-octopamine, and (R)-denopamine", Tetrahedron: Asymmetry, 20071112	<1%

31	epdf.pub Internet Source	<1%
32	Uwe T. Bornscheuer, Romas J. Kazlauskas. "Catalytic Promiscuity in Biocatalysis: Using Old Enzymes to Form New Bonds and Follow New Pathways", Angewandte Chemie International Edition, 2004 Publication	<1%
33	von Langermann, Jan, David M. Nedrud, and Romas J. Kazlauskas. "Increasing the Reaction Rate of Hydroxynitrile Lyase from Hevea brasiliensis toward Mandelonitrile by Copying Active Site Residues from an Esterase that Accepts Aromatic Esters", ChemBioChem, 2014. Publication	<1%
34	www.medsci.org Internet Source	<1%
35	www.pubfacts.com Internet Source	<1%
36	Surabhi Lata, Mohd. Akif. "Structure-based identification of natural compound inhibitor against thioredoxin reductase: insight from molecular docking and dynamics simulation ", Journal of Biomolecular Structure and Dynamics, 2020	<1%

37	dalspace.library.dal.ca Internet Source	<1%
38	Atoholi Sema, H., Ghanashyam Bez, and Sanjib Karmakar. "Asymmetric Henry reaction catalysed by L-proline derivatives in the presence of Cu(OAc)2: isolation and characterization of an in situ formed Cu(II) complex: Asymmetric Henry reaction catalysed by I-proline derivative", Applied Organometallic Chemistry, 2014.	<1%
39	patents.google.com Internet Source	<1%
40	portal.research.lu.se Internet Source	<1%
41	www.science.gov Internet Source	<1%
42	Thomas Purkarthofer, Karl Gruber, Mandana Gruber-Khadjawi, Kerstin Waich, Wolfgang Skranc, Daniel Mink, Herfried Griengl. "A Biocatalytic Henry Reaction—The Hydroxynitrile Lyase fromHevea brasiliensis Also Catalyzes Nitroaldol Reactions", Angewandte Chemie International Edition, 2006 Publication	<1%

43	archiv.ub.uni-marburg.de Internet Source	<1%
44	mafiadoc.com Internet Source	<1%
45	Submitted to Higher Education Commission Pakistan Student Paper	<1%
46	Nisha Jangir, Santosh Kumar Padhi. "Immobilized Baliospermum montanum hydroxynitrile lyase catalyzed synthesis of chiral cyanohydrins", Bioorganic Chemistry, 2018 Publication	<1%
47	Submitted to University College London Student Paper	<1%
48	www.freepatentsonline.com Internet Source	<1%
49	www.koreascience.or.kr Internet Source	<1%

Exclude quotes On Exclude bibliography On

Exclude matches

< 14 words

UNIVERSITY OF HYDERABAD SCHOOL OF LIFE SCIENCES DEPARTMENT OF BIOCHEMISTRY

PROFORMA FOR SURMISSION OF THE SIS/DISSEDITATION

	- Was a state of the state of t	ON OF THE SIS/DISSERTATION
1.	Name of the Candidate	: BADIPATLA VISHNU FRIMA
2.	Roll No.	: 17L6PH06
3,	Year of Registration	2017
4.	Topic	Photoin engineering of frabidops baliana Hydrogenthik lyase suproves promisculars suprocedulars attractables. Dr. SANTOSH KUMAR PATHT.
5.	Supervisor(s) and affiliations	: Dr. SANTOSH KUMAR PADHTI & METroutsoulders
6.	Whether extension/re-registration g (Specify below)	ranted: -
7.	Date of submission	: 23/11/2022
8.	Last class attended on (M.Phil/Pre-l	Ph.D): 08 06 2022
9.	Whether tuition fee for the current p	period Paid: Receipt No. & Dt: \$8115012 Date - 12/12/22
10.	Whether thesis submission fee paid	: Receipt No & Dt : Transaction 42 - 232605924930
11.	Whether hostel dues cleared	: Receipt No & Dt: UP? transaction 10.229061267548 Date 17/10/2022
12.	Whether a summary of the dissertation	The state of the s
Supervisor(s) Santesh Kumar Padhi Signature Department of Biochemistry School of Life Sciences University of Hyderabad Hyderabad-500 046. India Signature of the Dean, of the School DEAN Forwarded on Signature of the Head of the Department. Department. Department. Dept of Biochemistry School of Life Sciences SCHOOL OF LIFE SCIENCES SCHOOL OF HYDERABAD UNIVERSITY OF HYDERABAD UNIVERSITY OF HYDERABAD University of Hyderabad University of Hyderabad		
	Universi	ty of 1900 046.

Hyderabad-500 046.



Rs:

UNIVERSITY OF HYDERABAD

E-Receipt

Received With Thanks from: Transaction No.: 221122110718174

Name: BADIPATLA VISHNU PRIYA Date: Nov 22, 2022

Course: Ph.D.(Biochemistry) PG Reference No.: 221122136790896

Rupees: 1200 Application/Reg. No.: 17LBPH06

Purpose : Thesis Submission Payment Gateway ICICI

1200